Mechanism and Chirality Transfer in Cyclizations of Amides and Related Compounds

by

David B. Guthrie

B.S., St. Vincent College, 2003

Submitted to the Graduate Faculty of

Arts and Sciences in partial fulfillment

of the requirements for the degree of

Doctor of Philosophy

University of Pittsburgh

2008

UNIVERSITY OF PITTSBURGH

FACULTY OF ARTS AND SCIENCES

This dissertation was presented

by

David B. Guthrie

It was defended on

November 25, 2008

and approved by

Alexander S. Doemling, Associate Professor, Pharmaceutical Sciences

Paul E. Floreancig, Associate Professor, Chemistry

Craig S. Wilcox, Professor, Chemistry

Dissertation Advisor: Dennis P. Curran, Distinguished Service Professor, Chemistry

Mechanism and Chirality Transfer in Cyclizations of Amides and Related Compounds

David B. Guthrie, Ph.D.

University of Pittsburgh, 2008

The role of halogens in the 5-*endo-trig* cyclizations of radicals derived from *N*-cyclohexenyl-α-haloacetamides on the product distribution has been thoroughly investigated. Under reductive radical conditions, α-chloroamides produce octahydroindolones, while α-iodoamides primarily give a mixture of hexahydroindolones and *N*-cyclohexenylacetamides. Kinetic studies showed the rate constants of cyclization are not critically halogen-dependent, but the ratio of cyclized to oxidized products is dependent on the halogen used in the radical precursor. When the starting halide is easily reducible, a single electron transfer from cyclized intermediates to starting material overrides the normal reductive chain process. This process spurs an ionic, acid-driven reductive halogenation process, which disrupts the anticipated radical chain mechanism. Addition of excess base suppresses the reductive dehalogenation pathway.

Enantioenriched derivatives of *N*-allyl-*o*-iodoarylcarbamates undergo radical cyclizations to give enantioenriched dihydroindoles in 87-100% yields and 83-92% chirality transfers. Anionic cyclizations of these substrates proceed in 58-74% yields and 84-99% chirality transfers. *N*-Aryl barriers to rotation were measured and found to be comparable to similar *o*-iodoacetanilides. The radical and anionic cyclizations proceed with the same sense of chirality.

Radical cyclizations of *N*-cyclohexenyl-*o*-iodoanilides may only occur through the *syn* atropisomer when an additional *ortho* substituent is present on the aromatic ring. When a second *ortho* substituent is not present, *N*-aryl rotation of the intermediate radical is faster than all

competing processes. Heck cyclizations on these substrates proceed through the *anti* atropisomer, requiring simultaneous *N*-aryl and *N*-cyclohexenyl rotations to achieve the necessary transition state. The β-elimination step of these Heck reactions occurs with complete *syn* selectivity.

Radical cyclizations of axially chiral α-haloacetanilides which contain an *ortho*-radical acceptor produce dihydroquinolin-2-ones in high yields and with high levels of chirality transfer (80-100%). A model of chirality transfer has been determined by absolute configuration determination of a substrate / product pair by X-ray crystallography. Secondary α-haloamides faithfully cyclize with exclusive *trans* selectivity. This methodology has been applied to a tandem 6-*exo*-*trig*/5-*exo*-*trig* radical cyclization, which proceeds with good diastereo- and enantioselectivity.

TABLE OF CONTENTS

LIST OF TABLES

LIST OF FIGURES

LIST OF SCHEMES

LIST OF ABBREVIATIONS

ABCN	1,1'-azobis(cyclohexanecarbonitrile)
Ac	acetyl
AIBN	2,2-azobisisobutyronitrile
Alloc	allyloxycarbonyl
atm	atmosphere(s)
BINAP	2,2'-bis(diphenylphosphino)-1,1'-binaphthyl
Bn	benzyl
Boc	*tert*-butoxycarbonyl
brsm	based on recovered starting material
Bu	butyl
BuLi	butyllithium
Cbz	benzyloxycarbonyl
cod	1,5-cyclooctadiene
CSA	camphorsulfonic acid
ct	chirality transfer
dba	dibenzylideneacetone
DCC	*N*,*N*'-dicyclohexylcarbodiimide
DCE	1,2-dichloroethane

DEPT	distortionless enhancement by polarization transfer
DLP	dilauroyl peroxide
DMAP	*N*,*N*-dimethyl-4-aminopyridine
DMF	*N*,*N*-dimethylformamide
dppf	1,1'-bis(diphenylphosphino)ferrocene
dr	diastereomeric ratio
EDCI	1-ethyl-3-(3'-dimethylaminopropyl)carbodiimide
ee	enantiomeric excess
EI	electron ionization
equiv	equivalent(s)
er	enantiomeric ratio
ESI	electrospray ionization
Et	ethyl
FEE	first eluting enantiomer
FTIR	Fourier Transform infrared spectroscopy
GC	gas chromatography
h	hours
h	Planck's constant
HAT	hydrogen atom transfer
HMPA	hexamethylphosphoramide
HRMS	high resolution mass spectrometry
ID	inner diameter
***i*-Pr**	isopropyl

k_B	Boltzmann's constant
LDA	lithium diisopropylamide
LiHMDS	lithium bis(trimethylsilyl)amide
LRMS	low resolution mass spectrometry
m	*meta*
M	molar
***m*-CPBA**	*meta*-chloroperoxybenzoic acid
Me	methyl
Meoc	methoxycarbonyl
min	minutes
mM	millimolar
MOM	methoxymethyl
Ms	methanesulfonyl
NaHMDS	sodium bis(trimethylsilyl)amide
nd	not detected
NMR	nuclear magnetic resonance
o	*ortho*
ORTEP	Oak Ridge thermal ellipsoid plot
p	*para*
Ph	phenyl
PMB	*para*-methoxylbenzyl
ppm	parts per million
rac	racemic

rt	room temperature
sat	saturated
SCE	saturated calomel electrode
SEE	second eluting enantiomer
SET	single electron transfer
***t*-Bu**	*tert*-butyl
TFA	trifluoroacetic acid
THF	tetrahydrofuran
TLC	thin layer chromatography
TMS	trimethylsilyl
tol	tolyl
Ts	*para*-toluenesulfonyl
TTF	tetrathiafulvalene
TTMSS	tris(trimethylsilyl)silane
UV	ultraviolet
V	volt(s)
w/w	(percentage) by weight

PREFACE

I would like to take this opportunity to thank everyone who has been a part of my graduate studies. First and foremost, I would like to thank my advisor, Prof. Dennis Curran. My experience working with him has been both challenging and rewarding, and it has been an honor and a privilege to conduct research under his guidance. I have certainly learned much from him over the years, not only in chemistry knowledge but also how to conduct myself as a professional. I am grateful for the freedom he has given me to explore new ideas, as well as for his assistance in developing my writing technique. I will always owe a great deal to him for helping me develop and mature as a scientist.

I am also thankful to Profs. Paul Floreancig, Craig Wilcox, and Alexander Doemling for serving on my defense committee, and Prof. Peter Wipf for acting as my research proposal mentor. I appreciate all of the input and insight they have given me in my endeavors.

It has been wonderful to work with, and befriend, so many great people in the Curran group over the years. I am especially grateful to Dr. Jonathan Tripp and Dr. Andre Lapierre, who helped to familiarize me with radical chemistry and axially chiral amides. Over the years, I was also fortunate enough to have two of the best lab partners anyone could ask for, Dr. Cristian Harrison and Dr. Eveline Kumli.

I would like to thank Dr. Kasi Somayajula and Dr. John Williams, who both directed our excellent mass spectrometry facilities during my studies here. I am also very grateful to Dr. Futyan Lin and Dr. Damodaran Krishnan for their assistance in NMR studies, particularly variable temperature NMR experiments. The X-ray crystallography expertise of Dr. Steven Geib has also been crucial to the success of several of my projects, and has been greatly appreciated.

I would also like to give a special thanks to a group of people whose efforts are often underappreciated: everyone who works in the second floor office. The day-to-day operations of the department could never proceed so smoothly without their constant efforts. I am especially thankful to Mrs. Fran Nagy, who has done so much for me and every other graduate student in this department.

I could never have achieved so much in my life without the constant love and support from my family, especially my parents, Terry and Karen Guthrie. They have always believed in me, and made every effort to ensure that none of my goals or dreams were ever out of reach. I will always be grateful for everything they have done for me, and I can only hope that I will always make them proud.

Finally, I would like to thank Sarah Morrison, who has been a source of unending love and inspiration over the last few years. She has given me strength when I needed it most, and I am truly thankful that she is a part of my life.

1.0 EFFECT OF THE HALOGEN ATOM IN 5-*ENDO-TRIG* RADICAL CYCLIZATIONS OF α-HALOENAMIDES

1.1 INTRODUCTION

1.1.1 5-*Endo-trig* Radical Cyclizations in Organic Synthesis

A relatively new addition to the family of radical cyclizations, the 5-*endo-trig* ring closure is both an unusual and useful process.[1-17] A 4-pentenyl radical **1.1** can react in a 5-*endo-trig* fashion to produce a cyclopentyl radical **1.2**, or it can cyclize in a 4-*exo-trig* manner to produce a cyclobutylcarbinyl radical **1.3** (Scheme 1.1). Due to the ring strain present in **1.3**, 4-*exo-trig* processes are often reversible with the equilibrium greatly favoring the ring-opened form **1.1**,[4,17] except in special cases where R is a radical stabilizing group.[18] In contrast, the 5-*endo-trig* process is much less reversible due to the thermodynamic stability of cyclopentyl radical **1.2**.[3] However, formation of **1.2** is disfavored by Baldwin's rules because of the failure of **1.1** to meet the stereoelectronic requirements for cyclization.[19,20]

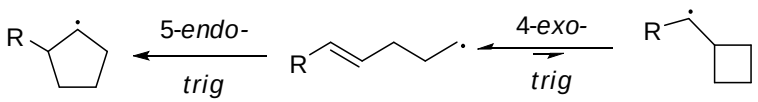

1.2 **1.1** **1.3**

Scheme 1.1 Cyclization Routes for a 4-Pentenyl Radical

Despite the inherently unfavorable nature of the 5-*endo-trig* process, addition of a high degree of substitution around the ring being formed can result in a beneficial Thorpe-Ingold effect,[21,22] accelerating cyclization. Malacria used this advantageous factor in the cascade radical cyclization of **1.4** to **1.5**, shown in Scheme 1.2. This is one of the first examples of formation of an all-carbon ring through a 5-*endo-trig* radical process.[1] The fused silacycle also assists in the final ring closure process by conformational fixation of the radical intermediate, an effect which has been observed in other, similar reactions.[23]

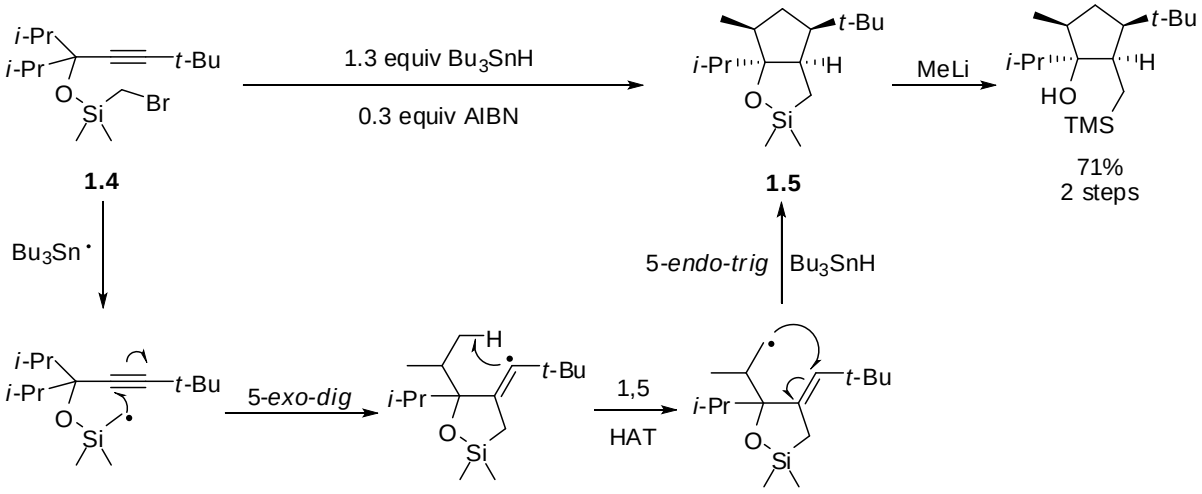

Scheme 1.2 Tandem Sequence Including an All-Carbon 5-*Endo-trig* Cyclization

The majority of effective 5-*endo-trig* cyclizations take advantage of a highly stabilized cyclized radical. Early studies toward the synthesis of fredericamycin A employed such an effect[14] by cyclizing the radical derived from **1.6** to form benzyl radical **1.7**, which abstracts a hydrogen atom from Ph_3SnH to give the 5-*endo-trig* product **1.8** in very high yield (Scheme 1.3). The synthetic tactic used on model compound **1.6** was successfully applied to a synthesis of the natural product.[13]

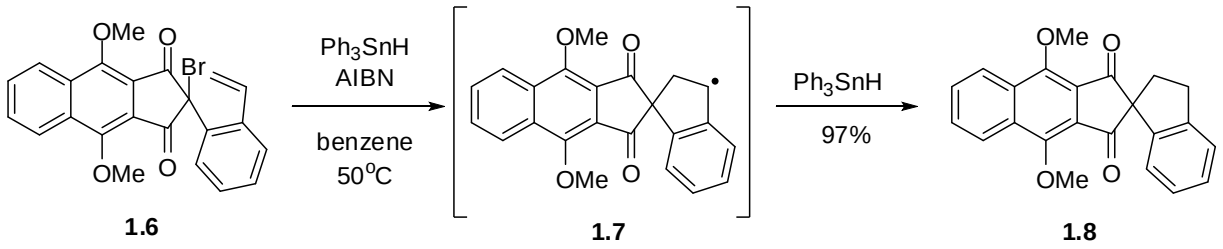

Scheme 1.3 5-*Endo-trig* Cyclization in Fredericamycin Model System

Radical 5-*endo-trig* cyclizations have also found widespread use in the formation of γ-lactam containing alkaloids and related compounds.[2,5-9,11,12,15,16,24-26] The Bu_3SnH-mediated cyclization of α-halo enamides is a useful way to form five-membered nitrogen-containing heterocycles. The precursors for these cyclizations contain four sp^2 carbons in the ring being formed, assisting in cyclization, and the resulting cyclized radical is heteroatom-stabilized. This methodology has been successfully applied to the synthesis of 4-arylglutamic acid **1.10** from α-chloroenamide **1.9**,[24] as seen in Scheme 1.4.

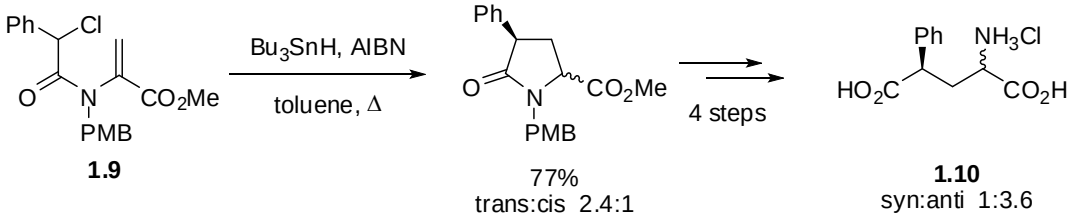

Scheme 1.4 Cyclization of α-Halo Enamide Towards Amino Acids

Radical cyclizations of α-halo enamides have been frequently used to construct fused ring systems found in natural alkaloids.[5-7,9,11,16] For example, chloride **1.11a** in Scheme 1.5 cyclizes under Bu_3SnH-mediated conditions to produce a mixture of lactams **1.13** and **1.14** in 77% total yield; the iodo congener **1.11b** gives similar results, cyclizing in 81% overall yield (Scheme 1.5).[5] The incorporation of the hydroxyl group in compound **1.14** is rationalized by

reaction of cyclized radical **1.12** with molecular oxygen, followed by reduction of the resulting peroxyl radical with Bu_3SnH.[27] The ability of intermediate **1.12** to react with adventitious oxygen, rather than Bu_3SnH, has been attributed to its relatively long-lived nature. Due to captodative stabilization[17,28,29] by the flanking nitrogen and carbonyl moieties, intermediate **1.12** reacts slowly with Bu_3SnH, and has ample lifetime to capture dissolved oxygen.

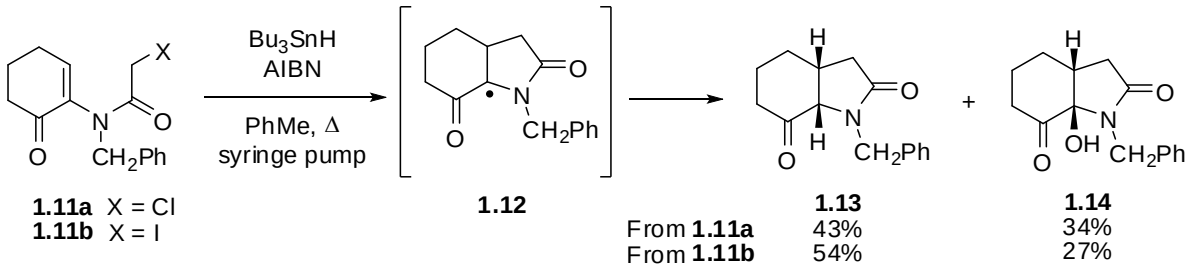

Scheme 1.5 Cyclization of α-Haloenamides to Produce Fused Lactams

1.1.2 Role of the Halogen Atom in 5-*Endo-trig* Cyclizations of α-Haloenamides

Recently, Ishibashi and co-workers reported anomalous results dealing with the Bu_3SnH-mediated radical cyclizations of substrates **1.15a-c**,[16] as summarized in Table 1.1. Chloride **1.15a** cyclized cleanly and efficiently to give octahydroindolone **1.16** as the sole product in 92% yield. Iodide **1.15c**, on the other hand, gave the product of direct reduction **1.19** in 68% yield, along with minor amounts of oxidized cyclized products **1.17** and **1.18**. Bromide **1.15b** gave a product distribution intermediate between the other two halides, producing **1.16** in a moderate yield of 55%, with small amounts of the oxidized cyclized compounds. These results were puzzling, as halogen abstraction from any substrate **1.15a-c** results in the same radical intermediate regardless of the identity of the halogen. A previous study on the *N*-methyl congeners of **1.15a** and **1.15c** showed a qualitatively similar trend in reactivity; only the chloride was able to cyclize, while the iodide was simply reduced.[8]

Table 1.1 Selected Examples of Halogen Effect in Ishibashi's Cyclizations of α-Haloenamides

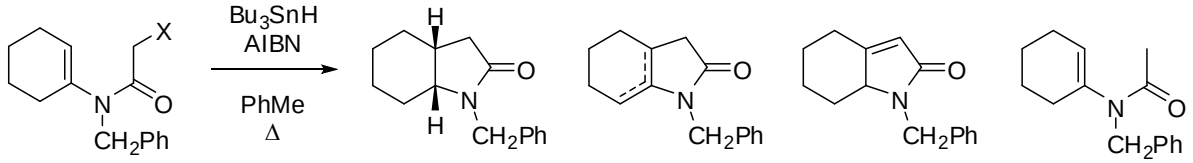

1.15a X = Cl
1.15b X = Br
1.15c X = I

1.16 **1.17** **1.18** **1.19**

			% yield of product[b]					
entry[a]	amide	X	**1.16**	**1.17**	**1.18**	**1.19**	total	cyc:red[c]
1	**1.15a**	Cl	92	0	0	0	92	> 99:1
2	**1.15b**	Br	55	11	11	0	77	> 99:1
3	**1.15c**	I	0	13	11	68	92	26:74

[a] conditions: Bu_3SnH (1.2 equiv) and AIBN (0.1 equiv) in toluene (12 mM in Bu_3SnH) was added via syringe pump to a refluxing mixture of the amide in toluene (10 mM) over 3 h. [b] Isolated yield after aq. KF workup and column chromatography. [c] Ratio of (**1.16 + 1.17 + 1.18**) to **1.19**.

Ishibashi postulated that steric differences among the different halogen atoms in **1.15a-c** were responsible for fixing the precursor in different *Z*/*E* amide rotamers as in Figure 1.1, consequently affecting the overall cyclization/reduction ratio of the products. It was proposed that, due to the greater internal steric hindrance caused by a shorter carbon-halogen bond length,[22] the α-chloro group (C−Cl = 1.78 Å) would have a significant repulsion by the *N*-benzyl group, forcing the molecule into rotamer (*E*)-**1.15a** ($K_X < 1$). The iodide, with a longer carbon-halogen bond length (2.14 Å), could preferentially populate the (*Z*)-**1.15c** rotamer ($K_X > 1$). The bromide (C−Br = 1.94 Å) would be expected to have an intermediate *Z*/*E* ratio.

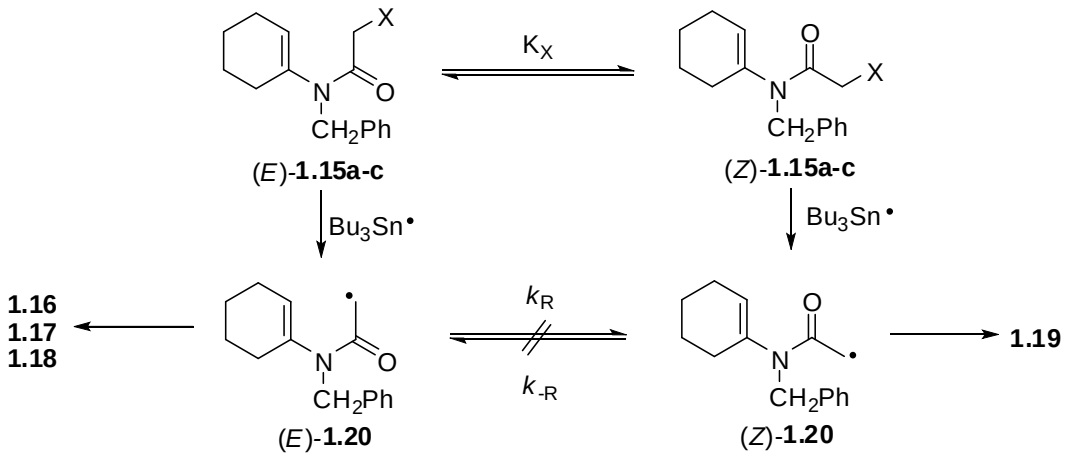

Figure 1.1 Postulated Rotamer Roles in Reactions of 11a-c

Upon halogen abstraction, rotamer (*E*)-**1.15** initially produces carbamoylmethyl radical (*E*)-**1.20**, which is in position to cyclize; similarly, halide rotamer (*Z*)-**1.15** would produce (*Z*)-**1.20** after halogen abstraction. Ishibashi postulated α-amide radical rotation rates k_R/k_{-R} to be slower than either intramolecular cyclization or reduction by Bu_3SnH. In this scenario, the fate of a given radical depends directly on the initial rotamer geometry of the starting material, which in turn is dependent on the identity of the halide used.

Rotamer geometry plays a vital role in the radical cyclization of various carbamoylmethyl radicals.[15,30-33] Previous studies by Curran[30,32] showed that, at ambient temperature, the 5-*exo*-*trig* atom-transfer cyclization of various α-halo amides gave a product distribution that reflected the starting *Z*/*E* amide rotamer ratio. Cyclization yields were increased by heating the reaction mixture, allowing the unreactive *Z*-α-amide radical intermediate to overcome the amide rotation barrier and isomerize to the reactive *E*-rotamer.

By using laser flash photolytic methods, Newcomb was able to determine absolute rate constants for the rotation of simple *N*,*N*-disubstituted α-amide radicals.[34] For primary α-amide radical **1.21**, carbonyl−N rotation rate constants of k_{rot} = 5.1 x 10^5 s^{-1} at 20 °C, and k_{rot} = 1.5 x

10^7 at 110 °C are derived from the experimentally determined Arrhenius equation. In comparison, Chatgilialoglu has determined absolute rate constants[3] for the 5-*endo-trig* cyclization of α-amide radical **1.22** to **1.23** as $k_C = 1.9 \times 10^4\ s^{-1}$ at 20 °C, and $k_C = 5.1 \times 10^5\ s^{-1}$ at 110 °C. Because k_{rot} of **1.22** is 25-30 times faster than k_C of **1.22** in this temperature range, the starting rotamer population is likely irrelevant, which makes Ishibashi's hypothesis flawed from a kinetic standpoint.

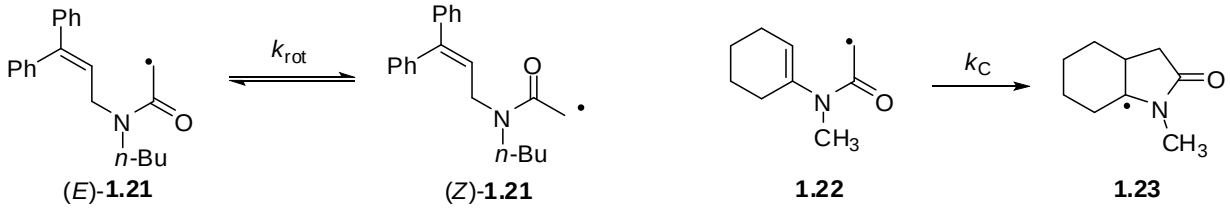

Figure 1.2 Previously Investigated α-Amide Radicals

1.1.3 Lewis Acids as Cyclization-Promoting Additives

In further studies of the reactions of **1.15c** with Bu_3SnH, Ishibashi also discovered that when 1 equiv of Bu_3SnCl was added to the reaction mixture, the ratio of cyclized products to directly reduced **1.19** was significantly increased, as seen in Table 1.2 (Entry 2).[16] Addition of 5 equiv of Bu_3SnCl resulted in an 88:12 cyclization:reduction ratio, albeit with a 17% decrease in total mass recovery (Entry 3). Interestingly, addition of Bu_3SnI had no effect on the product distribution, even though it should also behave as a Lewis acid (Entry 1).

Table 1.2 Representative Cyclizations of 1.15c With Tributyltin Additives

			% yield of product[b]					
entry[a]	additive	equiv.	**1.16**	**1.17**	**1.18**	**1.19**	total	cyc:red[c]
control[d]	--	--	0	13	11	68	92	26:74
1	Bu_3SnI	1	0	14	12	71	97	27:73
2	Bu_3SnCl	1	11	13	14	30	68	56:44
3	Bu_3SnCl	5	18	20	28	9	75	88:12

[a] conditions: Bu_3SnH (1.2 equiv) and AIBN (0.1 equiv) in toluene (12 mM in Bu_3SnH) was added via syringe pump to a refluxing mixture of the amide in toluene (10 mM) and additive over 3 h. [b] Isolated yield after aq. KF workup and column chromatography. [c] Ratio of (**1.16 + 1.17 + 1.18**) to **1.19**. [d] From Table 1.1, Entry 3.

Ishibashi proposed that Bu_3SnCl could act as a Lewis acid in this reaction by coordinating to the carbonyl oxygen of **1.15c**, greatly increasing the steric bulk around this center and forcing the amide bond to populate the *E*-rotamer.[16] This would result in nearly exclusive production of radical intermediate (*E*)-**1.20-Sn**, which is in position to cyclize, as shown in Scheme 1.8. It was also proposed that the coordinated Lewis acid could block any attempts by tin hydride to reduce the minor radical intermediate (*Z*)-**1.20-Sn**.

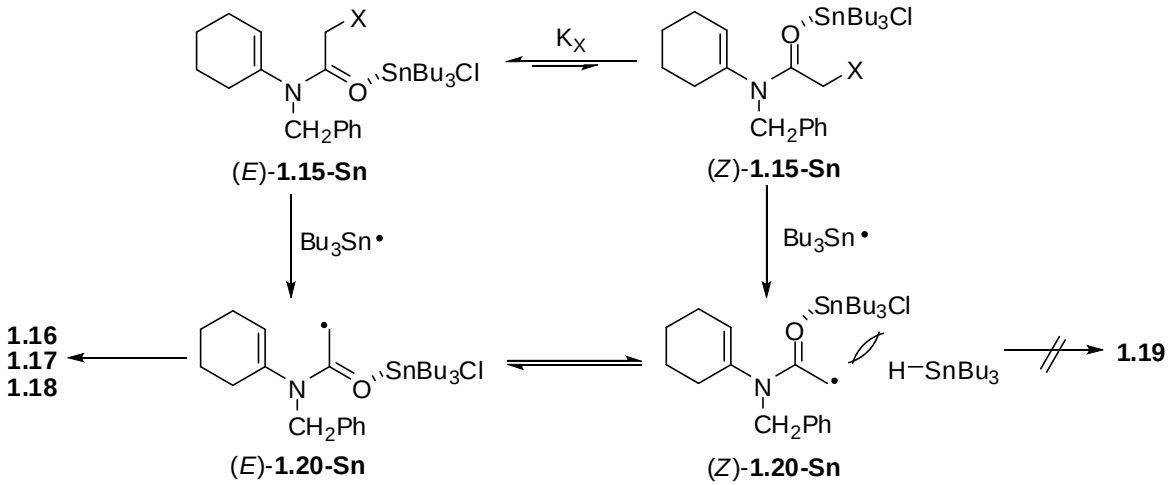

Figure 1.3 Postulated Role of Lewis Acids in Cyclization Behavior of 1.15c

Sibi and co-workers have used tributyltin halides[35] to fix the geometries of *N*-enoyloxazolidinones through bidentate chelation of the two carbonyl groups. Bu_3SnCl

presumably has a greater effect than Bu_3SnI, because it is a stronger Lewis acid.[36] However, it is curious that such a large excess of additive is needed to produce a relatively moderate increase in yields of the cyclized products. Lewis acids are known to significantly weaken the carbon-halogen bonds of α-halocarbonyl compounds, making them more susceptible to homolytic cleavage.[37,38] This implies that the complexed substrate (*E*)-**1.15-Sn** would be significantly more reactive towards halogen abstraction than uncomplexed **1.15**, resulting in preferential formation of complexed radical intermediate (*E*)-**1.20-Sn** (vs. uncomplexed **1.20**) even with substoichiometric Lewis acid additive.

1.1.4 Formation of Oxidized Cyclized Products by Single Electron Transfer

Under standard Bu_3SnH-mediated reaction conditions, no formal oxidants are present in the reaction mixture. However, the formation of oxidation products derived from intermediate cyclized α-amidoyl radicals is common nonetheless.[8,9,12,16,39] To justify the formation of oxidized cyclized products **1.17** and **1.18**, Ishibashi proposed[16] reaction of cyclized α-amidoyl radical **1.24** with starting material **1.15** via one of two routes, as shown in Scheme 1.6. A single electron transfer (SET) from **1.24** to halide **1.15** through an outer-sphere process[2,39-41] produces acyliminium ion **1.25**, which can deprotonate to give products **1.17** and **1.18**. The radical anion **1.26** produced by the SET will fragment extremely quickly to give iodide ion and α-amide radical **1.20**. Another viable pathway for oxidation of **1.24** is an inner-sphere halogen atom transfer,[30,42-44] where **1.24** is converted to halide **1.27**, which may then eliminate hydrogen halide to give the oxidized products **1.17** and **1.18**.

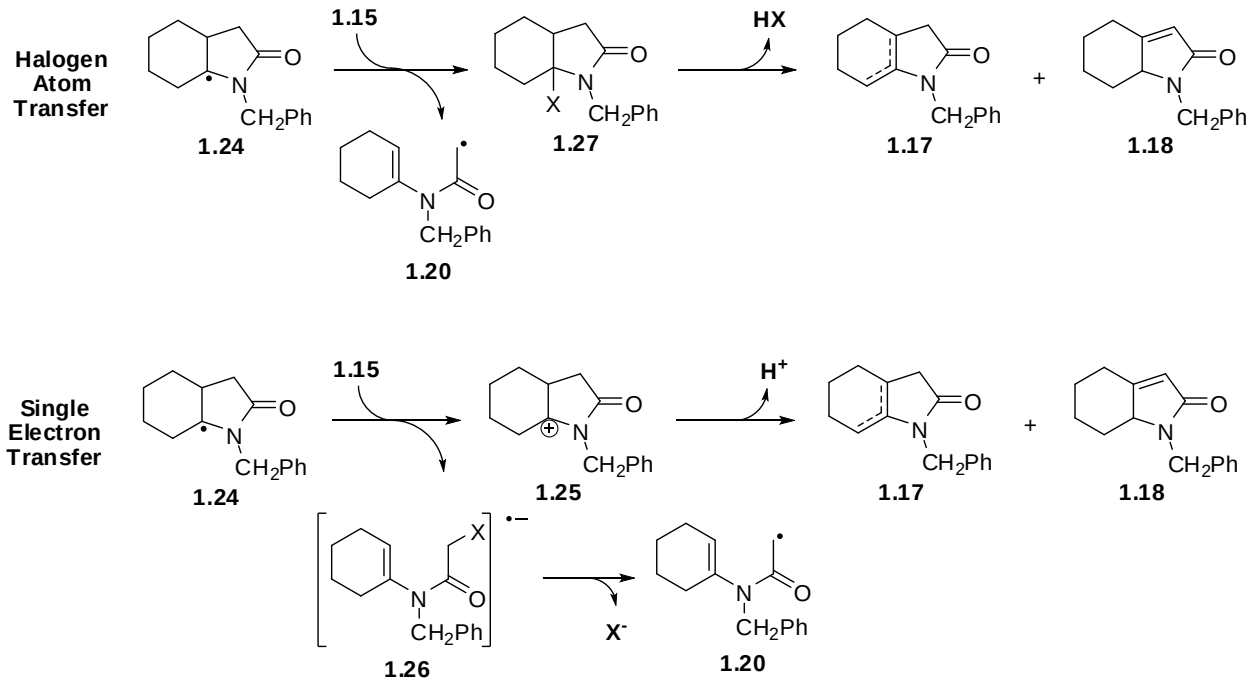

Scheme 1.6 Oxidative Mechanisms for Formation of Products 1.17-1.18

Bowman has previously found evidence for SET from cyclized radical intermediates to starting material[39] in cyclizations of alkyl radicals onto imidazole rings, where phenylselenides are the radical precursors. SET has also been implicated in reactions with easily reduced halides in the starting material,[40,41] but evidence for halogen atom transfer has been observed by Savéant in the electrochemical reduction of various α-halocarbonyl compounds.[42] Both mechanisms shown in Scheme 1.6 produce the same result: formation of oxidized products **1.17**/**1.18**, consumption of starting material **1.15** to give α-amide radical **1.20**, and release of hydrogen halide. Without a detailed kinetic analysis, these processes are practically indistinguishable from one another,[41,45] and for our purposes may be treated as similar. For simplicity, the remainder of this chapter will refer to these collective processes as "SET," though either mechanism outlined in Scheme 1.6 may actually be occurring.

The literature is filled with oxidative versions of 5-*endo-trig* cyclizations of enamide systems,[2,6,9,11,12] most of which take advantage of the easily oxidized α-amidoyl radical intermediates. Miranda and co-workers recently exploited the ease of oxidation of radical intermediate **1.20** by developing methodology[6] in which organic peroxides act as both chain initiators and single electron oxidants. Upon addition of 2 equiv of dibenzoyl peroxide to **1.15a** in toluene at 95 °C, the oxidized cyclized compounds **1.17** and **1.18** were isolated in 5% and 89% yield, respectively.

The proposed mechanism of this oxidative 5-*endo-trig* radical cyclization is shown in Scheme 1.7. Chlorine atom abstraction from **1.15a** by phenyl radical results in chlorobenzene and carbamoylmethyl radical **1.20**, which cyclizes in a typical fashion to give tertiary α-amidoyl radical **1.24**. A SET to dibenzoyl peroxide occurs, producing acyliminium ion **1.25**. The resulting peroxyl radical anion may then fragment to produce phenyl radical, carbon dioxide, and benzoate anion, the latter of which may assist in deprotonating **1.25**. A benzoic acid-catalyzed equilibrium can account for the product distribution between **1.17** and **1.18**.

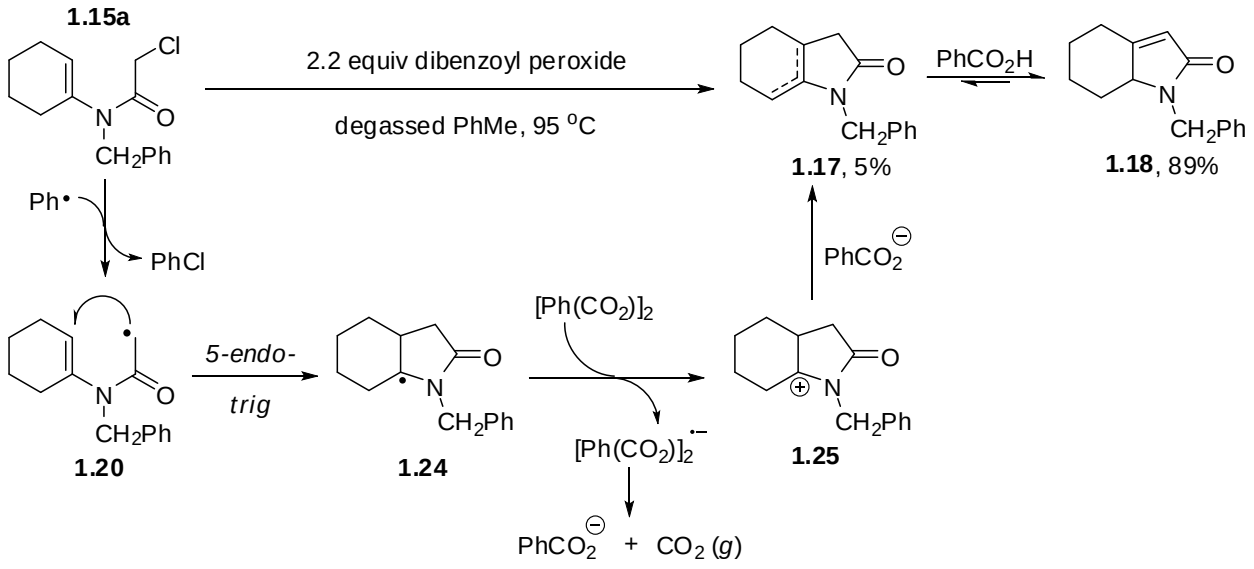

Scheme 1.7 Miranda's Oxidative 5-*Endo-trig* Cyclization Pathway

Despite the apparent ease of oxidation of intermediate **1.24** to **1.25**, Bu_3SnH-mediated conditions allow few reasonable mechanisms for this process. It has been proposed that AIBN[46] and various other azoalkanes[47] can act as oxidants by H-atom abstraction of a radical intermediate, a process that has been observed in reactions such as heterolytic aromatic substitution.[48] However, this requires a stoichiometric amount of AIBN. Because only catalytic amounts are used in Ishibashi's reaction conditions,[16] oxidation by AIBN cannot totally account for the formation of products **1.17** and **1.18**.

With this backdrop, we set out to investigate the halogen-dependent cyclization ability of α-haloenamides **1.15a-c**, specifically examining the roles of SET processes and amide rotamer behavior on the product distribution.

1.2 RESULTS AND DISCUSSION

1.2.1 Conformational Analysis of *N*-Benzyl α-Haloenamides

Ishibashi originally postulated that halides **1.15a** and **1.15c** had different rotamer ratios, but provided no experimental evidence to support this conclusion. Hence, we first turned our attention toward determining the *syn*/*anti* amide geometry of these substrates by dynamic ^{1}H NMR spectroscopic analysis. Previous studies[49] in this area have determined the barrier to amide rotation for α-chloroacetamide **1.28a** (Figure 1.4) in chlorobenzene to be $\Delta G^{\ddagger}_{298}$ = 16.4 kcal/mol, while the α-bromo congener **1.28b** has a slightly lower $\Delta G^{\ddagger}_{298}$ = 15.8 kcal/mol in chlorobenzene. These are within the range of typical amide rotation barriers[22] (15-17 kcal/mol), and the nonequivalent *N*-methyl groups in **1.28a-b** are well-defined in the ^{1}H NMR spectra.

Because **1.15a-c** contain an *N*-cyclohexenyl group, α-chloroacetanilide **1.29** is likely a better comparison due to the sp^2 carbon bonded to the amidic nitrogen. Unfortunately, the barrier to amide rotation of **1.28** cannot be determined, because the population of the minor rotamer is too small to measure by ^{1}H NMR spectroscopy.[50]

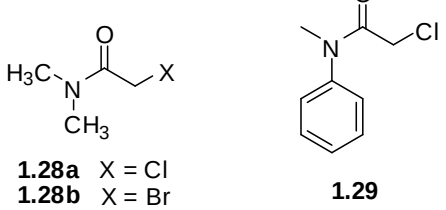

1.28a X = Cl
1.28b X = Br

1.29

Figure 1.4 Previously Studied α-Haloamides

To begin our conformational analysis, **1.15c** was dissolved in $CDCl_3$ with a small amount of tetramethylsilane to be used as a line width standard. ^{1}H NMR spectra were recorded at various temperatures in the range of 297 K – 215 K, and portions of these spectra are shown in Figure 1.5.

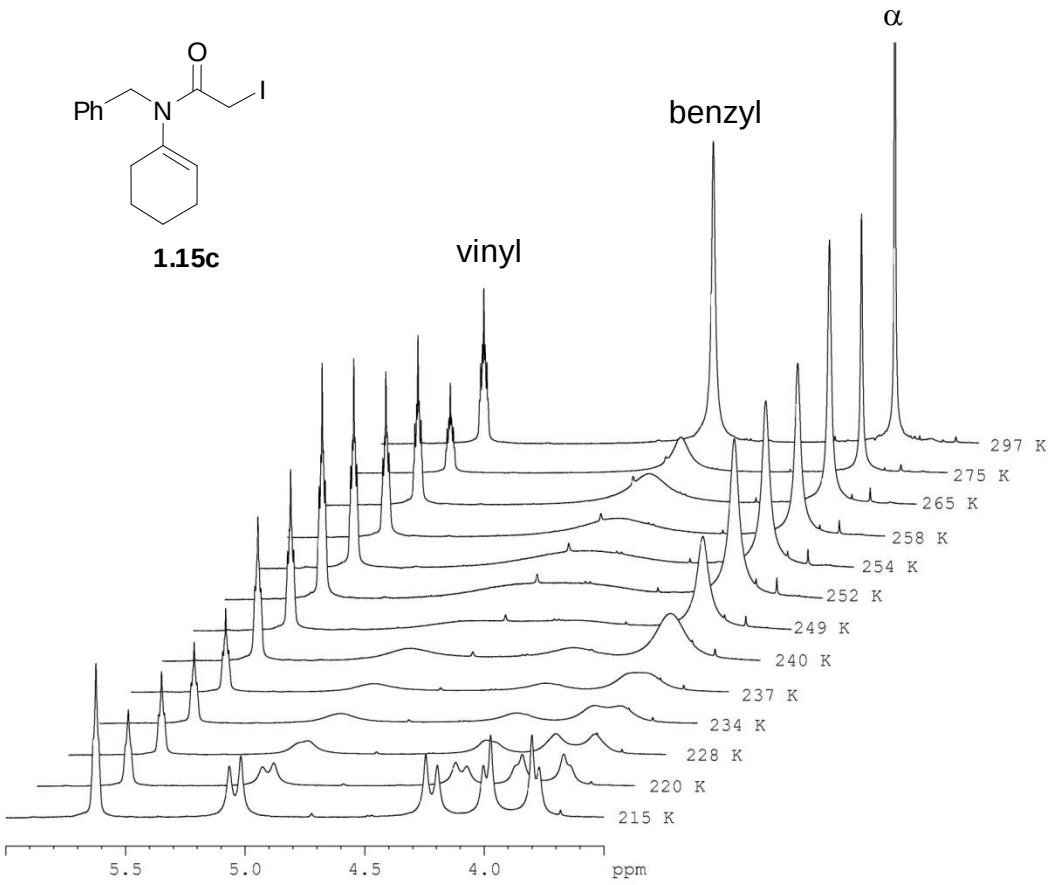

Figure 1.5 300 MHz ^{1}H NMR Spectra of 1.15c in $CDCl_3$ (297 K – 215 K)

The NMR spectrum of **1.15c** at 297 K shows one singlet apiece for the benzyl and α protons, suggesting either the presence of one major rotamer,[50] or the existence of an abnormally low barrier to rotation about the C–N bond resulting in a coalescence of the rotamer signals.[51] As the sample was cooled, decoalescence of the α protons and benzyl protons occurred. At 215 K, the benzyl protons give rise to mutually coupled doublets (J = 14.6 Hz) at 5.04 and 4.22 ppm; the α signal shows similar behavior, producing geminally coupled doublets (J = 9.3 Hz) at 3.99 and 3.79 ppm.

The spectroscopic behavior observed in Figure 1.5 is not consistent with locking out *Z*/*E* amide rotamers.[52] This process would result in a doubling of all signals near the C-N amide bond, which was not observed at any temperature. Furthermore, the *Z*/*E* rotamers would be expected to have homotopic methylene groups at the α- and benzyl positions. These results suggested that **1.15c** exists as a single amide rotamer in solution, and another rotational process causes both sets of protons to become diastereotopic.[53,54] The variable-temperature ^{1}H NMR spectra of chloride **1.15a** are not shown, but displayed temperature-dependent decoalescences and couplings similar to **1.15c**. At 212 K, the benzyl signal decoalesced into two doublets (J = 13.6 Hz) at 5.08 and 4.18 ppm. The α protons were partially obscured by one of the benzyl signals, but line-shape analysis with WINDNMR software[55] revealed two doublets (J = 12.4 Hz) at 4.30 and 4.18 ppm.

The low temperature NMR data strongly suggests that cooling the substrate slows the *N*-cyclohexenyl bond rotation, as shown in Figure 1.6. Slowing this rotation allows the element of asymmetry within the molecule to become visible on the NMR timescale. In this sense, compounds **1.15a-c** behave similarly to axially chiral anilides,[56] in which an asymmetrically substituted *N*-aryl group serves as a source of chirality. Mannschreck and coworkers were the first to recognize the axial chirality of enamides,[57] and used the coalescence temperature of diastereotopic protons in NMR spectra to determine the *N*-vinyl barrier to rotation for several enamides.[58]

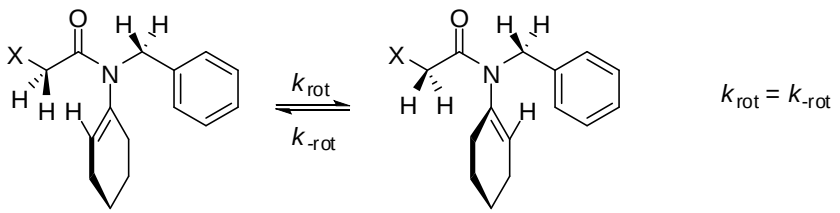

Figure 1.6 Rotational Dynamics of 1.15a-c

Using the WINDNMR 7.1 line-shape analysis program[55] to analyze the benzyl peaks of **1.15a,c**,[59] we determined the rotational rate constant k_{rot} at each temperature T. The $\Delta G^{\ddagger}$ at any temperature can be calculated from the experimentally determined rate using the Arrhenius equation (Equation 1.1), where h is Planck's constant and k_B is Boltzmann's constant.[60] The data was graphed in an Eyring plot (Figure 1.8) for further kinetic analysis. The plots for chloride **1.15a** and iodide **1.15c** nearly coincide, suggesting that their dynamics are similar.

$$\Delta G^{\ddagger} = -RT \ln\left(\frac{k \cdot h}{k_B \cdot T}\right) \qquad \text{(Equation 1.1)}$$

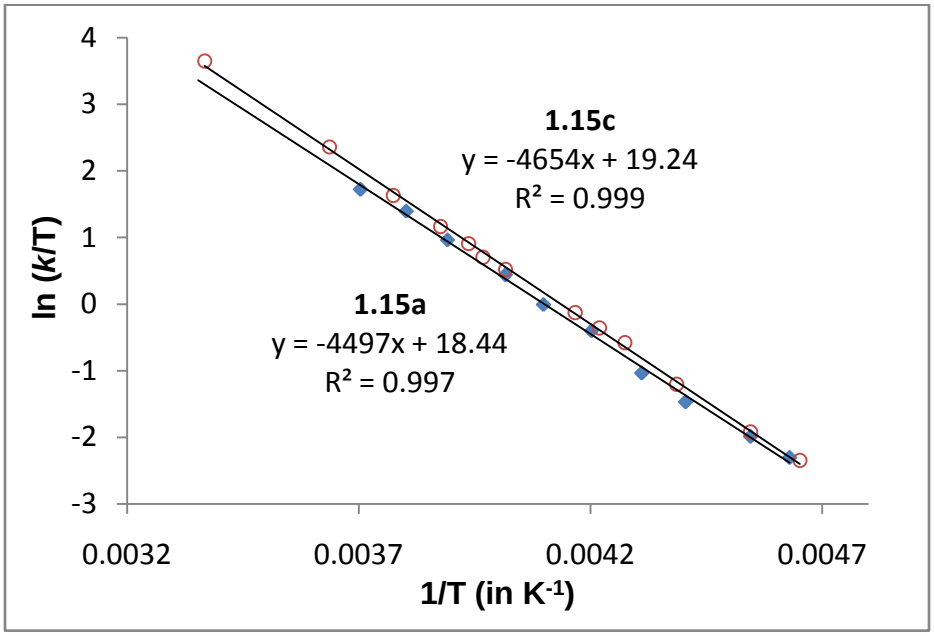

Figure 1.7 Eyring Plot of Chloride 1.15a (♦) and Iodide 1.15c (○)

Using equation 1.2[60] and the slope and intercept from the Eyring plot, we calculated thermodynamic values for the bond rotations. Chloride **1.15a** exhibited a $\Delta H^{\ddagger}$ of 8.9 kcal/mol for the *N*-cyclohexenyl rotation, and a significant $\Delta S^{\ddagger}$ of −10.6 cal/(mol K). The iodide **1.15c**

gave similar results, with $\Delta H^{\ddagger}$ = 9.3 kcal/mol and $\Delta S^{\ddagger}$ = −9.0 cal/(mol K). The Gibbs energies of activation for the rotations at room temperature were calculated, and were found to be $\Delta G^{\ddagger}_{298}$ = 12.1 kcal/mol for chloride **1.15a** and $\Delta G^{\ddagger}_{298}$ = 11.9 kcal/mol for iodide **1.15c**.

$$\ln\left(\frac{k}{T}\right)=\left(\frac{-\Delta H^{\ddagger}}{R}\right)\left(\frac{1}{T}\right)+\frac{\Delta S^{\ddagger}}{\mathrm{R}}+\ln\left(\frac{k_B}{h}\right) \qquad \text{(Equation 1.2)}$$

The measured $\Delta G^{\ddagger}_{298}$ values are much too small to represent amide bond rotation, but are reasonable for the *N*-cyclohexenyl bond rotation, a theory that was supported by the crystal structure of **1.15a**. X-ray quality crystals were grown by a vapor diffusion technique[61] in an ethyl acetate/hexanes solvent system, and an enantiopure single crystal of (*P*)-**1.15a** was deposited. The crystal structure in Figure 1.8 shows that the *N*-cyclohexenyl bond prefers to exist orthogonal to the plane of the N-C amide bond, with a torsional angle of 74°. Furthermore, the amide bond nitrogen clearly exhibits typical sp^2 character, with practically no pyramidalization: the sum of the bond angles to nitrogen is 359.9°. As expected, the amide exists as the (*E*)-**1.15** rotamer, extending the structural similarities between α-haloenamides and α-haloacetamides.

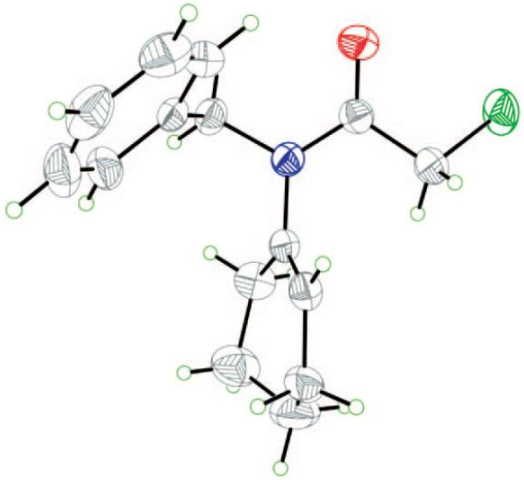

Figure 1.8 ORTEP Crystal Structure of 1.15a

We then extended our rotational studies to several other α-haloenamides, in collaboration with Dr. Andrew Clark at the University of Warwick. α-Bromo-α,α-dimethylenamides **1.30-1.33** (Figure 1.9) were synthesized in the laboratories of Dr. Clark. Samples of these compounds were dissolved in toluene-*d8* and analyzed with variable temperature ^{1}H NMR. In each case, coalescence and decoalescence of the benzyl proton signals was the focal point of analysis. At room temperature, **1.30a** and **1.31** displayed sharp singlets for the benzylic protons. Enamide **1.32** showed geminally coupled doublets for the benzylic protons in its room temperature spectrum. All other compounds displayed a very broad benzylic signal at room temperature, in some cases completely disappearing into the baseline.

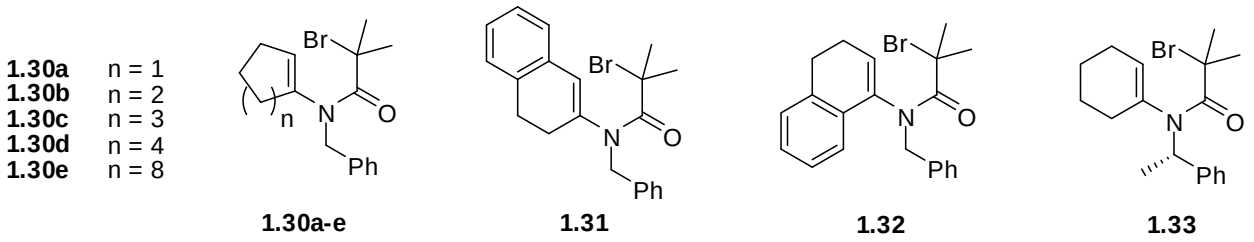

Figure 1.9 α-Haloenamides Used in Rotational Studies

Line-shape analysis was again performed with NUTS[62] and WINDNMR[55] programs. The rate of rotation at each temperature was calculated, and Eyring plots for each substrate afforded thermodynamic data (Table 1.3). Varying the size of the cycloalkenyl ring in the 6-12 carbon range did little to change the barriers to rotation among **1.30b-e**, with a narrow range of $\Delta G^{\ddagger}_{298}$ = 12.4–13.3 kcal/mol (Entries 4-7). However, a sharp decrease in rotational barrier was seen with cyclopentenyl substrate **1.30a**, with $\Delta G^{\ddagger}_{298}$ = 9.95 kcal/mol (Entry 3). Enamide **1.31**, a derivative of 2-tetralone, had a barrier of $\Delta G^{\ddagger}_{298}$ = 11.7 kcal/mol. In sharp contrast, 1-tetralone derivative **1.32** had a much higher barrier to rotation of $\Delta G^{\ddagger}_{298}$ = 18.0 kcal/mol, which can be

attributed to the additional substitution on the enamide double bond (Entry 9). Upon cooling, **1.33** decoalesced to a 2:1 mixture of diastereomers with two separate barriers to rotation (Entry 10); compared to **1.30b**, the barrier increase induced by the α-methyl group was about 1 kcal/mol.

Table 1.3 Barriers to Rotation of α-Haloenamides in Toluene-*d8*

entry	substrate	temp. range	k_{298} (s^{-1})	$\Delta H^{\ddagger}$ (kcal/mol)	$\Delta S^{\ddagger}$ (cal/mol K)	$\Delta G^{\ddagger}_{298}$ (kcal/mol)
1[a]	**1.15a**	297 – 215 K	8.49×10^{3}	8.9	−10.6	12.1
2[a]	**1.15c**	270 – 216 K	1.12×10^{4}	9.2	−9.0	11.9
3	**1.30a**	290 – 186 K	3.11×10^{5}	8.0	−6.6	9.95
4	**1.30b**	311 – 233 K	1.06×10^{3}	11.3	−6.6	13.3
5	**1.30c**	350 – 250 K	7.35×10^{2}	11.8	−5.7	13.5
6	**1.30d**	341 – 230 K	3.09×10^{3}	11.4	−4.3	12.7
7	**1.30e**	341 – 230 K	4.88×10^{3}	11.4	−3.5	12.4
8	**1.31**	311 – 220 K	1.59×10^{4}	9.7	−6.7	11.7
9	**1.32**	379 – 341 K	4.08×10^{-1}	11.9	−20.4	18.0
10[b]	**1.33**	350 – 271 K	1.83×10^{2} 3.64×10^{2}	12.7 12.7	−5.4 −4.0	14.4 14.0

[a] $CDCl_3$ was used as the solvent. [b] Forward and reverse rates for diastereomer interconversion were determined.

None of the α-haloenamides in this study had barriers to rotation high enough to allow for resolution of enantiomers at room temperature. Substitution on the carbons α to the carbonyl or α to the nitrogen did little to increase the barrier. In the case of **1.32**, however, substitution at the vinylic carbon brought the barrier close to a useful range for resolution. Further studies on developing resolvable α-haloenamides should, therefore, focus on substitution at the vinylic and allylic[58] position of the olefin to increase the barrier.

1.2.2 Rate Constant Determinations of 5-*Endo-trig* Cyclizations

Having eliminated amide rotamer behavior as the source of the halogen-dependent cyclization results, we next turned our attention to studying the radical cyclization kinetics of **1.15a-c**. A series of competition experiments were performed, measuring the ratio of direct reduction product **1.19** to the sum of cyclization products **1.16-1.18** as a function of Bu_3SnH concentration.[63] Because the Bu_3SnH trapping agent is added at the start (as opposed to by syringe pump), its initial concentration is known, and the relative cyclization rate can be determined. For an accurate determination of the product distribution, GC analysis was used for these reactions.

Substrates **1.15a-c** and authentic products **1.16-1.19** were synthesized as shown in Scheme 1.8. Literature procedures[16] were followed to make **1.15a-c** in 23-97% yields. Catalytic hydrogenation of 2-oxindole to produce octahydroindolone **1.34**, followed by *N*-benzylation, afforded an authentic sample of cyclized product **1.16** in 45% overall yield. Condensation of cyclohexanone and benzylamine, followed by *N*-acetylation, produced reduction product **1.19** in 66% yield. Basic hydrolysis of ester **1.35** and coupling of the resulting acid with benzylamine produced amide **1.36** in 80% yield over two steps. Acid-catalyzed intramolecular condensation of **1.36** afforded products **1.17** and **1.18**. While compound **1.18** was isolable as a stable compound by flash chromatography, **1.17** was extremely sensitive to isomerization. Even though it exhibited two spots on TLC, it was always recovered as a 2.3:1 mixture of the $\Delta^{7,7a}$ and $\Delta^{7a,3a}$ isomers after flash chromatography. A 2D TLC experiment showed that this isomerization occurs on silica gel on the timescale of flash chromatography (< 15 min).

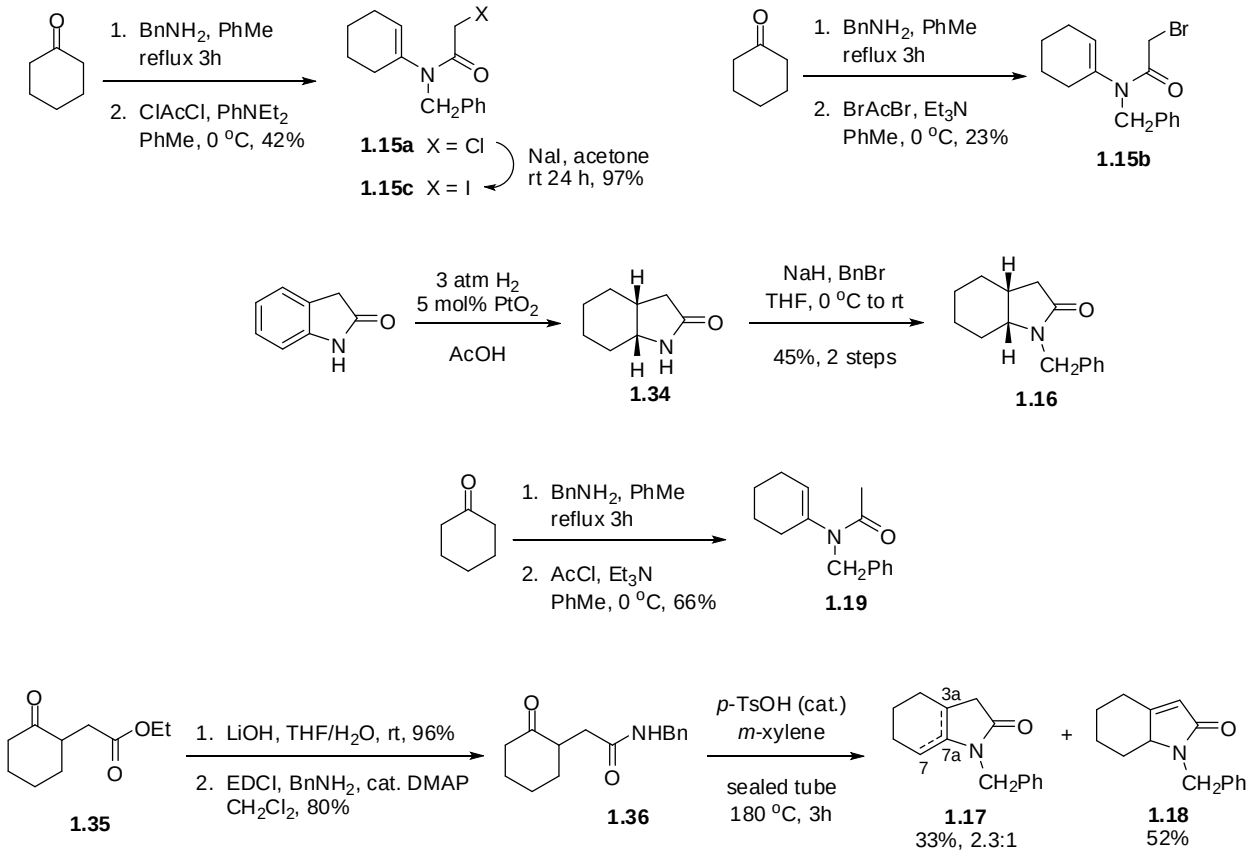

Scheme 1.8 Synthesis of Substrates 1.15a-c and Authentic Products 1.16-1.19

Competition experiments were conducted by heating an α-halo enamide **1.15a-c** (0.025 mmol), Bu_3SnH (1.2 equiv), and AIBN (0.2 equiv) in toluene at 110 °C in a sealed tube for 3 h. Reaction mixtures contained octadecane as an internal standard, and were analyzed by GC; the results are summarized in Table 2.1. Response factors of **1.15-1.19** versus octadecane were determined so that absolute GC yields could be calculated for each reaction. Oxidized products **1.17-1.18** gave a single peak in the GC method used, and authentic **1.18** was used to calculate the response factor for this peak. All reactions were clean; product peaks were well-defined and no significant side product peaks formed, even when mass balances were low.

The kinetic competition reactions of **1.15a-c** gave standard, highly reproducible results (Table 1.4). As the Bu_3SnH concentration was increased, the ratio of reduced **1.19** to cyclized **1.16-1.18** increased accordingly for all substrates. The mass balances were moderate to high (60-87%), and generally increased as the Bu_3SnH concentration was increased. Even at lower Bu_3SnH concentrations, only small amounts of unreacted starting material were present in the case of the chloride **1.15a** and bromide **1.15b**. Interestingly, the ratio of cyclized **1.16** to oxidized products **1.17/1.18** showed a halogen dependence, in qualitative agreement with Ishibashi's results.[8,16] Regardless of the tin hydride concentration, chloride **1.15a** yielded an average of 15:1 cyclized:oxidized in the product distribution. Cyclization of **1.15b** gave a ratio of about 8:1, and the iodide **1.15c** equalized the ratio to 1:1.

Table 1.4 Kinetic Competition Reactions for Substrates 1.15a-c

		% yield of product[b]				
substrate	$[Bu_3SnH]_i$[c]	**1.16**	**1.17+1.18**	**1.19**	total[d]	cyc : red[e]
1.15a	10.0 mM	33	2	15	60 (71)	70 : 30
	15.0 mM	32	3	22	57 (74)	61 : 39
	17.8 mM	36	3	29	68 (82)	57 : 43
	30.0 mM	29	2	39	70 (81)	44 : 66
	42.9 mM	28	2	56	86	35 : 65
1.15b	7.5 mM	34	5	18	57 (61)	68 : 32
	10.0 mM	29	5	22	56 (61)	61 : 39
	15.0 mM	39	4	38	81	53 : 47
	17.8 mM	35	4	41	80	49 : 51
	30.0 mM	27	3	52	82	36 : 64
	42.9 mM	20	2	55	77	29 : 71
1.15c	7.5 mM	16	18	31	65	52 : 48
	10.0 mM	13	14	33	60	45 : 55
	15.0 mM	12	14	46	72	36 : 64
	17.8 mM	11	14	55	80	31 : 69
	30.0 mM	9	10	68	87	22 : 78

[a] conditions: The appropriate substrate (1.0 equiv), Bu_3SnH (1.2 equiv), and AIBN (0.2 equiv) in toluene were combined in a sealed tube and heated at 110 °C for 3 h. [b] GC yield, using octadecane as an internal standard. Yields are an average of three trials. [c] Initial concentration of Bu_3SnH. [d] Yield in parentheses is based on recovered starting material. [e] Ratio of (**1.16 + 1.17 + 1.18**) to **1.19**.

Relative rates of cyclization for each system were established by a plot of the ratio of reduction product **1.19** to combined cyclization products **1.15-1.17**, versus the concentration of Bu_3SnH. In this plot, the slope is equal to the ratio k_H/k_c, representing the rate constants of competing reduction and unimolecular cyclization shown in Scheme 1.9. Because the conditions were not pseudo-first order in trapping agent, the mean concentration of tributyltin hydride $[Bu_3SnH]_c$ (equation 1.3) was used for the *k* calculations, as recommended by Newcomb.[63] The kinetic plot is depicted in Figure 1.10.

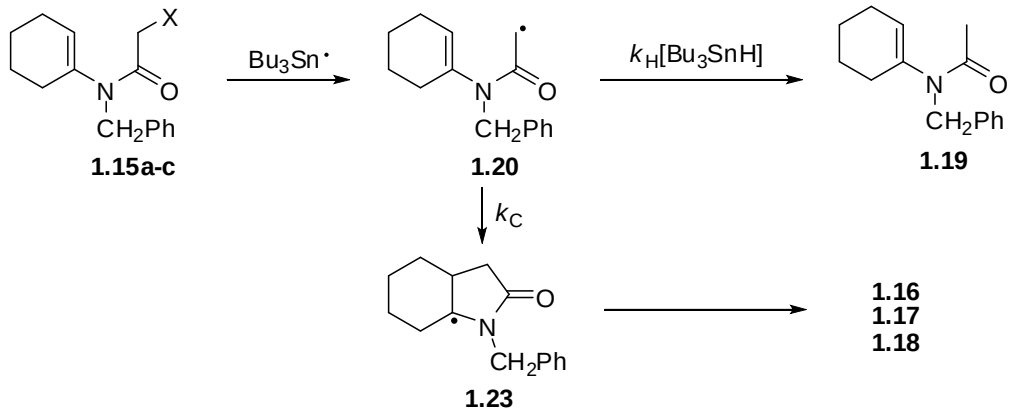

Scheme 1.9 Competing Pathways of α-Amidoyl Radical 1.20

$$[Bu_3SnH]_c = \frac{[Bu_3SnH]_i + ([Bu_3SnH]_i - [RX]_i)}{2} \qquad \text{(Equation 1.3)}$$

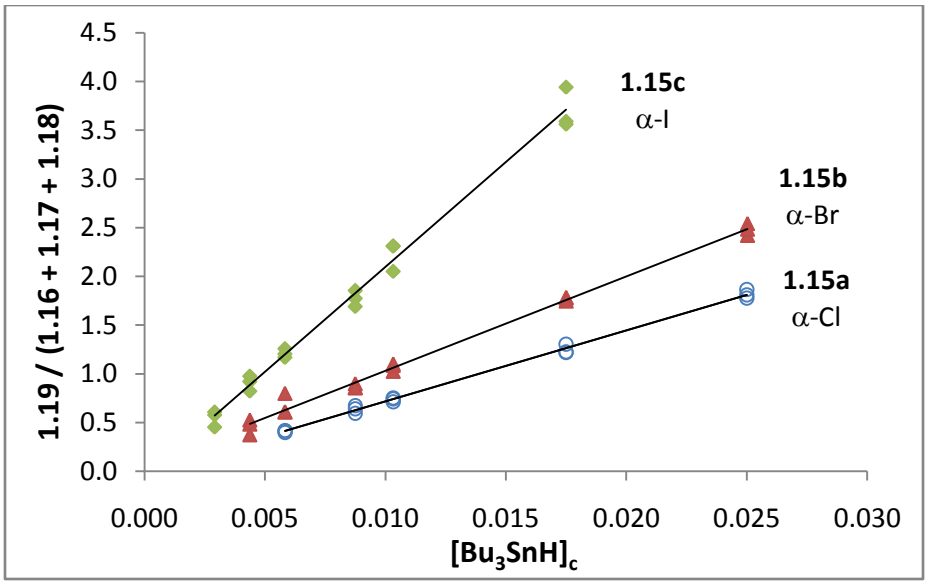

Figure 1.10 Kinetic Competition Plot of 1.15a (○), 1.15b (▲) and 1.15c (♦)

In principle, the three precursors should give the same radical intermediate **1.20**, and the plots in Figure 1.11 should overlap. In actuality, there is a four-fold difference between the slopes of the competition plots for chloride **1.15a** and iodide **1.15c**. This implies a *different* rate constant of cyclization k_c for the common intermediate **1.20**, depending on the substrate used.

Using the relative rate data, absolute rate constants for these cyclizations were determined. Absolute rate data for the direct Bu_3SnH reduction of carbon-centered alkyl radicals is abundant, and Newcomb has shown that α-amide radicals are reduced by Bu_3SnH at a rate comparable to their alkyl counterparts.[64] With the appropriate Arrhenius equations determined by Chatgilialoglu for primary carbon-centered radicals,[65,66] the k_H for α-carbamoylmethyl radical **1.20** can be reasonably approximated as $k_H = 9.3 \times 10^6\ M^{-1}s^{-1}$ at 383 K. Based on the relative rates garnered from Figure 2.9, we can calculate the 5-*endo-trig* cyclization rate constant of **1.20** produced by **1.15a** to be $k_c = 1.3 \times 10^5\ s^{-1}$, a value in reasonable agreement with Chatgilialoglu's experimentally determined rate constant of $5.1 \times 10^5\ s^{-1}$ at 383 K for the *N*-methyl radical **1.22**

(Chapter 1.1.2).[3] Our competition results also yielded cyclization rate constants of $k_c = 9.3 \times 10^4$ s^{-1} for **1.15b** and $k_c = 4.0 \times 10^4$ s^{-1} for **1.15c**.

The relatively small difference between k_c values, all within a factor of ~5, was unexpected given Ishibashi's previous results. Because Ishibashi's optimized conditions for the 5-*endo-trig* cyclization utilize a syringe pump, the Bu_3SnH concentration is always kept very low (<< 1 mM). At low Bu_3SnH concentrations, the competition plots in Figure 1.11 converge, theoretically yielding similar reduction/cyclization ratios. Ishibashi's preparative results (Table 1.1), therefore, cannot be explained by our kinetic findings. Although the kinetic plot slopes for **1.15a-c** are different, there is a common y-intercept value of zero for the competition plots of all three substrates. This rules out reversibility of the cyclization; in this case, the intercept would be positive.[63] Furthermore, the halogen-dependent cyclized:oxidized ratios suggest a mechanistic divergence *after* cyclization in these reactions.

1.2.3 Effects of Bu_3SnX Additives

We then briefly investigated the effect of the variable tributylstannyl halide byproduct on the reaction mixture, which in some cases had been posited to act as a Lewis acid. A room temperature ^1H NMR spectrum of a 1:1 mixture of Bu_3SnCl and **1.15c** in $CDCl_3$ produced no discernible change in chemical shifts of the substrate. We took this as evidence that little or no coordination was occurring, and Bu_3SnCl was not acting as a Lewis acid activator towards **1.15c**. Nevertheless, we ran several trials to determine if Bu_3SnX compounds could play a role in increasing the cyclization yield of **1.15c**. The results of some of these trials, which were run under the same conditions as the competition reactions (Table 1.4) at 10.0 mM Bu_3SnH, are outlined in Table 1.5.

Table 1.5 Reaction of 1.15c in the Presence of Bu_3SnX Additives

			% yield of products[b]				
entry[a]	additive	equiv	**1.16**	**1.17+1.18**	**1.19**	total	cyc:red[d]
control[c]	--	--	13	14	33	60	45 : 55
1	Bu_3SnCl	1.0	10	9	33	52	36 : 64
2	Bu_3SnCl	3.0	3	8	25	36	31 : 69
3	Bu_3SnCl	5.0	9	9	33	51	35 : 65
4	Bu_3SnI	1.0	13	12	34	59	42 : 58
5	Bu_3SnI	2.0	14	9	32	55	42 : 58
6	Bu_3SnI	3.0	13	8	31	52	41 : 59

[a] conditions: Iodide **1.15c** (1.0 equiv), Bu_3SnH (1.2 equiv), additive, and AIBN (0.2 equiv) in toluene were combined in a sealed tube and heated at 110 °C for 3 h. [b] GC yield, using octadecane as an internal standard. Yields are an average of three trials. [c] From Table 1.4. [d] Ratio of (**1.16 + 1.17 + 1.18**) to **1.19**.

In these trials, no increase in the cyclized:reduced product ratio was seen, regardless of the identity or quality of tin halide used. In fact, a slight *decrease* in mass balance and cyclization ability was noticed when 3 equiv of tributyltin chloride was employed (Entry 2); the reason for this is not currently known. Multiple other trials were run at varying Bu_3SnH concentrations with different amounts of Bu_3SnX (1-5 equiv), but no significant deviations from the control experiment (Entry 1) or noticeable trends were observed under any conditions.

Our results show that Bu_3SnX additives do not noticeably assist in cyclization by acting as Lewis acids. However, halogen exchange between trialkyltin halides and alkyl halides is known to occur,[67] resulting in an equilibrium based on the strengths of the carbon-halogen and tin-halogen bonds. This process is greatly accelerated by catalytic amounts of halide anions in solution.[67] Therefore, Bu_3SnCl may have been altering the behavior of iodide **1.15c** in Ishibashi's syringe pump experiments by a halogen exchange reaction.

This hypothesis was supported with a control experiment by refluxing 1 equiv of **1.15c** with 5 equiv of Bu_3SnCl in toluene. After 3 h, a small amount (< 5% by GC) of conversion to the chloride **1.15a** was seen. Addition of 5 mol% tetrabutylammonium iodide, however, caused the reaction to reach equilibrium (Figure 1.11) within 1 h (further refluxing did not change the

GC ratios of **1.15a**/**1.15c**). A ^{1}H NMR spectrum of the final equilibrium mixture in $CDCl_3$ showed a mixture of **1.15c**:**1.15a** in a 1.4:1.0 ratio (by integration of α proton peaks).

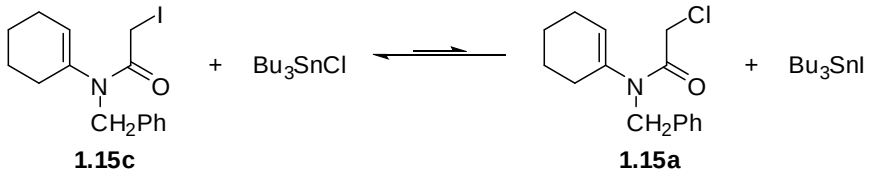

1.15c **1.15a**

Figure 1.11 Halogen Exchange Equilibrium for 1.15 and Tributyltin Halides

The equilibrium constant in Figure 1.11 favors the iodide **1.15c** and Bu_3SnCl, in keeping with other experimentally determined equilibria of this nature.[67] However, addition of a large excess of Bu_3SnCl can shift the equilibrium to produce a significant amount of chloride **1.15a**. Ishibashi observed that addition of Bu_3SnCl to iodide **1.15c** provided cyclization results similar to chloride **1.15a**. We suggest that this is not because Bu_3SnCl functions as a Lewis acid, but because it partially converts iodide **1.15c** to chloride **1.15a** under the conditions of the experiment, producing "chloride-like" results.

1.2.4 Preliminary Evidence for SET

A possible alternate mechanism in the radical reactions of **1.15a-c**, hypothesized by Ishibashi[16] but not investigated, involves an SET-type reaction between cyclized intermediate **1.23** and starting material **1.15** as previously outlined in Scheme 1.6. This secondary chain process can proceed in the absence of tin hydride, but it is not immediately clear how this would affect the reduction vs. cyclization product distribution.

It has previously been established that radical intermediates α to a heteroatom such as nitrogen or oxygen[68] are powerful reducing agents. This is commonly attributed to a three-

electron interaction, where the third electron lies in a higher-energy antibonding orbital and can thus be easily removed.[69,70] Yoshida has reported[71] an electrochemical single electron reduction potential of −0.85 V (vs. Ag/AgCl(CH_3CN)) for acyliminium ion **1.37**. Furthermore, tertiary alkyl radicals tend to have an oxidation potential 0.10-0.20 V lower than their secondary counterparts. These data give a good approximation of $E_{1/2}^{ox} = -1.0$ V for radical intermediate **1.24**, which is comparable to the substantial oxidation potential of α-aminyl radicals.[69]

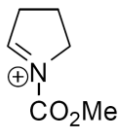

1.37

The reduction potential of α-halo carbonyl compounds is known to be much lower than most other alkyl halides, such as $E_{1/2}^{red} = -0.34$ V for bromoacetone (vs. SCE, H_2O pH 4.6) vs. $E_{1/2}^{red} = -2.23$ V for a typical alkyl bromide (vs. SCE, 75% dioxane/water).[72] A better comparison to **1.15** is ethyl bromoacetate, which has $E_{1/2}^{red} = -0.88$ V (vs. SCE) in anhydrous DMF.[73]

The efficiency of SET to the starting material is expected to be highly halogen-dependent as well. Literature trends indicate that alkyl chlorides tend to have a reduction potential approximately 0.75-0.85 V higher than bromides, while the easily reduced iodides have a typical 0.35-0.45 V decrease in reduction potential.[72,74-76] We can thus estimate a redox potential of −0.1 V (−2.3 kcal/mol) for the SET from **1.24** to **1.15b**, while SET to the iodide **1.15c** occurs at a more favorable potential of approximately −0.5 V (−11.5 kcal/mol). While these values cannot be quantitatively applied to our system due to estimations and solvent effects, they do show that SET from **1.23** to the starting halide **1.15** is a thermodynamically viable pathway. Furthermore, these values are equally applicable whether the oxidation/reduction is occurring via a stepwise (SET) mechanism, or concerted (halogen atom transfer) pathway.[77]

Our preliminary test for this mechanistic pathway was to *favor* the possible SET by adding excess **1.15c** substrate. As the concentration of iodide precursor **1.15c** is increased relative to that of Bu_3SnH, the reaction rate of cyclized radical intermediate **1.24** with starting material **1.15c** would increase relative to reduction by Bu_3SnH. In these reactions, 1-2 equiv of starting material were reacted with 1 equiv of Bu_3SnH (0.01 M) under our typical sealed-tube conditions, as in Table 1.6.

We observed an increasing ratio of oxidized cyclized products **1.17/1.18** to cyclized product **1.16** (1.1:1, 2.5:1, 4.0:1), as the amount of **1.15c** was increased from 1.0 to 1.5 to 2.0 equiv. Furthermore, substoichiometric amounts of Bu_3SnH were needed to consume **1.15c** in entries 2-3 of Table 1.6, implying that an SET pathway could be occurring. As shown previously in Scheme 1.6, the SET process regenerates α-carbamoylmethylradical **1.20** from **1.15c**. This allows the iodide precursor to be consumed in a "SET chain" mechanism, where Bu_3SnH is only involved in the intiation and termination steps. Control experiments showed that **1.15c** is stable under the reaction conditions, as well as in the presence of AIBN and/or Bu_3SnI, so simple thermal decomposition of the substrate itself can be effectively ruled out. Although the mass balances of these reactions were low (41-47%), no additional peaks appeared on the GC.

Table 1.6 Promotion of SET by Adding Excess 1.15c

		% yield of product[b]						
entry[a]	equiv **1.15c**	**1.16**	**1.17+1.18**	**1.19**	total	recovered **1.15c** (equiv)	cyc:red[c]	ox:cyc[d]
1	1.0	12	13	21	46	0.00	54 : 46	1.1 : 1
2	1.5	6	15	26	47	0.15	45 : 55	2.5 : 1
3	2.0	4	16	28	48	0.46	29 : 71	4.0 : 1

[a] conditions: Iodide **1.15c**, Bu_3SnH (1.0 equiv), and AIBN (0.2 equiv) in toluene were combined in a sealed tube and heated at 110°C for 3h. [b] GC yield, using octadecane as an internal standard. Yields are an average of three trials. Bu_3SnH was the limiting reagent [c] Ratio of **(1.16 + 1.17 + 1.18)** to **1.19**. [d] Ratio of **(1.17 + 1.18)** to **1.16**.

1.2.5 Attempt to Trap Post-SET Acyliminium Intermediate

Our next mechanistic probe for SET involved an intramolecular trap to intercept the posited acyliminium ion generated during the process. We envisioned tethering an electron-rich aromatic ring near the reactive site as in enamide **1.38** (Scheme 1.10). A 5-*endo-trig* cyclization of this substrate to give radical **1.39**, followed by SET, would produce acyliminium ion **1.40**, which could act as an electrophile in a Friedel-Crafts alkylation, producing alkaloid **1.41**. The cyclization of acyliminium ions such as **1.40** is well-known[78] and is a commonly used route to the *Erythrina* alkaloids.[6,11] α-Amidoyl radical **1.39** would not be expected to cyclize onto the aromatic ring,[11] allowing a differentiation between possible trapped intermediates.

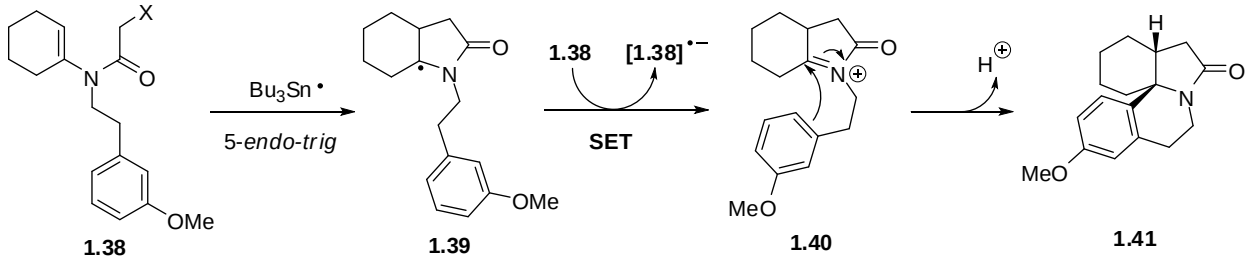

Scheme 1.10 Proposed Trapping of the Post-SET Acyliminium Intermediate

Substrates **1.38a-c** were synthesized according to Scheme 1.11. Condensation of 3-methoxyphenethylamine with cyclohexanone, followed by *N*-acylation with chloroacetyl chloride, afforded α-chloroenamide **1.38a** in 80% yield. Xanthate **1.38b** was synthesized from **1.38a** and potassium *O*-ethylxanthate in 96% yield, while treatment with NaI under Finkelstein conditions produced the α-iodide **1.38c**. An authentic sample of the expected Friedel-Crafts product **1.41** was made by condensation of 3-methoxyphenethylamine with ester **1.35**, followed by treatment with concentrated hydroiodic acid, in 73% yield over two steps.[10]

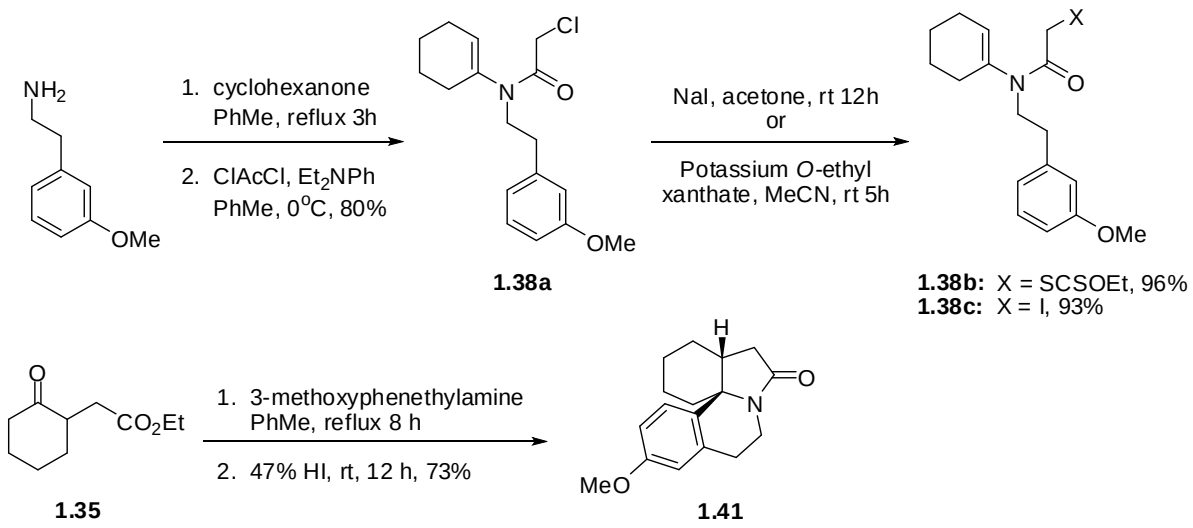

Scheme 1.11 Synthesis of Iminium "Trap" Substrates and Authentic Trapped Product

Initial testing on the Bu_3SnH-mediated cyclization yielded results similar to Ishibashi's results with the *N*-benzyl congeners.[16] A toluene solution of Bu_3SnH (1.2 equiv) and catalytic AIBN (0.1 equiv) was added over 2 h via syringe pump to a refluxing solution of precursors **1.38a-c** in toluene (2.0 mM). The mixtures were subjected to an aqueous KF workup[16] followed by flash chromatography to isolate the products shown in Scheme 1.12. Chloride **1.38a** required 2.4 equiv of Bu_3SnH to fully react, but afforded cyclization product **1.42** in 75% yield, along with 10% of reduced product **1.45**. Xanthate **1.38b** reacted similarly, producing **1.42** in 62% yield and **1.45** in 13% yield. In contrast, iodide **1.38c** gave a mixture of oxidized cyclized products **1.43** and **1.44** (9% and 43% yields, respectively), as well as ~12% of **1.45** (contaminated with tin byproducts). No evidence of the expected Friedel-Crafts product[10] **1.41** was seen in any reaction mixture.

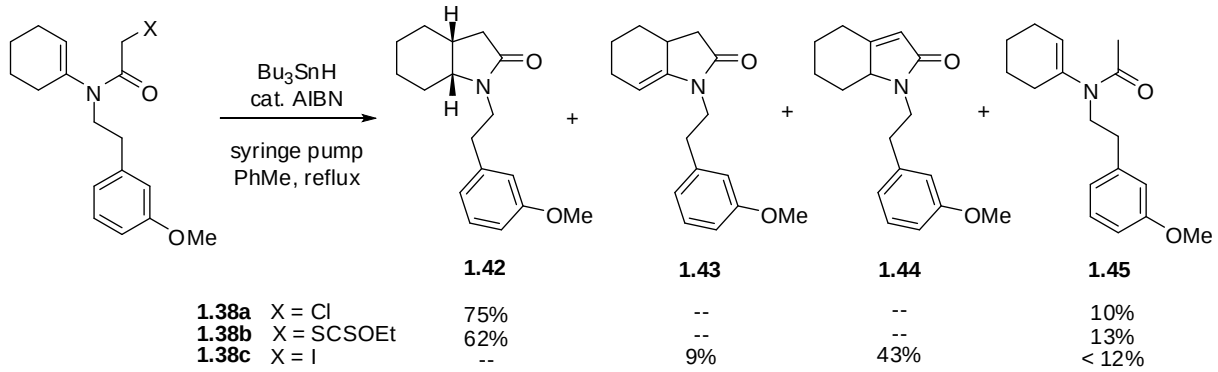

Scheme 1.12 Bu_3SnH-Mediated Cyclization of 1.38a-c

The absence of alkaloid **1.41** suggested either that acyliminium ion **1.40** was not being formed under our conditions, or that it *was* forming and its deprotonation was faster than the cyclization. Therefore, we tested the feasibility of cyclization onto the hypothesized acyliminium ion under various reaction conditions (Scheme 1.13). Xanthate **1.38b** was cyclized under oxidative radical conditions with dilauroyl peroxide,[6] followed by addition of catalytic *p*-toluenesulfonic acid in benzene. Surprisingly, compound **1.44** was the only compound isolated after column chromatography, in 67% yield. A literature search established that cyclizations onto an acyliminium ion which do not occur in nonpolar aprotic solvents proceed cleanly in more polar aprotic solvents.[79] Therefore, we resubmitted **1.44** to acidic conditions in 1,2-dichloroethane (DCE) to regenerate the acyliminium ion, shown in Scheme. This produced an inseparable mixture of alkaloid **1.41** in 81% yield along with 12% recovered starting material. Drawing on these results, iodide **1.38c** was subjected once again to Bu_3SnH-mediated radical cyclization, this time in DCE. No evidence of **1.41** was seen by NMR analysis of the crude reaction mixture, and only **1.44** (45%) and **1.45** (15%) were isolated by column chromatography.

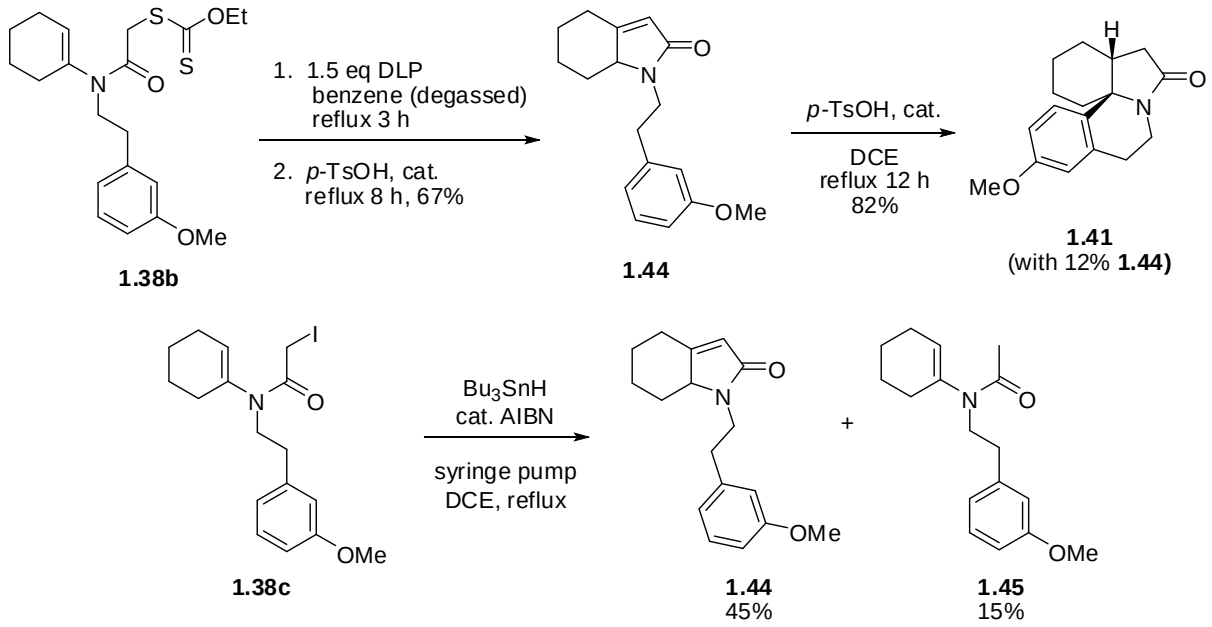

Scheme 1.13 Further Attempts to Trap Acyliminium Ion 1.40

At this point, the inability of the aromatic substituents to trap the postulated acyliminium ion was recognized, and this mechanistic probe was abandoned. While these experiments were unable to confirm the existence of acyliminium **1.40**, the results strongly suggest that if **1.40** does exist as an intermediate, the rate of its deprotonation is very fast. However, the complete isomerization from **1.43** to the thermodynamically favored **1.44** in some of our trials implies that residual acid was present in the reaction mixture. In these cases, a trapped iminium may not have come directly from the SET, but rather from reprotonation of **1.43/1.44**. The possibility of acid within the reaction is important, and will be discussed further in Chapter 1.2.7.

1.2.6 Attempts to Discourage SET by Substrate Control

We then turned our attention towards trapping an intermediate α-amidoyl radical in a tandem intramolecular cyclization before it could be oxidized. Ishibashi has previously shown

that chloride **1.46a** cyclizes under Bu_3SnH-mediated conditions in a predominant 5-*endo-trig* manner[26] as shown in Scheme 1.14, giving minor amounts of the 6-exo-trig product **1.49** (8%). Moreover, the intermediate **1.47** from initial cyclization react further via 5-*exo-trig* to give **1.51** (32% yield), or 6-*endo-trig* to produce **1.52** (27% yield). Small amounts of products from premature reduction are also formed: **1.48** in 6% yield, and **1.50** in 7% yield.

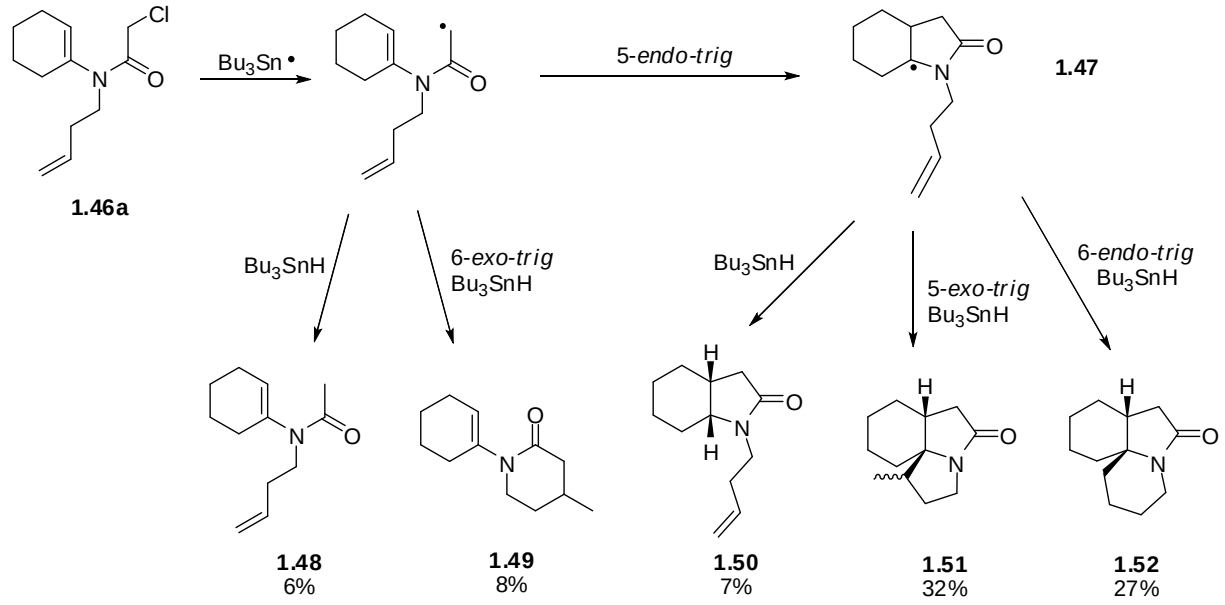

Scheme 1.14 Routes for Tandem Cyclization After a 5-*Endo-trig* Step

We hypothesized that the α-iodo congener **1.46b** would produce similar results as the chloride **1.46a**, cyclizing in a tandem fashion before SET could occur. Chloride **1.46a** was synthesized as shown in Scheme 1.15;[26] allyl cyanide was reduced to the corresponding amine, condensed with cyclohexanone, and acylated with chloroacetyl chloride in a three-step sequence (15% overall yield). Iodide **1.46b** was then made in 83% yield by treatment of **1.46a** with NaI in acetone. With both substrates in hand, radical cyclizations were performed under several conditions. Either Bu_3SnH or tris(trimethylsilyl)silane (TTMSS) with catalytic AIBN (0.1 equiv) in toluene was added via syringe pump to **1.46** in a refluxing toluene solution. After

removing the solvent, the crude mixture was directly chromatographed using 10% w/w KF/silica gel as the stationary phase to remove the tributyltin residues.[80]

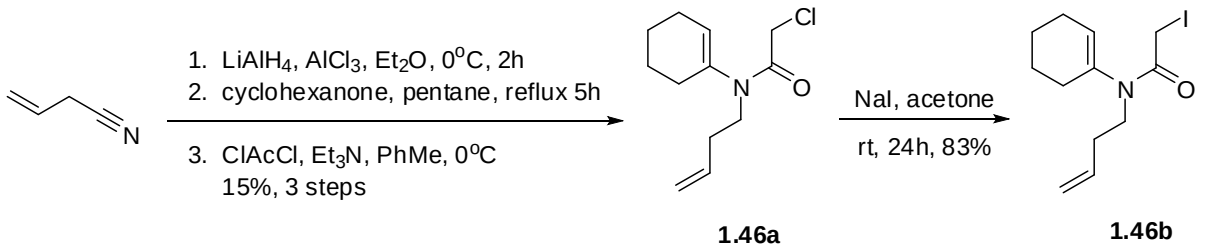

1.46a **1.46b**

Scheme 1.15 Synthesis of Tandem Cyclization Substrates

The Bu_3SnH-mediated cyclization of **1.46a** went in general accordance with literature results, giving good yields of tandem cyclization products **1.51** (14%) and **1.52** (51%), along with minor amounts of premature reduction product **1.48** and initial 6-*exo*-*trig* cyclization onto the terminal olefin to give **1.49** (Table 1.7, Entry 1). However, the α-iodo congener **1.46b**, under the same conditions, produced only reduction product **1.48** in excellent yield (83%), with trace amounts of cyclization product visible in the crude NMR spectrum (Entry 2). Lengthening the addition time of Bu_3SnH to **1.46b** had little effect on the product distribution (Entry 3), so TTMSS was considered as an alternative hydride source. TTMSS delivers hydrogen at a rate about one order of magnitude slower than tin hydride,[17,65] which in some cases may allow slower cyclizations to proceed more efficiently. Reaction of TTMSS with chloride **1.46a** resulted in recovered starting material, which was attributed to the inability of TTMSS to begin an efficient chain with the chloride (Entry 4). Reaction with iodide **1.46b**, however, immediately resulted in a persistent, dark red-colored reaction mixture that was highly acidic (pH approx. 1-3) to pH paper. The reaction mixture was exceedingly difficult to purify directly, and even after basic workup, column chromatography produced only **1.48**, contaminated with silicon-containing

byproducts, in less than 26% yield (Entry 5). Octahydroindolone **1.50** was not isolated in any of the reactions.

Table 1.7 Cyclization Reactions of 1.46a-b

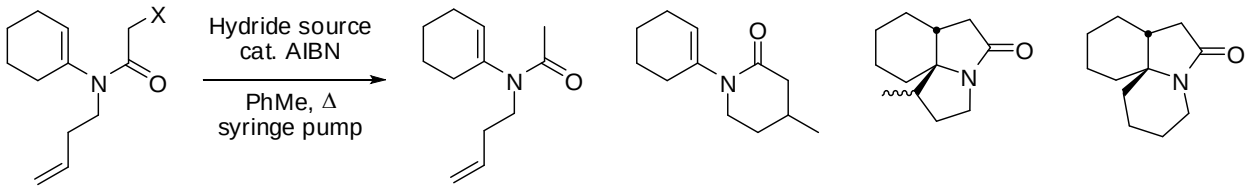

1.46 **1.48** **1.49** **1.51** **1.52**

				% yield of product[b]			
entry[a]	substrate	hydride	addn time	**1.48**	**1.49**	**1.51**	**1.52**
control[26]	**1.46a**	Bu_3SnH	1 h	6	8	32	27
1	**1.46a**	Bu_3SnH	3 h	9	< 5	14	51
2	**1.46b**	Bu_3SnH	3 h	83	trace	trace	trace
3	**1.46b**	Bu_3SnH	6 h	75	trace	trace	trace
4	**1.46a**	TTMSS	2 h		Recovered **1.46a**		
5	**1.46b**	TTMSS	3 h	< 26	0	0	0

[a] conditions: hydride (1.2 equiv) and AIBN (0.1 equiv) in toluene (24 mM in hydride) was added via syringe pump to a refluxing mixture of the amide in toluene (20 mM). [b] Isolated yield after 10% KF/silica gel column chromatography.

Iodide **1.46b** was unable to achieve the desired tandem cyclization, but its inability to form isolable amounts of *any* cyclized product is very interesting. An analogous reaction of the trichloroacetamide **1.53** has also failed to complete the tandem cyclization shown in Scheme 1.16.[2] Zard and coworkers observed that, after 5-*endo*-*trig* cyclization under Ni/AcOH conditions, intermediate **1.54** was oxidized by the easily-reduced starting material to eventually produce **1.55** in 51% yield. This astonishing result suggests that SET from the α-amidoyl radical **1.54** is *faster* than the possible cyclizations onto the available olefin, and is the favored pathway when a good oxidant is present. Furthermore, our results indicate that even a small amount of SET under typical Bu_3SnH-mediated conditions may be enough to terminate the radical chain

process, and initiate a competing mechanism to form reduced **1.48**. This possibility is explored further in Chapter 1.2.7.

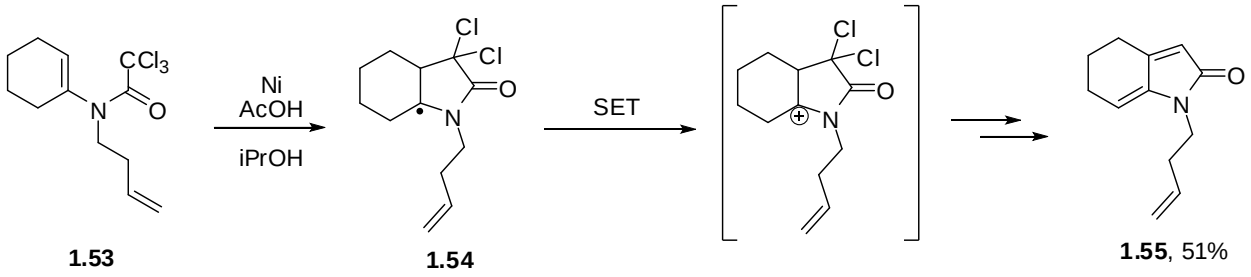

1.53 **1.54** **1.55**, 51%

Scheme 1.16 SET Under Oxidative Radical Conditions

1.2.7 Ionic Reductive Dehalogenation and Base Additive Studies

The presence of iodine and HI in the reaction of TTMSS with **1.46b** caused us to reevaluate the origin of reduced product **1.48**. Silyl iodides are known to perform reductive dehalogenations on α-halocarbonyl compounds.[81-84] It is possible that TTMSS iodide formed in the reaction of **1.46b** with TTMSS (Table 1.7, Entry 5) could react in this manner with starting material, as shown in Scheme 1.17. TTMSS also reacts with the necessary byproduct of I_2 to form $(TMS)_3Si\bullet$ which propagates the radical chain, and hydrogen iodide[85] which consumes TTMSS to release more iodine. So, in the presence of HI or I_2, this ionic sequence is self-propagating upon addition of further TTMSS. Ishibashi's reaction of **1.15c** with TTMSS resulted in recovering **1.19** as the sole product in 76% yield.[16]

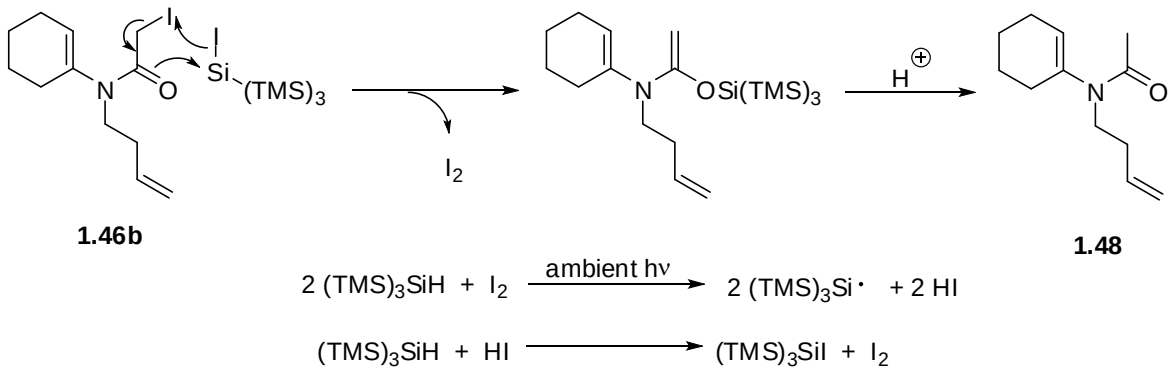

Scheme 1.17 Proposed TTMSI-Mediated Reductive Dehalogenation of 1.46b

Without a silyl iodide to begin this process, though, how does reductive dehalogenation occur in Bu_3SnH-mediated processes? Bearing in mind that the SET process occurring in Scheme 1.6 results in the overall elimination of HI, it is plausible that this Brønsted acid would react with an α-iodo substrate[86,87] like **1.15c**, as shown in Scheme 1.18. Furthermore, the distinctive color of molecular iodine, the necessary byproduct of this reaction, had been observed in all syringe pump additions involving α-iodo compounds thus far.

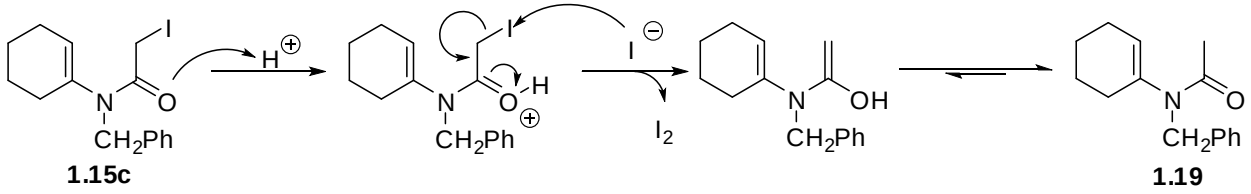

Scheme 1.18 Proposed Mechanism of Non-Radical Reductive Dehalogenation of 1.15c

To test the ability of an α-iodo enamide to undergo acidic reductive dehalogenation, we submitted substrate **1.15c** to several reaction conditions in refluxing toluene as shown in Table 1.8, and monitored for the formation of reduced compound **1.19**. A control experiment using Bu_4NI as an iodide source showed no reaction (Entry 1), and an attempt to generate HI *in situ* using iodine and alumina[88] led to complete decomposition (Entry 3). Refluxing with 1 equiv

camphorsulfonic acid (CSA) delivered **1.19** in 53% yield, albeit with a rather long reaction time (Entry 4). When 2 equiv each of CSA and Bu_4NI were used, however, the reaction proceeded cleanly and efficiently, giving **1.19** in 68% yield (Entry 5). Interestingly, extensive refluxing with CSA and Bu_3SnI showed no reaction (Entry 2), suggesting that Bu_3SnI does not act as source of iodide ion. No products of cyclization **1.16-1.18** were formed under any of these conditions.

Table 1.8 Non-Radical Reductive Dehalogenation of 1.15c

entry[a]	conditions	time	**1.19** (% yield)
1	1.0 equiv Bu_4NI	2 h	--
2	1.0 equiv CSA, 1.0 equiv Bu_3SnI	24 h	--
3	4.0 equiv I_2, alumina	5 h	Decomposition
4	1.0 equiv CSA	24 h	53
5	2.0 equiv CSA, 2.0 equiv Bu_4NI	2 h	68

[a] conditions: **1.15c** (0.01 M) and additive in toluene were refluxed under Ar.

The presence of iodide in an acidic medium not only promotes the formation of **1.19** via reductive dehalogenation, but it can also halt the radical chain. Past studies have shown that Bu_3SnH can be consumed by protic acids such as in Equation 1.4, disrupting the normal chain process.[17] The molecular iodine produced by the SET process also rapidly converts trialkyltin hydrides to their iodide counterparts as shown in Equation 1.5, releasing further protic acid.

$$Bu_3SnH + HI \rightarrow Bu_3SnI + H_2 \qquad \text{(Equation 1.4)}$$

$$Bu_3SnH + I_2 \rightarrow Bu_3SnI + HI \qquad \text{(Equation 1.5)}$$

With an eye towards removing the interfering HI being produced by SET, cyclization reactions were run on iodide **1.15c** with a variety of base additives. The use of bases, both homogeneous and heterogeneous, has been shown to increase the efficiency of other radical reactions involving the release of protic acid.[43] Typical syringe pump conditions were used:

Bu_3SnH (1.2 equiv) and AIBN (0.1 equiv) in toluene were added over 3 h to a refluxing solution of substrate **1.15c** and the appropriate base additive in toluene. After filtering the mixtures (when solid bases were used) and removing solvent, the crude reaction mixtures were directly chromatographed on a 10% w/w KF/silica column.[89] The results are summarized in Table 1.9.

Table 1.9 Bu_3SnH-Mediated Cyclization of 1.15c With Base Additives

			% yield of product[b]					
entry[a]	additive	equiv	**1.16**	**1.17**	**1.18**	**1.19**	total	cyc:red[c]
control[16]	--	--	0	13	11	68	92	26 : 74
1	--	--	4	13	21	35	73	52 : 48
2	pyridine	5	13	60	3	5	81	94 : 6
3	2,6-lutidine	5	4	45	22	5	76	93 : 7
4	Cs_2CO_3	5	4	44	5	0	53	> 100 : 1
5	K_2CO_3	10	10	41	20	0	71	> 100 : 1
6	Proton Sponge ®	5	0	32	0	0	32	> 100 : 1

[a] conditions: Bu_3SnH (1.2 equiv) and AIBN (.1 equiv) in toluene (12 mM in Bu_3SnH) was added via syringe pump to a refluxing mixture of the amide **1.15c** in toluene (10 mM) and additive over 3 h. [b] Isolated yield after 10% KF/silica column chromatography. [c] Ratio of (**1.16** + **1.17** + **1.18**) to **1.19**.

The base additives had the predicted effect on the product distribution: the normal radical chain and SET mechanisms were unhindered by competing acid-driven processes. The distinctive red color of iodine was not observed in any of the reactions with additives, suggesting that the pathway in Scheme 1.18 had been shut down. Under basic conditions, the total yield of cyclized products **1.16-1.18** could be increased to 76% in some cases, while only trace amounts of directly reduced products were observed in any of the reactions. Heterogeneous bases seemed to work as well as the soluble organic bases, though cesium carbonate produced a lower mass recovery (Entry 4). The use of Proton Sponge® resulted in a large amount of decomposition (Entry 6), which is likely due to its high basicity.

1.2.8 Conclusions

The role of halogens in the 5-*endo-trig* cyclization of α-haloenamides has been thoroughly investigated.[90] Low-temperature NMR analysis has shown that *N*-cyclohexenyl rotation, not amide rotation, is the major conformational process in these molecules. Kinetic studies showed the rate constants of cyclization are not critically halogen-dependent, but the ratio of cyclized to oxidized products is dependent on the halogen used in the radical precursor. Control experiments with Bu_3SnX additives showed no distinctive Lewis acid activity, but halogen exchange occurs under the reaction conditions. SET plays a substantial role as a competing mechanism when the starting halide is easily reducible. This process also spurs an ionic, acid-driven reductive halogenation process, which disrupts the anticipated radical chain mechanism. Addition of excess base to the reaction mixture suppresses the reductive dehalogenation pathway.

2.0 AN INTRODUCTION TO AXIALLY CHIRAL ANILIDES

2.1 AXIALLY CHIRAL AMIDES

2.1.1 Axial Chirality

Once a mere curiosity, axial chirality has become a major focal point of research in the last two decades.[54,91-139] Axially chiral compounds do not necessarily contain a stereogenic center, yet nevertheless possess an element of asymmetry. Eliel defines axial chirality as four substituents held in a non-planar arrangement around an axis, such that the molecule is not superimposable on its mirror image.[140,141] Like stereogenic centers, axes of chirality have two possible spatial arrangements that are mirror images of one another. Throughout the remainder of this document, the Cahn-Ingold-Prelog notation of *M*/*P* will be used to describe the absolute stereochemistry of chiral axes.[142]

Axial chirality is exemplified by allenes such as **2.1**, cumulated dienes which contain two orthogonal π-bonds (Figure 2.1). Biaryls such as **2.2** are also common, and their enantiomeric forms may interconvert by a 180° rotation about the aryl-aryl bond. In recent years, axially chiral natural products (Figure 2.2) have also been identified and synthesized. These include murrastifoline F,[95] which possesses an *N*-aryl axis, and the biaryl natural product kotanin.[114] The potent antibiotic vancomycin[129] also contains an axis of chirality, highlighted in Figure 2.2.

Figure 2.1 Axially Chiral Allenes and Biphenyls

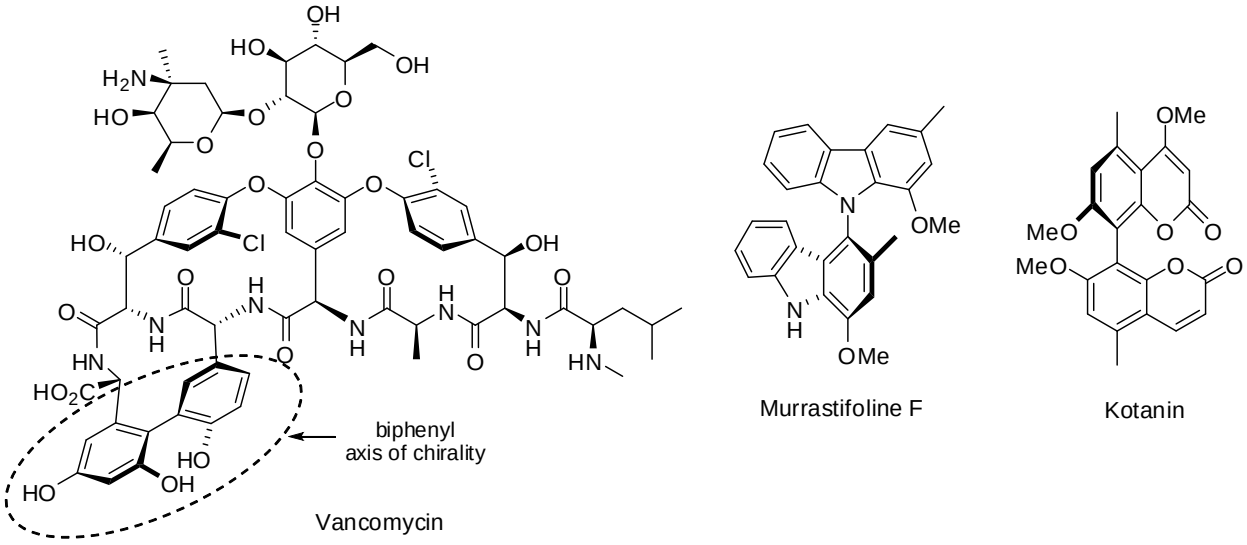

Figure 2.2 Representative Axially Chiral Natural Products

Axially chiral compounds have also enjoyed great synthetic utility, particularly as transition metal ligands for asymmetric synthesis. In 2001, Noyori shared the Nobel Prize in Chemistry for his accomplishments in asymmetric catalysis, specifically the use of axially chiral diphosphine ligands. Most notable is the industrial synthesis of menthol, which relies on a ruthenium-catalyzed asymmetric olefin isomerization with BINAP as a chiral ligand (Scheme 2.1). Isomerization of **2.3** is catalyzed by the (*S*)-BINAP-Rh^{I} complex formed *in situ*, producing intermediate **2.4** in 96-99% ee on a 9 ton scale.[130]

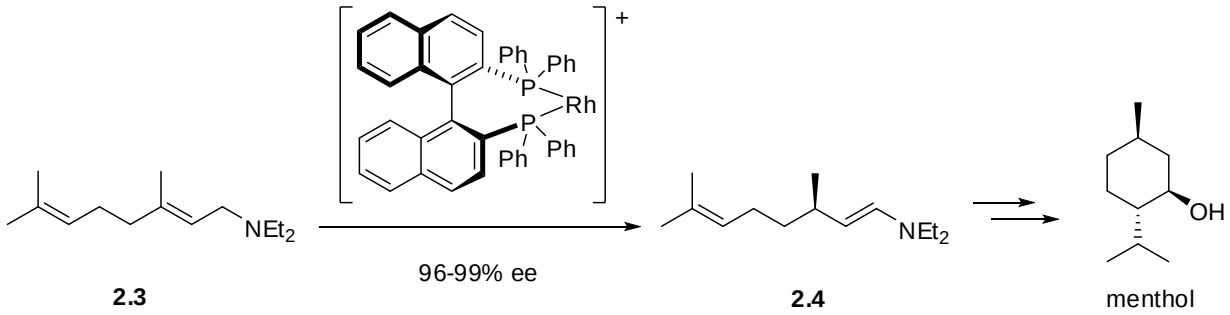

Scheme 2.1 Asymmetric Catalysis With an Axially Chiral Ligand

2.1.2 Atropisomerism

Axially chiral compounds that emanate from restricted rotation about a single bond are racemized through thermal, not chemical, means. While tetrahedral stereocenters require a bond-breaking event and subsequent bond forming to change configuration, an axially chiral compound needs only to overcome an energy barrier to undergo a 180° rotation about its axis. If this barrier is high enough, then the axially chiral enantiomers are classified as "atropisomers." Ōki defined an atropisomer[54] as a conformer which can retain its axial chirality with a half-life of racemization of $t_{1/2} \geq 1000$ s. This definition is temperature-dependent, however, as the half-life of racemization of an axially chiral compound will decrease with increasing temperature. By Ōki's definition, a compound at 25 °C requires a barrier to rotation of at least 22.2 kcal/mol to be considered atropisomeric, while a barrier of 26.4 kcal/mol is required at 80 °C. We propose a more practical definition of atropisomers as compounds whose axial chirality can be observed by spectroscopic means. Stable atropisomers, then, have a barrier high enough that they can be resolved by laboratory methods.

The first stable atropisomer to be isolated was 6,6′-dinitro-2,2′-diphenic acid **2.5** (Figure 2.3), which was resolved by cocrystallization with a chiral amine in 1922.[143] Since then,

thousands of atropisomeric compounds have been identified and resolved by numerous methods, including 2,2′-diiodobiphenyl **2.6**.[139] Biaryl **2.6** possesses an aryl-aryl rotation barrier of 23.1 kcal/mol, giving it a half-life to racemization of 80 min at room temperature.

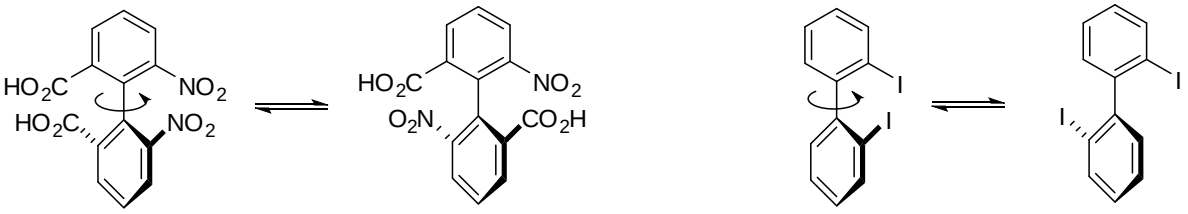

(*P*)-**2.5** (*M*)-**2.5** (*P*)-**2.6** (*M*)-**2.6**

Figure 2.3 Atropisomerism in Biaryl Compounds

2.1.3 Configurational and Rotational Behavior of Amides

The amide functional group contains a planar, sp^2-hybridized nitrogen resulting from conjugation of the nitrogen lone pair with the adjacent carbonyl functionality (Figure 2.4),[22,144] granting the carbonyl-nitrogen bond a partial double bond character. Unsymmetrically *N*,*N*-disubstituted amides **2.7** have two possible ground states that interconvert by a single rotation of the *N*-carbonyl bond. Because of the partial double bond character of the rotating bond, we refer to these two states as "Z" and "E" by analogy to the nomenclature rules for olefins. Tertiary *N*,*N*-dialkylamides nearly always prefer the (*Z*) configuration at equilibrium, because the larger *N*-substituent R^3 is *cis* to the smaller carbonyl oxygen.[145]

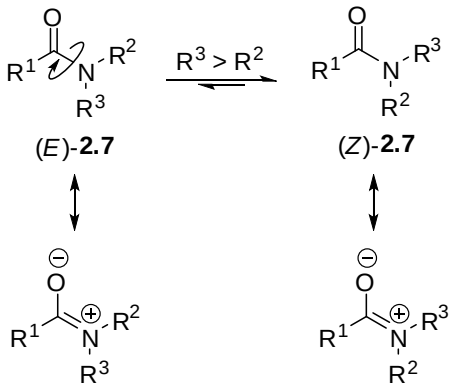

Figure 2.4 Rotation and Resonance of a Generic Tertiary Amide

The barrier to amide rotation is typically in the range of 15-20 kcal/mol,[22] and is subject to both steric and electronic effects of substituents. Sample barriers to amide *N*-carbonyl rotation are shown in Figure 2.5. Increasing the steric bulk of carbonyl substituent R^1 or *N*-substituents R^2 and R^3 leads to a decrease in the rotational barrier, as seen in comparisons of **2.8** to more highly substituted amides **2.9**-**2.11**.[49,146] In the ground state, all substituents are coplanar and thus have the most steric interaction with one another. Therefore, greater steric hindrance leads to a destabilization of the ground state energy. Substitution with multiple α-halogen atoms, as in **2.12**, raises the rotational barrier by withdrawing electron density from the carbonyl group, thereby stabilizing the ground state and offsetting the steric factor.[49]

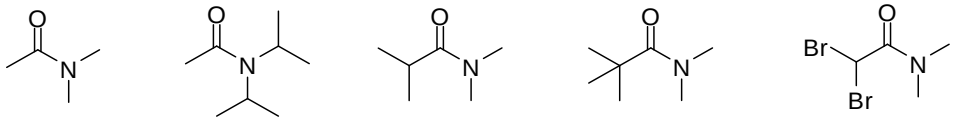

2.8 ΔG_{rot} = 18.5 kcal/mol

2.9 ΔG_{rot} = 16.3 kcal/mol

2.10 ΔG_{rot} = 16.5 kcal/mol

2.11 ΔG_{rot} = 10.5 kcal/mol

2.12 ΔG_{rot} = 17.3 kcal/mol

Figure 2.5 Representative Carbonyl-*N* Amide Barriers to Rotation

ortho-Substituted benzamides **2.13**, as in Figure 2.6, add a second element of stereochemistry to the amide.[147,148] The steric effect of *o*-substituents X and Y twists the aromatic ring out of planarity with the amide group, creating an axis of chirality. If R^2 and R^3 are non-equivalent, equilibrium favors the *E*-amide rotamer,[92] in contrast to the preferred *Z*-configuration of *o*-unsubstituted benzamides (X = Y = H). If alkyl groups R^2 and R^3 contain no additional stereocenters, then interconverting enantiomers (*M*)-**2.13** and (*P*)-**2.13** are formed. Some examples of experimentally determined barriers to rotation are shown in Figure 2.6.[92] When only one *ortho* substituent is present (Y = H), the barrier to carbonyl-aryl rotation is low enough that the amides cannot be resolved as stable atropisomers (for example, **2.14** and **2.15**).[54] However, a second substituent increases the barrier to rotation as in the cases of **2.16** and **2.17**, slowing interconversion to a rate that allows for resolution of the enantiomers under ambient conditions.[149,150] The rotational dynamics[91,92,94,97-101,104,151] and asymmetric reactions[94,97-101] of this class of compounds have been thoroughly studied by Clayden and coworkers.

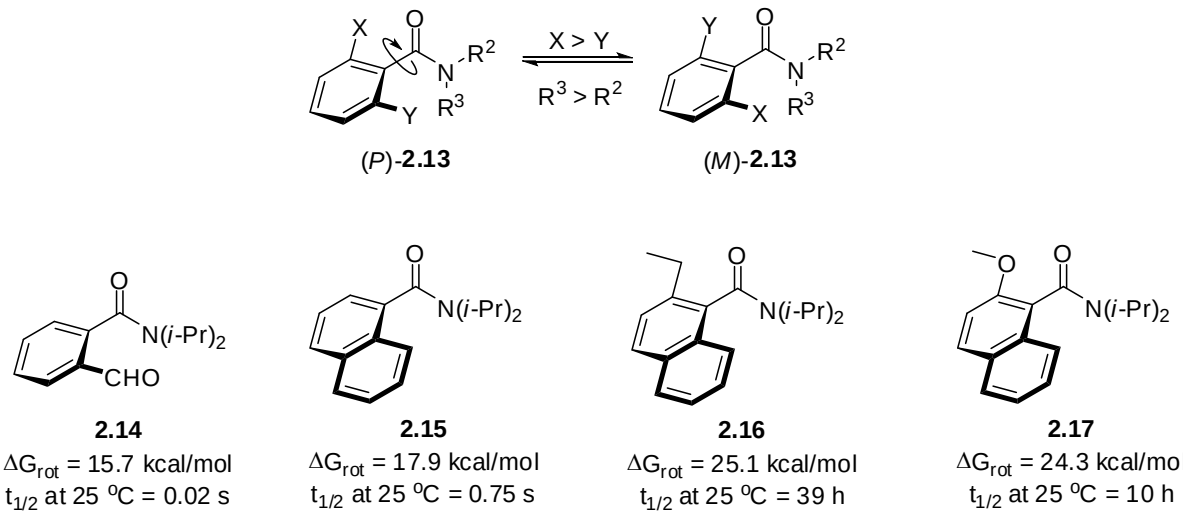

Figure 2.6 Rotational Dynamics and Barriers of Axially Chiral Benzamides

Aryl groups positioned on the amide nitrogen are also twisted out of planarity. An early crystal structure of *N*-methylacetanilide **2.18** showed that the amide and aryl planes were roughly perpendicular to one another (Figure 2.7).[152] Because the aryl group twists to avoid steric interactions, tertiary anilides prefer the *E*-configuration in solution, and most are able to readily equilibrate at room temperature with typical barriers to carbonyl-*N* rotation.[107] In one case, **2.18** has a 200:1 *E*:*Z* ratio in pyridine solution; in most systems, ratios of 10:1 *E*:*Z* or greater are typical.[48,105,107,109,127,132,133] In a rare example, extremely hindered system **2.19** is locked in either a *Z*- or *E*-configuration, only able to isomerize under prolonged heating.[153]

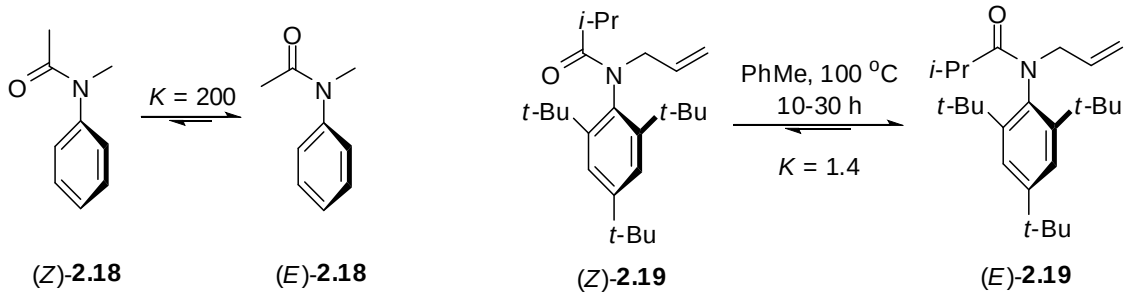

Figure 2.7 *E*/*Z* Configuration in Twisted Anilides

Substitution at the *ortho* position of an aryl group forms an axis of chirality along the aryl-*N* bond, producing stable atropisomers if steric hindrance is significant. The first axially chiral anilide **2.20** was discovered in 1937 by optical resolution of its brucine salt (Figure 2.8).[154] Since then, many other chiral anilides have been developed, each with a single large *ortho* substituent such as *t*-Bu (**2.21**, **2.22**) or I (**2.23**) to slow *N*-aryl rotation and allow for resolution. Addition of a second *ortho* substituent further increases the barrier (**2.24**), resulting in compounds that are atropisomerically stable for years, if not centuries, at ambient temperature. In general, greater steric hindrance on the *N* substituent, at either of the *ortho* positions, or alpha

to the carbonyl increases the barrier to rotation, as seen by the examples in Figure 2.8. Benzoyl and acryloyl anilides tend to have lower barriers than acetanilides, as observed in the 3.2 kcal/mol difference between the rotation of **2.21** and **2.22**. Unlike alkyl groups, aryl and vinyl groups may twist out of planarity with the carbonyl, thereby avoiding hindrance with *o*-substituents in the rotation transition state.[107]

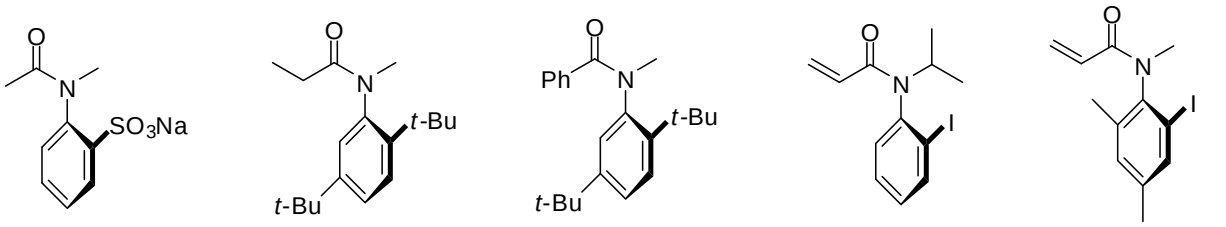

2.20
23.4 kcal/mol
$t_{1/2}$ at 25 °C =
134 min

2.21
29.6 kcal/mol
$t_{1/2}$ at 25 °C =
9 years

2.22
26.4 kcal/mol
$t_{1/2}$ at 25 °C =
15 days

2.23
22.8 kcal/mol
$t_{1/2}$ at 25 °C =
49 min

2.24
30.8 kcal/mol
$t_{1/2}$ at 25 °C =
69 years

Figure 2.8 Barriers to Rotation and Approximate Half-Lives of Selected Axially Chiral Anilides

2.1.4 Preparation of Enantioenriched Axially Chiral Anilides

The first synthesis of an enantioenriched axially chiral anilide was achieved by the chemical resolution of diastereomeric atropisomers.[120] EDCI-mediated coupling of *N*-allylaniline **2.25** with (*S*)-*O*-acetyl lactic acid produced **2.26** as a 3:1 mixture of diastereomers. These compounds were separable by column chromatography, and their relative configurations were identified by X-ray crystallography. The major diastereomer, (*S*,*P*)-**2.26**, was subjected to saponification, followed by formation of the mesylate and substitution to provide α-selenide **2.27**. This compound was oxidized to the selenoxide, and spontaneous β-elimination produced anilide (*P*)-**2.28** in 81% yield over 4 steps with 97% ee. This process[119,120,122] has also been applied to the preparation of enantioenriched *o*-iodoanilides,[132] but is somewhat limited in substrate scope.

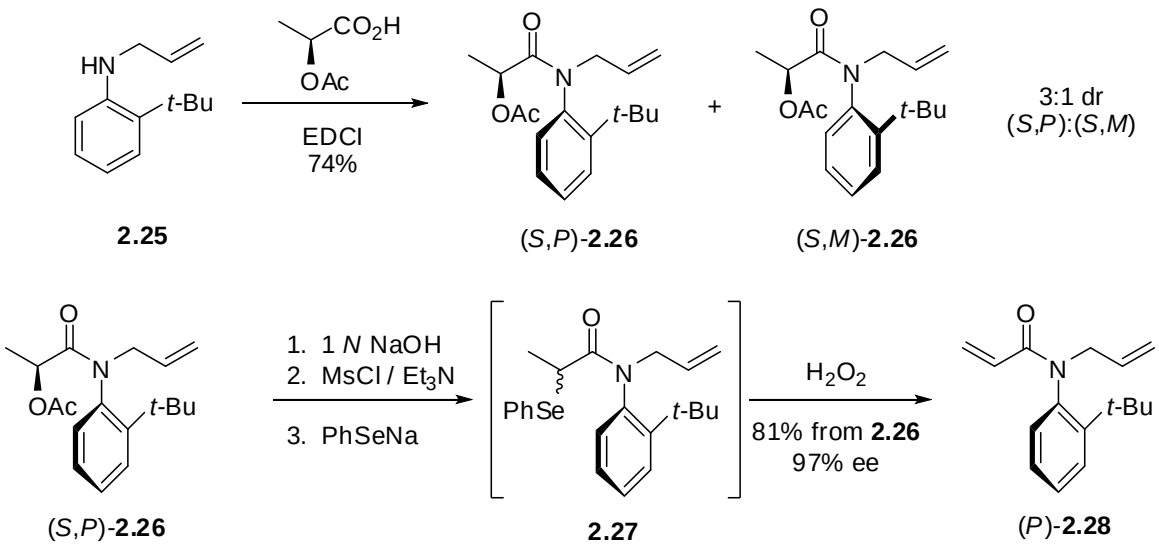

Scheme 2.2 Preparation of Enantioenriched Anilide *via* Chemical Resolution

To date, the most general access to enantioenriched axially chiral anilides is resolution of racemates by semipreparative chiral HPLC. Axially chiral benzamides with an aryl-carbonyl axis of chirality were among the first amides to be resolved by this method.[92,149,150] This chromatographic technique was first applied to anilides in 1997,[96,107] and has proven itself to be highly useful in the resolution of numerous anilides ever since.[105,108,128,132,133,155] Two columns are particularly efficient for resolution of anilides (Figure 2.9): the Chiralcel OD column, which has a cellulose-based coating on silica gel, and the (*S*,*S*)-Whelk O1 column, which contains a chiral amide-containing group covalently tethered to the silica. Both stationary phases possess chiral functionalities that act as hydrogen bond donors for axially chiral amide substrates. Additionally, the π-acidic dinitrobenzamide group and the π-basic naphthyl group in the Whelk column recognize aromatic analytes through π-π face-to-face as well as face-to-edge interactions.[156]

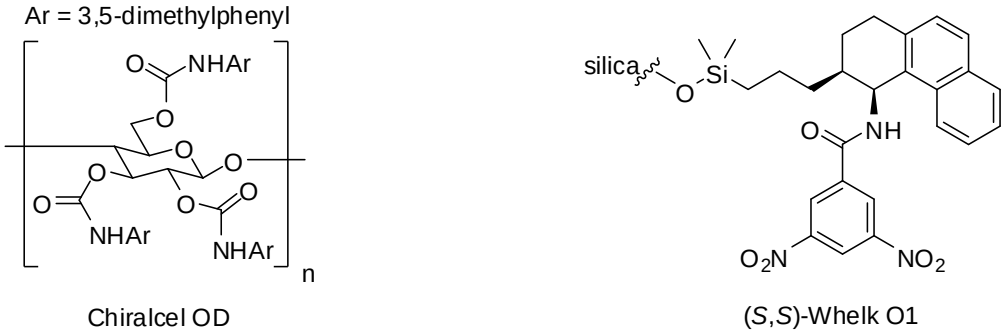

Figure 2.9 Chiral HPLC Stationary Phases

Recently, enantioselective syntheses of axially chiral anilides have also been developed. Uemura has developed a general procedure for the desymmetrization of 2,6-dimethylanilides by asymmetric deprotonation of tricarbonylchromium complexes such as **2.29**, followed by alkylation to give **2.30** in 97% ee.[112,113,125,126] Curran[137] and Taguchi[121] simultaneously disclosed methods for the asymmetric allylation of achiral anilides possessing an *ortho t*-butyl substituent (Scheme 2.3). In the allylation of **2.31**, Curran's procedure gave allylated product (*P*)-**2.32** in 27% yield and 43% ee, while Taguchi's conditions produce (*P*)-**2.32** in 94% yield and 40% ee. This strategy has been extended to catalytic asymmetric *N*-arylation, with significantly higher enantioselectivities (88-96% ee).[123,124]

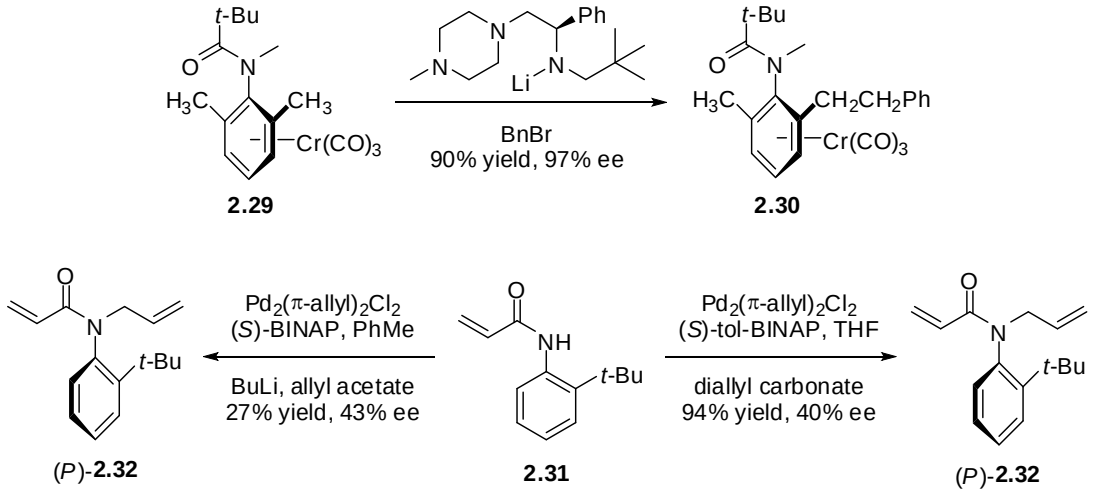

Scheme 2.3 Enantioselective Syntheses of Axially Chiral Anilides

While enantioselective synthesis is a promising route toward enantioenriched axially chiral anilides, the aforementioned methods in Scheme 2.3 are limited in scope. Presently, the most general means to efficiently access a variety of enantioenriched anilides is through resolution by chiral HPLC.

2.1.5 Asymmetric Induction by Axially Chiral Anilides

Many asymmetric reactions of atropisomeric anilides take advantage of the bulky *ortho* substituent as a stereodirecting group, preferentially shielding one face of the reactive site.[109] In an early example, the 1,3-dipolar cycloaddition of racemic **2.33** with benzonitrile oxide generated *in situ* gave cycloadducts **2.34a** and **2.34b** in a 92/8 dr (Scheme 2.4).[157] Because **2.33** exists primarily in the *E*-amide configuration, the *o*-*t*-butyl group effectively shields one face of the alkene, allowing cycloaddition to occur selectively from the back side to give **2.34a** as the primary product. Facial selectivity has also been observed in other nitrile oxide cycloadditions,[107] as well as iodine-mediated Diels-Alder reactions[119,120] and [2+2] photocycloadditions[158] of axially chiral anilides.

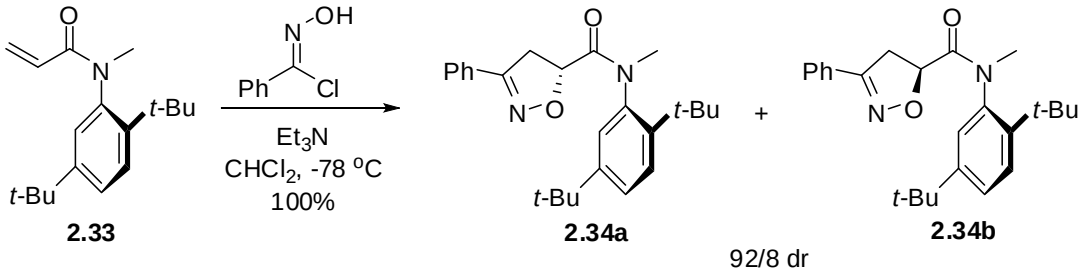

Scheme 2.4 Atroposelective Cycloaddition with Benzonitrile Oxide

Enolates of axially chiral amides undergo nucleophilic reactions with facial control imparted by the bulky *ortho* substituent (Scheme 2.5). The lithium enolate **2.36** is prepared by

treatment of **2.35** with LDA.[115] The *N*-methoxymethyl group is thought to fix the configuration of the amide *N*-carbonyl bond in enolate **2.36** by lithium coordination, as shown in Scheme 2.5. Treating **2.36** with BnBr gives alkylated product **2.37** in 83% yield and 25:1 dr.[115-117] This method has recently been extended to atropisomeric *N*-phenyl anilides with excellent diastereoselection (23:1 to 46:1 dr).[124] Alternatively, treating enolate **2.36** with benzaldehyde results in a 87% yield of *syn*-aldol product **2.38** as a single diastereomer.[115,116]

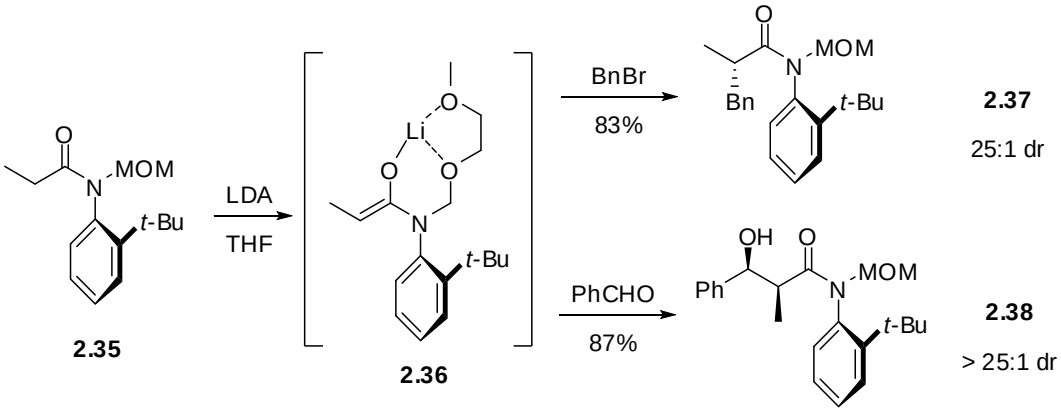

Scheme 2.5 Atroposelective Alkylation and Aldol Reaction

2.2 CHIRALITY TRANSFER OF AXIALLY CHIRAL *O*-IODOANILIDES

2.2.1 Chirality Transfer

"Memory of chirality" occurs when the reaction of a chiral starting material results in a chiral product, despite proceeding through a configurationally labile intermediate containing no permanent chiral features.[118,159-161] Chirality transfer is a subset of "memory of chirality" reactions, in which the element of stereochemistry in the product is at a different location than in the starting material.[160] An excellent example of chirality transfer was recently put forth by

Rychnovsky in the transannular radical cyclization of **2.39** (Scheme 2.6).[162] When enantioenriched oxalate **2.39** (94/6 er) was exposed to light at –15 °C, cyclization and thiopyridyl trapping produced **2.40** in 51% yield and 84/16 er (major enantiomer **2.40a**).

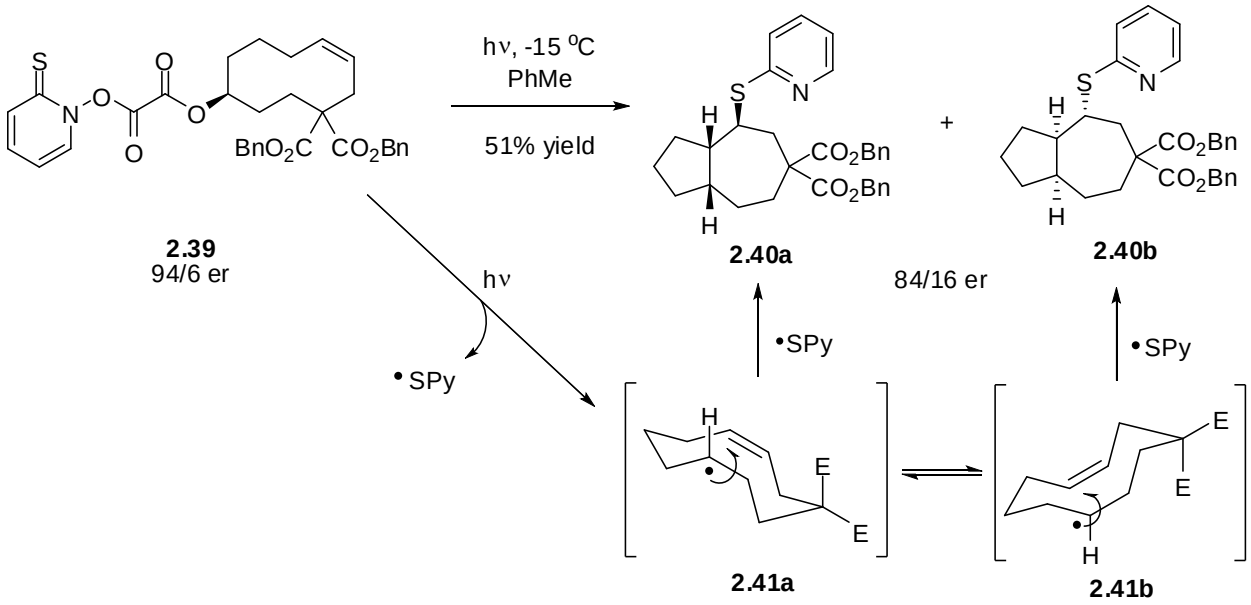

Scheme 2.6 Chirality Transfer in a Radical Transannulation

Cyclodecenyl radical **2.41a** is initially produced by deoxygenation of **2.39**. Radical **2.41a** may cyclize to give major enantiomer **2.40a**, or interconvert by a ring flip to radical **2.41b**, which cyclizes to minor enantiomer **2.40b**. Radical **2.41** is configurationally labile and lacks permanent chiral features, but the cyclization is faster than ring interconversion, and chirality transfer results. At higher temperatures, the yield of the reaction increased but the chirality transfer decreased, implying that conformational interconversion gradually becomes competitive with cyclization.

Chirality transfer is usually quantified by dividing the proportion of the major enantiomer in the product by the proportion of the major enantiomer in the starting material. This is a measurement of what percentage of the conformationally labile intermediate reacted while

retaining its memory of chirality. In the example above (Scheme 2.6), the chirality transfer is (84/94) x 100% = 89%. This value represents the percentage of the major enantiomer one would expect from reaction of enantiopure starting material. By definition, chirality transfer values range from 50% (racemization, complete loss of stereochemical information) to 100% (complete chirality transfer).

2.2.2 Chirality Transfer in Intramolecular Radical Reactions

Chirality transfer in radical cyclizations of *o*-iodoanilides was discovered by the Curran group in 1999.[108] Enantioenriched (*P*)-**2.42** was treated with Bu_3SnH and Et_3B in benzene at room temperature, producing dihydroindolone (*S*)-**2.43** in 86% yield and 90% chirality transfer (Scheme 2.7). Similarly, (*M*)-**2.42** gave (*R*)-**2.43** in 93% yield with 90% chirality transfer (not shown). Cyclizations of related substrates proceeded with 50-94% chirality transfer.[108,127]

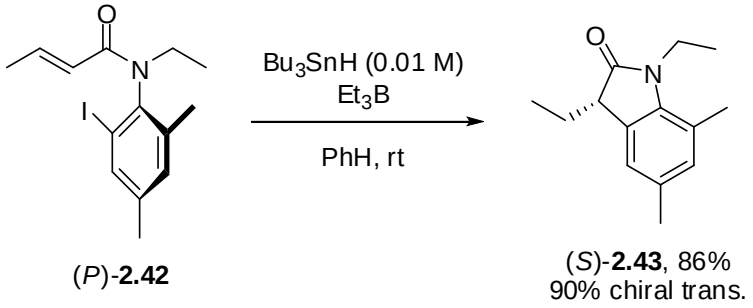

Scheme 2.7 Chirality Transfer in a 5-*exo* Radical Cyclization

Substrate (*P*)-**2.42** exists as a stable atropisomer at room temperature ($\Delta G^{\ddagger}_{rot} \approx 30.8$ kcal/mol),[108] but iodine atom abstraction produces an aryl radical **2.44a** whose barrier to rotation is significantly lower (Scheme 2.8). Radical **2.44a** is a labile intermediate that can rotate to **2.44b**, which destroys the chiral information in the starting material, or cyclize to **2.45a,** which

retains the memory of chirality. The transition state model for this class of cyclizations has the olefin twisting towards the incoming radical.[106,108,127,163]

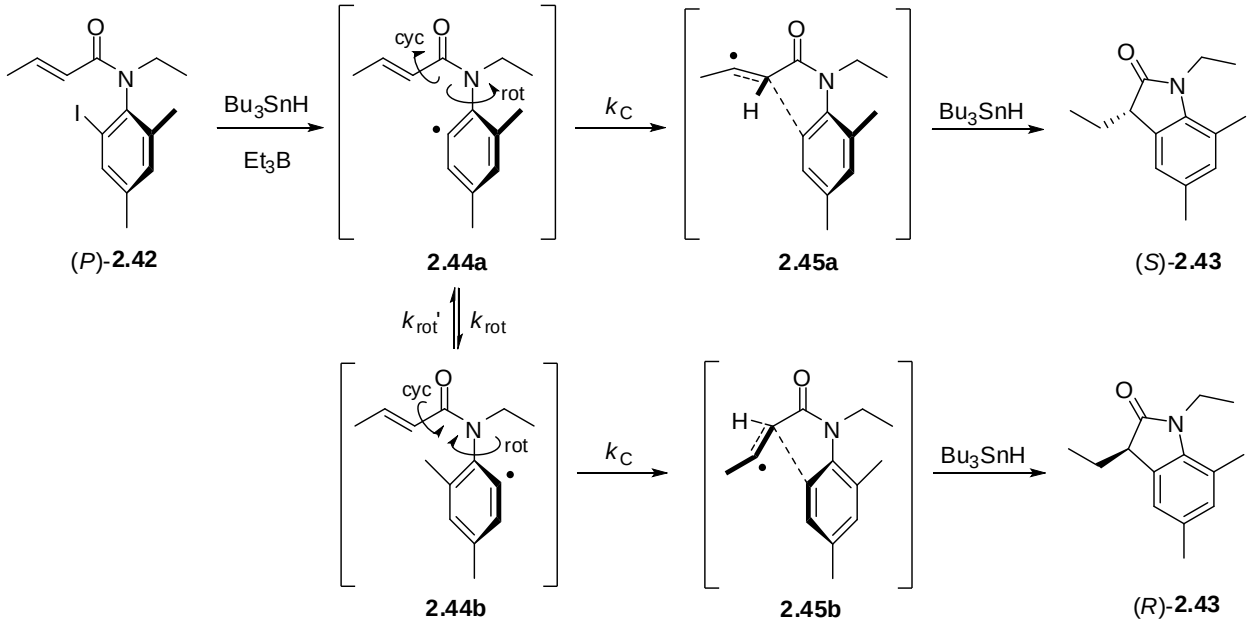

Scheme 2.8 Model for Chirality Transfer in Cyclizations of Acryloyl Anilides

The stereoselectivity of the radical cyclization depends on two factors: the facial selectivity of the attacking radical, and the ability of the intermediate radical **2.44** to cyclize before *N*-aryl rotation. The cyclization rate constant k_C of radical **2.44** has been estimated as $k_C = 7.8 \times 10^7\ s^{-1}$ at room temperature.[133,155] The high values of chirality transfer for this cyclization imply that, for the most part, cyclization events proceed before a rotation can occur ($k_C > k_{rot}$). The reaction also proceeds with moderate to excellent facial selectivity, preferring to react with one face of the olefin radical acceptor.

Chirality transfer has also been observed in radical cyclizations of *N*-allyl-*o*-iodoanilides. In a typical example, enantioenriched **2.46a** (99.5/0.5 er) was subjected to room temperature radical cyclization conditions with Bu_3SnH and Et_3B (Scheme 2.9).[105,127] After purification, dihydroindolone **2.47a** was obtained in 95% yield and in a 93/7 er, a chirality transfer of 93%.

The general model for chirality transfer was deduced by X-ray crystallographic analysis of a substrate-product pair. Iodine abstraction from **2.46a** produces aryl radical **2.48a**, and the *N*-allyl group twists towards the radical center. Attack of the radical on the bottom face of the alkene results in intermediate **2.49a**, which is reduced by Bu_3SnH to produce **2.47a**. According to this model, *P*-iodoanilides are expected to give *R*-indolines, and *M*-iodoanilides give *S*-indolines.

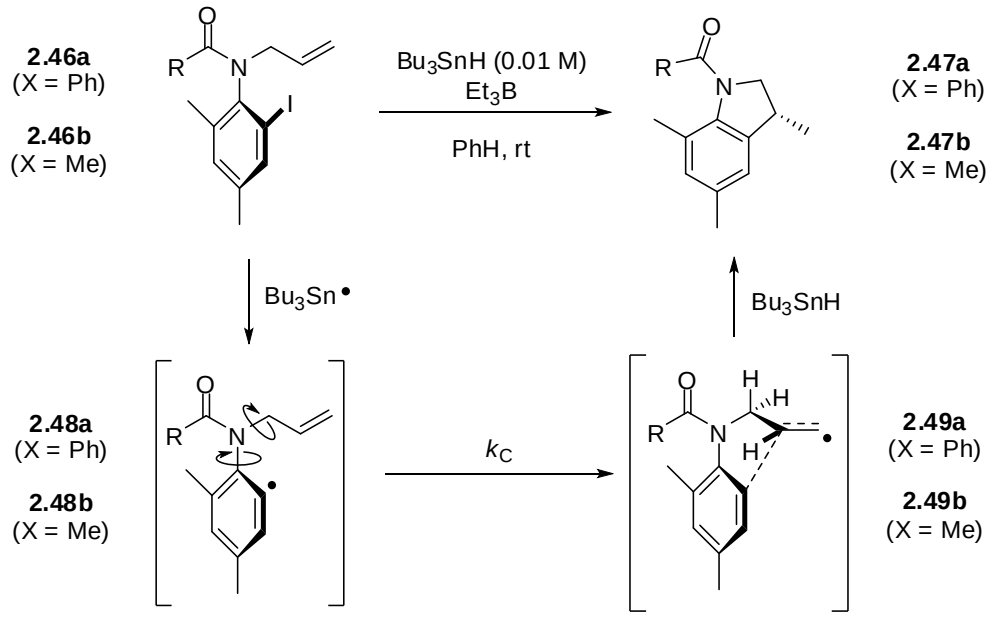

Scheme 2.9 Chirality Transfer in Cyclizations onto *N*-Allyl Groups

Chirality transfer in this class of cyclization is dependent upon both cyclization outpacing competitive *N*-aryl rotation, and facial selectivity in reaction with the olefin. The rate constant of cyclization k_C of radical **2.48b**, produced by halogen abstraction from racemic **2.46b**, was measured as $k_C = 3.0 \times 10^9\ s^{-1}$. Given that chirality transfer values for this class of reactions were moderate to high (74-95%),[105] cyclization must be significantly faster than rotation about the *N*-aryl bond, and facial selectivity must be high.

3.0 CHIRALITY TRANSFER IN RADICAL AND ANIONIC CYCLIZATIONS OF AXIALLY CHIRAL CARBAMATES

3.1 INTRODUCTION

3.1.1 Axially Chiral Carbamates

Axially chiral amides are among the most widely studied types of *N*-aryl atropisomeric compounds, particularly *o*-iodoanilides which undergo cyclizations with chirality transfer.[105,108,127,128,132,133] While axially chiral *o*-iodoanilides are useful substrates for forming indolines, a common subunit of alkaloids, the residual amide moiety in the product can be difficult to remove. Therefore, a more synthetically useful alternative to amides would be highly valuable. Among the reported yet little-studied classes of compounds possessing an *N*-aryl axis of chirality (Figure 3.1) are thiazolin-2-thiones,[138] thiazolin-2-ones,[138] iminothiazolines,[134] thioureas,[164] ureas,[102,103] thioamides,[110] and carbamates.[91]

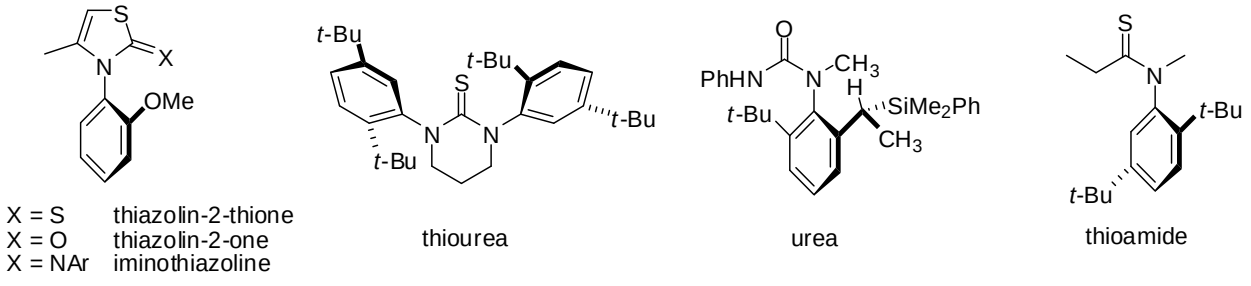

Figure 3.1 Some Axially Chiral Compounds with a C–N Axis

Surprisingly, axially chiral carbamates have received little attention, despite the vast synthetic utility of carbamates as easily removable protecting groups.[165] Like amides, carbamates (Figure 3.2) contain an sp^2-hybridized nitrogen atom whose lone pair is delocalized into the adjacent carbonyl, resulting in planarity of the functional group. Also like amides, carbamates are resistant to hydrolysis and nucleophilic attack. But unlike amides, carbamates undergo facile C−N bond cleavage under conditions dictated by the oxygen substituent R^3. In two examples of particular relevance to peptide chemistry, the *t*-butoxycarbonyl (Boc) group suffers deprotection under anhydrous acidic conditions, and the carbonylbenzyloxy (Cbz) group is susceptible to hydrogenolysis.[165]

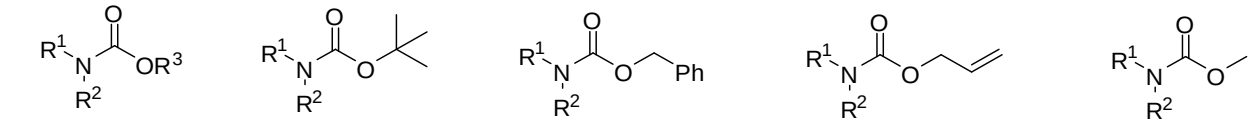

Figure 3.2 Representative Carbamate Structures

The radical cyclizations of *o*-iodoarylcarbamates have been used in syntheses of analogs of antitumor agents duocarmycin,[166-174] CC-1065,[167-169,171,174-176] and yatakemycin.[172] An example of this cyclization is shown in Scheme 3.1; aryl iodide **3.1** was treated with Bu_3SnH, cyclizing to give racemic indoline *rac*-**3.2** in 87% yield.[172] The product was then resolved by chiral HPLC to give enantiomerically pure (*S*)-**3.2**, which is carried forward in the synthesis. Because **3.1** only contains a single *o*-iodine substituent, its *N*-aryl barrier to rotation is estimated to be $\Delta G^{\ddagger}_{rot}$ = 19.2 kcal/mol,[91] making resolution of the enantiomers impossible under ambient laboratory conditions ($t_{1/2}$ for racemization = 15 s).

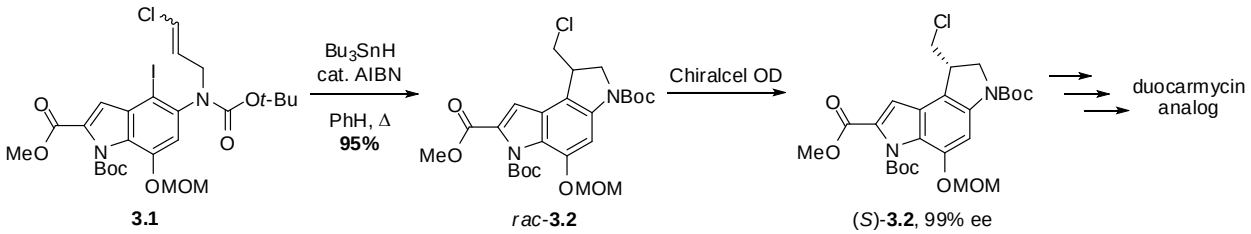

3.1 *rac*-**3.2** (*S*)-**3.2**, 99% ee

Scheme 3.1 Racemic Radical Cyclization of an *o*-Iodoarylcarbamate

The *N*-aryl barriers to rotation of *N*-aryl-*N*-benzyl carbamates containing various *ortho*-substituents have previously been measured by Annunziata and co-workers (Figure 3.3).[177] Predictably, increasing the steric bulk of the *o*-substituent leads to a gradual rise in barrier to rotation, as exemplified by substrates **3.3**-**3.5**. However, increasing the sterics of the *O*-substituent in the carbamate group does not noticeably affect the barrier, as seen by comparing *o*-Cl substrates **3.6**-**3.8**. None of the *o*-monosubstituted *N*-arylcarbamates studied possessed a barrier high enough to allow for resolution.

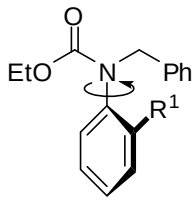

3.3 R^1 = Me 15.2 kcal/mol

3.4 R^1 = Et 18.9 kcal/mol

3.5 R^1 = *i*-Pr 21.4 kcal/mol

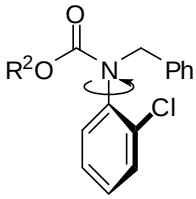

3.6 R^2 = Me 16.6 kcal/mol

3.7 R^2 = Et 16.6 kcal/mol

3.8 R^2 = *t*-Bu 16.6 kcal/mol

Figure 3.3 *N*-Aryl Barriers to Rotation of *o*-Monosubstituted Carbamates

N-Aryl carbamates containing two *ortho* substituents have a much higher *N*-aryl barrier to rotation, and therefore display atropisomeric behavior. Tanaka's group has recently reported the enantioselective synthesis of an axially chiral carbamate **3.11**, using an asymmetric Rh-catalyzed [2+2+2] cycloaddition of ynamide **3.9** and diyne **3.10** (Scheme 3.2).[136] Carbamate (*P*)-

3.11 was isolated in 69% yield and 98% ee, with a *syn*/*anti* rotamer ratio of 86/14. Hsung expanded upon this reaction by reacting aryl-substituted ynamide **3.12** and diyne **3.13** to produce diastereomeric biphenyls (*M*,*P*)-**3.14** and (*P*,*P*)-**3.14** in a 6:1 dr, containing both a C−C and a C−N axis of chirality.[131] These oxazolidinones, which are cyclic carbamates, are also configurationally stable. When (*M*,*P*)-**3.14** was heated to 85 °C in toluene-*d8* for 24 h, no *N*-aryl bond rotation was observed, implying a high barrier to rotation. When analogs of **3.14** containing only one *ortho* group were synthesized, C−N rotation was observed on the NMR timescale.[131]

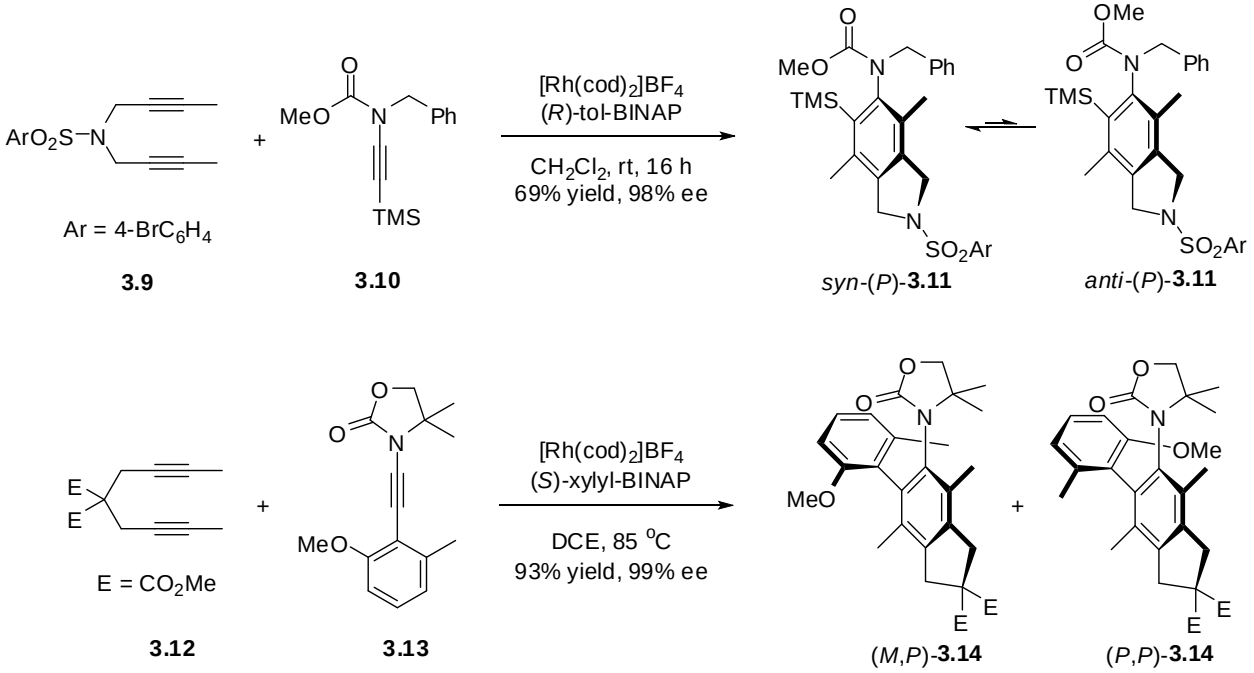

Scheme 3.2 Asymmetric Syntheses of Axially Chiral Carbamates

3.1.2 Intramolecular Conjugate Addition of Aryllithiums

Lithium-halogen (Li-X) exchange is an indispensable tool for creating a nucleophilic organolithium within a molecule, which can then undergo intramolecular conjugate addition. In

particular, conjugate additions of aryllithiums generated by Li-X exchange typically proceed without significant side reactions.[178,179] At low temperatures, Li-X exchange between alkyllithium reagents and aryl halides proceeds much more quickly than competing deprotonation or intermolecular addition processes.[180] The cyclizations themselves also tend to be very rapid for most medium-sized ring formations,[178] an effect of conformational control by the sp^2 carbons in the aromatic ring.[180] An example of efficient intramolecular aryllithium addition was recently developed by Piers (Scheme 3.3).[181] Lithium-iodine exchange with aryl iodide **3.15** was triggered at –78 °C by *t*-BuLi in the presence of TMSCl and HMPA in THF. Subsequent conjugate addition onto the enone produced racemic **3.16** in 80% yield. No complications from the potential aforementioned side reactions were observed.

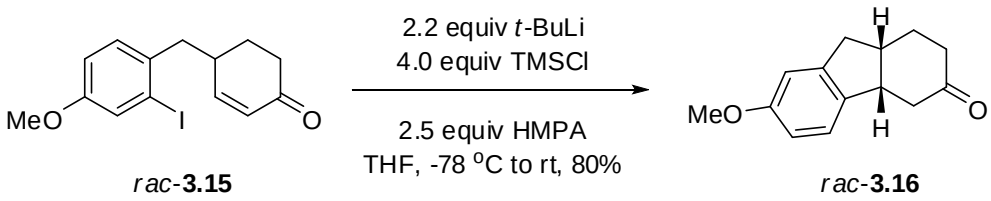

rac-**3.15** *rac*-**3.16**

Scheme 3.3 Intramolecular Conjugate Addition of an Aryllithium

Rodrigo and coworkers reported that fumaric ester amide **3.17** easily underwent anionic cyclization after lithium-halogen exchange, to give dihydroindol-2-one **3.18** in 85% yield (Scheme 3.4).[182] The optimal conditions involved addition of BuLi in a 4:1:1 THF : Et_2O : hexane solvent mixture, more commonly known as the Trapp solvent mixture,[183] at –100 °C. The presence of TMSCl was required to avoid polymerization of the cyclized enolate ester intermediate. Despite the excess of TMSCl present in the reaction, no *o*-silylation was observed, leading to the conclusion that the lifetime of the aryllithium intermediate is short indeed. A crystal structure of **3.17** revealed that the planes of the aromatic ring and amide groups are

perpendicular to one another, resulting in axial chirality about the *N*-aryl bond. We hypothesized that if compounds similar to **3.17** could be resolved, then the anionic cyclization would proceed with chirality transfer.

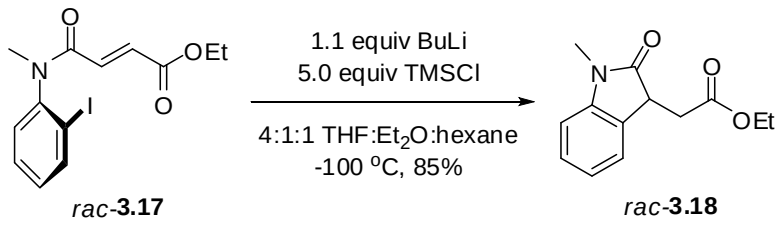

Scheme 3.4 Intramolecular Anionic Conjugate Addition of an Axially Chiral Anilide

Rodrigo's substrate **3.17** is unfit for chirality transfer experiments in anionic cyclizations for two reasons. First, the presence of only one *ortho* substituent implies the barrier to rotation of **3.17** is too low for convenient resolution (< 22 kcal/mol). Second, the pKa of the proton at the newly formed stereocenter in **3.18** is expected to be less than 18.5,[184] and its removal by BuLi during the reaction results in destruction of the product's chirality. To address these problems, we developed *N*-arylcarbamates **3.19** (Scheme 3.5) as substrates which contain a second *o*-substituent to facilitate resolution, and produce a non-epimerizable stereocenter upon cyclization to **3.20**. Our studies focused especially on the role of carbamate identity (R^1) and additional aromatic substituents (R^2, R^3) on reactivity, barriers to rotation, and chirality transfer.

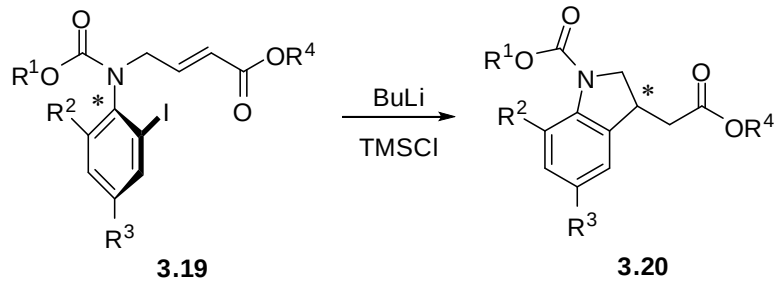

Scheme 3.5 Proposed Anionic Cyclization of Axially Chiral Carbamates

3.2 RESULTS AND DISCUSSION

3.2.1 Synthesis of Starting Materials

The preparation of carbamates **3.19** began with the synthesis of various *o*-iodoanilines with different substitution patterns (Scheme 3.6). Compound **3.21** was made in 68% yield by treating 2,4-dimethylaniline with $BnNEt_3 \bullet ICl_2$ and solid base in the presence of MeOH.[185] Similarly, *o*-bromo analog **3.22**[132] was prepared in 91% yield from 2-bromo-4-methylaniline and iodinating reagent $BnNMe_3 \bullet ICl_2$. The iodinations of 4-bromo-2-methylaniline and 2,4-dibromoaniline were effected with I_2 and Ag_2SO_4 in EtOH to furnish **3.23**[128] (65%) and **3.24**[186] (33%), respectively. The preparation of *o*-silylated **3.27** was accomplished by a three-step sequence. *bis*-Iodination of *p*-toluidine with ICl provided **3.25**[132] in 77% yield, followed by *bis*-TMS protection by two treatments with LDA and TMSCl to give **3.26**[132] in 87% yield. A lithium-halogen exchange with *s*-BuLi, followed by a C to N silyl migration[187] and hydrolysis of the remaining *N*-TMS group, furnished aniline **3.27** in 82% yield.

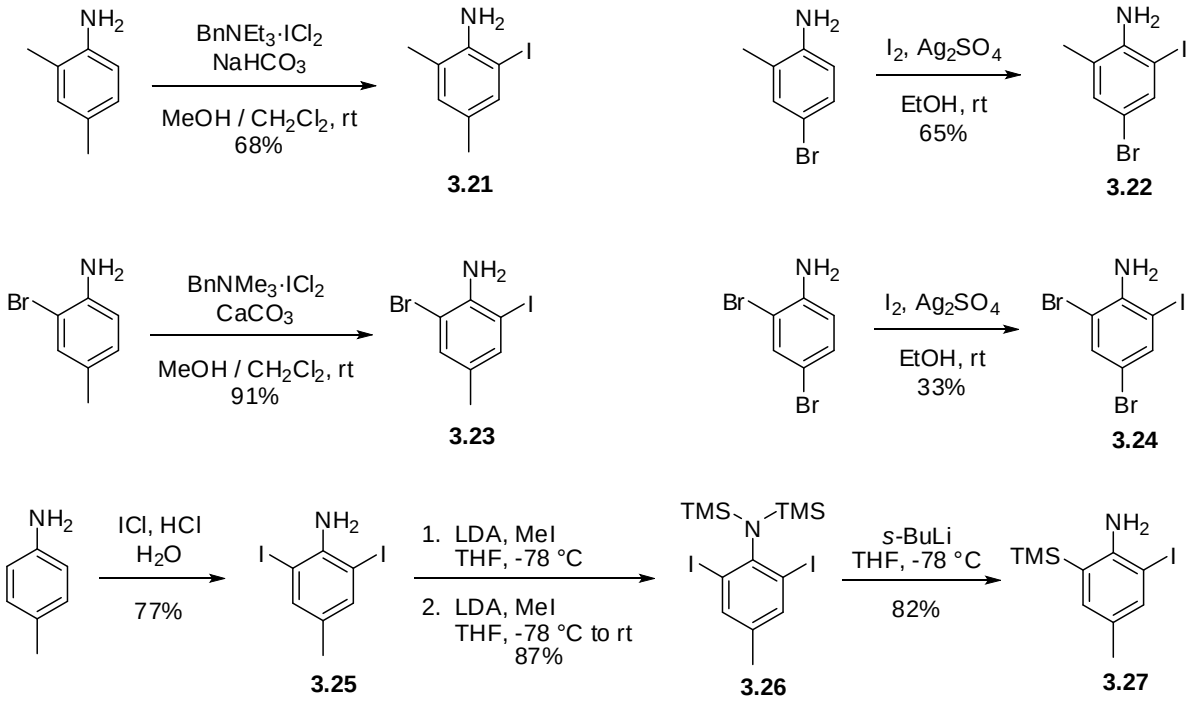

Scheme 3.6 Preparation of *o*-Iodoanilines

Next, various carbamate groups were installed on the nitrogen atoms of the *o*-iodoanilines (Scheme 3.7). Boc groups were easily installed by deprotonation of the appropriate aniline with NaHMDS at low temperatures, followed by treatment with di-*t*-butyldicarbonate, producing **3.28-3.33** in 62-94% yields. Alloc and methoxycarbonyl (Meoc) groups were installed on **3.21** by treatment with the appropriate chloroformate reagent in pyridine, to give **3.34** (93% yield) and **3.35** (92% yield), respectively. Treatment of **3.21** with benzyloxychloroformate under biphasic Schotten-Baumann conditions provided Cbz-protected **3.36** in 93% yield.

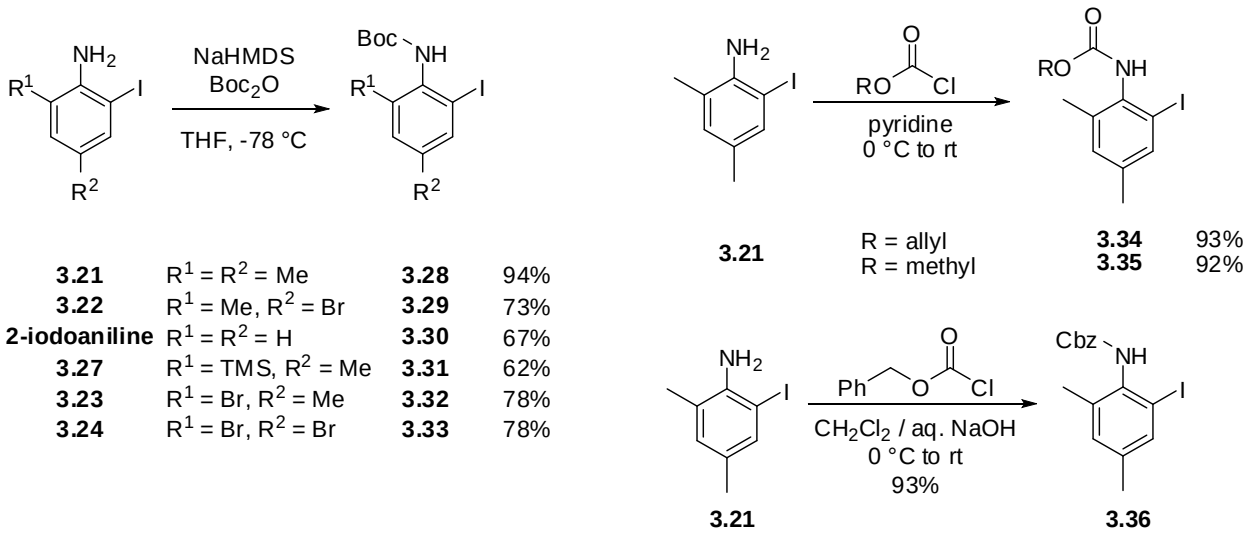

Scheme 3.7 Formation of Carbamates from *o*-Iodoanilines

Finally, the preparation of substrates **3.19a-i** was completed by installing the olefinic acceptor via *N*-alkylation (Table 3.1). We initially attempted deprotonation of carbamate **3.36** with NaHMDS followed by alkylation with methyl 4-bromocrotonate (Entry 1), but this led to incomplete reaction, low yield of **3.19c** (47%) and difficult purification. Changing the base to K_2CO_3 led to complete consumption of carbamates **3.28** and **3.36** (Entries 2-3), though multiple additions of base and alkylating agent were required, and numerous side products led to low isolated yields of **3.19a** (52%) and **3.19b** (67%). Use of Cs_2CO_3 as a base for **3.28** (Entry 4) accelerated the reaction, but side products were still a problem, increasing the yield of **3.19a** by only a small amount (68%). Alkylation of **3.28** with methyl 4-iodocrotonate eliminated the formation of side products, accelerated the reaction, and increased the yield of **3.19a** to 72% (Entry 5). Compounds **3.29**-**3.36** were alkylated with these conditions, furnishing **3.19b-i** in a range of 63 – 99% yields (Entries 6-13). Allyl ester **3.19j** was also prepared by hydrolysis of methyl ester **3.19a**, followed by DCC-mediated coupling of crude acid **3.37** with allyl alcohol (Scheme 3.8). Carbamate **3.19j** was isolated in 62% yield over two steps.

Table 3.1 Alkylation of *N*-Carbamate Protected Anilines

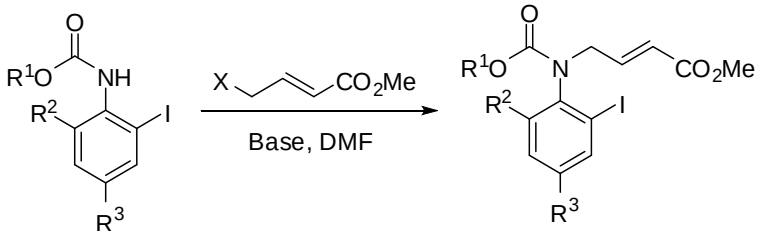

entry	substrate	R^1	R^2	R^3	X	base	product	% yield[a]
1	**3.36**	Bn	Me	Me	Br	NaHMDS[b]	**3.19c**	47
2	**3.28**	*t*-Bu	Me	Me	Br	K_2CO_3	**3.19a**	52
3	**3.36**	Bn	Me	Me	Br	K_2CO_3	**3.19c**	67
4	**3.28**	*t*-Bu	Me	Me	Br	Cs_2CO_3	**3.19a**	68
5	**3.28**	*t*-Bu	Me	Me	I	Cs_2CO_3	**3.19a**	72
6	**3.34**	Allyl	Me	Me	I	Cs_2CO_3	**3.19b**	99
7	**3.36**	Bn	Me	Me	I	Cs_2CO_3	**3.19c**	94
8	**3.29**	*t*-Bu	Me	Br	I	Cs_2CO_3	**3.19d**	63
9	**3.30**	*t*-Bu	H	H	I	Cs_2CO_3	**3.19e**	91
10	**3.35**	Me	Me	Me	I	Cs_2CO_3	**3.19f**	77
11	**3.31**	*t*-Bu	TMS	Me	I	Cs_2CO_3	**3.19g**	57
12	**3.32**	*t*-Bu	Br	Me	I	Cs_2CO_3	**3.19h**	65
13	**3.33**	*t*-Bu	Br	Br	I	Cs_2CO_3	**3.19i**	86

[a] Isolated by column chromatography. [b] THF was used as solvent.

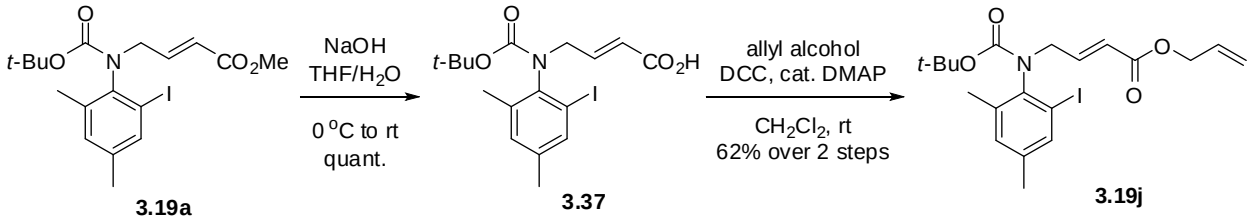

Scheme 3.8 Synthesis of Allyl Ester Substrate 3.19j

In contrast to *N*-allyl *o*-iodoanilides, which exist largely or exclusively as *E*-amide rotamers in solution,[105,155] carbamates **3.19a-j** exist as two rotamers in $CDCl_3$ as determined by ^{1}H NMR spectroscopy. Whereas *Z*/*E* nomenclature is typically used to describe amide rotamers, *syn*/*anti* designations are used for carbamates.[188] The rotamer ratios in **3.19a-j** range from 2:1 to 5:1, depending on the identity of the carbamate group R^1 as well as the ortho substituent R^2 (see

Chapter 6.3). Tertiary *N*-aryl carbamates containing at least one *o*-aryl substituent display a moderate preference for the *syn* rotamer (Figure 3.4),[136] so we determined that the major rotamer of substrates **3.19a-j** in solution was *syn*. For simplicity, only the *syn* isomer of substrates **3.19a-j** are depicted in future schemes. Both rotamers of **3.19a-j** are able to undergo cyclization.

The carbonyl-*N* barrier to rotation of *N*-aryl-*N*-alkyl carbamates is typically $\Delta G^{\ddagger}_{rot}$ = 10.7-13.2 kcal/mol when no *ortho* substituent is present on the aromatic ring.[189,190] The appearance of well-defined signals for two rotamers in the ^{1}H NMR spectra of **3.19a-j** suggest a minimum value of $\Delta G^{\ddagger}_{rot}$ > 16 kcal/mol, which is comparable to *N*,*N*-dialkylcarbamates[189,191,192] and *o*-monosubstituted *N*-alkyl-*N*-aryl carbamates.[177]

Figure 3.4 Rotamer Behavior of Axially Chiral Carbamates 3.19a-j

3.2.2 Reaction Optimization and Substrate Screening

We began the studies by optimizing the anionic cyclization conditions on racemic **3.19a-j** (Table 3.2). *t*-BuLi was slowly added to a solution of iodide **3.19a** and excess TMSCl in an HMPA/THF solvent mixture at –78 °C (Conditions "A3").[181] These conditions provided **3.20a** in 56% yield, along with numerous side products (Entry 1). The same conditions were applied to *N*-Cbz congener **3.19c**, producing **3.20c** in only 10% isolable yield (Entry 2). When BuLi/TMSCl was used in the reaction of **3.19a** in the Trapp solvent mixture[183] at –98 °C (Conditions "A"), the reaction proceeded much more cleanly and efficiently to give **3.20a** in

79% isolated yield (Entry 3). Similarly, the yield of **3.20c** was increased to 76% by cyclizing **3.19c** under these conditions (Entry 5). Application of these optimized conditions to iodides **3.19b,e,f,g,j** gave similar results, with yields ranging from 67-82% and no formation of major side products (Entries 4, 6-9). The lithium-halogen exchange therefore occurs more rapidly than the intermolecular conjugate addition of BuLi.[179] As in Rodrigo's findings,[182] no direct silylation of the intermediate aryllithium by TMSCl was observed, implying a rapid cyclization.

Table 3.2 Anionic and Radical Cyclizations of Racemic Carbamates

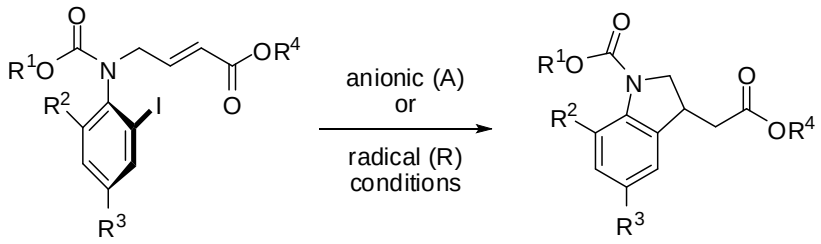

rac-**3.19a-j** *rac*-**3.20a-j**

entry	substrate	R^1	R^2	R^3	R^4	cond.[a]	prod.	% yield[b]
1	**3.19a**	*t*-Bu	Me	Me	Me	A3	**3.20a**	56
2	**3.19c**	Bn	Me	Me	Me	A3	**3.20c**	10
3	**3.19a**	*t*-Bu	Me	Me	Me	A	**3.20a**	79
4	**3.19b**	Allyl	Me	Me	Me	A	**3.20b**	82
5	**3.19c**	Bn	Me	Me	Me	A	**3.20c**	76
6	**3.19e**	*t*-Bu	H	H	Me	A	**3.20e**	67
7	**3.19f**	Me	Me	Me	Me	A	**3.20f**	79
8	**3.19g**	*t*-Bu	TMS	Me	Me	A	**3.20g**	76
9	**3.19j**	*t*-Bu	Me	Me	Allyl	A	**3.20j**	76
10	**3.19h**	*t*-Bu	Br	Me	Me	A	**3.20h**	18
11	**3.19h**	*t*-Bu	Br	Me	Me	A2	**3.20h**	59
12	**3.19d**	*t*-Bu	Me	Br	Me	A2	**3.20d**	51
13	**3.19i**	*t*-Bu	Br	Br	Me	A2	**3.20i**	42
14	**3.19a**	*t*-Bu	Me	Me	Me	R	**3.20a**	96
15	**3.19b**	Allyl	Me	Me	Me	R	**3.20b**	99
16	**3.19c**	Bn	Me	Me	Me	R	**3.20c**	96
17	**3.19d**	*t*-Bu	Me	Br	Me	R2	**3.20d**	99

[b] Conditions A: 1.2 equiv BuLi, 5.0 equiv TMSCl, Trapp solvent mix, –98 °C. A2: 1.2 equiv BuLi, 5.0 equiv TMSCl, PhMe, –91 °C. A3: 2.2 equiv *t*-BuLi, 5.0 equiv TMSCl, THF/HMPA, –78 °C. R: 1.5 equiv Bu_3SnH, Et_3B, PhH, rt. R2: 1.1 equiv Bu_3SnH, Et_3B, PhH, rt. [b] Isolated by column chromatography.

Bromide **3.19h** was reacted under the optimized conditions, but produced desired **3.20h** in only 18% yield (Entry 10). The multiple products seen in the reaction mixture, as well as the incomplete consumption of starting material, implied a competitive lithium-halogen exchange with the aryl bromide. Taking a cue from Fukuyama's previous work,[193,194] we curtailed the undesired Li-Br exchange by switching the reaction solvent to toluene at –91 °C (Conditions "A2"). These conditions led to a much cleaner reaction of **3.19h**, albeit with a modest 59% yield of **3.20h** (Entry 11). Brominated substrates **3.19d** and **3.19i** reacted cleanly under these conditions as well, producing **3.20d** in 51% yield and **3.20i** in 42% yield (Entries 12-13).

Racemic iodides **3.19a-d** were also subjected to radical cyclization reactions. In a typical experiment, Et_3B initiator was added to a stirred PhH solution of iodide **3.19a** and 1.5 equiv Bu_3SnH (10 mM) at room temperature (Conditions "R"). The iodide was consumed within 5 min, the solvent was removed, and the cyclized product **3.20a** was isolated by flash chromatography on 10% w/w KF/silica gel in 96% yield (Entry 14).[80] Iodides **3.19b-d** were reacted in the same fashion (Entries 15-17), and consistently gave nearly quantitative yields of **3.20b-d** (96-99%). Only 1.1 equiv Bu_3SnH was used in the reaction of **3.19d** to avoid over-reduction of the bromide (Conditions "R2").

3.2.3 Resolution of Substrates 3.19a-d

Substrates **3.19a-d** were resolved by dissolution in *i*-PrOH and injection onto the appropriate semipreparative HPLC column, eluting with the appropriate ratio of hexanes and *i*-PrOH (flow rate 10 mL/min). In this study, either an (*S*,*S*)-Whelk O1 (25 cm x 21.1 mm ID) or a Chiralcel OD (25 cm x 20.0 mm ID) column was used, depending on which gave the best separation. Typically, 40 mg of racemate were injected at once, and several injections were performed per

compound. After resolution, the solvent was removed from combined enantioenriched fractions, and the er was determined by analytical chiral HPLC – either on an (*S*,*S*)-Whelk O1 (250 mm x 4.6 mm ID) or Chiralcel OD (250 mm x 4.6 mm ID) column. The first eluting enantiomers of **3.19a-d** were recovered in 96-98% ee, but partial peak overlap led to poorer resolution of second eluting enantiomers (74-98% ee). The resolved compounds are quite stable to racemization at room temperature (see Chapter 3.2.4), but were generally stored in the freezer. The attempted resolutions of **3.19e-j** failed due to poor recognition by the chiral stationary phases; HPLC analysis showed either a single peak or nearly complete peak overlap of the two enantiomers.

3.2.4 Studies of *N*-Aryl Rotational Barriers

The barriers to rotation of the *N*-aryl bonds in **3.19a-c** were measured by thermally racemizing enantioenriched samples, and following the loss of enantiopurity by HPLC. In a typical procedure, a sample of the second eluting enantiomer of **3.19b** was dissolved in 9:1 hexanes:*i*-PrOH to make a ~2 mg/mL solution in a pressure tube. The tube was sealed and placed in a preheated oil bath at 115 °C with an electronic temperature controller. At various time intervals, the sealed tube was removed briefly (1-2 min) from the bath, unsealed, and a 10 μL aliquot was removed via syringe. The tube was resealed and replaced into the bath, and the aliquot was injected onto the Chiralcel OD column to measure the enantiomeric ratio (Table 3.3).

Table 3.3 Thermal Racemization Data for 3.19b

Time (min)	er
0	83.3/16.7
20	82.4/17.6
93	81.3/18.7
171	79.7/20.3
254	78.2/21.8
388	76.8/23.2
519	74.7/25.3
596	73.2/26.8

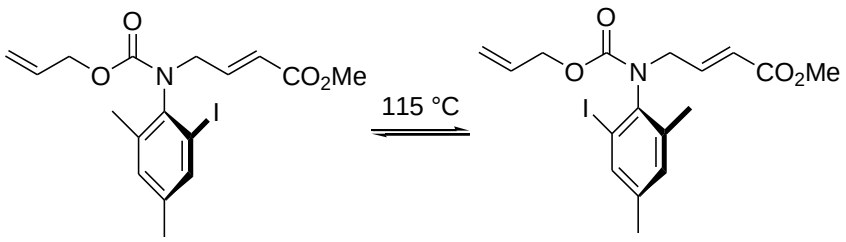

The decreasing ee of **3.19b** over time is a first-order process, and can therefore be quantified by the left-hand term in Equation 3.1.[141] Here, "F3.19b" denotes the mol % fraction of the first eluting enantiomer, and "S3.19b" denotes the fraction of the second eluting enantiomer at a given time *t*. The value of the left-hand side of the equation is plotted on the y-axis against time *t* on the x-axis as in Figure 3.5. In this plot, the slope is equal to the rate of racemization k_{rac}.

$$\ln\left[\frac{1+[\text{F3.19b}]/[\text{S3.19b}]}{1-[\text{F3.19b}]/[\text{S3.19b}]}\right] = k_{rac}t + c \qquad \text{(Equation 3.1)}$$

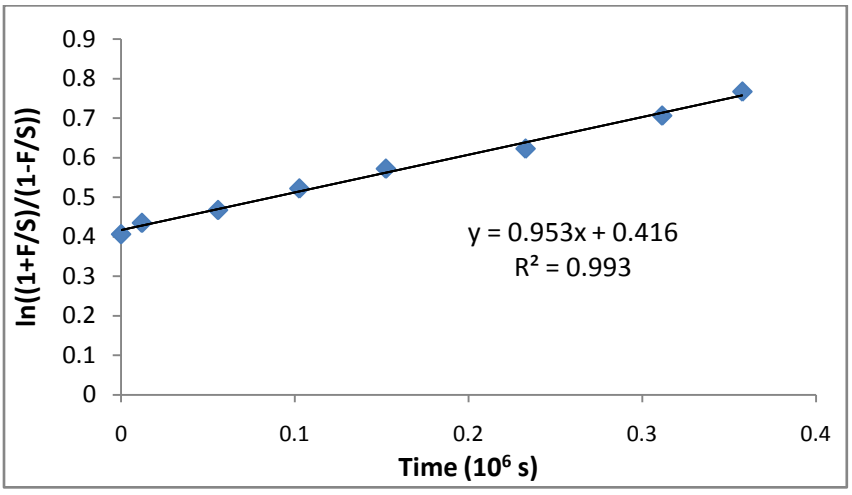

Figure 3.5 Thermal Racemization of 3.19b

From Figure 3.5, the slope is equal to the rate of racemization k_{rac} = 9.53 x 10^{-6} s^{-1}. However, the rate of racemization is equivalent to twice the rate of the rotation from one enantiomer to another.[141] Therefore, a "corrected" value of k_{rot} = 4.77 x 10^{-6} s^{-1} was used for the calculations. This value was entered into the Arrhenius equation[60] (Equation 3.2), and a $\Delta G^{\ddagger}_{rot}$ = 32.4 kcal/mol was obtained for **3.19b** at 388 K.

$$\Delta G^{\ddagger}_{rot} = -RT \ln\left(\frac{k_{rot}h}{k_B T}\right) \qquad \text{(Equation 3.2)}$$

The half-life to racemization at room temperature can be approximated by using the $\Delta G^{\ddagger}_{rot}$ value and Equation 3.2 to calculate k_{rac} at 298 K. With this value in hand, the half-life can be determined using Equation 3.3. At room temperature, **3.19b** has an approximate half-life to racemization of $t_{1/2}$ = 960 years.

$$t_{1/2} = \frac{\ln 2}{k_{rac}} \qquad \text{(Equation 3.3)}$$

N-Boc congener **3.19a** had a barrier of $\Delta G^{\ddagger}_{rot}$ = 32.2 kcal/mol at 115 °C, and *N*-Cbz compound **3.19c** was measured at $\Delta G^{\ddagger}_{rot}$ = 32.1 kcal/mol at 114 °C (Figure 3.6). These barriers are all high enough that the half-life for racemization is greater than $t_{1/2}$ = 600 years at ambient temperature. Changing the identity of the carbamate did not appreciably affect the barrier to rotation. We were pleased to see that the barriers to rotation are comparable to those of axially chiral amides **3.38a-c**. This implies that axially chiral carbamates will retain their configuration just as well as amides in reactions with chirality transfer, but will have the added feature of a removable exocyclic group after undergoing cyclization.

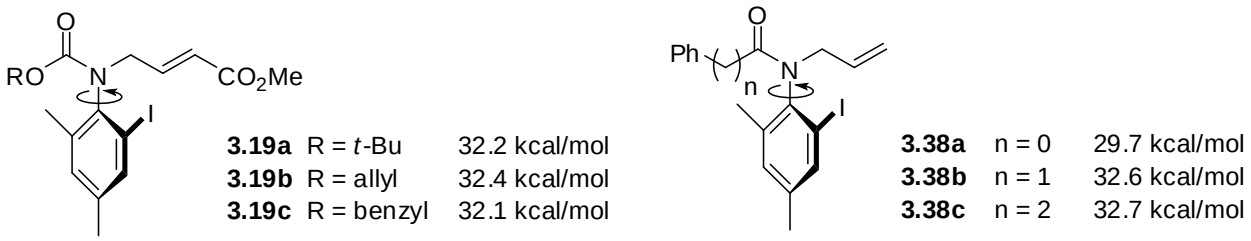

Figure 3.6 *N*-Aryl Rotational Barriers of Carbamates and Amides

3.2.5 Chirality Transfer in Cyclizations

After resolution of substrates **3.19a-d**, chirality transfer in both the optimized radical and anionic reactions was examined (Table 3.4). Radical cyclization of (+)-**3.19a** (99/1 er) under the optimized conditions produced (+)-**3.20a** in 87% yield and 86/14 er, a chirality transfer of 87% (Entry 1). Lithium-halogen exchange with (+)-**3.19a** effected anionic cyclization, producing (+)-**3.20a** in a slightly lower yield of 72%, but with 90/10 er, a higher chirality transfer of 91% (Entry 3).

Table 3.4 Chirality Transfer in Cyclizations of Axially Chiral Carbamates

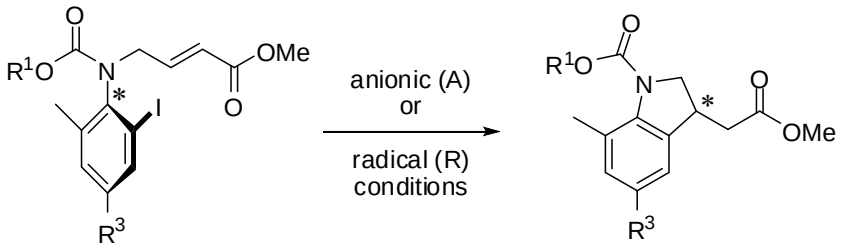

3.19a-d **3.20a-d**

entry	substrate[a]	R^1	R^3	er	cond.[b]	prod.[a]	% yield[c]	er	% ct[d]
1	(*P*)-(+)-**3.19a**	*t*-Bu	Me	99/1	R	(*S*)-(+)-**3.20a**	87	86/14	87
2	(*M*)-(–)-**3.19a**			90/10	R	(*R*)-(–)-**3.20a**	91	82/18	91
3	(*P*)-(+)-**3.19a**			99/1	A	(*S*)-(+)-**3.20a**	72	90/10	91
4	(*M*)-(–)-**3.19a**			87/13	A	(*R*)-(–)-**3.20a**	72	81/19	93
5	(*P*)-(–)-**3.19b**	Allyl	Me	99/1	R	(*S*)-(+)-**3.20b**	97	92/8	93
6	(*M*)-(+)-**3.19b**			87/13	R	(*R*)-(–)-**3.20b**	100	75/25	86
7	(*P*)-(–)-**3.19b**			99/1	A	(*S*)-(+)-**3.20b**	67	98/2	99
8	(*M*)-(+)-**3.19b**			87/13	A	(*R*)-(–)-**3.20b**	70	82/18	94
9	(*P*)-(+)-**3.19c**	Bn	Me	99/1	R	(*S*)-(+)-**3.20c**	93	91/9	92
10	(*M*)-(–)-**3.19c**			89/11	R	(*R*)-(–)-**3.20c**	97	77/23	87
11	(*P*)-(+)-**3.19c**			99/1	A	(*S*)-(+)-**3.20c**	74	97/3	98
12	(*M*)-(–)-**3.19c**			89/11	A	(*R*)-(–)-**3.20c**	71	82/18	92
13	(+)-**3.19d**	*t*-Bu	Br	98/2	R2	(+)-**3.20d**	97	81/19	83
14	(–)-**3.19d**			97/3	R2	(–)-**3.20d**	100	85/15	88
15	(+)-**3.19d**			98/2	A2	(+)-**3.20d**	63	82/18	84
16	(–)-**3.19d**			97/3	A2	(–)-**3.20d**	58	87/13	90

[a] Absolute stereochemical assignments are discussed in Section 3.2.6. [b] Conditions R: 1.5 equiv Bu_3SnH, Et_3B, PhH, rt. A: 1.2 equiv BuLi, 5.0 equiv TMSCl, Trapp solvent mix, –98 °C. R2: 1.1 equiv Bu_3SnH, Et_3B, PhH, rt. A2: 1.2 equiv BuLi, 5.0 equiv TMSCl, PhMe, –91 °C. [c] Isolated by column chromatography. [d] Chirality transfer.

The remaining radical reactions of enantioenriched **3.19a-d** (Entries 2, 5/6, 9/10, 13/14) proceeded in excellent yields (87-100%) of **3.20a-d** with chirality transfers in the range of 83-93%, which are comparable to values seen in the radical cyclizations of *o*-iodo-*N*-allylanilides.[127,133] Iodides **3.19a-c** gave lower yields of **3.20a-c** (67-74%) under anionic conditions, but proceeded with higher chirality transfers (91-99%) than radical conditions (Entries 3/4, 7/8, 11/12). This is undoubtedly partially due to the much lower temperature used for the Li-I exchange. Bromine-containing **3.19d**, which was subjected to anionic cyclization in

toluene (Entries 15/16), gave lower yields (58-63%) and chirality transfers (84-90%) only slightly better than those produced by radical reactions. The excellent chirality transfers in all cases show that both the radical and anionic ring closures are much faster than rotation of the *N*-aryl bond of the intermediate aryl radical or aryllithium. The assignment of absolute stereochemistries in the case of **3.19a-c** and **3.20a-c** is discussed in Section 3.2.6.

3.2.6 Determination of Absolute Configurations

The elution orders and signs of optical rotation of enantioenriched precursors **3.19a-d** and their products of cyclization **3.20a-d** are listed in Table 3.5. Unlike our previous work with axially chiral amides,[105,155] there was no correlation between the HPLC elution order or signs of optical rotation between substrates **3.19a-d** and their products **3.20a-d**. Matters were further complicated by the use of two HPLC columns with different chiral stationary phases, precluding correlations. Our attempts at crystallizing a precursor/product pair failed, so comparison of the absolute stereochemistry of indolines **3.20a-c** required derivatization. The first step in this process was to convert an enantioenriched cyclized product to a compound with a known absolute configuration.

Table 3.5 Chiral HPLC Analysis of Substrate/Product Pairs

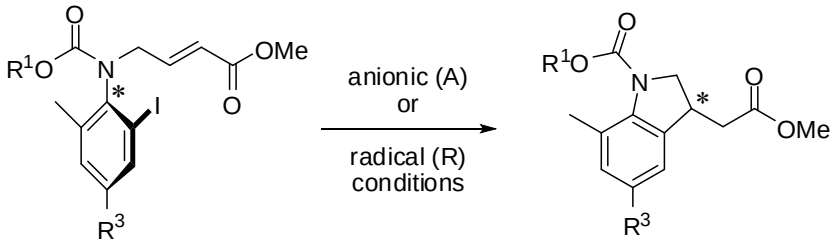

3.19a-d **3.20a-d**

iodide	R^1	R^3	column	elution	rot.	prod.	column	elution	rot.
3.19a	*t*-Bu	Me	Whelk	FEE[a]	+	**3.20a**	Whelk	FEE	+
				SEE[b]	–			SEE	–
3.19b	Allyl	Me	Chiralcel	FEE	–	**3.20b**	Whelk	FEE	+
				SEE	+			SEE	–
3.19c	Bn	Me	Chiralcel	FEE	+	**3.20c**	Chiralcel	SEE	+
				SEE	–			FEE	–
3.19d	*t*-Bu	Br	Whelk	FEE	+	**3.20d**	Whelk	FEE	+
				SEE	–			SEE	–

[a] FEE: first eluting enantiomer. [b] SEE: second eluting enantiomer.

Racemic **3.20b** was resolved using semipreparative HPLC on the (*S*,*S*)-Whelk O1 column (97:3 hexanes:*i*-PrOH, 10 mL/min). Enantioenriched (+)-**3.20b** (99/1 er) was hydrolyzed with aqueous NaOH in THF to produce the crude acid **3.39** in 89% yield (Scheme 3.9). The acid was converted to the acid chloride, and 2-mercaptopyridine *N*-oxide was added with exclusion of light to form the crude thiohydroxamate ester. This compound was immediately subjected to Barton radical decarboxylation[195] with Bu_3SnH to afford (+)-**3.40** in 47% yield over 3 steps from (+)-**3.20b**. Deprotection of the *N*-Alloc group with $Pd(PPh_3)_4$ and $NaBH_4$ proceeded efficiently to produce (+)-**3.41** in 80% yield. Finally, acylation with benzoyl chloride produced enantioenriched (+)-**3.42** in 61% yield. The ^1H NMR spectrum and optical rotation ($[\alpha]_D^{23}$ +3.0, *c* 6.0 mg/mL, $CHCl_3$) were identical with the previously reported enantioenriched compound ($[\alpha]_D^{23}$ +3.0, *c* 6.2 mg/mL, $CHCl_3$).[105,127] Comparison to an authentic sample, synthesized by Dr. Andre Lapierre, by analytical HPLC ((*S*,*S*)-Whelk O1, 85:15 hexane:*i*-PrOH, 1 mL/min)

confirmed the stereochemistry as (*S*)-**3.42**. The stereochemistry of (+)-**3.42** was originally assigned by comparison to a closely related analog whose absolute configuration was determined by X-ray crystallography.[105,127] The stereochemistry of (+)-**3.20b** can thus be assigned as (*S*).

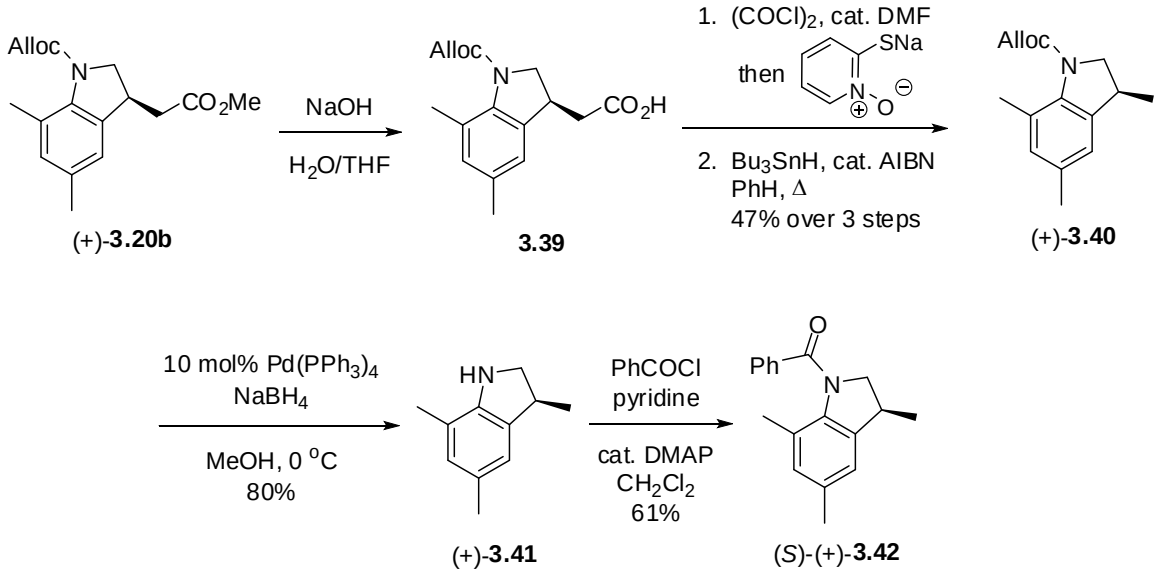

Scheme 3.9 Absolute Configuration of (+)-3.20b by Derivatization

Having determined the absolute configuration of (+)-**3.20b**, we performed *N*-deprotections to compare the configurations of (+)-**3.20a-c** (Scheme 3.10). The carbamate group was removed from each of the enantioenriched cyclized products, and the resulting compounds were compared by analytical HPLC. *N*-Boc derivative (+)-**3.20a** was treated with TFA to produce (+)-**3.43** in 75% yield. *N*-Cbz congener (+)-**3.20c** was deprotected by catalytic hydrogenation, giving (+)-**3.43** in 80% yield. *N*-Alloc derivative (+)-**3.20b** was treated with $Pd(PPh_3)_4$ and $NaBH_4$ to produce a reasonably pure sample of (+)-**3.43** which was analyzed by HPLC without further purification. Each compound (+)-**3.20a-c** gave the same enantiomer (+)-**3.43** as determined by chiral HPLC. Because (+)-**3.20b** was determined to be the (*S*)

enantiomer, all three indolines (+)-**3.20a-c** must be (*S*) as well. The experiments shown in Scheme 3.10 also demonstrate the ease of carbamate deprotection from cyclized indolines.

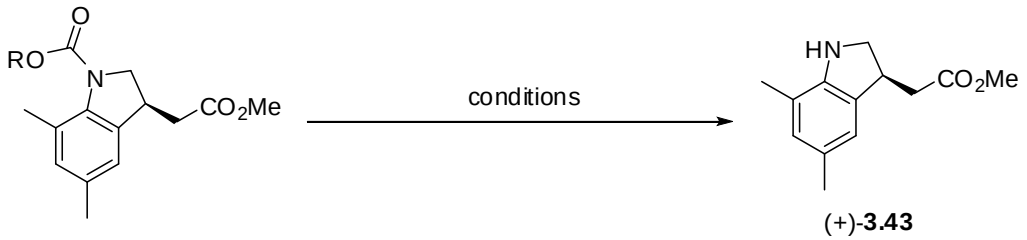

(+)-**3.20a** (R = *t*-Bu)	TFA, DCM	75%
(+)-**3.20b** (R = allyl)	10 mol% $Pd(PPh_3)_4$, $NaBH_4$, MeOH	nd
(+)-**3.20c** (R = benzyl)	H_2, Pd/C, EtOH	80%

(+)-**3.43**

Scheme 3.10 Comparison of Product Configurations by Deprotection

In all cyclizations, a given enantiomer of **3.19a-d** resulted in the same enantiomer of **3.20a-d** whether radical or anionic conditions were used, implying similar transition states. By analogy to cyclizations of *N*-allyl-*o*-iodoanilines (see Chapter 2.2.2),[105,155] we propose a likely model of chirality transfer for this system (Scheme 3.11). When the aryl radical or aryllithium is formed from (*M*)-**3.19**, *N*-aryl bond rotation towards the alkene allows it to attack one of two diastereotopic faces of the olefin acceptor. Based on the previously accepted model for anilides,[105] the alkene preferentially rotates away from the incoming radical (**3.44a**) rather than towards it (**3.44b**), ultimately resulting in (*R*)-**3.20**. Our results shown in Table 3 imply that the anionic and radical reactions likely proceed through similar transition states, though the anionic transition state is simplified by omitting the lithium ion.

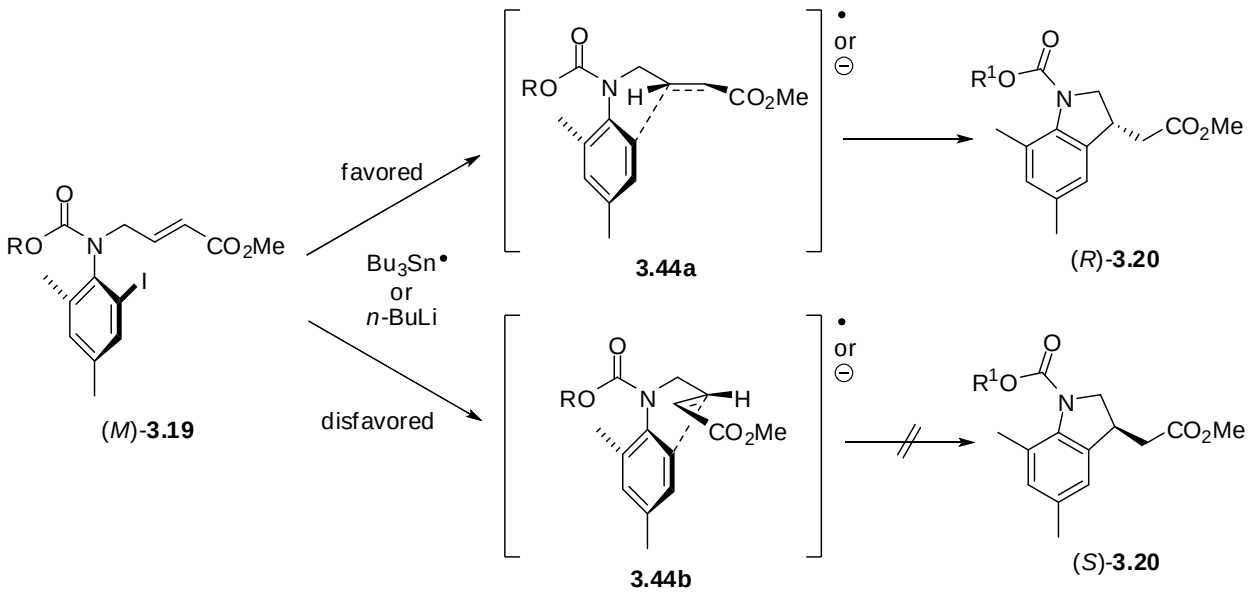

Scheme 3.11 Transition State Model for Chirality Transfer

Working backwards using the model of chirality transfer shown in Scheme 3.11, we identified the configuration of precursors to (*S*)-(+)-**3.20a-c** as (*P*)-**3.19a-c**. Consequently, the (*M*)-atropisomer of **3.19a-c** gives (*R*)-(–)-**3.20a-c** upon cyclization. Testing on additional substrates would be required to determine if the correlation between (+) and (*S*) in cyclized carbamates is a trend that can be used for predictive purposes.

3.2.7 Conclusions

We have developed the first anionic and radical cyclizations of enantiomerically enriched axially chiral carbamates. The radical cyclizations of *o*-iodoarylcarbamates **3.19a-d** proceed in 87-100% yield and 83-92% chirality transfer, while anionic reaction conditions on **3.19a-d** proceed in 58-74% yield and 84-99% chirality transfer. Chemoselective conditions for the Li-I exchange have been developed for bromine-containing compounds. The *N*-aryl barriers to rotation were

measured and found to be comparable to similar *o*-iodoacetanilides (~ 32 kcal/mol). Finally, the absolute configurations of three products were determined by derivatization and comparison to a compound of known stereochemistry.

4.0 RADICAL AND HECK CYCLIZATIONS OF DIASTEREOMERIC *O*-HALOANILIDE ATROPISOMERS

4.1 INTRODUCTION

4.1.1 Radical Cyclizations of Axially Diastereomeric *o*-Iodoanilides

Most stereoselective radical cyclizations rely on existing stereocenters in the chain between the radical and the olefin acceptor ("intraannular" stereocenters). By comparison, few reactions use a remote, or "extraannular," stereocenter to influence the stereochemical outcome.[4,196] The presence of such a stereocenter creates an energy difference between two or more transition states of the intermediate radical. Alternatively, extraannular stereocenters may fix the radical precursor in a specific conformation, leading to the generation of a radical intermediate which cyclizes before adopting a different conformation.

Recent work in the Curran group has focused on the latter strategy in cyclizations of *o*-iodoanilides (Scheme 4.1),[133] based on Jones' work.[197] An equilibrium mixture of 68/32 (*M*,*S*)/(*P*,*S*)-**4.1** was resolved by preparative HPLC to obtain (*M*,*S*)-**4.1** enriched to a 99/1 dr, and (*P*,*S*)-**4.1** in a 97/3 dr. Iodide (*M*,*S*)-**4.1** was then subjected to room temperature radical cyclization to obtain **4.2** as a mixture of diastereomers in 73% yield. The excellent diastereoselectivity of 94/6 (*R*,*S*)-**4.2**/(*S*,*S*)-**4.2** shows that the radical initially formed from (*M*,*S*)-

4.1 cyclizes faster than it interconverts. Similarly, (*P*,*S*)-**4.1** selectively produces (*S*,*S*)-**4.2** in 79% yield and 91/9 dr. In these reactions, the function of the extraannular stereocenter is not to create a significant energy difference between two configurationally labile intermediate radicals. Instead, it allows for the separation of two atropisomeric precursors, leading to the preferential generation of only one diastereomeric radical which cyclizes with good chirality transfer.

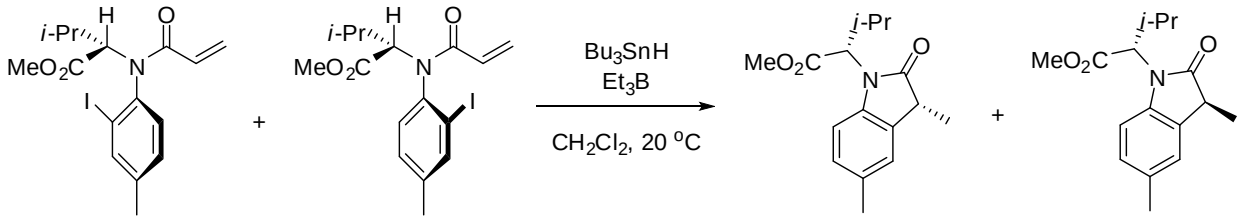

(*M*,*S*)-**4.1** (*P*,*S*)-**4.1** (*R*,*S*)-**4.2** (*S*,*S*)-**4.2**

4.1 (*M*,*S*)/(*P*,*S*)	yield **4.2**	**4.2** (*R*,*S*)/(*S*,*S*)
99/1	73%	94/6
3/97	79%	9/91

Scheme 4.1 Diastereoselective Radical Cyclizations at Room Temperature

4.1.2 Axially Chiral Anilides with Branching Near the Radical Acceptor

The effect of stereocenters within the forming ring of axially chiral *o*-haloanilide radical cyclizations has not been studied in depth. In one of the few existing examples, β-lactam **4.3** was reacted with Bu_3SnH to produce benzocarbanepam **4.4** as a single diastereomer in 65% yield (Scheme 4.2).[198,199] The reported ^1H NMR spectrum of **4.3** does not show discrete signals for the two diastereomeric atropisomers **4.3a** and **4.3b**, which suggests rapid *N*-aryl rotation at room temperature. Abstraction of the bromine atom by tributyltin radical produces aryl radicals **4.5a** and **4.5b**, which probably interconvert; however, only **4.5b** is predisposed to cyclize. Two

transition states are available for cyclization, but **4.6a** is the favored one, in which the olefin acceptor is held away from the incoming radical. This exclusively leads to **4.4** after Bu_3SnH reduction. In this case, the preexisting stereocenter controls the selectivity.

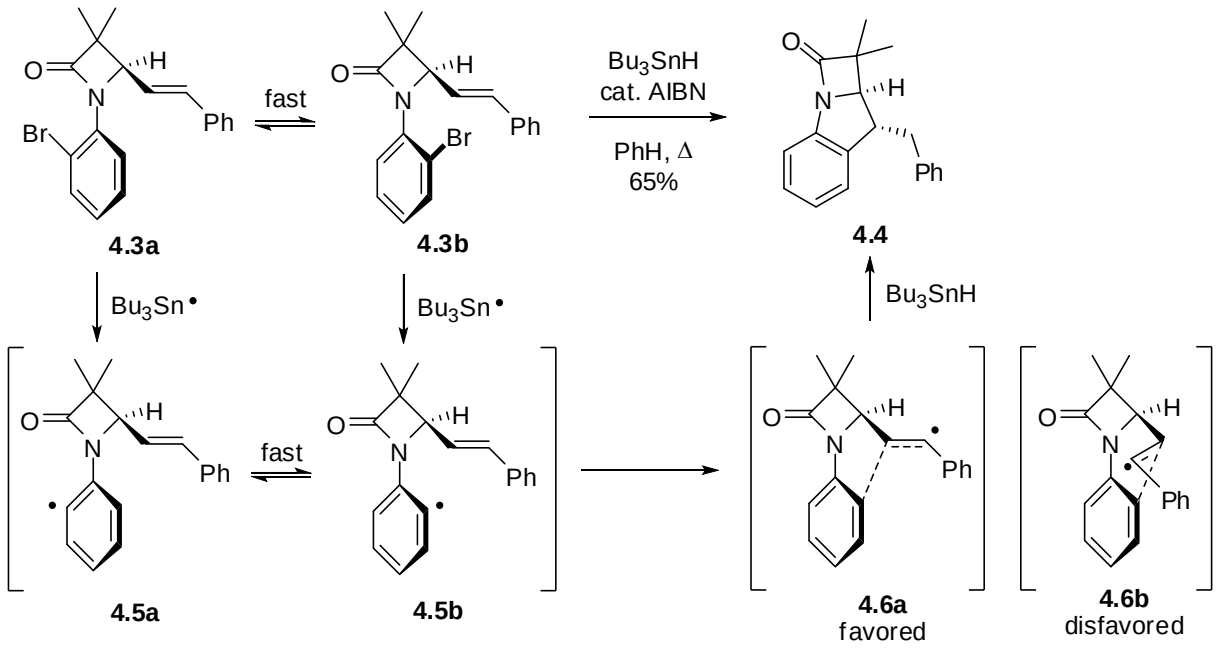

Scheme 4.2 Diastereoselectivity in Cyclizations of 2-Azetidinone 4.3

In another interesting example,[200] diazonium salt **4.7** cyclized under radical conditions to produce tricycle **4.8** in 65% yield (Scheme 4.3). SET from tetrathiafulvalene (TTF) produces the radical cation $TTF^{+\bullet}$, nitrogen gas, and aryl radical **4.9**. Cyclization onto the *N*-cyclohexenyl group gives alkyl radical **4.10**, which is trapped by $TTF^{+\bullet}$ to give sulfonium intermediate **4.11**.[201] Solvolysis by water produces alcohol **4.8** as a single diastereomer and regenerates TTF. The complete selectivity for *cis*-ring fusion suggests a favored transition state through a single axial diastereomer of radical **4.9**. Although diazonium **4.7** undoubtedly contains an element of axial chirality, the authors did not investigate this molecular feature. Because the conformation of **4.7**

and its resultant radical are unknown, they are drawn without explicit axial chirality in Scheme 4.3.

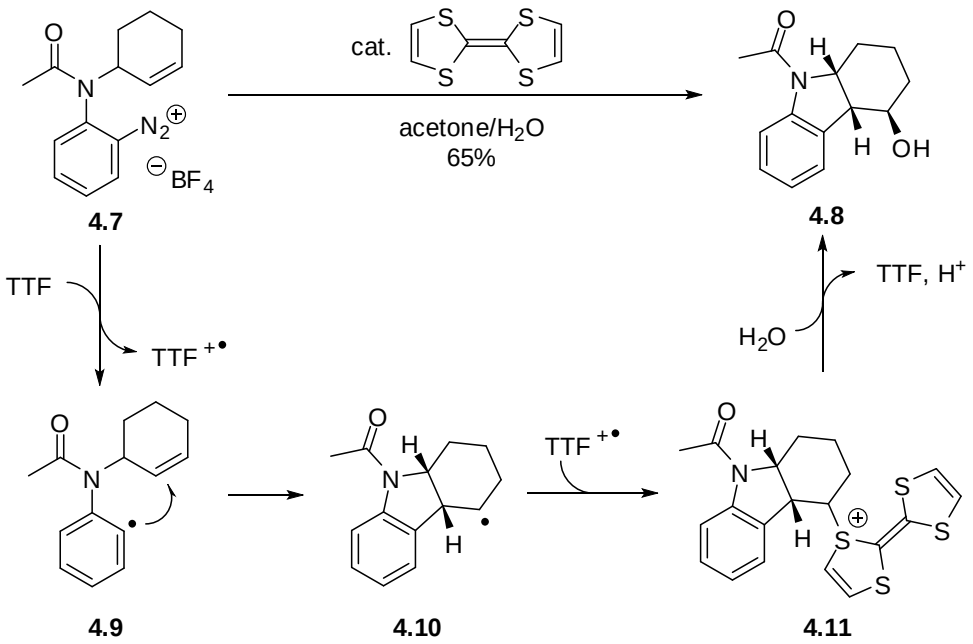

Scheme 4.3 Radical-Polar Crossover Cyclization of a Diazonium Salt

We envisioned using an *ortho* iodine atom in *N*-cyclohexenyl radical precursors similar to **4.7**. By increasing the steric bulk of the *o*-substituent, the barrier to rotation could be increased, allowing for isolation of the diastereomeric atropisomers at room temperature.[91,133] Furthermore, by adding a second *o*-substituent, the barriers to rotation of the atropisomers could be increased. Reaction of these compounds could give insight to both the cyclization transition states of radicals like **4.9**, as well as the rates of *N*-aryl bond rotation of the intermediate aryl radicals.

4.2 RESULTS AND DISCUSSION

4.2.1 Synthesis and Configuration of Diastereomeric *o*-Iodoanilides

The first series of diastereomeric anilides **4.13** was prepared as shown in Scheme 4.4. First, 2-iodoaniline was alkylated to produce *N*-cyclohexenyl aniline **4.12** in 87% yield. This compound was then acylated with acetyl chloride to produce a mixture of atropisomers **4.13**. The two diastereomers were partially separable by column chromatography; the first eluting compound, *anti*-**4.13**, was isolated in 58% yield in a 95/5 dr. The second eluting compound, *syn*-**4.13**, was collected in 22% yield in an 82/18 dr. A set of *o*-methylated substrates was made in the same fashion: alkylation of **3.21** with 3-bromocyclohexene afforded **4.14** in 61% yield. Acylation with acetyl chloride produced two stereopure diastereomers of **4.15** which were separable by flash chromatography. The first eluting diastereomer, pure *anti*-**4.15**, was collected in 45% yield, followed by pure *syn*-**4.15**, which was isolated in 40% yield.

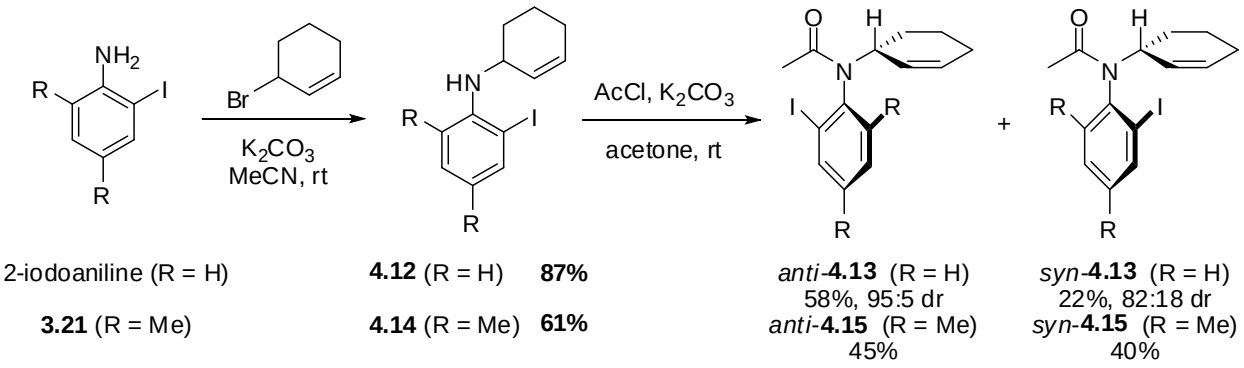

Scheme 4.4 Synthesis of Diastereomeric *o*-Iodoanilides

The relative configurations of the atropisomers of **4.15** were determined by X-ray crystallography. Single crystals of both *syn*- and *anti*-**4.15** were grown by slow evaporation from

a 3:1 hexane:CH_2Cl_2 solvent mixture, and the crystal structures were solved by Dr. Steven Geib. *Anti*-**4.15** crystallized with a pair of enantiomers in the unit cell; for clarity, only the (*P*,*R*) structure is shown in Figure 4.1. In this structure, the planes of the amide group and the aromatic ring are nearly perpendicular, with a dihedral angle of 84.1°. The *N*-cyclohexenyl bond is rotated such that the hydrogen α to the amide nitrogen is pointing toward the *o*-iodine. The dihedral angle between this C-H bond and the N-carbonyl amide bond is 46.6°. As expected, the cyclohexene ring exists in a half-chair conformation, with the amide group at the pseudoaxial position. The (*M*,*S*) structure, which is also contained in the unit cell, possesses a very similar structure, with differences in dihedral angles of less than 2° in all instances. In this structure, the iodine atom is held far from the olefin, implying that the radical derived from *anti*-**4.15** is not predisposed for cyclization.

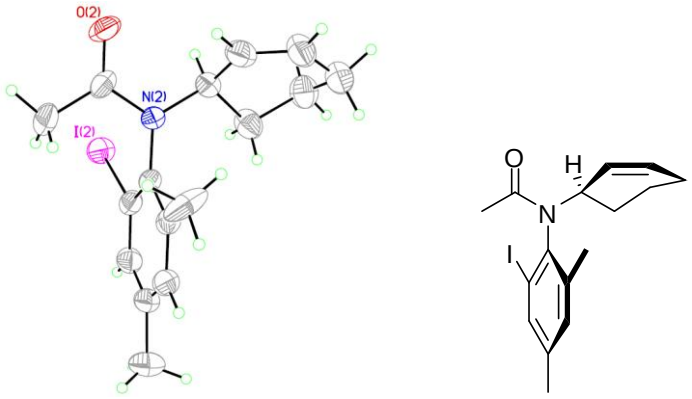

Figure 4.1 ORTEP Representation of *anti*-4.15

Slow evaporation of a solution containing racemic *syn*-**4.15** deposited several crystals, and the one chosen for analysis consisted of only the (*M*,*R*) enantiomer, containing two unique structures in the unit cell (Figure 4.2). As expected, both structures contained an *N*-aryl axis of chirality nearly perpendicular to the plane of the amide, with similar dihedral angles of 84.8° and 85.6°. However, the two structures differ in the orientation of the *N*-cyclohexenyl group. In the

left structure of Figure 4.2, the allylic hydrogen alpha to nitrogen is pointed toward the *o*-methyl group, with a dihedral C-H_α / N-carbonyl angle of 48.5°. In the other unique structure, the α-hydrogen is oriented towards the *o*-iodine, and the dihedral angle between the C-H_α bond and carbonyl-N bond is –41.5°. This molecule showed only one set of resonances in ^{1}H NMR spectra, so it is likely that these conformations rapidly interconvert in solution. Importantly, the *o*-iodine radical precursor is in proximity to the double bond, making the radical derived from *syn*-**4.15** predisposed to cyclize.

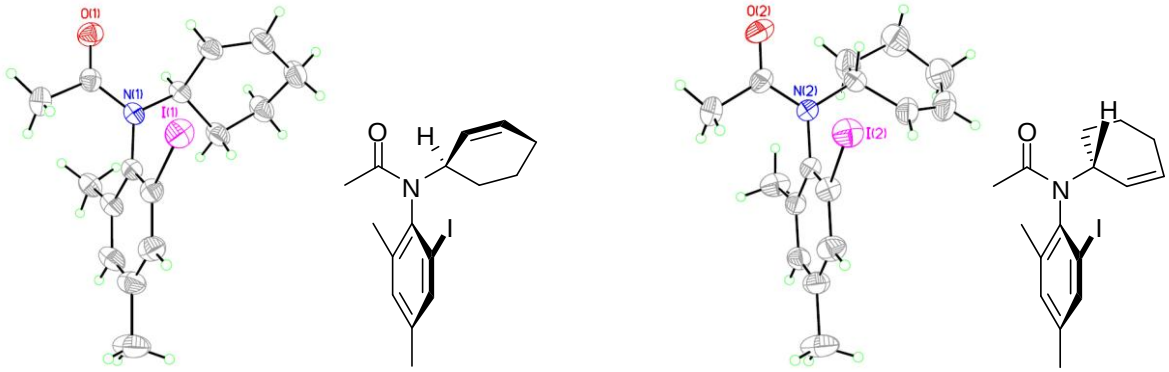

Figure 4.2 ORTEP Representations of *syn*-4.15

Chromatographic and spectroscopic behavior of *syn*- and *anti*-**4.15** allowed us to characterize atropisomeric compounds **4.13** as *anti* or *syn* by analogy. During column chromatography on silica gel, *anti*-**4.15** was less polar than *syn*-**4.15**. Furthermore, ^{1}H NMR spectroscopy showed that the olefinic and allylic (α to N) protons of *anti*-**4.15** were shifted downfield relative to those of *syn*-**4.15**. After separation of the atropisomers of **4.13**, the first eluting atropisomer indeed showed a downfield shift for the three diagnostic signals, making its assignment *syn*-**4.13**. This pattern held true for all *N*-cyclohexenyl-*o*-iodoanilides prepared for our studies.

4.2.2 Determination of *N*-Aryl Barriers To Rotation

Because *anti*-**4.13** and *syn*-**4.13** are diastereomers, interconversion by rotation of the *N*-aryl bond occurs with two different barriers to rotation if $K_{eq} \neq 1$. To determine the barriers, a sample of *syn*-**4.13** (72/28 dr) was first dissolved in a 9:1 hexanes:EtOAc solvent mixture (~2 mg/mL concentration) in a sealable tube. The cap was affixed, and the tube was placed in a pre-heated oil bath at 36 °C with digital temperature control. At various times, the cap was removed, and a 10 μL aliquot was collected and injected onto an analytical Waters NovaPak silica HPLC column (90:10 hexane:EtOAc, 1 mL/min). The ratio of diastereomers was measured over time until equilibrium was reached, and the final composition of the equilibrium mixture was confirmed by ^{1}H NMR to be 65/35 *anti*/*syn*. The first-order isomerization of *syn*-**4.13** to *anti*-**4.13** was plotted against time (Figure 4.3).

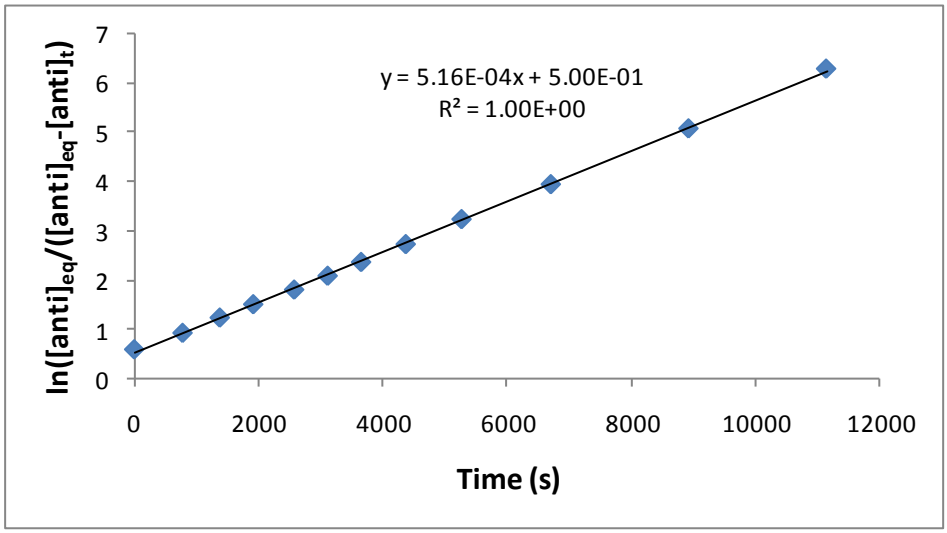

Figure 4.3 Equilibration Plot of *syn*-4.13 to *anti*-4.13 Conversion

The slope of the graph in Figure 4.3 corresponds to the rate constant of rotation from *syn*-**4.13** to *anti*-**4.13** (Figure 4.4) at 36 °C, $k_1 = 5.16 \times 10^{-4}$ s^{-1}. From the equilibrium values, the rate

constant for the reverse rotation is k_{-1} = 2.80 x 10^{-4} s^{-1}. By the Eyring equation,[60] the barriers to rotation for these two processes at 36 °C are $\Delta G^{\ddagger}_{rot}$ = 22.8 kcal/mol and $\Delta G^{\ddagger}_{rot}$ = 23.1 kcal/mol, respectively. These values are in line with the experimentally determined barrier to rotation for *N*-cyclohexyl *o*-iodoanilide **4.16** (Figure 4.4), which has $\Delta G^{\ddagger}_{rot}$ = 25.1 kcal/mol at 40 °C.[91] The barriers to rotation for **4.15** were determined in the same manner as for **4.13**, although heating to 153 °C was necessary to effect rotation on a practical timescale (data can be found in Chapter 6.6). The rotation of *syn*-**4.15** to *anti*-**4.15** has a barrier of $\Delta G^{\ddagger}_{rot}$ = 36.0 kcal/mol, and the reverse process has $\Delta G^{\ddagger}_{rot}$ = 36.6 kcal/mol.

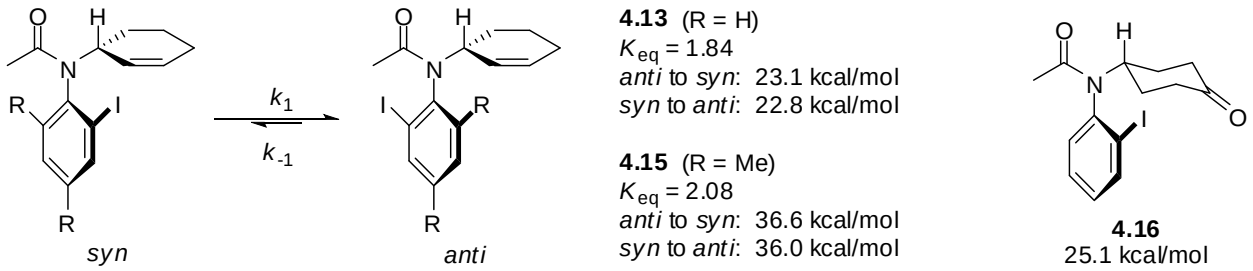

Figure 4.4 Barriers to Rotation for *N*-Cyclohexenyl Compounds

4.2.3 Radical Reactions of *N*-Cyclohexenyl Atropisomers

Having assigned the relative stereochemistry of the atropisomers of **4.15**, we subjected both compounds to radical conditions (Scheme 4.5). First, *syn*-**4.15** was reacted with Bu_3SnH (0.10 M) and Et_3B at rt, resulting in two products. Cyclized **4.18** was isolated as the major product in 92% yield. A minor product consisted of directly reduced **4.17** (4%) as an inseparable mixture of atropisomers in a 2/1 ratio – the configurations of the atropisomers were not assigned. To unambiguously confirm the identity of **4.17**, catalytic hydrogenation over Pd/C produced *N*-cyclohexylanilide **4.19**, a racemic compound with a simpler spectrum. Upon reacting *anti*-**4.15**

under radical cyclization conditions, **4.17** was obtained in 71% yield, again as a 2/1 mixture of atropisomers. Decreasing the Bu_3SnH concentration 100-fold at room temperature to $[Bu_3SnH]_i$ = 1.0 mM led to partial decomposition; crude NMR analysis showed significant formation of **4.17**, but no cyclized **4.18**. A radical reaction in refluxing benzene, initiated by AIBN, gave similar results to this room temperature experiment.

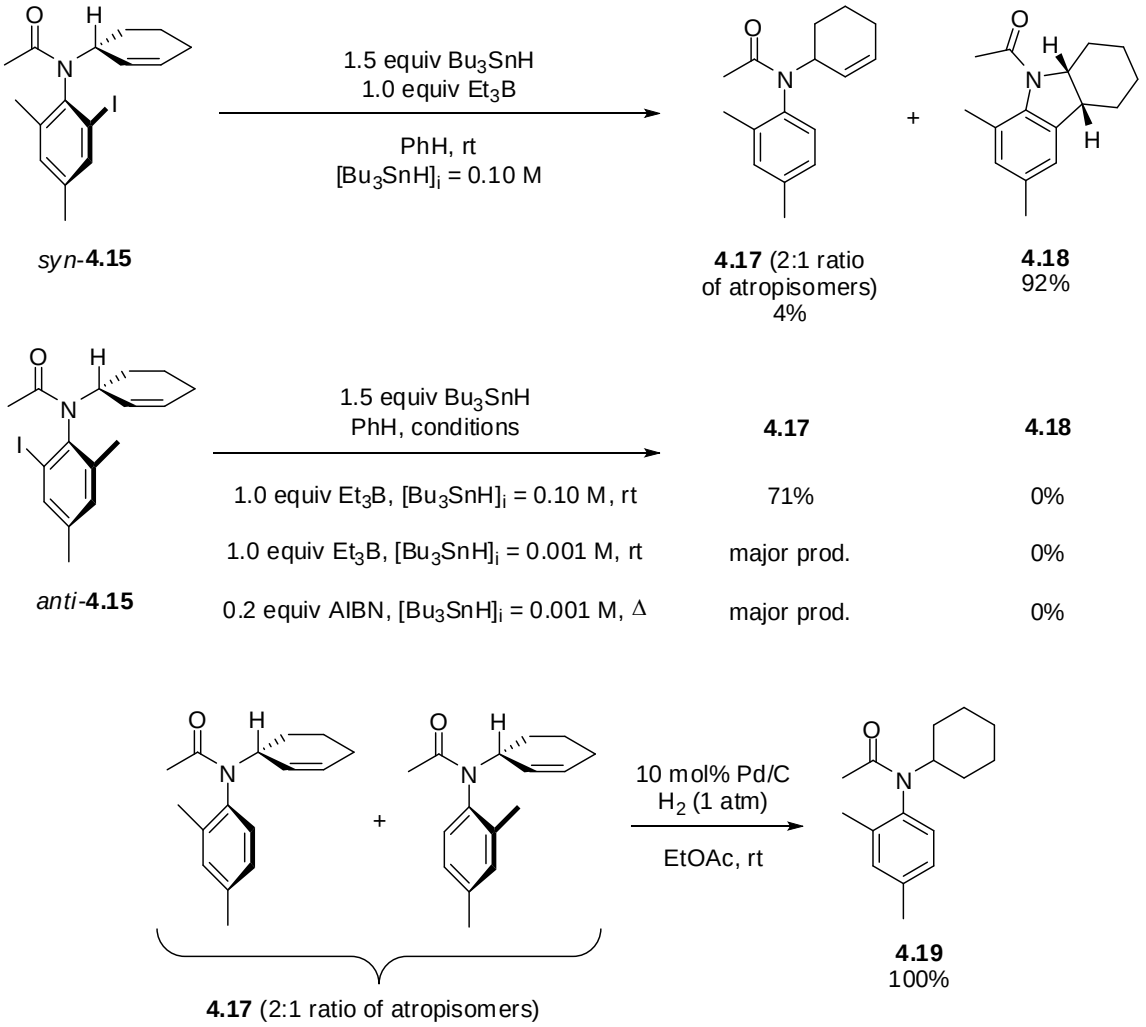

Scheme 4.5 Radical Reactions of *syn*- and *anti*-4.15

The preference for *syn*-**4.15** to cyclize can be explained by analogy to radical cyclizations of *N*-allyl-*o*-iodoacetamides,[105] discussed in Chapter 2.2.2. When radical **4.20** is formed (Scheme 4.6), the preferred conformation of the allyl group holds the olefin acceptor away from the radical center. This results in cyclization to **4.21**, which is eventually reduced by Bu_3SnH. The *N*-cyclohexenyl system likely goes through a similar transition state, except that the conformation of the olefin acceptor in radical **4.22a** is fixed. Cyclization to **4.23** can only occur from the "bottom" face of the olefin, accounting for the *cis* ring fusion in the product. The failure of *anti*-**4.13** to cyclize implies that the aryl radical **4.22b** generated by iodine abstraction cannot undergo *N*-aryl bond rotation to **4.22a** before undergoing some other process. Therefore, *N*-aryl rotation of the intermediate aryl radical must be slow relative to reduction, due to the steric hindrance of the *o*-methyl group.

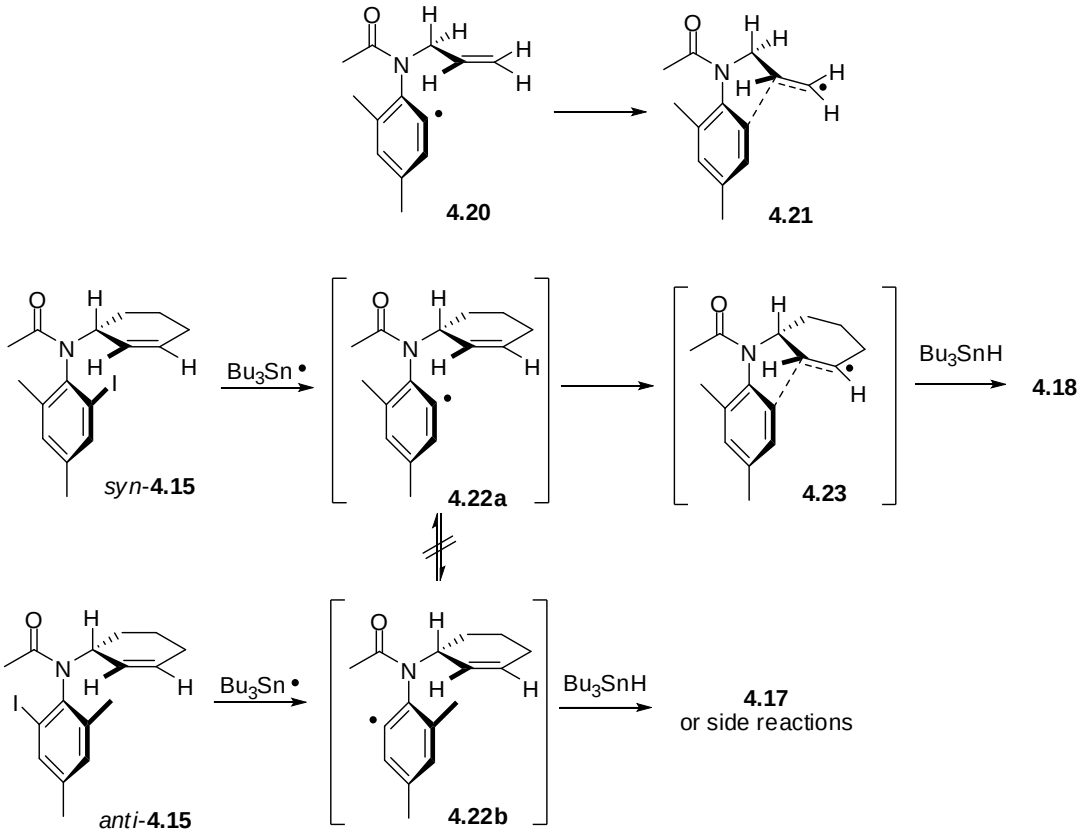

Scheme 4.6 Transition State Analysis for Cyclizations Onto *N*-Cyclohexenyl Group

The Bu_3SnH-mediated radical reactions of atropisomerically enriched **4.13** gave strikingly different results than those of **4.15**. A 12:82 *anti*:*syn* mixture of **4.13** was dissolved in a minimal amount of benzene with Bu_3SnH, and Et_3B initiator was added extremely rapidly to the stirred solution (Scheme 4.7). Despite the high initial concentration of hydride ($[Bu_3SnH]_i$ = 0.83 M), cyclization predominated, giving **4.23** in 81% yield and the product of direct reduction, **4.24**, in 6% isolated yield. When a 95:5 *syn*:*anti* mixture was reacted under the same conditions, similar results were obtained. Cyclized **4.23** was isolated in 76% yield, and directly reduced **4.24** was collected in 10% yield.

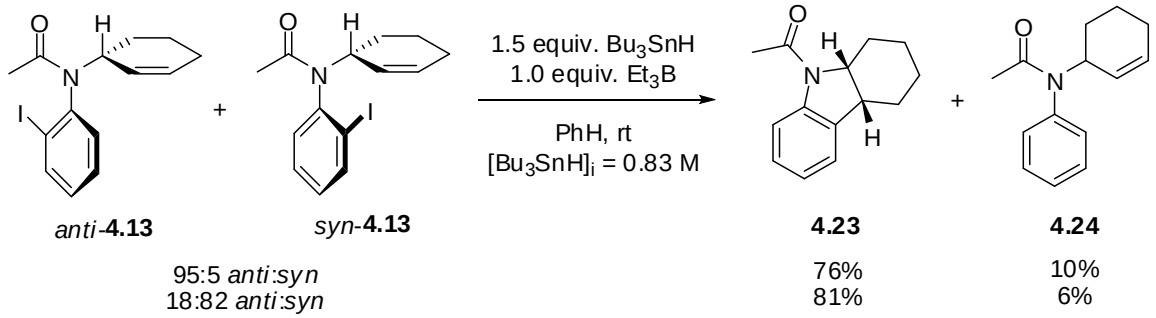

Scheme 4.7 Radical Reactions of *syn*- and *anti*-4.13

From our studies on **4.15**, we know that cyclization only occurs when the aryl radical formed is *syn* to the double bond in the cyclohexene group. Therefore, cyclization must occur via radical **4.25a**, which can be produced directly from *syn*-**4.13**, or by an *N*-aryl bond rotation of radical **4.25b** (Scheme 4.8). Because *anti*-**4.13** and *syn*-**4.13** give similar results at high $[Bu_3SnH]$, this rotation k_r must be rapid. In the reaction of 95/5 *anti*/*syn*-**4.13**, at least 75% of radical **4.25b** formed from *anti*-**4.13** must have undergone rotation to **4.25a** to account for the total yield of **4.23**. This implies that the rotation process is at least three times faster than the competing reduction by Bu_3SnH.

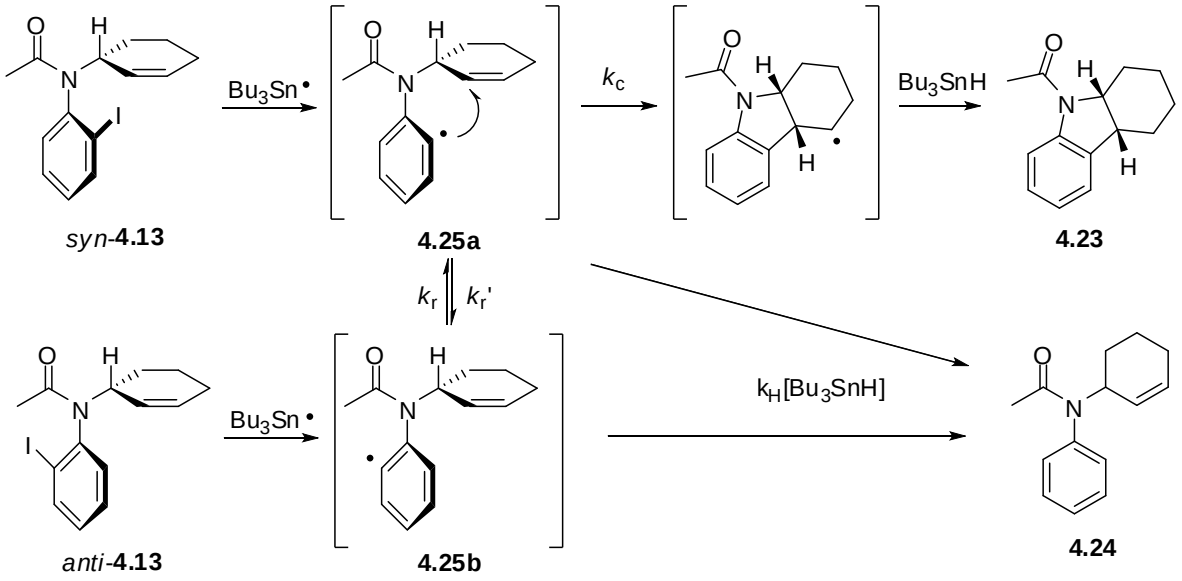

Scheme 4.8 Mechanism of Formation of 4.23 and 4.24

The rate constant k_H for reduction of the phenyl radical is 5.2 x 10^8 $M^{-1}s^{-1}$ at room temperature.[202] In the experiments shown in Scheme 2.7, the mean tributyltin hydride concentration[63] $[Bu_3SnH]_c$ = 0.55 M allows us to estimate the rate of reduction of **4.25** as 2.9 x 10^8 s^{-1} in both reactions. We can therefore identify a lower limit for the rotational rate constant of **4.25b** to **4.25a** of k_r = 8.7 x 10^8 s^{-1}.

4.2.4 Radical Reactions of Diastereomeric Atropisomers with Two Acceptors

We extended our studies on the kinetics of *N*-aryl bond rotation by developing substrates with a second radical acceptor. Work in the Jones[203] and Curran[105,127] groups has illustrated a regioselectivity effect in the cyclizations of compounds such as **4.26** and **4.27** (Scheme 4.9). When no second *ortho* substituent is present, as in **4.26**, cyclization occurs exclusively onto the acryloyl group to give **4.28**, with no trace of **4.29** in the product mixture. When an *o*-methyl group is present, however, **4.27** cyclizes preferentially onto the *N*-allyl group to give **4.31**, with

no **4.30** detected. This difference was attributed to steric hindrance between the second *o*-substituent and the *N*-allyl moiety, which slows the cyclization onto the crotonyl group.[105,127]

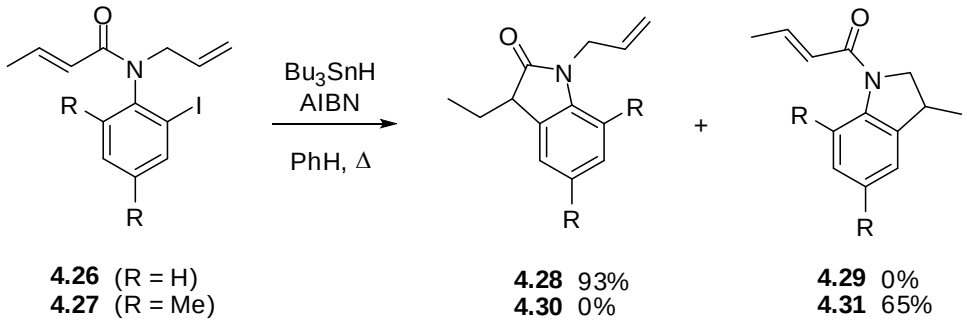

Scheme 4.9 Regioselective Cyclizations Dependent on *o*-Substituent

Substrates **4.32** and **4.33** were designed with an additional olefin acceptor at the amide carbonyl (Scheme 4.10). Acylation of **4.12** with *trans*-crotonyl chloride produced **4.32** in 49% yield as an inseparable mixture of *anti*/*syn* diastereomers in a 64/36 ratio. While both atropisomers were visible by TLC analysis, *N*-aryl bond rotation on the flash chromatography timescale made separation at room temperature impossible by this method. *o*-Methylated aniline **4.14** was also acylated with *trans*-crotonyl chloride to produce stable atropisomers of **4.33**, which were separable by column chromatography. The first eluting diastereomer, *anti*-**4.33**, was collected in 38% yield, followed by *syn*-**4.33**, which was isolated in 29% yield.

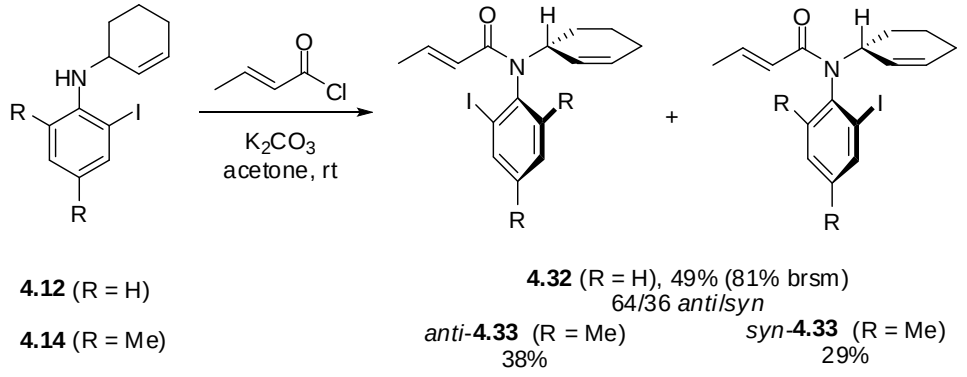

Scheme 4.10 Synthesis of Competition Substrates

These substrates were then reacted under radical conditions as shown in Scheme 4.11. Substrate *syn*-**4.33** was reacted with Bu_3SnH (0.01 M) and Et_3B at room temperature in benzene. Although the initially formed radical has two 5-*exo*-*trig* pathways available, **4.34** was obtained in 81% yield as the sole product, denoting exclusive cyclization onto the *N*-cyclohexenyl moiety. The reaction of *anti*-**4.33** under similar conditions gave decomposition to multiple inseparable products in poor mass balance. In both of these reactions, severe steric hindrance between the *o*-methyl group and branched *N*-cyclohexenyl group likely disfavors the transition state for cyclization onto the crotonyl olefin, in accordance with Curran's and Jones' work.[105,127,203]

When a 64/36 *anti*/*syn* mixture of **4.32** was treated with Bu_3SnH at room temperature, a mixture of products was obtained. The first eluting *N*-cyclohexenylindolone **4.35** was obtained in 46% yield as an inseparable 5:1 mixture of diastereomers. Tricyclic **4.36** was also collected in 53% yield.

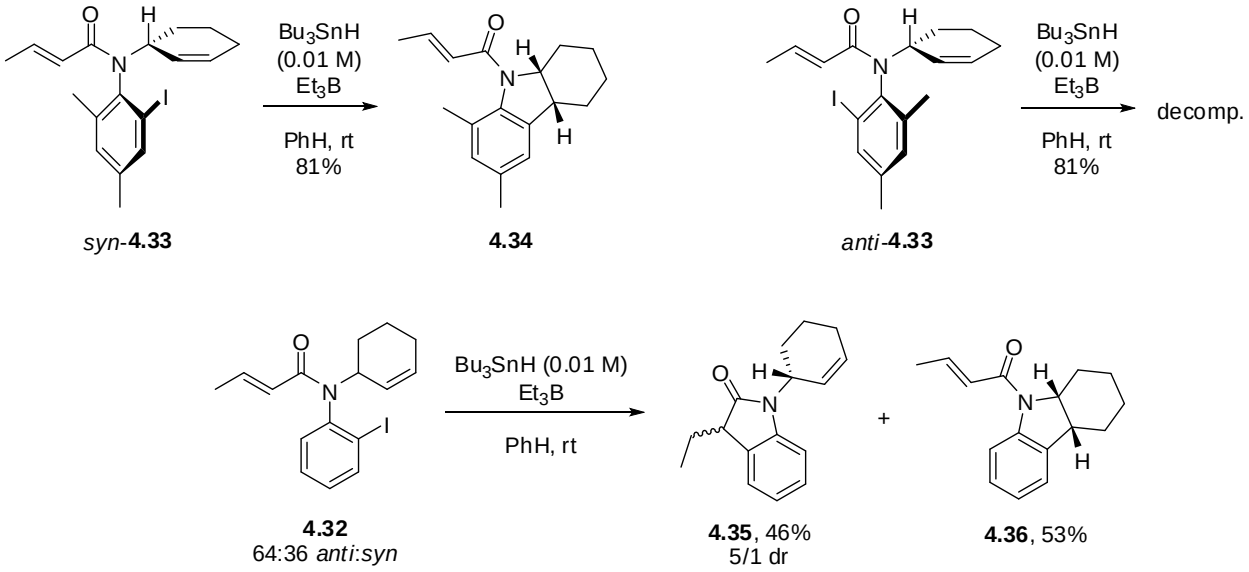

Scheme 4.11 Radical Reactions of Competition Substrates

The pathways for formation of **4.35** and **4.36** from **4.32** are shown in Scheme 4.12. Radical **4.37a**, formed directly from *anti*-**4.32**, can only cyclize onto the crotonyl group, preferentially giving cyclized radical **4.38a** according to the previously discussed transition state model (see Chapter 2.2.2). Bu_3SnH reduction of **4.38a** leads to product **4.35a**. Aryl radical **4.37b**, produced by iodine atom abstraction from *syn*-**4.32**, has two cyclization pathways available. Cyclization onto the crotonyl group gives radical **4.38b**, leading to product **4.35b**. Alternatively, cyclization of **4.37b** onto the cyclohexenyl group produces radical **4.39**, which leads to product **4.36**. Aryl radicals **4.37a** and **4.37b** may also interconvert by an *N*-aryl bond rotation, shown by the immediately preceding work (Section 4.2.3).

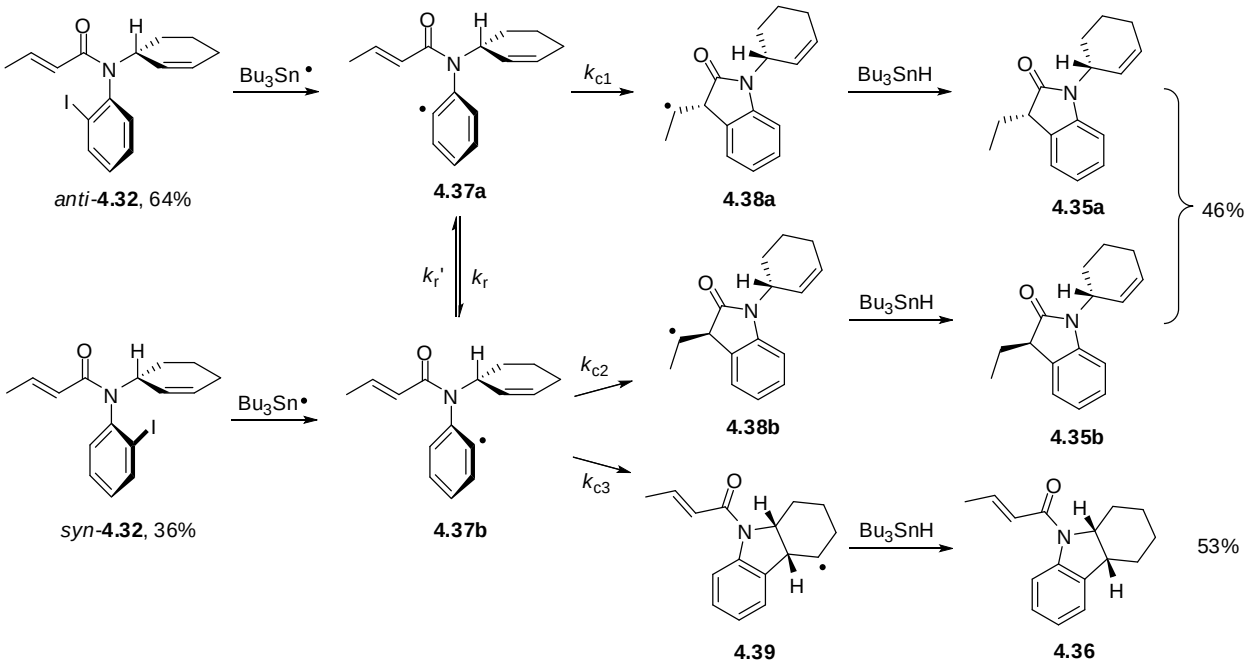

Scheme 4.12 Mechanistic Analysis for Radical Reaction of 4.32

If *N*-aryl rotation processes of **4.37a** and **4.37b** (k_r, k_r') are significantly slower than cyclization processes (k_{c1}, k_{c2}, k_{c3}) then the ratio of products **4.35a**/(**4.35b + 4.36**) should reflect the starting *anti*/*syn* ratio. However, this is not the case, and therefore **4.37a** and **4.37b** must

equilibrate to some degree before cyclizing at room temperature. Our inability to unambiguously identify the major diastereomer of **4.35** precludes comparison of the rate constants of cyclization (k_{c1}, k_{c2}, k_{c3}) to one another.

4.2.5 Heck Reactions of Axially Chiral Diastereomers

The Curran group has previously investigated chirality transfer in room temperature Heck reactions of axially chiral *o*-iodoanilide **4.40** (Scheme 4.13).[128] In these reactions, the axis of chirality of the substrates dictated the stereochemistry of the product **4.41**. After oxidative insertion, the arylpalladium intermediate was able to selectively coordinate with one face of a freely rotating olefin, leading to chirality transfers of 86-91%.

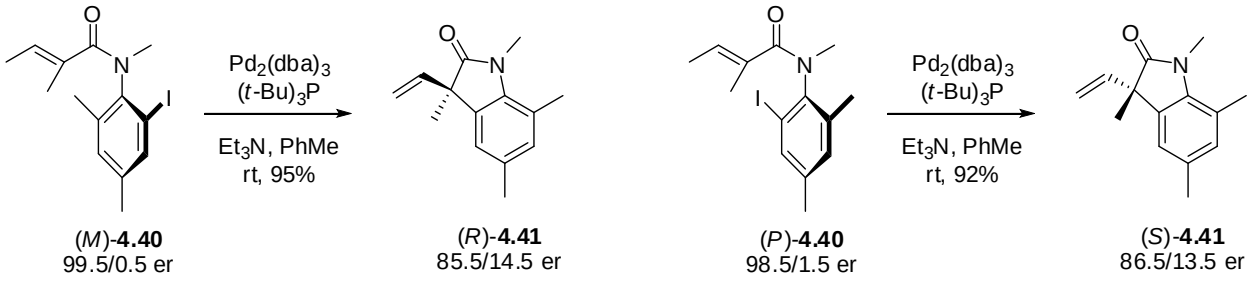

(*M*)-**4.40**
99.5/0.5 er

(*R*)-**4.41**
85.5/14.5 er

(*P*)-**4.40**
98.5/1.5 er

(*S*)-**4.41**
86.5/13.5 er

Scheme 4.13 Asymmetric Room Temperature Heck Reactions

Because substrates **4.15** have restricted rotation about both the *N*-aryl *and N*-cyclohexenyl bonds, we surmised that one atropisomer would cyclize under Heck conditions, while the other would fail to react. We subjected both diastereomers of **4.15** to room temperature Heck conditions (Scheme 4.14), which were developed by Hartwig,[204] in order to minimize rotational processes in the substrates and intermediates. Surprisingly, when *syn*-**4.15** was treated with catalytic $Pd_2(dba)_3$ and P(*t*-Bu)$_3$ ligand with Et_3N base, no cyclization to **4.42** occurred. When the same conditions were applied to *syn*-**4.15** in the presence of excess *t*-butyl

acrylate, intramolecular coupling product **4.43** was obtained in 69% yield. The room temperature Heck reaction of *anti*-**4.15** effected intramolecular cyclization, producing 74% of **4.42a/b** as an inseparable mixture of olefin isomers in a 55:45 ratio. Performing the Heck reaction of *anti*-**4.15** in the presence of 4.0 equiv *t*-butyl acrylate formed *t*-butyl adduct **4.44** in 31% yield, and **4.42a/b** was isolated as a 25:75 mixture in 68% yield.

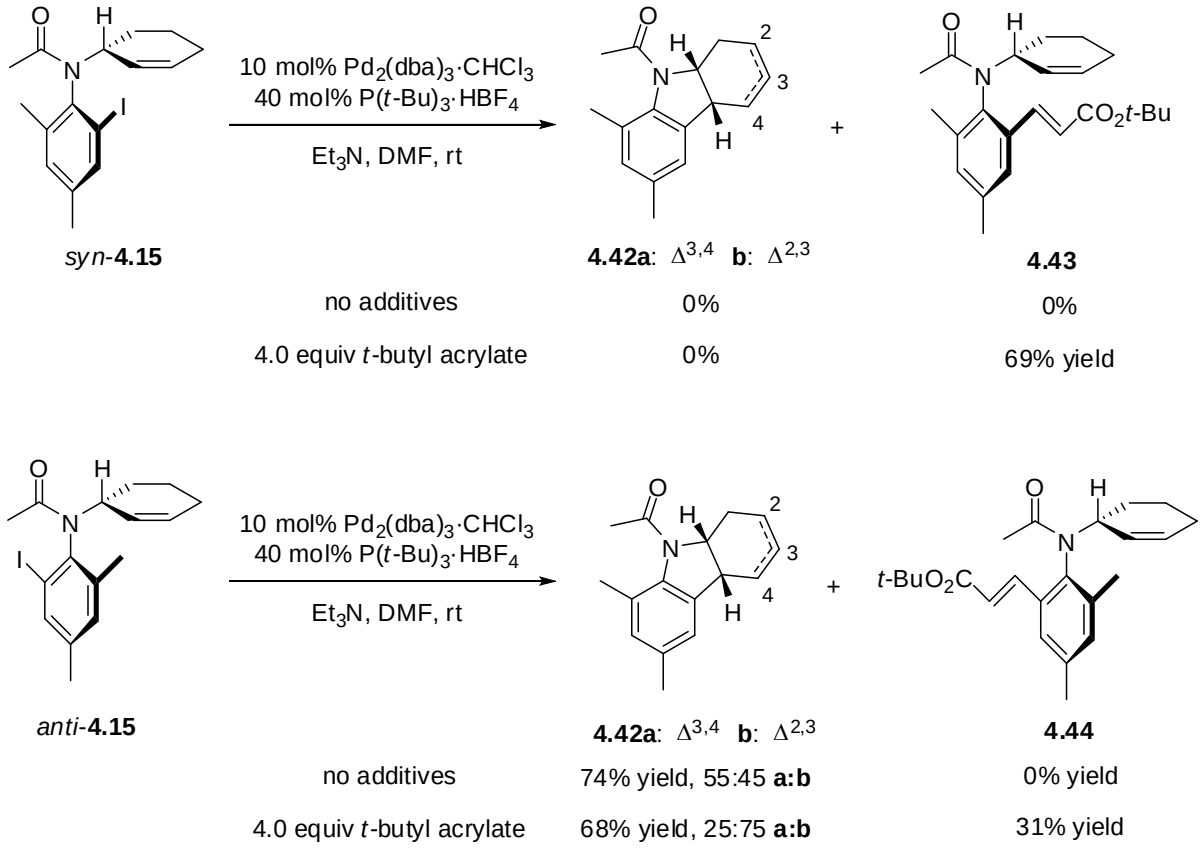

Scheme 4.14 Room-Temperature Heck Reactions of 4.15

In contrast to the radical reactions of **4.15**, in which only the *syn* atropisomer can cyclize, only *anti*-**4.15** is predisposed to cyclize under room-temperature Heck conditions. Based on these results, a transition state model for the Heck cyclization of *anti*-**4.15** was developed as shown in Scheme 4.15. Oxidative addition of the palladium catalyst into the carbon-iodine bond of *anti*-**4.15** produces arylpalladium intermediate **4.45**. *N*-Aryl rotation, concomitant with *N*-

cyclohexenyl bond rotation, allows for coordination between the palladium and the olefin on the concave face of the cyclohexene ring, as in **4.46**. Migratory insertion from this face results in the *cis* ring fusion observed in the product, and gives intermediate **4.47**. Only one hydrogen is available for *syn* β-hydride elimination, initially producing **4.42a**. Rapid palladium hydride reinsertion and elimination can migrate the double bond to the $\Delta^{2,3}$ position[205,206] to produce **4.42b**. The Pd^{II} species is then reduced to the active Pd^0 by the Et_3N base in solution.

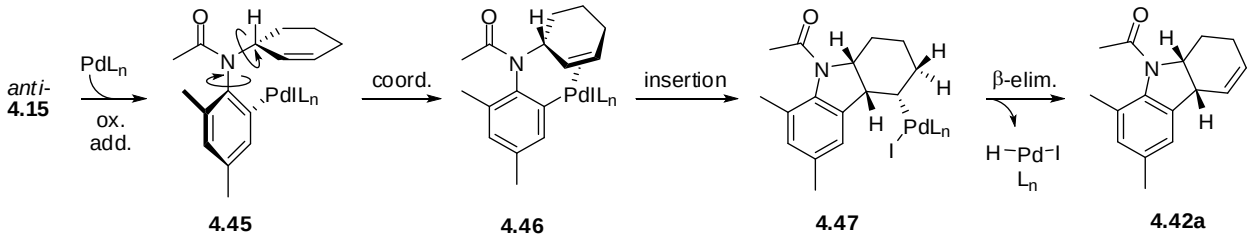

Scheme 4.15 Transition State Model for Heck Reaction

4.2.6 Synthesis of *N*-Cyclohexenyl Allylic Acetates

In the final step of the Heck reaction, the β-elimination of a heteroatomic leaving group (e.g., –Cl, –OAc, $–OCH_3$) typically proceeds more quickly than competing β-hydride elimination when both pathways are available.[207] Recently, Lautens and coworkers developed a procedure for the efficient Heck coupling of aryl iodides and allylic acetates.[208,209] The final step of the reaction presumably involved a chemoselective β-acetoxy elimination. Strikingly, very little isomerization of the double bond was seen in most products. We hypothesized that judicious placement of an acetoxy group in our substrates could avoid a palladium hydride intermediate, thereby circumventing isomerization.

With this in mind, disubstituted cyclohexenes **4.51**-**4.52** were prepared, containing a *cis*-acetoxy group relative to the anilide group (Scheme 4.16). First, 2-iodoaniline was oxidized to a

nitrosoarene using *m*-CPBA, and the crude nitroso compound was subjected to [4 + 2] cycloaddition with 1,3-cyclohexadiene to produce bicyclic oxazine **4.48**. The N-O bond of impure **4.48** was then reductively cleaved[210,211] using $Mo(CO)_6$ and $NaBH_4$ to produce pure alcohol **4.49** in 40% yield over three steps. *bis*-Acetylation of **4.49** gave desired **4.52** in 76% yield as a 3:2 mixture of *anti*:*syn* atropisomers. *o*-Methyl congeners **4.53** were prepared in the same fashion, beginning with oxidation of **3.21** to the nitroso compound followed by cycloaddition with 1,3-cyclohexadiene to produce impure oxazine **4.50**. Treatment of **4.50** with $Mo(CO)_6/NaBH_4$ failed to produce alcohol **4.51**; this is likely due to the additional steric hindrance near the nitrogen imposed by the *o*-methyl group.[210,211] The N-O bond cleavage was effected by reaction with TMSI in wet acetonitrile, producing pure **4.51** in 39% over three steps from **3.21**. *bis*-Acetylation of **4.51**, followed by careful column chromatography, yielded *anti*-**4.53** (32%) and *syn*-**4.53** (26%) as atropisomerically stable compounds.

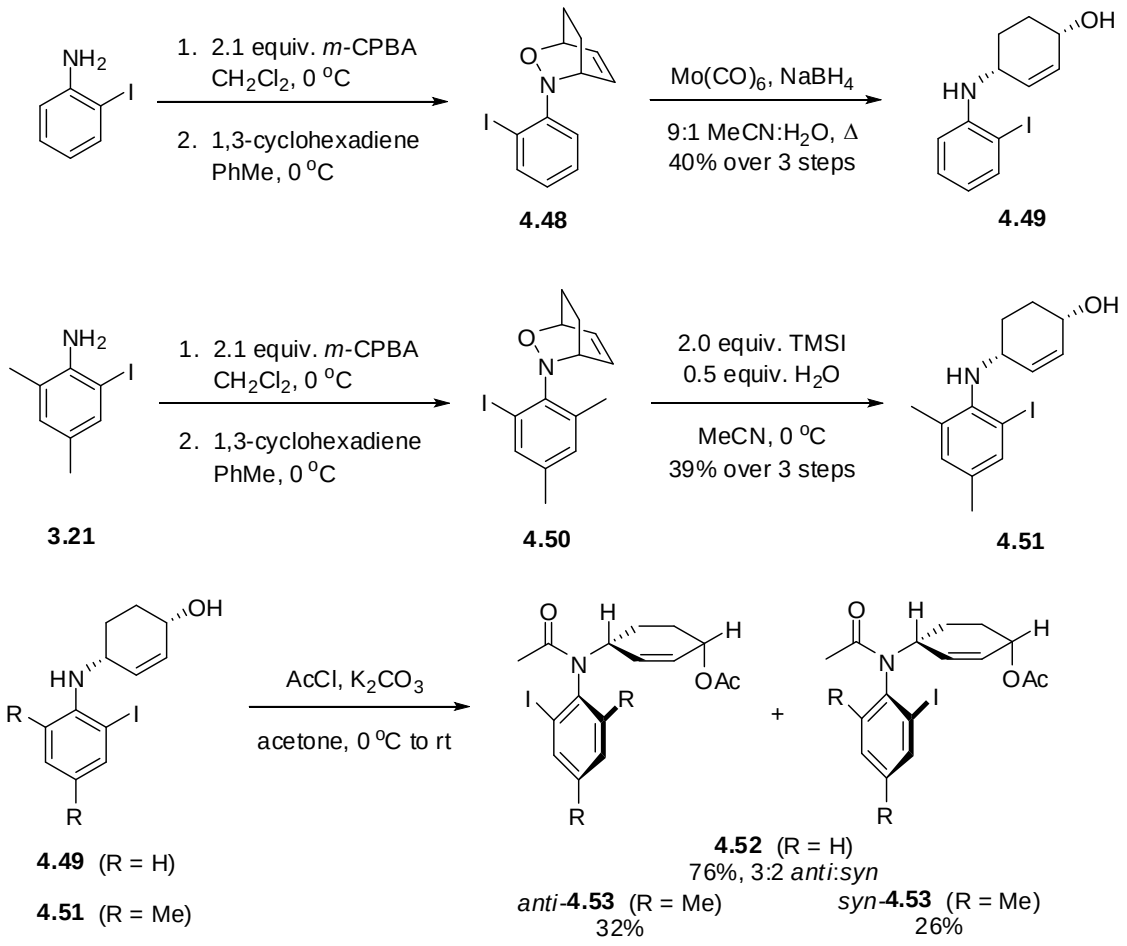

Scheme 4.16 Preparation of *cis*-Cyclohexenyl Acetate Substrates

Upon standing at room temperature, a sample of neat oil **4.52** (3:2 *anti*:*syn*) spontaneously formed crystals possessing an *anti* configuration (Figure 4.5). The selective crystallization of one diastereomeric atropisomer, a dynamic thermodynamic resolution, has been performed previously in our group[133] to produce diastereoenriched anilides from an equilibrium mixture. The torsion angle between the amide and aromatic planes is 83.8°, essentially perpendicular as expected. The cyclohexene ring exists in a half-chair conformation, with the bulkier amide group pseudo-equatorial and the acetate pseudo-axial. ^{1}H NMR analysis of a

crystal fragment confirmed that *anti*-**4.52** is the major atropisomer in $CDCl_3$ solution after equilibrium is reached.

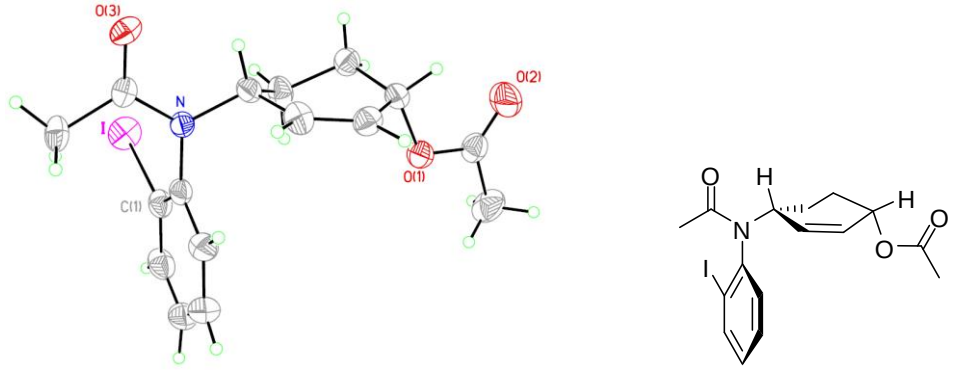

Figure 4.5 Crystal Structure of *anti*-4.52

Substrates **4.56** and **4.57**, possessing an acetoxy substituent *trans* relative to the anilide, were also prepared (Scheme 4.17). Anilide **4.54**[48] was deprotonated with NaH and alkylated with *cis*-4-chlorocyclohex-2-enyl acetate,[212] producing **4.56** in 76% yield as a 2:1 mixture of *anti*:*syn* atropisomers. The *N*-alkylation of anilide **4.55**[93,105] met with less success due to the steric hindrance imparted by the *o*-methyl group. The two atropisomers *anti*-**4.57** (17%) and *syn*-**4.57** (11%) were separable by column chromatography, and 42% of **4.55** was recovered.

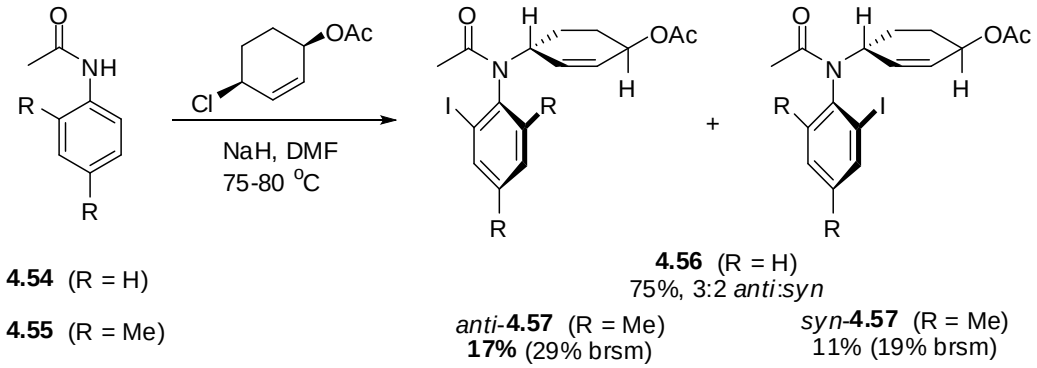

Scheme 4.17 Preparation of *trans*-Cyclohexenyl Acetate Substrates

4.2.7 Radical and Heck Reactions of *N*-Cyclohexenyl Allylic Acetates

Under radical conditions (Scheme 4.18), all compounds containing an allylic acetate group behaved similarly to unsubstituted analogs **4.13** and **4.15**. *trans*-Disubstituted **4.56** (3:2 *anti*:*syn*) was treated with Bu_3SnH and Et_3B at room temperature and cyclized to **4.58** in 89% yield. Similarly, *cis*-acetoxy compound **4.52** (3:2 *anti*:*syn*) efficiently cyclized to **4.59** in 92% yield without a trace of premature reduction. *o*-Methyl substrates *syn*-**4.57** and *syn*-**4.53** also underwent cyclization under these conditions, producing **4.60** (77% yield) and **4.61** (71% yield), respectively. When *anti*-**4.57** was treated with Bu_3SnH at an initial hydride concentration of 0.01 M, multiple inseparable products were formed. Increasing the $[Bu_3SnH]_i$ to 0.21 M avoided the formation of these compounds and produced **4.62** in 96% yield in a 2:1 ratio of atropisomers. Similarly, the radical reaction of *anti*-**4.53** afforded directly reduced **4.63** (96% yield) as a 2:1 mixture of atropisomers.

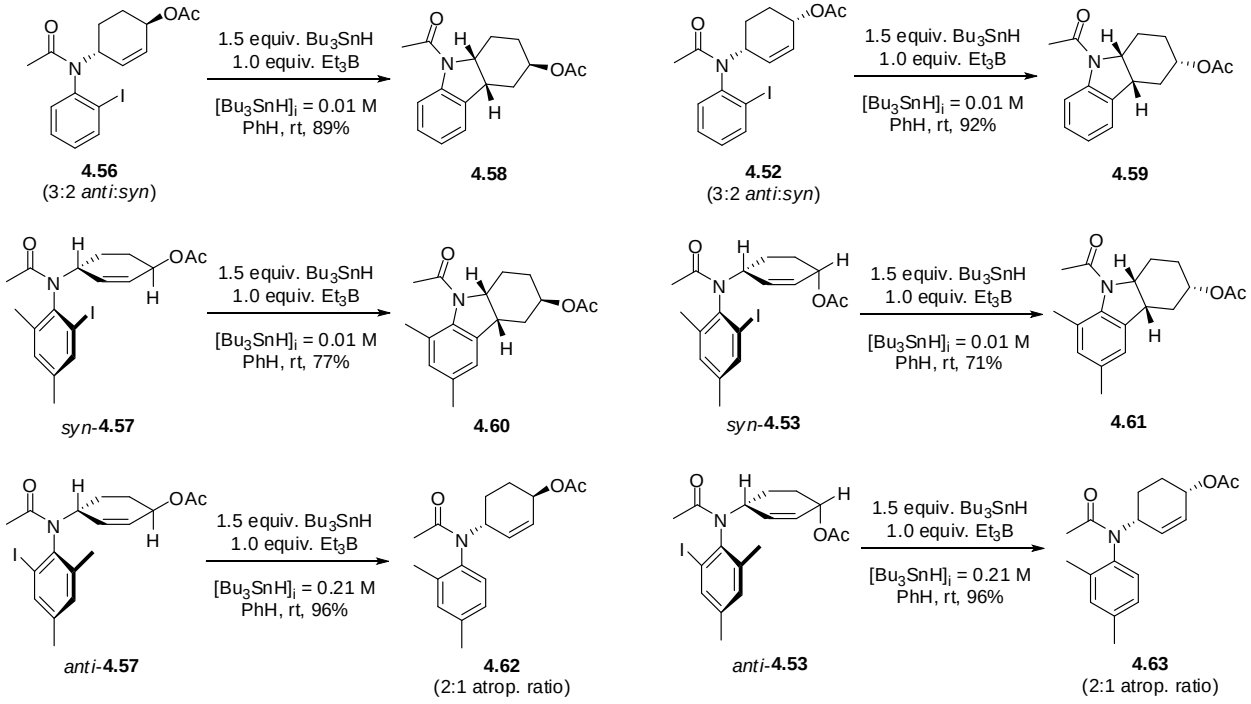

Scheme 4.18 Radical Reactions of Cyclohexenyl Acetates

The substrates were then subjected to Heck conditions according to a procedure developed by Lautens (Scheme 4.19).[208,209] Based on our results with **4.15**, the *syn* substrates were expected to be unreactive towards Heck cyclizations, and were not thoroughly examined. In a 10:1 MeCN:H_2O solvent system, **4.52** (3:2 *anti*:*syn*) was combined with $BuNMe_2$ base and catalytic $Pd_2(dba)_3$•$CHCl_3$ along with P(*o*-tol)$_3$ ligand. The mixture was placed in a sealed tube and heated at 80 °C until the reaction was complete, at which point Pd black precipitated from the mixture. After purification, **4.64** was obtained in 47% yield as a single olefin isomer. Under the same reaction conditions, *anti*-**4.53** produced **4.42a** in 73% yield as a single olefin isomer. The behavior of *trans*-disubstituted cyclohexene systems under these conditions was studied as well. Under Heck conditions, **4.56** (3:2 *anti*:*syn*) gave vinyl acetate **4.65** in 82% yield as the sole product. Similarly, *anti*-**4.57** produced vinyl acetate **4.66** in 73% yield.

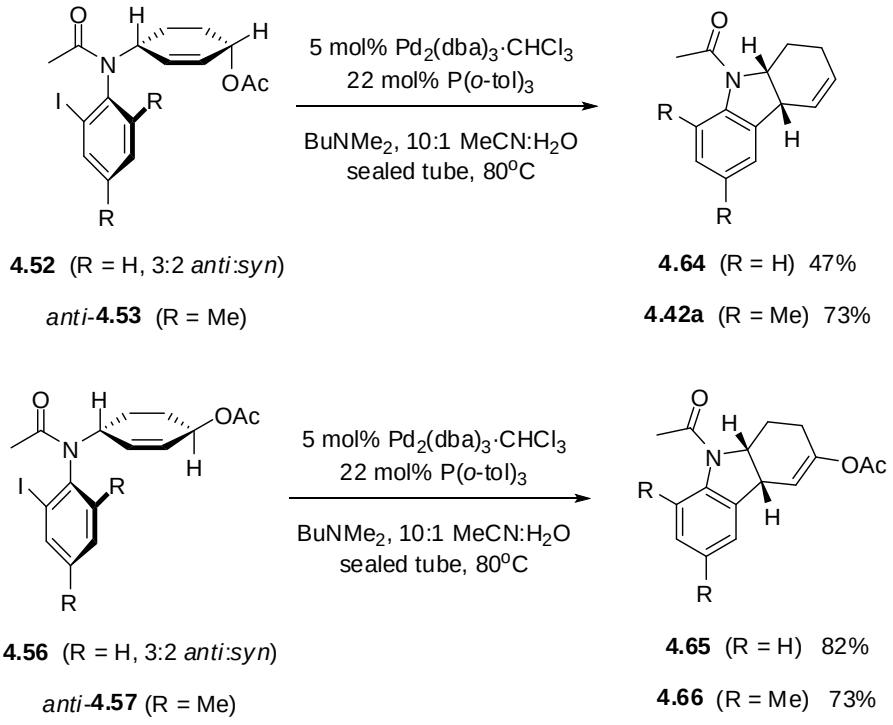

Scheme 4.19 Heck Reactions of Cyclohexenyl Acetates

The mechanistic rationale for these results is shown in Scheme 4.20, using substrates *anti*-**4.53** and *anti*-**4.57** as examples. Oxidative addition of the Pd^0 catalyst occurs to give aryl-Pd^{II} intermediate **4.67**, followed by concomitant *N*-aryl and *N*-cyclohexenyl rotation to allow coordination to the olefin (**4.68**). Insertion gives alkylpalladium intermediate **4.69**, which necessarily undergoes β-elimination with *syn* substituent R^2. In the reaction of *anti*-**4.53**, R^2 is an acetate group; $IPd^{II}OAc$ is eliminated and is subsequently reduced by tertiary amine base.[208] When *anti*-**4.57** is the substrate, R^2 is H, and β-hydride elimination occurs to give vinyl acetate **4.66**.

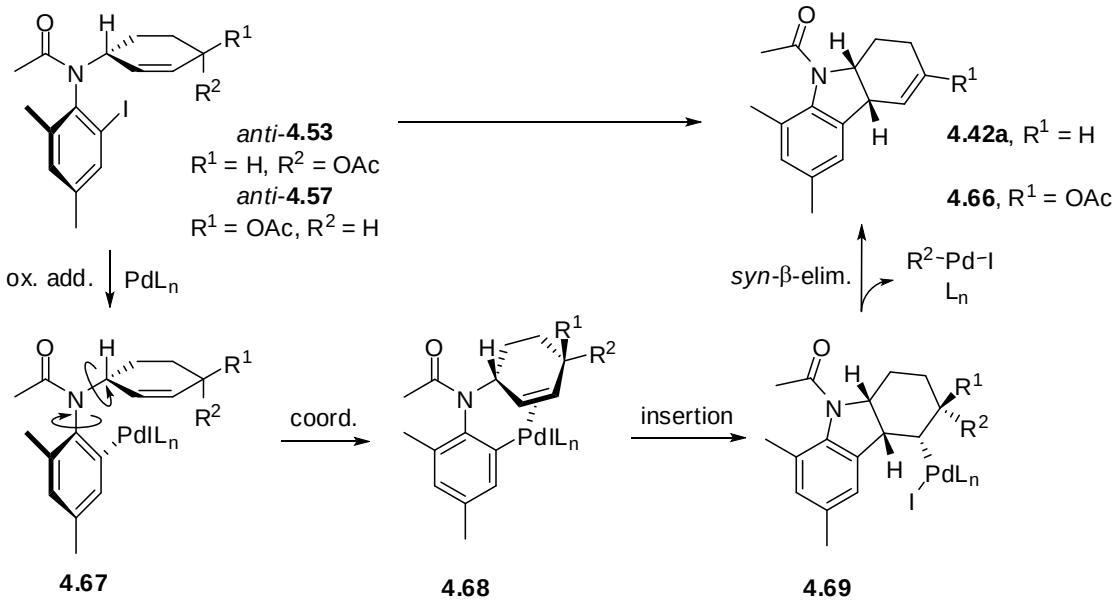

Scheme 4.20 Mechanism of Heck Reaction with Chemoselective β-Elimination

The ability of **4.69** to undergo β-acetoxy elimination when R^2 = OAc is unusual. Previous studies have shown that β-elimination of heteroatom substituents during the Heck reaction proceeds with the leaving group *anti*-periplanar to the palladium.[207,213] However, those studies were performed under acidic reaction conditions, with $Pd(OAc)_2$ catalyst in AcOH

solution. Both *anti*- and *syn*-eliminations of aryloxy groups have been observed during Heck reactions in the presence of trialkylamine base.[214] The propensity for our system to undergo *syn*-acetoxy elimination is indicative of a change in mechanism when switching to basic conditions.

4.2.8 Conclusions

The radical and Heck reactions of *N*-cyclohexenyl-*o*-iodoanilides were investigated. Radical cyclizations may only occur through the *syn* atropisomer when an additional *ortho* substituent is present on the aromatic ring. Heck cyclizations may only proceed through the *anti* isomer, requiring simultaneous *N*-aryl and *N*-cyclohexenyl rotation to achieve the necessary transition state. The β-elimination step of these Heck reactions occurs with complete *syn* selectivity.

5.0 CHIRALITY TRANSFER IN 6-*EXO-TRIG* CYCLIZATIONS OF α-HALO-(2-ALKENYL)ANILIDES

5.1 INTRODUCTION

5.1.1 Stereoselective Preparations of Dihydroquinolin-2-ones

The dihydroquinolin-2-one moiety is rarely present in natural products. Most of these natural compounds, such as pinolinone[215] and the penigequinolines,[216] display little to no biological activity. Exploration of non-natural dihydroquinolin-2-ones, however, has revealed structures with great medicinal potential. Recently, cyclopropanated quinolinones have shown promise as HIV-1 inhibitors.[217,218] Other compounds being developed include selective $\alpha_v\beta_3$ integrin antagonists, which may provide a treatment for osteoporosis or the angiogenesis phase of cancer.[219] Despite the recent advances made with this class of molecules, relatively few methods exist to synthesize substituted derivatives in a stereoselective fashion.

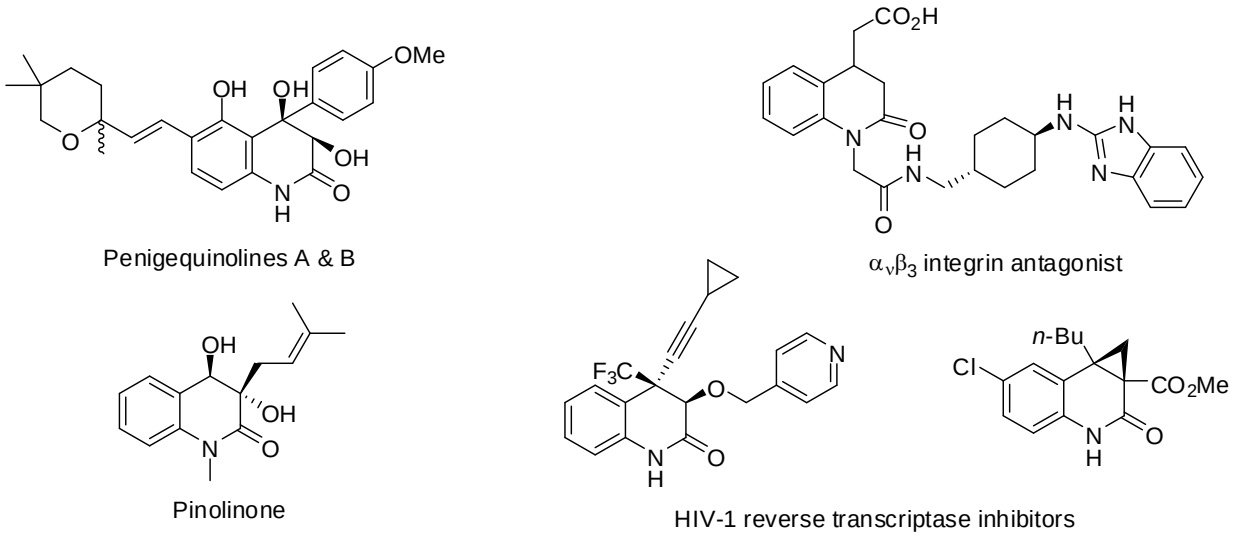

Figure 5.1 Representative Natural (Left) and Non-Natural (Right) Dihydroquinolin-2-ones

One of the first enantioselective routes towards dihydroquinolin-2-ones was introduced by Alper, who developed an asymmetric version of his palladium-catalyzed cyclocarbonylation.[220] By treating 2-vinylanilines with catalytic amounts of $Pd(OAc)_2$ and a chiral bidentate biphosphine ligand under a CO/H_2 atmosphere, enantioenriched dihydroquinolin-2-ones can be obtained in excellent yields and with varying substitution patterns.[221,222] However, this method is impractical for general use due to the high pressures and temperatures (> 40 atm, > 100 °C) required, as well as the modest and substrate-dependent enantioselectivities (0 – 84% ee).

More recently, new entries to dihydroquinolin-2-ones have been developed (Scheme 5.1), each with its own strengths and limitations. In the first example, dioxolanone **5.1**, derived from readily available mandelic acid, undergoes highly diastereoselective alkylation to produce **5.2**. A one-pot nitro group reduction and aminolysis affords enantiopure products **5.3** in excellent yields.[223] Despite the efficiency of this sequence, the scope is limited; the phenyl and hydroxy substituents at the 3-position are both derived from the mandelic acid starting material, and thus

must appear in the product. Procter's solid-phase approach to these systems holds more promise for molecular diversity.[224,225] A three-step procedure attaches α-bromoacetanilide **5.4** to solid support via a sulfonyl linker, and installs a Michael acceptor. Base-induced cyclization of **5.5**, followed by α-allylation and cleavage of the linker with SmI_2, produces disubstituted dihydroquinolinone **5.6**. This general procedure allows for alkyl substitution at the 3- and 4-positions. However, little to no diastereoselectivity is observed, and the method cannot be extended to enantioselective preparations. Harmata and co-workers have developed a more selective method, using chiral sulfoximines to effect diastereoselective cyclizations.[226] Coupling of aryl bromide **5.7** and sulfoximine **5.8**, followed by deprotonation and Michael addition, produces benzothiazine **5.9** as a single diastereomer. Subsequent alkylation of **5.9**, followed by reductive desulfurization and lactamization, affords enantiopure products **5.10** in good yields. This procedure allows introduction of a variety of functional groups at the 4-position of the dihydroquinolinone system, but does not tolerate substitution at the 3-position. While these approaches are useful, they are limited in scope and selectivity, and a need still exists for more general methods of enantioselective dihydroquinolin-2-one production.

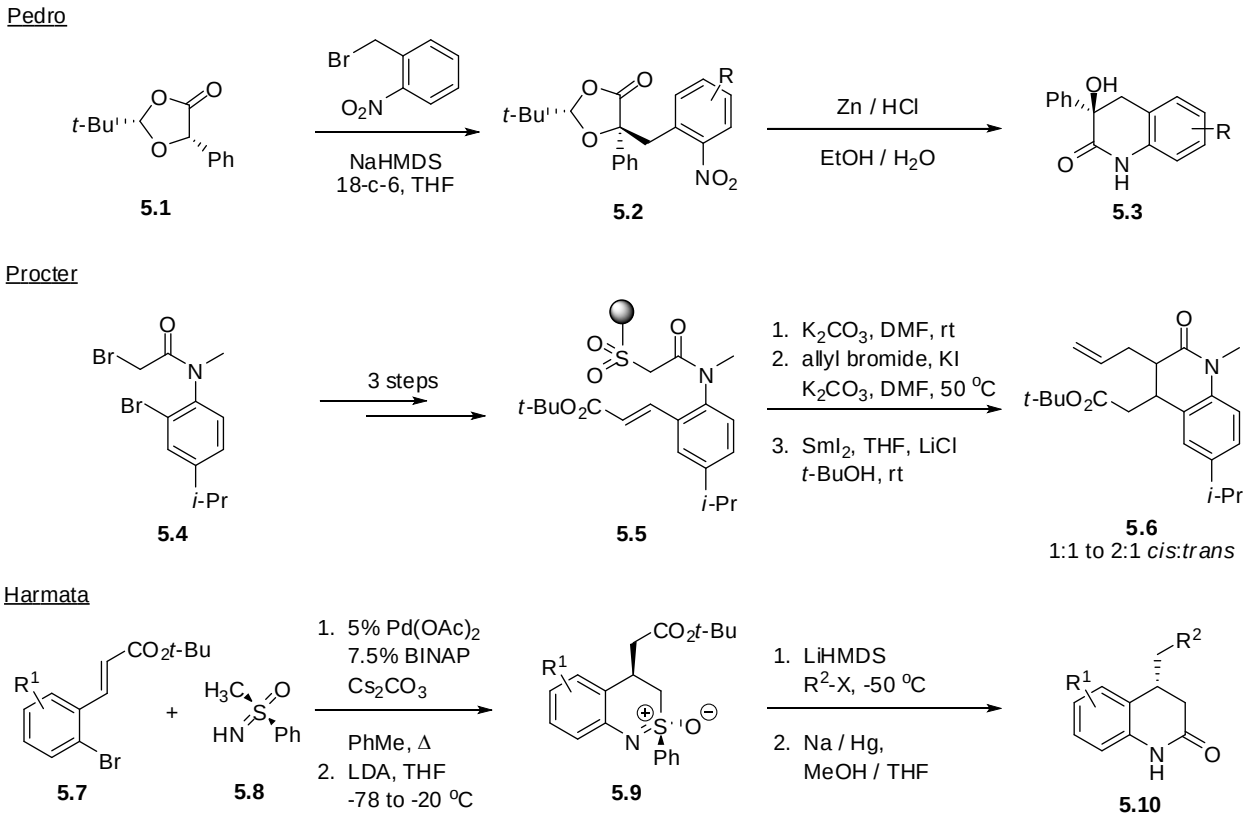

Scheme 5.1 Stereoselective Syntheses of Dihydroquinolin-2-ones

5.1.2 Dihydroquinolin-2-ones Via 6-*Exo*-*Trig* Radical Cyclizations

6-*Exo*-*trig*[227] and 6-*endo*-*trig*[228] radical cyclizations of *o*-iodoanilides have been used to construct dihydroquinolin-2-ones, but these reactions suffered from poor yields and regioselectivities. In these approaches, halogen abstraction at the *ortho* position generates an aryl radical, which cyclizes onto an olefin acceptor within the amide group. Greater success has been found in "reversed" systems, in which the *ortho* substituent is the radical acceptor group, and the radical is generated within the amide functionality. In the first examples of this type, Ikeda and co-workers reacted α,α-dichloroacetanilides **5.11a-d** with Bu_3SnH and catalytic AIBN in refluxing toluene, to cleanly produce cyclized products **5.12a-d** (Scheme 5.2).[229]

Regioselectivity for 6-*exo-trig* cyclization was typically excellent in these systems; no 7-*endo-trig* products were observed.

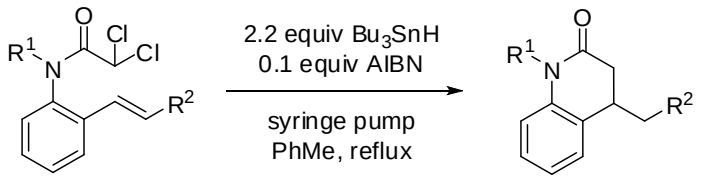

5.11a-d **5.12a-d**

Substrate	R^1	R^2	% yield **5.12**
5.11a	Me	H	49
5.11b	Me	Me	79
5.11c	H	Me	100
5.11d	H	CO_2t-Bu	100

Scheme 5.2 First Radical Cyclizations of *N*-(*o*-Alkenylphenyl)-α-Haloacetamides

More recently, Parsons and coworkers reported an undesired 6-*exo-trig* cyclization during their efforts to construct mitomycin systems by tandem radical cyclizations (Scheme 5.3).[230] When α-chloroamide **5.13** was subjected to Ph_3SnH and catalytic AIBN in refluxing toluene, 6-*exo* product **5.14** was obtained in 63% yield, along with tandem cyclization products **5.15** and target molecule **5.16** in 16% and 12% yields, respectively. The formation of **5.14** as the major product further supports the notion that this mode of cyclization is an efficient method of synthesizing dihydroquinolinones. However, the competitive formation of **5.15** and **5.16**, whose formations begin with a usually disfavored 5-*endo-trig* cyclization,[231] indicates that the 6-*exo-trig* cyclization is rather slow, despite the presence of the activating terminal ester substituent.

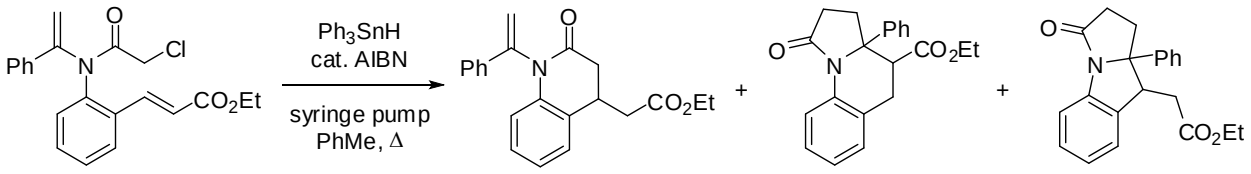

5.13 **5.14** 63% yield **5.15** 16% yield **5.16** 12% yield

Scheme 5.3 Competing 5-*Endo-Trig* and 6-*Exo-Trig* Radical Cyclizations

In the examples discussed in Schemes 5.2 and 5.3, the α-haloanilide precursors contain an element of *N*-aryl axial chirality.[50,152,232] Because **5.11a-d** and **5.13** do not possess a second *ortho* substituent, it is likely that their *N*-aryl barriers to rotation are low, precluding resolution. We envisioned a series of anilide precursors **5.17** (Scheme 5.4) with an additional *ortho* substituent to decrease the rate of racemization. We set out to learn whether substrates **5.17** could be resolved, and to determine whether radical cyclizations of enantioenriched **5.17** would proceed with chirality transfer to give enantioenriched cyclized products **5.18**.

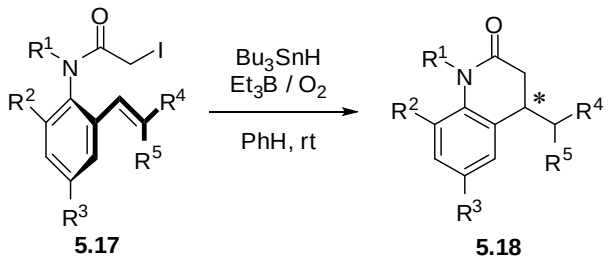

5.17 **5.18**

Scheme 5.4 Proposed 6-*Exo*-*Trig* Cyclization with Chirality Transfer

5.2 RESULTS AND DISCUSSION

5.2.1 Synthesis of Starting Materials

Preparation of substrates **5.17** began with the installation of a variety of *N*-substituents on an array of *o*-iodoanilines (Scheme 5.5). Deprotonation of **3.21** with LDA, followed by alkylation with methyl iodide, provided *N*-methylated **5.19** in 84% yield. Alternatively, *N*-PMB congener **5.20** was prepared in 83% yield from **3.21** by reductive amination at room temperature with *p*-anisaldehyde and $NaBH(OAc)_3$.[233] Boc-deprotection of **5.21**[234] with TFA, followed by reductive amination to install the *N*-PMB group, provided **5.22** (76% yield) in a simple one-pot operation.

Treatment of **3.21** with tosyl chloride in pyridine readily provided **5.23** in 90% yield. Synthesis of **5.24** via acid-mediated reductive amination failed, owing to the sensitivity of the *o*-TMS group to TFA. Success was achieved by deprotonation of **3.27** with LiHMDS and alkylation with *p*-methoxybenzyl bromide (81% yield). Condensation of **3.23** with *p*-anisaldehyde did not proceed at room temperature, but refluxing these compounds in toluene with azeotropic removal of water effected the transformation. Reduction of the resulting imine with TFA/$NaBH(OAc)_3$ cleanly provided **5.25** in 72% yield.

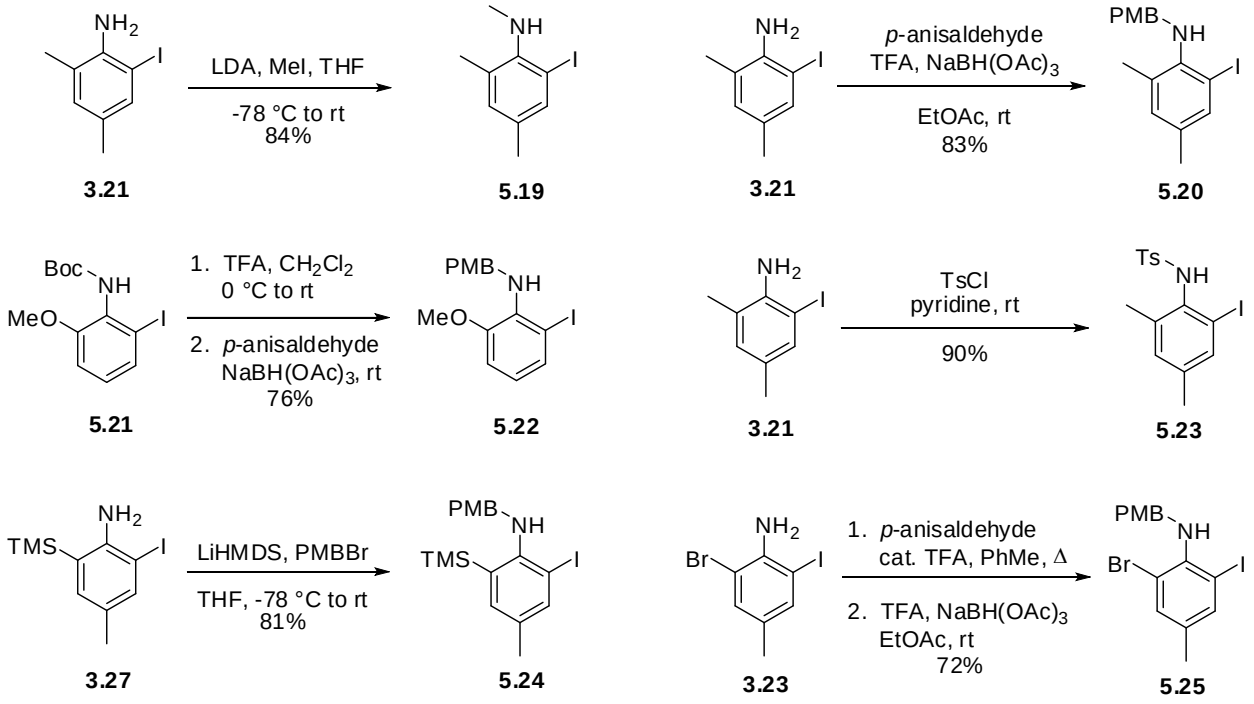

Scheme 5.5 Preparation of *N*-Substituted Anilines

Next, the aryl iodide was used as a handle to install various olefinic radical acceptors by palladium-mediated methods (Scheme 5.6). Ligand-free Heck reactions[235] coupled **5.19-5.24** with *tert*-butyl acrylate to cleanly produce **5.26a-e** (77-92% yields). With *o*-bromo compound **5.25**, the Jeffery-Larock protocol[236] effected chemoselective[237,238] coupling with *t*-butyl acrylate to furnish **5.26f** in 81% yield at room temperature. These conditions were also used to couple

5.20 with acrylonitrile; however, higher temperatures were required for reaction, and α,β-unsaturated nitrile **5.26g** was obtained in 45% yield. The ligand-free Heck conditions were applied to coupling with 4-bromostyrene; however, the reaction was not clean, and **5.26h** was only produced in 29% yield. Finally, a geminal-dimethyl olefin acceptor was installed through a Negishi coupling[239] of **5.20** and (2-methylprop-1-enyl)zinc halide formed from the corresponding Grignard reagent, producing **5.26i** in 98% yield.

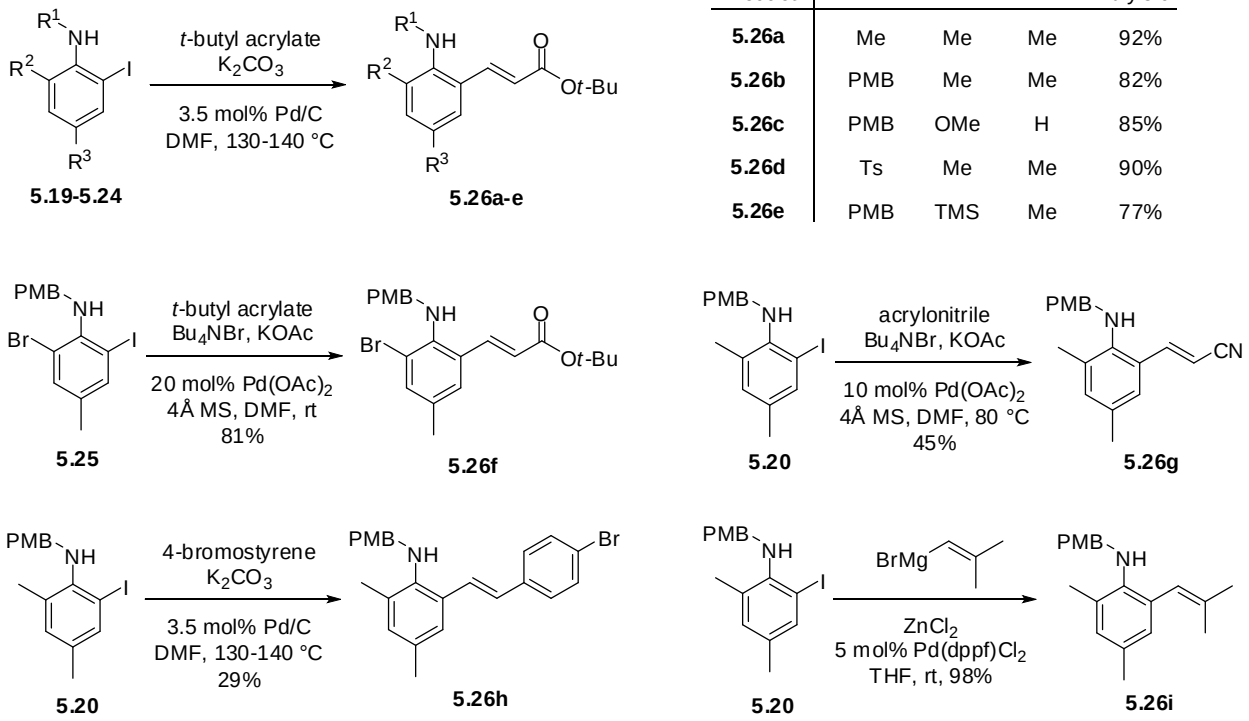

Product	R^1	R^2	R^3	% yield
5.26a	Me	Me	Me	92%
5.26b	PMB	Me	Me	82%
5.26c	PMB	OMe	H	85%
5.26d	Ts	Me	Me	90%
5.26e	PMB	TMS	Me	77%

Scheme 5.6 Installation of Radical Acceptor Groups

With **5.26a-i** in hand, a general two-step sequence gave access to racemic α-iodide precursors **5.17a-i** as depicted in Table 5.1. *N*-Acetylation of **5.26a-i** with chloroacetyl chloride provided α-chloroamides **5.27a-i** (74 – 98% yields) as racemates. These α-chloramides underwent halogen exchange under typical room temperature Finkelstein conditions to produce α-iodoamide substrates **5.17a-i** (78 – 96% yields). The reactions proceeded uneventfully in all

cases, except for the transformation of **5.27e** to **5.17e**, which required prolonged refluxing. It is likely that the *o*-TMS group of **5.27e** sterically hinders the reaction site, slowing the backside attack of iodide.

Table 5.1 Preparation of α-Haloacetamide Substrates

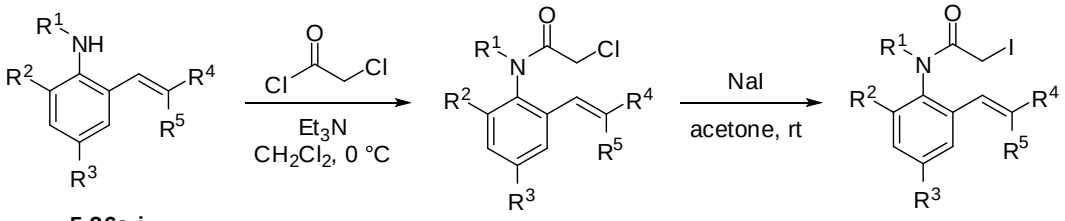

5.26a-i **5.27a-i** **5.17a-i**

substrate	R^1	R^2	R^3	R^4	R^5	α-Cl amide	% yield[a]	α-I amide	% yield[a]
5.26a	Me	Me	Me	CO_2t-Bu	H	**5.27a**	90	**5.17a**	93
5.26b	PMB	Me	Me	CO_2t-Bu	H	**5.27b**	97	**5.17b**	92
5.26c	PMB	OMe	H	CO_2t-Bu	H	**5.27c**	85	**5.17c**	98
5.26d	Ts	Me	Me	CO_2t-Bu	H	**5.27d**	89	**5.17d**	78
5.26e	PMB	TMS	Me	CO_2t-Bu	H	**5.27e**	99	**5.17e**	96[b]
5.26f	PMB	Br	Me	CO_2t-Bu	H	**5.27f**	90	**5.17f**	91
5.26g	PMB	Me	Me	4-BrC_6H_4	H	**5.27g**	89	**5.17g**	86
5.26h	PMB	Me	Me	CN	H	**5.27h**	74	**5.17h**	86
5.26i	PMB	Me	Me	Me	Me	**5.27i**	98	**5.17i**	88

[a] Yield of racemate after isolation by column chromatography. [b] The reaction mixture was refluxed for 40 h and reaction progress was monitored by GC.

5.2.2 Reaction Optimization and Substrate Screening

With α-iodides **5.17a-i** in hand, we set out to determine optimal cyclization conditions on racemic compounds, while also probing the scope of the reaction. To a solution of **5.17a** and Bu_3SnH (10 mM) in PhH at rt was added Et_3B initiator. After 5 min, TLC analysis of the reaction mixture showed complete consumption of **5.17a**. The solvent was removed, and the crude mixture was directly chromatographed on 10% w/w KF/silica gel[80] to efficiently remove

tributyltin byproducts. This reaction provided cyclized product **5.18a** in 55% yield, but purification was complicated by the presence of small amounts of directly reduced **5.28a**. The reaction of **5.17b** under similar conditions produced **5.18b** in 72% yield, along with small amounts of **5.28b**. To minimize premature reduction, we employed syringe pump conditions. Bu_3SnH and Et_3B initiator were dissolved in rigorously degassed PhH, and this solution was added dropwise over 2 h to a non-degassed PhH solution of substrates **5.17a-b** at room temperature. We were pleased to see that these conditions both increased the yields of **5.18a** and **5.18b** to 83% and 85%, respectively (Table 5.2, Entries 2 and 4), and no **5.28a-b** was observed in the product mixture.

Substrates **5.17c,e,f** behaved similarly, cyclizing in 61-97% yields (Entries 5, 7, 8). Especially notable is the surprising stability of *o*-silylated **5.18e** (Entry 7) to the chromatography conditions; no desilylation was observed despite the KF treatment. Unsaturated nitrile **5.17h** cyclized to **5.18h** under syringe pump conditions, but coeluted with numerous impurities that made purification impossible (Entry 11). Adding all Bu_3SnH at the outset of the reaction suppressed most of the side products, and allowed **5.18h** to be formed in 70% yield in ~ 95% purity. A lower yield in the cyclization of **5.17i** to **5.18i** (51%) was not surprising, as cyclizations onto olefins with terminal alkyl substituents are approximately 700 times slower[18,59] than those with terminal ester substituents. A small amount of the sole side product was isolated during purification and identified as the product of premature reduction **5.28i**.

Table 5.2 Cyclizations of Racemic α-Iodoamides 5.17a-i

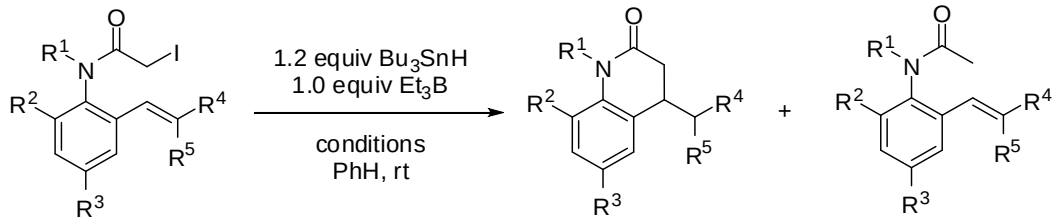

rac-**5.17a-i** *rac*-**5.18a-i** *rac*-**5.28a-i**

entry	α-I	R^1	R^2	R^3	R^4	R^5	cond.[a]	cyc. product	% yield[b]
1	**5.17a**	Me	Me	Me	CO_2t-Bu	H	B	**5.18a**	55[d]
2	**5.17a**	Me	Me	Me	CO_2t-Bu	H	A	**5.18a**	83
3	**5.17b**	PMB	Me	Me	CO_2t-Bu	H	B	**5.18b**	72[d]
4	**5.17b**	PMB	Me	Me	CO_2t-Bu	H	A	**5.18b**	85
5	**5.17c**	PMB	OMe	H	CO_2t-Bu	H	A	**5.18c**	97
6	**5.17d**	Ts	Me	Me	CO_2t-Bu	H	A	**5.18d**	nd[c,d]
7	**5.17e**	PMB	TMS	Me	CO_2t-Bu	H	A	**5.18e**	93
8	**5.17f**	PMB	Br	Me	CO_2t-Bu	H	A	**5.18f**	61
9	**5.17g**	PMB	Me	Me	4-BrC_6H_4	H	B	**5.18g**	nd[c]
10	**5.17g**	PMB	Me	Me	4-BrC_6H_4	H	A	**5.18g**	nd[c]
11	**5.17h**	PMB	Me	Me	CN	H	A	**5.18h**	< 71
12	**5.17h**	PMB	Me	Me	CN	H	C	**5.18h**	70
13	**5.17i**	PMB	Me	Me	Me	Me	A	**5.18i**	51[d]

[a] Conditions A: Bu_3SnH and Et_3B in 20 mL PhH were added over 2 h via syringe pump to a stirred 10 mM PhH solution of iodide. B: neat Bu_3SnH and Et_3B were added sequentially in one portion to a stirred PhH solution of iodide with $[Bu_3SnH]_i$ = 10 mM. C: Same as B with $[Bu_3SnH]_i$ = 5 mM. [b] Yield of racemic **5.18a-i** after isolation by column chromatography on 10% w/w KF/silica gel. [c] nd = not determined. [d] Directly reduced **5.28** was detected in crude reaction mixture by TLC or ^{1}H NMR.

Not all substrates were able to cyclize in an efficient manner. The reaction of *N*-tosyl compound **5.17d** gave an inseparable mixture of products in 90% mass balance after chromatography (Entry 6). Synthesis of the product of direct reduction **5.28d**[240] and comparison of ^{1}H NMR spectra showed that **5.28d** made up approximately 80% of the product mixture; little or no cyclization product was observed. The reaction of substrate **5.17g**, containing an aromatic olefin substituent, resulted in decomposition (Entry 9) with no major product identifiable by TLC or ^{1}H NMR analysis of the reaction mixture. Adding all Bu_3SnH reducing reagent at 10 mM concentration before Et_3B initiation led to similar results (Entry 10). It is likely that reduction of

the cyclized benzylic radical by Bu_3SnH is slow enough (k_H = 3.6 x 10^4 M^{-1} s^{-1} at 298 K)[241] that, under the low Bu_3SnH concentrations employed in this reaction, side reactions of the radical occur before reduction.

5.2.3 Rate Constant Measurements

The necessity of syringe pump conditions to avoid premature reduction in reactions of compounds **5.17a-i** implies a small rate constant of 6-*exo*-*trig* cyclization. The rate constant of 6-*exo*-*trig* cyclization of the parent 6-heptenyl radical[4,17,63] is k_C = 5.0 x 10^3 s^{-1}. However, because all atoms connecting the radical precursor and radical acceptor are sp^2-hybridized in **5.17a-i**, no direct comparison to the all-sp^3 6-heptenyl system can be made. Therefore, kinetic competition experiments[63] were undertaken to determine the cyclization rate constant k_C for the reaction of a representative compound **5.17b**, using GC analysis as described in Chapter 1.2.2.

An authentic sample of **5.28b** was prepared in 92% yield by treating **5.26b** with acetyl chloride.[240] The GC retention times of **5.18b** and **5.28b** were then determined with respect to eicosane, which was used as an internal standard in competition experiments. This allowed for determination of absolute yields in each reaction.

The competition experiments were performed by mixing stock PhH (non-degassed) solutions of **5.17b** (0.025 mmol), Bu_3SnH (0.030 mmol), and eicosane internal standard in round bottom flasks open to the atmosphere. A hexanes solution of Et_3B (0.010 mmol) was added all at once. The initiator solution was included in the total volume during calculations, but accounted for no more than 2.5% of the total reaction volume in any experiment. The reaction mixtures were stirred for 10 min, and were then injected onto the GC without workup or dilution. Three trials were performed at each concentration, and the results of these reactions are

summarized in Table 5.3. Reactions were very clean and went to completion in all cases, and no significant side peaks were observed in GC analysis.

Table 5.3 Kinetic Competition Experiments for 5.17b

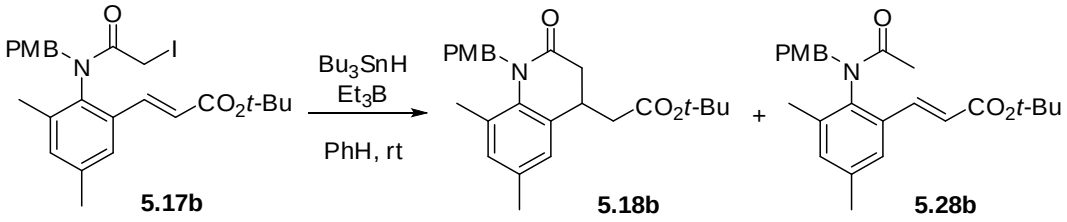

5.17b **5.18b** **5.28b**

		products (% yield)[a]			
$[Bu_3SnH]_i$[b]	$[Bu_3SnH]_c$[c]	**5.18b**	**5.28b**	total	red : cyc[d]
14.9 mM	8.7 mM	67	21	89	24 : 76
19.9 mM	11.6 mM	64	25	89	28 : 72
27.0 mM	15.8 mM	59	30	88	33 : 67
37.0 mM	21.6 mM	58	39	97	40 : 60
49.2 mM	28.7 mM	50	46	95	48 : 52
58.8 mM	34.3 mM	45	45	90	50 : 50
73.2 mM	42.7 mM	33	43	76	57 : 43

[a] GC yield, using eicosane as an internal standard. Yields are an average of three trials. [b] Initial concentration of Bu_3SnH. [c] Average concentration of Bu_3SnH during consumption of starting material. [d] The ratio of reduced **5.18b** to cyclized **5.28b**.

The reactions of **5.17b** gave highly reproducible results at all concentrations, with excellent mass balances (76-95%) throughout. As expected, the ratio of reduced product **5.28b** increased with respect to **5.18b** as the concentration of tin hydride reducing agent increased. As seen in Scheme 5.7, initially formed α-amide radical **5.29** may cyclize to α-ester radical **5.30** with rate constant k_C, eventually producing cyclized **5.18b**. Alternately, **5.29** may be directly reduced to **5.28b** in a process whose rate depends on Bu_3SnH concentration. The reduction:cyclization ratio was plotted against the mean tributyltin hydride concentration $[Bu_3SnH]_c$ as shown in Figure 5.2, in which the slope of the resulting line is equal to k_H/k_C.

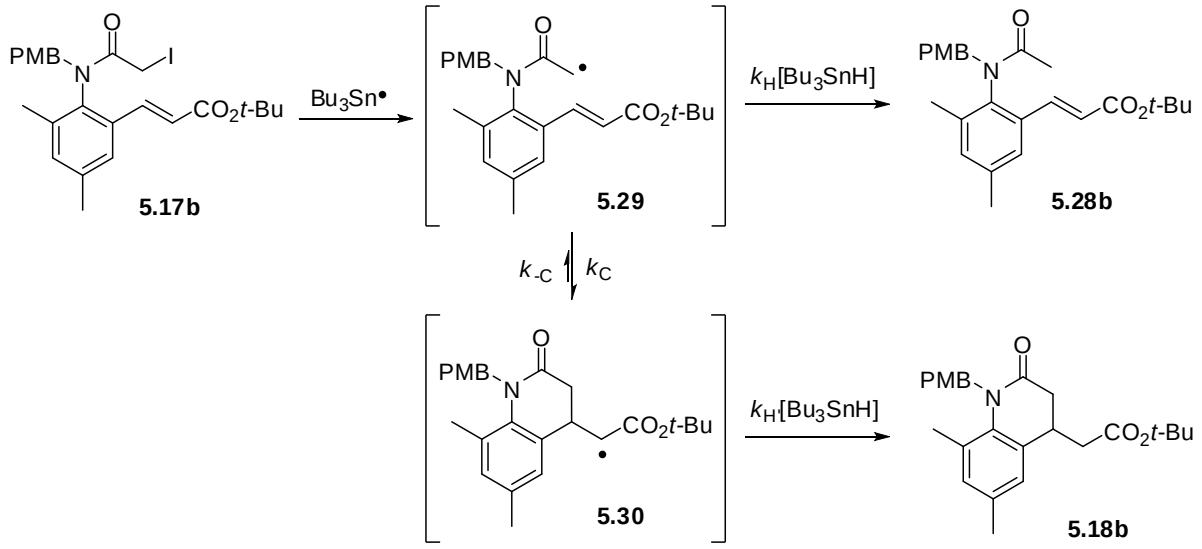

Scheme 5.7 Competing Reactions of Radical 5.29

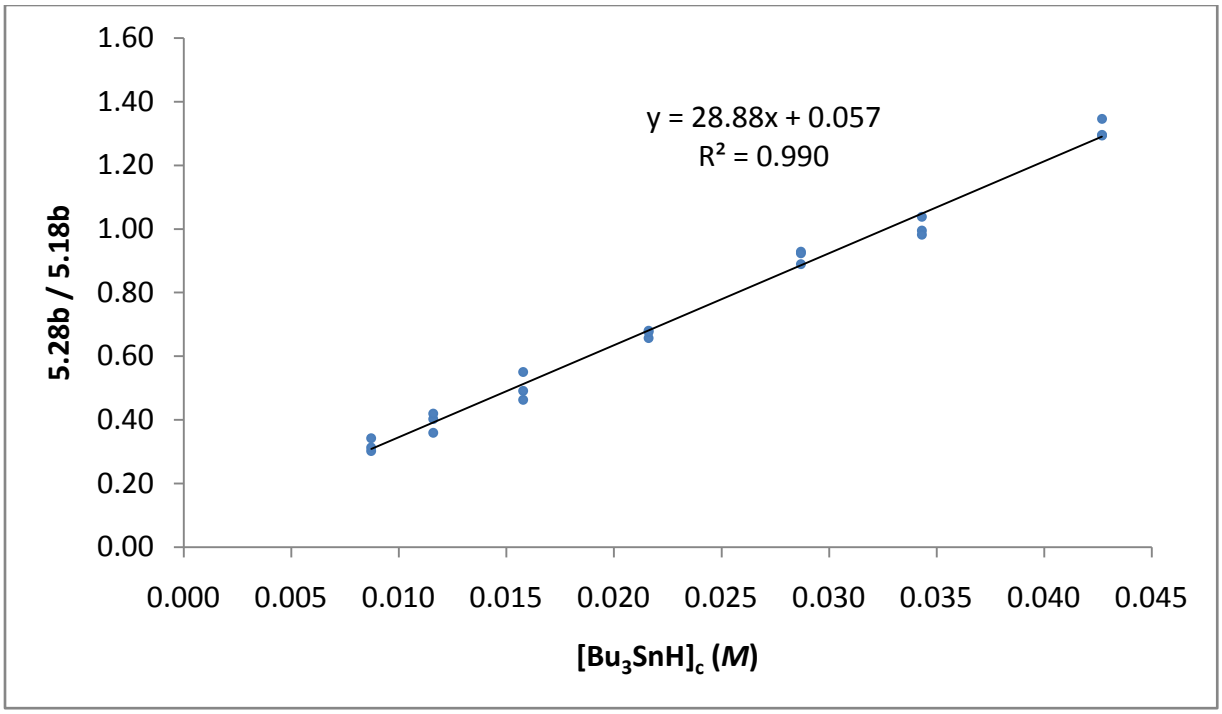

Figure 5.2 Kinetic Competition Plot of 5.17b

We calculated the cyclization rate constant k_C from the data in the kinetic plot. Because primary α-amidoyl radicals undergo reduction by Bu_3SnH at the same rate as primary alkyl radicals,[242] the rate constant for reduction of **5.29** at room temperature was taken to be k_H = 2.31

x 10^6 $M^{-1}s^{-1}$ based on existing rate data.[65,66] From this value and the slope of the kinetic plot, the rate constant for cyclization of radical **5.29** was calculated to be k_C = 8.0 x 10^4 s^{-1}. This cyclization is over an order of magnitude faster than the all-carbon 6-*exo-trig* cyclization of the 6-heptenyl radical (k_C = 5.0 x 10^3 s^{-1} at 298 K),[4,17,243] and is slightly faster than the 5-*endo-trig* cyclization of **1.22** from Chapter 1.1.2 (k_C = 1.9 x 10^4 s^{-1} at 298 K).[3] These findings are in line with the 5-*endo* / 6-*exo* competition experiments of Parsons (Scheme 5.3).[230]

The slightly positive value of the intercept in the kinetic plot raises the possibility that the cyclization may be reversible. The value of the intercept[63] in Figure 5.2 is equal to ($k_H \cdot k_{-C}$)/($k_C \cdot k_H'$) where k_{-C} is the rate constant of ring opening of **5.30** and k_H' is the rate constant for Bu_3SnH reduction of **5.30**, which is taken to be k_H' = 1.47 x 10^6 s^{-1} based on measurements by Chatgilialoglu.[65,66] Using these values, we calculated a ring opening rate constant for **5.30** of k_{-C} = 2.9 x 10^3 s^{-1}, almost 30 times slower than cyclization. Further experiments would be needed to verify the reversibility of 6-*exo-trig* cyclization in the reaction of **5.17b**.

5.2.4 Resolution of Substrates

In order to perform chirality transfer experiments, enantioenriched samples of **5.17a-c,e-f,h-i** were obtained by resolution on semipreparative chiral HPLC. Typically, samples of **5.17** were dissolved in *i*-PrOH, and injected onto either a Chiralcel OD or (*S*,*S*)-Whelk-O 1 column (25.0 cm x 21.1 mm ID) eluting with a hexane:*i*-PrOH solvent mixture. A hexane:EtOAc solvent system was used for **5.17h** because of complete insolubility in *i*-PrOH. Depending on the ease of separation, a 40–120 mg sample of racemic **5.17** was resolved per injection. After fraction collection and solvent removal, the enantiomeric ratios of the resolved compounds were

measured by analytical chiral HPLC. Most compounds were recovered in > 97% ee, and all resolved compounds were stored in a freezer to avoid racemization.

Most compounds were resolved without difficulty; however, the rotational dynamics of *N*-methyl congener **5.17a** led to complications. Iodide **5.17a** exists as a 14:1 *E*:*Z* ratio of amide rotamers which are visible by TLC analysis but not isolable under ambient laboratory conditions. Analytical HPLC (Whelk, 80:20 hexanes:*i*-PrOH, 1 mL/min) showed a small peak at 10.5 min, followed by two large peaks at 14.5 min and 18.5 min that were nearly equal in area. HPLC analysis of the resolved fractions allowed us to interpret the chromatogram of racemic **5.17a**. The peak at 10.5 min is the minor amide rotamer of (–)-**5.17a**, and the major amide rotamer of (+)-**5.17a** elutes at 14.5 min. The minor amide rotamer of (+)-**5.17a** and the major amide rotamer of (–)-**5.17a** overlap at 18.1 min. A plateau between the minor and major amide rotamer peaks of each enantiomer indicates slow interconversion at room temperature, and therefore a larger barrier to amide rotation than is typical ($\Delta G^{\ddagger}_{rot} \approx$ 22-23 kcal/mol).[50] While this introduced difficulties into determining the er of resolved **5.17a**, the relatively small proportion of the minor rotamer (6.7%) should keep the error at a reasonable amount.

After resolution, four substrates (**5.17b**, **5.17c**, **5.17f**, **5.27c**) were chosen for racemization studies to measure their respective barriers to *N*-aryl bond rotation. As described in Chapter 3.2.4, enantioenriched samples were dissolved in a 90:10 hexane:*i*-PrOH solvent mixture, and heated in a sealed tube at an appropriate temperature. The racemization was monitored by periodically measuring the er of aliquots of the solution by analytical chiral HPLC. Racemization data is available in the Experimental section (Chapter 6.6).

The barrier to rotation of *o*-methyl substrate **5.17b** was surprisingly high, with a $\Delta G^{\ddagger}_{rot}$ = 34.3 kcal/mol (143.7 kJ/mol). The *o*-Br substrate **5.17f** had an essentially similar barrier of 34.2

kcal/mol (142.9 kJ/mol), a result in line with previous observations.[108,132] The barrier to rotation of *o*-methoxy substrate **5.17c** was rather low, with $\Delta G^{\ddagger}_{rot}$ = 26.3 kcal/mol (109.9 kJ/mol). The experimental 8.0 kcal/mol barrier difference between **5.17b** and **5.17c** is significantly larger than that predicted by Sternhell's biphenyl model,[244] which predicts a 2.3 – 3.8 kcal/mol difference. Finally, replacing the α-iodine atom with a chlorine atom in **5.27c** led to only a 1.0 kcal/mol lowering of the barrier (Figure 5.3). The barriers to rotation are high enough that the enantioenriched iodides can all be handled at ambient temperature without rapid racemization; *o*-methoxy substrate **5.17c**, however, is much less stable and should be kept from sources of heat to avoid loss of enantiopurity.

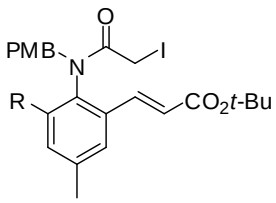

5.17b (R = Me)
34.3 kcal/mol at 140 °C
$t_{1/2}$ at 25 °C = 25,200 years

5.17f (R = Br)
34.2 kcal/mol at 143 °C
$t_{1/2}$ at 25 °C = 21,400 years

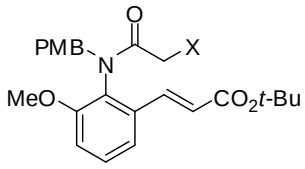

5.17c (X = I)
26.3 kcal/mol at 55 °C
$t_{1/2}$ at 25 °C = 12 days

5.27c (X = Cl)
25.3 kcal/mol at 52 °C
$t_{1/2}$ at 25 °C = 2.4 days

Figure 5.3 Barriers to Rotation and Half-Lives of Racemization for α-Haloacetamides

5.2.5 Chirality Transfer in 6-*Exo*-*trig* Cyclizations

Enantioenriched samples of **5.17a-c,e-f,h-i** were subjected to optimized reaction conditions for reductive cyclization. The cyclized products were isolated by column chromatography, and enantiopurities were determined by analytical chiral HPLC with comparison to racemic material. The results of this series of experiments are shown in Table 5.4. Both enantiomers of each substrate were tested, and resulted in similar chirality transfers within experimental error. Isolated yields of each reaction were comparable to yields of reactions with racemic substrate (Table 5.2) in each case. *N*-Methyl substrate **5.17a** cyclized with 92-99%

chirality transfer (Entries 1-2). *N*-PMB substrates **5.17b-f** with a terminal ester acceptor consistently cyclized to **5.18b-f** with chirality transfers of 94-96% (Entries 3-10) regardless of *ortho* substituent. Substrate **5.17h**, containing a terminal nitrile substituent, also cyclized to **5.18h** with excellent chirality transfer of 93-97% (Entries 11-12). Compound **5.17i** gave **5.18i** in modest chirality transfer of 80-81% (Entries 13-14), likely reflecting a longer time for the intermediate radical to racemize before the slower cyclization occurs. These values of chirality transfer are comparable to those observed in room temperature cyclizations of *N*-allyl-*o*-iodoacetamides (74-97%)[105] and *N*-acryloyl-*o*-iodoanilides (49-94%).[108]

Table 5.4 Chirality Transfer in Cyclizations of 5.17a-i

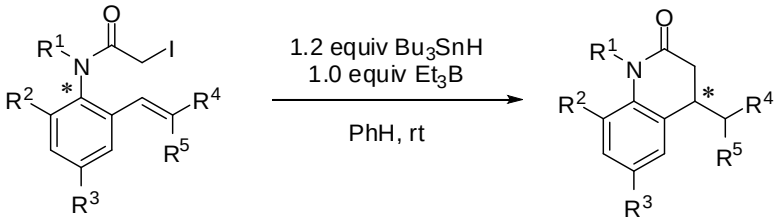

5.17a-i **5.18a-i**

entry	precursor	R^1	R^2	R^3	R^4	R^5	er	cond.[a]	product	% yield[b]	er	% ct[d]
1	(+)-**5.17a**	Me	Me	Me	CO_2t-Bu	H	98.5/1.5	A	(–)-**5.18a**	79	91/9	92
2	(–)-**5.17a**	Me	Me	Me	CO_2t-Bu	H	85/15	A	(+)-**5.18a**	81	84/16	99
3	(+)-**5.17b**	PMB	Me	Me	CO_2t-Bu	H	100/0	A	(–)-**5.18b**	87	95/5	95
4	(–)-**5.17b**	PMB	Me	Me	CO_2t-Bu	H	100/0	A	(+)-**5.18b**	85	96/4	96
5	(+)-**5.17c**	PMB	OMe	H	CO_2t-Bu	H	99/1	A	(–)-**5.18c**	94	93/7	94
6	(–)-**5.17c**	PMB	OMe	H	CO_2t-Bu	H	99/1	A	(+)-**5.18c**	96	93/7	94
7	(+)-**5.17e**	PMB	TMS	Me	CO_2t-Bu	H	100/0	A	(+)-**5.18e**	95	95/5	95
8	(–)-**5.17e**	PMB	TMS	Me	CO_2t-Bu	H	100/0	A	(–)-**5.18e**	93	94/6	96
9	(*P*)-**5.17f**[c]	PMB	Br	Me	CO_2t-Bu	H	99/1	A	(*S*)-**5.18f**[c]	63	95/5	96
10	(*M*)-**5.17f**[c]	PMB	Br	Me	CO_2t-Bu	H	0/100	A	(*R*)-**5.18f**[c]	66	94/6	94
11	(+)-**5.17h**	PMB	Me	Me	CN	H	99.5/0.5	C	(–)-**5.18h**	71	93/7	93
12	(–)-**5.17h**	PMB	Me	Me	CN	H	99/1	C	(+)-**5.18h**	68	96/4	97
13	(+)-**5.17i**	PMB	Me	Me	Me	Me	99/1	A	(+)-**5.18i**	57	80/20	81
14	(–)-**5.17i**	PMB	Me	Me	Me	Me	0/100	A	(–)-**5.18i**	55	80/20	80

[a] Conditions A: Bu_3SnH and Et_3B in 20 mL PhH were added over 2 h via syringe pump to a stirred 10 mM PhH solution of iodide. C: neat Bu_3SnH and Et_3B were added sequentially in one portion to a stirred PhH solution of iodide with $[Bu_3SnH]_i$ = 5 mM. [b] Yield of **5.18** after isolation by column chromatography on 10% w/w KF/silica gel. [c] Absolute stereochemistry determined by X-ray crystallography. [d] Percent chirality transfer.

5.2.6 Crystal Structures of a Precursor / Product Pair and Model of Chirality Transfer

To propose a model for chirality transfer, the absolute configurations of an enantioenriched precursor **5.17f** and its product **5.18f** were determined. Because **5.17f** exists as a non-crystallizable semisolid as either a racemate or a single atropisomer, conversion to a suitable derivative was necessary. To this end, a sample of (+)-**5.17f** (99/1 er) was treated with TFA in CH_2Cl_2 to cleave the *t*-butyl ester, producing solid α,β-unsaturated acid (+)-**5.31** in 71% yield (Figure 5.4).[240] This acid was crystallized by the slow vapor diffusion method, by first dissolving (+)-**5.31** in ethyl acetate and allowing hexanes to diffuse into this solution. The crystal structure was solved by Dr. Steven Geib, and the absolute configuration was determined by using the anomalous scattering method.[245,246]

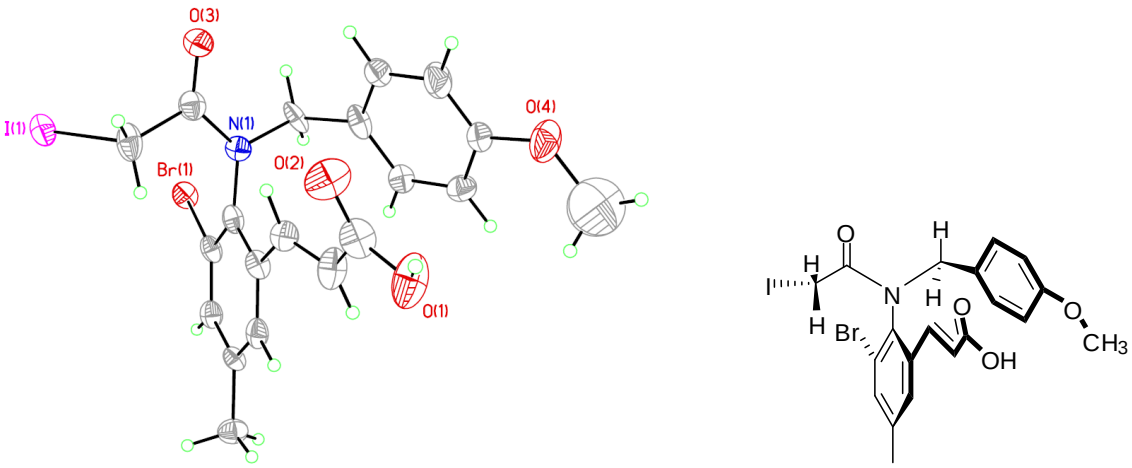

Figure 5.4 ORTEP Diagram of (*P*)-5.31

Acid (+)-**5.31** crystallized with four unique molecules in the unit cell, as two pairs of dimers displaying hydrogen bonding between the carboxylic acid groups. The differences in geometries between the four structures are small, and consist of different dihedral angles between either the PMB methoxy group and the aromatic ring, or the carbon-iodine single bond

with the double bond of the carbonyl group. For simplicity, only one of the four molecules is shown in Figure 5.4.

In this structure, the plane of the aromatic ring is almost completely orthogonal to the plane of the amide, with a torsion angle of 83.4°. The olefin acceptor exists in the *s*-trans conformation, and is twisted slightly out of planarity with the aromatic ring (torsion angle = 156.2°). Interestingly, the *N*-PMB group is twisted to the same side of the molecule as the α,β-unsaturated carboxylic acid function, with their planes nearly parallel. This can possibly be attributed to π-π stacking[247] between the electron-rich aromatic ring and the electron-deficient olefin. The 3.32–3.86 Å distance range between the two quasi-parallel planes is ideal for this interaction.[248] The other three unique structures in the crystal lattice displayed similar characteristics for these molecular features, and most importantly, all possess the same absolute configuration, allowing us to assign (+)-**5.17f** as (*P*).

Although racemic and enantioenriched **5.18f** were originally isolated as oils, (+)-**5.18f** (Table 5.4, Entry 9) spontaneously solidified upon standing. Slow vapor-phase diffusion in a $CHCl_3$ / hexane solvent system produced crystals of **5.18f** suitable for X-ray crystallography. This structure was also solved by Dr. Geib, and is shown in Figure 5.5. Due to the presence of the bromine heavy atom, the anomalous scattering method allowed us to determine the absolute stereochemistry of (+)-**5.18f** as (*S*).

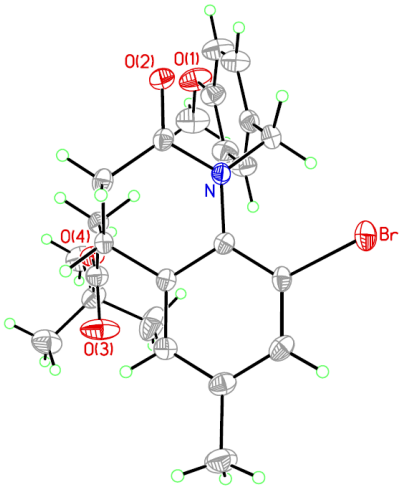

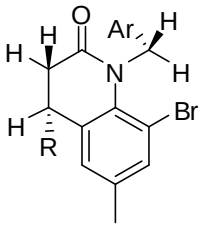

Ar = *p*-methoxyphenyl
R = -CH_2CO_2t-Bu

Figure 5.5 ORTEP Diagram of (*S*)-5.18f

Based on these results, a model of chirality transfer for the formation of (*S*)-**5.18f** from (*P*)-**5.17f** was put forth, shown in Scheme 5.8. Iodine abstraction by a tributyltin radical produces α-amidoyl radical **5.32**. While the *N*-aryl bond rotates to bring the olefin acceptor into proximity with the radical, a slight aryl-olefin bond rotation allows the double bond to twist towards the radical, resulting in cyclized intermediate **5.33**. Reduction of **5.33** produces cyclized product (*S*)-**5.18f**.

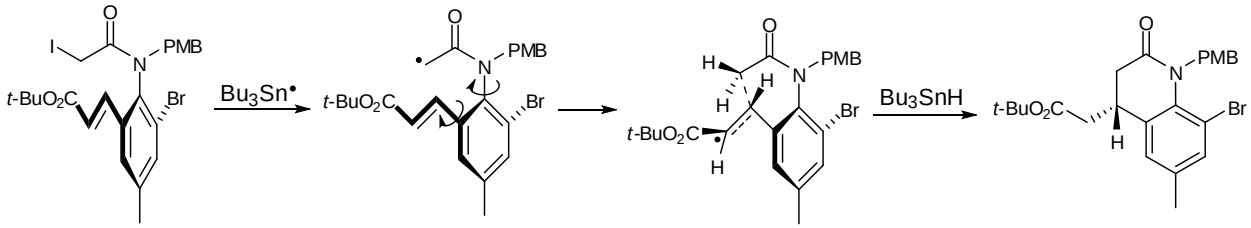

(*P*)-**5.17f** **5.32** **5.33** (*S*)-**5.18f**

Scheme 5.8 Model of Chirality Transfer for 6-*Exo-trig* Cyclizations

Unfortunately, there is no correlation between the optical rotation sign or HPLC elution order of substrates **5.17a-i** and the respective products of cyclization **5.18a-i**. Because no clear

pattern exists, the absolute configuration of the remaining precursor/product pairs cannot currently be determined.

5.2.7 Preparation and Chirality Transfer of a Secondary Radical Precursor

Encouraged by the excellent chirality transfer seen in cyclizations of primary α-iodoanilides, we extended our efforts toward secondary radical precursors to explore the potential for diastereoselectivity. Substrates **5.34a-b** were prepared by treating **5.26c** with 2-bromopropionyl bromide and Et_3N, producing two diastereomers **5.34a** (less polar) and **5.34b** (more polar) which were separable by column chromatography (Scheme 5.9). Attempts to convert these compounds to suitable crystalline derivatives were unsuccessful, and NMR spectroscopy was not informative enough to unambiguously assign the relative stereochemistry. Because halogen abstraction from **5.34a-b** destroys the α-stereocenter,[4,17] leaving only the *N*-aryl axis to influence chirality transfer, further examination of the relative stereochemistry of **5.34a-b** was not undertaken.

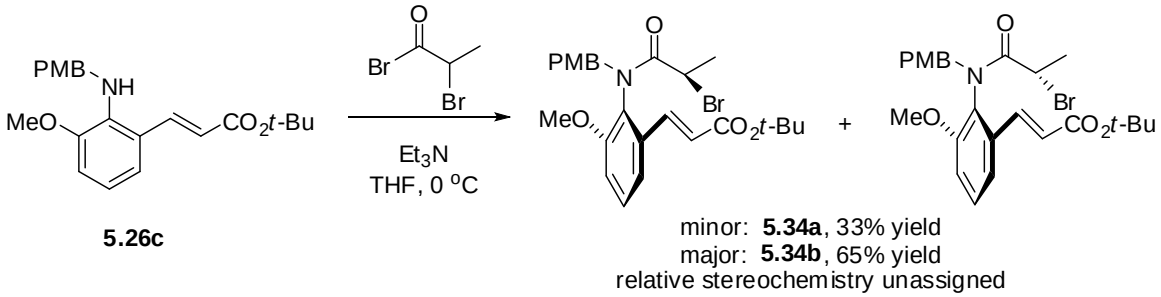

Scheme 5.9 Preparation of a Secondary Radical Precursor

Racemic samples of **5.34a-b** were reacted with Bu_3SnH and Et_3B at room temperature, according to the optimized syringe pump conditions, as seen in Table 5.5 (Entries 1-2). Both diastereomers gave the same product **5.35** in excellent yield (95-97%), and only one

diastereomer of the expected product was isolated. Samples of **5.34a-b** were also resolved by chiral HPLC, and the enantioenriched substrates were subjected to the same reaction conditions (Entries 3-6). Yields were reproducibly high (96-98%), and chirality transfers were even higher than those observed for the primary α-amide radical precursor series, at least 99% in all cases.

Table 5.5 Cyclizations of a Secondary Radical Precursor

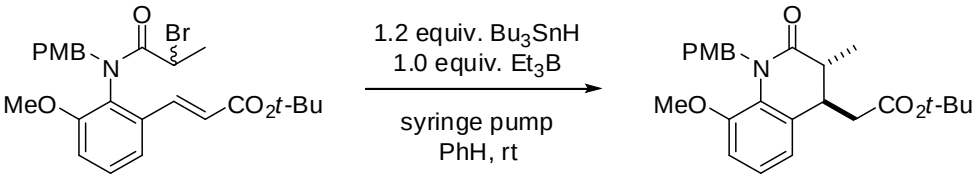

5.34a-b **5.35**

entry	substrate	er	product	% yield[a]	er	% chirality transfer
1	*rac*-**5.34a**	50/50	*rac*-**5.35**	95	50/50	--
2	*rac*-**5.34b**	50/50	*rac*-**5.35**	97	50/50	--
3	(+)-**5.34a**	98/2	(+)-**5.35**	98	98/2	100
4	(–)-**5.34a**	99/1	(–)-**5.35**	96	98/2	99
5	(+)-**5.34b**	100/0	(–)-**5.35**	98	99/1	99
6	(–)-**5.34b**	100/0	(+)-**5.35**	97	99.5/0.5	99.5

[a] Yield after isolation by column chromatography on 10% w/w KF/silica gel.

The product **5.35** was assigned with *trans* stereochemistry based on the transition state analysis shown in Scheme 5.10. Halogen abstraction from either diastereomer of **5.34** produces a mixture of α-amide radicals s-*cis*-**5.36** and s-*trans*-**5.36**, which interconvert by rotation of the C_α-carbonyl single bond. While s-*cis*/s-*trans* interconversion in **5.36** is relatively slow,[249] with $k_{rot} = 2.0 \times 10^4\ s^{-1}$, the slow rate of 6-*exo*-*trig* cyclization may allow time for thermodynamic equilibration to the favored s-*cis*-**5.36** conformer.[4] Cyclization of s-*cis*-**5.36** proceeds through transition state **5.37a**, which minimizes strain between the substituents and leads to the observed product **5.35**. Transition state **5.37b** is significantly less favored due to steric hindrance between the methyl group and the radical acceptor, and thus *cis*-disubstituted **5.38** is not formed in

appreciable amounts. The results continue an established trend; preferential-to-exclusive formation of *trans* products has also been observed in 4-*exo*-*trig*[250] and 5-*exo*-*trig*[251-253] cyclizations of substituted α-amidoyl radicals.

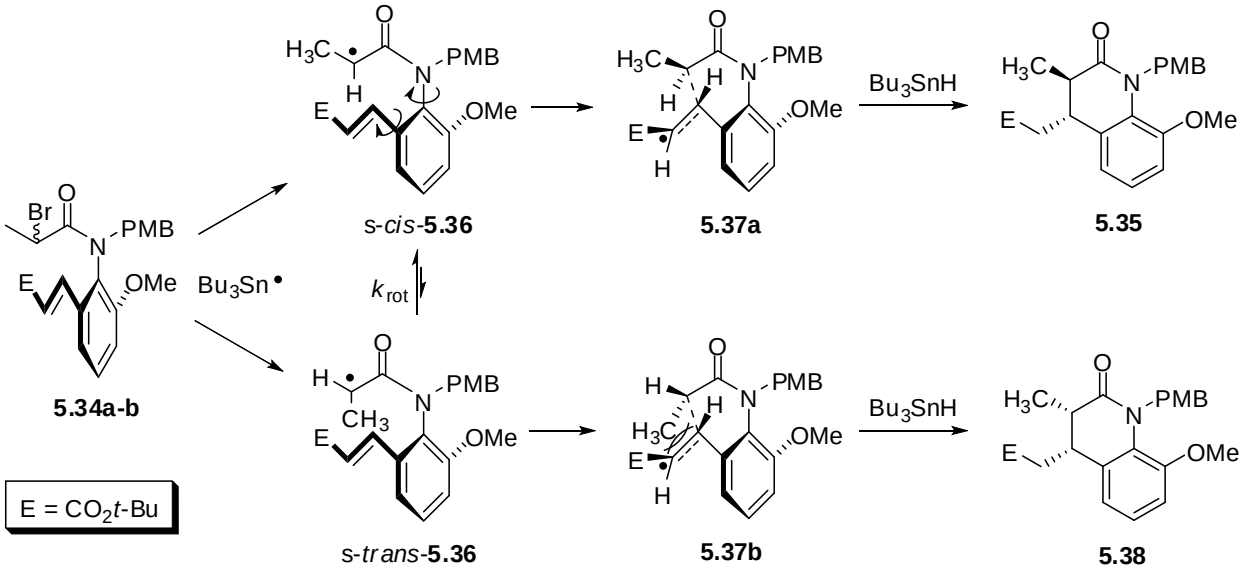

Scheme 5.10 Assignment of Configuration by Transition State Analysis

5.2.8 Preparation and Chirality Transfer of a Tandem Cyclization Precursor

Given our success with the reaction of **5.34**, we envisioned incorporating the highly diastereoselective 6-*exo*-*trig* cyclization into a tandem radical sequence. Cyclizations often proceed with high levels of diastereoselectivity when the radical and alkene acceptor are connected by a pre-formed ring.[4]

Scheme 5.11 illustrates the synthesis of tandem precursors **5.40a-b**. Racemic 2-aminopentenoic acid underwent diazotization of the amine, followed by bromine substitution, to produce α-bromoacid **5.39** in 58% yield. Acid **5.39** was converted to the acid chloride, which was added to **5.26c** followed by Et_3N, producing **5.40a** (35% yield) and **5.40b** (39% yield) as

diastereomers separable by column chromatography. The order of addition was crucial in this reaction: when Et_3N was added to **5.26c** before the acid chloride was introduced, the starting aniline was recovered unchanged. As with **5.34a-b**, the configurations of **5.40a-b** were not assigned.

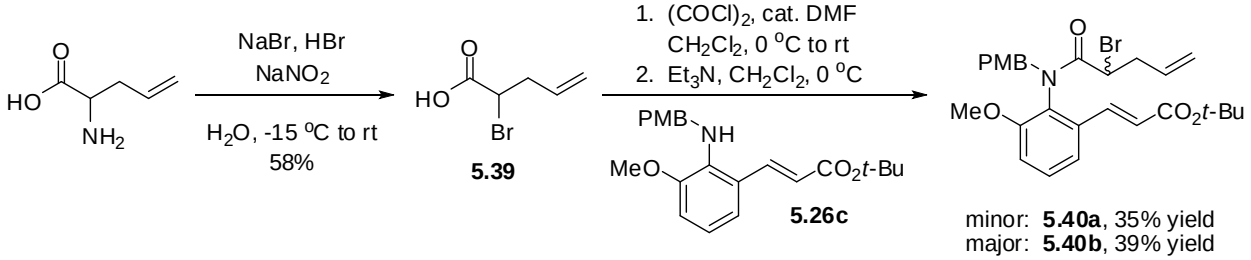

Scheme 5.11 Synthesis of a Tandem Precursor

Racemic **5.40a** was treated with Bu_3SnH under syringe pump conditions at room temperature (Table 5.6, Entry 1). After column chromatography, tricyclic product *rac*-**5.41** was isolated in 51% yield as a single diastereomer. Column fractions containing minor products, inseparable from one another, were also collected and comprised 30% of the mass balance. This mixture of side products contained, among other unidentified compounds, two minor diastereomers of the 6-*endo*-*trig* / 5-*exo*-*trig* sequence, as evidenced by two distinct doublets in the upfield region denoting the respective methyl signals of the diastereomers. Enantiopure samples of **5.40b** were accessed by resolution with chiral HPLC, and were also subjected to the reaction conditions (Entries 2-3). These reactions provided the same diastereomer of **5.41** in similar yields and excellent chirality transfer (98-99%). The final products of these reactions were contaminated by small amounts (~5%) of the minor cyclized products after purification as determined by ^{1}H NMR.

Table 5.6 Cyclization of a Tandem Radical Precursor

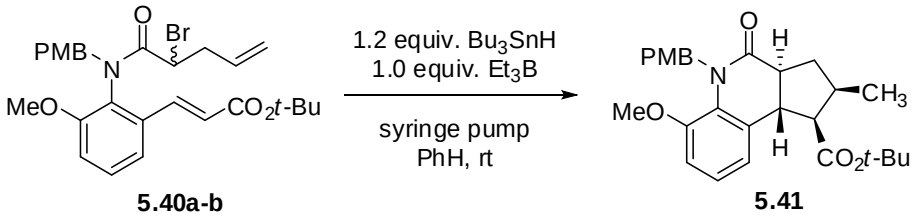

5.40a-b **5.41**

entry	substrate	er	product	% yield[a]	er	% chirality transfer
1	*rac*-**5.40a**	50/50	*rac*-**5.41**	51	50/50	--
2	(+)-**5.40b**	100/0	(–)-**5.41**	51[b]	99/1	99
3	(–)-**5.40b**	100/0	(+)-**5.41**	49[b]	98/2	98

[a] Yield after isolation by column chromatography on 10% w/w KF/silica gel. [b] 95% diastereomeric purity.

The assignment of the ring fusion **5.41** as *trans* was based on the 14.1 Hz coupling constant between the α-lactam and benzylic protons, indicating a nearly 180° dihedral angle between these protons.[254] The remaining stereocenters were unambiguously determined by X-ray crystallography. A $CDCl_3$ sample containing racemic **5.41**, upon slow evaporation, produced single crystals suitable for analysis. The structure, which was solved by Dr. Steve Geib, is shown in Figure 5.6.

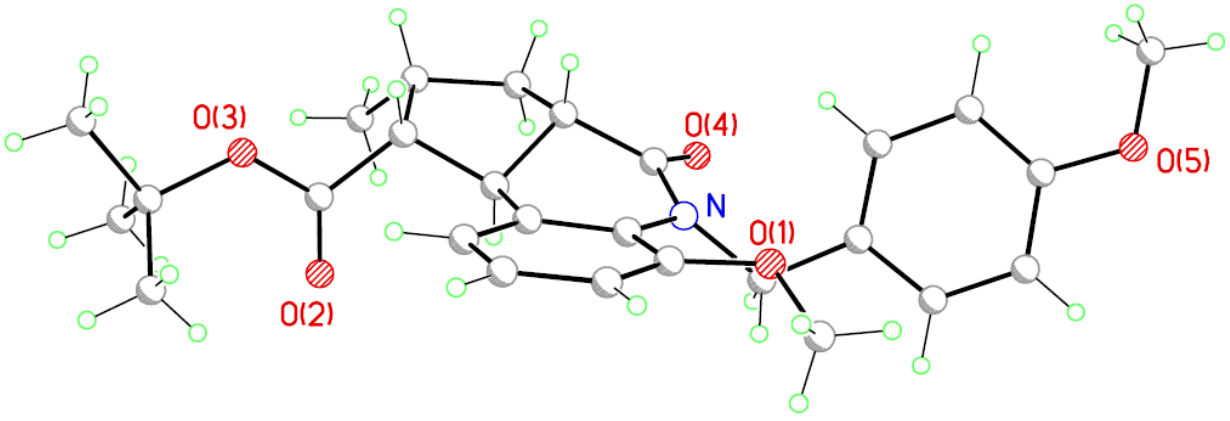

Figure 5.6 Crystal Structure of *rac*-5.41

The transition state analysis for formation of **5.41** is shown in Scheme 5.12. Reaction of either diastereomer of **5.40a-b** with tributyltin radical produces α-amide radical **5.44** in the s-*cis* geometry. This radical is unlikely to undergo 3-*exo-trig* cyclization onto the pendant terminal olefin. 3-exo-trig cyclization in the parent 3-butenyl system **5.42** is slow (k_C = 9 x 10^3 s^{-1}), and the reverse ring opening of the resulting cyclopropylmethyl radical **5.43** is fast enough (k_{open} > 1 x 10^8 s^{-1}) that **5.42** exists almost exclusively in the open-chain form.[17,63,255-259] As discussed in Section 5.2.7, **5.44** cyclizes with *trans* selectivity through transition state **5.45**, forming α-ester radical **5.46**.

The final 5-*exo-trig* cyclization occurs in accordance with the Beckwith-Houk model; the four possible transition states **5.46** are shown in Scheme 5.12.[4,260,261] The major product **5.41** arises from chair-equatorial-**5.46**, which minimizes steric strain. Because the ester substituent is relatively small, eclipsing interactions between it and the olefin are minimal. Boat-equatorial-**5.46** and chair-axial-**5.46** transition states are higher in energy due to unfavorable gauche interactions, and produce a *trans* relationship between the methyl and ester functionalities in the product. The resulting products of these transition states, **5.47** and **5.48**, could be the minor products seen during purification of the reaction mixture. Finally, **5.49** could potentially be formed through the boat-axial conformation; however, this transition state is high enough in energy that **5.49** will likely not be formed.

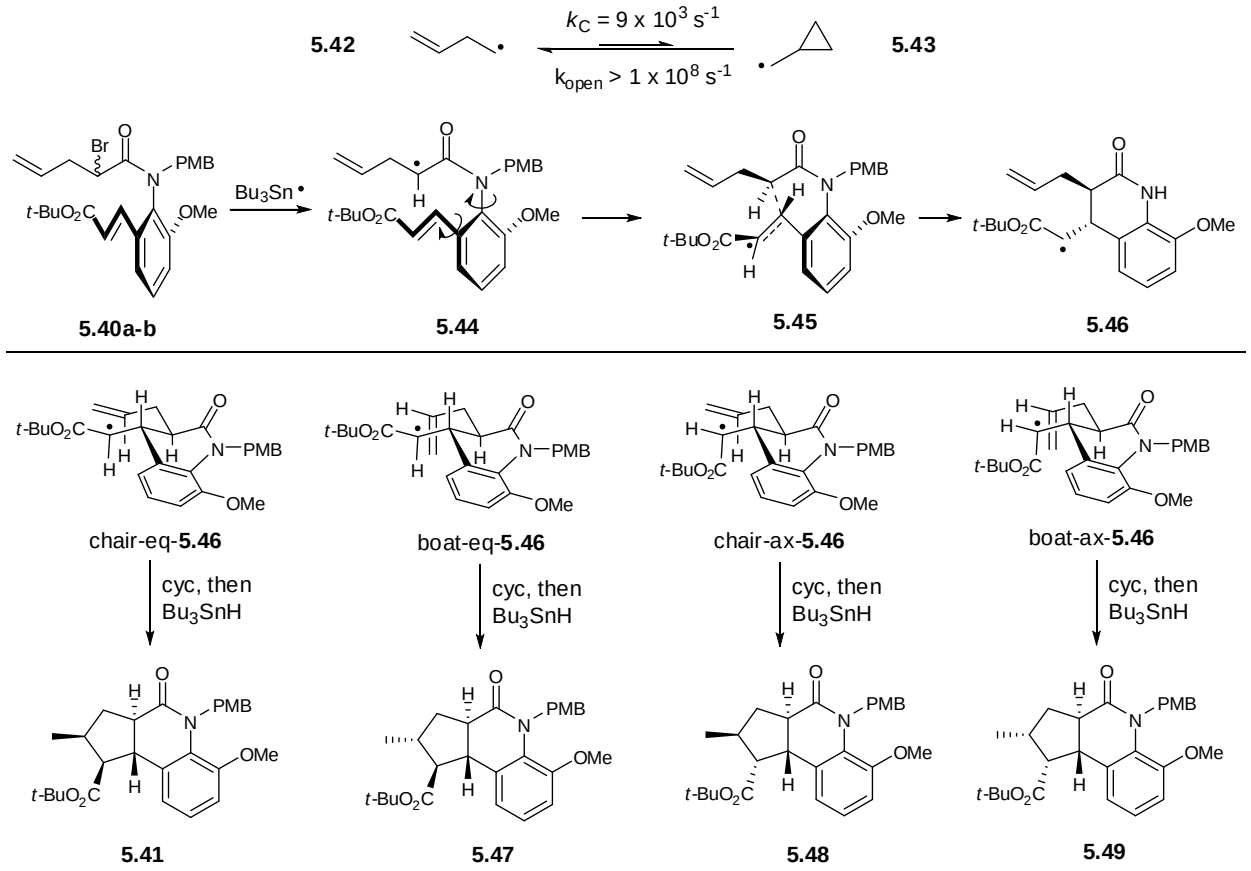

Scheme 5.12 Transition State Analysis of Tandem Cyclization

The excellent enantio- and diastereoselectivities of this tandem reaction hold great promise for future exploration. Further development of this methodology could provide swift access to the ring system of the *Melodinus* alkaloids (Figure 5.7).[262-265]

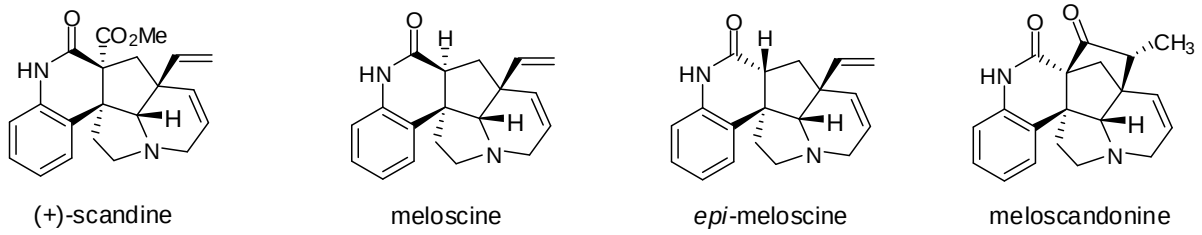

Figure 5.7 *Melodinus* Alkaloids

5.2.9 Conclusions

Axially chiral α-haloamides in which an *ortho*-substituent is a radical acceptor are easily prepared and resolved. The radical cyclizations of these α-haloamides to dihydroquinolin-2-ones proceed in high yields and with high levels of chirality transfer (80-100%). A model of chirality transfer has been determined by absolute configuration determination of a substrate / product pair by X-ray crystallography. Secondary α-haloamides, upon cyclization, faithfully do so with exclusively *trans* selectivity. This methodology has been applied to a tandem 6-*exo-trig*/5-*exo-trig* radical cyclization, which proceeds with good diastereo- and enantioselectivity.

6.0 EXPERIMENTAL

6.1 GENERAL INFORMATION AND PROCEDURES

All reactions were performed in oven-dried glassware under an argon atmosphere, except where noted. Chemicals and solvents were purchased from commercial suppliers and used as received, excepting as follows. Dichloromethane, THF, ether, and toluene were dried by passing through an activated alumina column. When necessary, DMF, MeCN, and H_2O were degassed by sparging with Ar for at least 2 h. Benzene was also degassed when necessary by the freeze-pump-thaw method (at least 5 cycles). Trimethylsilyl chloride (TMSCl) was distilled over CaH_2 before use. Solutions of BuLi were titrated regularly against diphenylacetic acid in THF. Benzyltriethylammonium dichloroiodate was prepared as described in the literature.[185]

All reactions were followed by TLC to completion, unless stated otherwise. TLC analysis was performed by illumination with a UV lamp (254 nm) or staining with $KMnO_4$ and heating. All flash chromatography was performed with 230-400 mesh silica gel purchased from Sorbent Technologies as the stationary phase. "Gradient column chromatography" refers to packing the column with the initial eluent, and initially filling the solvent reservoir with ~4 column volumes of the initial eluent. After elution of one column volume, the solvent reservoir is refilled with the second eluent. This process is continued after every eluted column volume until the final compound has completely eluted.

^{1}H NMR spectra were measured on a Bruker Avance 300 MHz instrument in $CDCl_3$, and chemical shifts were measured relative to residual solvent peak (δ 7.27). The following abbreviations were used to describe coupling: s = singlet, d = doublet, t = triplet, q = quartet, m = multiplet, br = broad. ^{13}C NMR spectra were measured on Bruker Avance instruments at 75 MHz with chemical shifts relative to residual solvent peak (δ 77.0). In ^{13}C spectra, a notation of (*x*C) is used to denote *x* equivalent carbons for a multi-carbon signal. In some compounds containing rotamers, complicated ^{13}C spectra were deconvoluted by comparison with DEPT-135 spectra to determine peaks corresponding to the major and minor rotamers.

IR spectra were recorded as thin films ($CHCl_3$) or neat on NaCl plates on a Nicolet Avatar 360 FTIR spectrometer. Melting ranges were determined using a Mel-Temp II apparatus and are uncorrected. Compounds listed as having a melting point at a single temperature had a sharp melting range of < 0.5 °C. Optical rotations were measured on a Perkin-Elmer 241 Polarimeter using a 1 dm cell length. All quoted optical rotation values are corrected for 100% ee samples, and have the units (deg cm^2 g^{-1}). Mass spectra were obtained on a VG-7070 or Fisons Autospec high-resolution magnetic sector mass spectrometer.

Analytical chiral HPLC analysis was conducted using either an (*S*,*S*)-Whelk-O 1 column (Pirkle, 250 mm x 4.6 mm ID) or a Chiralcel OD column (Daicel, 250 mm x 4.6 mm ID) typically eluting with hexanes:*i*-PrOH at 1.0 mL/min, 10-20 μg per injection. Analytical normal phase HPLC analysis was conducted using a Waters Nova-Pak Silica column (150 mm x 3.9 mm ID) eluting with hexanes:EtOAc at 1.0 mL/min, 10-20 μg per injection. Preparatory chiral HPLC resolutions were performed on either an (*S*,*S*)-Whelk-O 1 column (Pirkle, 25 cm x 21.1 mm ID) or a Chiralcel OD column (Daicel, 250 mm x 20.0 mm ID) eluting with hexanes:iPrOH at 10.0 mL/min, 40-150 mg per injection. All HPLC injections were monitored with a Waters

model 440 UV detector at wavelength 254 nm, when the solvent system was hexane:*i*-PrOH. In the cases where a hexane:EtOAc solvent system was used, the injections were monitored at wavelength 270 nm.

All gas chromatography analysis was performed with an Agilent 6850 GC under the following conditions: Initial oven temp. 100 °C, first ramp 10 °C/min to 250 °C, second ramp 15 °C/min to 315 °C, held at this temperature for 8 min. All GC yields were determined by calculation of response factors, using a straight-chain alkane internal standard. For each compound analyzed, three standard mixtures of a measured amount of the compound and a known amount of internal standard from a stock solution were analyzed by GC. Response factors were calculated using the equation:[266]

$$RF_X = \frac{M_{IS} \cdot A_X}{A_{IS} \cdot M_X}$$

RF_X = response factor of compound X

M_{IS} = moles of internal standard

M_X = moles of compound X

A_{IS} = area of internal standard GC peak

A_X = area of compound X GC peak

For each compound X, the three trials were graphed with the M_{IS}/M_X value on the y-axis, and the corresponding A_{IS}/A_X value on the x-axis. The slope of the line was taken to be the RF_X value. All compounds gave excellent linear plots with intercepts ≈ 0, showing that the response factor for each compound was consistent over varying molar ratios of compound to internal standard.

6.2 COMPOUND DATA FOR CHAPTER 1

Experimental procedures and spectroscopic data have been previously reported in the literature for compounds **1.15a-c**,[16] **1.16**,[8,16] **1.17**,[6,16] **1.18**,[6,16] **1.19**,[8,16] **1.34**,[267] **1.35**,[268,269] **1.36**,[270] **1.41**,[10] **1.46a**,[26] **1.48**,[26] **1.49**,[26] **1.51**,[26] and **1.52**.[26] These procedures were followed, and the products' physical properties and spectroscopic data were consistent with those previously reported, except as outlined below. Compounds **1.29-1.32** were synthesized in the labs of Dr. Andrew Clark at the University of Warwick, and were graciously donated to us.

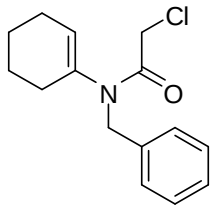

***N*-Benzyl-2-chloro-*N*-cyclohex-1-enylacetamide (1.15a):** The literature procedure[16] was followed: benzylamine (3.21 g, 30.0 mmol) and cyclohexanone (2.94 g, 30.0 mmol) were condensed in refluxing toluene (150 mL) for 4 h. The crude imine was *N*-acylated (again, following the literature procedure) using chloroacetyl chloride (6.78 g, 60.0 mmol), and *N*,*N*-diethylaniline (13.43 g, 90.0 mmol) as the base instead of Et_3N. After workup, chromatography on silica gel (hexanes:Et_2O 5:2) gave the title compound (42%) as a white solid, mp 92-93 °C (previously reported as an oil). Spectroscopic data was consistent with the previously reported results.[16]

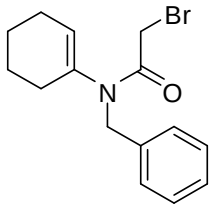

***N*-Benzyl-2-bromo-*N*-cyclohex-1-enylacetamide (1.15b)**: The literature procedure[16] was followed: benzylamine (1.07 g, 10.0 mmol) and cyclohexanone (0.98 g, 10.0 mmol) were condensed in refluxing toluene (50 mL) for 4 h. The crude imine was *N*-acylated (again, following the literature procedure) with bromoacetyl bromide (2.20 g, 11.0 mmol) and triethylamine (2.97 g, 30.0 mmol). After workup, chromatography on silica gel (hexanes:Et_2O 5:2) gave the title compound (23%) as a white solid, mp 35-36 °C (previously reported as an oil). Spectroscopic data was consistent with the previously reported results.[16]

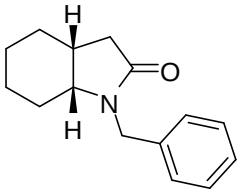

***rac*-*N*-Benzyl-*cis*-octahydroindol-2-one (1.16):** Solid 95% NaH (29 mg, 1.2 mmol) was slurried with THF (1.0 mL) and cooled to 0 °C. Octahydroindolone **1.34**[267] (139 mg, 1.0 mmol, > 95% purity by ^{1}H NMR) was dissolved in THF (1.0 mL) and added dropwise to the stirred reaction mixture. Stirring continued for another 30 min, at which point a solution of benzyl bromide (205 mg, 1.2 mmol) in THF (1.0 mL) was added dropwise to the reaction mixture. The ice bath was removed, and the mixture was stirred at room temperature for 3 h before being quenched with sat. aq. NH_4Cl (5 mL). The mixture was extracted with CH_2Cl_2 (3 x 10 mL), and the combined organic layers were dried over $MgSO_4$, filtered, and solvent was evaporated. The crude residue was chromatographed (2:1 hexanes:EtOAc) to afford 144 mg of the title compound

as a colorless oil (45% yield over 2 steps from 2-oxindole). Spectroscopic data matched previously reported results.[16]

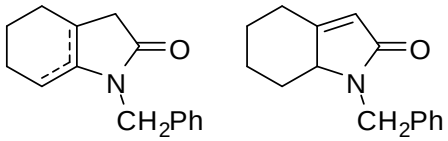

Intramolecular condensation of **1.36**: In a pressure tube, amide **1.36** (0.245 g, 1.0 mmol) and *p*-TsOH (3 mg, 0.016 mmol) were combined with *m*-xylene (2.0 mL) and a stir bar. The tube was tightly sealed with a screw cap, and heated at 180 °C for 2 h. The reaction mixture was cooled to room temperature, solvent was removed by rotary evaporation, and the crude residue was chromatographed (1:1 hexanes:Et_2O). The first eluting product **1.17** was collected as an inseparable mixture of olefin isomers (0.076 g, 33%): **1-benzyl-3a,4,5,6-tetrahydro-1*H*-indol-2(3*H*)-one** and **1-benzyl-4,5,6,7-tetrahydro-1*H*-indol-2(3*H*)-one** in a 2.3:1.0 ratio. These compounds were extremely sensitive to isomerization and interconverted rapidly to one another on silica gel. The second eluting compound, **1-benzyl-5,6,7,7a-tetrahydro-1*H*-indol-2(4*H*)-one** (**1.18**) was collected as a light yellow oil (0.119 g, 52% yield). Spectra were consistent with previously reported results.[6,16]

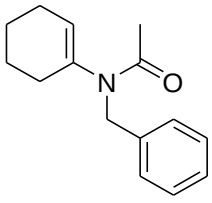

***N*-Benzyl-*N*-cyclohex-1-enylacetamide (1.19)**: Benzylamine (1.07 g, 10.0 mmol) and cyclohexanone (0.98 g, 10.0 mmol) were dissolved in toluene (50 mL) in a round-bottomed flask fitted with a Dean-Stark apparatus. The solution was refluxed for 3 h with azeotropic removal of

water, cooled to room temperature, and the reaction volume was reduced by half by rotary evaporation. The solution containing the crude imine was cooled to 0 °C, and a solution of acetyl chloride (1.18 g, 15.0 mmol) in toluene (50 mL) was added dropwise to the reaction mixture. After stirring for 2 h at this temperature, triethylamine (2.97 g, 30.0 mmol) was added dropwise to the reaction mixture, and stirring was continued for another 2 h at 0 °C. The reaction mixture was then washed with saturated $NaHCO_3$ (3 x 100 mL) and brine (3 x 100 mL) solutions, dried over $MgSO_4$, and solvent was removed by using rotary evaporation. Chromatography on silica gel (3:2 hexanes:Et_2O) gave the title compound (1.51 g, 66%) as a white solid, mp 50-51 °C (previously reported as an oil). Spectroscopic data was consistent with the previously reported results.[16]

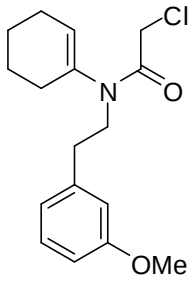

***N*-Cyclohex-1-enyl-2-chloro-*N*-(2-(3-methoxyphenyl)ethyl)acetamide (1.38a)**: A stirred solution of cyclohexanone (0.79 g, 8.0 mmol) and 3-methoxyphenethylamine (1.21 g, 8.0 mmol) in toluene (50 mL) was refluxed for 3 h in a round-bottomed flask fitted with a Dean-Stark apparatus. The reaction mixture was then cooled to room temperature, and the solvent volume was reduced by half by using rotary evaporation. The mixture containing the imine was added dropwise to a solution of chloroacetyl chloride (1.36 g, 12.0 mmol) in toluene (25 mL) at 0 °C. The reaction mixture was stirred for 2 h at 0°C, at which point *N*,*N*-diethylaniline (2.39 g, 16.0 mmol) was added dropwise, and stirring at 0 °C was continued for 2 h. The reaction was

quenched by addition of H_2O (100 mL), and the organic layer was washed with saturated aq. $NaHCO_3$ (3 x 50 mL) and brine (3 x 50 mL) solutions. The organic layer was dried over $MgSO_4$, concentrated by rotary evaporation, and chromatographed on silica gel (hexanes:EtOAc 3:1) to give the title compound (1.98 g, 80%) as a yellow oil: ^{1}H NMR (300 MHz, $CDCl_3$) δ 7.21 (t, *J* = 7.7 Hz, 1H), 6.83-6.74 (m, 3H), 5.62 (m, 1H), 4.09 (s, 2 H), 3.80 (s, 3H), 3.63 (t, *J* = 7.2 Hz, 2H), 2.85 (t, *J* = 7.9 Hz, 2H), 2.18-2.04 (m, 4H), 1.78-1.67 (m, 2H), 1.66-1.55 (m, 2H); ^{13}C NMR (75 MHz, $CDCl_3$) δ 165.3, 159.4, 140.0, 137.6, 129.1, 128.2, 120.8, 114.0, 111.6, 54.8, 47.3, 41.5, 33.6, 27.3, 24.4, 22.3, 21.1; FTIR (neat, cm^{-1}) 2935, 2837, 1655, 1603, 1402, 1043, 783; HRMS calcd for $C_{17}H_{22}NO_2Cl$ $[M]^+$: 307.1339, found: 307.1338.

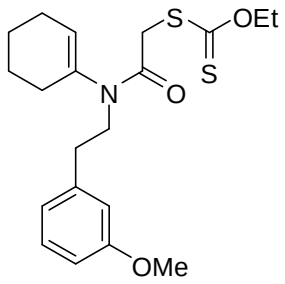

***N*-Cyclohex-1-enyl-2-(*O*-ethylxanthate)-*N*-(2-(3-methoxyphenyl)ethyl)acetamide (1.38b):** Enamide **1.38a** (616 mg, 2.0 mmol) was dissolved in dry MeCN (50 mL), and solid potassium *O*-ethyl xanthate (320 mg, 2.0 mmol) was added portionwise (approximately 0.1 equiv per addition) over 5 minutes. The mixture was stirred for 5 h, and then solvent was removed by rotary evaporation. The crude residue was partitioned between ether and water (25 mL each), and the aqueous layer was extracted with ether (3 x 25 mL). The combined organic layers were dried over $MgSO_4$, the solvent was evaporated, and the crude residue was chromatographed on silica gel (hexanes:EtOAc 3:1) to give the title compound (756 mg, 96%) as a viscous, light yellow oil: ^{1}H NMR (300 MHz, $CDCl_3$) δ 7.20 (t, *J* = 7.7 Hz, 1H), 6.83-6.74 (m,

3H), 5.66 (m, 1H), 4.65 (q, *J* = 7.1 Hz, 2H), 4.08 (s, 2H), 3.80 (s, 3H), 3.63 (t, *J* = 7.5 Hz, 2H), 2.85 (t, *J* = 7.8 Hz, 2H), 2.20-2.10 (m, 4H), 1.81-1.73 (m, 2H), 1.68-1.60 (m, 2H), 1.42 (t, *J* = 7.1 Hz, 3H); ^{13}C NMR (75 MHz, $CDCl_3$) δ 214.0, 165.6, 159.5, 140.3, 138.2, 129.2, 128.5, 121.0, 114.2, 111.7, 70.2, 55.0, 47.6, 39.6, 34.0, 27.6, 24.7, 22.6, 21.3, 13.7; FTIR (neat, cm^{-1}) 2935, 1649, 1601, 1055, 783; HRMS calcd for $C_{17}H_{22}NO_2S$ $[M - CSOEt]^+$: 304.1371, found: 304.1370.

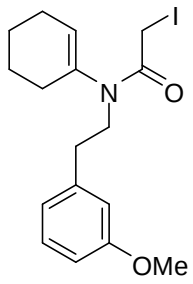

***N*-Cyclohex-1-enyl-2-iodo-*N*-(2-(3-methoxyphenyl)ethyl)acetamide (1.38c)**: Enamide **1.38a** (616 mg, 2.0 mmol) was dissolved in dry acetone (50 mL) in a round-bottomed flask covered with aluminum foil. Excess sodium iodide (3.00 g, 20.0 mmol) was added, and the mixture was stirred for 16 h under argon. The solvent was removed by rotary evaporation, and the residue was partitioned between ether and water (30 mL each). The organic layer was successively washed with 10% aq. $Na_2S_2O_3$ (2 x 30 mL) and water (2 x 30 mL), and dried over Na_2SO_4. The resulting mixture was filtered, concentrated by rotary evaporation, and the residue was chromatographed on silica gel (hexanes:EtOAc 2:1) to give the title compound (743 mg, 93%) as a viscous, bright yellow oil: ^{1}H NMR (300 MHz, $CDCl_3$) δ 7.21 (t, *J* = 7.7 Hz, 1H), 6.84-6.74 (m, 3H), 5.73 (m, 1H), 3.82 (s, 2H), 3.81 (s, 3H), 3.61 (br m, 2H), 2.85 (t, *J* = 7.9 Hz, 2H), 2.21-2.11 (m, 4H), 1.80-1.71 (m, 2H), 1.67-1.58 (m, 2H); ^{13}C NMR (75 MHz, $CDCl_3$) δ 167.1, 159.6, 140.3, 138.7, 129.3, 128.0, 121.1, 114.3, 111.8, 55.1, 47.7, 33.7, 27.3, 24.6, 22.7, 21.3, −2.3.

FTIR (neat, cm^{-1}) 2933, 2834, 1649, 1415, 1039, 783: HRMS calcd for $C_{17}H_{22}NO_2$ $[M - I]^+$: 272.1651, found: 272.1646.

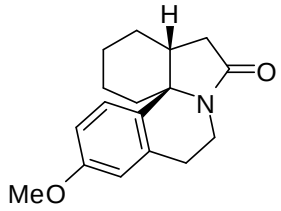

16-Methoxy-8-oxoerythrinane (1.41): Ester **1.35** (0.179 g, 0.97 mmol) and 3-methoxyphenethylamine (0.147 g, 0.97 mmol) were refluxed in toluene (3.0 mL) for 8 h. The reaction mixture was cooled to room temperature, 47% aq. HI (0.70 mL) was added, and the mixture was stirred overnight open to the atmosphere. The mixture was diluted with EtOAc (20 mL), and washed successively with saturated $NaHCO_3$ (2 x 20 mL) and 10% $Na_2S_2O_3$ (1 x 20 mL) solutions. The organic phase was dried over $MgSO_4$, filtered, and solvent was removed to give a pale yellow oil. Flash chromatography with EtOAc furnished the title compound as a white solid (192 mg, 73%), mp 109-110 °C (lit. 109-110.5 °C).[10] Spectroscopic data agreed with the previously reported partial characterization:[10] ^{1}H NMR (300 MHz, $CDCl_3$) δ 7.32 (d, *J* = 8.6 Hz, 1H), 6.77 (dd, *J* = 8.6 Hz, 2.6 Hz, 1H), 6.65 (d, *J* = 2.5 Hz, 1H), 4.05 (ddd, *J* = 13.1 Hz, 7.0 Hz, 4.0 Hz, 1H), 3.79 (s, 3H), 3.28 (ddd, *J* = 13.1 Hz, 9.4 Hz, 5.8 Hz, 1H), 3.02 (ddd, *J* = 16.4 Hz, 9.2 Hz, 7.2 Hz, 1H), 2.78 (ddd, *J* = 16.4 H, 4.8 Hz, 4.8 Hz, 1H), 2.62-2.54 (m, 1H), 2.36 (d, *J* = 8.4 Hz, 2H), 2.12-2.00 (m, 1H), 1.92-1.47 (m, 7H); ^{13}C NMR (75 MHz, $CDCl_3$) δ 173.9, 158.0, 135.5, 134.9, 125.6, 113.9, 112.2, 62.1, 55.1, 37.8, 36.4, 36.0, 34.8, 27.9, 26.8, 20.6, 20.1; FTIR (thin film, cm^{-1}) 3006, 2939, 2862, 1668, 1441, 1041, 667; HRMS calcd for $C_{17}H_{21}NO_2$ $[M]^+$: 271.1572, found: 271.1570.

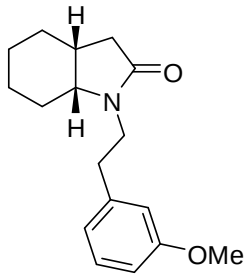

1-(2-(3-Methoxyphenyl)ethyl)octahydroindol-2-one (1.42): Enamide **1.38a** (128 mg, 0.416 mmol) was dissolved in toluene (22 mL) and the solution was brought to reflux. A solution of Bu_3SnH (292 mg, 0.500 mmol) and AIBN (6.2 mg, 0.042 mmol) in toluene (22 mL) was added to the reaction mixture via syringe pump over 2 h, and the mixture was refluxed an additional 2 h. GC analysis showed that approximately half of the starting material remained, so a second portion of Bu_3SnH (292 mg, 0.500 mmol) and AIBN (6.2 mg, 0.042 mmol) in toluene solution (11 mL) was added via syringe pump over 1 h, and reflux was continued for a further 2 h. The mixture was cooled to room temperature, the solvent was removed by rotary evaporation, and the residue was partitioned between Et_2O (20 mL) and 8% aq. KF (50 mL),[271] and the mixture was stirred for 15 h. The aqueous layer was removed, and the organic layer was dried over $MgSO_4$, filtered through a Celite pad, and solvent was removed. Gradient column chromatography (exhaustive 100% hexane flush to remove tin impurities, followed by 1:1 hexanes:EtOAc) furnished the title compound as a light yellow oil (84 mg, 74%): ^{1}H NMR (300 MHz, $CDCl_3$) δ 7.19 (t, *J* = 8.1 Hz, 1H), 6.81-6.72 (m, 3H), 3.87 (ddd, *J* = 14.1 Hz, 9.3 Hz, 6.4 Hz, 1H), 3.78 (s, 3H), 3.40 (q, *J* = 5.3 Hz, 1H), 3.05 (ddd, *J* = 14.0 Hz, 9.1 Hz, 6.1 Hz, 1H), 2.86-2.68 (m, 2H), 2.32-2.18 (m, 2H), 2.17-2.06 (m, 1H), 1.81-1.67 (m, 1H), 1.64-1.50 (m, 2H), 1.49-1.25 (m, 5H); ^{13}C NMR (75 MHz, $CDCl_3$) δ 175.2, 159.6, 140.5, 129.3, 120.9, 114.2, 111.7, 56.6, 55.1, 41.3, 36.9, 33.9, 32.3, 27.0, 26.7, 22.3, 21.0; HRMS calcd for $C_{17}H_{23}NO_2$ $[M]^+$: 273.1729, found: 273.1728.

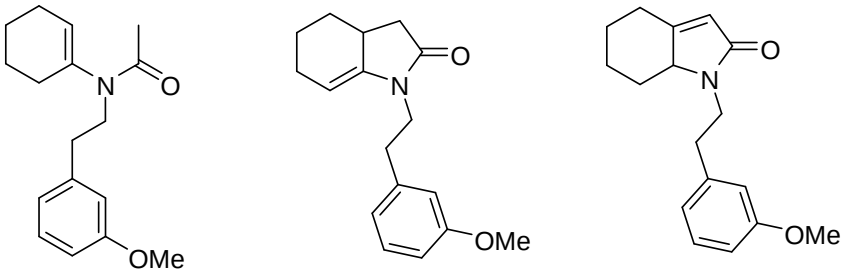

Cyclization of **1.38c**: Enamide **1.38c** (200. mg, 0.50 mmol) was dissolved in toluene (25 mL) and the solution was brought to reflux. A solution of Bu_3SnH (175 mg, 0.60 mmol) and AIBN (8 mg, 0.05 mmol) in toluene (25 mL) was added to the reaction mixture via syringe pump over 2.5 h, and the mixture was refluxed an additional 1 h. The mixture was cooled to room temperature, solvent was removed by rotary evaporation, the residue was partitioned between Et_2O (20 mL) and 8% aq. KF (50 mL), and the mixture was stirred 15 h. The aqueous layer was removed, and the organic layer was dried over $MgSO_4$, filtered through a Celite pad, and solvent was removed by rotary evaporation. Gradient column chromatography (exhaustive hexane flush to remove tin impurities, followed by 1:1 hexanes:EtOAc) furnished three products:

***N*-Cyclohex-1-enyl-*N*-(2-(3-methoxyphenyl)ethyl)acetamide (1.45)** was the first eluting compound, yielding 17 mg (12% yield) as a light yellow oil: ^{1}H NMR (300 MHz, $CDCl_3$) δ 7.20 (t, *J* = 7.8 Hz, 1H), 6.83-6.73 (m, 3H), 5.55 (m, 1H), 3.80 (s, 3H), 3.60 (m, 2H), 2.83 (t, *J* = 8.5 Hz, 2H), 2.15-2.09 (m, 2H), 2.07-2.01 (m, 2H), 2.02 (s, 3H), 1.77-1.69 (m, 2H), 1.64-1.56 (m, 2H); ^{13}C NMR (75 MHz, $CDCl_3$): δ 169.6, 159.5, 140.7, 139.1, 129.1, 127.3, 121.0, 114.2, 111.5, 55.0, 46.9, 34.2, 27.6, 24.6, 22.7, 21.7, 21.4; FTIR (neat, cm^{-1}) 2933, 2837, 1651, 1398, 1045; HRMS calcd for $C_{17}H_{23}NO_2$ $[M]^+$: 273.1729, found: 273.1727.

1-(2-(3-Methoxyphenyl)ethyl)-1,3,3a,4,5,6-hexahydroindol-2-one (1.43) eluted second and consisted of 12 mg (9% yield) as a bright yellow oil: ^{1}H NMR (300 MHz, $CDCl_3$) δ 7.22

(dd, *J* = 8.9 Hz, 7.5 Hz, 1H), 6.83-6.75 (m, 3H), 4.85 (br m, 1H), 3.85-3.75 (overlapping m with clear d, *J* = 7.1 Hz, 1H), 3.81 (s, 3H), 3.48 (ddd, *J* = 13.8 Hz, 9.3 Hz, 5.9 Hz, 1H), 2.92-2.84 (overlapping m with clear dd, *J* = 13.3 Hz, 5.7 Hz, 1H), 2.85-2.74 (overlapping with clear ddd, *J* = 13.3 Hz, 9.1 Hz, 7.1 Hz, 1H), 2.73-2.60 (m, 1H), 2.53 (dd, *J* = 16.0 Hz, 8.8 Hz, 1H), 2.30-2.00 (m, 4H), 1.96-1.84 (br m, 1H), 1.67-1.49 (m, 1H), 1.39-1.27 (m, 1H); ^{13}C NMR (75 MHz, $CDCl_3$) δ 173.8, 159.4, 141.6, 139.9, 129.1, 120.8, 114.1, 111.5, 96.5, 54.8, 40.5, 36.5, 34.4, 32.7, 27.6, 22.9, 22.0; FTIR (thin film, cm^{-1}) 2933, 2837, 1721, 1678, 1602, 1454, 1403, 1323, 1260, 1164.

1-(2-(3-Methoxyphenyl)ethyl)-1,4,5,6,7,7a-hexahydroindol-2-one (1.44) was the final eluting product, collected by an EtOAc flush of the column, and consisted of 58 mg (43% yield) of a clear oil: ^{1}H NMR (300 MHz, $CDCl_3$) δ 7.21 (t, *J* = 8.2 Hz, 1H), 6.83-6.74 (m, 3H), 5.78 (s, 1H), 3.91 (ddd, *J* = 14.3 Hz, 8.4 Hz, 6.4 Hz, 1H), 3.80 (s, 3H), 3.54 (dd, *J* = 11.6 Hz, 6.1 Hz, 1H), 3.33 (ddd, *J* = 14.3 Hz, 8.5 Hz, 6.8 Hz, 1H), 2.86 (m, 2H), 2.75-2.70 (m, 1H), 2.39-1.78 (m, 4H), 1.45-1.21 (m, 2H) 1.05-0.92 (m, 1H); ^{13}C NMR (75 MHz, $CDCl_3$) δ 171.8, 162.1, 160.1, 141.0, 129.8, 121.4, 118.7, 114.6, 112.3, 62.6, 55.5, 41.7, 35.6, 33.4, 28.6, 27.7, 23.4; FTIR (neat, cm^{-1}) ν_{max} 2933, 2862, 1686, 1500, 1241, 1158, 1040, 751.

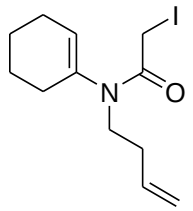

***N*-(But-3-enyl)-*N*-cyclohexenyl-2-iodoacetamide (1.46b)**: α-Chloroenamide **1.46a** (454 mg, 2.0 mmol) was dissolved in dry acetone (20 mL) in a round-bottomed flask covered with aluminum foil. Excess sodium iodide (3.00 g, 20.0 mmol) was added, and the mixture was

stirred for 15 h under argon. The solvent was removed by rotary evaporation, and the residue was partitioned between ethyl acetate (100 mL) and 10% aq. $Na_2S_2O_3$ (50 mL each). The organic layer was successively washed with 10% aq. $Na_2S_2O_3$ (50 mL) and brine (50 mL), and dried over Na_2SO_4. The resulting solution was concentrated by rotary evaporation, and the residue was chromatographed on silica gel (4:1 hexanes:EtOAc) to give the title compound (530 mg, 83%) as a viscous, bright yellow oil: ^{1}H NMR (300 MHz, $CDCl_3$) δ 5.84 (m, 1H), 5.78 (ddt, *J* = 17.1 Hz, 10.3 Hz, 6.8 Hz, 1H), 5.11-5.00 (m, 2H), 3.80 (s, 2H), 3.46 (br s, 2H), 2.30 (m with clear q, *J* = 7.0 Hz, 2H), 2.22-2.13 (m, 4H), 1.82-1.71 (m, 2H), 1.68-1.58 (m, 2H); ^{13}C NMR (75 MHz, $CDCl_3$) δ 167.0, 138.3, 135.0, 128.1, 116.5, 45.1, 31.8, 27.3, 24.6, 22.6, 21.3, −2.4; FTIR (neat, cm^{-1}) 2932, 1650. 1416. 1393, 921.

6.3 COMPOUND DATA FOR CHAPTER 3

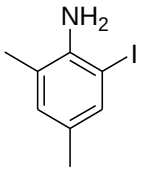

2-Iodo-4,6-dimethylaniline (3.21): 2,4-Dimethylaniline (9.69 g, 80.0 mmol) was dissolved in a magnetically stirred mixture of MeOH (80 mL) and CH_2Cl_2 (80 mL), and solid $NaHCO_3$ (13.44 g, 160. mmol) was added. A solution of benzyltriethylammonium dichloroiodate[185] (31.2 g, 80.0 mmol) in CH_2Cl_2 was added dropwise via an addition funnel to the stirred mixture over 30 min at room temperature. After stirring for 1 hour, the mixture was poured into 240 mL water. The organic layer was separated and washed further with water (3 x 160 mL), dried over $MgSO_4$, filtered, and concentrated by rotary evaporation. The resulting semisolid material was stirred in 200 mL of a 10:1 hexane:EtOAc mixture for 15 minutes, and the resulting supernatant solution was decanted away from the insoluble material. This was repeated a total of four times. The supernatant solutions were combined and concentrated by rotary evaporation, and the resulting crude was passed through a plug of silica gel using 25:1 petroleum ether:Et_2O to afford the title compound[272] (13.42 g, 68%) as a pink solid, mp 64–65 °C (lit. 66–67 °C): ^{1}H NMR (300 MHz, $CDCl_3$) δ 7.37 (s, 1H), 6.85 (s, 1H), 4.11 (br s, 2H), 2.21 (s, 3H), 2.19 (s, 3H); ^{13}C NMR (75 MHz, $CDCl_3$) δ 142.1, 136.5, 131.2, 128.8, 122.2, 84.6, 19.7, 18.7; FTIR (thin film, $CHCl_3$, cm^{-1}) 3399, 3307 (broad), 3016, 2918, 1622, 1480, 1287, 1239, 1061, 854, 755, 722; LRMS (EI) *m/z* 247 (M^+, 79), 120 (100), 104 (76), 91 (85), 77 (82); HRMS (EI) calcd for $C_8H_{10}IN$ $[M]^+$: 246.9858, found: 246.9863.

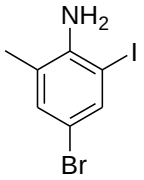

4-Bromo-2-iodo-6-methylaniline (3.22): To a magnetically stirred solution of 4-bromo-2-methylaniline (2.08 g, 11.2 mmol) in EtOH (37 mL) was added I_2 (2.83 g, 11.2 mmol) all at once. The mixture was stirred for 5 min, Ag_2SO_4 (3.49 g, 11.2 mmol) was added in one portion, and the mixture was stirred at room temperature for 3 h. Upon completion of the reaction, solids were removed by vacuum filtration, and the filtrate was concentrated by rotary evaporation. The crude mixture was redissolved in CH_2Cl_2 (30 mL) and washed sequentially with 5% aqueous NaOH, water, and brine (25 mL each), dried over $MgSO_4$, filtered, and concentrated by rotary evaporation. Flash chromatography (10:1 pentane:Et_2O) afforded the title compound[128] (2.26 g, 65%) as a tan solid, mp 59–60 °C (lit. 55–57 °C): ^{1}H NMR (300 MHz, $CDCl_3$) δ 7.62 (d, J = 2.1 Hz, 1H), 7.12 (d, J = 1.5 Hz, 1H), 4.04 (br s, 2H), 2.16 (s, 3H); ^{13}C NMR (75 MHz, $CDCl_3$) δ 143.9, 137.8, 132.6, 123.6, 109.4, 84.2, 18.6; FTIR (thin film, $CHCl_3$, cm^{-1}) 3391, 3303 (broad), 3221, 2930, 1620, 1462, 1438, 1238, 861, 720, 668; LRMS (EI) *m/z* 313 (M^+ (^{81}Br), 38), 128 (50), 83 (56), 69 (95), 55 (100); HRMS (EI) calcd for $C_7H_7{}^{79}BrIN$ $[M]^+$: 310.8807, found: 310.8812.

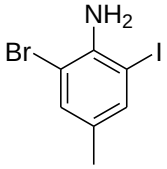

2-Bromo-6-iodo-4-methylaniline (3.23): To a stirred mixture of 2-bromo-4-methylaniline (4.65 g, 25.0 mmol) and $CaCO_3$ (5.00 g, 50.0 mmol) in CH_2Cl_2 (50 mL) and MeOH (25 mL) was

added portionwise $BnNMe_3•ICl_2$ (9.57 g, 27.5 mmol) over 5 min. The reaction was stirred at room temperature for 9 h, and was determined to have stalled by TLC analysis. A second portion of $BnNMe_3•ICl_2$ (4.35 g, 12.5 mmol) and $CaCO_3$ (2.50 g, 25.0 mmol) were added with MeOH (75 mL), and the mixture was stirred overnight (12 h). The reaction mixture was filtered through a pad of Celite and concentrated by rotary evaporation. The crude was partitioned between 5% aqueous $NaHSO_3$ (250 mL) and Et_2O (300 mL), the organic layer was removed, and the aqueous layer was extracted with Et_2O (3 x 300 mL). The combined organic layers were dried over $MgSO_4$, filtered, and concentrated by rotary evaporation. Flash chromatography of the crude residue (25:1 pentane:Et_2O) gave the title compound[132] (7.09 g, 91%) as a white solid, mp 91 °C (lit. 85–88 °C): ^{1}H NMR (300 MHz, $CDCl_3$) δ 7.44 (s, 1H), 7.24 (s, 1H), 4.43 (br s, 2H), 2.20 (s, 3H); ^{13}C NMR (75 MHz, $CDCl_3$) δ 141.6, 138.5, 133.2, 130.1, 107.0, 83.1, 19.5; FTIR (thin film, $CHCl_3$, cm^{-1}) 3419, 3321 (broad), 1614, 1575, 1469, 1053, 849, 716, 706; LRMS (EI) *m/z* 313 (M^+ (^{81}Br), 61), 104 (49), 52 (100); HRMS (EI) calcd for $C_7H_7{}^{79}BrIN$ $[M]^+$: 310.8807, found: 310.8810.

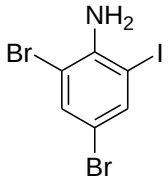

2,4-Dibromo-6-iodoaniline (3.24): To a magnetically stirred solution of I_2 (2.79 g, 11.0 mmol) in EtOH (50 mL) was added solid Ag_2SO_4 (3.43 g, 11.0 mmol) all at once. The mixture was stirred for 5 min at room temperature, 2,4-dibromoaniline (2.51 g, 10.0 mmol) was added all at once, and the mixture was stirred for 3 h. Upon completion of the reaction, the mixture was filtered through a Celite pad, the pad was rinsed with EtOH, and the filtrate was concentrated by

rotary evaporation. The residue was dissolved in CH_2Cl_2 (200 mL), washed once with 10% aqueous $Na_2S_2O_3$ solution (50 mL), dried over $MgSO_4$, filtered, and concentrated by rotary evaporation. Flash chromatography (97.5:2.5 pentane:Et_2O) gave the title compound[186] (1.23 g, 33%) as a light pink solid, mp 120-121 °C (lit. 124–125 °C): ^{1}H NMR (300 MHz, $CDCl_3$) δ 7.71 (d, *J* = 2.1 Hz, 1H), 7.54 (d, *J* = 2.1 Hz, 1H), 4.61 (br s, 1H); ^{13}C NMR (75 MHz, $CDCl_3$) δ 143.4, 139.8, 134.7, 109.4, 107.1, 82.6; FTIR (thin film, $CHCl_3$, cm^{-1}) 3250 (broad), 2949, 1693, 1514, 1245, 1062, 995, 941, 846, 694; LRMS (EI) *m/z* 379 (M^+ (^{81}Br, ^{81}Br), 88), 252 ((^{81}Br, ^{81}Br), 56), 168 (74); HRMS (EI) calcd for $C_6H_4{}^{79}Br_2IN$ $[M]^+$: 374.7755, found: 374.7748.

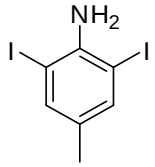

2,6-Diiodo-4-methylaniline (3.25): To a room temperature solution of 37% w/w aq. HCl (250 mL) and water (1.75 L) in a round bottom flask equipped with a mechanical stirrer was added *p*-toluidine (11.50 g, 107.3 mmol) all at once. After all solid had dissolved, solid ICl (34.84 g, 214.6 mmol) was added all at once, and the mixture was stirred open to the atmosphere for 20 h. The mixture was vacuum filtered, and the solids were washed with water (1.0 L). The crude wet solid was taken up in 300 mL CH_2Cl_2, the aqueous layer that formed was removed, and the organic layer was dried over $MgSO_4$, filtered, and concentrated by rotary evaporation. The crude product was taken up in CH_2Cl_2, and "short" flash column chromatography (400 g silica, 4:1 hexanes:EtOAc) afforded the title compound[132] (29.59 g, 77%) as a yellow-brown solid whose spectra matched that previously reported: ^{1}H NMR (300 MHz, $CDCl_3$) δ 7.47 (s, 2H), 4.46 (br s, 2H), 2.18 (s, 3H).

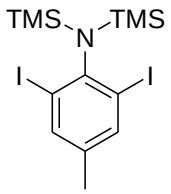

2,6-Diiodo-4-methyl-*N*,*N*-bis(trimethylsilyl)aniline (3.26): To a stirred solution of **3.25** (1.84 g, 5.13 mmol) in THF (50 mL) at –78 °C was quickly added a heptane/PhEt/THF solution of LDA (2.69 mL, 5.39 mmol) via syringe. The mixture was stirred at this temperature for 15 min, TMSCl (0.585 g, 5.39 mmol) was quickly added via syringe, and the mixture was stirred at –78 °C for 15 min. In the same fashion, a second portion of LDA solution (2.69 mL, 5.39 mmol) was added, followed by stirring 20 min, and a second addition of TMSCl (0.585 g, 5.39 mmol). The mixture was allowed to warm to room temperature, was stirred for 30 min, and saturated aqueous NH_4Cl solution (50 mL) was added. The mixture was extracted with Et_2O (3 x 50 mL), and the combined organic layers were washed with brine (2 x 50 mL), dried over $MgSO_4$, filtered, and concentrated by rotary evaporation. The crude product was filtered through a plug of silica gel with hexanes to afford the title compound[132] (2.24 g, 87%) as a white solid, mp 122-123 °C (lit. 125–128 °C): ^{1}H NMR (300 MHz, $CDCl_3$) δ 7.69 (s, 2H), 2.20 (s, 3H), 0.27 (s, 18H); ^{13}C NMR (75 MHz, $CDCl_3$) δ 150.4, 140.6 (2C), 136.6, 103.3 (2C), 19.3, 3.6 (6C); FTIR (thin film, $CHCl_3$, cm^{-1}) 2954, 1427, 1249, 1232, 910, 837, 821, 758, 703; LRMS (EI) *m/z* 503 (M^+, 7), 488 (60), 361 (100), 73 (90); HRMS (EI) calcd for $C_{13}H_{23}I_2NSi_2$ $[M]^+$: 502.9459, found: 502.9458.

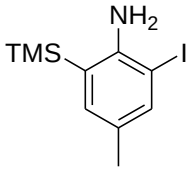

2-Iodo-4-methyl-6-(trimethylsilyl)aniline (3.27): To a stirred solution of **3.26** (2.01 g, 4.00 mmol) in THF (120 mL) at –78 °C was added a solution of *s*-BuLi in cyclohexane (6.3 mL, 8.80 mmol) quickly via syringe. The mixture was stirred at this temperature for 30 min, saturated aqueous NH_4Cl (40 mL) was added, and the mixture was warmed to rt and stirred 2 h. The mixture was extracted with Et_2O (3 x 120 mL), and the combined organic layers were washed with brine (2 x 120 mL), dried over $MgSO_4$, filtered, and concentrated by rotary evaporation. Flash chromatography of the crude residue (99:1 hexanes:EtOAc) afforded the title compound (0.997 g, 82%) as an orange oil: ^{1}H NMR (300 MHz, $CDCl_3$) δ 7.53 (s, 1H), 7.06 (s, 1H), 4.12 (br s, 2H), 2.21 (s, 3H), 0.34 (s, 9H); ^{13}C NMR (75 MHz, $CDCl_3$) δ 148.1, 140.6, 135.8, 129.0, 123.5, 86.8, 19.9, –0.8 (3C); FTIR (neat, cm^{-1}) 3473, 3375, 2954, 1611, 1441, 1250, 1064, 902, 840, 761; LRMS (EI) *m/z* 305 (M^+, 89), 290 (99), 250 (84), 162 (33), 73 (100); HRMS (EI) calcd for $C_{10}H_{16}INSi$ $[M]^+$: 305.0097, found: 305.0088.

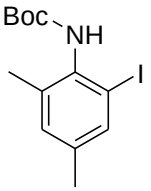

***tert*-Butyl 2-iodo-4,6-dimethylphenylcarbamate (3.28):** To a stirred solution of aniline **3.21** (3.71 g, 15.0 mmol) in THF (60 mL) at –78 °C was added a solution of NaHMDS in THF (1.0 M, 30.0 mL) dropwise via syringe. The mixture was warmed to room temperature over 30 min, stirred at room temperature an additional 30 min, and recooled to –78 °C. A solution of Boc_2O

(3.60 g, 16.5 mmol) in THF (30 mL) was added dropwise via syringe, and the mixture was stirred at –78 °C for 15 min. The reaction was quenched with sat. aqueous NH_4Cl solution (60 mL), warmed to room temperature, and extracted with EtOAc (3 x 150 mL). The combined organic layers were washed with brine (1 x 150 mL), dried over $MgSO_4$, filtered, and concentrated by rotary evaporation. Flash chromatography (10:1 hexanes:EtOAc) afforded the title compound (4.88 g, 94%) as a red viscous oil: ^1H NMR (300 MHz, $CDCl_3$) δ 7.52 (s, 1H), 7.01 (s, 1H), 5.97 (br s, 1H), 2.30 (s, 3H), 2.26 (s, 3H), 1.51 (br s, 9H); ^{13}C NMR (75 MHz, $CDCl_3$) δ 153.0, 137.9, 136.9, 136.5, 134.5, 131.1, 100.1, 79.6, 28.0 (3C), 20.0, 19.1; FTIR (neat, cm^{-1}) 3310 (broad), 2978, 2926, 1706, 1367, 1246, 1167, 1050, 910, 851, 733; HRMS (ESI) calcd for $C_{13}H_{18}INNaO_2$ $[M + Na]^+$: 370.0280, found: 370.0273.

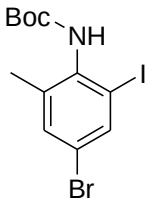

***tert*-Butyl 4-bromo-2-iodo-6-methylphenylcarbamate (3.29):** To a stirred solution of aniline **3.22** (1.56 g, 5.00 mmol) in THF (10.0 mL) at –78 °C was added a solution of NaHMDS in THF (1.0 M, 10.0 mL) dropwise via syringe. The mixture was warmed to room temperature over 30 min, stirred at room temperature an additional 30 min, and recooled to –78 °C. A solution of Boc_2O (1.20 g, 5.50 mmol) in THF (10.0 mL) was added dropwise via syringe, and the mixture was stirred at –78 °C for 1 h. Saturated aqueous NH_4Cl solution (20 mL) was added, the mixture was warmed to room temperature, and extracted with EtOAc (3 x 50 mL). The combined organic layers were washed with brine (1 x 25 mL), dried over $MgSO_4$, filtered, and concentrated by rotary evaporation. Flash chromatography (9:1 pentane:Et_2O) afforded the title compound

(1.51 g, 73%) as a tan solid, mp 83-84 °C: ^{1}H NMR (300 MHz, $CDCl_3$) δ 7.80 (d, *J* = 1.8 Hz, 1H), 7.34 (d, *J* = 1.8 Hz, 1H), 6.08 (br s, 1H), 2.30 (s, 3H), 1.50 (s, 9H); ^{13}C NMR (75 MHz, $CDCl_3$) δ 153.00, 139.2, 138.4, 136.7, 133.6, 120.8, 100.7, 80.7, 28.3 (3C), 19.4; FTIR (thin film, $CHCl_3$, cm^{-1}) 3284 (broad), 2978, 2929, 1695, 1498, 1391, 1367, 1249, 1153, 1059, 915, 855, 757, 682; LRMS (EI) *m/z* 413 (M^+ (^{81}Br), 25), 313 ((^{81}Br) 99), 311 ((^{79}Br) 100), 230 ((^{81}Br) 69), 104 (91), 77 (93); HRMS (EI) calcd for $C_{12}H_{15}{}^{79}BrINO_2$ $[M]^+$: 410.9331, found: 410.9327.

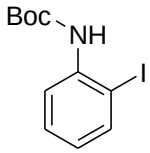

***tert*-Butyl 2-iodophenylcarbamate (3.30):** To a stirred solution of 2-iodoaniline (2.19 g, 10.0 mmol) in THF (10 mL) at –78 °C was added a solution of NaHMDS in THF (1.0 M, 20.0 mL) dropwise via syringe. The mixture was warmed to room temperature over 30 min, stirred at room temperature an additional 30 min, and recooled to –78 °C. A solution of Boc_2O (2.40 g, 11.0 mmol) in THF (10 mL) was added dropwise via syringe, and the mixture was stirred at –78 °C for 1 h. Saturated aqueous NH_4Cl solution (40 mL) was added, the mixture was warmed to room temperature, and extracted with EtOAc (100 mL). The combined organic layers were washed with brine (1 x 50 mL), dried over $MgSO_4$, filtered, and concentrated by rotary evaporation. Flash chromatography (20:1 pentane:Et_2O) afforded the title compound[273] (2.14 g, 67%) as an orange liquid: ^{1}H NMR (300 MHz, $CDCl_3$) δ 8.06 (d, *J* = 8.1 Hz, 1H), 7.75 (dd, *J* = 7.8 Hz, 1.2 Hz, 1H), 7.32 (t, *J* = 8.1 Hz, 1H), 6.83 (br s, 1H), 6.78 (td, *J* = 7.8 Hz, 1.2 Hz, 1H), 1.55 (s, 9H); ^{13}C NMR (75 MHz, $CDCl_3$) δ 152.5, 138.8, 129.1, 124.6, 120.1, 88.7, 81.0, 28.2 (3C); FTIR (neat, cm^{-1}) 3394, 2978, 2931, 1734, 1588, 1516, 1431, 1367, 1298, 1246, 1223,

1156, 1011, 898, 830, 749; LRMS (EI) *m/z* 319 (M^+, 63), 263 (76), 219 (80), 136 (71), 57 (100); HRMS (EI) calcd for $C_{11}H_{14}INO_2$ $[M]^+$: 319.0069, found: 319.0077.

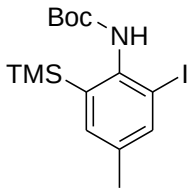

***tert*-Butyl 2-iodo-4-methyl-6-(trimethylsilyl)phenylcarbamate (3.31):** To a stirred solution of aniline **3.27** (305 mg, 1.00 mmol) in THF (4.0 mL) at –78 °C was added a solution of NaHMDS in THF (1.0 M, 2.00 mL) dropwise via syringe. The mixture was warmed to room temperature over 30 min, stirred at room temperature an additional 30 min, and recooled to –78 °C. A solution of Boc_2O (240. mg, 1.10 mmol) in THF (1.00 mL) was added dropwise via syringe, the mixture was stirred at –78 °C for 3 h, warmed to room temperature, and stirred overnight (16 h). The reaction was quenched with sat. aqueous NH_4Cl solution (5 mL), and extracted with EtOAc (3 x 10 mL). The combined organic layers were washed with brine (2 x 10 mL), dried over $MgSO_4$, filtered, and concentrated by rotary evaporation. Flash chromatography (10:1 hexanes:EtOAc) afforded the title compound (253 mg, 62%) as a cream-colored solid, mp 132-133 °C, in a 2.2:1 ratio of rotamers: ^{1}H NMR (300 MHz, $CDCl_3$) δ 7.72 (s, 1H), 7.25 (s, 1H), 6.05 (br s, 1H, major), 5.90 (br s, 1H, minor), 2.30 (s, 3H), 1.53 (s, 9H, major), 1.42 (s, 9H, minor), 0.28 (s, 9H); ^{13}C NMR (75 MHz, $CDCl_3$) δ 153.8, 141.2, 140.8, 140.3, 138.5, 135.6, 102.9, 80.0, 28.4 (3C), 20.4, –0.6 (3C); FTIR (thin film, $CHCl_3$, cm^{-1}) 3220, 2976, 1704, 1366, 1250, 1164, 1086, 887, 840, 757, 627; HRMS (ESI) calcd for $C_{15}H_{20}NNaO_2SiI$ $[M + Na]^+$: 428.0157, found: 428.0169.

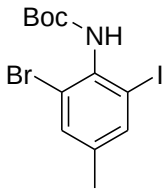

***tert*-Butyl 2-bromo-6-iodo-4-methylphenylcarbamate (3.32):** To a stirred solution of aniline **3.23** (0.624 g, 2.00 mmol) in THF (5.0 mL) at –78 °C was added a solution of NaHMDS in THF (1.0 M, 4.00 mL) dropwise via syringe. The mixture was warmed to room temperature over 30 min, stirred at room temperature an additional 30 min, and recooled to –78 °C. A solution of Boc_2O (0.480 g, 2.20 mmol) in THF (3.00 mL) was added dropwise via syringe, the mixture was stirred at –78 °C for 1 h, warmed to room temperature, and stirred for 1 h further. The mixture was quenched at 0 °C with sat. aqueous NH_4Cl solution (10 mL), warmed to room temperature, and extracted with EtOAc (3 x 20 mL). The combined organic layers were washed with brine (2 x 20 mL), dried over $MgSO_4$, filtered, and concentrated by rotary evaporation. Flash chromatography (6:1 hexanes:EtOAc) afforded the title compound (0.645 g, 78%) as a tan solid, mp 77-79 °C, in an 8:1 ratio of rotamers: ^{1}H NMR (300 MHz, $CDCl_3$) δ 7.64 (s, 1H), 7.42 (s, 1H), 6.13 (br s, 1H, major), 5.84 (br s, 1H, minor), 2.29 (s, 3H), 1.52 (br s, 9H, major), 1.42 (s, 1H, minor); ^{13}C NMR (75 MHz, $CDCl_3$) δ 152.7, 140.0, 138.8, 135.0, 133.5, 122.4, 100.4, 80.6, 28.2 (3C), 20.0; FTIR (thin film, $CHCl_3$, cm^{-1}) 3300 (broad), 2977, 2927, 1709, 1483, 1450, 1367, 1251, 1161, 1072, 1045, 1023, 852, 758, 725; LRMS (EI) *m/z* 413 (M^+ (^{81}Br), 17), 313 ((^{81}Br) 99), 311 ((^{79}Br) 100), 184 (35), 77 (65); HRMS (EI) calcd for $C_{12}H_{15}{}^{79}BrINO_2$ $[M]^+$: 410.9331, found: 410.9310.

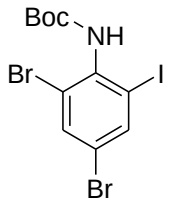

***tert*-Butyl 2,4-dibromo-6-iodophenylcarbamate (3.33):** To a stirred solution of aniline **3.24** (1.13 g, 3.00 mmol) in THF (12.0 mL) at –78 °C was added a solution of NaHMDS in THF (1.0 M, 6.00 mL) dropwise via syringe. The mixture was warmed to room temperature over 30 min, stirred at room temperature an additional 30 min, and recooled to –78 °C. A solution of Boc_2O (0.720 g, 3.30 mmol) in THF (6.00 mL) was added dropwise via syringe, the mixture was stirred at –78 °C for 2 h, warmed to room temperature, and stirred for 4 h further. The mixture was quenched at 0 °C with sat. aqueous NH_4Cl solution (15 mL), warmed to room temperature, and extracted with EtOAc (3 x 15 mL). The combined organic layers were washed with brine (3 x 15 mL), dried over $MgSO_4$, filtered, and concentrated by rotary evaporation. Flash chromatography (10:1 hexanes:EtOAc) afforded the title compound (0.645 g, 78%) as a pinkish-orange solid, mp 82 °C: ^{1}H NMR (300 MHz, $CDCl_3$) δ 7.96 (d, J = 2.1 Hz, 1H), 7.77 (d, J = 2.1 Hz, 1H), 6.12 (br s, 1H), 1.52 (br s, 9H); ^{13}C NMR (75 MHz, $CDCl_3$) δ 152.3, 140.5, 137.2, 135.4, 123.3, 121.3, 101.0, 81.3, 28.2 (3C); FTIR (thin film, $CHCl_3$, cm^{-1}) 3267 (broad), 2979, 1702, 1498, 1367, 1278, 1253, 1167, 857, 759, 722, 677; LRMS (EI) *m/z* 479 (M^+ (^{81}Br, ^{81}Br), 3), 379 (^{81}Br, ^{81}Br) 70), 88 (71), 59 (100); HRMS (EI) calcd for $C_{11}H_{12}{}^{79}Br_2INO_2$ $[M]^+$: 474.8280, found: 474.8288.

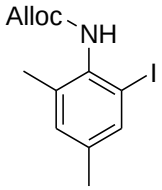

Allyl 2-iodo-4,6-dimethylphenylcarbamate (3.34): To a stirred solution of aniline **3.21** (0.988 g, 4.00 mmol) in pyridine (10 mL) at 0 °C was added allyl chloroformate (1.45 g, 12.0 mmol) dropwise via syringe over 5 min. The mixture was warmed to room temperature, stirred overnight (16 h), and poured into water (40 mL). The mixture was extracted with EtOAc (3 x 40 mL), and the combined organic layers were washed sequentially with water, sat. $CuSO_4$ solution, 0.20 M HCl, and brine (1 x 40 mL each), dried over $MgSO_4$, filtered, and concentrated by rotary evaporation. Flash chromatography (6:1 hexanes:EtOAc) afforded the title compound (1.23 g, 93%) as a cream-colored solid, mp 77–78 °C: ^{1}H NMR (300 MHz, $CDCl_3$) δ 7.53 (s, 1H), 7.03 (s, 1H), 6.28-5.79 (m, 2H), 5.50-5.15 (m, 2H), 4.68 (br s, 2H), 2.31 (s, 3H), 2.28 (s, 3H); ^{13}C NMR (75 MHz, $CDCl_3$) δ 153.8, 138.9, 137.2, 137.0, 134.1, 132.5, 131.6, 117.7, 99.8, 65.9, 20.3, 19.3; FTIR (thin film, $CHCl_3$, cm^{-1}) 3270 (broad), 2921, 1707, 1508, 1232, 1056, 994, 936, 847, 771; HRMS (ESI) calcd for $C_{12}H_{14}INNaO_2$ $[M + Na]^+$: 353.9967, found: 353.9964.

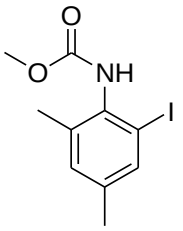

Methyl 2-iodo-4,6-dimethylphenylcarbamate (3.35): To a stirred solution of aniline **3.21** (1.24 g, 5.00 mmol) in pyridine (10 mL) at 0 °C was added methyl chloroformate (0.709 g, 7.5 mmol) dropwise via syringe over 5 min. The solution was warmed to room temperature and stirred 9 h. The mixture was recooled to 0 °C, a second portion of methyl chloroformate (0.709

g, 7.5 mmol) was added in the same manner, and the mixture was stirred at room temperature overnight (15 h). A final portion of methyl chloroformate (0.709 g, 7.5 mmol) was again added at 0 °C, the mixture was stirred for 2 h at room temperature, and water (50 mL) was slowly added. The mixture was extracted with EtOAc (3 x 50 mL) and the combined organic layers were washed sequentially with water, sat. $CuSO_4$ solution, 0.20 M HCl, and brine (50 mL each), dried over $MgSO_4$, filtered, and concentrated with rotary evaporation. Flash chromatography (4:1 hexanes:EtOAc) afforded the title compound (1.40 g, 92%) as a white solid, mp 91-92 °C in a 2.3:1 ratio of rotamers: ^{1}H NMR (300 MHz, $CDCl_3$) δ 7.54 (s, 1H), 7.03 (s, 1H), 6.14 (br s, 1H, major), 5.95 (br s, 1H, minor), 3.79 (br s, 3H), 2.30 (s, 3H), 2.28 (s, 3H); ^{13}C NMR (75 MHz, $CDCl_3$) δ 154.5, 138.6, 137.0, 136.8, 134.1, 131.4, 99.8, 52.5, 20.1, 19.1; FTIR (thin film, $CHCl_3$, cm^{-1}) 3286 (broad), 2953, 2921, 1710, 1502, 1449, 1349, 1241, 1068, 851, 771; LRMS (EI) *m/z* 305 (M^+, 28), 178 (100), 163 (62), 118 (27); HRMS (EI) calcd for $C_{10}H_{12}INO_2$ $[M]^+$: 304.9913, found: 304.9904.

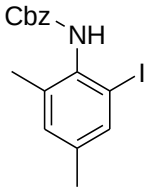

Benzyl 2-iodo-4,6-dimethylphenylcarbamate (3.36): To a stirred solution of aniline **3.21** (0.988 g, 4.00 mmol) in CH_2Cl_2 (5.0 mL) at 0 °C was added via syringe an aqueous NaOH solution (1.0 M, 5.0 mL) followed by dropwise addition of benzyl chloroformate (0.853 g, 5.00 mmol), and the mixture was stirred overnight (16 h) at room temperature. The mixture was then extracted with EtOAc (3 x 25 mL), and the combined organic layers were washed with brine (2 x 25 mL), dried over $MgSO_4$, filtered, and concentrated by rotary evaporation. Flash

chromatography of the crude material (5:1 hexanes:EtOAc) afforded the title compound (1.40 g, 92%) as a pink solid, mp 102-103 °C, in a 3:1 ratio of rotamers: ^{1}H NMR (300 MHz, $CDCl_3$) δ 7.54 (s, 1H), 7.50-7.24 (m, 5H), 7.03 (s, 1H), 6.31 (br s, 1H, major), 6.15 (br s, 1H, minor), 5.23 (s, 2H), 2.29 (br s, 3H), 2.28 (s, 3H); ^{13}C NMR (75 MHz, $CDCl_3$) δ 154.0, 139.0, 137.3, 137.1 (2C), 136.3, 134.1, 131.8, 128.4 (2C), 128.0 (2C, accidental isochrony, confirmed by DEPT-135), 99.8, 67.2, 20.3, 19.3; FTIR (thin film, $CHCl_3$, cm^{-1}) 3267 (broad), 3032, 2955, 1700, 1516, 1243, 1061, 847, 746, 699; HRMS (ESI) calcd for $C_{16}H_{16}INNaO_2$ $[M + Na]^+$: 404.0124, found: 404.0121.

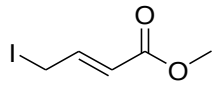

Methyl 4-iodocrotonate: Methyl 4-bromocrotonate (8.06 g, 45.0 mmol) was dissolved in dry acetone (100 mL), and NaI (13.5 g, 90.0 mmol) was added to the reaction mixture. The mixture was refluxed for 2 h, cooled to room temperature, and poured into 1 L CH_2Cl_2. The resulting mixture was washed successively with 10% $Na_2S_2O_3$ aqueous solution, water, saturated $NaHCO_3$ solution, and brine (250 mL each), dried over $MgSO_4$, filtered, and concentrated by rotary evaporation. Flash chromatography of the residue (10:1 pentane:Et_2O) gave the title compound[274] (7.43 g, 73%) as a red mobile oil: ^{1}H NMR (300 MHz, $CDCl_3$) δ 7.07 (dt, *J* = 15.0 Hz, 8.4 Hz, 1H), 5.95 (d, *J* = 15.3 Hz, 1H), 5.94 (d, 8.4 Hz, 2H), 3.76 (s, 3H); ^{13}C NMR (75 MHz, $CDCl_3$) δ 165.7, 143.6, 122.6, 51.6, 0.8; FTIR (neat, cm^{-1}) 2950, 1721, 1650, 1322, 1277, 1206, 1128, 973, 867, 723; LRMS (EI) *m/z* 226 (M^+, 20), 195 (28), 127 (57), 99 (100); HRMS (EI) calcd for $C_5H_7IO_2$ $[M]^+$: 225.9491, found: 225.9500.

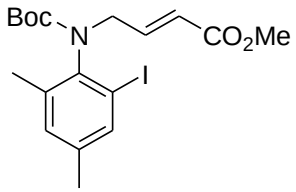

Representative procedure for **4-[*t*-butyloxycarbonyl-(2-iodo-4,6-dimethylphenyl)-amino]-but-2-enoic acid methyl ester (3.19a):** Carbamate **3.28** (0.694 g, 2.00 mmol) was dissolved in DMF (6.0 mL) with stirring at 0 °C. In one portion, Cs_2CO_3 (1.30 g, 4.00 mmol) was added and the mixture was stirred for 10 min. A solution of methyl 4-iodocrotonate (0.678 g, 3.00 mmol) in DMF (3.0 mL) was then added dropwise over 5 min. The mixture was slowly warmed to room temperature and stirred overnight, then poured into water (90 mL) and extracted with Et_2O (3 x 90 mL). The combined organic layers were washed sequentially with water and brine (2 x 90 mL each), dried over $MgSO_4$, filtered, and concentrated by rotary evaporation. Flash chromatography of the residue (5:1 hexanes:EtOAc) gave the title compound (0.641 g, 99%) as a clear solid, mp 66-68 °C, in a 2.8:1 ratio of rotamers. The racemate was submitted to preparative chiral HPLC separation ((*S*,*S*)-Whelk-O1, 99:1 hexanes:*i*-PrOH), first eluting enantiomer (*P*) $[\alpha]_D^{23}$ +1, 99/1 er (*c* 2.4 mg/mL, $CHCl_3$); second eluting enantiomer (*M*) $[\alpha]_D^{23}$ –1, 90/10 er (*c* 8.0 mg/mL, $CHCl_3$): ^{1}H NMR (300 MHz, $CDCl_3$) major rotamer δ 7.52 (m, 1H), 7.08 (ddd, *J* = 15.6 Hz, 7.5 Hz, 6.6 Hz, 1H), 6.98 (m, 1H), 5.83 (dt, *J* = 15.6 Hz, 1.5 Hz, 1H), 4.47 (ddd, *J* = 15.3 Hz, 6.3 Hz, 1.5 Hz, 1H), 3.97 (ddd, *J* = 15.3 Hz, 7.5 Hz, 1.5 Hz, 1H), 3.72 (s, 3H), 2.27 (s, 3H), 2.21 (s, 3H), 1.36 (s, 9H), minor rotamer δ 7.54 (m, 1H), 7.09 (ddd, *J* = 15.6 Hz, 7.2 Hz, 6.3 Hz, 1H), 7.00 (m, 1H), 5.86 (dt, *J* = 15.6 Hz, 1.5 Hz, 1H), 4.40 (ddd, *J* = 15.9 Hz, 6.3 Hz, 1.5 Hz, 1H), 3.91 (ddd, *J* = 15.9 Hz, 7.5 Hz, 1.5 Hz, 1H), 3.75 (s, 3H), 2.25 (s, 3H), 2.23 (s, 3H), 1.54 (s, 9H), ^{13}C NMR (75 MHz, $CDCl_3$) major rotamer δ 165.9, 153.5, 143.1, 139.8, 138.7, 137.4, 137.1, 131.3, 122.7, 100.1, 80.0, 51.2, 50.1, 27.9 (3C), 20.1, 19.08, additional peaks from the

minor rotamer seen at δ 166.0, 152.9, 143.5, 140.4, 137.62, 137.59, 131.6, 122.4, 100.3, 80.7, 51.4, 51.3, 28.1 (3C), 19.14; FTIR (thin film, $CHCl_3$, cm^{-1}) 2977, 2927, 1703, 1437, 1389, 1367, 1316, 1167, 1024, 981, 914, 855, 765, 733; HRMS (ESI) calcd for $C_{18}H_{24}NNaIO_4$ $[M + Na]^+$: 468.0648, found: 468.0685.

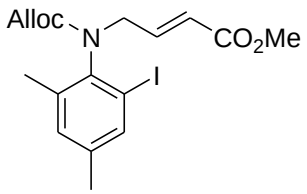

4-[Allyloxycarbonyl-(2-iodo-4,6-dimethylphenyl)-amino]-but-2-enoic acid methyl ester (3.19b): Carbamate **3.34** (1.01 g, 3.00 mmol) was alkylated in the manner of **3.19a** and purified with flash chromatography (5:1 hexanes:EtOAc) to give the title compound (1.28 g, 99%) as a clear colorless oil, in a 4.0:1 rotamer ratio. The racemate was submitted to preparative chiral HPLC separation (Chiralcel OD, 97:3 hexanes:*i*-PrOH), first eluting enantiomer (*P*) $[\alpha]_D^{23}$ –3.4, 100/0 er (*c* 13.4 mg/mL, $CHCl_3$); second eluting enantiomer (*M*) $[\alpha]_D^{23}$ +2.7, 87/13 er (*c* 26.2 mg/mL, $CHCl_3$): ^{1}H NMR (300 MHz, $CDCl_3$) major rotamer δ 7.55 (m, 1H), 7.09 (ddd, *J* = 15.6 Hz, 7.5 Hz, 6.6 Hz, 1H), 7.01 (m, 1H), 5.87 (dt, *J* = 15.6 Hz, 1.2 Hz, 1H), 5.83 (ddt, *J* = 17.1 Hz, 10.5 Hz, 5.4 Hz, 1H), 5.14 (dq, *J* = 17.1 Hz, 1.5 Hz, 1H), 5.12 (dq, *J* = 10.5 Hz, 1.5 Hz, 1H), 4.58 (dt, *J* = 5.4 Hz, 1.5 Hz, 1H), 4.52 (ddd, *J* = 15.3 Hz, 6.3 Hz, 1.2 Hz, 1H), 4.03 (ddd, *J* = 15.6 Hz, 7.5 Hz, 1.2 Hz, 1H), 3.73 (s, 3H), 2.28 (s, 3H), 2.22 (s, 3H), minor rotamer δ 7.55 (m, 1H), 7.09 (ddd, *J* = 15.6 Hz, 7.5 Hz, 6.6 Hz, 1H), 7.01 (m, 1H), 5.90-5.83 (m, 1H), 6.01 (ddt, *J* = 17.1 Hz, 10.5 Hz, 5.4 Hz, 1H), 5.39 (dq, *J* = 17.1 Hz, 1.5 Hz, 1H), 5.27 (dq, *J* = 10.5 Hz, 1.5 Hz, 1H), 4.75 (ddt, *J* = 13.5 Hz, 5.7 Hz, 1.5 Hz), 4.69 (ddt, *J* = 13.5 Hz, 5.7 Hz, 1.5 Hz, 1H), 4.56-4.47 (m, 1H), 4.05-3.95 (m, 1H), 3.75 (s, 3H), 2.27 (s, 3H), 2.23 (s, 3H); ^{13}C NMR (75 MHz, $CDCl_3$)

major rotamer δ 165.8, 154.3, 142.3, 139.3, 139.2, 137.6, 137.2, 132.2, 131.6, 123.2, 117.1, 100.0, 66.1, 51.2, 50.7, 20.1, 19.1, additional peaks from the minor rotamer seen at δ 153.6, 142.6, 139.8, 139.4, 137.7, 132.3, 131.7, 122.9, 117.5, 99.9, 66.2, 51.3,; FTIR (neat, cm^{-1}) 2950, 1716, 1437, 1394, 1308, 1173, 1029, 987, 929, 854, 798, 766; LRMS (EI) *m/z* 429 (M^+, 22), 344 (34), 165 (73), 158 (100), 98 (53); HRMS (EI) calcd for $C_{17}H_{20}INO_4$ $[M]^+$: 429.0437, found: 429.0443.

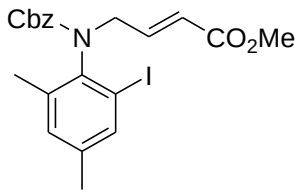

4-[Benzyloxycarbonyl-(2-iodo-4,6-dimethylphenyl)-amino]-but-2-enoic acid methyl ester (3.19c): Carbamate **3.36** (1.14 g, 3.00 mmol) was alkylated in the manner of **3.19a** and purified with flash chromatography (4:1 hexanes:EtOAc) to give the title compound (1.35 g, 94%) as a clear colorless oil in a 3.3:1 rotamer ratio. The racemate was submitted to preparative chiral HPLC separation (Chiralcel OD, 96:4 hexanes:*i*-PrOH), first eluting enantiomer (*P*) $[\alpha]_D^{23}$ +8.5, 99.5/0.5 er (*c* 8.9 mg/mL, $CHCl_3$); second eluting enantiomer (*M*) $[\alpha]_D^{23}$ –8.0, 89/11 er (*c* 28.2 g/mL, $CHCl_3$): ^{1}H NMR (300 MHz, $CDCl_3$) major rotamer δ 7.55 (m, 1H), 7.45-7.18 (m, 5H), 7.08 (ddd, *J* = 15.6 Hz, 7.5 Hz, 6.6 Hz, 1H), 6.99 (m, 1H), 5.87 (dt, *J* = 15.6 Hz, 1.5 Hz, 1H), 5.16 (d, *J* = 12.6 Hz, 1H), 5.10 (d, *J* = 12.6 Hz, 1H), 4.53 (ddd, *J* = 15.3 Hz, 6.6 Hz, 1.2 Hz, 1H), 4.04 (ddd, *J* = 15.6 Hz, 7.5 Hz, 1.2 Hz, 1H), 3.73 (s, 3H), 2.28 (s, 3H), 2.15 (s, 3H), minor rotamer δ 7.55 (m, 1H), 7.45-7.18 (m, 5H), 7.12-7.00 (m, 1H), 7.02 (m, 1H), 5.82 (dt, *J* = 15.3 Hz, 1.5 Hz, 1H), 5.31 (d, *J* = 12.3 Hz, 1H), 5.22 (d, *J* = 12.3 Hz, 1H), 4.55-4.45 (m, 1H), 4.04-3.94 (m, 1H), 3.74 (s, 3H), 2.27 (s, 3H), 2.22 (s, 3H); ^{13}C NMR (75 MHz, $CDCl_3$) major rotamer

δ 166.2, 154.9, 142.5, 139.6, 139.5, 137.9, 137.5, 136.3, 131.9, 128.2, 127.8, 127.6, 123.5, 100.3, 67.5, 51.5, 51.1, 20.4, 19.3, additional peaks from minor rotamer seen at δ 154.1, 142.9, 140.0, 139.7, 138.0, 137.8, 136.2, 132.0, 128.4, 128.1, 123.2, 100.1, 67.8, 51.6; FTIR (neat, cm^{-1}) 3031, 2951, 1710, 1437, 1399, 1173, 1127, 1027, 986, 911, 855, 733; LRMS (EI) *m/z* 479 (M^+, 17), 388 (53), 344 (62), 158 (62), 91 (100); HRMS calcd for $C_{21}H_{22}INO_4$ $[M]^+$: 479.0594, found: 479.0589.

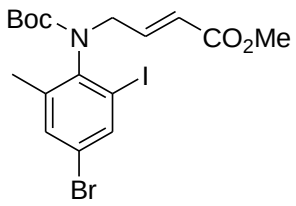

4-[*t*-Butyloxycarbonyl-(4-bromo-2-iodo-6-methylphenyl)-amino]-but-2-enoic acid methyl ester (3.19d): Carbamate **3.29** (0.412 g, 1.00 mmol) was alkylated in the manner of **3.19a** and purified with flash chromatography (4:1 hexanes:EtOAc) to give the title compound (320. mg, 63%) as a white solid, mp 45-46 °C, in a 3.1:1 ratio of rotamers. The racemate was submitted to preparative chiral HPLC separation ((*S*,*S*)-Whelk-O1, 98:2 hexanes:*i*-PrOH), first eluting enantiomer $[\alpha]_D^{23}$ +0.5, 98/2 er (*c* 6.2 mg/mL, $CHCl_3$); second eluting enantiomer $[\alpha]_D^{23}$ –0.6, 97/3 (*c* 30.0 mg/mL, $CHCl_3$): ^{1}H NMR (300 MHz, $CDCl_3$) major rotamer δ 7.84 (d, *J* = 2.1 Hz, 1H), 7.35 (d, *J* = 1.5 Hz, 1H), 7.05 (ddd, *J* = 15.6 Hz, 7.5 Hz, 6.6 Hz, 1H), 5.84 (dt, *J* = 15.6 Hz, 1.5 Hz, 1H), 4.46 (ddd, *J* = 15.6 Hz, 6.3 Hz, 1.5 Hz, 1H), 3.96 (ddd, *J* = 15.6 Hz, 7.5 Hz, 1.2 Hz, 1H), 3.73 (s, 3H), 2.23 (s, 3H), 1.37 (s, 9H), minor rotamer δ 7.85 (m, 1H), 7.36 (d, *J* = 2.1 Hz, 1H), 7.06 (ddd, *J* = 15.9 Hz, 7.2 Hz, 6.0 Hz, 1H), 5.86 (dt, *J* = 15.6 Hz, 1.5 Hz, 1H), 4.39 (ddd, *J* = 15.6 Hz, 6.0 Hz, 1.5 Hz, 1H), 3.90 (ddd, *J* = 15.9 Hz, 7.5 Hz, 1.2 Hz, 1H), 3.76 (s, 3H), 2.25 (s, 3H), 1.54 (s, 9H); ^{13}C NMR (75 MHz, $CDCl_3$) major rotamer δ 166.15, 153.3, 142.7, 142.1,

139.6, 139.3, 133.6, 123.4, 121.5, 101.2, 80.9, 51.6, 50.1, 28.1 (3C), 19.3, additional peaks from minor rotamer seen at δ 166.21, 152.9, 143.1, 142.5, 140.2, 139.5, 133.9, 123.1, 121.9, 101.4, 81.6, 51.7, 51.4, 28.3 (3C), 19.4; FTIR (thin film, $CHCl_3$, cm^{-1}) 2976, 1707, 1435, 1392, 1367, 1317, 1154, 980, 861, 756; HRMS (ESI) calcd for $C_{17}H_{21}{}^{79}BrINNaO_4$ $[M + Na]^+$: 531.9596, found: 531.9625.

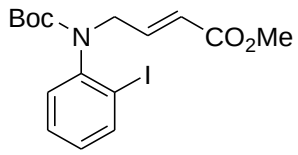

4-[*t*-Butyloxycarbonyl-(2-iodophenyl)-amino]-but-2-enoic acid methyl ester (3.19e): Carbamate **3.30** (0.638 g, 2.00 mmol) was alkylated in the manner of **3.19a** and purified with flash chromatography (3:1 pentane:Et_2O) to give the title compound in quantitative yield (843 mg) as a clear colorless oil containing ~5% of an inseparable impurity. For further purification, 400. mg of the oil was purified by preparative HPLC ((*S*,*S*)-Whelk O 1, 90:10 hexanes:*i*-PrOH, 4 injections) to afford the title compound (0.364 g, 91% overall yield) as a clear colorless oil, with a 2.4:1 ratio of rotamers: ^{1}H NMR (300 MHz, $CDCl_3$) major rotamer δ 7.87 (d, *J* = 7.5 Hz, 1H), 7.33 (t, *J* = 7.5 Hz, 1H), 7.15 (d, *J* = 7.5 Hz, 1H), 7.02 (ddd, *J* = 15.6 Hz, 6.6 Hz, 5.7 Hz, 1H), 7.03-6.97 (m, 1H), 5.90 (d, *J* = 15.6 Hz, 1H), 4.66 (dd, *J* = 16.5 Hz, 5.4 Hz, 1H), 3.85 (dd, *J* = 16.2 Hz, 6.6 Hz, 1H), 3.73 (s, 3H), 1.36 (s, 9H), minor rotamer 7.93-7.85 (br m, 1H), 7.40-7.33 (br m, 1H), 7.24 (d, *J* = 7.5 Hz, 1H), 7.02 (ddd, *J* = 15.6 Hz, 6.6 Hz, 5.7 Hz, 1H), 7.03-6.97 (m, 1H), 6.00-5.90 (br m, 1H), 4.65-4.53 (br m, 1H), 3.87-3.79 (m, 1H), 3.76 (s, 3H), 1.53 (s, 9H); ^{13}C NMR (75 MHz, $CDCl_3$) major rotamer δ 166.4, 153.7, 143.4, 139.5, 129.7, 129.2, 129.0 (2C, accidental isochrony), 122.7, 100.1, 80.8, 51.5, 50.2, 28.1 (3C), peaks from minor rotamer were

broadened; FTIR (neat, cm^{-1}) 2979, 1705, 1472, 1435, 1386, 1316, 1278, 1166, 1019, 980, 863, 761; HRMS calcd for $C_{16}H_{20}INO_4$ $[M]^+$: 417.0437, found: 417.0445.

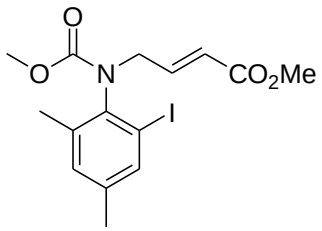

4-[Methyloxycarbonyl-(2-iodo-4,6-methylphenyl)-amino]-but-2-enoic acid methyl ester (3.19f): Carbamate **3.35** (0.915 g, 3.00 mmol) was alkylated in the manner of **3.19a** and purified with flash chromatography (2:1 pentane:Et_2O) to give the title compound (0.934 g, 77%) as a clear colorless oil in a 5.0:1 ratio of rotamers: ^{1}H NMR (300 MHz, $CDCl_3$) major rotamer δ 7.56 (m, 1H), 7.09 (ddd, 15.6 Hz, 7.5 Hz, 6.6 Hz, 1H), 7.02 (m, 1H), 5.87 (dt, *J* = 15.6 Hz, 1.5 Hz, 1H), 4.49 (ddd, *J* = 15.6 Hz, 6.6 Hz, 1.5 Hz, 1H), 4.04 (ddd, *J* = 15.6 Hz, 7.5 Hz, 1.5 Hz, 1H), 3.73 (s, 3H), 3.68 (s, 3H), 2.28 (s, 3H), 2.21 (s, 3H), minor rotamer δ 7.56 (m, 1H), 7.08 (ddd, *J* = 15.6 Hz, 7.5 Hz, 6.3 Hz, 1H), 7.02 (m, 1H), 5.85 (dt, *J* = 15.6 Hz, 1.5 Hz, 1H), 4.51-4.42 (m, 1H), 4.01-3.93 (m, 1H), 3.84 (s, 3H), 3.75 (s, 3H), 2.27 (s, 3H), 2.22 (s, 3H); ^{13}C NMR (75 MHz, $CDCl_3$) major rotamer δ 165.85, 155.2, 142.4, 139.4, 139.3, 137.7, 137.3, 131.7, 123.2, 100.1, 53.1, 51.3, 50.9, 20.2, 19.1, additional signals from the minor rotamer were seen at δ 165.91, 154.4, 142.8, 139.8, 137.8, 137.6, 131.8, 122.8, 100.0, 53.0, 51.4; FTIR (neat, cm^{-1}) 2952, 1717, 1447, 1313, 1193, 1174, 992, 916, 854, 732; LRMS (EI) *m/z* 403 (M^+, 46), 276 (100), 216 (32), 177 (78), 158 (40); HRMS (EI) calcd for $C_{15}H_{18}INO_4$ $[M]^+$: 403.0281, found: 403.0299.

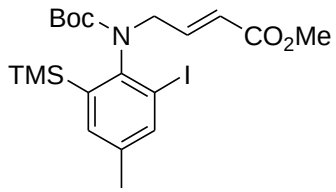

4-[*t*-Butyloxycarbonyl-(2-iodo-4-methyl-6-(trimethylsilyl)phenyl)-amino]-but-2-enoic acid methyl ester (3.19g): Carbamate **3.31** (0.203 g, 0.500 mmol) was alkylated in the manner of **3.19a** and purified with flash chromatography (6:1 hexanes:EtOAc) to give the title compound (143 mg, 57%) as a white solid, mp 69-71 °C, with a 2.75:1 ratio of rotamers: ^{1}H NMR (300 MHz, $CDCl_3$) major rotamer δ 7.69 (s, 1H), 7.26 (s, 1H), 7.09 (dt, *J* = 15.6 Hz, 7.2 Hz, 1H), 5.80 (d, *J* = 15.6 Hz, 1H), 4.43 (dd, *J* = 15.3 Hz, 6.6 Hz, 1H), 4.08 (dd, *J* = 15.3 Hz, 7.5 Hz, 1H), 3.70 (s, 3H), 2.30 (s, 3H), 1.39 (s, 9H), 0.28 (s, 9H), minor rotamer δ 7.69 (s, 1H), 7.26 (s, 1H), 7.19 (dt, *J* = 15.6 Hz, 7.2 Hz, 1H), 5.80 (d, *J* = 15.6 Hz, 1H), 4.31 (dd, *J* = 15.6 Hz, 6.9 Hz, 1H), 4.15-4.00 (m, 1H), 3.73 (s, 3H), 2.28 (s, 3H), 1.53 (s, 9H), 0.28 (s, 9H); ^{13}C NMR (75 MHz, $CDCl_3$) major rotamer δ 166.1, 154.0, 144.7, 143.2, 141.2, 141.0, 138.2, 136.3, 122.8, 102.1, 80.7, 51.4, 51.3, 28.2 (3C), 20.4, 0.17 (3C), additional peaks from the minor rotamer seen at δ 166.2, 153.5, 145.6, 143.9, 141.6, 141.3, 138.5, 136.5, 122.3, 102.4, 80.9, 52.6, 51.5, 28.3 (3C), –0.0 (3C); FTIR (thin film, $CHCl_3$, cm^{-1}) 2976, 1727, 1704, 1435, 1366, 1316, 1251, 1165, 895, 839, 757; LRMS (EI) *m/z* 503 (M^+, 1), 447 (95), 356 (69), 320 (100), 288 (81), 200 (86); HRMS (EI) calcd for $C_{20}H_{30}INO_4Si$ $[M]^+$: 503.0989, found: 503.0977.

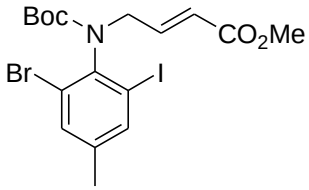

4-[*t*-Butyloxycarbonyl-(6-bromo-2-iodo-4-methylphenyl)-amino]-but-2-enoic acid methyl ester (3.19h): Carbamate **3.32** (0.412 g, 1.00 mmol) was alkylated in the manner of **3.19a** and purified with flash chromatography (4:1 pentane:Et_2O) to give the title compound (0.332 g, 65%) as a white solid, mp 92-94 °C, with a 3.76:1 ratio of rotamers: ^{1}H NMR (300 MHz, $CDCl_3$) major rotamer δ 7.63 (m, 1H), 7.41 (m, 1H), 7.18 (dt, *J* = 15.6 Hz, 6.9 Hz, 1H), 5.87 (dt, *J* = 15.6 Hz, 1.5 Hz, 1H), 4.30 (ddd, *J* = 15.6 Hz, 6.9 Hz, 1.5 Hz, 1H), 4.23 (m, 1H), 3.72 (s, 3H), 2.30 (s, 3H), 1.38 (s, 9H), minor rotamer δ 7.65 (m, 1H), 7.42 (m, 1H), 7.22 (dt, *J* = 15.6 Hz, 6.6 Hz, 1H), 5.86 (dt, *J* = 15.6 Hz, 1.5 Hz, 1H), 4.25-4.19 (m, 1H), 4.15 (ddd, *J* = 15.9 Hz, 6.9 Hz, 1.5 Hz, 1H), 3.75 (s, 3H), 2.28 (s, 3H), 1.54 (s, 9H); ^{13}C NMR (75 MHz, $CDCl_3$) major rotamer δ 166.4, 153.2, 143.5, 140.7, 140.0, 139.3, 134.0, 123.4, 123.1, 101.0, 80.9, 51.5, 50.1, 28.1 (3C), 20.2, additional signals from the minor rotamer were seen at δ 166.5, 144.1, 141.1, 139.5, 134.2, 122.6, 101.2, 81.6, 51.6, 28.4 (3C); FTIR (thin film, $CHCl_3$, cm^{-1}) 2976, 1708, 1461, 1435, 1367, 1315, 1164, 978, 855, 763, 723; HRMS (ESI) calcd for $C_{17}H_{21}{}^{79}BrINNaO_4$ $[M + Na]^+$: 531.9596, found: 531.9586.

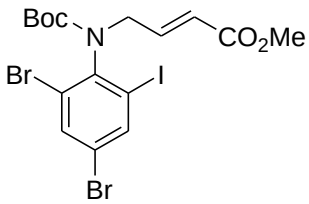

4-[*t*-Butyloxycarbonyl-(4,6-dibromo-2-iodo-6-phenyl)-amino]-but-2-enoic acid methyl ester (3.19i): Carbamate **3.33** (0.715 g, 1.50 mmol) was alkylated in the manner of **3.19a** and purified

with flash chromatography (6:1 hexanes:EtOAc) to give the title compound (0.742 g, 86%) as a white solid, mp 78-79 °C, in a 3.8:1 ratio of rotamers: ^{1}H NMR (300 MHz, $CDCl_3$) Major rotamer δ 7.96 (d, *J* = 2.4 Hz, 1H), 7.76 (d, *J* = 2.1 Hz, 1H), 7.15 (dt, *J* = 15.6 Hz, 7.2 Hz, 1H), 5.85 (dt, *J* = 15.6 Hz, 1.5 Hz, 1H), 4.29 (ddd, *J* = 15.6 Hz, 6.9 Hz, 1.5 Hz), 4.22 (ddd, *J* = 15.6 Hz, 6.9 Hz, 1.5 Hz), 3.73 (s, 3H), 1.38 (s, 9H), minor rotamer δ 7.97 (d, *J* = 2.1 Hz, 1H), 7.77 (d, *J* = 2.1 Hz, 1H), 7.19 (dt, *J* = 15.9 Hz, 6.9 Hz, 1H), 5.87 (dt, *J* = 15.6 Hz, 1.5 Hz, 1H), 4.21-4.15 (m, 2H), 3.76 (s, 3H), 1.54 (s, 9H); ^{13}C NMR (75 MHz, $CDCl_3$) major rotamer δ 165.8, 152.3, 142.7, 141.9, 140.6, 135.6, 124.1, 123.2, 121.9, 101.8, 81.1, 51.4, 49.6, 27.8 (3C), additional peaks from the minor rotamer seen at δ 165.9, 152.2, 143.2, 142.5, 140.8, 135.8, 124.5, 122.8, 122.2, 102.0, 81.7, 51.5, 51.1, 28.1 (3C); FTIR (thin film, $CHCl_3$, cm^{-1}) 3400 (broad), 2977, 1714, 1555, 1527, 1443, 1367, 1317, 1163, 978, 860, 814, 759, 718; LRMS (EI) *m/z* 577 (M^+ (^{81}Br, ^{81}Br), < 1), 521 ((^{81}Br, ^{81}Br) 44), 290 ((^{81}Br, ^{81}Br) 19), 99 (39), 91 (71), 57 (100); HRMS (EI) calcd for $C_{16}H_{18}Br_2INO_4$ $[M]^+$: 572.8647, found: 572.8649.

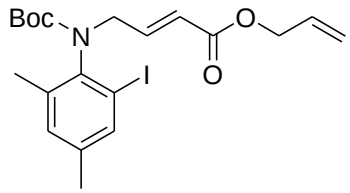

4-[*t*-Butyloxycarbonyl-(2-iodo-4,6-dimethylphenyl)-amino]-but-2-enoic acid allyl ester (3.19j): To a stirred solution of methyl ester **3.19a** (0.891 g, 2.00 mmol) in THF (10 mL) at 0 °C was added aqueous NaOH solution (1.0 M, 6.0 mL). The mixture was warmed to room temperature and stirred overnight, volatiles were removed by rotary evaporation, and the mixture was acidified to pH 1 at 0 °C with 1 N HCl. The mixture was extracted with CH_2Cl_2 (3 x 50 mL) and EtOAc (1 x 50 mL), and the combined organic layers were dried over Na_2SO_4, filtered, and

concentrated by rotary evaporation. This yielded the crude acid **3.37** as a sticky yellow solid in quantitative yield (~95% pure by ^{1}H NMR), which was used directly in the next step without further purification.

The crude acid **3.37** (0.866 g, ~2.00 mmol) and allyl alcohol (0.139 g, 2.40 mmol) were dissolved in CH_2Cl_2 (10 mL) with stirring. DCC (0.495 g, 2.40 mmol) was added all at once, followed by DMAP (12 mg, 0.1 mmol), and the reaction was stirred for 3 h at room temperature. The mixture was filtered through Celite and washed with CH_2Cl_2 (3 x 20 mL), washed with water (1 x 50 mL), dried over $MgSO_4$, filtered, and concentrated by rotary evaporation. Flash chromatography (5:1 hexanes:EtOAc) gave the title compound (0.584 g, 62% over 2 steps) as a clear colorless oil in a 3:1 ratio of rotamers: ^{1}H NMR (300 MHz, $CDCl_3$) major rotamer δ 7.52 (s, 1H), 7.10 (ddd, *J* = 15.6 Hz, 7.5 Hz, 6.6 Hz, 1H), 6.98 (s, 1H), 6.00-5.83 (m, 1H), 5.86 (dt, *J* = 15.3 Hz, 1.2 Hz), 5.31 (dq, *J* = 17.1 Hz, 1.5 Hz, 1H), 5.23 (dq, *J* = 10.5 Hz, 1.5 Hz, 1H), 4.63 (dt, *J* = 5.7 Hz, 1.2 Hz, 2H), 4.47 (ddd, *J* = 15.3 Hz, 6.3 Hz, 1.2 Hz, 1H), 3.99 (ddd, *J* = 15.6 Hz, 7.5 Hz, 1.2 Hz, 1H), 2.27 (s, 3H), 2.21 (s, 3H), 1.36 (s, 9H), minor rotamer δ 7.54 (s, 1H), 7.10 (ddd, *J* = 15.6 Hz, 7.5 Hz, 6.6 Hz, 1H), 7.00 (s, 1H), 6.00-5.85 (m, 2H), 5.33 (dq, *J* = 17.1 Hz, 1.5 Hz, 1H), 5.28-5.23 (m, 1H), 4.66 (dt, *J* = 5.4 Hz, 1.2 Hz, 1H), 4.40 (ddd, *J* = 15.9 Hz, 6.3 Hz, 1.5 Hz, 1H), 3.92 (ddd, *J* = 15.7 Hz, 7.2 Hz, 1.2 Hz, 1H), 2.25 (s, 3H), 2.23 (s, 3H), 1.53 (s, 9H); ^{13}C NMR (75 MHz, $CDCl_3$) major rotamer δ 165.4, 153.7, 143.5, 140.0, 138.9, 137.6, 137.3, 132.1, 131.5, 123.0, 117.8, 100.3, 80.3, 64.8, 50.2, 28.1 (3C), 20.3, 19.2, additional peaks from the minor rotamer seen at δ 153.2, 144.0, 140.5, 139.3, 137.8, 131.8, 122.6, 100.5, 81.0, 64.9, 51.6, 28.3 (3C), 19.3; FTIR (neat, cm^{-1}) 2976, 2927, 1703, 1472, 1367, 1312, 1257, 1166, 1021, 987, 935, 855, 768; HRMS (ESI) calcd for $C_{20}H_{26}INNaO_4$ $[M + Na]^+$: 494.0804, found: 494.0796.

General procedures for the cyclizations of racemic and enantioenriched **3.19a-j** to **3.20a-j** follow. These procedures describe the experiments outlined in Table 3.2 in Chapter 3.2.2, and Table 3.4 in Chapter 3.2.5. Characterization data for cyclized products **3.20a-j** are given below; for the associated procedures and yields, refer to these tables in the main text.

General procedure (R) for radical mediated cyclizations: To a non-degassed, stirred solution of the appropriate aryl iodide in benzene, open to the atmosphere, was added Bu_3SnH (0.01 M, 1.5 equiv) at room temperature. A solution of Et_3B in hexane (1.0 M, 1.0 equiv) was added via syringe, and the reaction was stirred until completion (< 5 min). Solvent was removed by rotary evaporation, and the crude residue was purified using flash chromatography on 10% w/w KF/silica gel[80] with a hexane/EtOAc solvent system.

General procedure (R2) for radical cyclizations of Br-containing compounds: To a non-degassed, stirred solution of the appropriate aryl iodide in benzene was added Bu_3SnH (0.01 M, 1.1 equiv) at room temperature. A solution of Et_3B in hexane (1.0 M, 1.0 equiv) was added via syringe, and the reaction was completed and purified as described in general procedure R.

General procedure (A) for lithium-halogen exchange mediated cyclizations: The appropriate aryl iodide was dissolved in a Trapp solvent mixture (4:1:1 THF : Et_2O : pentane) with stirring to make a ~0.10 M solution. TMSCl (5.0 equiv) was added via syringe, the mixture was stirred for 5 min, and then cooled to –98 °C with a MeOH / liquid nitrogen bath. A solution of BuLi in hexanes (1.29 M, 1.2 equiv) was added dropwise over 10 min, and the reaction was stirred until complete (< 10 min). The reaction was quenched with rapid addition of sat. aqueous NH_4Cl solution (1 mL), and the mixture was allowed to warm to room temperature and stirred for 1 h. Water (4 mL) was added, and the mixture was extracted with Et_2O (3 x 10 mL). The

combined organic layers were washed with brine (1 x 10 mL), dried over $MgSO_4$, filtered, and concentrated by rotary evaporation. The crude residue was purified using flash chromatography with the appropriate solvent system.

General procedure (A2) for lithium-halogen exchange on Br-containing compounds: The appropriate aryl iodide was dissolved in toluene with stirring to make a ~0.05 M solution. TMSCl (5.0 equiv) was added via syringe, the mixture was stirred for 5 min, and then cooled to –91 °C with a heptane / liquid nitrogen bath. A solution of BuLi in hexanes (1.29 M, 1.2 equiv) was added dropwise over 10 min, and the reaction was stirred until complete. The reaction mixture was then quenched, worked up and purified as described in procedure A.

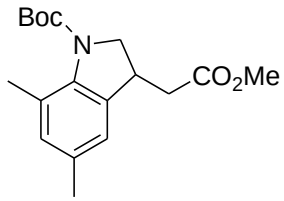

***tert*-Butyl 3-(2-methoxy-2-oxoethyl)-5,7-dimethylindoline-1-carboxylate (3.20a):** After cyclization of **3.19a**, flash chromatography (5:1 hexanes:EtOAc) afforded the title compound as a clear, colorless oil. Chiral analysis was performed on the analytical (*S*,*S*)-Whelk-O1 column (98:2 hexanes:*i*-PrOH). The atropisomer (*P*)-(+)-**3.19a** cyclized to give (*S*)-(+)-**3.20b** (first eluting enantiomer), $[\alpha]_D^{23}$ +8.2 (*c* 29.8 mg/mL, $CHCl_3$): The atropisomer (*M*)-(–)-**3.20a** cyclized to give (*R*)-(–)-**3.19b** (second eluting enantiomer), $[\alpha]_D^{23}$ –9.2 (*c* 19.5 mg/mL, $CHCl_3$). ^{1}H NMR (300 MHz, $CDCl_3$) δ 6.86 (s, 1H), 6.80 (s, 1H), 4.24 (dd, *J* = 11.4 Hz, 7.5 Hz, 1H), 3.78 (dd, *J* = 11.4 Hz, 5.7 Hz, 1H), 3.74 (s, 3H), 3.56 (m, 1H), 2.71 (dd, *J* = 16.2 Hz, 5.1 Hz, 1H), 2.45 (dd, *J* = 16.2 Hz, 9.3 Hz, 1H), 2.28 (s, 3H), 2.27 (s, 3H), 1.53 (s, 9H); ^{13}C NMR (75 MHz, $CDCl_3$) δ 172.2, 153.9, 139.2, 136.4, 134.0, 130.8, 127.8, 121.4, 80.5, 56.8, 51.6, 38.1, 37.9, 28.2

(3C), 20.8, 19.6; FTIR (neat, cm^{-1}) 2976, 1739, 1708, 1479, 1366, 1246, 1163, 1010, 856, 770, 733; HRMS (ESI) calcd for $C_{18}H_{25}NNaO_4$ $[M + Na]^+$: 342.1681, found: 342.1671.

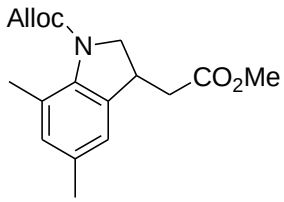

Allyl 3-(2-methoxy-2-oxoethyl)-5,7-dimethylindoline-1-carboxylate (3.20b): After cyclization of **3.19b**, flash chromatography (4:1 hexanes:EtOAc) afforded the title compound as a clear, colorless oil. Chiral analysis was performed on the analytical (*S*,*S*)-Whelk-O1 column (99:1 hexanes:*i*-PrOH). The atropisomer (*P*)-(–)-**3.19b** cyclized to give (*S*)-(+)-**3.20b** (first eluting enantiomer), $[\alpha]_D^{23}$ +5.0 (*c* 9.8 mg/mL, $CHCl_3$): The atropisomer (*M*)-(+)-**3.19b** cyclized to give (*R*)-(–)-**3.20b** (second eluting enantiomer), $[\alpha]_D^{23}$ –6.4 (*c* 14.3 mg/mL, $CHCl_3$). ^1H NMR (300 MHz, $CDCl_3$) δ 6.87 (s, 1H), 6.82 (s, 1H), 5.99 (ddt, *J* = 17.1 Hz, 10.5 Hz, 6.0 Hz, 1H), 5.34 (dq, *J* = 17.1 Hz, 1.2 Hz, 1H), 5.25 (dd, *J* = 10.5 Hz, 1.2 Hz, 1H), 4.70 (dd, *J* = 17.1 Hz, 1H), 4.68 (dt, *J* = 6.0 Hz, 1.2 Hz, 1H), 4.35 (dd, *J* = 11.4 Hz, 7.5 Hz, 1H), 3.83 (dd, *J* = 11.4 Hz, 6.0 Hz, 1H), 3.73 (s, 3H), 3.61 (m, 1H), 2.75 (dd, *J* = 16.2 Hz, 5.1 Hz, 1H), 2.47 (dd, *J* = 16.2 Hz, 9.6 Hz, 1H), 2.29 (s, 3H), 2.27 (s, 3H); ^{13}C NMR (75 MHz, $CDCl_3$) δ 172.2, 154.2, 138.8, 136.3, 134.4, 132.5, 131.1, 127.7, 121.5, 118.0, 66.4, 56.6, 51.7, 38.1, 37.8, 20.8, 19.8; FTIR (neat, cm^{-1}) 2952, 1715, 1478, 1416, 1382, 1327, 1239, 1169, 1029, 934, 857, 766; HRMS (ESI) calcd for $C_{17}H_{21}NNaO_4$ $[M + Na]^+$: 326.1368, found: 326.1360.

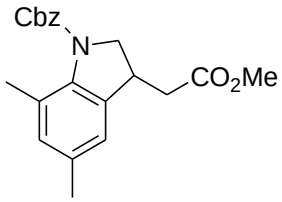

Benzyl 3-(2-methoxy-2-oxoethyl)-5,7-dimethylindoline-1-carboxylate (3.20c): After cyclization of **3.19c**, flash chromatography (4:1 hexanes:EtOAc) afforded the title compound as a clear, colorless oil. Chiral analysis was performed on the analytical Chiralcel OD column (98:2 hexane:*i*-PrOH). The atropisomer (*P*)-(+)-**3.19c** cyclized to give (*S*)-(+)-**3.20c** (second eluting enantiomer), $[\alpha]_D^{23}$ +9.0 (*c* 12.3 mg/mL, $CHCl_3$): The atropisomer (*M*)-(–)-**3.19c** cyclized to give (*R*)-(–)-**3.20c** (first eluting enantiomer), $[\alpha]_D^{23}$ –11 (*c* 12.4 mg/mL, $CHCl_3$). ^{1}H NMR (300 MHz, $CDCl_3$) δ 7.38-7.32 (m, 5H), 6.86 (s, 1H), 6.81 (s, 1H), 5.27 (d, *J* = 12.3 Hz, 1H), 5.20 (d, *J* = 12.3 Hz, 1H), 4.33 (dd, *J* = 11.4 Hz, 7.8 Hz, 1H), 3.86 (dd, *J* = 11.4 Hz, 6.0 Hz, 1H), 3.71 (s, 3H), 3.58 (m, 1H), 2.71 (dd, *J* = 16.5 Hz, 5.7 Hz, 1H), 2.44 (dd, *J* = 16.2 Hz, 9.3 Hz, 1H), 2.28 (s, 3H), 2.24 (s, 3H); ^{13}C NMR (75 MHz, $CDCl_3$) δ 172.1, 154.4, 138.8, 136.3, 136.2, 134.5, 131.1, 128.4 (2C), 128.1 (2C), 128.1, 127.8, 121.5, 67.5, 56.6, 51.7, 38.1, 37.8, 20.8, 19.9; FTIR (neat, cm^{-1}) 3031, 2952, 1715, 1478, 1390, 1355, 1219, 1169, 1023, 856, 754; HRMS (ESI) calcd for $C_{21}H_{23}NNaO_4$ $[M + Na]^+$: 376.1525, found: 376.1529.

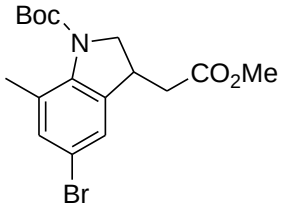

***tert*-Butyl 3-(2-methoxy-2-oxoethyl)-5-bromo-7-methylindoline-1-carboxylate (3.20d):** After cyclization of **3.19d**, flash chromatography (5:1 hexanes:EtOAc) afforded the title compound as a clear, colorless oil. Chiral analysis was performed on the analytical (*S*,*S*)-Whelk-O1 column

(99:1 hexanes:*i*-PrOH). The atropisomer (+)-**3.19d** cyclized to give (+)-**3.20d** (first eluting enantiomer), $[\alpha]_D^{23}$ +1.9 (*c* 5.7 mg/mL, $CHCl_3$). The atropisomer (–)-**3.19d** cyclized to give (–)-**3.20d** (second eluting enantiomer), $[\alpha]_D^{23}$ –2.2 (*c* 19.8 mg/mL, $CHCl_3$). ^{1}H NMR (300 MHz, $CDCl_3$) δ 7.18 (s, 1H), 7.11 (s, 1H), 4.24 (dd, *J* = 11.7 Hz, 8.1 Hz, 1H), 3.79 (dd, *J* = 11.7 Hz, 5.7 Hz, 1H), 3.74 (s, 3H), 3.59 (m, 1H), 2.69 (dd, *J* = 16.2 Hz, 5.4 Hz, 1H), 2.46 (dd, *J* = 16.2 Hz, 9.0 Hz, 1H), 2.27 (s, 3H), 1.52 (s, 9H); ^{13}C NMR (75 MHz, $CDCl_3$) δ 171.9, 153.6, 141.1, 138.5, 133.0, 130.3, 124.1, 117.1, 81.2, 56.9, 51.9, 38.0, 37.9, 28.3 (3C), 19.7; FTIR (neat, cm^{-1}) 3011, 2978, 1737, 1707, 1459, 1366, 1238, 1161, 1009, 859, 757; LRMS (EI) *m/z* 385 (M^+ (^{81}Br), 4), 285 ((^{81}Br) 40), 144 (40), 131 (100); HRMS (EI) calcd for $C_{17}H_{22}{}^{79}BrNO_4$ $[M]^+$: 383.0732, found: 383.0726.

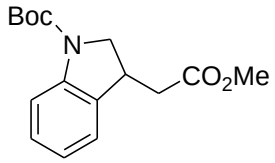

***rac-tert*-Butyl 3-(2-methoxy-2-oxoethyl)-indoline-1-carboxylate (3.20e):** After cyclization of *rac*-**3.19e**, flash chromatography (4:1 hexanes:EtOAc) afforded the title compound as a clear, colorless oil: ^{1}H NMR (300 MHz, $CDCl_3$) δ 7.86 (br, 1H), 7.20 (t, *J* = 7.8 Hz, 1H), 7.13 (d, *J* = 7.5 Hz, 1H), 6.95 (td, *J* = 7.5 Hz, 1.2 Hz, 1H), 4.21 (dd, *J* = 11.4 Hz, 9.6 Hz, 1H), 3.83-3.73 (m, 1H), 3.74 (s, 3H), 3.73- 3.62 (m, 1H), 2.79 (dd, *J* = 16.5 Hz, 4.8 Hz, 1H), 2.59 (dd, *J* = 16.5 Hz, 9.3 Hz, 1H), 1.57 (s, 9H); ^{13}C NMR (75 MHz, $CDCl_3$) δ 172.2, 152.4, 128.2, 123.8, 122.3, 114.8, 80.8 (br), 53.9, 51.2, 39.9, 35.7, 28.4 (3C), 2 aromatic signals missing, attributed to peak broadening from N-CO rotation; FTIR (neat, cm^{-1}) 2977, 1738, 1703, 1486, 1393, 1167, 1146, 1016, 753; HRMS (ESI) calcd for $C_{16}H_{21}NNaO_4$ $[M + Na]^+$: 314.1368, found: 314.1368.

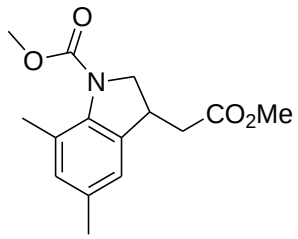

***rac*-Methyl 3-(2-methoxy-2-oxoethyl)-5,7-dimethylindoline-1-carboxylate (3.20f):** After cyclization of *rac*-**3.19f**, flash chromatography (4:1 hexanes:EtOAc) afforded the title compound as a clear, colorless oil: ^{1}H NMR (300 MHz, $CDCl_3$) δ 6.88 (s, 1H), 6.81 (s, 1H), 4.33 (dd, *J* = 11.4 Hz, 7.8 Hz, 1H), 3.80 (s, 3H), 3.80 (dd, *J* = 11.4 Hz, 6.3 Hz, 1H), 3.73 (s, 3H), 3.60 (m, 1H), 2.75 (dd, *J* = 16.5 Hz, 5.1 Hz, 1H), 2.47 (dd, *J* = 16.2 Hz, 9.3 Hz, 1H), 2.29 (s, 3H), 2.26 (s, 3H); ^{13}C NMR (75 MHz, $CDCl_3$) δ 172.0, 154.9, 138.7, 136.1, 134.3, 130.9, 127.6, 121.4, 56.5, 52.5, 51.6, 37.9, 37.6, 20.7, 19.6; FTIR (neat, cm^{-1}) 2954, 1716, 1441, 1367, 1243, 1194, 1169, 1122, 1055, 857, 767; HRMS (ESI) calcd for $C_{15}H_{19}NNaO_4$ $[M + Na]^+$: 300.1212, found: 300.1208.

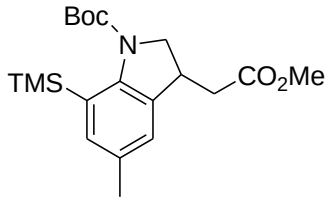

***rac-tert*-Butyl 3-(2-methoxy-2-oxoethyl)-5-methyl-7-(trimethylsilyl)indoline-1-carboxylate (3.20g):** After cyclization of *rac*-**3.19g**, flash chromatography (6:1 hexanes:EtOAc) afforded the title compound as a clear, colorless oil: ^{1}H NMR (300 MHz, $CDCl_3$) δ 7.23 (s, 1H), 6.97 (s, 1H), 4.23 (dd, *J* = 11.7 Hz, 8.1 Hz, 1H), 3.75 (dd, *J* = 11.4 Hz, 6.0 Hz, 1H), 3.75 (s, 3H), 2.74 (dd, *J* = 16.2 Hz, 4.8 Hz, 1H), 2.45 (dd, *J* = 16.2 Hz, 9.9 Hz, 1H), 2.32 (s, 3H), 1.54 (s, 9H), 0.29 (s,

9H); ^{13}C NMR (75 MHz, $CDCl_3$) δ 172.5, 154.8, 145.0, 135.3, 134.9, 133.0, 129.6, 124.8, 80.5, 55.5, 51.7, 38.6, 37.6, 28.4 (3C), 21.0, 0.3 (3C); FTIR (neat, cm^{-1}) 2952, 2899, 1740, 1707, 1398, 1364, 1246, 1164, 1010, 885, 840, 778; HRMS (ESI) calcd for $C_{20}H_{31}NNaO_4Si$ $[M + Na]^+$: 400.1920, found: 400.1918.

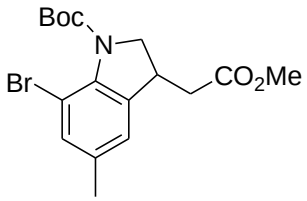

***rac-tert*-Butyl 3-(2-methoxy-2-oxoethyl)-7-bromo-5-methylindoline-1-carboxylate (3.20h):** After cyclization of *rac*-**3.19h**, flash chromatography (4:1 hexanes:EtOAc) afforded the title compound as a clear, colorless oil: ^{1}H NMR (300 MHz, $CDCl_3$) δ 7.22 (s, 1H), 6.91 (s, 1H), 4.27 (dd, *J* = 11.7 Hz, 7.5 Hz, 1H), 3.81 (dd, *J* = 11.7 Hz, 5.7 Hz, 1H), 3.74 (s, 3H), 3.62 (m, 1H), 2.69 (dd, *J* = 16.5 Hz, 5.7 Hz, 1H), 2.47 (dd, *J* = 16.2 Hz, 9.0 Hz, 1H), 2.29 (s, 3H), 1.54 (s, 9H); ^{13}C NMR (75 MHz, $CDCl_3$) δ 171.9, 153.5, 140.0, 139.1, 135.9, 132.8, 123.4, 112.6, 81.5, 57.4, 51.8, 38.6, 38.0, 28.2 (3C), 20.7; FTIR (neat, cm^{-1}) 2977, 1703, 1473, 1366, 1249, 1161, 1117, 1040, 1006, 855, 787, 735; HRMS (ESI) calcd for $C_{17}H_{22}{}^{79}BrNNaO_4$ $[M + Na]^+$: 406.0630, found: 406.0641.

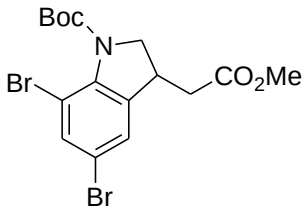

***rac-tert*-Butyl 3-(2-methoxy-2-oxoethyl)-5,7-dibromoindoline-1-carboxylate (3.20i):** After cyclization of *rac*-**3.19i**, flash chromatography (4:1 hexanes:EtOAc) afforded the title compound

as a white solid, mp 101-103 °C: ^{1}H NMR (300 MHz, $CDCl_3$) δ 7.56 (s, 1H), 7.25 (s, 1H), 4.29 (dd, *J* = 11.7 Hz, 7.8 Hz, 1H), 3.82 (dd, 11.7 Hz, 6.0 Hz), 3.74 (s, 3H), 3.66 (m, 1H), 2.68 (dd, *J* = 16.5 Hz, 6.0 Hz, 1H), 2.50 (dd, *J* = 16.5 Hz, 8.4 Hz, 1H), 1.54 (s, 9H); ^{13}C NMR (75 MHz, $CDCl_3$) δ 171.5, 152.9, 141.9, 140.8, 134.7, 126.0, 117.3, 113.5, 82.0, 57.3, 51.9, 38.4, 37.7, 28.1 (3C); FTIR (thin film, $CHCl_3$, cm^{-1}) 2979, 1709, 1447, 1368, 1335, 1248, 1160, 858, 759; LRMS (EI) *m/z* 451 (M^+ (^{81}Br, ^{81}Br), 7), 351 ((^{81}Br, ^{81}Br) 65), 290 ((^{81}Br, ^{81}Br) 34), 210 ((^{81}Br) 49), 197 ((^{81}Br) 68), 57 (100); HRMS (EI) calcd for $C_{16}H_{19}{}^{79}Br_2NO_4$ $[M]^+$: 446.9681, found: 446.9670.

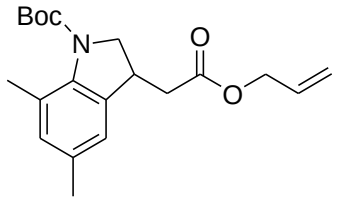

***rac-tert*-Butyl 3-(2-allyloxy-2-oxoethyl)-5,7-dimethylindoline-1-carboxylate (3.20j):** After cyclization of *rac*-**3.19j**, flash chromatography (4:1 hexanes:EtOAc) afforded the title compound as a clear, colorless oil: ^{1}H NMR (300 MHz, $CDCl_3$) δ 6.86 (s, 1H), 6.81 (s, 1H), 5.94 (ddt, *J* = 17.1 Hz, 10.5 Hz, 5.7 Hz, 1H), 5.34 (dd, *J* = 17.1 Hz, 1.2 Hz, 1H), 5.27 (dd, *J* = 10.5 Hz, 1.2 Hz, 1H), 4.64 (dt, *J* = 5.7 Hz, 1.2 Hz, 2H), 4.24 (dd, *J* = 11.4 Hz, 7.5 Hz, 1H), 3.79 (dd, *J* = 11.4 Hz, 6.0 Hz, 1H), 3.57 (m, 1H), 2.73 (dd, *J* = 16.2 Hz, 5.4 Hz, 1H), 2.47 (dd, *J* = 16.2 Hz, 9.3 Hz, 1H), 2.28 (s, 3H), 2.27 (s, 3H), 1.52 (s, 9H); ^{13}C NMR (75 MHz, $CDCl_3$) δ 171.5, 154.0, 139.3, 136.4, 134.1, 131.9, 130.9, 127.8, 121.5, 118.4, 80.6, 65.3, 56.9, 38.3, 37.9, 28.2 (3C), 20.8, 19.6; FTIR (neat, cm^{-1}) 2976, 2929, 1737, 1709, 1479, 1366, 1245, 1163, 1007, 932, 856, 770; HRMS (ESI) calcd for $C_{20}H_{27}NNaO_4$ $[M + Na]^+$: 368.1838, found: 368.1837.

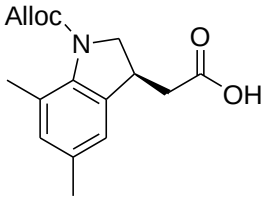

(*S*)-2-(1-(Allyloxycarbonyl)-5,7-dimethylindolin-3-yl)acetic acid (3.39): To a stirred solution of enantioenriched ester (+)-**3.20b** (236 mg, 0.778 mmol, 99/1 er) in THF (5.0 mL) at 0 °C was added dropwise an aqueous solution of NaOH (1.0 M, 2.33 mL). The mixture was allowed to warm to room temperature and was stirred overnight. Organic solvents were removed *in vacuo*, the mixture was cooled to 0 °C with stirring, and acidified to pH 2 with dropwise addition of 1 N HCl. The mixture was extracted with CH_2Cl_2 (3 x 25 mL), and the combined organic layers were dried over Na_2SO_4, filtered, and concentrated by rotary evaporation to afford the crude title compound (201 mg, ~95% pure, ~89% crude yield) as a clear colorless oil. The acid was not purified further and was used directly in the next step. ^{1}H NMR (300 MHz, $CDCl_3$) δ 10.88 (br s, 1H), 6.89 (s, 1H), 6.86 (s, 1H), 6.01 (ddt, *J* = 17.1 Hz, 10.2 Hz, 6.0 Hz, 1H), 5.34 (dd, *J* = 17.1 Hz, 1.2 Hz, 1H), 5.27 (dd, *J* = 10.5 Hz, 0.9 Hz, 1H), 4.72 (dd, *J* = 5.7 Hz, 0.9 Hz, 2H), 4.39 (dd, *J* = 11.7 Hz, 7.8 Hz, 1H), 3.87 (dd, *J* = 11.7 Hz, 6.3 Hz, 1H), 3.62 (m, 1H), 2.82 (dd, *J* = 16.5 Hz, 4.8 Hz, 1H), 2.53 (dd, *J* = 16.5 Hz, 9.6 Hz, 1H), 2.31 (s, 3H), 2.29 (s, 3H); ^{13}C NMR (75 MHz, $CDCl_3$) δ 177.5, 154.4, 138.7, 136.0, 134.6, 132.4, 131.2, 127.8, 121.5, 118.2, 66.6, 56.6, 38.1, 37.5, 20.9, 19.9.

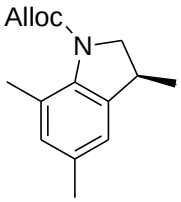

(*S*)-Allyl 3,5,7-trimethylindoline-1-carboxylate (3.40): Crude acid **3.39** (~195 mg, ~0.674 mmol) was dissolved in CH_2Cl_2 (2.0 mL) at 0 °C, to which oxalyl chloride (171 mg, 1.35 mmol) and DMF (1 drop) were added sequentially via syringe. The reaction mixture was warmed to room temperature and stirred for 1 h, after which all volatiles were removed *in vacuo*.

The crude acid chloride was redissolved in CH_2Cl_2 (2.0 mL) at room temperature in a round-bottom flask shielded from light with Al foil. With stirring, 2-mercaptopyridine *N*-oxide sodium salt (111 mg, 0.741 mmol) was added all at once, and the mixture was stirred in the dark for 1 h. Upon completion, solids were removed by rapid filtration into a second Al-foil shielded round-bottom flask, and solvent was removed.

The crude Barton ester was redissolved in benzene (6.75 mL), and to this solution Bu_3SnH (589 mg, 2.02 mmol) and AIBN (11 mg, 0.067 mmol) were added. The flask was fitted with a condenser, and the reaction vessel was placed into a preheated oil bath and refluxed for 5 h in the dark. After cooling to room temperature and removal of solvent by rotary evaporation, the crude residue was subjected to flash chromatography on 10% w/w KF/silica gel (8:1 hexanes:EtOAc) to obtain the title compound (90. mg, 47% from ester (+)-**3.19b**) as a clear colorless oil, $[\alpha]_D^{23}$ +24 (*c* 8.4 mg/mL, $CHCl_3$): ^{1}H NMR (300 MHz, $CDCl_3$) δ 6.85 (s, 1H), 6.82 (s, 1H), 5.99 (ddd, *J* = 16.2 Hz, 10.5 Hz, 5.7 Hz, 1H), 5.37 (d, *J* = 17.4 Hz, 1H), 5.27 (d, 10.2 Hz, 1H), 4.68 (d, *J* = 5.7 Hz, 2H), 4.33 (dd, *J* = 11.1 Hz, 7.8 Hz, 1H), 3.57 (dd, *J* = 11.1 Hz, 7.8 Hz, 1H), 3.30 (m, 1H), 2.30 (s, 3H), 2.27 (s, 3H), 1.26 (d, *J* = 6.6 Hz, 3H); ^{13}C NMR (75 MHz, $CDCl_3$) δ 154.4, 139.5, 138.7, 134.4, 132.7, 130.4, 127.5, 121.2, 118.0, 66.4, 58.6, 36.1,

20.9, 19.9, 18.1; FTIR (neat, cm^{-1}) 2960, 2925, 2876, 1715, 1477, 1414, 1382, 1326, 1214, 1128, 1031, 995, 931, 854, 764; LRMS (EI) *m/z* 245 (M^+, 51), 188 (76), 161 (93), 144 (100), 130 (83), 91 (67); HRMS (EI) calcd for $C_{15}H_{19}NO_2$ $[M]^+$: 245.1416, found: 245.1407.

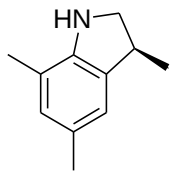

(*S*)-3,5,7-Trimethylindoline (3.41): To a stirred solution of **3.40** (57 mg, 0.232 mmol) in MeOH (2.5 mL) was added $Pd(PPh_3)_4$ (27 mg, 0.0232 mmol) in one portion, and the mixture was stirred at room temperature for 5 min. Solid $NaBH_4$ (18 mg, 0.464 mmol) was added in one portion, the reaction was stirred for 5 min, cooled to 0 °C, quenched with 2 mL saturated aqueous NH_4Cl, and warmed to room temperature. Another 5 mL water was added, and the mixture was extracted with CH_2Cl_2 (3 x 10 mL), the combined organic layers were washed with brine (2 x 10 mL), dried over $MgSO_4$, filtered, and concentrated using rotary evaporation. Flash chromatography (4:1 hexanes:EtOAc) yielded the title compound[105] (30 mg, 80%) as a bright yellow oil, $[\alpha]_D^{23}$ +34 (*c* 4.3 mg/mL, $CHCl_3$): ^{1}H NMR (300 MHz, $CDCl_3$) δ 6.80 (s, 1H), 6.72 (s, 1H), 3.72 (t, *J* = 8.7 Hz, 1H), 3.37 (m, 1H), 3.11 (t, *J* = 8.7 Hz, 1H), 2.27 (s, 3H), 2.13 (s, 3H), 1.32 (d, *J* = 6.9 Hz, 3H); ^{13}C NMR (75 MHz, $CDCl_3$) δ 147.3, 134.1, 128.8, 128.4, 121.5, 119.0, 55.6, 37.0, 20.8, 18.7, 16.6; FTIR (neat, cm^{-1}) 3366 (broad), 2959, 2922, 2860, 1485, 1266, 1225, 1140, 1012, 855, 751; LRMS (EI) *m/z* 161 (M^+, 56), 146 (100), 69 (77), 57 (95); HRMS (EI) calcd for $C_{11}H_{15}N$ $[M]^+$: 161.1204, found: 161.1211.

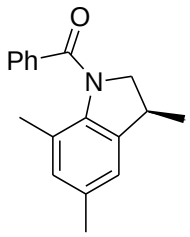

(*S*)-Phenyl(3,5,7-trimethylindolin-1-yl)methanone (3.42): To a stirred solution of indoline **3.41** (14 mg, 0.0868 mmol), pyridine (14 mg, 0.174 mmol) and DMAP (1 mg) in CH_2Cl_2 (2 mL) at 0 °C was added benzoyl chloride (18 mg, 0.130 mmol) via syringe. The mixture was warmed to room temperature and stirred for 15 min. Upon completion, the reaction mixture was quenched with sat. aq. NH_4Cl (5 mL), extracted with CH_2Cl_2 (3 x 5 mL), and the combined organic layers were washed with brine (2 x 5 mL), dried over $MgSO_4$, filtered, and concentrated in vacuo. Flash chromatography of the crude residue (3:1 hexanes:EtOAc) afforded the title compound (14 mg, 61%) as a white solid. Chiral analysis was performed on the analytical (*S*,*S*)-Whelk-O1 column (85:15 hexanes:iPrOH) to give (*S*)-**3.42** (first eluting enantiomer), $[\alpha]_D^{23}$ +3.0 (*c* 6.0 mg/mL, $CHCl_3$). The HPLC analysis was performed against an enantioenriched authentic sample previously made by Dr. Andre Lapierre.[105] The compound's optical rotation matched that previously reported ($[\alpha]_D^{23}$ +3.0, (*c* 6.2 mg/mL, $CHCl_3$)), as did the spectral data: ^{1}H NMR (300 MHz, $CDCl_3$) δ 7.79-7.70 (m, 2H), 7.55-7.40 (m, 3H), 6.90 (s, 1H), 6.87 (s, 1H), 4.21 (dd, *J* = 10.5 Hz, 7.8 Hz, 1H), 3.64 (dd, *J* = 10.5 Hz, 8.1 Hz, 1H), 3.33 (sextet, *J* = 6.9 Hz, 1H), 2.33 (s, 3H), 2.19 (s, 3H), 1.24 (d, *J* = 6.9 Hz, 3H).

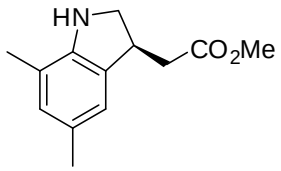

(*S*)-Methyl 2-(5,7-dimethylindolin-3-yl)acetate (3.43): This compound was prepared by the three procedures shown below. Analysis was performed on the analytical (*S*,*S*)-Whelk O1 column, eluting with 90:10 hexane:*i*-PrOH. In each case, the major enantiomer (+)-**3.43** was the first eluting enantiomer, $[\alpha]_D^{23}$ +23 (*c* 6.0 mg/mL, $CHCl_3$). ^{1}H NMR (300 MHz, $CDCl_3$) δ 6.78 (s, 1H), 6.74 (s, 1H), 3.81 (t, *J* = 8.7 Hz, 1H), 3.73 (s, 3H), 3.71 (m, 1H), 3.47 (br s, 1H), 3.27 (dd, *J* = 8.7 Hz, 6.3 Hz, 1H), 2.78 (dd, *J* = 15.9 Hz, 5.1 Hz, 1H), 2.57 (dd, *J* = 15.9 Hz, 9.0 Hz, 1H), 2.25 (s, 1H), 2.12 (s, 1H); ^{13}C NMR (75 MHz, $CDCl_3$) δ 172.8, 147.2, 130.8, 129.4, 128.2, 121.2, 119.1, 53.4, 51.5, 38.74, 38.66, 20.6, 16.6; FTIR (neat, cm^{-1}) 3371, 3002, 2950, 2859, 1734, 1486, 1437, 1326, 1227, 1165, 1011, 856, 755; LRMS (EI) *m/z* 219 (M^+, 32), 158 (25), 146 (100), 131 (25), 130 (17); HRMS (EI) calcd for $C_{13}H_{17}NO_2$ $[M]^+$: 219.1259, found: 219.1259.

Procedure 1: *N*-Boc (*S*)-(+)-**3.20a** (0.029 g, 0.091 mmol, 86/14 er) was dissolved in CH_2Cl_2 (0.90 mL) at room temperature with stirring. Trifluoroacetic acid (0.10 mL) was added dropwise via syringe, and the reaction mixture was stirred at room temperature for 7 h. The mixture was concentrated by rotary evaporation, and to the crude residue was sequentially added water (1 mL) and $NaHCO_3$ (4 mL). The mixture was extracted with EtOAc (3 x 5 mL), and the combined organic layers were washed with brine (2 x 5 mL), dried over $MgSO_4$, filtered, and concentrated by rotary evaporation. The residue consisted of indoline (*S*)-(+)-**3.43** (0.015 g, 75%) as a yellow oil, determined to be pure by ^{1}H NMR.

Procedure 2: *N*-Cbz (*S*)-(+)-**3.20c** (0.012 g, 0.034 mmol, 91/9 er) was dissolved in EtOH (1.5 mL) at room temperature with stirring. Solid 10% w/w Pd/C (2.0 mg, 0.0019 mmol)

was added, and the mixture was placed under a H_2 atmosphere. After stirring for 6 h, the mixture was filtered through a pad of Celite, rinsing the pad with EtOH, and the filtrate was concentrated in vacuo. Short column chromatography (2:1 hexanes:EtOAc) furnished (*S*)-(+)-**3.43** (0.006 g, 80%) as a yellow oil.

Procedure 3: *N*-Alloc (*S*)-(+)-**3.20b** (0.010 g, 0.033 mmol, 98/2 er) was dissolved in MeOH (1.0 mL) with stirring at 0 °C. Solid $Pd(PPh_3)_4$ (0.003 g, 0.0026 mmol) was added all at once, followed by solid $NaBH_4$ (0.005 g, 0.132 mmol). The mixture was stirred for 10 min, and saturated aqueous NH_4Cl solution (1 mL) was added, followed by water (4 mL). The mixture was extracted with CH_2Cl_2 (3 x 5 mL), and the combined organic layers were washed with brine (3 x 5 mL), dried over $MgSO_4$, filtered, and concentrated in vacuo. The mostly pure crude (~9 mg) indoline (*S*)-(+)-**3.43** was directly analyzed by chiral HPLC without further purification. The same conditions, when applied to (*R*)-(–)-**3.20b** on a 0.500 mmol scale, produced (*R*)-(–)-**3.43** in 94% yield after purification by column chromatography.

6.4 COMPOUND DATA FOR CHAPTER 4

Experimental procedures and spectroscopic data have been previously reported in the literature for compounds **4.54**,[48] **4.55**,[93,105] and *trans*-4-chlorocyclohex-2-enyl acetate.[212] These procedures were followed, and the products' physical properties and spectroscopic data were consistent with those previously reported. The preparation of **3.21** is described in Chapter 6.3.

General procedure for radical reactions: To a stirred PhH solution of the appropriate substrate (1.0 equiv) at room temperature, open to the atmosphere, was added Bu_3SnH (1.5 equiv) all at once. The initial hydride concentration $[Bu_3SnH]_i$ is detailed for each individual reaction. A 1.0 M hexanes solution of Et_3B (1.0 equiv) was added all at once, and the reaction was stirred until the starting material was completely consumed (usually < 5 min). The reaction mixture was concentrated by rotary evaporation, and the crude residue was directly chromatographed on 10% w/w KF/silica gel,[80] using the appropriate eluent.

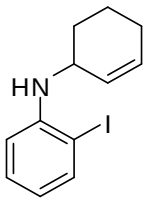

***rac*-*N*-(Cyclohex-2-enyl)-2-iodoaniline (4.12):** A stirred mixture of 2-iodoaniline (5.26 g, 24.0 mmol) and K_2CO_3 (8.30 g, 60.0 mmol) in MeCN (25 mL) was cooled to 0 °C. By syringe, 3-bromocyclohex-1-ene (3.22 g, 20.0 mmol) was added dropwise over 10 min, and the mixture was allowed to warm to room temperature and stir for 12 h. The reaction mixture was filtered through a Celite pad, rinsing with a small amount of MeCN, and the filtrate was concentrated by

rotary evaporation. Column chromatography (20:1 hexanes:EtOAc) afforded the title compound (5.21 g, 87%) as a yellow oil: ^{1}H NMR (300 MHz, $CDCl_3$) δ 7.67 (dd, *J* = 7.8 Hz, 1.5 Hz, 1H), 7.20 (m with clear d, *J* = 1.5 Hz, 1H), 6.63 (dd, *J* = 8.1 Hz, 1.2 Hz, 1H), 6.43 (ddd, *J* = 7.8 Hz, 7.2 Hz, 1.5 Hz, 1H), 5.91 (dtd, *J* = 9.9 Hz, 3.6 Hz, 1.8 Hz, 1H), 5.77 (ddt, *J* = 9.9 Hz, 3.0 Hz, 2.1 Hz, 1H), 4.17 (br d, 1H), 4.04 (br m, 1H), 2.20-1.98 (m, 2H), 1.98-1.83 (m, 1H), 1.83-1.59 (m, 3H); ^{13}C NMR (75 MHz, $CDCl_3$) δ 146.2, 139.1, 130.6, 129.2, 127.7, 118.3, 111.0, 85.8, 48.1, 28.5, 25.0, 19.4; FTIR (neat, cm^{-1}) 3390, 3021, 2934, 2859, 1587, 1500, 1450, 1313, 1279, 1170, 1088, 1004, 741; LRMS (EI) *m/z* 299 (M^+, 83), 271 (37), 219 (100), 172 (38), 144 (35), 81 (82); HRMS (EI) calcd for $C_{12}H_{14}IN$: 299.0171, found: 299.0167.

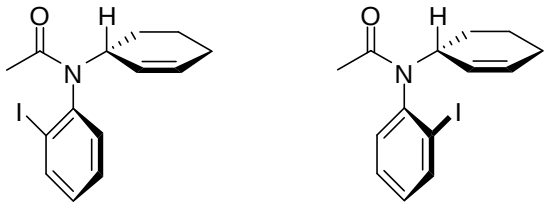

***rac*-*N*-(Cyclohex-2-enyl)-*N*-(2-iodophenyl)acetamide (4.13):** To a stirred solution of **4.12** (1.50 g, 5.00 mmol) in acetone (5 mL) was added solid K_2CO_3 (2.76 g, 20.0 mmol) all at once, and the mixture was cooled to 0 °C. To this mixture, acetyl chloride (1.18 g, 15.0 mmol) was added dropwise via syringe, and the mixture was warmed to room temperature and stirred for 24 h. The mixture was recooled to 0 °C, and saturated aqueous $NaHCO_3$ solution (50 mL) was added. This mixture was extracted with EtOAc (3 x 50 mL), and the combined organic layers were washed with brine (3 x 50 mL), dried over $MgSO_4$, filtered, and concentrated by rotary evaporation. Exhaustive gradient column chromatography (2 columns, hexanes to 2:1 hexanes:EtOAc) provided acylated products enriched in one atropisomer. The first eluting compound was collected as a mixture of 95:5 *anti*:*syn* atropisomers (0.992 g, 58%) as a white

solid: ^{1}H NMR (300 MHz, $CDCl_3$) δ 7.96 (dd, *J* = 8.1 Hz, 1.5 Hz, 1H), 7.39 (td, *J* = 7.5 Hz, 1.5 Hz, 1H), 7.23 (dd, *J* = 7.8 Hz, 1.8 Hz, 1H), 7.07 (td, *J* = 7.8 Hz, 1.5 Hz, 1H), 5.83 (dq, *J* = 10.2 Hz, 2.1 Hz, 1H), 5.77 (m, 1H), 5.32 (m, 1H), 2.10-1.98 (m, 1H), 1.93-1.80 (m, 1H), 1.82 (s, 3H), 1.63-1.53 (m, 2H), 1.22-1.08 (m, 1H); ^{13}C NMR (75 MHz, $CDCl_3$) δ 169.3, 142.4, 139.5, 129.5, 129.3, 129.1, 128.9, 128.8, 103.1, 52.6, 25.3, 23.8, 23.2, 20.8; FTIR (thin film, $CHCl_3$, cm^{-1}) 3022, 2933, 2864, 1660, 1468, 1432, 1378, 1308, 1081, 1019, 753. The second eluting compound was collected as a mixture of 18:82 *anti*:*syn* atropisomers (0.370 g, 22%) as a white solid: ^{1}H NMR (300 MHz, $CDCl_3$) δ 7.95 (dd, *J* = 7.8 Hz, 1.5 Hz, 1H), 7.40 (td, *J* = 7.5 Hz, 1.5 Hz, 1H), 7.26 (dd, *J* = 7.8 Hz, 1.5 Hz, 1H), 7.07 (td, *J* = 7.8 Hz, 1.5 Hz, 1H), 5.68-5.57 (m, 2H), 5.23-5.14 (m, 1H), 2.30-2.18 (m, 1H), 1.97-1.87 (m, 2H), 1.80 (s, 3H), 1.78-1.65 (m, 2H); ^{13}C NMR (75 MHz, $CDCl_3$) δ 169.9, 143.6, 139.9, 130.3 (2C, accidental isochrony), 129.5, 129.2, 126.6, 103.9, 53.4, 28.4, 24.5, 23.7, 20.9; FTIR (thin film, $CHCl_3$, cm^{-1}) 3029, 2931, 2862, 1661, 1468, 1377, 1308, 1082, 1019, 752, 724; HRMS (ESI) calcd for $C_{14}H_{16}INNaO$ $[M + Na]^+$: 364.0174, found: 364.0152.

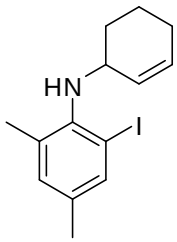

***rac*-*N*-(Cyclohex-2-enyl)-2-iodo-4,6-dimethylaniline (4.14):** To a stirred mixture of **3.21** (4.94 g, 20.0 mmol) and K_2CO_3 (8.30 g, 60.0 mmol) in MeCN (20 mL) was added 3-bromocyclohex-1-ene (3.22 g, 20.0 mmol) dropwise via syringe over 10 min, and the mixture was stirred for 18 h. The reaction mixture was filtered through a Celite pad, rinsing with MeCN (3 x 20 mL), and

the filtrate was concentrated by rotary evaporation. Column chromatography (40:1 pentane:Et_2O) afforded the title compound (4.02 g, 61%) as a yellow oil: ^{1}H NMR (300 MHz, $CDCl_3$) δ 7.46 (s, 1H), 6.92 (s, 1H), 5.85-5.78 (m, 1H), 5.76 (m with clear d, *J* = 11.7 Hz, 1H), 3.76 (br m, 1H), 3.39 (br s, 1H), 2.31 (s, 3H), 2.22 (s, 3H), 2.17-1.92 (m, 2H), 1.91-1.75 (m, 2H), 1.66-1.51 (m, 2H); ^{13}C NMR (75 MHz, $CDCl_3$) δ 144.6, 137.2, 132.8, 132.5, 130.2, 129.7, 129.1, 95.7, 52.9, 30.0, 25.1, 20.3, 19.87, 19.85; FTIR (neat, cm^{-1}) 3332, 3020, 2925, 2857, 1473, 1441, 1273, 1234, 1126, 1074, 984, 852, 777, 723; LRMS (EI) *m/z* 327 (M^+, 43), 247 (100), 200 (33), 120 (29), 81 (75); HRMS (EI) calcd for $C_{14}H_{18}IN$: 327.0484, found: 327.0484.

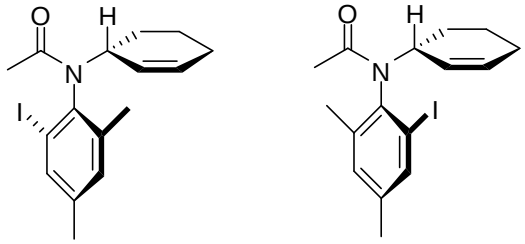

***rac*-*N*-(Cyclohex-2-enyl)-*N*-(2-iodo-4,6-dimethylphenyl)acetamide (4.15):** To a stirred mixture of **4.14** (1.64 g, 5.00 mmol) and K_2CO_3 (2.76 g, 20.0 mmol) in acetone (10 mL) at 0 °C was added acetyl chloride (1.18 g, 15.0 mmol) dropwise via syringe. The mixture was warmed to room temperature and stirred for 5 days, recooled to 0 °C, and saturated aqueous $NaHCO_3$ solution (50 mL) was added. The mixture was extracted with EtOAc (3 x 50 mL), and the combined organic layers were washed with brine (3 x 50 mL), dried over $MgSO_4$, filtered, and concentrated by rotary evaporation. Exhaustive gradient column chromatography (2 columns, hexanes to 3:1 hexanes:EtOAc) afforded the acylated compound as two separate atropisomers. The first eluting compound consisted of *anti*-**4.15** (0.830 g, 45%) as a white solid, mp 66-68 °C: ^{1}H NMR (300 MHz, $CDCl_3$) δ 7.58 (s, 1H), 7.06 (s, 1H), 6.02 (dt, *J* = 10.2 Hz, 1.8 Hz, 1H), 5.70

(m with clear d, 10.2 Hz, 1H), 4.91 (m, 1H), 2.30 (s, 3H), 2.27 (s, 3H), 1.99-1.79 (m, 2H), 1.75 (s, 3H), 1.71-1.52 (m, 2H), 1.02 (qd, *J* = 11.7 Hz, 3.9 Hz, 1H); ^{13}C NMR (75 MHz, $CDCl_3$) δ 169.9, 139.6, 139.4, 138.1, 137.4, 131.5, 129.8, 127.1, 103.7, 53.3, 26.1, 24.3, 23.1, 21.2, 20.3, 20.0; FTIR (thin film, $CHCl_3$, cm^{-1}) 3002, 2929, 2863, 1659, 1468, 1375, 1324, 1304, 1270, 1240, 1070, 1036, 855, 754; LRMS (EI) *m/z* 369 (M^+, 100), 289 (81), 247 (48), 232 (41), 200 (56), 162 (48), 81 (71); HRMS (EI) calcd for $C_{16}H_{20}INO$: 369.0590, found: 369.0585. The second eluting compound consisted of *syn*-**4.15** (0.737 g, 40%) as an off-white solid, mp 82-83 °C: ^{1}H NMR (300 MHz, $CDCl_3$) δ 7.60 (s, 1H), 7.06 (s, 1H), 5.78 (dt, *J* = 10.2 Hz, 1.8 Hz, 1H), 5.65 (m with clear d, *J* = 10.5 Hz, 1H), 4.78 (m, 1H), 2.30 (s, 3H), 2.26 (s, 3H), 2.17-2.05 (m, 1H), 2.03-1.93 (m, 2H), 1.79-1.60 (m, 2H), 1.75 (s, 3H), 1.55-1.43 (m with clear d, *J* = 3.3 Hz, 1H); ^{13}C NMR (75 MHz, $CDCl_3$) δ 170.2, 140.3, 139.3, 137.8, 137.7, 131.7, 128.2, 128.0, 103.4, 54.6, 27.2, 24.3, 23.3, 21.3, 20.0, 19.9; FTIR (thin film, $CHCl_3$, cm^{-1}) 2929, 1662, 1466, 1373, 1331, 1303, 1135, 855, 789, 755; LRMS (EI) *m/z* 369 (M^+, 100), 289 (98), 247 (91), 200 (67), 162 (55), 81 (68); HRMS (EI) calcd for $C_{16}H_{20}INO$: 369.0590, found: 369.0572.

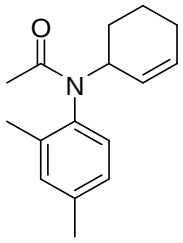

***rac*-*N*-(Cyclohex-2-enyl)-*N*-(2,4-dimethylphenyl)acetamide (4.17):** Iodide *anti*-**4.15** (0.111 g, 0.30 mmol) was reacted according to the general radical procedure, with $[Bu_3SnH]_i$ = 0.10 M. Column chromatography (2:1 hexanes:EtOAc) provided the title compound (0.052 g, 71%) as a white solid, mp 95-97 °C, in a 3:2 ratio of atropisomers: ^{1}H NMR (300 MHz, $CDCl_3$) δ 7.09 (m,

1H, both), 7.00 (m with clear d, *J* = 8.1 Hz, 1H, both), 6.95 (d, *J* = 8.1 Hz, 1H, minor), 6.94 (d, *J* = 7.8 Hz, 1H, major), 5.79 (dq, *J* = 10.2 Hz, 1.8 Hz, 1H, major), 5.77-5.70 (m, 1H, major), 5.64 (dq, *J* = 10.2 Hz, 2.7 Hz, 1H, minor), 5.51 (d of pentets, *J* = 10.5 Hz, 1.8 Hz, 1H, minor), 5.40-5.29 (m, 1H, major), 5.25-5.15 (m, 1H, minor), 2.34 (s, 3H, both), 2.23 (s, 3H, minor), 2.21 (s, 3H, major), 2.10-2.00 (m, 1H, minor), 1.95-1.76 (m, 3H, both), 1.74 (s, 3H, major), 1.72 (s, 3H, minor), 1.65-1.47 (m, 2H, both), 1.27-1.12 (m, 1H, major); ^{13}C NMR (75 MHz, $CDCl_3$) all signals, both atropisomers δ 170.7, 170.6, 137.9, 137.8, 137.1, 136.5, 136.4, 131.8, 131.7, 129.59, 129.55, 129.45, 129.4, 129.1, 127.5, 127.4, 127.3, 52.9, 52.7, 28.2, 25.8, 24.5, 24.2, 22.9, 22.8, 21.3, 21.2, 20.9, 18.4, 18.0; FTIR (thin film, $CHCl_3$, cm^{-1}) 3024, 2935, 2864, 1657, 1503, 1380, 1309, 1053, 754; LRMS (EI) *m/z* 243 (M^+, 44), 200 (20), 163 (37), 121 (100), 81 (30), 79 (39), 77 (41); HRMS (EI) calcd for $C_{16}H_{21}NO$: 243.1623, found: 243.1620.

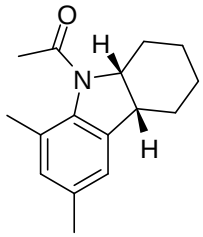

***rac*-1-(*cis*-6,8-dimethyl-2,3,4,4a-tetrahydro-1*H*-carbazol-9(9a*H*)-yl)ethanone (4.18):** Iodide *syn*-**4.15** (0.111 g, 0.30 mmol) was reacted according to the general radical procedure, with $[Bu_3SnH]_i$ = 0.10 M. Gradient column chromatography (hexanes to 3:2 hexanes:EtOAc) gave **4.17** (3 mg, 4%) as a first eluting minor byproduct. The second eluting compound consisted of the title compound (0.066 g, 92%) as a white solid, mp 90-91°C: ^{1}H NMR (300 MHz, $CDCl_3$) δ 6.86 (s, 1H), 6.81 (s, 1H), 4.31 (br s, 1H), 3.51 (br m, 1H), 2.32 (s, 3H), 2.26 (s, 3H), 2.23 (s, 3H), 1.95 (m, 1H), 1.85-1.70 (m with clear dd, *J* = 5.7 Hz, 3.9 Hz, 1H), 1.60-1.47 (m, 2H), 1.30-1.00 (m, 4H); ^{13}C NMR (75 MHz, $CDCl_3$) δ 167.3 (br), 138.7, 136.6 (br), 134.7, 129.9, 129.2

(br), 120.5, 63.6, 41.0, 27.6, 24.5, 23.0 (br), 22.9, 21.0, 20.5, 20.1; FTIR (thin film, $CHCl_3$, cm^{-1}) 2928, 2858, 1664, 1473, 1412, 1388, 1275, 853, 757; LRMS (EI) *m/z* 243 (M^+, 57), 201 (60), 158 (100); HRMS (EI) calcd for $C_{16}H_{21}NO$ $[M]^+$: 243.1623, found: 243.1628.

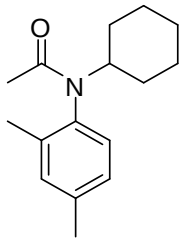

***rac*-*N*-Cyclohexyl-*N*-(2,4-dimethylphenyl)acetamide (4.19):** A mixture of **4.17** (0.061 g, 0.250 mmol) and 10% Pd on C (0.027 g, 0.025 mmol) in EtOAc (4 mL) was stirred under a H_2 atmosphere (1 atm) at room temperature for 3 days. The mixture was filtered a Celite pad, which was washed with a few mL of EtOAc. The filtrate was concentrated by rotary evaporation. Column chromatography (3:2 hexanes:EtOAc) furnished the title compound (0.061 g, 100%) as a white solid, mp 69-70 °C: ^{1}H NMR (300 MHz, $CDCl_3$) δ 7.10 (s, 1H), 7.02 (d, *J* = 7.8 Hz, 1H), 6.93 (d, *J* = 7.8 Hz, 1H), 4.52 (tt, *J* = 12.0 Hz, 3.6 Hz, 1H), 2.35 (s, 3H), 2.20 (s, 3H), 2.02 (m with clear d, *J* = 11.7 Hz, 1H), 1.70-1.53 (m, 3H), 1.69 (s, 3H), 1.63-1.52 (m, 1H), 1.45-1.20 (m, 3H), 0.95 (qt, *J* = 12.9 Hz, 3.6 Hz, 1H), 0.90 (qd, *J* = 12.6 Hz, 4.5 Hz, 1H); ^{13}C NMR (75 MHz, $CDCl_3$) δ 170.3, 137.9, 136.6, 136.5, 131.9, 129.7, 127.3, 55.3, 32.0, 30.1, 25.7 (2C, accidental isochrony), 25.4, 23.0, 20.9, 18.2; FTIR (thin film, $CHCl_3$, cm^{-1}) 2931, 2855, 1655, 1503, 1387, 1315, 1262, 1227, 1075; LRMS (EI) *m/z* 245 (M^+, 10), 202 (17), 163 (100), 160 (45), 132 (28), 121 (63), 83 (25), 77 (20); HRMS (EI) calcd for $C_{16}H_{23}NO$: 245.1780, found: 245.1769.

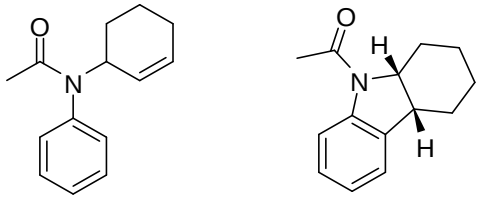

Iodide *anti*-**4.13** (0.171 g, 0.50 mmol) was reacted according to the general radical procedure, with $[Bu_3SnH]_i$ = 0.83 M. Column chromatography (3:2 hexanes:EtOAc) gave the first eluting product, ***rac*-*N*-(cyclohex-2-enyl)-*N*-phenylacetamide (4.24)**, as an orange oil (0.011 g, 10%): ^{1}H NMR (300 MHz, $CDCl_3$) δ 7.44-7.32 (m, 3H), 7.17-7.08 (m, 2H), 5.73 (ddt, *J* = 10.2 Hz, 4.2 Hz, 2.4 Hz, 1H), 5.62 (*J* = 10.2 Hz, 1H), 5.45 (m, 1H), 1.95-1.80 (m, 3H), 1.76 (s, 3H), 1.66-1.54 (m, 2H), 1.42-1.30 (m, 1H); ^{13}C NMR (75 MHz, $CDCl_3$) δ 170.4, 140.1, 130.1, 129.9 (2C), 129.1 (2C), 128.6, 128.0, 51.4, 27.6, 24.3, 23.4, 21.2; FTIR (neat, cm^{-1}) 3027, 2935, 2864, 1656, 1594, 1494, 1385, 1314, 747; LRMS (EI) *m/z* 215 (M^+, 56), 172 (26), 81 (49), 77 (100); HRMS (EI) calcd for $C_{14}H_{17}NO$: 215.1310, found: 215.1319. The second eluting compound consisted of ***rac*-1-(*cis*-2,3,4,4a-tetrahydro-1*H*-carbazol-9(9a*H*)-yl)ethanone (4.23)** as a white solid (0.082 g, 76%), mp 96-97 °C (lit. 98 °C).[275] The compound exists in a 3:1 amide rotamer ratio: ^{1}H NMR (300 MHz, $CDCl_3$) δ 8.13 (br d, *J* = 7.5 Hz, 1H, major), 7.26-7.13 (m, 2H, both), 7.20-7.13 (m, 1H, minor), 7.08 (td, *J* = 7.5 Hz, 0.9 Hz, both), 4.79 (br s, 1H, minor), 4.25 (br q, *J* = 5.7 Hz, major), 3.53 (m, 1H, major), 3.41 (br s, 1H, minor), 2.37 (s, 3H, minor), 2.30 (s, 3H, major), 2.35-2.25 (m, 1H, both), 2.05-1.92 (br m, 1H, both), 1.90-1.75 (m, 1H, both), 1.70-1.50 (br m, 2H, both), 1.35-1.00 (m, 3H, both); ^{13}C NMR (75 MHz, $CDCl_3$) major rotamer δ 167.8, 142.1, 133.8, 127.3, 123.8, 122.3, 118.1, 61.8, 40.0, 28.0, 24.0, 23.2, 22.6, 20.7, additional peaks from the minor rotamer were seen at δ 127.0, 123.6, 60.9, 39.0, 26.7; FTIR (thin film, $CHCl_3$, cm^{-1}) 2930, 2858, 1657, 1477, 1460, 1401, 1358, 1276, 1128, 759; LRMS (EI) *m/z* 215 (M^+, 36), 173 (31), 130 (100), 117 (23); HRMS (EI) calcd for $C_{14}H_{17}NO$: 215.1310, found: 215.1311.

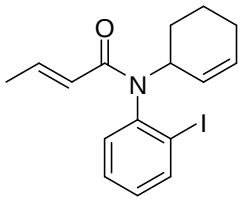

***rac*-(*E*)-*N*-(Cyclohex-2-enyl)-*N*-(2-iodophenyl)but-2-enamide (4.32):** To a stirred mixture of **4.13** (1.20 g, 4.00 mmol) and K_2CO_3 (2.21 g, 16.0 mmol) in acetone (4 mL) at 0 °C was added *trans*-crotonyl chloride (1.25 g, 12.0 mmol) dropwise via syringe over 10 min. The mixture was warmed to room temperature and stirred for 20 h, recooled to 0 °C, and saturated aqueous $NaHCO_3$ solution (20 mL) was added. The mixture was extracted with EtOAc (3 x 40 mL), and the combined organic layers were washed with brine (3 x 40 mL), dried over $MgSO_4$, filtered, and concentrated by rotary evaporation. Column chromatography (4:1 hexanes:EtOAc) furnished unreacted starting material (0.475 g, 40%), and the title compound (0.717 g, 49%) as a white solid, mp 106-108 °C. The compound was isolated as an inseparable 2:1 *anti*:*syn* mixture of atropisomers. ^{1}H NMR (300 MHz, $CDCl_3$) δ 7.96 (dd, *J* = 8.1 Hz, 1.2 Hz, 1H, major), 7.94 (dd, *J* = 7.8 Hz, 1.2 Hz, 1H, minor), 7.40 (td, *J* = 7.8 Hz, 1.5 Hz, 1H, minor), 7.39 (td, *J* = 7.5 Hz, 1.5 Hz, 1H, major), 7.24 (dt, *J* = 7.5 Hz, 1.2 Hz, 1H, both), 7.08 (dt, *J* = 7.5 Hz, 1.5 Hz, 1H, both), 6.98 (dq, *J* = 15.0 Hz, 6.9 Hz, 1H, major), 6.97 (dq, *J* = 15.0 Hz, 6.9 Hz, 1H, minor), 5.88-5.76 (m, 2H, major), 5.65 (dq, *J* = 10.2 Hz, 2.4 Hz, 1H, minor), 5.59 (m with clear d, *J* = 10.8 Hz, 1H, minor), 5.44 (dq, *J* = 15.0 Hz, 1.8 Hz, 1H, major), 5.42 (dq, *J* = 15.0 Hz, 1.8 Hz, 1H, minor), 5.37-5.28 (m, 1H, major), 5.27-5.17 (m, 1H, minor), 2.33-2.23 (m, 1H, minor), 2.08-1.98 (m, 1H, major), 1.98-1.80 (m, 2H, both), 1.78-1.55 (m, 2H both and 1H minor), 1.72 (dq, *J* = 6.9 Hz, 1.5 Hz, 3H, both), 1.31-1.15 (m, 1H, major); ^{13}C NMR (75 MHz, $CDCl_3$) all signals, both atropisomers δ 165.12, 165.06, 142.6, 142.0, 141.4, 141.2, 139.7, 139.6, 130.5, 130.2, 130.0, 129.35, 129.30, 129.28, 129.2, 128.9, 126.6, 123.1, 123.0, 104.2, 103.6, 53.5, 53.2, 28.3, 25.6,

24.3, 24.1, 21.1, 20.9, 17.7; FTIR (thin film, $CHCl_3$, cm^{-1}) 3023, 2934, 2863, 1665, 1627, 1466, 1443, 1374, 1350, 1294, 1239, 1065, 1019, 963, 927, 738; HRMS (EI) calcd for $C_{16}H_{18}INO$: 367.0433, found: 367.0429.

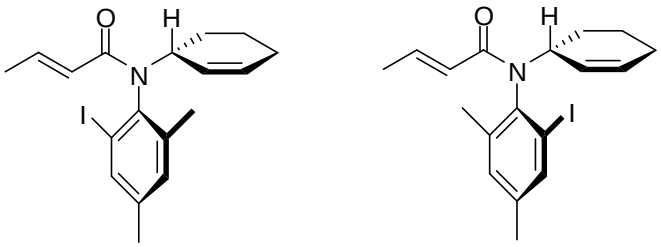

***rac*-(*E*)-*N*-(Cyclohex-2-enyl)-*N*-(2-iodo-4,6-dimethylphenyl)but-2-enamide (4.33):** To a stirred mixture of **4.15** (0.327 g, 1.00 mmol) and K_2CO_3 (0.553 g, 4.00 mmol) in acetone (1 mL) at 0 °C was added *trans*-crotonyl chloride (0.314 g, 3.00 mmol) dropwise via syringe. The reaction mixture was allowed to warm to room temperature, and stirring was continued for 1 h. The mixture was recooled to 0 °C, and saturated aqueous $NaHCO_3$ solution (5 mL) was added. The mixture was extracted with EtOAc (3 x 10 mL), and the combined organic layers were washed with brine (3 x 10 mL), dried over $MgSO_4$, filtered, and concentrated by rotary evaporation. Gradient column chromatography (hexanes to 5:1 hexanes:EtOAc) provided the acylated product as two separable atropisomers. The first eluting compound consisted of *anti*-**4.33** (0.152 g, 38%) as a white solid, mp 90-91 °C: ^{1}H NMR (300 MHz, $CDCl_3$) δ 7.58 (s, 1H), 7.05 (s, 1H), 6.97 (dq, *J* = 15.0 Hz, 6.9 Hz, 1H), 6.04 (dt, *J* = 10.2 Hz, 1.8 Hz, 1H), 5.70 (dq, *J* = 10.2 Hz, 2.4 Hz, 1H), 5.41 (dq, *J* = 15.0 Hz, 1.8 Hz, 1H), 4.89 (m, 1H), 2.32 (s, 3H), 2.24 (s, 3H), 1.95 (m, 2H), 1.84 (m, 1H), 1.71 (dd, *J* = 6.9 Hz, 1.8 Hz, 3H), 1.74-1.50 (m, 2H), 1.16 (qd, *J* = 11.4 Hz, 3.6 Hz, 1H); ^{13}C NMR (75 MHz, $CDCl_3$) δ 166.0, 141.6, 139.8, 139.5, 139.2, 137.9, 131.7, 130.3, 127.4, 123.1, 104.4, 54.4, 26.7, 24.8, 21.8, 20.7, 20.4, 18.0; FTIR (thin film,

$CHCl_3$, cm^{-1}) 2931, 1666, 1630, 1445, 1358, 1235, 963, 926, 855, 753; LRMS (EI) *m/z* 395 (M^+, 100), 315 (20), 247 (28), 200 (28), 188 (50), 158 (24), 121 (30), 104 (36); HRMS (EI) calcd for $C_{18}H_{22}INO$: 395.0746, found: 395.0733. The second eluting compound consisted of *syn*-**4.33** (0.114 g, 29%) as a white solid, mp 128 °C: ^1H NMR (300 MHz, $CDCl_3$) δ 7.60 (s, 1H), 7.05 (s, 1H), 6.96 (dq, *J* = 15.0 Hz, 6.9 Hz, 1H), 5.80 (d, *J* = 10.2 Hz, 1H), 5.65 (dq, *J* = 10.2 Hz, 3.0 Hz, 1H), 5.42 (dq, *J* = 15.0 Hz, 1.8 Hz, 1H), 4.75 (m, 1H), 2.31 (s, 3H), 2.22 (s, 3H), 2.11 (m, 1H), 2.05-1.90 (m, 2H), 1.80-1.73 (m, 1H), 1.71 (dd, *J* = 6.9 Hz, 1.8 Hz, 3H), 1.68-1.56 (m, 2H); ^{13}C NMR (75 MHz, $CDCl_3$) δ 166.2, 141.4, 140.1, 139.7, 138.7, 138.1, 131.9, 128.9, 128.2, 123.3, 104.0, 55.6, 27.6, 24.7, 21.9, 20.42, 20.35, 18.0; FTIR (thin film, $CHCl_3$, cm^{-1}) 2932, 2862, 1667, 1630, 1444, 1355, 1293, 1235, 963, 855, 754; LRMS (EI) *m/z* 395 (M^+, 100), 315 (17), 247 (19), 200 (25), 188 (37), 158 (23); HRMS (EI) calcd for $C_{18}H_{22}INO$: 395.0746, found: 395.0742.

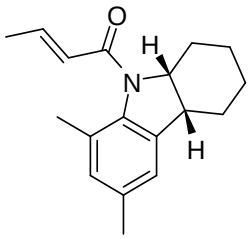

***rac*-(*E*)-1-(*cis*-6,8-Dimethyl-2,3,4,4a-tetrahydro-1*H*-carbazol-9(9a*H*)-yl)but-2-en-1-one (4.33):** Iodide *syn*-**4.33** (0.099 g, 0.25 mmol) was reacted according to the general radical procedure, with $[Bu_3SnH]_i$ = 0.01 M. Column chromatography (3:1 hexanes:EtOAc) provided the title compound (0.054 g, 81%) as a white solid, mp 117-119 °C: ^1H NMR (300 MHz, $CDCl_3$) δ 7.02 (dq, *J* = 15.0 Hz, 6.9 Hz, 1H), 6.86 (s, 1H), 6.82 (s, 1H), 6.16 (br d, *J* = 14.4 Hz, 1H), 4.49 (br s, 1H), 3.49 (t, *J* = 6.0 Hz, 1H), 2.33 (s, 3H), 2.31-2.22 (m, 1H), 2.20 (s, 3H), 2.05-1.95 (m, 1H), 1.93 (dd, *J* = 6.9 Hz, 1.2 Hz, 3H), 1.77 (tdd, *J* = 14.1 Hz, 5.7 Hz, 4.5 Hz, 1H),

1.65-1.45 (m, 2H), 1.23 (t, J = 9.3 Hz, 2H), 1.14 (m with clear q, J = 12.6 Hz, 1H); ^{13}C NMR (75 MHz, $CDCl_3$) δ 164.3, 141.5, 138.7, 137.2 (br), 134.8, 130.0, 128.9 (br), 124.3, 120.7, 63.5, 41.2, 27.9, 24.6, 23.0, 21.1, 20.6, 20.0, 18.0; FTIR (thin film, $CHCl_3$, cm^{-1}) 2928, 2857, 1667, 1630, 1472, 1446, 1413, 1378, 1237, 966, 854, 754; LRMS (EI) *m/z* 269 (M^+, 38), 201 (63), 158 (57), 69 (100); HRMS (EI) calcd for $C_{18}H_{23}NO$: 269.1780, found: 269.1776.

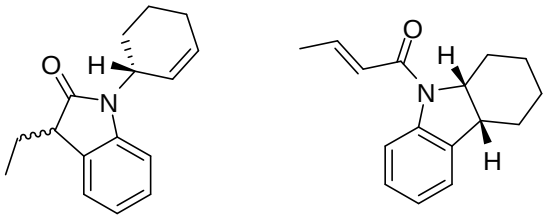

Iodide **4.32** (0.184 g, 0.50 mmol, 2:1 *anti*:*syn*) was reacted according to the general radical procedure, with $[Bu_3SnH]_i$ = 0.01 M. Column chromatography (3:1 hexanes:EtOAc) gave two products. The first eluting product, ***rac*-1-(Cyclohex-2-enyl)-3-ethylindolin-2-one (4.35)**, was isolated as a yellow oil in a 5:1 dr: ^{1}H NMR (300 MHz, $CDCl_3$) δ 7.24 (d, J = 7.2 Hz, 1H, both), 7.20 (d, J = 7.8 Hz, 1H, minor), 7.18 (d, J = 7.8 Hz, 1H, major), 7.08 (d, J = 7.8 Hz, 1H, major), 7.60 (d, J = 8.1 Hz, 1H, minor), 7.02 (t, J = 7.5 Hz, 1H, both), 6.05-5.95 (m, 1H, both), 5.63 (m with clear d, J = 9.9 Hz, 1H, major), 5.57 (m with clear d, J = 10.2 Hz, 1H, minor), 5.25-5.13 (m, 1H, both), 3.43 (t, J = 5.4 Hz, 1H, both), 2.23-2.13 (m, 2H, both), 2.10-2.00 (m, 2H, both), 2.00-1.70 (m, 4H, both), 0.88 (t, J = 7.5 Hz, 3H, minor), 0.84 (t, J = 7.5 Hz, 3H, major); ^{13}C NMR (75 MHz, $CDCl_3$) Major diastereomer δ 177.6, 143.0, 130.9, 129.2, 127.6, 127.3, 123.7, 121.7, 110.7, 48.2, 46.2, 25.8, 24.5, 23.8, 21.7, 9.6; additional non-overlapping signals for the minor diastereomer were also seen at δ 177.5, 143.0, 129.2, 127.8, 123.8, 48.1, 46.3, 25.7, 23.9, 9.8; FTIR (neat, cm^{-1}) 3029, 2935, 2874, 1695, 1609, 1484, 1357, 1196, 1059, 1025, 750; LRMS (EI) *m/z* 241 (M^+, 76), 162 (87), 161 (100), 133 (61), 81 (41); HRMS (EI) calcd for $C_{16}H_{19}NO$:

241.1467, found: 241.1466. The second eluting product, ***rac*-(*E*)-1-(*cis*-2,3,4,4a-tetrahydro-1*H*-carbazol-9(9a*H*)-yl)but-2-en-1-one (4.36)**, was isolated as a white solid, mp 95-97 °C, in a 2:1 amide rotamer ratio: ^{1}H NMR (300 MHz, $CDCl_3$) δ 8.20 (br s, 1H, major), 7.45-7.30 (br s, 1H, minor), 7.25-7.15 (m with clear d, *J* = 7.5 Hz, 2H, both), 7.15-7.03 (m, 2H, both), 6.34 (br d, *J* = 14.4 Hz, 1H, both), 4.46 (br s, 1H, both), 3.51 (br t, *J* = 6.6 Hz, 1H, both), 2.35 (m with clear d, *J* = 14.7 Hz, 1H, both), 2.10-1.95 (m, 1H, both), 1.96 (dd, *J* = 6.9 Hz, 1.5 Hz, 3H, both), 1.95-1.72 (m, 2H, both), 1.66-1.54 (m, 2H, both), 1.30-1.18 (m, 2H, both); ^{13}C NMR (75 MHz, $CDCl_3$) δ 163.8, 142.4, 142.2 (br), 127.3, 123.8, 123.5, 123.3 (br), 122.5, 118.3 (br), 60.9 (br), 39.9, 28.5 (br), 24.0, 22.6, 20.8, 18.2; FTIR (thin film, $CHCl_3$, cm^{-1}) 2931, 2858, 1663, 1624, 1475, 1460, 1402, 1273, 1242, 962, 756; LRMS (EI) *m/z* 241 (M^+, 45), 173 (51), 130 (55), 86 (65), 84 (100), 69 (43); HRMS (EI) calcd for $C_{16}H_{19}NO$: 241.1467, found: 241.1465.

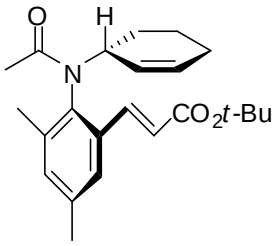

***rac-syn*-(*E*)-*t*-Butyl 3-(2-(*N*-(cyclohex-2-enyl)acetamido)-3,5-dimethylphenyl)acrylate (4.43):** To a solid mixture of $Pd_2(dba)_3$•$CHCl_3$ (0.041 g, 0.040 mmol) and P(*t*-Bu)$_3$•HBF_4 (0.046 g, 0.160 mmol) was added degassed DMF (2.0 mL) via syringe. The mixture was stirred for 10 min, at which point *syn*-**4.15** (0.148 g, 0.40 mmol) was added as a solid all at once, followed by *t*-butyl acrylate (0.205 g, 1.60 mmol) via syringe. Finally, Et_3N (0.061 mg, 0.600 mmol) was added via syringe, and the mixture was stirred at room temperature for 24 h. The mixture was quenched with brine (5 mL) and extracted with Et_2O (3 x 10 mL). The combined organic layers were dried over $MgSO_4$, filtered, and concentrated by rotary evaporation. Column

chromatography (2:1 hexanes:EtOAc) furnished the title compound (0.102 g, 69%) as a clear colorless oil: ^{1}H NMR (300 MHz, $CDCl_3$) δ 7.70 (d, *J* = 15.9 Hz, 1H), 7.33 (s, 1H), 7.13 (s, 1H), 6.26 (d, *J* = 15.9 Hz, 1H), 5.97 (m with clear d, *J* = 9.9 Hz, 1H), 5.73 (dq, *J* = 9.6 Hz, 2.4 Hz, 1H), 4.91 (m, 1H), 2.36 (s, 3H), 2.21 (s, 3H), 1.95-1.85 (m, 2H), 1.75-1.40 (m, 3H), 1.68 (s, 3H), 1.53 (s, 9H), 1.27-1.12 (m, 1H); ^{13}C NMR (75 MHz, $CDCl_3$) δ 170.7, 165.6, 139.9, 138.1, 137.4, 137.2, 134.2, 133.4, 128.8, 128.6, 125.2, 122.4, 80.5, 54.4, 28.1 (3C), 26.3, 24.6, 23.2, 21.4, 21.0, 18.5; FTIR (neat, cm^{-1}) 2976, 2932, 1708, 1656, 1472, 1370, 1328, 1303, 1256, 1154, 983, 919, 855, 731; LRMS (EI) *m/z* 369 (M^+, 11), 312 (25), 270 (100), 252 (25), 174 (43), 158 (30), 121 (25), 81 (58); HRMS (EI) calcd for $C_{23}H_{31}NO_3$: 369.2304, found: 369.2289.

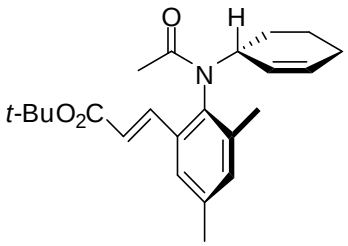

***rac-anti*-(*E*)-*t*-Butyl-3-(2-(*N*-(cyclohex-2-enyl)acetamido)-3,5-dimethylphenyl)acrylate (4.44):** To a solid mixture of $Pd_2(dba)_3$•$CHCl_3$ (0.026 g, 0.025 mmol) and P(*t*-Bu)$_3$•HBF_4 (0.029 g, 0.10 mmol) was added degassed DMF (1.5 mL) via syringe. The mixture was stirred for 10 min, at which point *syn*-**4.15** (0.092 g, 0.25 mmol) was added as a solid all at once, followed by *t*-butyl acrylate (0.128 g, 1.00 mmol) via syringe. Finally, Et_3N (0.038 mg, 0.375 mmol) was added via syringe, and the mixture was stirred at room temperature for 20 h. The mixture was quenched with saturated aqueous LiCl (5 mL) and extracted with Et_2O (3 x 10 mL). The combined organic layers were dried over $MgSO_4$, filtered, and concentrated by rotary evaporation. Gradient column chromatography (hexanes to 3:2 hexanes:EtOAc) gave the title compound (0.029 g, 31%), the first eluting product, as a light yellow oil: ^{1}H NMR (300 MHz,

$CDCl_3$) δ 7.60 (d, *J* = 15.9 Hz, 1H), 7.34 (s, 1H), 7.12 (s, 1H), 6.32 (d, *J* = 15.9 Hz, 1H), 5.81 (dt, *J* = 10.2 Hz, 1.2 Hz, 1H), 5.68 (dq, *J* = 10.2 Hz, 2.7 Hz, 1H), 4.93 (m, 1H), 2.35 (s, 3H), 2.22 (s, 3H), 1.95-1.78 (m, 3H), 1.75-1.55 (m, 2H), 1.67 (s, 3H), 1.53 (s, 9H), 1.38-1.22 (m, 1H); ^{13}C NMR (75 MHz, $CDCl_3$) δ 170.7, 165.7, 139.3, 138.1, 137.9, 137.4, 134.0, 133.5, 128.8, 128.7, 125.5, 122.5, 80.7, 54.6, 28.2 (3C), 27.1, 24.6, 23.2, 21.6, 21.0, 19.2; FTIR (neat, cm^{-1}) 2977, 2933, 1709, 1657, 1370, 1329, 1291, 1258, 1154, 984, 855, 754; LRMS (EI) *m/z* 369 (M^+, 50), 312 (78), 270 (98), 268 (78), 252 (73), 191 (63), 190 (73), 174 (90), 156 (56), 146 (70), 81 (88), 57 (100); HRMS (EI) calcd for $C_{23}H_{31}NO_3$: 369.2304, found: 369.2295. The second eluting product consisted of a mixture of **4.42a**/**4.42b** (0.41 mg, 68%) in a 25:75 ratio. Spectral data for this product is listed later in the chapter.

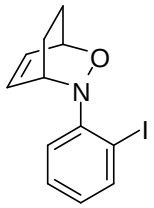

***rac*-3-(2-Iodophenyl)-2-oxa-3-azabicyclo[2.2.2]oct-5-ene (4.48):** In a round bottom flask fitted with an addition funnel, 2-iodoaniline (5.48 g, 25.0 mmol) was dissolved in CH_2Cl_2 (125 mL) at 0 °C with stirring. To this, a solution of 77% w/w *m*-CPBA (9.06 g, 52.5 mmol) in CH_2Cl_2 (250 mL) was added dropwise over 1 h at 0 °C. Immediately after addition was complete, the mixture was successively washed with saturated aqueous $NaHCO_3$ solution (3 x 400 mL) and brine (400 mL), dried over $MgSO_4$, filtered, and concentrated by rotary evaporation. The crude nitroso compound was immediately used in the next reaction without further purification.

The crude nitroso compound was dissolved in PhMe (50 mL) at 0 °C with stirring. To this mixture was added 1,3-cyclohexadiene (3.01 g, 37.5 mmol) dropwise via syringe over 10

min. The mixture was stirred for 30 min at 0 °C, at which point the entire reaction mixture was loaded directly onto a short silica gel column. Column chromatography (9:1 pentane:Et_2O) afforded the title compound as a red oil (4.60 g, ~59%) of approximate 80-90% purity by ^1H NMR. This compound was characterized solely by ^1H NMR, and the entirety of the product was taken forward to the next step: ^1H NMR (300 MHz, $CDCl_3$) δ 7.74 (dd, *J* = 7.8 Hz, 1.5 Hz, 1H), 7.21 (ddd, *J* = 8.1 Hz, 7.2 Hz, 1.5 Hz, 1H), 7.07 (dd, *J* = 8.1 Hz, 1.5 Hz, 1H), 6.82-6.73 (m, 2H), 6.05 (ddd, *J* = 8.1 Hz, 6.0 Hz, 1.5 Hz, 1H), 4.77 (ddt, *J* = 5.4 Hz, 3.9 Hz, 1.5 Hz, 1H), 4.48 (m, 1H), 2.44 (ddt, *J* = 12.6 Hz, 9.6 Hz, 3.3 Hz, 1H), 2.29 (ddt, *J* = 12.6 Hz, 9.0 Hz, 3.3 Hz, 1H), 1.56 (tt, *J* = 12.0 Hz, 3.0 Hz, 1H), 1.40 (tdd, *J* = 12.0 Hz, 3.0 Hz, 1.5 Hz, 1H).

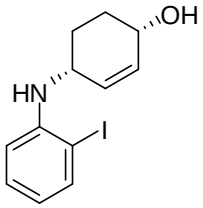

***rac-cis*-4-(2-Iodophenylamino)cyclohex-2-enol (4.49):** In a round bottom flask fitted with a reflux condenser, crude **4.48** (4.60 g, ~14.7 mmol) was dissolved in 9:1 MeCN:H_2O (150 mL) with stirring at room temperature. Solid $Mo(CO)_6$ (3.88 g, 14.7 mmol) was added all at once, followed by addition of solid $NaBH_4$ (0.613 g, 16.2 mmol) in one portion, and the mixture was refluxed for 4 h. At this time, a second equivalent portion of $NaBH_4$ (0.613 g, 16.2 mmol) was added, and the mixture was refluxed another 4 h. A final portion of $NaBH_4$ (0.613 g, 16.2 mmol) was added, and the stirred mixture was refluxed for 12 h. The mixture was cooled to room temperature, filtered through a Celite pad followed by a small rinse of the pad with MeCN, and the filtrate was concentrated by rotary evaporation. The crude residue was mixed with 2:1 hexanes:EtOAc, and the soluble material was subjected to column chromatography (2:1

hexanes:EtOAc) to furnish the title compound (3.13 g, 40% over 3 steps from 2-iodoaniline) as a red oil: ^{1}H NMR (300 MHz, $CDCl_3$) δ 7.68 (dd, *J* = 7.8 Hz, 1.5 Hz, 1H), 7.21 (ddd, *J* = 8.1 Hz, 7.2 Hz, 1.5 Hz, 1H), 6.62 (dd, *J* = 8.4 Hz, 1.2 Hz, 1H), 6.46 (ddd, *J* = 7.8 Hz, 7.2 Hz, 1.5 Hz, 1H); ^{13}C NMR (75 MHz, $CDCl_3$) δ 146.1, 139.4, 132.9, 130.6, 129.5, 118.8, 111.1, 86.0, 65.3, 48.2, 28.9, 24.8; FTIR (neat, cm^{-1}) 3386 (broad), 3062, 3024, 2941, 2862, 1586, 1499, 1450, 1313, 1130, 1052, 1004, 947, 739; LRMS (EI) *m/z* 315 (M^+, 100), 287 (52), 271 (46), 219 (100), 144 (41), 130 (79), 117 (32), 91 (65), 77 (67); HRMS (EI) calcd for $C_{12}H_{14}INO$: 315.0120, found: 315.0118.

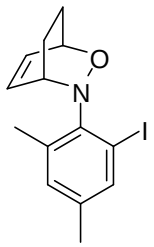

***rac*-3-(2-Iodo-4,6-dimethylphenyl)-2-oxa-3-azabicyclo[2.2.2]oct-5-ene (4.50):** In a round bottom flask fitted with an addition funnel, **3.21** (7.41 g, 30.0 mmol) was dissolved in CH_2Cl_2 (125 mL) at 0 °C with stirring. To this, a solution of 77% w/w *m*-CPBA (10.87 g, 63.0 mmol) in CH_2Cl_2 (250 mL) was added dropwise over 1 h at 0 °C. Immediately after addition was complete, the mixture was successively washed with saturated aqueous $NaHCO_3$ solution (3 x 400 mL) and brine (400 mL), dried over $MgSO_4$, filtered, and concentrated by rotary evaporation. The crude nitroso compound was immediately used in the next reaction without further purification.

The crude nitroso compound was dissolved in PhMe (25 mL) at 0 °C with stirring. To this mixture was added 1,3-cyclohexadiene (3.61 g, 45.0 mmol) dropwise via syringe over 10

min. The mixture was stirred for 3 h at 0 °C, at which point the entire reaction mixture was loaded directly onto a short silica gel column. Column chromatography (19:1 pentane:Et_2O) afforded the title compound as a red oil (8.31 g, ~81%) of approximate 90% purity by ^{1}H NMR. This compound was characterized solely by ^{1}H NMR, and the entirety of the product was taken forward to the next step: ^{1}H NMR (300 MHz, $CDCl_3$) δ 7.51 (s, 1H), 6.78 (s, 1H), 6.70 (ddd, *J* = 8.1 Hz, 5.7 Hz, 1.5 Hz, 1H), 6.58 (ddd, *J* = 8.1 Hz, 6.3 Hz, 1.5 Hz, 1H), 4.75 (td, *J* = 3.6 Hz, 1.8 Hz, 1H), 4.25 (m, 1H), 2.59 (td, *J* = 9.3 Hz, 3.3 Hz, 1H), 2.40 (s, 3H), 2.38-2.28 (m, 1H), 2.18 (s, 3H), 1.49-1.34 (m, 2H).

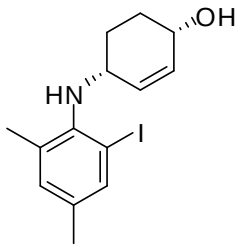

***rac-cis*-4-(2-Iodo-4,6-dimethylphenylamino)cyclohex-2-enol (4.51):** To a stirred mixture of NaI (7.49 g, 50.0 mmol) in MeCN (500 mL) at room temperature was added trimethylsilyl chloride (5.43 g, 50.0 mmol) via syringe. The mixture was stirred at room temperature for 1 h, and then cooled to 0 °C. Crude **4.50** (8.31 g, ~24.4 mmol) in MeCN (50 mL) was added to the stirred mixture dropwise via syringe over 10 min, followed by addition of water (0.225 g, 12.5 mmol) via syringe all at once. The mixture was stirred at 0 °C for 4 h, at which time water (250 mL) and brine (250 mL) were added, and the mixture was extracted with EtOAc (3 x 500 mL). The combined organic layers were washed successively with saturated aqueous $NaHCO_3$ solution (3 x 500 mL), 10% w/w aqueous $Na_2S_2O_3$ solution (2 x 500 mL), and brine (2 x 500 mL), dried over $MgSO_4$, filtered, and concentrated by rotary evaporation. Column chromatography (2:1 hexanes:EtOAc) furnished the title compound (4.03 g, 39% over 3 steps

from **3.21**) as a viscous red oil: ^{1}H NMR (300 MHz, $CDCl_3$) δ 7.46 (s, 1H), 6.93 (s, 1H), 5.92 (dd, *J* = 10.2 Hz, 1.8 Hz, 1H), 5.86 (dd, *J* = 10.2 Hz, 2.1 Hz, 1H), 4.20 (br m, 1H), 3.68 (br m, 1H), 3.41 (br s, 1H), 2.31 (s, 3H), 2.22 (s, 3H), 1.90-1.71 (m, 4H); ^{13}C NMR (75 MHz, $CDCl_3$) δ 144.3, 137.3, 133.3, 132.7, 132.6, 131.1, 130.4, 95.9, 64.9, 53.0, 29.4, 25.7, 19.9, 19.8; FTIR (neat, cm^{-1}) 3335 (broad), 3022, 2938, 2857, 1473, 1440, 1271, 1233, 1064, 989, 851, 727; LRMS (EI) *m/z* 343 (M^+, 77), 315 (16), 299 (22), 247 (100), 216 (17), 172 (16), 158 (30), 120 (37); HRMS (EI) calcd for $C_{14}H_{18}INO$: 343.0433, found: 343.0444.

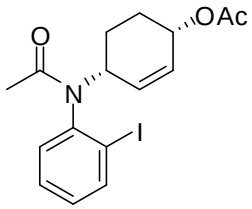

***rac-cis*-4-(*N*-(2-Iodophenyl)acetamido)cyclohex-2-enyl acetate (4.52):** A stirred mixture of **4.49** (2.21 g, 7.00 mmol) and K_2CO_3 (14.5 g, 105 mmol) in acetone (20 mL) was cooled to 0 °C. Acetyl chloride (4.12 g, 52.5 mmol) was added dropwise via syringe over 5 min, and the mixture was warmed to room temperature and stirred for 60 h. The mixture was recooled to 0 °C, water (50 mL) was added, and the mixture was extracted with EtOAc (3 x 50 mL). The combined organic layers were washed with brine (3 x 50 mL), dried over $MgSO_4$, filtered, and concentrated by rotary evaporation. Column chromatography (1:1 hexanes:EtOAc) furnished the title compound (2.11 g, 75%) as a yellow viscous oil in a 3:2 *anti*:*syn* atropisomer ratio: ^{1}H NMR (300 MHz, $CDCl_3$) δ 7.98 (dd, *J* = 7.8 Hz, 1.2 Hz, 1H, major), 7.97 (dd, *J* = 8.1 Hz, 1.2 Hz, 1H, minor), 7.43 (dt, *J* = 7.8 Hz, 1.5 Hz, 1H, minor), 7.42 (dt, *J* = 7.5 Hz, 1.8 Hz, 1H, major), 7.30-7.25 (m with clear d, *J* = 1.5 Hz, minor), 7.21 (dd, *J* = 7.8 Hz, 1.5 Hz, 1H, major), 7.11 (td, *J* = 7.8 Hz, 1.5 Hz, minor), 7.10 (td, *J* = 7.8 Hz, 1.5 Hz, 1H, major), 6.12 (m with clear d, *J* = 9.9 Hz,

1H, major), 5.94 (m with clear d, *J* = 10.8 Hz, 1H, minor), 5.90 (dddd, *J* = 10.2 Hz, 4.5 Hz, 2.4 Hz, 1.2 Hz, 1H, major), 5.70 (dq, *J* = 10.5 Hz, 2.4 Hz, 1H, minor), 5.23-5.05 (m, 2H, both), 2.18-2.09 (m, 1H, major), 1.99 (s, 3H, minor), 1.92 (s, 3H, major), 1.91-1.86 (m, 1H both and 1H minor), 1.84 (s, 3H, major), 1.81 (s, 3H, minor), 1.80-1.68 (m, 1H both and 1H minor), 1.40 (qd, *J* = 11.7 Hz, 3.9 Hz, 1H, major); ^{13}C NMR (75 MHz, $CDCl_3$) All signals, both atropisomers δ 170.27, 170.26, 170.2, 170.0, 143.3, 142.8, 140.2, 140.1, 135.2, 132.8, 130.3, 130.0, 129.83, 129.75, 129.4, 129.3, 127.2, 126.6, 103.7, 103.2, 65.6, 65.2, 53.2, 53.0, 26.9, 26.7, 23.8, 23.5, 21.1, 21.0, 20.8; FTIR (neat, cm^{-1}) 3056, 2950, 2872, 1729, 1661, 1468, 1433, 1373, 1305, 1242, 1078, 1017, 968, 899, 760, 726; HRMS (ESI) calcd for $C_{16}H_{18}INNaO_3$ $[M + Na]^+$: 422.0229, found: 422.0246.

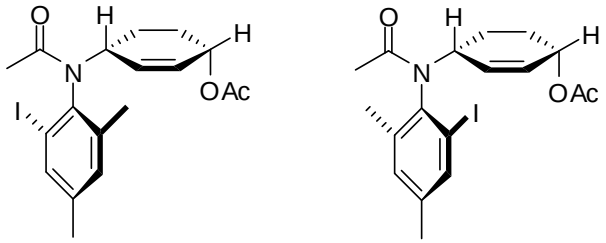

***rac-cis*-4-(*N*-(2-Iodo-4,6-dimethylphenyl)acetamido)cyclohex-2-enyl acetate (4.53):** To a stirred mixture of **4.50** (2.06 g, 6.00 mmol) and K_2CO_3 (12.44 g, 90.0 mmol) in acetone (40 mL) at 0 °C was added acetyl chloride (3.53 g, 45.0 mmol) dropwise via syringe. The mixture was stirred at 0 °C for 2 h, warmed to room temperature, and stirred an additional 16 h. The mixture was then recooled to 0 °C, and saturated aqueous $NaHCO_3$ solution (50 mL) was added. The mixture was extracted with EtOAc (3 x 50 mL), and the combined organic layers were washed with brine (50 mL), dried over $MgSO_4$, filtered, and concentrated by rotary evaporation. Exhaustive gradient column chromatography (2 columns, hexanes to 2:1 hexanes:EtOAc) provided the acylated compound as two separable atropisomers. The first eluting compound

consisted of *anti*-**4.53** (0.812 g, 32%) as a cream-colored solid, mp 120-121 °C: ^{1}H NMR (300 MHz, $CDCl_3$) δ 7.60 (s, 1H), 7.09 (s, 1H), 6.37 (d, *J* = 10.2 Hz, 1H), 5.79 (ddd, *J* = 10.2 Hz, 4.2 Hz, 1.8 Hz, 1H), 5.13 (q, *J* = 3.3 Hz, 1H), 4.86-4.75 (m, 1H), 2.32 (s, 3H), 2.27 (s, 3H), 1.99 (s, 3H), 1.86-1.79 (m, 2H), 1.77 (s, 3H), 1.72-1.62 (m, 1H), 1.34-1.19 (m, 1H); ^{13}C NMR (75 MHz, $CDCl_3$) δ 170.11, 169.8, 139.8, 139.3, 138.2, 137.6, 135.8, 131.7, 124.1, 103.6, 65.1, 53.1, 26.9, 23.1, 21.2, 20.8, 20.3, 20.1; FTIR (thin film, $CHCl_3$, cm^{-1}) 3007, 2955, 2871, 1731, 1660, 1468, 1373, 1243, 1073, 1013, 960, 901, 754; HRMS (ESI) calcd for $C_{18}H_{22}INNaO_3$ $[M + Na]^+$: 450.0542, found: 450.0555. The second eluting compound consisted of *syn*-**4.53** (0.670 g, 26%) as a cream-colored solid, mp 87-88 °C: ^{1}H NMR (300 MHz, $CDCl_3$) δ 7.62 (s, 1H), 7.08 (s, 1H), 6.11 (d, *J* = 10.2 Hz, 1H), 5.76-5.70 (m, 1H), 5.12 (m, 1H), 4.73-4.63 (m, 1H), 2.31 (s, 3H), 2.27 (s, 3H), 2.02 (s, 3H), 2.00-1.79 (m, 3H), 1.76 (s, 3H), 1.75-1.65 (m, 1H); ^{13}C NMR (75 MHz, $CDCl_3$) δ 170.3, 169.9, 139.8, 139.7, 137.8, 137.7, 134.3, 131.8, 124.6, 103.3, 65.0, 54.1, 26.9, 23.1, 22.2, 20.8, 20.0, 19.8; FTIR (thin film, $CHCl_3$, cm^{-1}) 2954, 1730, 1661, 1468, 1373, 1243, 1043, 1012, 966, 899, 754; LRMS (EI) *m/z* 427 (M^+, 7), 368 (78), 367(77), 325 (100), 272 (35), 198 (48), 158 (32), 79 (65); HRMS (EI) calcd for $C_{18}H_{22}INO_3$: 427.0644, found: 427.0643.

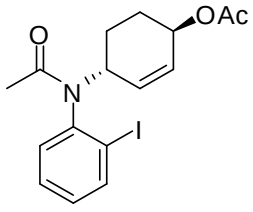

***rac-trans*-4-(*N*-(2-Iodophenyl)acetamido)cyclohex-2-enyl acetate (4.56):** In a round bottom flask fitted with a reflux condenser, solid 60% w/w NaH/mineral oil (0.336 g, 8.40 mmol) was slurried in DMF (3 mL) at 0 °C with stirring. A solution of **4.54**[48] (1.83 g, 7.0 mmol) in DMF (10 mL) was added to this slurry dropwise via syringe over 10 min. The resulting mixture was

warmed to room temperature, stirred for 30 min, and recooled to 0 °C. A solution of *trans*-4-chlorocyclohex-2-enyl acetate[212] (1.83 g, 10.5 mmol) in DMF (2 mL) was added dropwise via syringe over 5 min, and the stirred mixture was then heated at 80 °C for 40 h. The mixture was cooled to room temperature, and saturated aqueous NH_4Cl solution (150 mL) was added. The mixture was extracted with Et_2O (3 x 150 mL), and the combined organic layers were washed successively with water (3 x 150 mL) and brine (3 x 150 mL), dried over $MgSO_4$, filtered, and concentrated by rotary evaporation. Column chromatography (1:1 hexanes:EtOAc) furnished the title compound (2.21 g, 79%) as a yellow oil, in a 3:2 *anti*:*syn* ratio of atropisomers: ^{1}H NMR (300 MHz, $CDCl_3$) δ 7.97 (dd, *J* = 8.1 Hz, 1.5 Hz, 1H, major), 7.96 (dd, *J* = 8.1 Hz, 1.2 Hz, 1H, minor), 7.45-7.37 (m, 1H, both), 7.21 (dd, *J* = 7.8 Hz, 1.5 Hz, 1H, minor), 7.17 (dd, *J* = 7.8 Hz, 1.5 Hz, major), 7.09 (td, *J* = 7.8 Hz, 1.5 Hz, 1H, both), 5.97 (dq, *J* = 10.5 Hz, 1.5 Hz, 1H, major), 5.82 (dq, *J* = 10.5 Hz, 1.5 Hz, 1H, minor), 5.74 (dq, *J* = 10.2 Hz, 1.8 Hz, 1H, major), 5.54 (dq, *J* = 10.5 Hz, 1.5 Hz, 1H, minor), 5.41-5.31 (m, 1H, major), 5.31-5.18 (m, 2H, minor), 5.18-5.09 (m, 1H, major), 2.45-2.33 (m, 1H, minor), 2.23-2.10 (m, 1H, both), 2.04 (s, 3H, both), 2.03-1.93 (m, 1H, major), 1.83 (s, 3H, major), 1.80 (s, 3H, minor), 1.78-1.56 (m, 1H both and 1H minor), 1.30 (ddd, *J* = 13.2 Hz, 10.5 Hz, 2.7 Hz, 1H, major); ^{13}C NMR (75 MHz, $CDCl_3$) all signals, both atropisomers δ 170.6, 170.2, 170.1, 143.2, 142.6, 140.3, 140.2, 132.8, 130.6, 130.2, 130.0, 129.9, 129.82, 129.78, 129.53, 129.47, 103.7, 103.3, 68.9, 53.3, 52.9, 27.7, 27.0, 24.3, 23.6, 21.1; FTIR (neat, cm^{-1}) 3037, 2937, 2870, 1732, 1659, 1468, 1373, 1306, 1235, 1084, 1029, 901, 759; HRMS (ESI) calcd for $C_{16}H_{18}INNaO_3$ $[M + Na]^+$: 422.0229, found: 422.0238.

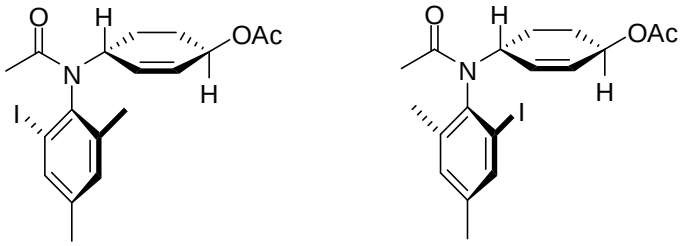

***rac-trans*-4-(*N*-(2-Iodo-4,6-dimethylphenyl)acetamido)cyclohex-2-enyl acetate (4.57):** Solid 60% w/w NaH (0.173 g, 7.20 mmol) was slurried in DMF (3 mL) at 0 °C with stirring. A solution of **4.55**[93,105] (1.74 g, 6.00 mmol) in DMF (10 mL) was added dropwise via syringe over 10 min, and the mixture was warmed to room temperature and stirred for 1 h. The mixture was then recooled to 0 °C, and a solution of *trans*-4-chlorocyclohex-2-enyl acetate[212] (1.57 g) in DMF (2 mL) was added via syringe over 5 min. The mixture was then stirred at 75 °C for 15 h, cooled to 0 °C, and water (150 mL) was added. The mixture was extracted with Et_2O (3 x 150 mL), and the combined organic layers were washed with water (3 x 150 mL) and brine (1 x 150 mL), dried over $MgSO_4$, filtered, and concentrated by rotary evaporation. Exhaustive column chromatography (2 columns, 1:1 hexanes:EtOAc) provided the pure atropisomers. The first eluting compound, *anti*-**4.57** (0.440 g, 17%) was isolated as a white solid, mp 124-126 °C: ^{1}H NMR (300 MHz, $CDCl_3$) δ 7.58 (s, 1H), 7.07 (s, 1H), 6.22 (dq, *J* = 10.2 Hz, 1.8 Hz, 1H), 5.64 (dq, *J* = 10.5 Hz, 1.8 Hz, 1H), 5.23 (m, 1H), 4.94 (m, 1H), 2.31 (s, 3H), 2.24 (s, 3H), 2.11-2.01 (m, 1H), 2.05 (s, 3H), 2.01-1.89 (m, 1H), 1.76 (s, 3H), 1.63 (m with clear d, *J* = 2.4 Hz, 1H), 1.19 (m with clear d, *J* = 2.4 Hz, 1H); ^{13}C NMR (75 MHz, $CDCl_3$) δ 170.81, 170.75, 140.3, 139.7, 138.5, 138.2, 133.9, 132.1, 127.5, 103.9, 69.6, 53.6, 28.2, 25.5, 23.5, 21.3, 20.7, 20.4; FTIR (thin film, $CHCl_3$, cm^{-1}) 2953, 2871, 1730, 1659, 1467, 1372, 1238, 1031, 905, 733; HRMS (ESI) calcd for $C_{18}H_{22}INNaO_3$ $[M + Na]^+$: 450.0542, found: 450.0551. The second eluting compound, *syn*-**4.57** (0.281 g, 11%), was isolated as a white solid, mp 139-141 °C: ^{1}H

NMR (300 MHz, $CDCl_3$) δ 7.60 (s, 1H), 7.06 (s, 1H), 5.97 (dq, *J* = 10.5 Hz, 2.1 Hz, 1H), 5.56 (dq, *J* = 10.2 Hz, 1.5 Hz, 1H), 5.37-5.27 (m, 1H), 4.87-4.76 (m, 1H), 2.29 (s, 3H), 2.24 (s, 3H), 2.22-2.05 (m, 2H), 2.03 (s, 3H), 1.74 (s, 3H), 1.66-1.58 (m with clear d, *J* = 2.4 Hz, 1H); ^{13}C NMR (75 MHz, $CDCl_3$) δ 170.9, 170.7, 140.2, 140.1, 138.4, 138.1, 132.4, 132.2, 128.0, 103.6, 69.6, 54.6, 28.2, 26.5, 23.5, 21.2, 20.4, 20.3; FTIR (thin film, $CHCl_3$, cm^{-1}) 2935, 2870, 1731, 1662, 1466, 1372, 1303, 1239, 1030, 904, 732; HRMS (ESI) calcd for $C_{18}H_{22}INNaO_3$ $[M + Na]^+$: 450.0542, found: 450.0527. The third eluting compound, starting material **4.55**, was also recovered (0.723 g, 42%).

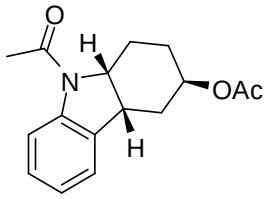

***rac*-(3*R*,4a*R*,9a*R*)-9-Acetyl-2,3,4,4a,9,9a-hexahydro-1*H*-carbazol-3-yl acetate (4.58):** Iodide **4.56** (0.160 g, 0.40 mmol, 2:1 *anti*:*syn*) was reacted according to the general radical procedure, with $[Bu_3SnH]_i$ = 0.01 M. Column chromatography (1:2 hexanes:EtOAc) provided the title compound (0.097 g, 89%) as a white solid, mp 146 °C, in a 2:1 rotamer ratio: ^1H NMR (300 MHz, $CDCl_3$) δ 8.11 (br d, *J* = 5.7 Hz, 1H, major), 7.31-7.25 (m, 1H, both), 7.22 (d, *J* = 7.8 Hz, 1H, both), 7.10 (t, *J* = 7.5 Hz, 1H, both), 4.77 (br m, 1H, minor), 4.70 (br m, 1H, both), 4.27 (br m, 1H, major), 3.72 (br m, 1H, major), 3.61 (br m, 1H, minor), 2.70-2.52 (m, 1H, both), 2.39 (br s, 3H, minor), 2.31 (br s, 3H, major), 2.07 (s, 3H, both), 1.94 (dq, *J* = 13.5 Hz, 6.3 Hz, 1H, both), 1.90 (dq, *J* = 13.5 Hz, 6.3 Hz, 1H, both), 1.60-1.32 (m, 3H, both); ^{13}C NMR (75 MHz, $CDCl_3$) δ 170.2, 167.6, 141.3, 132.4, 127.6, 124.1, 122.4, 118.0, 68.9, 60.3, 40.2, 29.2, 27.9, 26.1, 23.1, 21.1; additional signals from the minor amide rotamer were seen at 140.5, 135.1, 123.6, 115.4,

59.3, 39.0, 24.8, 23.8; FTIR (thin film, $CHCl_3$, cm^{-1}) 3009, 2945, 2866, 1731, 1658, 1599, 1478, 1402, 1246, 1038, 964, 930, 755; HRMS (ESI) calcd for $C_{16}H_{19}NNaO_3$ $[M + Na]^+$: 296.1263, found: 296.1252.

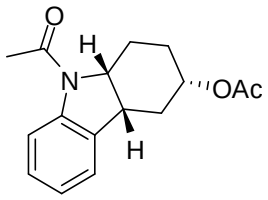

***rac*-(3*R*,4a*R*,9a*S*)-9-Acetyl-2,3,4,4a,9,9a-hexahydro-1*H*-carbazol-3-yl acetate (4.59):** Iodide **4.52** (0.16 g, 0.40 mmol, 3:2 *anti*:*syn*) was reacted according to the general radical procedure, with $[Bu_3SnH]_i$ = 0.01 M. Column chromatography (100% EtOAc) provided the title compound (0.101 g, 92%) as a white solid, mp 127-128 °C, in a 2:1 rotamer ratio: ^1H NMR (300 MHz, $CDCl_3$) δ 8.14 (br s, 1H, major), 7.45-7.20 (br s, 1H, minor), 7.21 (t, *J* = 7.5 Hz, 1H, both), 7.13 (d, *J* = 7.2 Hz, 1H, both), 7.05 (t, *J* = 7.5 Hz, 1H, both), 5.03 (m, 1H, both), 4.78 (br s, 1H, minor), 3.57 (br s, 1H, major), 3.68 (m with clear d, *J* = 15.3 Hz, 1H, both), 2.34 (br s, 3H, both), 2.04 (ddd, *J* = 15.3 Hz, 6.9 Hz, 3.3 Hz, 1H, both), 1.95-1.78 (m, 2H, both), 1.76 (s, 3H, both), 1.75-1.57 (m, 2H, both); ^{13}C NMR (75 MHz, $CDCl_3$) δ 170.5, 167.6, 140.9 (br), 134.5 (br), 127.1, 123.4, 122.6 (br), 117.8 (br), 67.3, 60.4 (br), 37.5 (br), 27.0, 26.3, 23.2 (br), 21.9 (br), 21.0; FTIR (thin film, $CHCl_3$, cm^{-1}) 2947, 2862, 1732, 1656, 1479, 1403, 1238, 1023, 994, 755; HRMS (ESI) calcd for $C_{16}H_{20}NO_3$ $[M + H]^+$: 274.1443, found: 274.1451.

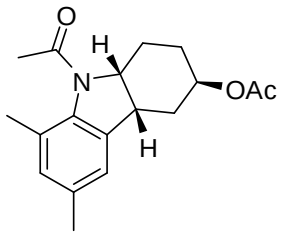

***rac*-(3*R*,4a*R*,9a*R*)-9-Acetyl-6,8-dimethyl-2,3,4,4a,9,9a-hexahydro-1*H*-carbazol-3-yl acetate (4.60):** Iodide *syn*-**4.57** (0.107 g, 0.250 mmol) was reacted according to the general radical procedure, with $[Bu_3SnH]_i$ = 0.01 M. Column chromatography (3:1 hexanes:EtOAc) provided the title compound (0.058 g, 77%) as a white solid, mp 134-136 °C: ^{1}H NMR (300 MHz, $CDCl_3$) δ 6.89 (s, 1H), 6.87 (s, 1H), 4.56 (tt, *J* = 11.4 Hz, 3.6 Hz, 1H), 4.37 (br s, 1H), 3.69 (br m, 1H), 2.56 (m with clear d, *J* = 14.1 Hz, 1H), 2.32 (s, 3H), 2.24 (br s, 3H), 2.21 (s, 3H), 2.10-2.00 (m, 1H), 2.05 (s, 3H), 1.88 (dd, *J* = 11.7 Hz, 6.0 Hz, 1H), 1.83 (dd, *J* = 11.7 Hz, 6.3 Hz, 1H), 1.53-1.23 (m, 2H); ^{13}C NMR (75 MHz, $CDCl_3$) δ 170.4, 167.7 (br), 138.1, 135.6 (br), 135.3, 130.5, 129.3 (br), 120.7, 69.0, 62.3, 41.5, 29.9, 28.4, 25.9, 23.0, 21.3, 21.0, 20.0; FTIR (thin film, $CHCl_3$, cm^{-1}) 2944, 2865, 1732, 1665, 1412, 1379, 1244, 1038, 754; LRMS (EI) *m/z* 301 (M^+, 36), 259 (29), 256 (15), 199 (15), 158 (40), 81 (100); HRMS (ESI) calcd for $C_{18}H_{23}NNaO_3$ $[M + Na]^+$: 324.1576, found: 324.1575.

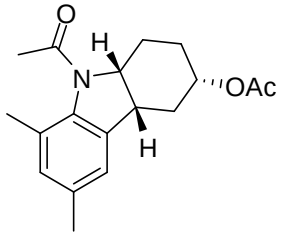

***rac*-(3*S*,4a*R*,9a*R*)-9-Acetyl-6,8-dimethyl-2,3,4,4a,9,9a-hexahydro-1*H*-carbazol-3-yl acetate (4.61):** Iodide *syn*-**4.53** (0.085 g, 0.200 mmol) was reacted according to the general radical procedure, with $[Bu_3SnH]_i$ = 0.01 M. Column chromatography (3:1 hexanes:EtOAc) provided

the title compound (0.043 g, 71%) as a white solid, mp 121-122 °C: ^{1}H NMR (300 MHz, $CDCl_3$) δ 6.84 (s, 1H), 6.73 (s, 1H), 4.96 (pentet, *J* = 3.0 Hz, 1H), 4.48 (br s, 1H), 3.56 (t, *J* = 6.6 Hz, 1H), 2.92 (m with clear d, *J* = 15.6 Hz, 1H), 2.29 (s, 3H), 2.25 (s, 3H), 2.24 (s, 3H), 1.97 (ddd, *J* = 15.6 Hz, 6.9 Hz, 3.3 Hz, 1H), 1.87-1.75 (m, 2H), 1.71 (s, 3H), 1.65-1.55 (m , 2H); ^{13}C NMR (75 MHz, $CDCl_3$) δ 170.5, 167.9 (br), 137.8, 137.5 (br), 134.3, 129.8, 128.7 (br), 120.8, 67.4, 62.4, 38.7, 27.2, 26.6, 22.9, 21.5, 20.9 (2C, accidental isochrony), 20.1; FTIR (thin film, $CHCl_3$, cm^{-1}) 2945, 2862, 1732, 1663, 1413, 1378, 1257, 1234, 1023, 904, 855, 755; LRMS (EI) *m/z* 301 (M^+, 79), 259 (57), 145 (25), 140 (23), 93 (23), 86 (62), 84 (100); HRMS (EI) calcd for $C_{18}H_{23}NO_3$ $[M]^+$: 301.1678, found: 301.1682.

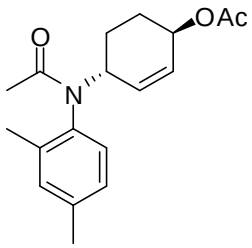

***rac-trans*-4-(*N*-(2,4-Dimethylphenyl)acetamido)cyclohex-2-enyl acetate (4.62):** Iodide *anti*-**4.57** (0.100 g, 0.234 mmol) was reacted according to the general radical procedure, with $[Bu_3SnH]_i$ = 0.21 M. Column chromatography (2:1 hexanes:EtOAc) provided the title compound (0.068 g, 96%) as a yellow oil in a 2:1 ratio of atropisomers: ^{1}H NMR (300 MHz, $CDCl_3$) δ 7.10 (m, 1H, both), 7.05-6.96 (m, 1H, both), 6.91 (d, *J* = 9.0 Hz, 1H, minor), 6.88 (d, *J* = 8.1 Hz, 1H, major), 5.92 (dq, *J* = 10.2 Hz, 1.5 Hz, 1H, major), 5.75-5.66 (m with clear d, 10.2 Hz, 1H, both), 5.56 (dq, *J* = 10.5 Hz, 1.5 Hz, 1H, minor), 5.32-5.24 (m, 1H, minor), 5.24-5.08 (m, 1H, both), 2.34 (s, 3H, both), 2.22 (s, 3H, minor), 2.20 (s, 3H, major), 2.03 (s, 3H, both), 2.01-1.84 (m, 1H both and 1H minor), 1.75 (s, 3H, major), 1.73 (s, 3H, minor), 1.70-1.55 (m,

2H, both), 1.41-1.25 (m, 1H, major); ^{13}C NMR (75 MHz, $CDCl_3$) all signals, both atropisomers δ 170.9, 170.8, 170.6, 138.4, 138.3, 136.5, 136.4, 136.3, 136.0, 132.9, 132.0, 131.9, 131.3, 129.5, 129.24, 129.19, 129.1, 127.7, 127.6, 69.1, 69.0, 52.7, 52.2, 27.80, 27.78, 26.6, 24.2, 22.8, 22.7, 21.2, 20.9, 18.4, 18.0; FTIR (neat, cm^{-1}) 2946, 2871, 1732, 1656, 1502, 1375, 1309, 1239, 1030; HRMS (ESI) calcd for $C_{18}H_{23}NNaO_3$ $[M + Na]^+$: 324.1576, found: 324.1549.

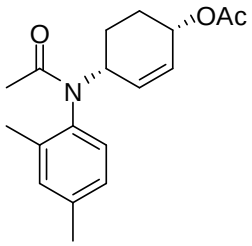

***rac-cis*-4-(*N*-(2,4-Dimethylphenyl)acetamido)cyclohex-2-enyl acetate (4.63):** Iodide *anti*-**4.53** (0.107 g, 0.250 mmol) was reacted according to the general radical procedure, with $[Bu_3SnH]_i$ = 0.21 M. Column chromatography (1:1 hexanes:EtOAc) provided the title compound (0.072 g, 96%) as a yellow oil in a 2:1 ratio of atropisomers: ^{1}H NMR (300 MHz, $CDCl_3$) δ 7.13 (m, 1H, both), 7.05-6.99 (m, 1H, both), 6.96 (d, *J* = 8.1 Hz, 1H, minor), 6.92 (d, *J* = 7.8 Hz, 1H, major),6.08 (d, *J* = 9.9 Hz, 1H, major), 5.90-5.83 (m, 1H, major), 6.85 (d, *J* = 10.2 Hz, 1H, minor), 5.71 (dq, *J* = 10.2 Hz, 2.7 Hz, 1H, minor), 5.25-5.15 (m, 1H, minor), 5.15-5.05 (m, 1H, major), 2.35 (s, 3H, both), 2.24 (s, 3H, minor), 2.23 (s, 3H, major), 1.98 (s, 3H, minor), 1.92 (s, 3H, major), 1.90-1.60 (m, 3H from both, 1H from minor), 1.76 (s, 3H, major), 1.74 (s, 3H, minor), 1.53-1.38 (m, 1H, minor); ^{13}C NMR (75 MHz, $CDCl_3$) All signals, both atropisomers δ 170.9, 170.8, 170.4, 138.3, 138.1, 136.8, 136.4, 136.30, 136.26, 135.5, 133.8, 131.94, 131.88, 129.5, 129.1, 127.6, 127.5, 126.5, 126.3, 65.6, 65.3, 52.9, 52.6, 26.9, 23.4, 22.8, 22.7, 21.2, 21.1,

20.9, 18.4, 18.0; FTIR (neat, cm^{-1}) 2950, 1731, 1657, 1502, 1376, 1310, 1242, 1046, 1014, 967, 898, 769, 733; HRMS (ESI) calcd for $C_{18}H_{23}NNaO_3$ $[M + Na]^+$: 324.1576, found: 324.1596.

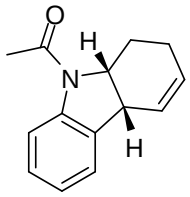

***rac*-1-(*cis*-1*H*-Carbazol-9(2*H*,4a*H*,9a*H*)-yl)ethanone (4.64):** In a sealable pressure tube were placed a stir bar, **4.56** (0.200 g, 0.500 mmol, 3:2 *anti*:*syn*), $Pd_2(dba)_3$•$CHCl_3$ (0.026 g, 0.025 mmol), and P(*o*-tol)$_3$ (0.040 g, 0.132 mmol). A degassed 10:1 MeCN:H_2O solvent mixture (6 mL) was added, followed by Me_2NBu (0.121 g, 1.20 mmol). The tube was sealed, heated at 80 °C for 6 h, and recooled to room temperature. Saturated aqueous NH_4Cl (10 mL) was added, and the mixture was extracted with EtOAc (3 x 10 mL). The combined organic layers were washed with brine (1 x 10 mL), dried over $MgSO_4$, filtered, and concentrated by rotary evaporation. Column chromatography (2 columns, 1:3 pentane:Et_2O) provided the title compound (0.061 g, 47%) as a yellow oil in a 3:1 ratio of amide rotamers: ^{1}H NMR (300 MHz, $CDCl_3$) δ 8.14 (br d, *J* = 7.5 Hz, 1H, major), 7.19 (t, *J* = 7.5 Hz, 2H, both), 7.17 (br m, minor), 7.05 (t, *J* = 7.5 Hz, 1H, both), 6.17-6.02 (br m, 1H, both), 6.00-5.90 (m, 1H, both), 4.88 (br s, 1H, minor), 4.39 (m, 1H, major), 3.94 (br s, 1H, major), 3.80 (br s, 1H, minor), 2.41 (s, 3H, minor), 2.31 (s, 3H, major), 2.21-1.91 (m, 3H, both), 1.63-1.45 (m, 1H, major), 1.38-1.20 (br m, 1H, minor); ^{13}C NMR (75 MHz, $CDCl_3$) δ 167.9, 140.7, 128.1, 127.4, 123.9 (2C, accidental isochrony), 123.2, 118.1, 60.4, 40.6, 25.0, 23.2, 22.8, peaks from the minor rotamer were also seen at 129.0, 124.5, 115.3, 59.6, 39.2, 24.2; FTIR (neat, cm^{-1}) 3031, 2935, 2841, 1650, 1480, 1403, 1319, 1080, 1015, 912, 730;

LRMS (EI) *m/z* 213 (M^+, 60), 171 (72), 170 (55), 156 (52), 143 (42), 130 (100), 77 (30); HRMS (EI) calcd for $C_{14}H_{15}NO$ $[M]^+$: 213.1154, found: 213.1153.

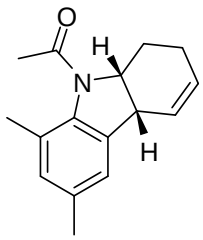

***rac*-1-(*cis*-6,8-Dimethyl-1*H*-carbazol-9(2*H*,4a*H*,9a*H*)-yl)ethanone (4.42a):** In a sealable pressure tube were placed a stir bar, *anti*-**4.53** (0.107 g, 0.250 mmol), $Pd_2(dba)_3$•$CHCl_3$ (0.013 g, 0.0125 mmol), and P(*o*-tol)$_3$ (0.017 g, 0.055 mmol). A degassed 10:1 MeCN:H_2O solvent mixture (2.5 mL) was added, followed by Me_2NBu (0.051 g, 0.500 mmol). The tube was sealed, heated at 80 °C for 4 h, and recooled to room temperature. Saturated aqueous NH_4Cl (5 mL) was added, and the mixture was extracted with EtOAc (3 x 5 mL). The combined organic layers were dried over $MgSO_4$, filtered, and concentrated by rotary evaporation. Gradient column chromatography (7:1 pentane:Et_2O to 1:2 pentane:Et_2O) provided the title compound (0.044 g, 73%) as a white solid, mp 136-137 °C: ^{1}H NMR (300 MHz, $CDCl_3$) δ 6.85 (s, 1H), 6.82 (s, 1H), 6.06 (m with clear d, *J* = 9.9 Hz, 1H), 5.94-5.85 (m, 1H), 4.50 (br s, 1H), 3.90 (br s, 1H), 2.30 (s, 3H), 2.27 (s, 3H), 2.23 (s, 3H), 2.17-2.04 (m, 2H), 2.03-1.90 (m, 1H), 1.58-1.38 (br m, 1H); ^{13}C NMR (75 MHz, $CDCl_3$) δ 168.2 (br), 138.1, 137.5 (br), 137.3, 135.0, 130.2, 128.1, 124.5, 121.5, 61.9, 41.2, 24.5, 23.0, 22.9, 20.9, 20.3; FTIR (thin film, $CHCl_3$, cm^{-1}) 3025, 2924, 2840, 1666, 1412, 1385, 1350, 853, 783; LRMS (EI) *m/z* 241 (M^+, 100), 199 (98), 184 (50), 158 (52); HRMS (EI) calcd for $C_{16}H_{19}NO$ $[M]^+$: 241.1467, found: 241.1461.

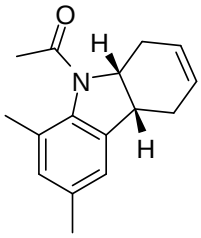

***rac*-1-((4a*R*,9a*R*)-6,8-dimethyl-4,4a-dihydro-1*H*-carbazol-9(9a*H*)-yl)ethanone (4.42b):** This compound was never isolated as a pure isomer, but co-eluted with **4.42a** in several reactions: ^{1}H NMR (300 MHz, $CDCl_3$) δ 6.86 (s, 1H), 6.79 (s, 1H), 5.76 (dq, *J* = 10.2 Hz, 3.0 Hz, 1H), 5.72-5.57 (m, 1H), 4.44 (br s, 1H), 3.66 (br t, *J* = 6.6 Hz, 1H), 2.73-2.58 (m, 1H), 2.58-2.48 (m, 1H), 2.43 (dt, *J* = 16.8 Hz, 6.3 Hz, 1H), 2.31 (s, 3H), 2.27 (s, 3H), 2.24 (s, 3H), 1.95-1.85 (m, 1H).

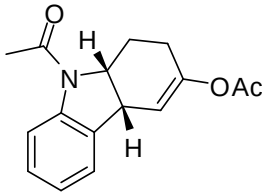

***rac-cis*-9-Acetyl-2,4a,9,9a-tetrahydro-1*H*-carbazol-3-yl acetate (4.65):** In a sealable pressure tube were placed a stir bar, **4.52** (0.240 g, 0.250 mmol, 3:2 *anti*:*syn*), $Pd_2(dba)_3$•$CHCl_3$ (0.031 g, 0.030 mmol), and P(*o*-tol)$_3$ (0.033 g, 0.110 mmol). A degassed 10:1 MeCN:H_2O solvent mixture (5 mL) was added, followed by Me_2NBu (0.101 g, 1.00 mmol). The tube was sealed, heated at 80 °C for 3 h, and recooled to room temperature. Saturated aqueous NH_4Cl (5 mL) was added, and the mixture was extracted with EtOAc (3 x 10 mL). The combined organic layers were washed with brine (1 x 10 mL), dried over $MgSO_4$, filtered, and concentrated by rotary evaporation. Gradient column chromatography (hexanes to 2:3 hexanes:EtOAc) provided the title compound (0.111 g, 82%) as a white solid, mp 132-133 °C, in a 2:1 amide rotamer ratio: ^{1}H NMR (300 MHz, $CDCl_3$) δ 8.14 (br d, *J* = 6.9 Hz, 1H, major), 7.22 (t, *J* = 7.5 Hz, 1H, both),

7.18 (br m, 1H, minor), 7.18-7.11 (m, 1H, both), 7.07 (td, *J* = 7.5 Hz, 1.2 Hz, 1H, both), 5.82 (br s, 1H, both), 4.89 (m, 1H, minor), 4.42 (m, 1H, major), 4.13 (br m, 1H, major), 4.00 (br m, 1H, minor), 2.60-2.237 (m, 1H both and 1H minor), 2.33 (br s, 3H, both), 2.16 (s, 3H, both), 2.12-1.98 (m, 2H, both), 1.87-1.67 (br m, 1H, minor); ^{13}C NMR (75 MHz, $CDCl_3$) major rotamer δ 169.0, 168.1, 149.2, 140.4, 133.1, 127.7, 124.2, 123.3, 118.1, 115.5, 110.6, 59.5, 40.0, 25.4, 25.1, 23.0, 20.9, additional signals from the minor rotamer also seen at δ 168.6, 131.0, 124.7, 58.8, 24.1, 20.5; FTIR (thin film, $CHCl_3$, cm^{-1}) 3011, 2847, 1752, 1656, 1479, 1401, 1369, 1275, 1208, 1132, 1014, 915, 755; HRMS (ESI) calcd for $C_{16}H_{18}NO_3$ $[M + Na]^+$: 272.1287, found: 272.1311.

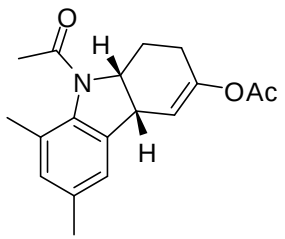

***rac-cis*-9-Acetyl-6,8-dimethyl-2,4a,9,9a-tetrahydro-1*H*-carbazol-3-yl acetate (4.66):** In a sealable pressure tube were placed a stir bar, *syn*-**4.57** (0.092 g, 0.250 mmol), $Pd_2(dba)_3$•$CHCl_3$ (0.013 g, 0.0125 mmol), and P(*o*-tol)$_3$ (0.017 g, 0.055 mmol). A degassed 10:1 MeCN:H_2O solvent mixture (2.5 mL) was added, followed by Me_2NBu (0.063 g, 0.625 mmol). The tube was sealed, heated at 80 °C for 1 h, and recooled to room temperature. Saturated aqueous NH_4Cl (5 mL) was added, and the mixture was extracted with EtOAc (3 x 5 mL). The combined organic layers were washed with brine (1 x 10 mL), dried over $MgSO_4$, filtered, and concentrated by rotary evaporation. Column chromatography (1:1 hexanes:EtOAc) provided an inseparable mixture (63 mg total) of the title compound (0.054 g, 0.182 mmol, 73%) and tri(*o*-tolyl)phosphine oxide[276] (0.009 g, 0.027 mmol): ^{1}H NMR (300 MHz, $CDCl_3$) δ 6.86 (s, 1H),

6.79 (s, 1H), 5.76 (dd, *J* = 4.8 Hz, 2.4 Hz, 1H), 4.53 (br s, 1H), 4.06 (br m, 1H), 2.58-2.43 (m, 1H), 2.28 (s, 3H), 2.26 (s, 3H), 2.22 (s, 3H), 2.14 (s, 3H), 2.08-1.95 (m, 2H), 1.70 (dq, *J* = 12.6 Hz, 4.5 Hz, 1H); HRMS (EI) calcd for $C_{18}H_{21}NNaO_3$ $[M + Na]^+$: 322.1419, found: 322.1440.

6.5 COMPOUND DATA FOR CHAPTER 5

Experimental procedures and spectroscopic data have been previously reported in the literature for compound **5.21**.[234] These procedures were followed, and the product's physical properties and spectroscopic data were consistent with those previously reported. The preparations of **3.21**, **3.23**, and **3.27** are described in Chapter 6.3.

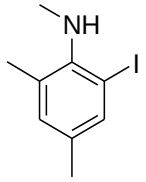

2-Iodo-*N*-4,6-trimethylaniline (5.19): LDA was made by dissolving *N*,*N*-diisopropylamine (2.43 g, 24.0 mmol) in THF (10 mL) at −78 °C with stirring, and adding a hexanes solution of BuLi (15.7 mL, 22.0 mmol) dropwise. The reaction mixture was stirred at this temperature for 40 min, warmed to 0 °C and stirred for 10 min. The resulting solution of LDA was then added dropwise over 10 min to a stirred solution of *o*-iodoaniline **3.21** (4.94 g, 20.0 mmol) in THF (150 mL) at −78 °C, and the mixture was stirred for an additional 20 min. Methyl iodide (2.98 g, 21.0 mmol) was added dropwise via syringe, the reaction mixture was warmed to room temperature, and stirred for 1 h. The mixture was quenched with saturated aqueous NH_4Cl solution (200 mL) and diluted with Et_2O (250 mL). The organic layer was separated and washed with saturated aqueous NH_4Cl (3 x 250 mL) and brine (250 mL) solutions, dried over $MgSO_4$, filtered, and concentrated by rotary evaporation. Flash chromatography (25:1 pentane:Et_2O) afforded the title compound (4.40 g, 84%) as a red-brown, acrid-smelling liquid: ^{1}H NMR (300 MHz, $CDCl_3$) δ 7.44 (s, 1H), 6.93 (s, 1H), 3.31 (br s, 1H), 2.73 (s, 3H), 2.35 (s, 3H), 2.22 (s, 3H); ^{13}C NMR (75 MHz, $CDCl_3$) δ 146.8, 136.8, 133.6, 132.5, 130.8, 95.3, 35.3, 19.9, 19.5; FTIR (neat, cm^{-1}) 3348,

2949, 2917, 2860, 1481, 1411, 1277, 1108, 1028, 852, 790, 726; LRMS (EI) *m/z* 261 (M^+, 75), 246 (32), 134 (29), 118 (27), 105 (45), 91 (100), 78 (87), 76 (99); HRMS (EI) calcd for $C_9H_{12}IN$: 261.0015, found: 261.0019.

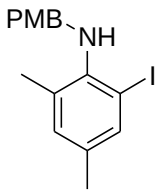

2-Iodo-*N*-(4-methoxybenzyl)-4,6-dimethylaniline (5.20): To a stirred solution of **3.21** (6.18 g, 25.0 mmol) and *p*-anisaldehyde (3.57 g, 26.3 mmol) in EtOAc (75 mL) was added trifluoroacetic acid (5.70 g, 50.0 mmol). The mixture was stirred at room temperature for 30 min, and solid $NaBH(OAc)_3$ (9.54 g, 45.0 mmol) was added portionwise over 5 min. The reaction mixture was stirred for 3 h, cooled to 0 °C, and quenched with 10% w/w aqueous NaOH solution (*very* slowly at first, until gas production stopped) until two distinct layers formed. The organic layer was separated and washed with brine (2 x 100 mL), dried over $MgSO_4$, filtered, and concentrated by rotary evaporation. Column chromatography (10:1 hexanes:EtOAc) afforded the title compound (7.59 g, 83%) as an off-white solid, mp 69-70 °C: ^{1}H NMR (300 MHz, $CDCl_3$) δ 7.47 (s, 1H), 7.36 (d, *J* = 8.7 Hz, 2H), 6.95 (s, 1H), 6.90 (d, *J* = 8.7 Hz, 2H), 4.02 (s, 2H), 3.83 (s, 3H), 3.44 (br s, 1H), 2.37 (s, 3H), 2.23 (s, 3H); ^{13}C NMR (75 MHz, $CDCl_3$) δ 158.7, 145.2, 137.0, 133.9, 132.3, 131.6, 131.3, 129.3 (2C), 113.7 (2C), 96.2, 55.0, 52.1, 19.9, 19.4; FTIR (thin film, $CHCl_3$, cm^{-1}) 3326, 2928, 2832, 1509, 1471, 1462, 1275, 1179, 1055, 1029, 831, 820, 738; LRMS (EI) *m/z* 368 (26), 367 (M^+, 82), 238 (37), 122 (65), 121 (100), 91 (32), 77 (40); HRMS (EI) calcd for $C_{16}H_{18}INO$: 367.0433, found: 367.0430.

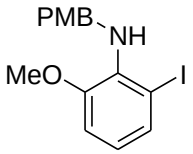

2-Iodo-6-methoxy-*N*-(4-methoxybenzyl)aniline (5.22): To a stirred solution of *N*-Boc aniline **5.21**[234] (4.36 g, 12.5 mmol) in CH_2Cl_2 (60 mL) at 0 °C was added trifluoroacetic acid (14.25 g, 125 mmol) in one portion via syringe. The reaction mixture was warmed to room temperature and stirred for 1.5 h, at which time *p*-anisaldehyde (1.79 g, 13.1 mmol) was added in one portion via syringe. The reaction was stirred for 10 min, and solid $NaBH(OAc)_3$ (7.95 g, 37.5 mmol) was added portionwise over 10 min. The mixture was stirred for 1 h, cooled to 0 °C, and quenched (*very* slowly at first, until gas production stopped) with 10% w/w aqueous NaOH solution (50 mL). The organic layer was separated and washed with brine (50 mL), dried over $MgSO_4$, filtered, and concentrated by rotary evaporation. Column chromatography (6:1 pentane:Et_2O) afforded the title compound (3.36 g, 76%) as a yellow oil: ^{1}H NMR (300 MHz, $CDCl_3$) δ 7.35 (dd, *J* = 8.1 Hz, 1.2 Hz, 1H), 7.30 (d, *J* = 8.7 Hz, 2H), 6.86 (d, *J* = 8.7 Hz, 2H), 6.81 (dd, *J* = 8.1 Hz, 1.2 Hz, 1H), 6.64 (t, *J* = 8.1 Hz, 1H), 4.32 (s, 2H), 4.02 (br s, 1H), 3.82 (s, 3H), 3.81 (s, 3H); ^{13}C NMR (75 MHz, $CDCl_3$) δ 158.6, 151.2, 139.0, 132.1, 131.2 (2C), 129.3, 123.1, 113.6 (2C), 111.4, 92.3, 55.7, 55.1, 51.4; FTIR (neat, cm^{-1}) 3347, 2934, 2833, 1611, 1582, 1512, 1463, 1247, 1175, 1031, 830, 760, 726; LRMS (EI) *m/z* 369 (M^+, 25), 240 (5), 121 (100), 91 (6), 77 (7); HRMS (EI) calcd for $C_{15}H_{16}INO_2$: 369.0226, found: 369.0227.

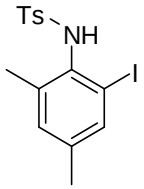

***N*-(2-Iodo-4,6-dimethylphenyl)-4-methylbenzenesulfonamide (5.23):** To a stirred solution of **3.21** (2.47 g, 10.0 mmol) in pyridine (10 mL) was added *p*-toluenesulfonyl chloride (2.29 g, 12.0 mmol) all at once. The reaction mixture was stirred at room temperature for 5 h, at which point saturated aqueous NH_4Cl solution (40 mL) was added to quench the reaction. The mixture was extracted with CH_2Cl_2 (4 x 40 mL), and the combined organic layers were washed with 1 N HCl (3 x 40 mL) and brine (3 x 40 mL), dried over $MgSO_4$, filtered, and concentrated by rotary evaporation. Column chromatography (4:1 hexanes:EtOAc) afforded the title compound (3.63 g, 90%) as a white solid, mp 157-158 °C: ^{1}H NMR (300 MHz, $CDCl_3$) δ 7.56 (d, *J* = 8.1 Hz, 2H), 7.39 (s, 1H), 7.25 (d, *J* = 8.1 Hz, 2H), 7.07 (s, 1H), 6.04 (s, 1H), 2.49 (s, 3H), 2.44 (s, 3H), 2.26 (s, 3H); ^{13}C NMR (75 MHz, $CDCl_3$) δ 143.9, 139.4, 139.2, 137.5, 137.2, 133.2, 132.7, 129.5 (2C), 127.9 (2C), 100.2, 21.6, 20.7, 20.3; FTIR (thin film, $CHCl_3$, cm^{-1}) 3270 (broad), 2922, 1598, 1465, 1387, 1330, 1162, 1091, 891, 813, 756, 709; HRMS (ESI) calcd for $C_{15}H_{16}INNaO_2S$ $[M + Na]^+$: 423.9844, found: 423.9849.

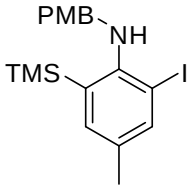

2-Iodo-*N*-(4-methoxybenzyl)-4-methyl-6-(trimethylsilyl)aniline (5.24): To a stirred solution of **3.27** (5.26 g, 17.2 mmol) in THF (85 mL) at −78 °C was added a hexanes solution of LiHMDS (19.0 mL, 19.0 mmol) dropwise via syringe. The reaction mixture was warmed to

room temperature, stirred for 30 min, and recooled to −78 °C. A solution of 4-methoxybenzyl bromide (4.16 g, 20.7 mmol) in THF (15 mL) was added to the reaction mixture dropwise via syringe, the mixture was warmed to room temperature and stirred for 3 h. Saturated aqueous NH_4Cl solution (100 mL) was added, and the mixture was extracted with Et_2O (3 x 100 mL). The combined organic layers were washed with brine (100 mL), dried over $MgSO_4$, filtered, and concentrated by rotary evaporation. Column chromatography (98:2 pentane:Et_2O) furnished the title compound (5.94 g, 81%) as an orange oil: ^{1}H NMR (300 MHz, $CDCl_3$) δ 7.71 (dd, *J* = 1.8 Hz, 0.6 Hz, 1H), 7.44 (d, *J* = 8.7 Hz, 2H), 7.24 (d, *J* = 1.5 Hz, 1H), 6.92 (d, *J* = 8.7 Hz, 2H), 4.05 (d, *J* = 6.9 Hz, 2 H), 3.84 (s, 3H), 3.26 (br t, *J* = 6.9 Hz, 1H), 2.29 (s, 3H), 0.34 (s, 9H); ^{13}C NMR (75 MHz, $CDCl_3$) δ 158.8, 151.7, 141.3, 136.6, 136.2, 134.9, 131.6, 129.1 (2C), 113.8 (2C), 98.9, 55.2, 54.6, 20.2, 0.4 (3C); FTIR (neat, cm^{-1}) 3297, 2952, 2899, 2833, 1611, 1584, 1513, 1426, 1301, 1247, 1173, 1074, 1037, 905, 839, 766; HRMS (ESI) calcd for $C_{18}H_{25}INOSi$ [M + H]$^+$: 426.0750, found: 426.0788.

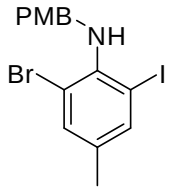

2-Bromo-6-iodo-*N*-(4-methoxybenzyl)-4-methylaniline (5.25): A solution of **3.23** (3.12 g, 10.0 mmol), *p*-anisaldehyde (1.36 g, 10.0 mmol), and trifluoroacetic acid (.228 g, 2.00 mmol) in toluene (10 mL) was stirred in a round-bottom flask fitted with a Dean-Stark trap and a reflux condenser. The reaction mixture was refluxed for 12 h with azeotropic removal of water, cooled to room temperature, and solvent was removed by rotary evaporation. The crude residue was redissolved in EtOAc (30 mL) with stirring, trifluoroacetic acid (2.28 g, 20.0 mmol) was added,

and the mixture was stirred for 30 min. Solid $NaBH(OAc)_3$ (4.24 g, 20.0 mmol) was added portionwise over 5 min, and the reaction mixture was stirred for 2 h at room temperature. The mixture was cooled to 0 °C, and quenched with 10% w/w aqueous NaOH solution (*very* slowly at first, until gas production stopped) until two distinct layers formed. The organic layer was separated and washed with brine (2 x 20 mL), dried over $MgSO_4$, filtered, and concentrated by rotary evaporation. Column chromatography (20:1 pentane:Et_2O) afforded the title compound (3.12 g, 72%) as a pink solid, mp 41-42 °C: ^{1}H NMR (300 MHz, $CDCl_3$) δ 7.59 (s, 1H), 7.39 (d, J = 8.7 Hz, 2H), 7.37 (s, 1H), 6.89 (d, J = 8.7 Hz, 2H), 4.22 (s, 2H, 3.82 (s, 3H), 2.25 (s, 3H); ^{13}C NMR (75 MHz, $CDCl_3$) δ 158.9, 144.5, 139.5, 135.6, 134.1, 131.3, 129.6 (2C), 117.0, 113.8 (2C), 94.6, 55.2, 52.1, 19.7; FTIR (thin film, $CHCl_3$, cm^{-1}) 3332, 2993, 2958, 2927, 2831, 1610, 1584, 1510, 1455, 1244, 1173, 1034, 852, 826, 745, 714; LRMS (EI) *m/z* 433 (M^+ (^{81}Br), 7), 431 (M^+ (^{79}Br), 7), 313 (5), 311 (5), 121 (100); HRMS (EI) calcd for $C_{15}H_{15}{}^{79}BrINO$: 430.9382, found: 430.9379.

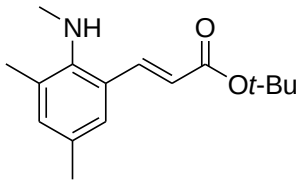

(*E*)-*tert*-Butyl 3-(3,5-dimethyl-2-(methylamino)phenyl)acrylate (5.26a): In a round-bottom flask fitted with a reflux condenser were combined **5.19** (1.31 g, 5.00 mmol), K_2CO_3 (1.04 g, 7.50 mmol), *tert*-butyl acrylate (0.961 g, 7.50 mmol), and 10% Pd/C (0.186 g, 0.175 mmol) in DMF (10 mL). The stirred mixture was heated at 140 °C for 2 h, cooled to room temperature, and filtered through a pad of Celite, followed by rinsing the pad with Et_2O (100 mL). The combined filtrates were washed with water (3 x 100 mL) and brine (100 mL), dried over $MgSO_4$,

filtered, and concentrated by rotary evaporation. Column chromatography (5:1 hexanes:EtOAc) afforded the title compound (1.20 g, 92%) as a bright yellow solid, mp 76 °C: ^{1}H NMR (300 MHz, $CDCl_3$) δ 7.91 (d, *J* = 15.9 Hz, 1H), 7.17 (s, 1H), 6.98 (s, 1H), 6.29 (d, *J* = 15.9 Hz, 1H), 3.17 (br s, 1H), 2.81 (3H, s), 2.26 (s, 3H), 2.25 (s, 3H), 1.55 (s, 9H); ^{13}C NMR (75 MHz, $CDCl_3$) δ 166.6, 146.2, 141.3, 132.9, 130.7, 129.1, 126.4, 126.0, 119.4, 79.9, 37.3, 28.1 (3C), 20.4, 17.6; FTIR (thin film, $CHCl_3$, cm^{-1}) 3390, 2976, 2931, 1705, 1628, 1480, 1367, 1332, 1278, 1151, 984, 757, 714; LRMS (EI) *m/z* 262 ($M+H^+$, 1), 206 (65), 188 (100), 173 (66), 160 (96), 145 (41); HRMS (EI) calcd for $C_{16}H_{24}NO_2$ $[M + H]^+$: 262.1807, found: 262.1794.

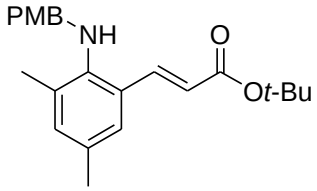

(*E*)-*tert*-Butyl 3-(2-(4-methoxybenzylamino)-3,5-dimethylphenyl)acrylate (5.26b): In a round-bottom flask fitted with a reflux condenser were combined **5.20** (3.67 g, 10.0 mmol), K_2CO_3 (2.07 g, 15.0 mmol), *tert*-butyl acrylate (1.92 g, 15.0 mmol), and 10% Pd/C (0.372 g, 0.350 mmol) in DMF (20 mL). The stirred mixture was heated at 130 °C for 4 h, cooled to room temperature, diluted with Et_2O (200 mL), and filtered through a pad of Celite, followed by rinsing the pad with Et_2O (50 mL). The filtrate was washed with water (3 x 200 mL) and brine (200 mL), dried over $MgSO_4$, filtered, and concentrated by rotary evaporation. Column chromatography (10:1 hexanes:EtOAc) gave the title compound (3.02 g, 82%) as a bright yellow-green solid, mp 68-70 °C: ^{1}H NMR (300 MHz, $CDCl_3$) δ 8.00 (d, *J* = 15.9 Hz, 1H), 7.25 (d, *J* = 9.3 Hz, 2H), 7.21 (s, 1H), 6.97 (s, 1H), 6.86 (d, *J* = 8.7 Hz, 2H), 6.31 (d, *J* = 15.9 Hz, 1H), 4.04 (s, 2H), 3.81 (s, 2H), 3.27 (br s, 1H), 2.28 (s, 3H), 2.14 (s, 3H), 1.54 (s, 9H); ^{13}C NMR (75

MHz, $CDCl_3$) δ 166.6, 158.8, 144.4, 141.3, 133.0, 132.2, 131.4, 129.8 (2C), 129.2, 127.2, 126.1, 119.8, 113.8 (2C), 80.0, 55.2, 54.7, 28.2 (3C), 20.6, 17.8; FTIR (thin film, $CHCl_3$, cm^{-1}) 3368, 2975, 2933, 2835, 1703, 1628, 1611, 1512, 1476, 1278, 1248, 1153, 1036, 983, 854, 823, 757; LRMS (EI) *m/z* 367 (M^+, 14), 310 (6), 256 (9), 146 (11), 121 (100), 69 (55); HRMS (EI) calcd for $C_{23}H_{29}NO_3$: 367.2147, found: 367.2144.

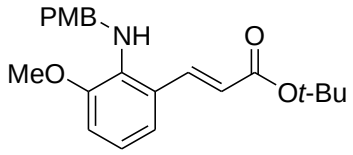

(*E*)-*tert*-Butyl 3-(3-methoxy-2-(4-methoxybenzylamino)phenyl)acrylate (5.26c): In a round-bottom flask fitted with a reflux condenser were combined **5.22** (3.32 g, 9.00 mmol), K_2CO_3 (1.87 g, 13.5 mmol), *tert*-butyl acrylate (1.73 g, 13.5 mmol), and 10% Pd/C (0.335 g, 0.315 mmol) in DMF (18 mL). The stirred mixture was heated at 130 °C for 4 h, cooled to room temperature, and filtered through a pad of Celite, followed by rinsing the pad with Et_2O (180 mL). Water (180 mL) was added to the filtrate, the organic layer was removed, and the aqueous layer was extracted with Et_2O (3 x 180 mL). The combined organic layers were washed with water (3 x 180 mL) and brine (180 mL), dried over $MgSO_4$, filtered, and concentrated by rotary evaporation. Column chromatography (3:1 hexanes:EtOAc) afforded the title compound (2.83 g, 85%) as a bright yellow-green solid, mp 67-68 °C: ^{1}H NMR (300 MHz, $CDCl_3$) δ 8.00 (d, *J* = 15.9 Hz, 1H), 7.27 (d, *J* = 9.0 Hz, 2H), 7.09 (dd, *J* = 7.8 Hz, 1.2 Hz, 1H), 6.88 (t, *J* = 8.1 Hz, 1H), 6.86 (d, *J* = 8.7 Hz, 2H), 6.81 (dd, *J* = 7.8 Hz, 1.2 Hz, 1H), 6.30 (d, *J* = 15.9 Hz, 1H), 4.29 (br s, 1H), 4.16 (s, 2H), 3.81 (s, 3H), 3.79 (s, 3H), 1.53 (s, 9H); ^{13}C NMR (75 MHz, $CDCl_3$) δ 166.3, 158.6, 150.9, 141.0, 138.5, 132.1, 128.9 (2C), 125.9, 120.8, 119.8, 119.5, 113.6 (2C), 111.0, 79.9, 55.6, 54.9, 54.2, 28.0 (3C); FTIR (thin film, $CHCl_3$, cm^{-1}) 3359, 2976, 2935, 2835,

1701, 1628, 1581, 1513, 1456, 1243, 1147, 1078, 1036, 983, 852, 824, 759; HRMS (ESI) calcd for $C_{22}H_{27}NNaO_4$ $[M + Na]^+$: 392.1838, found: 392.1832.

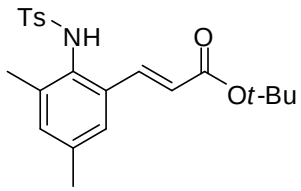

(*E*)-*tert*-Butyl 3-(3,5-dimethyl-2-(4-methylphenylsulfonamido)phenyl)acrylate (5.26d): In a round-bottom flask fitted with a reflux condenser were combined **5.23** (2.01 g, 5.00 mmol), K_2CO_3 (1.04 g, 7.50 mmol), *tert*-butyl acrylate (0.961 g, 7.50 mmol), and 10% Pd/C (0.186 g, 0.175 mmol) in DMF (10 mL). The stirred mixture was heated at 140 °C for 1 h, cooled to room temperature and filtered through a pad of Celite, followed by rinsing the pad with Et_2O (100 mL). Water (100 mL) was added to the filtrate, the organic layer was removed, and the aqueous layer was extracted with Et_2O (3 x 100 mL). The combined organic layers were washed with water (3 x 100 mL) and brine (100 mL), dried over $MgSO_4$, filtered, and concentrated by rotary evaporation. Column chromatography (3:1 hexanes:EtOAc) afforded the title compound (1.80 g, 90%) as a white solid, mp 150-152 °C: ^{1}H NMR (300 MHz, $CDCl_3$) δ 7.52 (d, *J* = 8.1 Hz, 2H), 7.39 (d, *J* = 15.9 Hz, 2H), 7.18 (s, 1H), 7.17 (d, *J* = 7.8 Hz, 2H), 7.09 (s, 1H), 6.49 (s, 1H), 5.99 (d, *J* = 15.9 Hz, 2H), 2.38 (s, 3H), 2.31 (s, 3H), 2.28 (s, 3H), 1.49 (s, 9H); ^{13}C NMR (75 MHz, $CDCl_3$) δ 165.8, 143.5, 139.3, 139.0, 137.9, 136.3, 133.9, 133.6, 130.5, 129.6 (2C), 127.5 (2C), 125.2, 120.5, 80.3, 28.1 (3C), 21.6, 21.0, 18.8; FTIR (thin film, $CHCl_3$, cm^{-1}) 3256 (broad), 2978, 2928, 1691, 1633, 1331, 1258, 1160, 1092, 982, 899, 855, 814, 756; HRMS (ESI) calcd for $C_{22}H_{27}NNaO_4S$ $[M + Na]^+$: 424.1559, found: 424.1542.

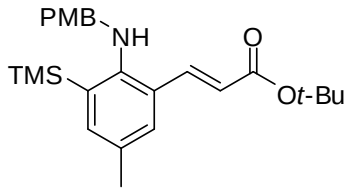

(*E*)-*tert*-Butyl-3-(2-(4-methoxybenzylamino)-5-methyl-3-(trimethylsilyl)phenyl)acrylate (5.26e): In a round-bottom flask fitted with a reflux condenser were combined **5.24** (3.40 g, 8.00 mmol), K_2CO_3 (1.54 g, 12.0 mmol), *tert*-butyl acrylate (1.54 g, 12.0 mmol), and 10% Pd/C (0.298 g, 0.280 mmol) in DMF (16 mL). The stirred mixture was heated at 130 °C for 8 h, cooled to room temperature and filtered through a pad of Celite, followed by rinsing the pad with Et_2O (160 mL). Water (160 mL) was added to the filtrate, the organic layer was removed, and the aqueous layer was extracted with Et_2O (3 x 160 mL). The combined organic layers were washed with water (3 x 160 mL) and brine (160 mL), dried over $MgSO_4$, filtered, and concentrated by rotary evaporation. Column chromatography (10:1 pentane:Et_2O) afforded the title compound (2.62 g, 77%) as a bright yellow-green oil: ^{1}H NMR (300 MHz, $CDCl_3$) δ 8.06 (d, *J* = 16.2 Hz, 1H), 7.38 (d, *J* = 8.7 Hz, 2H), 7.37 (s, 1H), 7.21 (d, *J* = 1.5 Hz, 1H), 6.31 (d, *J* = 16.2 Hz, 1H), 4.02 (br d, *J* = 5.1 Hz, 2H), 3.83 (s, 3H), 3.37 (br m, 1H), 2.32 (s, 3H), 1.53 (s, 9H), 0.30 (s, 9H); ^{13}C NMR (75 MHz, $CDCl_3$) δ 166.5, 158.9, 151.1, 141.8, 137.5, 131.8, 131.6, 131.4, 129.9, 129.4 (2C), 127.5, 119.8, 113.9 (2C), 80.0, 56.0, 55.2, 28.2 (3C), 20.7, 0.2 (3C); FTIR (neat, cm^{-1}) 3391, 2955, 2836, 1705, 1629, 1514, 1455, 1320, 1250, 1152, 1037, 910, 883, 837, 734; LRMS (EI) *m/z* 425 (M^+, 15), 369 (12), 309 (8), 216 (8), 121 (100); HRMS (EI) calcd for $C_{25}H_{35}NO_3Si$: 425.2386, found: 425.2389.

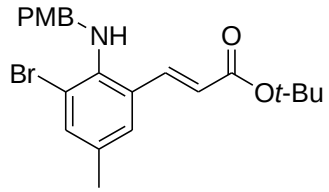

(*E*)-*tert*-Butyl 3-(3-bromo-2-(4-methoxybenzylamino)-5-methylphenyl)acrylate (5.26f): To a stirred solution of *o*-iodoaniline **5.25** (1.73 g, 4.00 mmol) in DMF (20. mL) were added Bu_4NBr (1.29 g, 4.00 mmol), KOAc (1.18 g, 12.0 mmol), $Pd(OAc)_2$ (0.180 g, 0.80 mmol), and crushed activated 4Å molecular sieves (~2 g). Finally, *tert*-butyl acrylate (2.56 g, 20.0 mmol) was added, and the reaction mixture was stirred at room temperature for 2 days. The mixture was vacuum filtered through a Celite pad, and the pad was rinsed with Et_2O (200 mL). The filtrate was washed with saturated aqueous $NaHCO_3$ solution (200 mL), water (3 x 200 mL), and brine (200 mL), dried over $MgSO_4$, filtered, and concentrated by rotary evaporation. Gradient column chromatography (hexanes to 10:1 hexanes:EtOAc) furnished the title compound (1.40 g, 81%) as a bright yellow oil: ^{1}H NMR (300 MHz, $CDCl_3$) δ 7.97 (d, *J* = 15.9 Hz, 1H), 7.34 (d, *J* = 1.5 Hz, 1H), 7.29 (d, *J* = 8.4 Hz, 2H), 7.25 (s, 1H), 6.87 (d, *J* = 8.7 Hz, 2H), 6.31 (d, *J* = 15.9 Hz, 1H), 4.07 (d, *J* = 6.6 Hz, 2H), 3.97 (br t, *J* = 6.6 Hz, 1H), 3.82 (s, 3H), 2.28 (s, 3H), 1.54 (s, 9H); ^{13}C NMR (75 MHz, $CDCl_3$) δ 166.1, 158.9, 143.5, 140.9, 134.0, 132.7, 131.5, 129.4 (2C), 128.4, 128.0, 120.8, 118.1, 113.8 (2C), 80.4, 55.2, 54.6, 28.2 (3C), 20.3; FTIR (neat, cm^{-1}) 3344, 2975, 2932, 2835, 1705, 1631, 1611, 1513, 1460, 1321, 1249, 1150, 1036, 980, 854, 828, 736; HRMS (ESI) calcd for $C_{22}H_{26}{}^{79}BrNNaO_3$ $[M + Na]^+$: 454.0994, found: 454.0996.

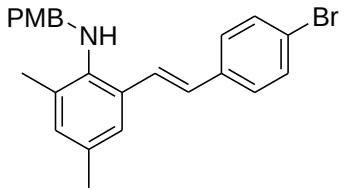

(*E*)-2-(4-Bromostyryl)-*N*-(4-methoxybenzyl)-4,6-dimethylaniline (5.26g): In a round-bottom flask fitted with a reflux condenser were combined **5.20** (1.84 g, 5.00 mmol), K_2CO_3 (1.04 g, 7.50 mmol), 4-bromostyrene (1.37 g, 7.50 mmol), and 10% Pd/C (0.186 g, 0.175 mmol) in DMF (10 mL). The stirred mixture was heated at 130 °C for 2 h, cooled to room temperature and filtered through a pad of Celite, followed by rinsing the pad with Et_2O (100 mL). Water (100 mL) was added to the filtrate, the organic layer was removed, and the aqueous layer was extracted with Et_2O (3 x 100 mL). The combined organic layers were washed with water (3 x 100 mL) and brine (100 mL), dried over $MgSO_4$, filtered, and concentrated by rotary evaporation. Gradient column chromatography (hexanes to 6:1 hexanes:EtOAc) gave the title compound (0.602 g, 29%) as a bright yellow solid, mp 63-65 °C: ^{1}H NMR (300 MHz, $CDCl_3$) δ 7.48 (d, *J* = 8.4 Hz, 2H), 7.47 (d, *J* = 15.9 Hz, 1H), 7.35 (d, *J* = 8.7 Hz, 2H), 7.29 (s, 1H), 7.26 (d, *J* = 8.7 Hz, 2H), 6.95 (d, *J* = 16.2 Hz, 1H), 6.95 (s, 1H), 6.89 (d, *J* = 8.4 Hz, 2H), 4.13 (s, 2H), 3.82 (s, 3H), 2.35 (s, 3H), 2.21 (s, 3H); ^{13}C NMR (75 MHz, $CDCl_3$) δ 158.8, 143.2, 136.9, 131.6 (2C), 131.5, 131.1, 129.9, 129.7, 129.0 (2C), 127.8 (2C), 127.3, 127.2, 125.3, 120.8, 113.9 (2C), 55.2, 54.1, 20.8, 17.9; FTIR (thin film, $CHCl_3$, cm^{-1}) 3363, 3001, 2912, 2834, 1610, 1511, 1487, 1246, 1175, 1072, 1035, 1007, 977, 908, 811, 732; HRMS (ESI) calcd for $C_{24}H_{25}NO^{79}Br$ $[M + H]^+$: 422.1120, found: 422.1133.

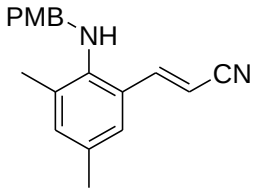

(*E*)-3-(2-(4-Methoxybenzylamino)-3,5-dimethylphenyl)acrylonitrile (5.26h): To a stirred solution of **5.20** (1.84 g, 5.00 mmol) in DMF (25 mL) were added Bu_4NBr (1.61 g, 5.00 mmol), KOAc (1.47 g, 15.0 mmol), $Pd(OAc)_2$ (0.112 g, 0.50 mmol), and crushed activated 4Å molecular sieves (~2.5 g). Finally, acrylonitrile (1.33 g, 25.0 mmol) was added, and the reaction mixture was heated at 80 °C for 8 h. The mixture was cooled to room temperature, diluted with Et_2O (250 mL), and filtered through Celite, rinsing with Et_2O (25 mL). The filtrate was washed with saturated aqueous $NaHCO_3$ solution (250 mL), water (3 x 250 mL), and brine (250 mL), dried over $MgSO_4$, filtered, and concentrated by rotary evaporation. Column chromatography (4:1 hexanes:EtOAc) afforded the title compound (0.660 g, 45%) as a bright yellow-green oil, containing ~5% of an inseparable impurity by ^{1}H NMR: ^{1}H NMR (300 MHz, $CDCl_3$) δ 7.78 (d, *J* = 16.8 Hz, 1H), 7.17 (d, *J* = 8.7 Hz, 2H), 7.10 (s, 1H), 7.02 (s, 1H), 6.87 (d, *J* = 8.7 Hz, 2H), 5.86 (d, *J* = 16.8 Hz, 1H), 4.01 (br s, 2H), 3.82 (s, 3H), 3.27 (br s, 1H), 2.29 (s, 3H), 2.09 (s, 3H); ^{13}C NMR (75 MHz, $CDCl_3$) δ 159.1, 148.8, 144.5, 134.1, 131.9, 131.8, 130.4, 129.1 (2C), 126.4, 125.6, 119.0, 114.1 (2C), 95.1, 55.3, 55.2, 20.6, 17.7; FTIR (neat, cm^{-1}) 3362, 3011, 2933, 2836, 2214, 1610, 1512, 1475, 1248, 1175, 1033, 982, 822, 755; HRMS (ESI) calcd for $C_{19}H_{21}N_2O$ [M + H]$^+$: 293.1654, found: 293.1678.

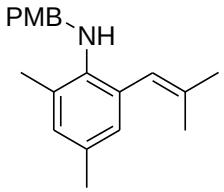

***N*-(4-Methoxybenzyl)-2,4-dimethyl-6-(2-methylprop-1-enyl)aniline (5.26i):** To a stirred solution of 2-methyl-1-propenylmagnesium bromide (7.17 g, 45.0 mmol) in THF (90. mL) at room temperature was added $ZnCl_2$ (6.13 g, 45.0 mmol) dropwise via syringe over 15 min. The mixture was stirred for 2 h, solid $Pd(dppf)Cl_2 \bullet CH_2Cl_2$ (0.184 g, 0.225 mmol) was added all at once, and the mixture was stirred an additional 5 min. **5.20** (1.65 g, 4.50 mmol) in THF (20 mL) was added dropwise via syringe, the reaction mixture was stirred for 2.5 h at rt, cooled to 0 °C, and saturated aqueous NH_4Cl solution (200 mL) was added to quench the reaction. The mixture was extracted with Et_2O (3 x 200 mL), and the combined organic layers were washed with brine (200 mL), dried over $MgSO_4$, filtered, and concentrated by rotary evaporation. Column chromatography (10:1 hexanes:EtOAc) afforded the title compound (1.30 g, 98%) as a light yellow oil: ^{1}H NMR (300 MHz, $CDCl_3$) δ 7.24 (d, *J* = 8.7 Hz, 2H), 6.86 (d, *J* = 8.7 Hz, 2H), 6.85 (s, 1H), 6.79 (s, 1H), 6.15 (s, 1H), 4.03 (s, 2H), 3.81 (s, 3H), 3.33 (br s, 1H), 2.26 (s, 3H), 2.25 (s, 3H), 1.88 (d, *J* = 1.5 Hz, 3H), 1.73 (d, *J* = 1.2 Hz, 3H); ^{13}C NMR (75 MHz, $CDCl_3$) δ 158.5, 142.8, 135.3, 132.7, 130.3, 129.9, 129.8, 128.9 (2C), 128.7, 128.5, 122.9, 113.5 (2C), 54.8, 52.2, 25.8, 20.5, 19.2, 18.2; FTIR (neat, cm^{-1}) 3369, 2911, 1611, 1512, 1475, 1247, 1174, 1036, 861, 823, 737; LRMS (EI) *m/z* 295 (M^+, 10), 252 (9), 174 (37), 121 (100); HRMS (EI) calcd for $C_{20}H_{25}NO$: 295.1936, found: 295.1925.

General acylation procedure (compounds 5.27a-i): To a stirred solution of **5.26a-i** (1.0 equiv.) in CH_2Cl_2 (10 mL/mmol = *X* mL) at 0 °C was added Et_3N (2.0 equiv.) all at once,

followed by chloroacetyl chloride (1.5 equiv.) dropwise via syringe. The mixture was stirred at 0 °C until completion, at which point saturated aqueous NH_4Cl solution (*X* mL) was added. The mixture was extracted with CH_2Cl_2 (3 x *X* mL), and the combined organic layers were washed with brine (*X* mL), dried over $MgSO_4$, filtered, and concentrated by rotary evaporation. The crude residue was subjected to column chromatography, using the appropriate eluent, to furnish the desired α-Cl amide **5.27a-i**.

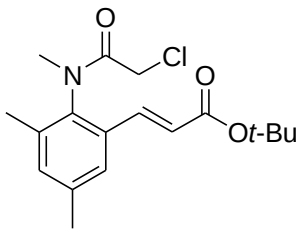

***rac*-(*E*)-*tert*-Butyl 3-(2-(2-chloro-*N*-methylacetamido)-3,5-dimethylphenyl)acrylate (5.27a):** Aniline **5.26a** (1.05 g, 4.00 mmol) was reacted according to the general procedure, and the reaction was complete after 2 h. After workup, column chromatography (2:1 hexanes:EtOAc) provided the title compound (1.21 g, 90%) as a white solid, mp 87 °C, as a mixture of amide rotamers in a 19:1 ratio: ^{1}H NMR (300 MHz, $CDCl_3$) Major rotamer δ 7.48 (d, *J* = 15.9 Hz, 1H), 7.35 (s, 1H), 7.16 (s, 1H), 6.36 (d, *J* = 15.9 Hz, 1H), 3.69 (d, *J* = 13.5 Hz, 1H), 3.64 (d, *J* = 13.5 Hz, 1H), 3.21 (s, 3H), 2.36 (s, 3H), 2.22 (s, 3H), 1.52 (s, 9H); minor rotamer δ 7.52 (d, *J* = 15.9 Hz, 1H), 7.35 (s, 1H), 7.12 (s, 1H), 6.35 (d, *J* = 15.9 Hz, 1H), 4.31 (d, *J* = 12.0 Hz, 1H), 4.23 (d, *J* = 12.0 Hz, 1H), 3.34 (s, 3H), 2.33 (s, 3H), 2.19 (s, 3H), 1.52 (s, 9H); ^{13}C NMR (75 MHz, $CDCl_3$) δ 166.2, 165.2, 138.9, 137.22, 137.17, 136.0, 133.8, 132.3, 125.8, 123.4, 80.6, 41.3, 36.0, 27.9 (3C), 20.8, 17.2; FTIR (thin film, $CHCl_3$, cm^{-1}) 2978, 2931, 1712, 1475, 1368, 1330, 1256, 1154, 1110, 983, 855, 755; HRMS (ESI) calcd for $C_{18}H_{24}ClNNaO_3$ $[M + Na]^+$: 360.1342, found: 360.1325.

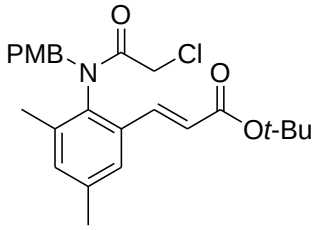

***rac*-(*E*)-*tert*-Butyl-3-(2-(2-chloro-*N*-(4-methoxybenzyl)acetamido)-3,5-dimethylphenyl) acrylate (5.27b):** Aniline **5.26b** (1.84 g, 7.00 mmol) was reacted according to the general procedure, and the reaction was complete after 3 h. After workup, column chromatography (3:1 hexanes:EtOAc) provided the title compound (3.01 g, 97%) as a yellow oil: ^{1}H NMR (300 MHz, $CDCl_3$) δ 7.12 (d, *J* = 15.9 Hz, 2H), 7.09 (s, 1H), 7.07 (d, *J* = 8.4 Hz, 2H), 6.73 (d, *J* = 8.7 Hz, 2H), 6.14 (d, *J* = 15.9 Hz, 2H), 4.87 (d, *J* = 13.8 Hz, 1H), 4.58 (d, *J* = 13.5 Hz, 1H), 3.76 (s, 3H), 3.69 (d, *J* = 13.8 Hz, 1H), 3.64 (d, *J* = 13.8 Hz, 1H), 2.35 (s, 3H), 1.93 (s, 3H), 1.49 (s, 9 H); ^{13}C NMR (75 MHz, $CDCl_3$) δ 165.6, 164.7, 159.0, 138.6, 137.4, 136.3, 135.1, 133.6, 132.8, 131.1 (2C), 127.1, 125.4, 122.2, 113.3 (2C), 80.0, 54.6, 52.0, 41.6, 27.6 (3C), 20.7, 17.2; FTIR (neat, cm^{-1}) 2977, 2933, 2837, 1708, 1667, 1513, 1469, 1327, 1248, 1152, 1035, 984, 851, 792, 733; HRMS (ESI) calcd for $C_{25}H_{30}ClNNaO_4$ $[M + Na]^+$: 466.1761, found: 466.1730.

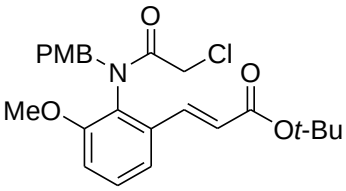

***rac*-(*E*)-*t*-Butyl 3-(2-(2-chloro-*N*-(4-methoxybenzyl)acetamido)-3-methoxyphenyl) acrylate (5.27c):** Aniline **5.26c** (1.35 g, 3.65 mmol) was reacted according to the general procedure, and the reaction was complete after 1 h. After workup, column chromatography (2:1 hexanes:EtOAc) provided the title compound (1.39 g, 85%) as a yellow oil: ^{1}H NMR (300 MHz, $CDCl_3$) δ 7.33 (t, *J* = 8.1 Hz, 1H), 7.24 (d, *J* = 16.8 Hz, 1H), 7.18 (d, *J* = 7.8 Hz, 1H), 7.01 (d, *J*

= 8.4 Hz, 2H), 6.91 (d, *J* = 8.4 Hz, 1H), 6.69 (d, *J* = 8.4 Hz, 2H), 6.18 (d, *J* = 15.9 Hz, 1H), 4.85 (d, *J* = 13.8 Hz, 1H), 4.63 (d, *J* = 13.8 Hz, 1H), 3.76 (d, *J* = 15.3 Hz, 1H), 3.74 (s, 3H), 3.71 (d, *J* = 14.7 Hz, 1H), 3.64 (s, 3H), 1.50 (s, 9H); ^{13}C NMR (75 MHz, $CDCl_3$) δ 166.7, 165.1, 159.0, 155.5, 137.3, 134.6, 131.2 (2C), 129.9, 127.8, 127.6, 123.3, 118.8, 113.3 (2C), 112.7, 80.7, 55.7, 55.0, 51.8, 42.5, 27.8 (3C); FTIR (neat, cm^{-1}) 2977, 2937, 2838, 2249, 1708, 1674, 1578, 1513, 1476, 1392, 1249, 1153, 1070, 1035, 984, 913, 849, 790, 733; HRMS (ESI) calcd for $C_{24}H_{28}ClNNaO_5$ $[M + Na]^+$: 468.1554, found: 468.1530.

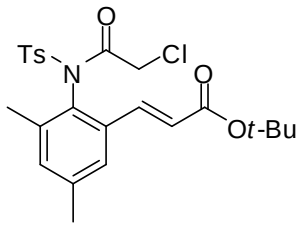

***rac*-(*E*)-*tert*-Butyl 3-(2-(2-chloro-*N*-tosylacetamido)-3,5-dimethylphenyl)acrylate (5.27d):** Aniline **5.26d** (1.20 g, 3.00 mmol) was reacted according to the general procedure, and the reaction was complete after 1 h. After workup, column chromatography (4:1 hexanes:EtOAc) provided the title compound (1.27 g, 89%) as a white solid, mp 170 °C (decomp.): ^{1}H NMR (300 MHz, $CDCl_3$) δ 8.02 (d, *J* = 8.4 Hz, 2H), 7.43 (s, 1H), 7.34 (d, *J* = 8.4 Hz, 2H), 7.27 (d, *J* = 15.9 Hz, 1H), 7.24 (s, 1H), 6.38 (d, *J* = 15.9 Hz, 1H), 3.66 (s, 2H), 2.46 (s, 3H), 2.404 (s, 3H), 2.396 (s, 3H), 1.47 (s, 9H); ^{13}C NMR (75 MHz, $CDCl_3$) δ 165.0, 164.7, 145.5, 140.8, 139.4, 137.2, 134.3, 134.1 (2C, accidental isochrony), 130.6, 130.2 (2C), 129.3 (2C), 125.9, 123.9, 80.6, 43.2, 27.8 (3C), 21.6, 21.1, 18.7; FTIR (thin film, $CHCl_3$, cm^{-1}) 2979, 1709, 1367, 1307, 1264, 1170, 1085, 983, 886, 814, 757; HRMS (ESI) calcd for $C_{24}H_{28}ClNNaO_5S$: $[M + Na]^+$: 500.1274, found: 500.1273.

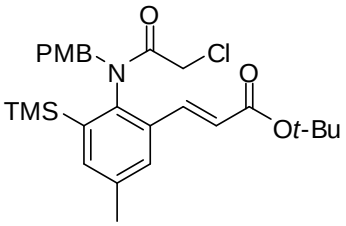

***rac*-(*E*)-*t*-Butyl 3-(2-(2-chloro-*N*-(4-methoxybenzyl)acetamido)-5-methyl-3-(trimethylsilyl) phenyl)acrylate (5.27e):** Aniline **5.26e** was reacted according to the general procedure, and the reaction was complete after 7 h. After workup, column chromatography (5:1 hexanes:EtOAc) provided the title compound (2.50 g, 99%) as a white solid, mp 69-71 °C: ^{1}H NMR (300 MHz, $CDCl_3$) δ 7.47 (d, *J* = 1.8 Hz, 1H), 7.34 (s, 1H), 7.03 (d, *J* = 8.4 Hz, 2H), 6.71 (d, *J* = 8.4 Hz, 2H), 6.68 (d, *J* = 15.9 Hz, 1H), 5.92 (d, *J* = 15.9 Hz, 1H), 5.76 (d, *J* = 13.5 Hz, 1H), 3.76 (d, *J* = 11.7 Hz, 3.74 (s, 3H), 3.73 (d, *J* = 14.1 Hz, 1H), 3.67 (d, *J* = 13.8 Hz, 1H), 2.39 (s, 3H), 1.44 (s, 9H), 0.35 (s, 9H); ^{13}C NMR (75 MHz, $CDCl_3$) δ 165.1, 164.5, 159.1, 140.8, 139.3, 139.2, 138.1, 137.5, 133.6, 131.3 (2C), 128.5, 126.7, 121.9, 113.5 (2C), 79.9, 54.7, 54.1, 42.2, 27.7 (3C), 20.9, 0.1 (t, $J_{Si\text{-}C}$ = 26.3 Hz, 3C); FTIR (thin film, $CHCl_3$, cm^{-1}) 2977, 1707, 1670, 1512, 1437, 1320, 1252, 1155, 982, 874, 839, 757; HRMS (ESI) calcd for $C_{27}H_{36}ClNNaO_4Si$ $[M + Na]^+$: 524.2000, found: 524.1974.

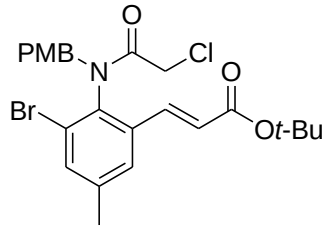

***rac*-(*E*)-*tert*-Butyl 3-(3-bromo-2-(2-chloro-*N*-(4-methoxybenzyl)acetamido)-5-methylphenyl) acrylate (5.27f):** Aniline **5.26f** (2.34 g, 5.50 mmol) was reacted according to the general procedure, and the reaction was complete after 2 h. After workup, column chromatography (3:1

hexanes:EtOAc) provided the title compound (2.51 g, 90%) as a white solid, mp 117 °C: ^{1}H NMR (300 MHz, $CDCl_3$) δ 7.53 (d, *J* = 1.2 Hz, 1H), 7.31 (d, *J* = 1.2 Hz, 1H), 7.03 (d, *J* = 8.7 Hz, 2H), 6.97 (d, *J* = 15.9 Hz, 1H), 6.71 (d, *J* = 8.7 Hz, 2H), 6.01 (d, *J* = 15.9 Hz, 1H), 5.38 (d, *J* = 13.8 Hz, 1H), 4.21 (d, *J* = 14.1 Hz, 1H), 3.78 (d, *J* = 13.8 Hz, 1H), 3.75 (s, 3H), 3.66 (d, *J* = 14.1 Hz, 1H), 2.38 (s, 3H), 1.48 (s, 9H); ^{13}C NMR (75 MHz, $CDCl_3$) δ 165.6, 164.5, 159.3, 140.8, 136.9, 135.9, 135.4, 134.9, 131.5 (2C), 127.0, 126.7, 124.6, 123.3, 113.6 (2C), 80.6, 54.9, 51.9, 42.3, 27.9 (3C), 20.8; FTIR (thin film, $CHCl_3$, cm^{-1}) 3007, 2978, 2934, 1709, 1513, 1459, 1323, 1249, 1152, 1036, 983, 851, 826, 756; HRMS (ESI) calcd for $C_{24}H_{27}{}^{79}BrClNNaO_4$ [M + Na]$^{+}$: 530.0710, found: 530.0761.

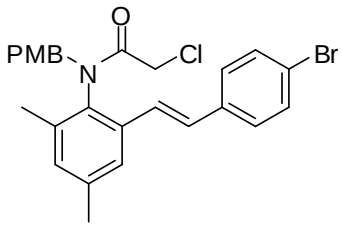

***rac*-(*E*)-*N*-(2-(4-Bromostyryl)-4,6-dimethylphenyl)-2-chloro-*N*-(4-methoxybenzyl)acetamide (5.27g):** Aniline **5.26g** (0.472 g, 1.12 mmol) was reacted according to the general procedure, and the reaction was complete after 2 h. After workup, column chromatography (4:1 hexanes:EtOAc) provided the title compound (0.498 g, 89%) as a yellow solid, mp 130-131 °C: ^{1}H NMR (300 MHz, $CDCl_3$) δ 7.38 (d, *J* = 8.4 Hz, 2H), 7.33 (s, 1H), 7.20 (d, *J* = 8.7 Hz, 2H), 7.06 (s, 1H), 6.99 (d, *J* = 8.4 Hz, 2H), 6.81 (d, *J* = 16.2 Hz, 1H), 6.71 (d, *J* = 8.7 Hz, 2H), 6.41 (d, *J* = 16.2 Hz, 2H), 5.24 (d, *J* = 13.5 Hz, 1H), 4.24 (d, *J* = 13.5 Hz, 1H), 3.68 (s, 2H), 3.65 (s, 3H), 2.38 (s, 3H), 2.08 (s, 3H); ^{13}C NMR (75 MHz, $CDCl_3$) δ 166.5, 159.3, 138.8,136.1, 135.6, 135.4, 134.9, 132.0, 131.54 (2C), 131.50 (2C), 129.8, 128.2, 128.1 (2C), 124.5, 124.1, 121.7, 113.7 (2C), 55.0, 52.6, 42.3, 21.2, 17.8; FTIR (thin film, $CHCl_3$, cm^{-1}) 3001, 2932, 2835, 1667,

1512, 1488, 1394, 1325, 1303, 1247, 1176, 1035, 1008, 965, 910, 849, 810, 732; HRMS (ESI) calcd for $C_{26}H_{25}{}^{79}BrClNNaO_2$ $[M + Na]^+$: 520.0655, found: 520.0690.

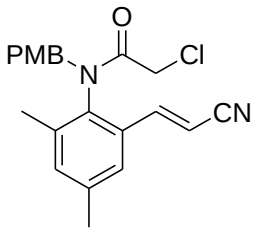

***rac*-(*E*)-2-Chloro-*N*-(2-(2-cyanovinyl)-4,6-dimethylphenyl)-*N*-(4-methoxybenzyl)acetamide (5.27h):** Aniline **5.26h** (0.731 g, 2.50 mmol) was reacted according to the general procedure, and the reaction was complete after 5 h. After workup, column chromatography (2:1 hexanes:EtOAc) provided the title compound (0.687 g, 74%) as a white solid, mp 159-160 °C: ^{1}H NMR (300 MHz, $CDCl_3$) δ 7.22 (s, 1H), 7.16 (s, 1H), 7.06 (d, *J* = 8.4 Hz, 2H), 6.80 (d, *J* = 8.7 Hz, 2H), 6.70 (d, *J* = 16.5 Hz, 1H), 5.56 (d, *J* = 16.8 Hz, 1H), 5.31 (d, *J* = 13.5 Hz, 1H), 4.13 (d, *J* = 13.5 Hz, 1H), 3.83 (s, 3H), 3.64 (d, *J* = 13.2 Hz, 1H), 3.59 (d, *J* = 13.5 Hz, 1H), 2.37 (s, 3H), 2.10 (s, 3H); ^{13}C NMR (75 MHz, $CDCl_3$) δ 166.0, 159.7, 144.8, 139.4, 136.9, 135.2, 135.1, 132.2, 131.4 (2C), 127.0, 124.6, 117.4, 114.0 (2C), 97.8, 55.2, 52.2, 41.6, 21.0, 17.6; FTIR (thin film, $CHCl_3$, cm^{-1}) 3012, 2936, 2837, 2218, 1669, 1612, 1513, 1467, 1392, 1249, 1176, 1111, 1033, 966, 849, 761; LRMS (EI) *m/z* 368 (M^+, 8), 304 (12), 291 (15), 183 (10), 169 (15), 155 (18), 121 (100), 91 (37), 84 (50); HRMS (EI) calcd for $C_{21}H_{21}ClN_2O_2$: 368.1292, found: 368.1295.

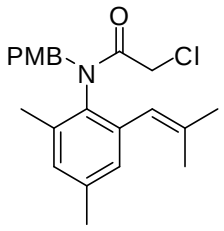

***rac*-2-Chloro-*N*-(2,4-dimethyl-6-(2-methylprop-1-enyl)phenyl)-*N*-(4-methoxybenzyl) acetamide (5.27i):** Aniline **5.26i** (0.886 g, 3.00 mmol) was reacted according to the general procedure, and the reaction was complete after 90 min. After workup, column chromatography (4:1 hexanes:EtOAc) provided the title compound (1.09 g, 98%) as a yellow oil: ^{1}H NMR (300 MHz, $CDCl_3$) δ 7.13 (d, *J* = 8.4 Hz, 2H), 6.90 (s, 2H), 6.75 (d, *J* = 8.4 Hz, 2H), 5.60 (s, 1H), 4.74 (d, *J* = 13.8 Hz, 1H), 4.62 (d, *J* = 13.8 Hz, 1H), 3.78 (s, 3H), 3.67 (d, 2H), 2.32 (s, 3H), 1.84 (s, 3H), 1.72 (s, 6H); ^{13}C NMR (75 MHz, $CDCl_3$) δ 166.1, 158.9, 137.7, 137.4, 136.5, 135.5, 134.7, 131.1 (2C), 130.1, 129.5, 128.4, 121.2, 113.3 (2C), 54.9, 51.7, 41.9, 26.2, 20.8, 19.0, 17.4; FTIR (neat, cm^{-1}) 2933, 2836, 1667, 1512, 1441, 1247, 1176, 1110, 1035, 915, 849, 822, 791, 733; HRMS (ESI) calcd for $C_{22}H_{26}ClNNaO_2$ $[M + Na]^+$: 394.1550, found: 394.1529.

General procedure for Finkelstein reactions (Compounds 5.17a-i): To a solution of α-Cl amide **5.27a-i** (1.0 equiv.) in acetone (10 mL/mmol = *X* mL) was added NaI (10.0 equiv.) all at once, and the reaction mixture was stirred at room temperature overnight (16-20 h). The mixture was diluted with Et_2O (10*X* mL) and washed with 10% aqueous $Na_2S_2O_3$ (3 x *X* mL), dried over $MgSO_4$, filtered, and concentrated by rotary evaporation. The crude residue was subjected to column chromatography, using the appropriate eluent, to furnish the desired product.

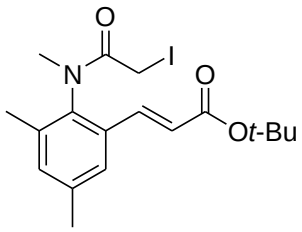

(*E*)-*t*-Butyl 3-(2-(2-iodo-*N*-methylacetamido)-3,5-dimethylphenyl)acrylate (5.17a): Chloride *rac*-**5.27a** (1.01 g, 3.00 mmol) was reacted according to the general procedure. Column chromatography (2:1 hexanes:EtOAc) furnished *rac*-**5.17a** (1.20 g, 93%) as a yellow oil in a 14:1 ratio of amide rotamers. The racemate was submitted to preparative chiral HPLC separation ((*S*,*S*)-Whelk-O1, 80:20 hexanes:*i*-PrOH), first eluting enantiomer $[\alpha]_D^{23}$ –153, 85/15 er (*c* 6.7 mg/mL, $CHCl_3$), second eluting enantiomer $[\alpha]_D^{23}$ +131, 98.5/1.5 er (*c* 4.7 mg/mL, $CHCl_3$): ^{1}H NMR (300 MHz, $CDCl_3$) major rotamer δ 7.55 (d, *J* = 15.9 Hz, 1H), 7.36 (s, 1H), 7.15 (s, 1H), 6.35 (d, *J* = 15.9 Hz, 1H), 3.48 (d, *J* = 10.2 Hz, 1H), 3.44 (d, *J* = 10.2 Hz, 1H), 3.17 (s, 3H), 2.36 (s, 3H), 2.26 (s, 3H), 1.52 (s, 9H); minor rotamer δ 7.55 (d, *J* = 15.9 Hz, 1H), 7.31 (s, 1H), 7.09 (s, 1H), 6.34 (d, *J* = 15.9 Hz, 1H), 3.96 (d, *J* = 9.6 Hz, 1H), 3.88 (d, *J* = 9.6 Hz, 1H), 3.28 (s, 3H), 2.32 (s, 3H), 2.26 (s, 3H), 1.52 (s, 9H); ^{13}C NMR (75 MHz, $CDCl_3$) major rotamer only δ 167.7, 165.1, 138.6, 137.6, 135.6, 133.7, 131.9, 125.7, 123.1, 80.3, 36.2, 27.9, 27.9 (3C), 20.8, 17.5, −3.7; FTIR (neat, cm^{-1}) 2977, 2930, 2246, 1708, 1662, 1474, 1427, 1367, 1329, 1300, 1253, 1153, 1096, 983, 916, 855, 732; HRMS (ESI) calcd for $C_{18}H_{24}INNaO_3$ $[M + Na]^+$: 452.0699, found: 452.0661.

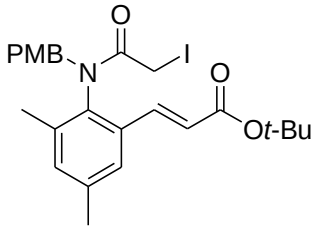

(*E*)-*tert*-Butyl 3-(2-(2-iodo-*N*-(4-methoxybenzyl)acetamido)-3,5-dimethylphenyl)acrylate (5.17b): Chloride *rac*-**5.27b** (2.00 g, 4.50 mmol) was reacted according to the general procedure. Column chromatography (2:1 hexanes:EtOAc) furnished *rac*-**5.17b** (2.22 g, 92%) as a yellow oil. The racemate was submitted to preparative chiral HPLC separation ((*S*,*S*)-Whelk-O1, 70:30 hexanes:iPrOH), first eluting enantiomer $[\alpha]_D^{23}$ –16, 100/0 er (*c* 16.7 mg/mL, $CHCl_3$), second eluting enantiomer $[\alpha]_D^{23}$ +15, 100/0 er (*c* 9.5 mg/mL, $CHCl_3$): ^{1}H NMR (300 MHz, $CDCl_3$) δ 7.27 (s, 1H), 7.19 (d, *J* = 15.9 Hz, 1H), 7.10 (s, 1H), 7.05 (d, *J* = 8.7 Hz, 2H), 6.72 (d, *J* = 8.7 Hz, 2H), 6.13 (d, *J* = 15.9 Hz, 1H), 3.76 (s, 3H), 3.47 (s, 2H), 2.35 (s, 3H), 1.98 (s, 3H), 1.49 (s, 9H); ^{13}C NMR (75 MHz, $CDCl_3$) δ 167.5, 165.2, 159.2, 138.6, 138.3, 136.5, 136.4, 133.8, 132.9, 131.4 (2C), 127.5, 125.7, 122.4, 113.6 (2C), 80.4, 55.0, 52.4, 28.0 (3C), 21.0, 18.0, −2.5; FTIR (thin film, $CHCl_3$, cm^{-1}) 2977, 2933, 2836, 1707, 1655, 1512, 1469, 1368, 1326, 1303, 1249, 1158, 1036, 984, 912, 852, 732; HRMS (ESI) calcd for $C_{25}H_{30}INNaO_4$ $[M + Na]^+$: 558.1117, found: 558.1071.

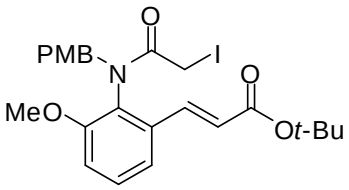

(*E*)-*t*-Butyl 3-(2-(2-Iodo-*N*-(4-methoxybenzyl)acetamido)-3-methoxyphenyl)acrylate (5.17c): Chloride *rac*-**5.27c** (0.981 g, 2.20 mmol) was reacted according to the general procedure.

Column chromatography (2:1 hexanes:EtOAc) furnished *rac*-**5.17c** (1.16 g, 98%) as a yellow oil. The racemate was submitted to preparative chiral HPLC separation (Chiralcel OD, 90:10 hexanes:*i*-PrOH), first eluting enantiomer $[\alpha]_D^{23}$ –27, 99/1 er (*c* 9.5 mg/mL, $CHCl_3$), second eluting enantiomer $[\alpha]_D^{23}$ +28, 99/1 er (*c* 13.6 mg/mL, $CHCl_3$): ^{1}H NMR (300 MHz, $CDCl_3$) δ 7.32 (t, *J* = 7.8 Hz, 1H), 7.30 (d, *J* = 16.2 Hz, 1H), 7.18 (d, *J* = 7.8 Hz, 1H), 7.00 (d, *J* = 8.7 Hz, 2H), 6.90 (d, *J* = 8.1 Hz, 1H), 6.69 (d, *J* = 8.7 Hz, 2H), 6.16 (d, *J* = 16.2 Hz, 1H), 4.87 (d, *J* = 13.8 Hz, 1H), 4.56 (d, *J* = 13.8 Hz, 1H), 3.74 (s, 3H), 3.67 (s, 3H), 3.50 (s, 2H), 1.50 (s, 9H); ^{13}C NMR (75 MHz, $CDCl_3$) δ 168.0, 165.0, 158.8, 155.2, 137.6, 134.1, 131.0 (2C), 129.6, 128.5, 127.7, 122.7, 118.5, 113.1 (2C), 112.7, 80.3, 55.5, 54.9, 51.6, 27.9, –2.1; FTIR (neat, cm^{-1}) 2976, 2935, 2837, 1708, 1659, 1577, 1513, 1368, 1248, 1153, 1070, 1035, 983, 849, 913, 849, 800, 732; HRMS (ESI) calcd for $C_{24}H_{28}INNaO_5$ $[M + Na]^+$: 560.0910, found: 560.0901.

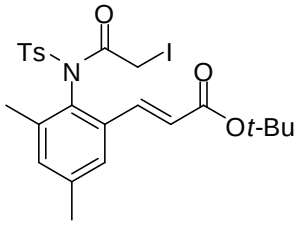

(*E*)-*tert*-Butyl 3-(2-(2-iodo-*N*-tosylacetamido)-3,5-dimethylphenyl)acrylate (5.17d): Chloride *rac*-**5.27d** (0.717 g, 1.50 mmol) was reacted according to the general procedure. Column chromatography (2:1 hexanes:EtOAc) furnished *rac*-**5.17d** (0.662 g, 78%) as a white solid, mp 205 °C (decomp.): ^{1}H NMR (300 MHz, $CDCl_3$) δ 8.00 (d, *J* = 8.1 Hz, 2H), 7.43 (s, 1H), 7.33 (d, *J* = 8.4 Hz, 2H), 7.33 (d, *J* = 15.6 Hz, 1H), 7.25 (s, 1H), 6.37 (d, *J* = 15.9 Hz, 1H), 3.48 (s, 2H), 2.46 (2 overlapping s, 2 x 3H), 2.41 (s, 3H), 1.47 (s, 9H); ^{13}C NMR (75 MHz, $CDCl_3$) δ 166.7, 165.0, 145.5, 140.6, 139.6, 137.9, 134.5, 134.3, 134.1, 132.0, 130.4 (2C), 129.4 (2C), 125.9, 123.7, 80.6, 28.0 (3C), 21.8, 21.2, 19.3, −2.2; FTIR (thin film, $CHCl_3$, cm^{-1}) 2978, 1705, 1365,

1275, 1171, 1083, 982, 885, 815, 758; HRMS (ESI) calcd for $C_{24}H_{28}INNaO_5S$ $[M + Na]^+$: 592.0631, found: 592.0616.

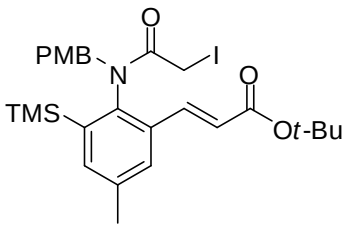

(*E*)-*t*-Butyl 3-(2-(2-iodo-*N*-(4-methoxybenzyl)acetamido)-5-methyl-3-(trimethylsilyl)phenyl) acrylate (5.17e): In a round bottom flask equipped with a reflux condenser, chloride *rac*-**5.27e** (1.51 g, 3.00 mmol) was mixed with NaI (4.50 g, 30.0 mmol) in acetone (30 mL). The stirred mixture was refluxed for 40 h until complete conversion had been achieved (monitored using GC). The mixture was cooled to room temperature, and was worked up according to the general procedure. Column chromatography (5:1 hexanes:EtOAc) furnished *rac*-**5.17e** (2.88 g, 96%) as a glassy yellow solid, mp 51-53 °C. The racemate was submitted to preparative chiral HPLC separation ((*S*,*S*)-Whelk-O1, 70:30 hexanes:*i*-PrOH), first eluting enantiomer $[\alpha]_D^{23}$ +86, 100/0 er (*c* 8.8 mg/mL, $CHCl_3$), second eluting enantiomer $[\alpha]_D^{23}$ –87, 100/0 er (*c* 12.2 mg/mL, $CHCl_3$-): ^{1}H NMR (300 MHz, $CDCl_3$) δ 7.47 (d, *J* = 1.8 Hz, 1H), 7.35 (d, *J* = 1.8 Hz, 1H), 7.02 (d, *J* = 8.7 Hz, 2H), 6.78 (d, *J* = 15.9 Hz, 1H), 6.70 (d, *J* = 8.7 Hz, 2H), 5.92 (d, *J* = 15.9 Hz, 1H), 5.70 (d, *J* = 13.5 Hz, 1H), 3.77 (d, *J* = 13.5 Hz, 1H), 3.74 (s, 3H), 3.55 (d, *J* = 11.1 Hz, 1H), 3.51 (d, *J* = 11.4 Hz, 1H), 2.39 (s, 3H), 1.45 (s, 9H), 0.36 (s, 9H); ^{13}C NMR (75 MHz, $CDCl_3$) δ 165.5, 164.3, 158.9, 141.7, 138.9, 137.8, 137.6, 133.2, 131.1 (2C), 128.2, 126.5, 121.3, 113.3 (2C), 79.5, 54.5, 54.2, 27.6 (3C), 20.8, 0.18 (3C), −0.6; FTIR (thin film, $CHCl_3$, cm^{-1}) 2976, 2836, 1706, 1659, 1512, 1437, 1367, 1320, 1250, 1161, 1109, 1036, 1007, 983, 874, 838, 757; HRMS (ESI) calcd for $C_{27}H_{36}INNaO_4Si$ $[M + Na]^+$: 616.1356, found: 616.1395.

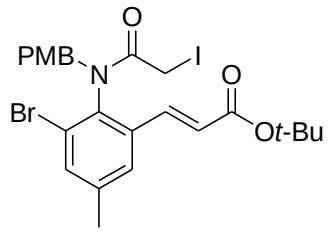

(*E*)-*t*-Butyl 3-(3-bromo-2-(2-iodo-*N*-(4-methoxybenzyl)acetamido)-5-methylphenyl) acrylate (5.17f): Chloride *rac*-**5.27f** (2.20 g, 4.32 mmol) was reacted according to the general procedure. Column chromatography (3:1 hexanes:EtOAc) furnished *rac*-**5.17f** (2.35 g, 91%) as a sticky yellow semi-solid. The racemate was submitted to preparative chiral HPLC separation ((*S*,*S*)-Whelk-O1, 70:30 hexanes:*i*-PrOH), first eluting enantiomer $[\alpha]_D^{23}$ +21, 99/1 er (*c* 14.4 mg/mL, $CHCl_3$), second eluting enantiomer $[\alpha]_D^{23}$ –19, 100/0 er (*c* 10.9 mg/mL, $CHCl_3$): ^{1}H NMR (300 MHz, $CDCl_3$) δ 7.50 (d, *J* = 1.2 Hz, 1H), 7.33 (s, 1H), 7.11 (d, *J* = 15.9 Hz, 1H), 7.02 (d, *J* = 8.7 Hz, 2H), 6.70 (d, *J* = 8.7 Hz, 2H), 6.01 (d, *J* = 15.9 Hz, 1H), 5.27 (d, *J* = 14.1 Hz, 1H), 4.26 (d, *J* = 13.8 Hz, 1H), 3.74 (s, 3H), 3.58 (d, *J* = 10.8 Hz, 1H), 3.44 (d, *J* = 10.5 Hz, 1H), 2.38 (s, 3H), 1.48 (s, 9H); ^{13}C NMR (75 MHz, $CDCl_3$) δ 166.9, 164.3, 159.0, 140.4, 137.3, 135.8, 135.3, 135.2, 131.2 (2C), 126.8, 126.6, 124.3, 122.7, 113.4 (2C), 80.2, 54.7, 51.8, 27.7 (3C), 20.7, −2.5; FTIR (thin film, $CHCl_3$, cm^{-1}) 2977, 2932, 2836, 1708, 1665, 1513, 1459, 1368, 1321, 1248, 1154, 1035, 982, 851, 822, 756; HRMS (ESI) calcd for $C_{24}H_{27}{}^{79}BrINNaO_4$ $[M + Na]^+$: 622.0066, found: 622.0031.

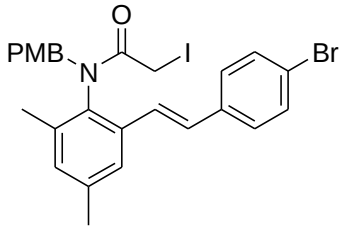

(*E*)-*N*-(2-(4-Bromostyryl)-4,6-dimethylphenyl)-2-iodo-*N*-(4-methoxybenzyl)acetamide (5.17g): Chloride *rac*-**5.27g** (0.399 g, 0.800 mmol) was reacted according to the general procedure. Column chromatography (4:1 hexanes:EtOAc) furnished *rac*-**5.17g** (0.408 g, 86%) as a yellow-orange solid, mp 97-98 °C: ^{1}H NMR (300 MHz, $CDCl_3$) δ 7.39 (d, *J* = 8.4 Hz, 2H), 7.34 (s, 1H), 7.17 (d, *J* = 8.7 Hz, 2H), 7.05 (s, 1H), 7.04 (d, *J* = 8.4 Hz, 2H), 6.80 (d, *J* = 16.2 Hz, 1H), 6.70 (d, *J* = 8.4 Hz, 2H), 6.51 (d, *J* = 16.2 Hz, 1H), 5.14 (d, *J* = 13.5 Hz, 1H), 4.28 (d, *J* = 13.5 Hz, 1H), 3.64 (s, 3H), 3.50 (d, *J* = 10.2 Hz, 1H), 3.46 (d, *J* = 10.2 Hz, 1H), 2.38 (s, 3H), 2.10 (s, 3H); ^{13}C NMR (75 MHz, $CDCl_3$) δ 168.1, 159.2, 138.6, 136.0, 135.9, 135.7, 135.0, 132.0, 131.5 (4C = two overlapping 2C), 129.4, 128.2, 128.1 (2C), 124.7, 124.5, 121.6, 113.7 (2C), 55.0, 52.6, 21.2, 18.1, −2.1; FTIR (thin film, $CHCl_3$, cm^{-1}) 3002, 2933, 2835, 1651, 1512, 1487, 1386, 1322, 1302, 1249, 1176, 1107, 1073, 1035, 1008, 909, 849, 810, 732; HRMS (ESI) calcd for $C_{26}H_{25}{}^{79}BrINNaO_2$ $[M + Na]^+$: 612.0011, found: 612.0002.

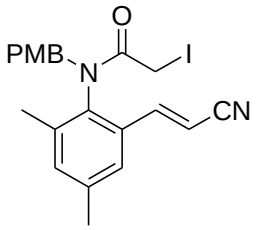

(*E*)-*N*-(2-(2-cyanovinyl)-4,6-dimethylphenyl)-2-iodo-*N*-(4-methoxybenzyl)acetamide (5.17h): To a solution of chloride *rac*-**5.27h** (0.619 g, 1.60 mmol) in acetone (65 mL) was added NaI (2.40 g, 16.0 mmol) all at once and the reaction mixture was stirred at room temperature

overnight. After 16 h, 10% aqueous $Na_2S_2O_3$ (65 mL) was added and the mixture was extracted with EtOAc (3 x 160 mL). The combined organic layers were dried over $MgSO_4$, filtered, and concentrated by rotary evaporation. Column chromatography (2:1 hexanes:EtOAc) furnished *rac*-**5.17h** (0.633 g, 86%) as a white solid, mp 144-145 °C. The racemate was submitted to preparative chiral HPLC separation ((*S*,*S*)-Whelk-O1, 80:20 hexanes:EtOAc), first eluting enantiomer $[\alpha]_D^{23}$ –0.4, 99/1 er (*c* 11.2 mg/mL, $CHCl_3$), second eluting enantiomer $[\alpha]_D^{23}$ +0.5, 99.5/0.5 er (*c* 43.9 mg/mL, $CHCl_3$): ^{1}H NMR (300 MHz, $CDCl_3$) δ 7.27 (s, 1H), 7.21 (s, 1H), 7.04 (d, *J* = 8.7 Hz, 2H), 6.81 (d, *J* = 16.8 Hz, 1H), 6.80 (d, *J* = 7.8 Hz, 2H), 5.56 (d, *J* = 16.5 Hz, 1H), 5.22 (d, *J* = 13.5 Hz, 1H), 4.16 (d, *J* = 13.8 Hz, 1H), 3.82 (s, 3H), 3.44 (d, *J* = 10.2 Hz, 1H), 3.39 (d, *J* = 10.2 Hz, 1H), 2.37 (s, 3H), 2.11 (s, 3H); ^{13}C NMR (75 MHz, $CDCl_3$) δ 167.5, 159.6, 145.3, 139.1, 136.7, 136.1, 135.2, 131.8, 131.3 (2C), 127.1, 124.6, 117.5, 113.9 (2C), 97.4, 55.2, 52.2, 21.0, 17.9, −3.2; FTIR (thin film, $CHCl_3$, cm^{-1}) 3004, 2934, 2217, 1655, 1512, 1385, 1304, 1250, 1176, 1107, 1033, 1007, 965, 849, 822, 755; HRMS (ESI) calcd for $C_{21}H_{21}IN_2NaO_2$ [M + Na]$^+$: 483.0545, found: 483.0533.

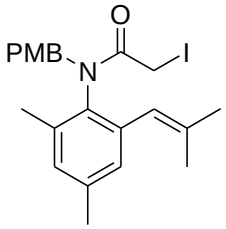

***N*-(2,4-Dimethyl-6-(2-methylprop-1-enyl)phenyl)-2-iodo-*N*-(4-methoxybenzyl)acetamide (5.17i):** Chloride *rac*-**5.27i** (0.744 g, 2.00 mmol) was reacted according to the general procedure. Column chromatography (4:1 hexanes:EtOAc) furnished *rac*-**5.17i** (0.816 g, 88%) as a white solid, mp 73-74 °C. The racemate was submitted to preparative chiral HPLC separation ((*S*,*S*)-Whelk-O1, 80:20 hexanes:*i*-PrOH), first eluting enantiomer $[\alpha]_D^{23}$–4.4, 99/1 er (*c* 2.8

mg/mL, $CHCl_3$), second eluting enantiomer $[\alpha]_D^{23}$ +4.2, 100/0 er (*c* 5.2 mg/mL, $CHCl_3$): ^{1}H NMR (300 MHz, $CDCl_3$) δ 7.11 (d, *J* = 8.7 Hz, 2H), 6.90 (br s, 2H), 6.74 (d, *J* = 8.7 Hz, 2H), 5.69 (s, 1H), 4.70 (d, *J* = 13.5 Hz, 1H), 4.61 (d, *J* = 13.8 Hz, 1H), 3.77 (s, 3H), 3.47 (s, 2H), 2.32 (s, 3H), 1.89 (s, 3H), 1.72 (s, 6H); ^{13}C NMR (75 MHz, $CDCl_3$) δ 167.5, 158.9, 137.4, 137.2, 136.3, 135.8, 135.3, 131.1 (2C), 130.1, 129.4, 128.4, 121.6, 113.3 (2C), 54.9, 51.7, 26.3, 20.9, 19.1, 17.8, −1.6; FTIR (thin film, $CHCl_3$, cm^{-1}) 2931, 2857, 2835, 1655, 1612, 1512, 1440, 1385, 1303, 1247, 1176, 1107, 1035, 849, 835, 822, 756; HRMS (ESI) calcd for $C_{22}H_{26}INNaO_2$ [M + Na]$^+$: 486.0906, found: 486.0867.

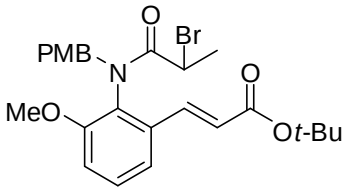

(*E*)-*t*-Butyl 3-(2-(2-bromo-*N*-(4-methoxybenzyl)propanamido)-3-methoxyphenyl) acrylate (**5.34a** and **5.34b**): To a stirred solution of **5.26c** (1.11 g, 3.00 mmol) and Et_3N (0.455 g, 4.50 mmol) in THF (6.0 mL) at 0 °C was added 2-bromopropionyl bromide (0.971 g, 4.50 mmol) dropwise via syringe. The mixture was stirred at 0 °C for 30 min, and saturated aqueous NH_4Cl (15 mL) was added. The mixture was extracted with Et_2O (3 x 30 mL), and the combined organic layers were washed with brine (30 mL), dried over $MgSO_4$, filtered, and concentrated by rotary evaporation. Column chromatography (3:1 hexanes:EtOAc) provided two diastereomers. The first eluting diastereomer, *rac*-**5.34a**, was isolated (0.497 g, 33%) as a clear, pale yellow oil. This racemate was submitted to preparative chiral HPLC separation ((*S*,*S*)-Whelk-O1, 75:25 hexanes:*i*-PrOH), first eluting enantiomer $[\alpha]_D^{23}$ +47, 98/2 er (*c* 13.4 mg/mL, $CHCl_3$), second eluting enantiomer $[\alpha]_D^{23}$ –48, 99/1 er (*c* 15.1 mg/mL, $CHCl_3$): ^{1}H NMR (300 MHz, $CDCl_3$) δ

7.34 (t, *J* = 8.1 Hz, 1H), 7.12 (d, *J* = 7.8 Hz, 1H), 7.03 (d, *J* = 8.7 Hz, 2H), 7.00 (d, *J* = 8.7 Hz, 2H), 6.90 (d, *J* = 15.9 Hz, 1H), 6.69 (d, *J* = 8.7 Hz, 1H), 5.43 (d, *J* = 15.9 Hz, 1H), 4.15 (d, *J* = 13.8 Hz, 1H), 4.01 (q, *J* = 6.6 Hz, 1H), 3.84 (s, 3H), 3.73 (s, 3H), 1.69 (d, *J* = 6.6 Hz, 3H), 1.46 (s, 9H); ^{13}C NMR (75 MHz, $CDCl_3$) δ 169.7, 165.0, 159.1, 155.7, 137.3, 134.7, 131.3 (2C), 129.7, 128.0, 127.9, 123.2, 118.0, 113.5 (2C), 113.1, 80.5, 55.7, 55.0, 51.3, 39.1, 28.0 (3C), 22.1; FTIR (neat, cm^{-1}) 2975, 2936, 2838, 2249, 1708, 1666, 1612, 1578, 1513, 1477, 1394, 1272, 1248, 1175, 1154, 1072, 1036, 984, 912, 849, 800, 733; HRMS (ESI) calcd for $C_{25}H_{30}BrNNaO_5$ $[M + Na]^+$: 526.1205, found: 526.1214. The second eluting diastereomer, *rac*-**5.34b**, was isolated (0.983 g, 65%) as a clear, colorless oil. This racemate was submitted to preparative chiral HPLC separation ((*S*,*S*)-Whelk-O1, 70:30 hexanes:*i*-PrOH), first eluting enantiomer $[\alpha]_D^{23}$ +66, 100/0 er (*c* 9.9 mg/mL, $CHCl_3$), second eluting enantiomer $[\alpha]_D^{23}$ –67, 100/0 er (*c* 6.3 mg/mL, $CHCl_3$): ^{1}H NMR (300 MHz, $CDCl_3$) δ 7.55 (d, *J* = 15.9 Hz, 1H), 7.31 (t, *J* = 8.1 Hz, 1H), 7.23 (d, *J* = 8.1 Hz, 1H), 6.98 (d, *J* = 8.7 Hz, 2H), 6.85 (d, *J* = 7.8 Hz, 1H), 6.68 (d, *J* = 8.4 Hz, 2H), 6.20 (d, *J* = 15.9 Hz, 1H), 4.82 (d, *J* = 13.8 Hz, 1H), 4.56 (d, *J* = 13.8 Hz, 1H), 4.11 (q, *J* = 6.6 Hz, 1H), 3.74 (s, 3H), 3.53 (s, 3H), 1.74 (d, *J* = 6.6 Hz, 3H), 1.51 (s, 9H); ^{13}C NMR (75 MHz, $CDCl_3$) δ 170.8, 165.2, 158.9, 155.3, 138.2, 134.4, 131.0 (2C), 129.5, 128.3, 127.9, 122.6, 119.0, 113.1 (2C), 112.3, 80.3, 55.5, 54.9, 51.7, 39.6, 27.9 (3C), 21.7; FTIR (neat, cm^{-1}) 2976, 2934, 2839, 1708, 1670, 1577, 1513, 1475, 1394, 1368, 1271, 1248, 1152, 1068, 984, 849, 801, 732; HRMS (ESI) calcd for $C_{25}H_{30}BrNNaO_5$ $[M + Na]^+$: 526.1205, found: 526.1206.

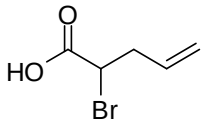

***rac*-2-Bromopent-4-enoic acid (5.39):** To a stirred solution of NaBr (6.47 g, 62.9 mmol) in aqueous HBr (0.75 M, 60 mL) at −15 °C was added, in one portion, $NaNO_2$ (1.52 g, 22.1 mmol). After stirring at this temperature for 15 min, (±)-2-amino-4-pentenoic acid (1.96 g, 17.0 mmol) was added in one portion. The reaction mixture was stirred at −15 °C for 1 h, 0 °C for 1 h, and at room temperature for 2 h, and was then extracted with EtOAc (3 x 125 mL). The combined organic layers were dried over $MgSO_4$, filtered, and concentrated by rotary evaporation. Column chromatography (50:50:1 hexanes:EtOAc:AcOH) provided the title compound (1.75 g, 58%) as a mobile red liquid: ^{1}H NMR (300 MHz, $CDCl_3$) δ 5.79 (ddt, *J* = 16.8 Hz, 10.2 Hz, 6.9 Hz, 1H), 5.23 (d, *J* = 16.5 Hz, 1H), 5.22 (d, *J* = 10.5 Hz, 1H), 4.28 (t, *J* = 7.2 Hz, 1H), 2.89 (dt, *J* = 14.4 Hz, 7.2 Hz, 1H), 2.76 (dd, *J* = 14.4 Hz, 7.2 Hz, 1H); ^{13}C NMR (75 MHz, $CDCl_3$) δ 175.3, 132.5, 119.5, 43.7, 38.6; FTIR (neat, cm^{-1}) 3083, 3000 (broad), 1720, 1430, 1253, 1201, 1171, 993, 927; HRMS (EI) calcd for $C_5H_7{}^{79}BrO_2$ $[M]^+$: 177.9629, found: 177.9626.

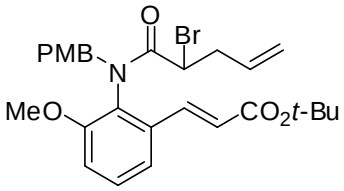

(*E*)-*t*-Butyl 3-(2-(2-bromo-*N*-(4-methoxybenzyl)pent-4-enamido)-3-methoxyphenyl) acrylate (**5.40a** and **5.40b**): To a stirred solution of *rac*-**5.39** (0.896 g, 5.00 mmol) in CH_2Cl_2 (20 mL) at 0 °C was added oxalyl chloride (0.635 g, 5.00 mmol) via syringe, followed by catalytic DMF (~1 drop). The mixture was warmed to room temperature and stirred for 2 h. This mixture containing the crude acid chloride was transferred dropwise over 10 min via syringe to a stirred

solution of **5.26c** (0.739 g, 2.00 mmol) in CH_2Cl_2 at 0 °C. After 10 min of stirring, Et_3N (0.202 g, 2.00 mmol) was added to this mixture via syringe, and the mixture was stirred at room temperature for 1 h. Saturated aqueous NH_4Cl (35 mL) was added, and the mixture was extracted with CH_2Cl_2 (3 x 35 mL). The combined organic layers were washed with brine (35 mL), dried over $MgSO_4$, filtered, and concentrated by rotary evaporation. Column chromatography (4:1 hexanes:EtOAc) provided two diastereomers. The first eluting diastereomer, *rac*-**5.40a**, was isolated (0.370 g, 35%) as a clear, colorless oil: ^{1}H NMR (300 MHz, $CDCl_3$) δ 7.34 (t, *J* = 8.1 Hz, 1H), 7.12 (d, *J* = 7.2 Hz, 1H), 7.03 (d, *J* = 8.4 Hz, 2H), 6.98 (d, *J* = 8.1 Hz, 1H), 6.95 (d, *J* = 15.9 Hz, 1H), 6.70 (d, *J* = 8.4 Hz, 2H), 6.06 (d, *J* = 15.9 Hz, 1H), 5.60 (ddt, *J* = 14.1 Hz, 9.9 Hz, 7.2 Hz, 1H), 5.40 (d, *J* = 13.8 Hz, 1H), 5.10-5.01 (m, 2H), 4.20 (d, *J* = 14.1 Hz, 1H), 3.83 (s, 3H), 3.79 (t, *J* = 7.2 Hz, 1H), 3.73 (s, 3H), 2.86 (dt, 14.1 Hz, 7.2 Hz, 1H), 2.62 (dt, *J* = 14.1 Hz, 7.2 Hz, 1H), 1.47 (s, 9H); ^{13}C NMR (75 MHz, $CDCl_3$) δ 168.7, 164.9, 159.0, 155.7, 137.7, 134.6, 133.6, 131.1 (2C), 129.7, 127.9, 127.8, 123.0, 118.8, 117.9, 113.4 (2C), 113.0, 80.3, 55.6, 54.9, 51.3, 43.1, 39.7, 27.9 (3C); FTIR (neat, cm^{-1}) 2977, 2936, 2837, 1708, 1666, 1612, 1578, 1513, 1476, 1439, 1393, 1271, 1248, 1152, 1071, 1035, 983, 929, 849, 798; HRMS (ESI) calcd for $C_{27}H_{32}{}^{79}BrNNaO_5$ $[M + Na]^+$: 552.1362, found: 552.1337. The second eluting diastereomer, *rac*-**5.40b**, was isolated (0.413 g, 39%) as a clear, colorless oil. The racemate was submitted to preparative chiral HPLC separation ((*S*,*S*)-Whelk-O1, 80:20 hexanes:*i*-PrOH), first eluting enantiomer $[\alpha]_D^{23}$ +84, 100/0 er (*c* 3.4 mg/mL, $CHCl_3$), second eluting enantiomer $[\alpha]_D^{23}$ –83, 100/0 er (*c* 4.1 mg/mL, $CHCl_3$): ^{1}H NMR (300 MHz, $CDCl_3$) δ 7.53 (d, *J* = 15.9 Hz, 1H), 7.31 (t, *J* = 8.1 Hz, 1H), 7.22 (d, *J* = 7.8 Hz, 1H), 6.99 (d, *J* = 8.7 Hz, 2H), 6.84 (d, *J* = 8.1 Hz, 1H), 6.68 (d, *J* = 8.7 Hz, 2H), 6.18 (d, *J* = 16.2 Hz, 1H), 5.67 (dddd, *J* = 16.8 Hz, 10.2 Hz, 7.5 Hz, 6.6 Hz, 1H), 5.06 (d, *J* = 17.1 Hz, 1H), 5.05 (d, *J* = 9.9 Hz, 1H), 4.77

(d, J = 13.8 Hz, 1H), 4.64 (d, J = 13.8 Hz, 1H), 3.89 (t, J = 7.2 Hz, 1H), 3.74 (s, 3H), 3.54 (s, 3H), 2.89 (dt, J = 14.4 Hz, 6.9 Hz, 1H), 2.68 (dt, J = 14.4 Hz, 7.5 Hz, 1H), 1.50 (s, 9H); ^{13}C NMR (75 MHz, $CDCl_3$) δ 169.7, 165.2, 158.9, 155.1, 138.3, 134.5, 134.1, 131.1 (2C), 129.6, 128.1, 127.9, 122.5, 118.8, 117.7, 113.1 (2C), 112.1, 80.3, 55.2, 54.9, 51.7, 43.6, 39.4, 28.0 (3C); FTIR (neat, cm^{-1}) 2977, 2934, 2837, 1707, 1670, 1577, 1513, 1475, 1438, 1394, 1270, 1247, 1152, 1070, 1035, 984, 921, 848, 800, 732; HRMS (ESI) calcd for $C_{27}H_{32}{}^{79}BrNNaO_5$ $[M + Na]^+$: 552.1362, found: 552.1349.

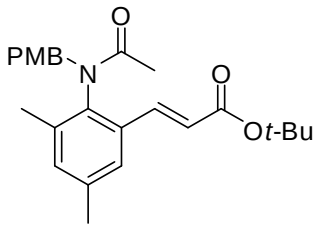

(*E*)-*tert*-Butyl 3-(2-(*N*-(4-methoxybenzyl)acetamido)-3,5-dimethylphenyl)acrylate (5.28b): To a stirred solution of **5.26b** (0.147 g, 0.400 mmol) and Et_3N (0.080 g, 0.800 mmol) in CH_2Cl_2 (4.0 mL) at 0 °C was added acetyl chloride (0.047 g, 0.600 mmol) dropwise via syringe. The mixture was stirred at this temperature for 15 min, and saturated aqueous NH_4Cl solution (5 mL) was added. The mixture was extracted with CH_2Cl_2 (3 x 5 mL), and the combined organic layers were washed with brine (10 mL), dried over $MgSO_4$, filtered, and concentrated by rotary evaporation. Column chromatography (2:1 hexanes:EtOAc) provided the title compound (0.150 g, 92%) as a clear, colorless oil: ^{1}H NMR (300 MHz, $CDCl_3$) δ 7.26 (s, 1H), 7.17 (d, J = 15.9 Hz, 1H), 7.07 (s, 1H), 7.05 (d, J = 8.7 Hz, 1H), 7.72 (d, J = 8.4 Hz, 1H), 6.13 (d, J = 15.9 Hz, 1H), 4.83 (d, J = 13.8 Hz, 1H), 4.55 (d, J = 13.5 Hz, 1H), 3.76 (s, 3H), 2.34 (s, 3H), 1.91 (s, 3H), 1.72 (s, 3H), 1.50 (s, 9H); ^{13}C NMR (75 MHz, $CDCl_3$) δ 170.3, 165.4, 159.0, 138.4, 138.0, 137.5, 136.6, 133.6, 133.0, 131.3 (2C), 128.4, 125.5, 122.0, 113.5 (2C), 80.3, 55.0, 51.2, 28.0

(3C), 22.0, 21.0, 17.5; FTIR (neat, cm^{-1}) 2977, 2931, 2836, 1708, 1659, 1612, 1512, 1471, 1391, 1326, 1247, 1151, 1035, 984, 851, 731; HRMS (ESI) calcd for $C_{25}H_{31}NNaO_4$ $[M + Na]^+$: 432.2151, found: 432.2149.

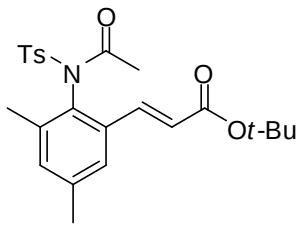

***rac*-(*E*)-*tert*-Butyl 3-(3,5-dimethyl-2-(*N*-tosylacetamido)phenyl)acrylate (5.28d):** To a stirred solution of **5.26d** (0.402 g, 1.00 mmol) and Et_3N (0.202 g, 2.00 mmol) in CH_2Cl_2 (5.0 mL) at 0 °C was added AcCl (0.118 g, 1.50 mmol) dropwise via syringe. The reaction mixture was stirred at this temperature for 30 min, and saturated aqueous NH_4Cl solution (10 mL) was added. The mixture was extracted with CH_2Cl_2 (3 x 10 mL), and the combined organic layers were washed with brine (10 mL), dried over $MgSO_4$, filtered, and concentrated by rotary evaporation. Column chromatography (3:1 hexanes:EtOAc) furnished the title compound (0.400 g, 90%) as a flaky white solid, mp 144-145 °C: ^{1}H NMR (300 MHz, $CDCl_3$) δ 7.99 (d, *J* = 8.4 Hz, 2H), 7.41 (s, 1H), 7.32 (d, *J* = 8.1 Hz, 2H), 7.31 (d, *J* = 16.2 Hz, 1H), 7.23 (s, 1H), 6.37 (d, *J* = 15.6 Hz, 1H), 2.45 (s, 3H), 2.40 (s, 3H), 2.39 (s, 3H), 1.78 (s, 3H), 1.47 (9H); ^{13}C NMR (75 MHz, $CDCl_3$) δ 169.5, 164.8, 144.8, 139.8, 139.1, 137.8, 135.0, 133.7 (2C, accidental isochrony), 132.6, 129.9 (2C), 129.0 (2C), 125.5, 123.1, 80.2, 27.7 (3C), 23.9, 21.4, 20.9, 18.6; FTIR (thin film, $CHCl_3$, cm^{-1}) 2978, 2929, 1709, 1635, 1366, 1332, 1258, 1169, 1086, 1011, 983, 881, 853, 814, 756; HRMS (ESI) calcd for $C_{24}H_{29}NNaO_5S$ $[M + Na]^+$: 466.1664, found: 466.1634.

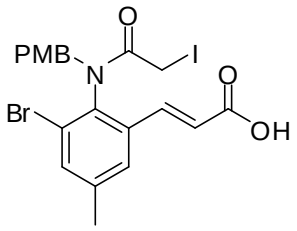

(*P*)-(*E*)-3-(3-Bromo-2-(2-iodo-*N*-(4-methoxybenzyl)acetamido)-5-methylphenyl)acrylic acid (5.31): To a stirred solution of (+)-**5.17f** (0.284 g, 0.473 mmol, 99/1 er) in CH_2Cl_2 (2.0 mL) at room temperature was added trifluoroacetic acid (2.0 mL) via syringe all at once. The reaction mixture was stirred for 1 h, at which point solvent was removed by rotary evaporation. The crude residue was directly subjected to column chromatography (40:60:1 hexanes:EtOAc:AcOH) to furnish the title compound (0.183 g, 71%) as a pale yellow solid, mp 109-110 °C, $[\alpha]_D^{23}$ +21, 99/1 er (*c* 14.9 mg/mL, $CHCl_3$): ^{1}H NMR (300 MHz, $CDCl_3$) δ 7.59 (s, 1H), 7.36 (s, 1H), 7.26 (d, *J* = 15.9 Hz, 1H), 7.04 (d, *J* = 8.4 Hz, 2H), 6.72 (d, *J* = 8.4 Hz, 2H), 6.07 (d, *J* = 15.9 Hz, 1H), 5.38 (d, *J* = 14.1 Hz, 1H), 4.21 (d, *J* = 14.1 Hz, 1H), 3.75 (s, 3H), 3.60 (d, *J* = 10.5 Hz, 1H), 3.43 (d, *J* = 10.8 Hz, 1H), 2.41 (s, 3H); ^{13}C NMR (75 MHz, $CDCl_3$) δ 170.6, 167.7, 159.4, 140.8 (2C, accidental isochrony), 136.1, 136.0, 135.0, 131.5 (2C), 127.2, 126.8, 124.7, 120.1, 113.8 (2C), 55.1, 52.1, 20.9, −2.6; FTIR (thin film, $CHCl_3$, cm^{-1}) 2999 (broad), 2836, 1693, 1662, 1512, 1461, 1383, 1320, 1283, 1250, 1176, 1106, 1034, 982, 910, 851, 822, 732; HRMS (ESI) calcd for $C_{20}H_{19}{}^{79}BrINNaO_4$ $[M + Na]^+$: 565.9440, found: 565.9465.

General procedure for radical cyclizations (Compounds 5.18a-c,e,f,i, 5.35, 5.41): Bu_3SnH (0.122 g, 0.42 mmol) and Et_3B (0.35 mL of a 1.0 M hexane solution, 0.35 mmol) were dissolved in degassed benzene (20 mL). This solution was added via syringe pump over a period of 2 h to a stirred solution of the appropriate α-halo amide (0.35 mmol) in benzene (35 mL). Upon completion of the reaction, solvent was removed by rotary evaporation, and the crude residue

was directly subjected to flash chromatography on 10% w/w KF/silica gel[80] using the appropriate eluent.

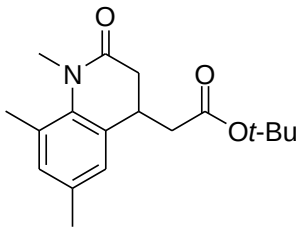

***t*-Butyl 2-(1,6,8-trimethyl-2-oxo-1,2,3,4-tetrahydroquinolin-4-yl)acetate (5.18a):** According to the general procedure, **5.18a** was prepared from the reaction of **5.17a** and chromatographed eluting with 3:1 hexanes:EtOAc. Chiral analysis was performed on the analytical (*S*,*S*)-Whelk-O1 column (75:25 hexanes:*i*-PrOH). *rac*-**5.17a** yielded *rac*-**5.18a** as a clear, colorless oil (0.088 g, 83%). The atropisomer (–)-**5.17a** yielded (+)-**5.18a** as a clear, colorless oil (0.086 g, 81%), $[\alpha]_D^{23}$ +6.3 (*c* 9.6 mg/mL, $CHCl_3$), 84/16 er, first eluting enantiomer. The atropisomer (+)-**5.17a** yielded (–)-**5.18a** as a clear, colorless oil (0.084 g, 79%), $[\alpha]_D^{23}$ –6.0 (*c* 8.5 mg/mL, $CHCl_3$), 91/9 er, second eluting enantiomer: ^{1}H NMR (300 MHz, $CDCl_3$) δ 6.90 (s, 1H), 6.88 (s, 1H), 3.34 (s, 3H), 3.29 (tt, *J* = 7.5 Hz, 4.8 Hz, 1H), 2.67 (dd, *J* = 15.3 Hz, 4.8 Hz, 1H), 2.54 (dd, *J* = 15.3 Hz, 4.5 Hz, 1H), 2.44 (dd, *J* = 15.3 Hz, 7.5 Hz, 1H), 2.38 (dd, *J* = 15.6 Hz, 7.2 Hz, 1H), 2.33 (s, 3H), 2.27 (s, 3H), 1.45 (s, 9H); ^{13}C NMR (75 MHz, $CDCl_3$) δ 171.8, 170.7, 138.3, 133.6, 132.3, 131.8, 127.6, 125.3, 80.9, 38.9, 37.8, 35.7, 33.4, 28.0 (3C), 20.6, 20.4; FTIR (neat, cm^{-1}) 2976. 2929, 1728, 1674, 1482, 1426, 1366, 1309, 1256, 1148, 1082, 1039, 961, 859, 844, 733; HRMS (ESI) calcd for $C_{18}H_{25}NNaO_3$ $[M + Na]^+$: 326.1732, found: 326.1756.

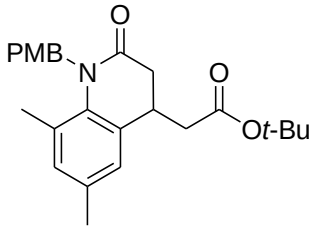

***t*-Butyl 2-(1-(4-methoxybenzyl)-6,8-dimethyl-2-oxo-1,2,3,4-tetrahydroquinolin-4-yl) acetate (5.18b):** According to the general procedure, **5.18b** was prepared from the reaction of **5.17b** and chromatographed eluting with 3:1 hexanes:EtOAc. Chiral analysis was performed on the analytical (*S*,*S*)-Whelk-O1 column (80:20 hexanes:*i*-PrOH). *rac*-**5.17b** yielded *rac*-**5.18b** as a clear, pale yellow oil (0.126 g, 88%). The atropisomer (+)-**5.17b** yielded (+)-**5.18b** as a clear, pale yellow oil (0.122 g, 85%), $[\alpha]_D^{23}$ +64 (*c* 9.5 mg/mL, $CHCl_3$), 96/4 er, first eluting enantiomer. The atropisomer (–)-**5.17b** yielded (–)-**5.18b** as a clear, pale yellow oil (0.126 g, 87%), $[\alpha]_D^{23}$ –64 (*c* 16.7 mg/mL, $CHCl_3$), 95/5 er, second eluting enantiomer: ^{1}H NMR (300 MHz, $CDCl_3$) δ 7.07 (d, *J* = 8.4 Hz, 2H), 6.90 (s, 1H), 6.82 (s, 1H), 6.75 (d, *J* = 8.7 Hz, 2H), 5.15 (d, *J* = 14.7 Hz, 1H), 4.87 (d, *J* = 14.7 Hz, 1H), 3.75 (s, 3H), 3.17 (tt, *J* = 7.5 Hz, 5.1 Hz, 1H), 2.63 (dd, *J* = 15.0 Hz, 5.1 Hz, 1H), 2.46 (dd, *J* = 15.0 Hz, 5.1 Hz, 1H), 2.34 (s, 3H), 2.26 (s, 3H), 2.08 (dd, *J* = 15.6 Hz, 7.8 Hz, 1H), 2.01 (dd, *J* = 15.6 Hz, 7.5 Hz, 1H), 1.41 (s, 9H); ^{13}C NMR (75 MHz, $CDCl_3$) δ 172.1, 170.8, 158.6, 137.1, 133.7, 133.5, 131.8, 129.5, 129.4 (2C), 127.9, 125.5, 113.5 (2C), 80.5, 55.0, 48.6, 38.2, 33.5, 27.9 (3C), 21.0, 20.5, missing peak due to accidental isochrony; FTIR (neat, cm^{-1}) 2976, 2932, 2836, 1727, 1674, 1611, 1513, 1479, 1368, 1248, 1147, 1035, 911, 845, 733; HRMS (ESI) calcd for $C_{25}H_{31}NNaO_4$ $[M + Na]^+$: 432.2151, found: 432.2142.

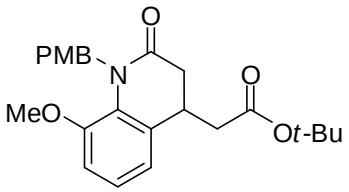

***tert*-Butyl 2-(8-methoxy-1-(4-methoxybenzyl)-2-oxo-1,2,3,4-tetrahydroquinolin-4-yl)acetate (5.18c):** According to the general procedure, **5.18c** was prepared from the reaction of **5.17c** and chromatographed eluting with 2:1 hexanes:EtOAc. Chiral analysis was performed on the analytical (*S*,*S*)-Whelk-O1 column (50:50 hexanes:*i*-PrOH). *rac*-**5.17c** yielded *rac*-**5.18c** as a clear, colorless oil (0.140 g, 97%). The atropisomer (–)-**5.17c** yielded (+)-**5.18c** as a clear, colorless oil (0.138 g, 96%), $[\alpha]_D^{23}$ +86 (*c* 4.1 mg/mL, $CHCl_3$), 93/7 er, first eluting enantiomer. The atropisomer (+)-**5.17c** yielded (–)-**5.18c** as a clear, colorless oil (0.136 g, 94%), $[\alpha]_D^{23}$ –87 (*c* 7.3 mg/mL, $CHCl_3$), 93/7 er, second eluting enantiomer: ^{1}H NMR (300 MHz, $CDCl_3$) δ 7.11 (d, *J* = 8.7 Hz, 2H), 7.01 (t, *J* = 7.8 Hz, 1H), 6.81 (d, *J* = 8.4 Hz, 1H), 6.79 (d, *J* = 7.8 Hz, 1H), 6.74 (d, *J* = 8.7 Hz, 2H), 5.38 (d, *J* = 14.4 Hz, 1H), 5.22 (d, *J* = 14.7 Hz, 1H), 3.81 (s, 3H), 3.74 (s, 3H), 3.27 (m, 1H), 2.70 (dd, *J* = 15.0 Hz, 5.1 Hz, 1H), 2.54 (dd, *J* = 15.0 Hz, 4.8 Hz, 1H), 2.22 (dd, *J* = 15.9 Hz, 7.8 Hz, 1H), 2.17 (dd, *J* = 16.2 Hz, 7.8 Hz, 1H), 1.40 (s, 9H); ^{13}C NMR (75 MHz, $CDCl_3$) δ 170.8, 170.7, 158.4, 149.9, 133.9, 130.4, 129.3 (2C), 128.1, 124.7, 119.6, 113.3 (2C), 111.5, 80.7, 55.5, 55.0, 46.7, 38.2, 37.7, 33.4, 28.0 (3C); FTIR (neat, cm^{-1}) 2976, 2936, 2837, 2248, 1727, 1674, 1612, 1589, 1513, 1484, 1462, 1368, 1248, 1148, 1102, 1033, 912, 845, 784, 733; HRMS (ESI) calcd for $C_{24}H_{29}NNaO_5$ $[M + Na]^+$: 434.1943, found: 434.1945.

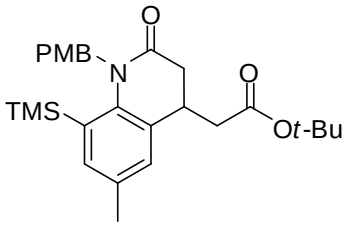

***tert*-Butyl 2-(1-(4-methoxybenzyl)-6-methyl-2-oxo-8-(trimethylsilyl)-1,2,3,4-tetrahydroquinolin-4-yl) acetate (5.18e):** According to the general procedure, **5.18e** was prepared from the reaction of **5.17e** and chromatographed eluting with 3:1 hexanes:EtOAc. Chiral analysis was performed on the analytical (*S*,*S*)-Whelk-O1 column (80:20 hexanes:*i*-PrOH). *rac*-**5.17e** yielded *rac*-**5.18e** as a clear, colorless oil (0.152 g, 93%). The atropisomer (+)-**5.17e** yielded (+)-**5.18e** as a clear, colorless oil (0.155 g, 95%), $[\alpha]_D^{23}$ +122 (*c* 4.8 mg/mL, $CHCl_3$), 95/5 er, first eluting enantiomer. The atropisomer (–)-**5.17e** yielded (–)-**5.18e** as a clear, colorless oil (0.152 g, 93%), $[\alpha]_D^{23}$ –120 (*c* 15.2 mg/mL, $CHCl_3$), 94/6 er, second eluting enantiomer: ^{1}H NMR (300 MHz, $CDCl_3$) δ 7.29 (d, *J* = 1.8 Hz, 1H), 7.02 (d, *J* = 8.7 Hz, 2H), 6.97 (d, *J* = 1.8 Hz, 1H), 6.71 (d, *J* = 8.7 Hz, 2H), 5.34 (d, *J* = 13.5 Hz, 1H), 4.69 (d, *J* = 13.5 Hz, 1H), 3.73 (s, 3H), 3.08 (m, 1H), 2.59 (dd, *J* = 15.0 Hz, 5.1 Hz, 1H), 2.41 (dd, *J* = 15.0 Hz, 4.2 Hz, 1H), 2.31 (s, 3H), 1.73 (m, 2H), 0.41 (s, 9H); ^{13}C NMR (75 MHz, $CDCl_3$) δ 171.0, 170.9, 158.9, 143.5, 136.0, 133.1, 132.6, 130.3, 130.2 (2C), 129.1, 129.0, 113.5 (2C), 80.3, 55.0, 51.7, 37.9, 37.8, 33.4, 27.9 (3C), 20.7, 0.6 (3C); FTIR (thin film, $CHCl_3$, cm^{-1}) 2975, 2836, 1727, 1675, 1611, 1513, 1452, 1368, 1249, 1151, 1112, 1037, 922, 864, 838, 757; HRMS (ESI) calcd for $C_{27}H_{37}NNaO_4Si$ $[M + Na]^+$: 490.2390, found: 490.2409.

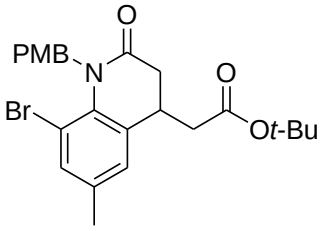

***tert*-Butyl 2-(8-bromo-1-(4-methoxybenzyl)-6-methyl-2-oxo-1,2,3,4-tetrahydroquinolin-4-yl) acetate (5.18f):** According to the general procedure, **5.18f** was prepared from the reaction of **5.17f** and chromatographed eluting with 3:1 hexanes:EtOAc. Chiral analysis was performed on the analytical (*S*,*S*)-Whelk-O1 column (70:30 hexanes:*i*-PrOH). *rac*-**5.17f** yielded *rac*-**5.18f** as a clear, colorless oil (0.102 g, 61%). The atropisomer (+)-**5.17f** yielded (+)-**5.18f** as a white solid (0.104 g, 63%), $[\alpha]_D^{23}$ +100 (*c* 7.0 mg/mL, $CHCl_3$), 95/5 er, first eluting enantiomer. The atropisomer (–)-**5.17f** yielded (–)-**5.18f** as a clear, colorless oil (0.109 g, 66%), $[\alpha]_D^{23}$ –100 (*c* 10.3 mg/mL, $CHCl_3$), 96/4 er, second eluting enantiomer: ^{1}H NMR (300 MHz, $CDCl_3$) δ 7.34 (s, 1H), 7.11 (d, *J* = 8.7 Hz, 2H), 6.93 (s, 1H), 6.74 (d, *J* = 8.4 Hz, 2H), 5.42 (d, *J* = 14.7 Hz, 1H), 5.34 (d, *J* = 15.3 Hz, 1H), 3.74 (s, 3H), 3.15 (m, 1H), 2.62 (dd, *J* = 15.0 Hz, 4.8 Hz, 1H), 2.47 (dd, *J* = 15.0 Hz, 5.1 Hz, 1H), 2.27 (s, 3H), 1.97 (d, *J* = 7.5 Hz, 2H), 1.39 (s, 9H); ^{13}C NMR (75 MHz, $CDCl_3$) δ 171.5, 170.5, 158.8, 136.3, 135.5, 133.9, 130.2 (2C), 129.3, 127.3, 113.5, 113.4 (2C), 80.7, 55.0, 47.5, 38.0, 37.7, 33.6, 27.9 (3C), 20.3, missing peak due to accidental isochrony; FTIR (neat, cm^{-1}) 2977, 2932, 2836, 1725, 1685, 1611, 1513, 1467, 1366, 1302, 1248, 1153, 1035, 917, 827, 761, 734; HRMS (ESI) calcd for $C_{24}H_{28}{}^{79}BrNNaO_4$ $[M + Na]^+$: 496.1099, found: 496.1104.

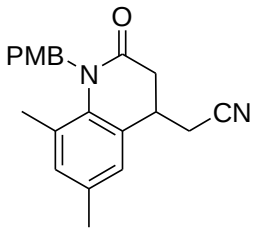

2-(1-(4-Methoxybenzyl)-6,8-dimethyl-2-oxo-1,2,3,4-tetrahydroquinolin-4-yl)acetonitrile (5.18h): To a stirred solution of **5.17h** (0.161 g, 0.35 mmol) in non-degassed benzene (84 mL) were added sequentially Bu_3SnH (0.122 g, 0.42 mmol) and Et_3B in hexane (0.35 mL of a 1.0 M solution, 0.35 mmol). The reaction was stirred for 5 min, and solvent was removed by rotary evaporation. The crude residue was directly chromatographed on 10% w/w KF/silica gel, eluting with 3:2 hexanes:EtOAc. The fractions containing the desired product were collected and concentrated, and a second flash column (silica gel only) was performed, eluting with 3:2 hexanes:EtOAc to remove residual impurities. The products were ~95% pure by ^{1}H NMR, containing trace unidentifiable impurities. Chiral analysis was performed on the analytical (*S*,*S*)-Whelk-O1 column (80:20 hexanes:EtOAc). *rac*-**5.17h** yielded *rac*-**5.18h** as a white solid (0.082 g, 70%), mp 101-102 °C. The atropisomer (–)-**5.17h** yielded (+)-**5.18h** as a white solid (0.080 g, 68%), $[\alpha]_D^{23}$ +99 (*c* 19.8 mg/mL, $CHCl_3$), 96/4 er, first eluting enantiomer. The atropisomer (+)-**5.17h** yielded (–)-**5.18h** as a white solid (0.083 g, 71%), $[\alpha]_D^{23}$ –97 (*c* 4.5 mg/mL, $CHCl_3$), 93/7 er, second eluting enantiomer: ^{1}H NMR (300 MHz, $CDCl_3$) δ 7.03 (s, 1H), 6.87 (s, 1H), 7.02 (d, *J* = 8.4 Hz, 2H), 6.76 (d, *J* = 8.7 Hz, 2H), 5.25 (d, *J* = 14.4 Hz, 1H), 4.73 (d, *J* = 14.4 Hz, 1H), 3.75 (s, 3H), 2.97 (m, 1H), 2.71 (dd, *J* = 15.3 Hz, 4.8 Hz, 1H), 2.50 (dd, *J* = 15.3 Hz, 4.2 Hz, 1H), 2.41 (s, 3H), 2.33 (s, 3H), 2.03 (dd, *J* = 16.8 Hz, 6.6 Hz, 1H), 1.75 (dd, *J* = 16.8 Hz, 9.0 Hz, 1H); ^{13}C NMR (75 MHz, $CDCl_3$) δ 170.7, 159.0, 136.8, 134.5, 132.8, 130.7, 129.8 (2C), 129.1, 128.5, 125.9, 117.5, 113.7 (2C), 55.1, 48.6, 37.7, 34.0, 20.8, 20.6, 20.3; FTIR (thin film, $CHCl_3$,

cm^{-1}) 3012, 2959, 2837, 1673, 1513, 1479, 1376, 1249, 1176, 1033, 859, 757; HRMS (ESI) calcd for $C_{21}H_{22}N_2NaO_2$ $[M + Na]^+$: 357.1579, found: 357.1612.

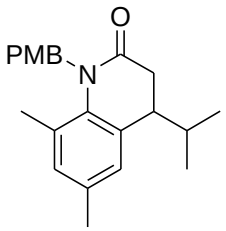

4-Isopropyl-1-(4-methoxybenzyl)-6,8-dimethyl-3,4-dihydroquinolin-2(1*H*)-one (5.18i):

According to the general procedure, **5.18i** was prepared from the reaction of **5.17i** and chromatographed eluting with 3:1 pentane:Et_2O. Chiral analysis was performed on the analytical (*S,S*)-Whelk-O1 column (80:20 hexanes:*i*-PrOH). *rac*-**5.17i** yielded *rac*-**5.18i** as a clear, colorless oil (0.060 g, 51%). The atropisomer (–)-**5.17i** yielded (–)-**5.18i** as a clear, colorless oil (0.065 g, 55%), $[\alpha]_D^{23}$ –44 (*c* 6.3 mg/mL, $CHCl_3$), 80/20 er, second eluting enantiomer. The atropisomer (+)-**5.17i** yielded (+)-**5.18i** as a clear, colorless oil (0.067 g, 57%), $[\alpha]_D^{23}$ +44 (*c* 8.6 mg/mL, $CHCl_3$), 80/20 er, first eluting enantiomer: ^{1}H NMR (300 MHz, $CDCl_3$) δ 7.04 (d, *J* = 8.7 Hz, 2H), 6.90 (s, 1H), 6.73 (d, *J* = 8.7 Hz, 2H), 6.71 (s, 1H), 5.22 (d, *J* = 14.7 Hz, 1H), 4.74 (d, *J* = 14.7 Hz, 1H), 3.75 (s, 3H), 2.65 (dd, *J* = 15.0 Hz, 3.6 Hz, 1H), 2.54 (dd, *J* = 14.7 Hz, 4.8 Hz, 1H), 2.33 (s, 3H), 2.28 (s, 3H), 2.19 (dt, *J* = 9.3 Hz, 4.2 Hz, 1H), 1.06 (d of septets, *J* = 9.3 Hz, 6.6 Hz, 2.7 Hz, 1H), 0.84 (d, *J* = 6.6 Hz, 3H), 0.66 (d, *J* = 6.6 Hz, 3H); ^{13}C NMR (75 MHz, $CDCl_3$) δ 172.9, 158.6, 137.3, 134.8, 133.2, 131.3, 129.7, 129.5 (2C), 128.1, 127.3, 113.3 (2C), 55.2, 48.6, 44.8, 36.3, 28.2, 21.5, 21.1, 20.6, 19.8; FTIR (neat, cm^{-1}) 2957, 2868, 2835, 1673, 1611, 1513, 1477, 1365, 1295, 1247, 1177, 1162, 1112, 1035, 860, 812; HRMS (ESI) calcd for $C_{22}H_{27}NNaO_2$ $[M + Na]^+$: 360.1939, found: 360.1911.

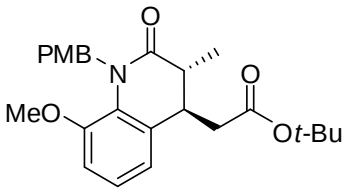

***trans-tert*-Butyl 2-(8-methoxy-1-(4-methoxybenzyl)-3-methyl-2-oxo-1,2,3,4-tetrahydroquinolin-4-yl)acetate (5.35):** According to the general procedure, **5.35** was prepared from the reaction of **5.34b** and chromatographed eluting with 2:1 hexanes:EtOAc. Chiral analysis was performed on the analytical (*S*,*S*)-Whelk-O1 column (70:30 hexanes:*i*-PrOH). *rac*-**5.34b** yielded *rac*-**5.35** as a clear, colorless oil (0.145 g, 97%). The atropisomer (+)-**5.34b** yielded (–)-**5.35** as a clear, colorless oil (0.146 g, 98%), $[\alpha]_D^{23}$ –109 (*c* 13.2 mg/mL, $CHCl_3$), 99/1 er, second eluting enantiomer. The atropisomer (–)-**5.34b** yielded (+)-**5.35** as a clear, colorless oil (0.145 g, 97%), $[\alpha]_D^{23}$ +111 (*c* 20.4 mg/mL, $CHCl_3$), 99.5/0.5 er, first eluting enantiomer: ^{1}H NMR (300 MHz, $CDCl_3$) δ 7.12 (d, *J* = 8.7 Hz, 2H), 7.01 (t, *J* = 8.4 Hz, 1H), 6.82 (d, *J* = 8.4 Hz, 1H), 6.80 (d, *J* = 8.1 Hz, 1H), 6.75 (d, *J* = 8.7 Hz, 2H), 5.41 (d, *J* = 14.4 Hz, 1H), 5.17 (d, *J* = 14.7 Hz, 1H), 3.79 (s, 3H), 3.74 (s, 3H), 2.97 (m with clear d, *J* = 2.7 Hz, 1H), 2.68 (qd, *J* = 7.2 Hz, 2.7 Hz, 1H), 2.21 (dd, *J* = 15.6 Hz, 6.9 Hz, 1H), 2.10 (dd, *J* = 15.6 Hz, 8.1 Hz, 1H), 1.38 (s, 9H), 1.05 (d, *J* = 7.5 Hz, 3H); ^{13}C NMR (75 MHz, $CDCl_3$) δ 173.6, 170.7, 158.3, 149.5, 131.2, 130.6, 129.2 (2C), 127.1, 124.7, 121.5, 113.2 (2C), 111.7, 80.5, 55.4, 54.9, 46.7, 41.8, 40.4, 39.0, 27.9 (3C), 14.9; FTIR (thin film, $CHCl_3$, cm^{-1}) 2974, 2934, 2837, 1727, 1669, 1612, 1590, 1512, 1483, 1461, 1365, 1248, 1175, 1150, 1107, 1085, 1036, 976, 935, 846, 790, 740; HRMS (ESI) calcd for $C_{25}H_{31}NNaO_5$ $[M + Na]^+$: 448.2100, found: 448.2128.

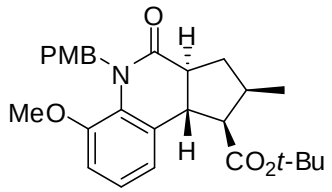

(±)-(1*S*,2*S*,3a*R*,9b*S*)-*t*-Butyl 6-methoxy-5-(4-methoxybenzyl)-2-methyl-4-oxo-2,3,3a,4,5,9b-hexahydro-1*H*-cyclopenta[*c*]quinoline-1-carboxylate (5.41): According to the general procedure, **5.41** was prepared from the reaction of **5.40** (0.143 g, 0.270 mmol) and chromatographed eluting with 3:1 hexanes:EtOAc on 10% w/w KF/silica. A second flash column was run with 3:2 pentane:Et_2O on silica only to remove residual impurities. Chiral analysis was performed on the analytical (*S*,*S*)-Whelk-O1 column (60:40 hexanes:*i*-PrOH). The atropisomer (+)-**5.40** yielded (–)-**5.41** as a clear, colorless oil (0.062 g, 51%, ~95% diastereomeric purity), $[\alpha]_D^{23}$ –113 (*c* 12.3 mg/mL, $CHCl_3$), 99/1 er, first eluting enantiomer. The atropisomer (–)-**5.40** yielded (+)-**5.41** as a clear, colorless solid, (0.060 g, 49%, ~95% diastereomeric purity), $[\alpha]_D^{23}$ +110 (*c* 10.4 mg/mL, $CHCl_3$), 98/2 er, second eluting enantiomer: ^{1}H NMR (75 MHz, $CDCl_3$) δ 7.07 (d, *J* = 8.7 Hz, 2H), 7.00 (t, *J* = 7.5 Hz, 1H), 6.76 (d, *J* = 7.8 Hz, 1H), 6.73 (d, *J* = 8.7 Hz, 2H), 6.53 (d, *J* = 7.5 Hz,1H), 5.51 (d, *J* = 15.0 Hz, 1H), 5.01 (d, *J* = 15.0 Hz, 1H), 3.77 (s, 3H), 3.73 (s, 3H), 3.30 (dd, *J* = 14.1 Hz, 10.8 Hz, 1H), 2.89 (t, *J* = 10.8 Hz, 1H), 2.69 (d of sextets, *J* = 10.5 Hz, 7.2 Hz, 1H), 2.40 (ddd, *J* = 14.4 Hz, 11.1 Hz, 7.2 Hz, 1H), 2.30 (dt, *J* = 12.6 Hz, 7.2 Hz, 1H), 1.68 (m, 1H), 1.51 (s, 9H), 1.10 (d, *J* = 7.2 Hz, 3H); ^{13}C NMR (75 MHz, $CDCl_3$) δ 173.3, 172.4, 158.2, 149.9, 135.3, 130.9, 129.1, 128.4 (2C), 125.0, 116.2, 113.4 (2C), 111.1, 80.9, 55.4, 55.0, 50.7, 46.9, 46.8, 44.2, 35.1, 33.7, 28.1 (3C), 18.2; FTIR (thin film, $CHCl_3$, cm^{-1}) 2971, 2837, 1724, 1678, 1513, 1459, 1368, 1280, 1247, 1148, 1067, 1036, 800, 763; HRMS (ESI) calcd for $C_{27}H_{33}NNaO_5$ $[M + Na]^+$: 474.2256, found: 474.2293.

6.6 *N*-ARYL BOND ROTATION STUDIES

Racemization of 3.19a-c, 5.17a,c,f, 5.27c: The appropriate compound, enantiomerically enriched in the second eluting enantiomer, was dissolved in a 9:1 hexanes:*i*-PrOH solvent mixture to make a ~2 mg/mL solution in a sealable tube. The tube was sealed and placed in a pre-heated oil bath with an electronic temperature controller. At various time intervals, the sealed tube was removed briefly (1-2 minutes) from the bath, opened, and a 10 μL aliquot was removed via syringe and injected onto the appropriate analytical HPLC column to measure the enantiomeric ratio. The decrease in enantiomeric excess (y-axis) was plotted against time (x-axis), and the barrier to rotation was calculated from the plot.[141] In the y-axis term of the plot, "F" denotes the fraction of the first eluting enantiomer, and "S" denotes the fraction of the second eluting enantiomer. A conversion factor of 1 cal = 4.184 J was used in all calculations.[60] The half-life for racemization at ambient temperature is determined by first calculating the rate of racemization (k_{rac}) from the barrier to rotation at 25 °C, assuming that $\Delta G^{\ddagger}_{rot}$ is mostly constant over a large temperature range.

$$k_{rac} = 2k_{rot} = \frac{2k_B T}{h} e^{\left(\frac{-\Delta G^{\ddagger}_{rot}}{RT}\right)} \qquad t_{1/2} = \frac{\ln 2}{k_{rac}}$$

A sample full data treatment is shown for **3.19a**.

Table 6.1 Thermal Racemization of 3.19a

time (min)	% ee
0	100.0
30	97.0
80	93.0
143	86.9
258	79.3
370	75.2
439	70.1
500	67.7
569	66.2

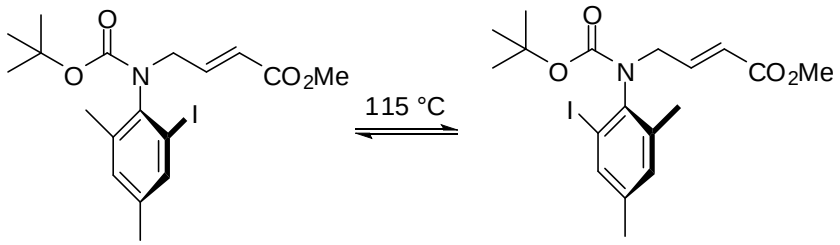

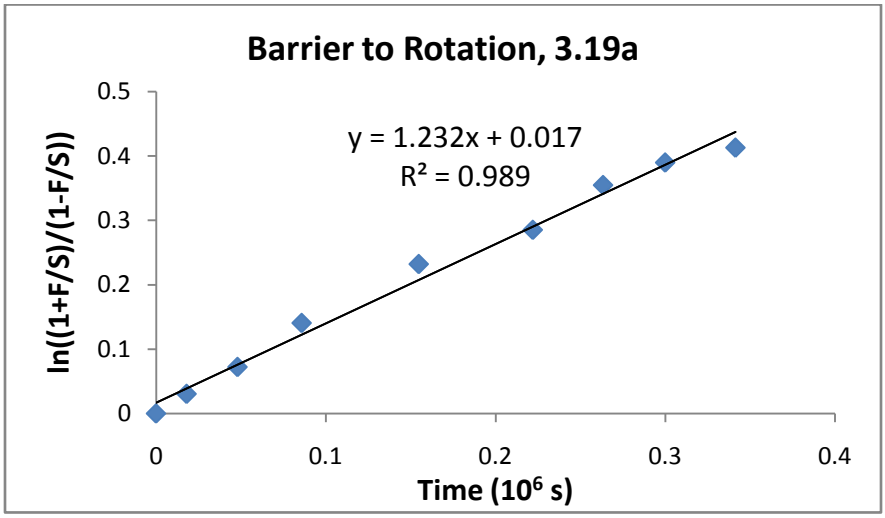

Equation for racemization: $$\ln\left[\frac{1+[F3.19a]/[S3.19a]}{1-[F3.19a]/[S3.19a]}\right] = k_{rac}t + c = 2k_{rot}t + c$$

Corresponding plot: $\ln\left[\frac{1+[F3.19a]/[S3.19a]}{1-[F3.19a][S3.19a]}\right]$ vs. time, where slope = $2k_{rot}$

$$k_{rot} = \frac{slope}{2} = \frac{9.533\times10^{-5}\,s^{-1}}{2} = 6.16\times10^{-6}\,s^{-1}$$

$$\Delta G^{\ddagger}_{rot} = -RT\ln\left(\frac{k_{rot}h}{k_BT}\right) = 134.6kJ/mol = 32.2kcal/mol$$

$t_{1/2}$ for racemization at 25 °C = 690 years

Table 6.2 Thermal Racemization of 3.19b

time (min)	% ee
0	66.6
20	64.7
93	62.6
171	59.3
254	56.4
388	53.6
519	49.3
596	46.4

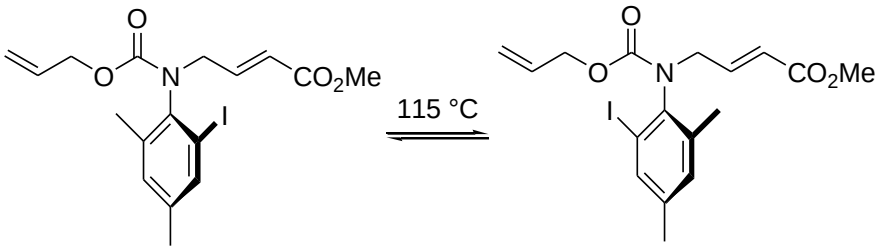

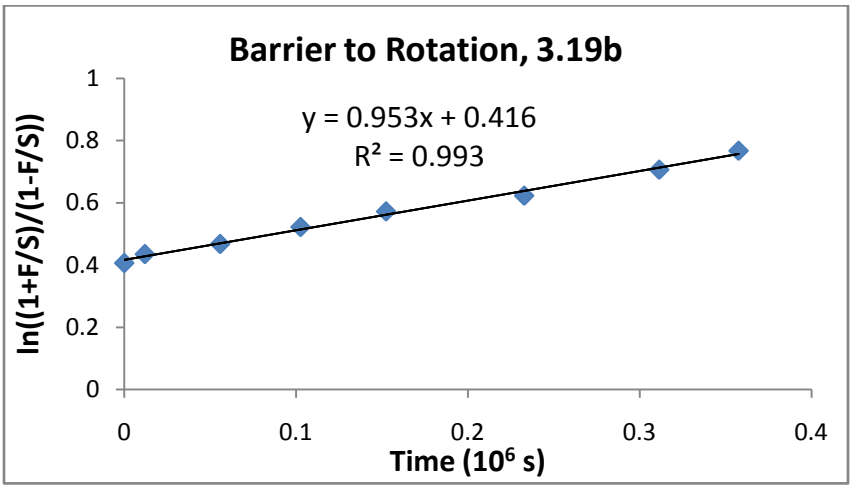

k_{rot} = 4.77 x 10^{-6} s^{-1}

$\Delta G^{\ddagger}_{rot}$ = 32.4 kcal/mol

$t_{1/2}$ at 25 °C = 960 years

Table 6.3 Thermal Racemization of 3.19c

time (min)	% ee
0	78.5
37	75.0
78	73.6
114	71.0
185	67.1
263	63.7
352	61.1
554	49.4
1252	31.2

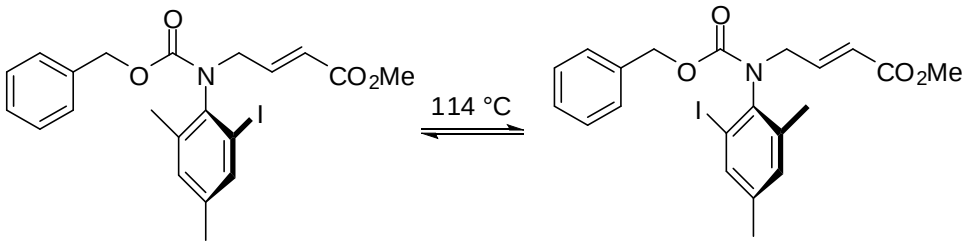

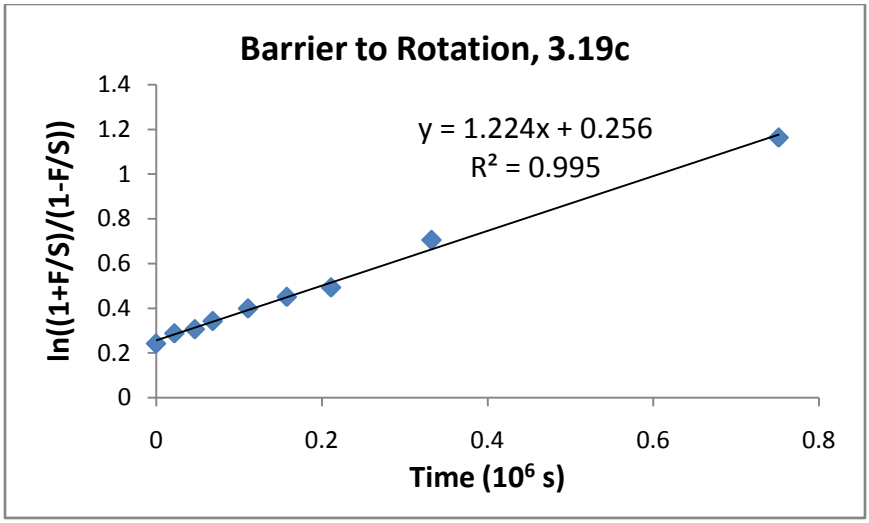

k_{rot} = 6.12 x 10^{-6} s^{-1}

$\Delta G^{\ddagger}_{rot}$ = 32.1 kcal/mol

$t_{1/2}$ at 25 °C = 601 years

Table 6.4 Thermal Racemization of 5.17b

time (min)	% ee
0	99.7
39	95.6
90	93.4
190	89.5
276	81.8
367	80.3
481	72.5
575	66.4
670	62.1

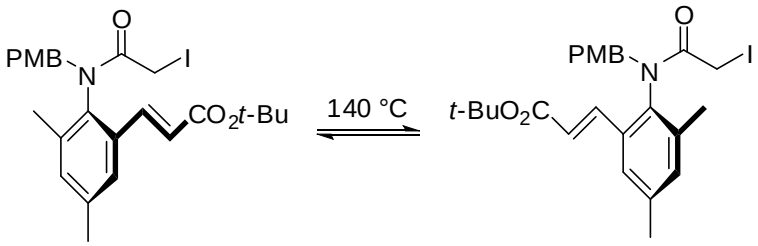

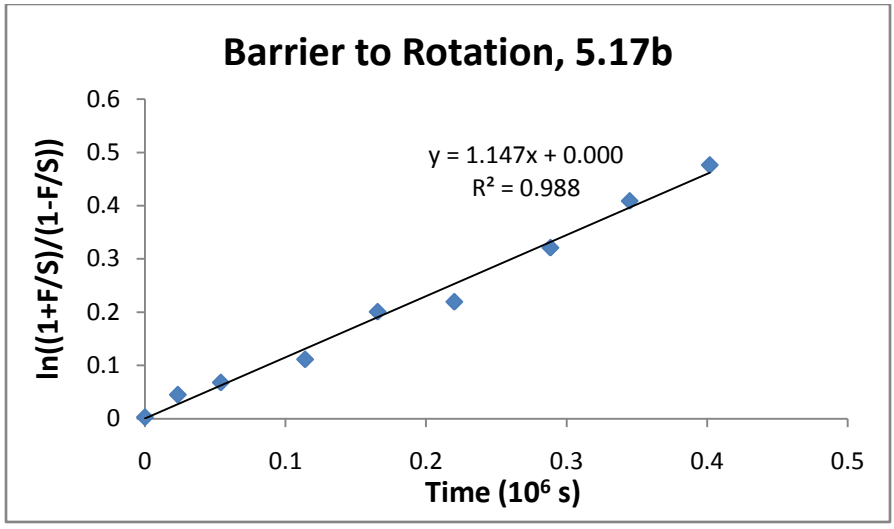

k_{rot} = 5.74 x 10^{-6} s^{-1}

$\Delta G^{\ddagger}_{rot}$ = 34.3 kcal/mol

$t_{1/2}$ at 25 °C = 27,500 years

Table 6.5 Thermal Racemization of 5.17c

time (min)	% ee
0	96.2
22	91.3
57	82.9
125	69.1
201	56.2
284	46.1
378	35.8
489	27.7

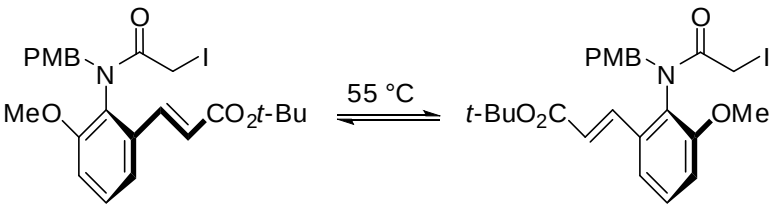

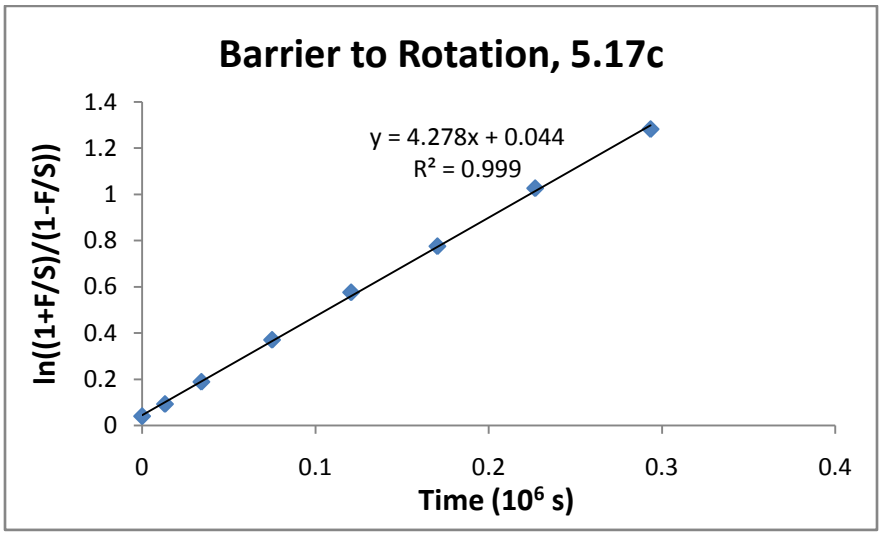

k_{rot} = 2.14 x 10^{-5} s^{-1}

$\Delta G^{\ddagger}_{rot}$ = 26.3 kcal/mol

$t_{1/2}$ at 25 °C = 12 days

Table 6.6 Thermal Racemization of 5.17f

time (min)	% ee
0	99.5
23	95.3
63	91.9
133	86.3
200	76.2
274	71.1
348	66.7
397	60.7
469	57.4

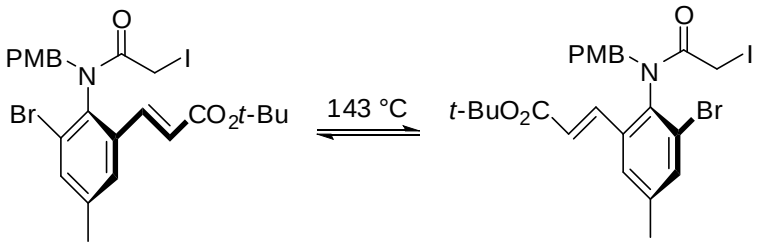

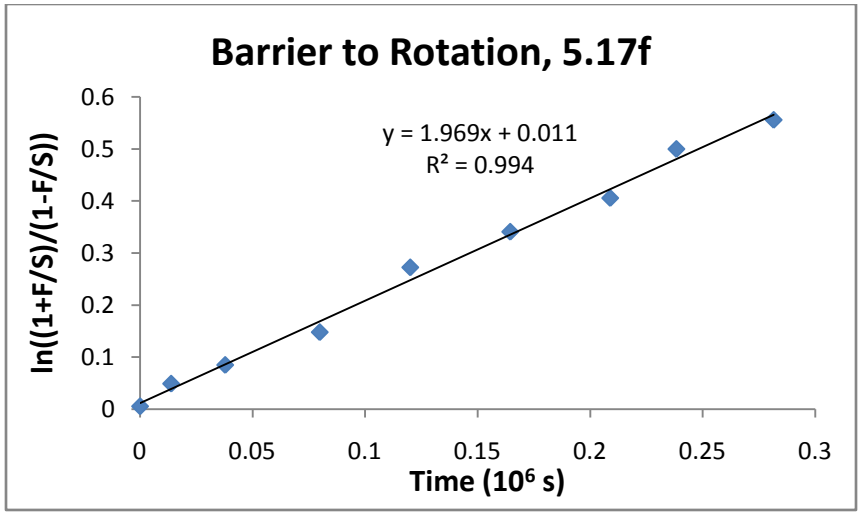

k_{rot} = 9.85 x 10^{-6} s^{-1}

$\Delta G^{\ddagger}_{rot}$ = 34.2 kcal/mol

$t_{1/2}$ at 25 °C = 19,900 years

Table 6.7 Thermal Racemization of 5.27c

time (min)	% ee
0	94.1
9	91.1
29	77.1
49	65.9
86	47.9
122	35.1
172	23.5
232	14.4

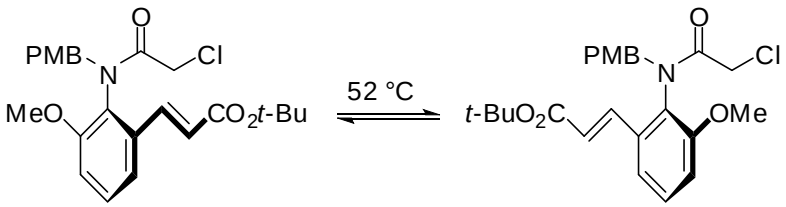

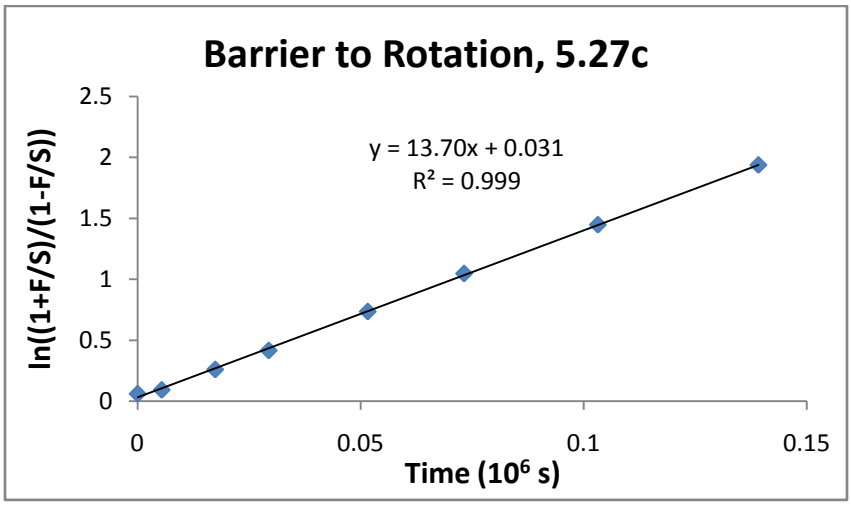

k_{rot} = 6.85 x 10^{-5} s^{-1}

$\Delta G^{\ddagger}_{rot}$ = 25.3 kcal/mol

$t_{1/2}$ at 25 °C = 2.2 days

Thermal equilibration of 4.13, 4.15: The appropriate compound, enriched in the *syn* diastereomer, was dissolved in a 9:1 hexanes:EtOAc solvent mixture to make a ~2 mg/mL solution in a sealable tube. The tube was sealed and placed in a pre-heated oil bath with an electronic temperature controller. At various time intervals, the sealed tube was removed briefly (1-2 minutes) from the bath, opened, and a 10 μL aliquot was removed via syringe and injected onto an analytical Waters NovaPak silica HPLC column to measure the dr. The sample was heated until equilibrium was reached, and the solution was concentrated and analyzed by ^{1}H NMR to ensure that the final ratio as determined by HPLC analysis was accurate. The first-order conversion of the *syn* isomer to the *anti* isomer, approaching equilibrium, was plotted against time.[60] In the resulting plot, the slope is equal to k_1, the conversion rate of *syn* to *anti*. The reverse rate k_{-1} was calculated from the equilibrium value ($k_{-1} = k_1 / K$). Finally, the barrier to rotation for each process was determined from the experimentally determined rate and the Eyring equation. A conversion factor of 1 cal = 4.184 J was used in all calculations.[60]

$$syn \underset{k_{-1}}{\overset{k_1}{\rightleftharpoons}} anti$$

$$\Delta G^{\ddagger}_{rot} = -RT \ln\left(\frac{kh}{k_B T}\right)$$

Table 6.8 Thermal Equilibration of 4.13

time (min)	% anti	% syn
0	28.3	71.7
13	38.7	61.3
23	45.7	54.3
32	50.3	49.7
43	54.0	46.0
52	56.7	43.3
61	58.7	41.3
73	60.5	39.5
88	62.2	37.8
112	63.6	36.4
149	64.4	35.6
186	64.7	35.3
247	64.9	35.1
312	64.8	35.2

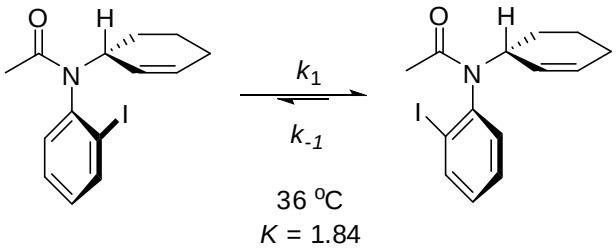

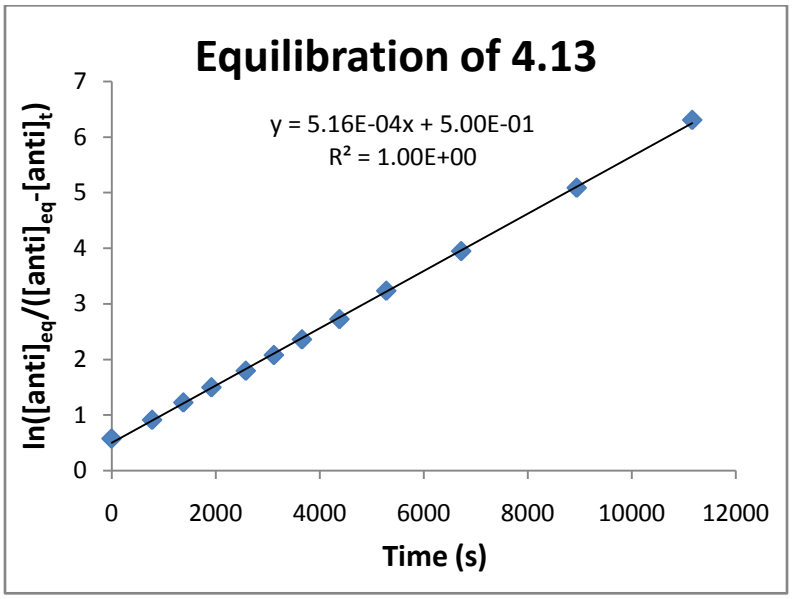

$k_1 = 5.16 \times 10^{-4}\ s^{-1}$

$k_{-1} = 2.80 \times 10^{-4}\ s^{-1}$

$\Delta G^{\ddagger}_{rot}$ (*syn* to *anti*) = 22.8 kcal/mol

$\Delta G^{\ddagger}_{rot}$ (*syn* to *anti*) = 23.1 kcal/mol

Table 6.9 Thermal Equilibration of 4.15

time (min)	% anti	% syn
0	4.3	95.7
95	5.0	95.0
245	5.8	94.2
645	12.7	87.3
1430	22.2	77.8
1728	23.7	76.3
2054	26.0	74.0
2847	30.5	69.5
3485	35.6	64.4
4345	40.2	59.8
4939	42.5	57.5
5807	45.7	54.3
21699	67.4	32.6
30340	67.6	32.4

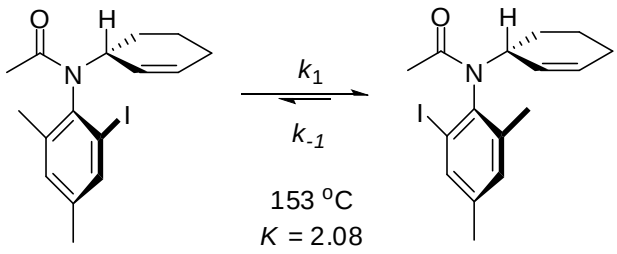

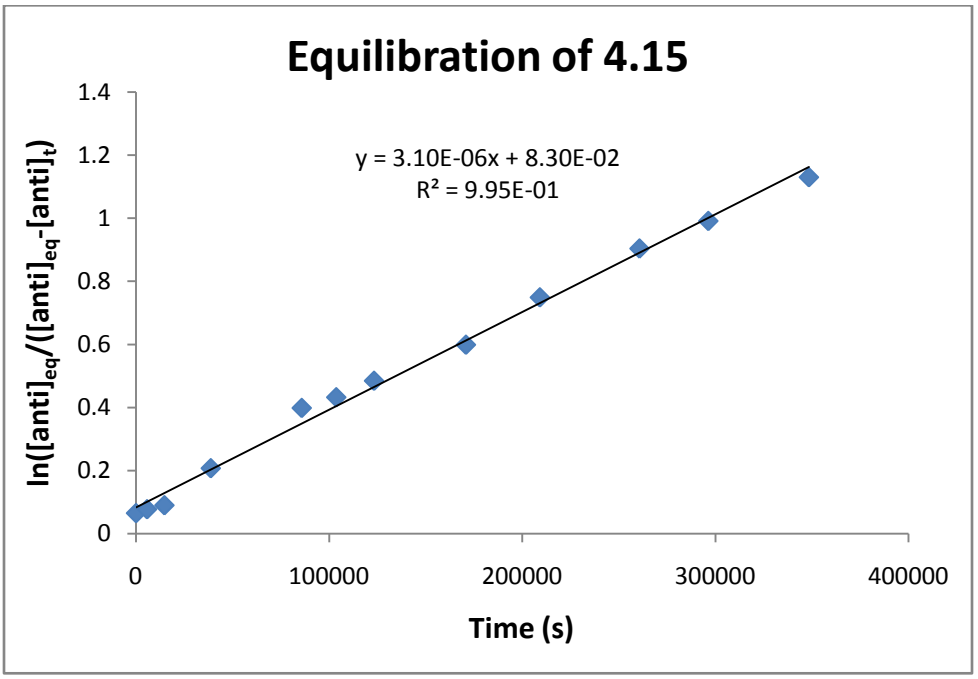

k_1 = 3.10 x 10^{-6} s^{-1}

k_{-1} = 1.49 x 10^{-6} s^{-1}

$\Delta G^{\ddagger}_{rot}$ (*syn* to *anti*) = 36.0 kcal/mol

$\Delta G^{\ddagger}_{rot}$ (*syn* to *anti*) = 36.6 kcal/mol

6.7 *N*-VINYL BOND ROTATION STUDIES

For each compound **1.15a,c** and **1.29-1.32**, a sample of the α-haloenamide was dissolved in the appropriate solvent ($CDCl_3$ or toluene-*d*8) with a small amount of tetramethylsilane, and the solution was placed in a standard 5 mm NMR sample tube. The samples were loaded into the NMR spectrometer and the probe was heated or cooled, allowing ~10 min equilibration time at each temperature before the spectrum was collected. The spectra for **1.29-1.32** were collected by Dr. Damodaran Krishnan Achary. Fourier transforms were performed using NUTS data processing software (www.acornnmr.com).[62] For each compound, the benzylic signals were used for line-shape analysis. For these signals, all compounds analyzed showed geminally coupled doublets at lower temperatures, coalescing to a singlet as temperature was increased. The only exception to this was **1.32**, which decoalesced to two quartets in a 2:1 ratio upon cooling.

At all temperatures, the standard peak width was determined by measuring the peak width at half-height of the tetramethylsilane internal standard. For at least two low-temperature spectra in the decoalesced temperature region, the ν_A and ν_B of the benzylic signals in Hz were also measured. By plotting the log $\Delta\nu$ (y-axis) vs. 1/T (x-axis) at these temperatures, the $\Delta\nu$ for the spectra at higher temperatures could be calculated.

Line-shape analysis of each spectrum was accomplished with WINDNMR-Pro software.[55] At each temperature, the appropriate line width and $\Delta\nu$ were entered, and line-shape analysis was performed by changing the *k* variable until the best fit was achieved. Simulation near the coalescence temperature was typically not performed, due to low accuracy (signals had

typically disappearing into the baseline). An Eyring plot was then derived from the data by plotting 1/T on the x-axis vs. ln (*k*/T) on the y-axis, according to the equation:

$$\ln\left(\frac{k}{T}\right)=\left(\frac{-\Delta H^{\ddagger}}{R}\right)\left(\frac{1}{T}\right)+\frac{\Delta S^{\ddagger}}{\mathrm{R}}+\ln\left(\frac{k_B}{h}\right)$$

From the Eyring plot, the thermodynamic parameters for the rotation were calculated using the following equations:

$$k_{298}=298K\cdot e^{\left(\frac{slope}{298K}+\mathrm{int.}\right)}$$

$$\Delta H^{\ddagger}=-R\cdot slope$$

$$\Delta S^{\ddagger}=R\cdot\left(\mathrm{int.}-\ln\left(\frac{k_B}{h}\right)\right)$$

$$\Delta G^{\ddagger}_{298}=-R\cdot 298K\cdot\ln\left(\frac{k_{298}\cdot h}{k_B\cdot 298K}\right)$$

A conversion factor of 1 cal = 4.184 J was used in all calculations.[60] The calculated thermodynamic values for all compounds analyzed are listed in Table 1.3, Chapter 1.2.1.

Table 6.10 Rotational Data for 1.15a in $CDCl_3$

temp. (K)	k (s^{-1})	calc. ν_a-ν_b (Hz)	actual ν_a-ν_b (Hz)
216	21.5	263.0	263.0
220	30.1	259.5	259.5
227	52.2	253.8	253.8
232	82.2	250.0	250.0
238	159	245.8	245.8
244	242	241.8	241.8
249	386	238.7	238.7
257	673	234.0	234.0
263	1.06×10^3	230.8	230.8
270	1.51×10^3	227.2	227.2

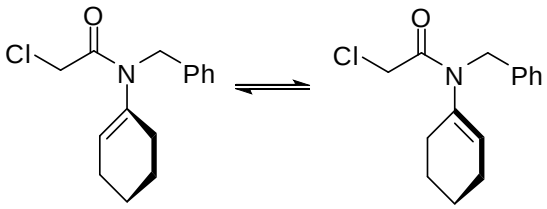

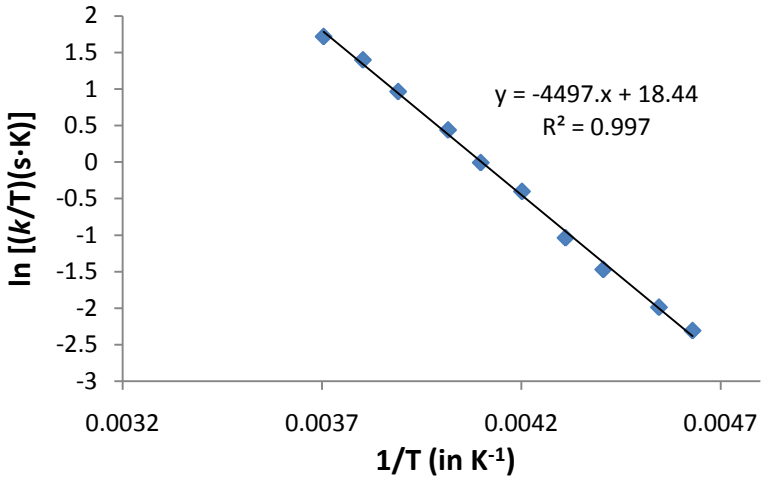

Figure 6.1 Eyring Plot for 1.15a

Table 6.11 Rotational Data for 1.15c in $CDCl_3$

temp. (K)	k (s^{-1})	calc. ν_a-ν_b (Hz)	actual ν_a-ν_b (Hz)
215	20.5	246.5	246.5
220	32.2	242.6	242.6
228	68.2	236.8	236.8
234	131	232.9	232.9
237	166	231.0	231.0
240	211	229.2	229.2
249	418	224.0	224.0
252	508	222.4	222.4
254	632	221.4	221.4
258	826	219.3	219.3
265	1.35×10^3	216.0	216.0
275	2.92×10^3	211.6	211.6
297	1.14×10^4	203.2	203.2

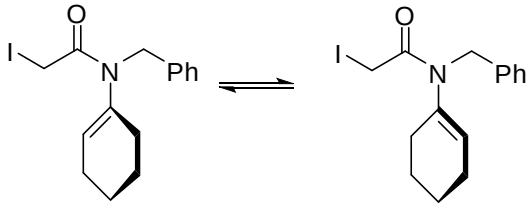

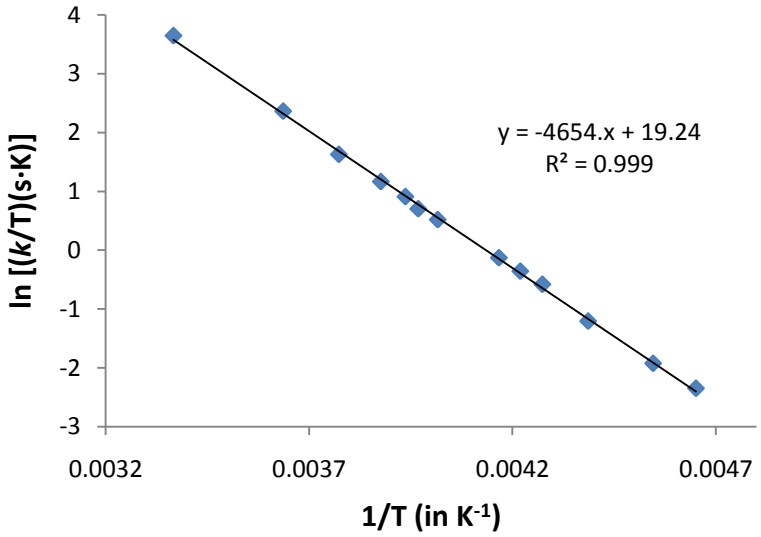

Figure 6.2 Eyring Plot for 1.15c

Table 6.12 Rotational Data for 1.29a in Toluene-*d*8

temp. (K)	*k* (s^{-1})	calc. ν_a-ν_b (Hz)	actual ν_a-ν_b (Hz)
186	57.7	546.3	546.5
191	102	533.3	533.5
202	303	507.9	507.9
222	2.40×10^3	470.6	470.6
233	6.90×10^3	453.8	453.8
245	1.42×10^4	437.7	437.7
256	2.90×10^4	424.8	424.8
266	5.75×10^4	414.3	414.3
279	1.05×10^5	402.0	402.0
290	1.97×10^5	392.8	392.8

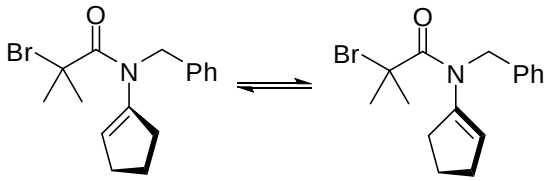

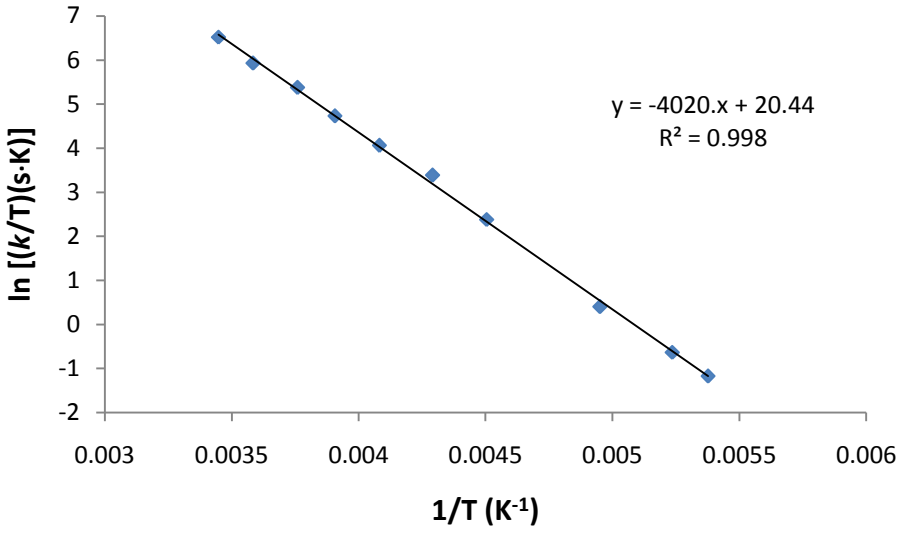

Figure 6.3 Eyring Plot for 1.29a

Table 6.13 Rotational Data for 1.29b in Toluene-*d*8

temp. (K)	*k* (s^{-1})	calc. ν_a-ν_b (Hz)	actual ν_a-ν_b (Hz)
233	5.4	431.8	432.8
245	15.0	409.7	411.1
256	31.9	392.1	391.8
266	80.0	378.0	366.9
279	207	361.9	346.7
311	2.43×10^3	330.0	331.2
327	5.99×10^3	317.3	318.2
339	1.67×10^4	308.9	308.2

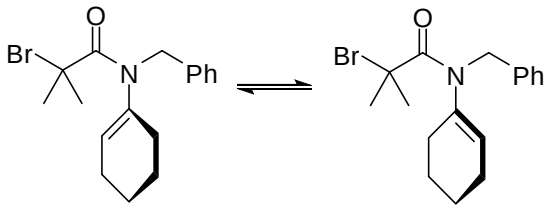

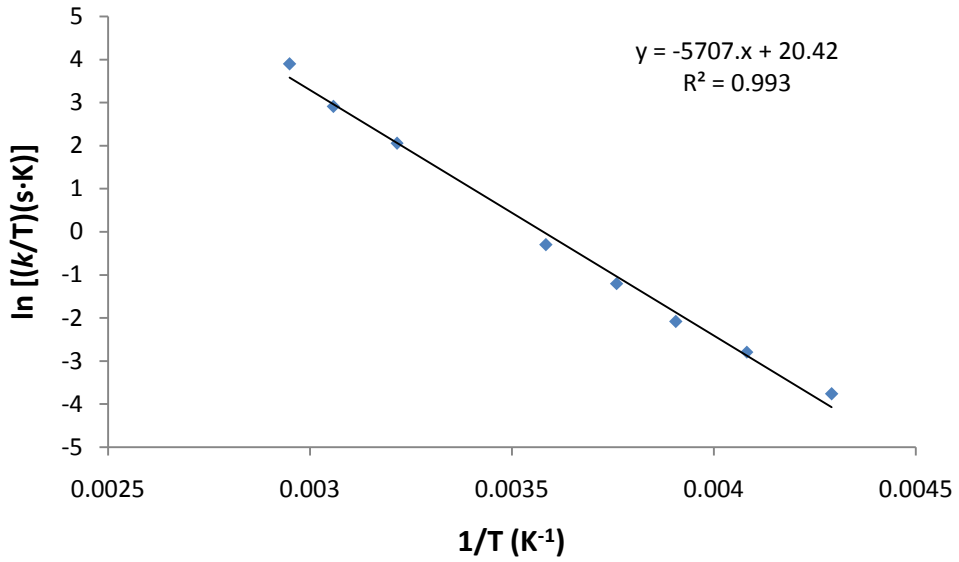

Figure 6.4 Eyring Plot for 1.29b

Table 6.14 Rotational Data for 1.29c in Toluene-*d*8

temp. (K)	*k* (s^{-1})	calc. ν_a-ν_b (Hz)	actual ν_a-ν_b (Hz)
250	16.7	548.5	549.2
261	40.5	522.8	522.3
271	91.5	489.3	491.6
281	172	460.1	459.6
292	374	432.1	412.6
311	1.62×10^3	391.8	392.4
321	3.12×10^3	373.8	374.4
331	5.76×10^3	357.7	356.4
341	1.19×10^4	343.1	344.4
350	2.11×10^4	331.2	331.6

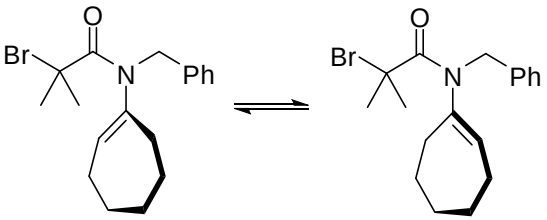

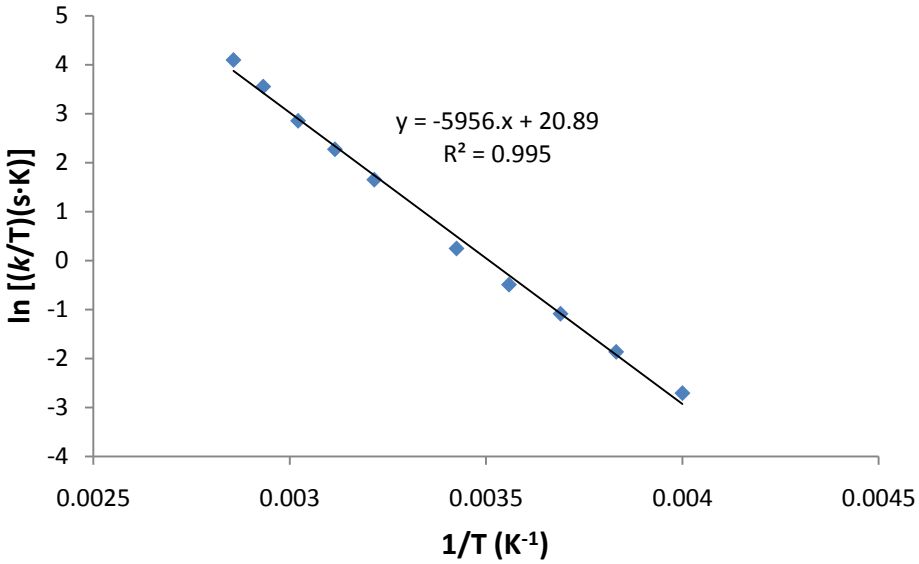

Figure 6.5 Eyring Plot for 1.29c

Table 6.15 Rotational Data for 1.29d in Toluene-*d*8

temp. (K)	k (s^{-1})	calc. ν_a-ν_b (Hz)	actual ν_a-ν_b (Hz)
230	11.0	506.6	508.5
240	22.5	483.5	484.1
250	60.0	463.2	461.6
261	161	443.6	440.6
271	365	427.7	426.1
292	1.73×10^3	399.5	399.6
301	3.43×10^3	389.1	388.6
311	7.33×10^3	378.6	379.6
321	1.41×10^4	369.0	369.6
331	2.63×10^4	360.1	359.9
341	4.62×10^4	352.0	350.9

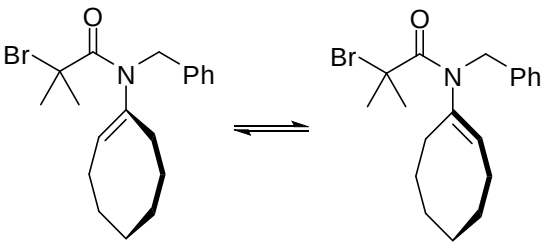

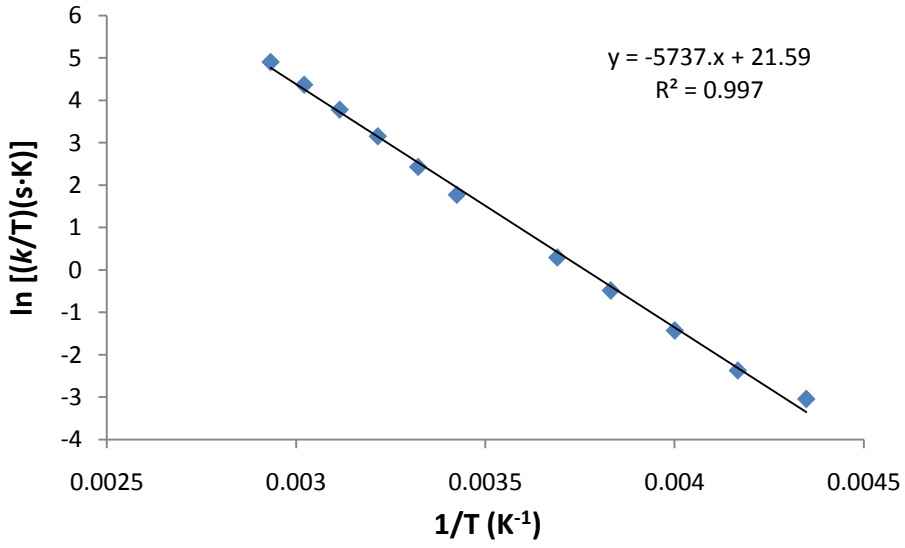

Figure 6.6 Eyring Plot for 1.29d

Table 6.16 Rotational Data for 1.29e in Toluene-*d*8

temp. (K)	*k* (s^{-1})	calc. ν_a-ν_b (Hz)	actual ν_a-ν_b (Hz)
230	15.1	603.9	604.8
240	35.4	584.2	583.8
250	101	566.7	565.9
261	280	549.4	549.9
292	2.80×10^3	510.0	510.0
301	5.17×10^3	500.5	500.0
311	1.06×10^4	490.8	490.0
321	2.36×10^4	481.9	481.7
331	3.94×10^4	473.6	473.4
341	7.01×10^4	466.0	467.1

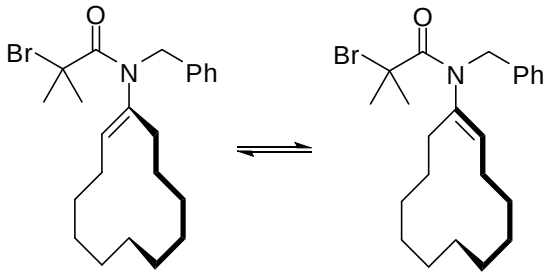

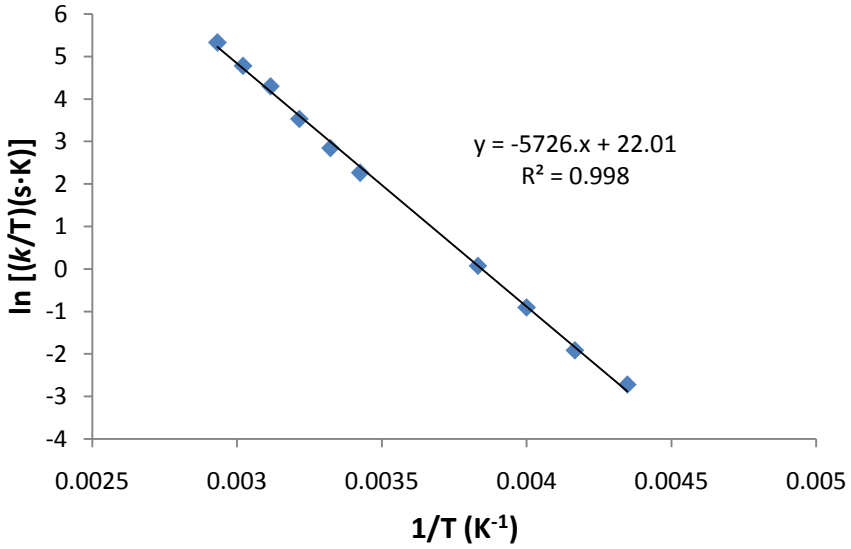

Figure 6.7 Eyring Plot for 1.29e

Table 6.17 Rotational Data for 1.30 in Toluene-*d*8

temp. (K)	*k* (s^{-1})	calc. ν_a-ν_b (Hz)	actual ν_a-ν_b (Hz)
220	8.0	110.9	111.2
230	17.8	105.8	105.8
240	42.8	101.3	101.4
250	106	97.4	97.4
271	432	90.4	90.4
281	836	87.6	87.6
292	1.80×10^3	84.9	84.9
301	3.03×10^3	82.8	82.7
311	5.58×10^3	80.7	80.6

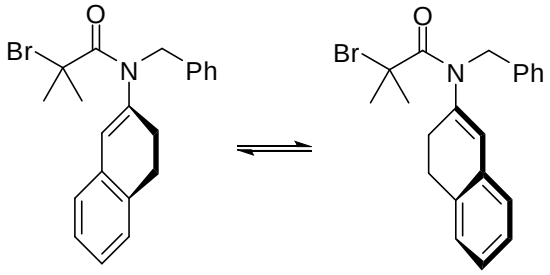

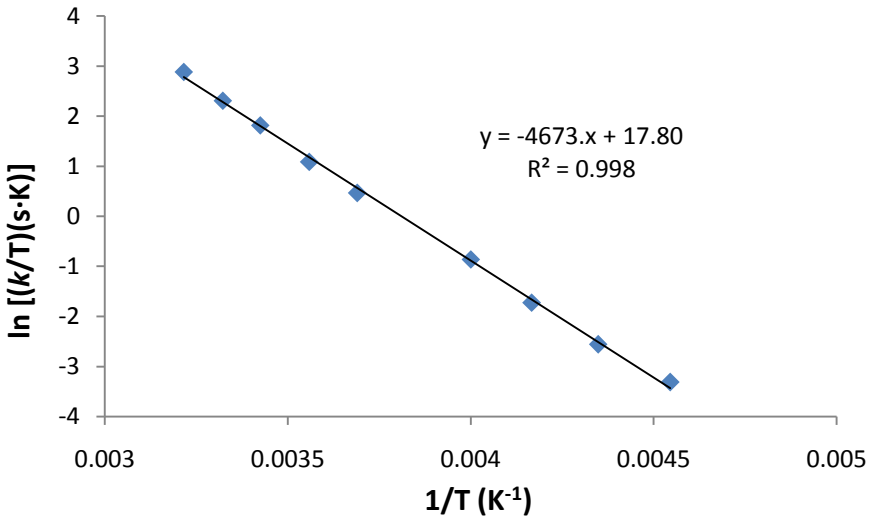

Figure 6.8 Eyring Plot for 1.30

Table 6.18 Rotational Data for 1.31 in Toluene-*d*8

temp. (K)	*k* (s^{-1})	calc. ν_a-ν_b (Hz)	actual ν_a-ν_b (Hz)
341	6.0	600.5	599.3
349	8.9	592.4	587.0
359	14.6	582.9	576.6
369	23.6	574.1	564.7
379	38.9	565.9	553.5

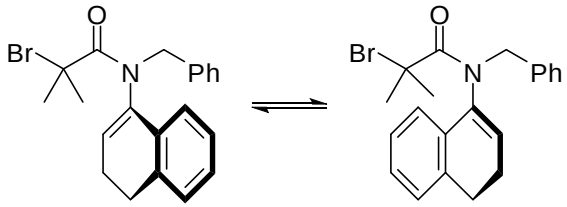

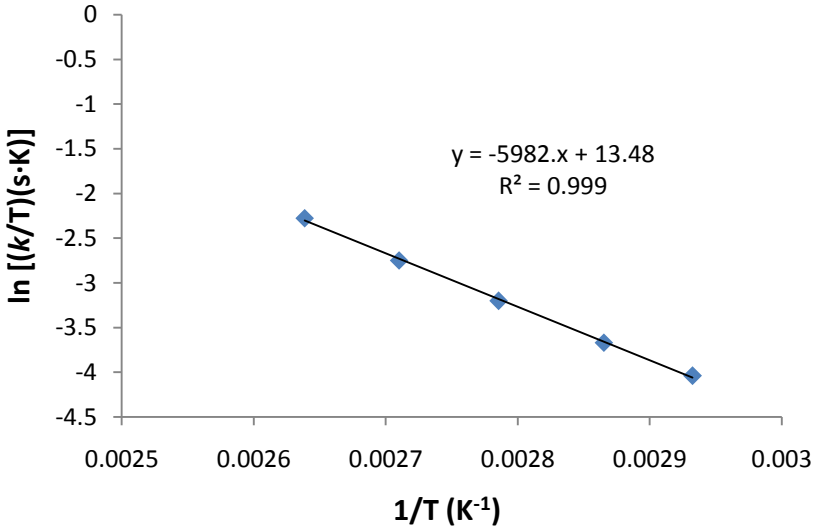

Figure 6.9 Eyring Plot for 1.31

Table 6.19 Rotational Data for 1.32 in Toluene-*d*8

temp. (K)	$k_1 + k_{-1}$ (s^{-1})	calc. ν_a-ν_b (Hz)	actual ν_a-ν_b (Hz)
271	67.0	182.9	180.7
281	136	175.5	175.5
292	316	168.1	168.3
301	656	162.7	162.7
311	1.39×10^3	157.3	157.1
321	2.66×10^3	152.3	152.4
331	4.88×10^3	147.9	148.0
341	1.02×10^4	143.7	143.7
350	1.70×10^4	140.3	140.2

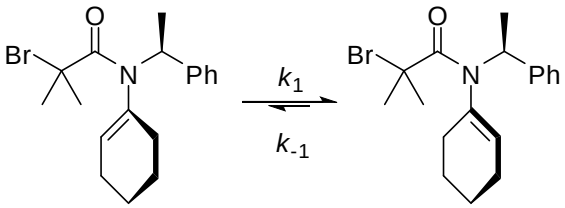

** Note: actual configuration of major diastereomer is unknown.

Upon cooling, two diastereomers were seen in a 2:1 ratio.

Therefore, $k_1 = (1/3)(k_1 + k_{-1})$, and $k_{-1} = (2/3)(k_1 + k_{-1})$ for each temperature.

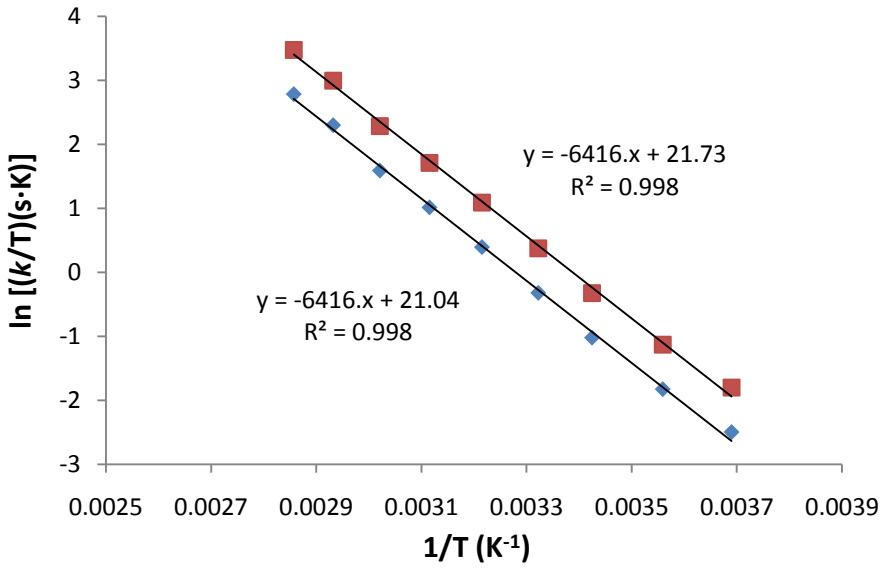

Figure 6.10 Eyring Plot for 1.32

APPENDIX A

X-RAY CRYSTALLOGRAPHY DATA

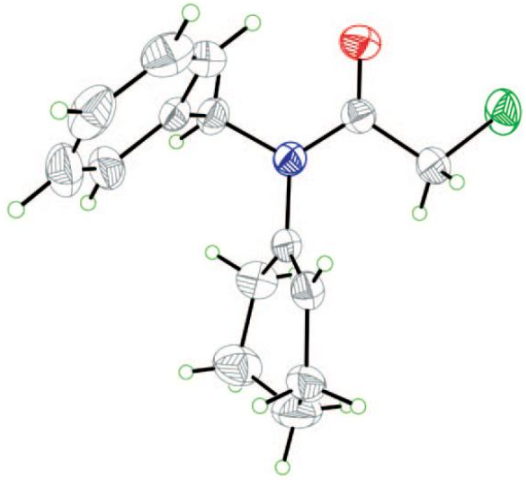

The corresponding CIF file for **1.15a** is shown below, between the lines of "+" symbols.

```
++++++++++++++++++++++++++++++++++++++++++++++++++++++++++++++++++++++++++++++

data_dguth1

_audit_creation_method           SHELXL-97
_chemical_name_systematic        ?
_chemical_name_common            ?
_chemical_melting_point          ?
_chemical_formula_moiety         'C15 H18 Cl N O'
_chemical_formula_sum            'C15 H18 Cl N O'
_chemical_formula_weight         263.75

loop_
_atom_type_symbol
_atom_type_description
_atom_type_scat_dispersion_real
```

```
_atom_type_scat_dispersion_imag
_atom_type_scat_source
C C 0.0033 0.0016 'International Tables Vol C Tables 4.2.6.8 and 6.1.1.4'
H H 0.0000 0.0000 'International Tables Vol C Tables 4.2.6.8 and 6.1.1.4'
N N 0.0061 0.0033 'International Tables Vol C Tables 4.2.6.8 and 6.1.1.4'
O O 0.0106 0.0060 'International Tables Vol C Tables 4.2.6.8 and 6.1.1.4'
Cl Cl 0.1484 0.1585 'International Tables Vol C Tables 4.2.6.8 and
6.1.1.4'

_symmetry_cell_setting           monoclinic
_symmetry_space_group_name_H-M   'P 21'
_symmetry_int_tables_number      4

loop_
_symmetry_equiv_pos_as_xyz
'x, y, z'
'-x, y+1/2, -z'

_cell_length_a                   8.852(5)
_cell_length_b                   9.106(5)
_cell_length_c                   9.389(5)
_cell_angle_alpha                90.00
_cell_angle_beta                 113.263(9)
_cell_angle_gamma                90.00
_cell_volume                     695.2(6)
_cell_formula_units_Z            2
_cell_measurement_temperature    295(2)
_cell_measurement_reflns_used    999
_cell_measurement_theta_min      5
_cell_measurement_theta_max      25

_exptl_crystal_description       plate
_exptl_crystal_colour            colorless
_exptl_crystal_size_max          0.49
_exptl_crystal_size_mid          0.33
_exptl_crystal_size_min          0.06
_exptl_crystal_density_meas      ?
_exptl_crystal_density_diffrn    1.260
_exptl_crystal_density_method    'not measured'
_exptl_crystal_F_000             280
_exptl_absorpt_coefficient_mu    0.263
_exptl_absorpt_correction_type   multi-scan
_exptl_absorpt_correction_T_min  0.8820
_exptl_absorpt_correction_T_max  0.9844
_exptl_absorpt_process_details   'Bruker Sadabs'

_exptl_special_details
;
 ?
;

_diffrn_ambient_temperature      295(2)
_diffrn_radiation_probe          x-ray
_diffrn_radiation_type           MoK\a
```

```
_diffrn_radiation_wavelength     0.71073
_diffrn_source                   'fine-focus sealed tube'
_diffrn_source_type              'Bruker AXS Smart Apex CDD'
_diffrn_radiation_monochromator  graphite
_diffrn_measurement_device_type  'CCD area detector'
_diffrn_measurement_method       'phi and omega scans'
_diffrn_detector_area_resol_mean ?
_diffrn_standards_number         ?
_diffrn_standards_interval_count ?
_diffrn_standards_interval_time  ?
_diffrn_standards_decay_%        ?
_diffrn_reflns_number            6450
_diffrn_reflns_av_R_equivalents  0.0354
_diffrn_reflns_av_sigmaI/netI    0.0511
_diffrn_reflns_limit_h_min       -11
_diffrn_reflns_limit_h_max       11
_diffrn_reflns_limit_k_min       -11
_diffrn_reflns_limit_k_max       11
_diffrn_reflns_limit_l_min       -12
_diffrn_reflns_limit_l_max       12
_diffrn_reflns_theta_min         2.50
_diffrn_reflns_theta_max         27.50
_reflns_number_total             3132
_reflns_number_gt                2471
_reflns_threshold_expression     >2sigma(I)

_computing_data_collection       'Bruker SMART'
_computing_cell_refinement       'Bruker SMART'
_computing_data_reduction        'Bruker SAINT'
_computing_structure_solution    'SHELXS-97 (Sheldrick, 1990)'
_computing_structure_refinement  'SHELXL-97 (Sheldrick, 1997)'
_computing_molecular_graphics    'Bruker SHELXTL'
_computing_publication_material  'Bruker SHELXTL'

_refine_special_details
;
 Refinement of F^2^ against ALL reflections.  The weighted R-factor wR and
 goodness of fit S are based on F^2^, conventional R-factors R are based
 on F, with F set to zero for negative F^2^. The threshold expression of
 F^2^ > 2sigma(F^2^) is used only for calculating R-factors(gt) etc. and
is
 not relevant to the choice of reflections for refinement.  R-factors
based
 on F^2^ are statistically about twice as large as those based on F, and
R-
 factors based on ALL data will be even larger.
;

_refine_ls_structure_factor_coef Fsqd
_refine_ls_matrix_type           full
_refine_ls_weighting_scheme      calc
_refine_ls_weighting_details
'calc w=1/[\s^2^(Fo^2^)+(0.0820P)^2^+0.0000P] where P=(Fo^2^+2Fc^2^)/3'
_atom_sites_solution_primary     direct
```

```
_atom_sites_solution_secondary   difmap
_atom_sites_solution_hydrogens   geom
_refine_ls_hydrogen_treatment    constr
_refine_ls_extinction_method     none
_refine_ls_extinction_coef       ?
_refine_ls_abs_structure_details
'Flack H D (1983), Acta Cryst. A39, 876-881, 1434 Friedel pairs'
_refine_ls_abs_structure_Flack   0.03(8)
_refine_ls_number_reflns         3132
_refine_ls_number_parameters     164
_refine_ls_number_restraints     1
_refine_ls_R_factor_all          0.0643
_refine_ls_R_factor_gt           0.0511
_refine_ls_wR_factor_ref         0.1386
_refine_ls_wR_factor_gt          0.1313
_refine_ls_goodness_of_fit_ref   0.999
_refine_ls_restrained_S_all      0.999
_refine_ls_shift/su_max          0.000
_refine_ls_shift/su_mean         0.000

loop_
_atom_site_label
_atom_site_type_symbol
_atom_site_fract_x
_atom_site_fract_y
_atom_site_fract_z
_atom_site_U_iso_or_equiv
_atom_site_adp_type
_atom_site_occupancy
_atom_site_symmetry_multiplicity
_atom_site_calc_flag
_atom_site_refinement_flags
_atom_site_disorder_assembly
_atom_site_disorder_group
Cl Cl 0.75491(10) 0.74726(7) 0.65329(10) 0.0778(3) Uani 1 1 d . . .
O O 0.7614(3) 0.5602(2) 0.4044(2) 0.0684(5) Uani 1 1 d . . .
N N 0.8214(2) 0.3496(2) 0.5397(2) 0.0480(5) Uani 1 1 d . . .
C1 C 0.9909(3) 0.2263(4) 0.7891(3) 0.0644(7) Uani 1 1 d . . .
H1A H 1.0366 0.3139 0.8497 0.077 Uiso 1 1 calc R . .
H1B H 1.0634 0.1971 0.7391 0.077 Uiso 1 1 calc R . .
C2 C 0.9846(4) 0.1050(5) 0.8962(4) 0.0914(11) Uani 1 1 d . . .
H2A H 0.9779 0.0109 0.8456 0.110 Uiso 1 1 calc R . .
H2B H 1.0849 0.1062 0.9895 0.110 Uiso 1 1 calc R . .
C3 C 0.8403(5) 0.1223(5) 0.9390(5) 0.0948(12) Uani 1 1 d . . .
H3A H 0.8407 0.0434 1.0085 0.114 Uiso 1 1 calc R . .
H3B H 0.8503 0.2143 0.9940 0.114 Uiso 1 1 calc R . .
C4 C 0.6824(4) 0.1206(3) 0.8024(4) 0.0703(8) Uani 1 1 d . . .
H4A H 0.5964 0.1574 0.8324 0.084 Uiso 1 1 calc R . .
H4B H 0.6552 0.0200 0.7677 0.084 Uiso 1 1 calc R . .
C5 C 0.6860(3) 0.2105(3) 0.6714(3) 0.0519(6) Uani 1 1 d . . .
H5A H 0.5872 0.2319 0.5892 0.062 Uiso 1 1 calc R . .
C6 C 0.8245(3) 0.2614(3) 0.6674(2) 0.0449(5) Uani 1 1 d . . .
C7 C 0.8700(3) 0.2771(3) 0.4252(3) 0.0530(6) Uani 1 1 d . . .
H7A H 0.9690 0.2203 0.4788 0.064 Uiso 1 1 calc R . .
```

```
H7B H 0.8952 0.3512 0.3637 0.064 Uiso 1 1 calc R . .
C8 C 0.7385(3) 0.1774(3) 0.3192(3) 0.0480(6) Uani 1 1 d . . .
C9 C 0.7523(4) 0.0264(3) 0.3392(4) 0.0639(7) Uani 1 1 d . . .
H9A H 0.8443 -0.0127 0.4184 0.077 Uiso 1 1 calc R . .
C10 C 0.6327(5) -0.0662(4) 0.2440(5) 0.0772(9) Uani 1 1 d . . .
H10A H 0.6430 -0.1672 0.2599 0.093 Uiso 1 1 calc R . .
C11 C 0.4994(5) -0.0100(4) 0.1265(4) 0.0772(10) Uani 1 1 d . . .
H11A H 0.4201 -0.0728 0.0598 0.093 Uiso 1 1 calc R . .
C12 C 0.4807(4) 0.1416(4) 0.1054(4) 0.0738(8) Uani 1 1 d . . .
H12A H 0.3879 0.1803 0.0269 0.089 Uiso 1 1 calc R . .
C13 C 0.6011(3) 0.2329(3) 0.2021(3) 0.0591(6) Uani 1 1 d . . .
H13A H 0.5894 0.3340 0.1880 0.071 Uiso 1 1 calc R . .
C14 C 0.7709(3) 0.4906(2) 0.5168(3) 0.0487(5) Uani 1 1 d . . .
C15 C 0.7258(4) 0.5560(3) 0.6432(3) 0.0638(7) Uani 1 1 d . . .
H15A H 0.7934 0.5122 0.7421 0.077 Uiso 1 1 calc R . .
H15B H 0.6117 0.5341 0.6220 0.077 Uiso 1 1 calc R . .

loop_
_atom_site_aniso_label
_atom_site_aniso_U_11
_atom_site_aniso_U_22
_atom_site_aniso_U_33
_atom_site_aniso_U_23
_atom_site_aniso_U_13
_atom_site_aniso_U_12
Cl 0.0953(5) 0.0447(3) 0.1103(6) -0.0148(4) 0.0586(5) -0.0098(3)
O 0.0942(15) 0.0537(11) 0.0656(11) 0.0091(9) 0.0404(10) 0.0001(10)
N 0.0520(10) 0.0454(11) 0.0513(11) -0.0008(8) 0.0256(9) -0.0006(8)
C1 0.0541(14) 0.0692(19) 0.0618(15) 0.0029(14) 0.0142(11) -0.0066(13)
C2 0.077(2) 0.101(3) 0.087(2) 0.032(2) 0.0236(18) 0.017(2)
C3 0.103(3) 0.108(3) 0.083(2) 0.046(2) 0.046(2) 0.024(2)
C4 0.0782(18) 0.0528(16) 0.099(2) 0.0161(16) 0.0553(18) 0.0041(14)
C5 0.0522(13) 0.0442(13) 0.0603(14) -0.0031(11) 0.0233(11) 0.0011(10)
C6 0.0511(12) 0.0384(11) 0.0467(11) -0.0037(10) 0.0210(9) -0.0003(10)
C7 0.0560(14) 0.0527(15) 0.0597(14) -0.0058(12) 0.0328(12) -0.0015(11)
C8 0.0609(15) 0.0447(13) 0.0517(13) -0.0006(10) 0.0363(12) 0.0032(10)
C9 0.0672(18) 0.0524(16) 0.0782(18) 0.0048(13) 0.0353(15) 0.0143(12)
C10 0.087(2) 0.0494(15) 0.111(3) -0.0177(17) 0.057(2) -0.0073(15)
C11 0.082(2) 0.083(2) 0.080(2) -0.0334(18) 0.0467(18) -0.0331(18)
C12 0.0663(17) 0.098(3) 0.0549(15) 0.0028(16) 0.0221(13) -0.0038(17)
C13 0.0726(16) 0.0557(16) 0.0516(13) 0.0073(13) 0.0273(12) 0.0047(14)
C14 0.0512(14) 0.0424(12) 0.0523(13) -0.0024(11) 0.0202(11) -0.0066(10)
C15 0.0881(19) 0.0401(13) 0.0739(17) -0.0010(13) 0.0436(16) -0.0005(13)

_geom_special_details
;
 All esds (except the esd in the dihedral angle between two l.s. planes)
 are estimated using the full covariance matrix.  The cell esds are taken
 into account individually in the estimation of esds in distances, angles
 and torsion angles; correlations between esds in cell parameters are only
 used when they are defined by crystal symmetry.  An approximate
(isotropic)
 treatment of cell esds is used for estimating esds involving l.s. planes.
;
```

```
loop_
_geom_bond_atom_site_label_1
_geom_bond_atom_site_label_2
_geom_bond_distance
_geom_bond_site_symmetry_2
_geom_bond_publ_flag
Cl C15 1.757(3) . ?
O C14 1.206(3) . ?
N C14 1.348(3) . ?
N C6 1.434(3) . ?
N C7 1.463(3) . ?
C1 C6 1.499(4) . ?
C1 C2 1.510(5) . ?
C1 H1A 0.9700 . ?
C1 H1B 0.9700 . ?
C2 C3 1.491(5) . ?
C2 H2A 0.9700 . ?
C2 H2B 0.9700 . ?
C3 C4 1.478(6) . ?
C3 H3A 0.9700 . ?
C3 H3B 0.9700 . ?
C4 C5 1.488(4) . ?
C4 H4A 0.9700 . ?
C4 H4B 0.9700 . ?
C5 C6 1.325(3) . ?
C5 H5A 0.9300 . ?
C7 C8 1.501(4) . ?
C7 H7A 0.9700 . ?
C7 H7B 0.9700 . ?
C8 C13 1.374(4) . ?
C8 C9 1.386(4) . ?
C9 C10 1.373(5) . ?
C9 H9A 0.9300 . ?
C10 C11 1.358(5) . ?
C10 H10A 0.9300 . ?
C11 C12 1.395(5) . ?
C11 H11A 0.9300 . ?
C12 C13 1.373(4) . ?
C12 H12A 0.9300 . ?
C13 H13A 0.9300 . ?
C14 C15 1.515(4) . ?
C15 H15A 0.9700 . ?
C15 H15B 0.9700 . ?

loop_
_geom_angle_atom_site_label_1
_geom_angle_atom_site_label_2
_geom_angle_atom_site_label_3
_geom_angle
_geom_angle_site_symmetry_1
_geom_angle_site_symmetry_3
_geom_angle_publ_flag
C14 N C6 124.18(19) . . ?
```

```
C14 N C7 119.2(2) . . ?
C6 N C7 116.6(2) . . ?
C6 C1 C2 112.3(2) . . ?
C6 C1 H1A 109.1 . . ?
C2 C1 H1A 109.1 . . ?
C6 C1 H1B 109.1 . . ?
C2 C1 H1B 109.1 . . ?
H1A C1 H1B 107.9 . . ?
C3 C2 C1 111.3(3) . . ?
C3 C2 H2A 109.4 . . ?
C1 C2 H2A 109.4 . . ?
C3 C2 H2B 109.4 . . ?
C1 C2 H2B 109.4 . . ?
H2A C2 H2B 108.0 . . ?
C4 C3 C2 112.5(3) . . ?
C4 C3 H3A 109.1 . . ?
C2 C3 H3A 109.1 . . ?
C4 C3 H3B 109.1 . . ?
C2 C3 H3B 109.1 . . ?
H3A C3 H3B 107.8 . . ?
C3 C4 C5 112.9(3) . . ?
C3 C4 H4A 109.0 . . ?
C5 C4 H4A 109.0 . . ?
C3 C4 H4B 109.0 . . ?
C5 C4 H4B 109.0 . . ?
H4A C4 H4B 107.8 . . ?
C6 C5 C4 122.5(3) . . ?
C6 C5 H5A 118.7 . . ?
C4 C5 H5A 118.7 . . ?
C5 C6 N 120.5(2) . . ?
C5 C6 C1 123.1(2) . . ?
N C6 C1 116.4(2) . . ?
N C7 C8 112.57(18) . . ?
N C7 H7A 109.1 . . ?
C8 C7 H7A 109.1 . . ?
N C7 H7B 109.1 . . ?
C8 C7 H7B 109.1 . . ?
H7A C7 H7B 107.8 . . ?
C13 C8 C9 118.4(3) . . ?
C13 C8 C7 121.2(2) . . ?
C9 C8 C7 120.4(3) . . ?
C10 C9 C8 121.1(3) . . ?
C10 C9 H9A 119.4 . . ?
C8 C9 H9A 119.4 . . ?
C11 C10 C9 119.8(3) . . ?
C11 C10 H10A 120.1 . . ?
C9 C10 H10A 120.1 . . ?
C10 C11 C12 120.3(3) . . ?
C10 C11 H11A 119.8 . . ?
C12 C11 H11A 119.8 . . ?
C13 C12 C11 119.2(3) . . ?
C13 C12 H12A 120.4 . . ?
C11 C12 H12A 120.4 . . ?
C8 C13 C12 121.1(3) . . ?
```

```
C8 C13 H13A 119.4 . . ?
C12 C13 H13A 119.4 . . ?
O C14 N 123.0(2) . . ?
O C14 C15 122.0(2) . . ?
N C14 C15 115.0(2) . . ?
C14 C15 Cl 110.72(18) . . ?
C14 C15 H15A 109.5 . . ?
Cl C15 H15A 109.5 . . ?
C14 C15 H15B 109.5 . . ?
Cl C15 H15B 109.5 . . ?
H15A C15 H15B 108.1 . . ?

_diffrn_measured_fraction_theta_max 0.985
_diffrn_reflns_theta_full        27.50
_diffrn_measured_fraction_theta_full 0.985
_refine_diff_density_max         0.331
_refine_diff_density_min         -0.193
_refine_diff_density_rms         0.044
```

++

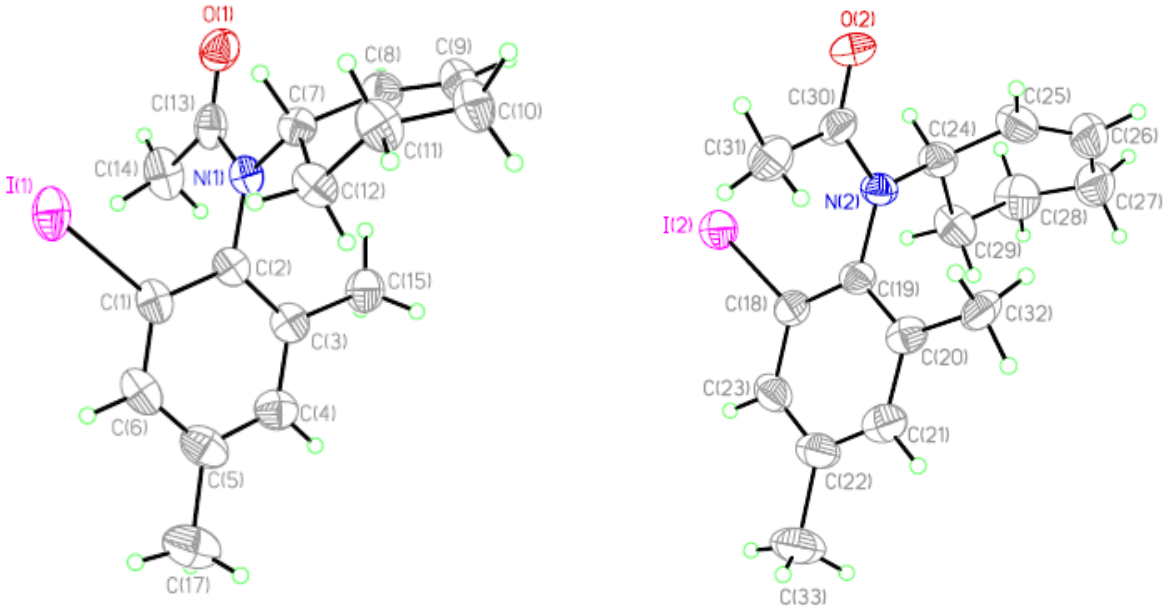

The corresponding CIF file for *anti*-**4.15** is shown below, between the lines of "+" symbols.

++

```
data_dg1009s

_audit_creation_method            SHELXL-97
_chemical_name_systematic
```

```
;
 ?
;
_chemical_name_common              ?
_chemical_melting_point            ?
_chemical_formula_moiety           ?
_chemical_formula_sum
 'C16 H20 I N O'
_chemical_formula_weight           369.23

loop_
 _atom_type_symbol
 _atom_type_description
 _atom_type_scat_dispersion_real
 _atom_type_scat_dispersion_imag
 _atom_type_scat_source
 'C'  'C'   0.0033   0.0016
 'International Tables Vol C Tables 4.2.6.8 and 6.1.1.4'
 'H'  'H'   0.0000   0.0000
 'International Tables Vol C Tables 4.2.6.8 and 6.1.1.4'
 'N'  'N'   0.0061   0.0033
 'International Tables Vol C Tables 4.2.6.8 and 6.1.1.4'
 'O'  'O'   0.0106   0.0060
 'International Tables Vol C Tables 4.2.6.8 and 6.1.1.4'
 'I'  'I'  -0.4742   1.8119
 'International Tables Vol C Tables 4.2.6.8 and 6.1.1.4'

_symmetry_cell_setting             Triclinic
_symmetry_space_group_name_H-M     P-1

loop_
 _symmetry_equiv_pos_as_xyz
 'x, y, z'
 '-x, -y, -z'

_cell_length_a                     9.0294(5)
_cell_length_b                     9.6581(5)
_cell_length_c                     19.4301(10)
_cell_angle_alpha                  79.2830(10)
_cell_angle_beta                   79.3550(10)
_cell_angle_gamma                  79.7700(10)
_cell_volume                       1618.13(15)
_cell_formula_units_Z              4
_cell_measurement_temperature      203(2)
_cell_measurement_reflns_used      5413
_cell_measurement_theta_min        2.16
_cell_measurement_theta_max        32.33

_exptl_crystal_description         ?
_exptl_crystal_colour              ?
_exptl_crystal_size_max            0.26
_exptl_crystal_size_mid            0.21
_exptl_crystal_size_min            0.13
_exptl_crystal_density_meas        0
```

```
_exptl_crystal_density_diffrn     1.516
_exptl_crystal_density_method     'not measured'
_exptl_crystal_F_000              736
_exptl_absorpt_coefficient_mu     1.972
_exptl_absorpt_correction_type    none
_exptl_absorpt_correction_T_min   0.6281
_exptl_absorpt_correction_T_max   0.7836
_exptl_absorpt_process_details    ?

_exptl_special_details
;
 ?
;

_diffrn_ambient_temperature       203(2)
_diffrn_radiation_wavelength      0.71073
_diffrn_radiation_type            MoK\a
_diffrn_radiation_source          'fine-focus sealed tube'
_diffrn_radiation_monochromator   graphite
_diffrn_measurement_device_type   'CCD area detector'
_diffrn_measurement_method        'phi and omega scans'
_diffrn_detector_area_resol_mean  ?
_diffrn_standards_number          ?
_diffrn_standards_interval_count  ?
_diffrn_standards_interval_time   ?
_diffrn_standards_decay_%         ?
_diffrn_reflns_number             15820
_diffrn_reflns_av_R_equivalents   0.0195
_diffrn_reflns_av_sigmaI/netI     0.0291
_diffrn_reflns_limit_h_min        -11
_diffrn_reflns_limit_h_max        11
_diffrn_reflns_limit_k_min        -12
_diffrn_reflns_limit_k_max        12
_diffrn_reflns_limit_l_min        -25
_diffrn_reflns_limit_l_max        25
_diffrn_reflns_theta_min          2.16
_diffrn_reflns_theta_max          27.50
_reflns_number_total              7401
_reflns_number_gt                 5740
_reflns_threshold_expression      >2sigma(I)

_computing_data_collection        'Bruker SMART'
_computing_cell_refinement        'Bruker SMART'
_computing_data_reduction         'Bruker SAINT'
_computing_structure_solution     'SHELXS-97 (Sheldrick, 1990)'
_computing_structure_refinement   'SHELXL-97 (Sheldrick, 1997)'
_computing_molecular_graphics     'Bruker SHELXTL'
_computing_publication_material   'Bruker SHELXTL'

_refine_special_details
;
 Refinement of F^2^ against ALL reflections.  The weighted R-factor wR and
 goodness of fit S are based on F^2^, conventional R-factors R are based
 on F, with F set to zero for negative F^2^. The threshold expression of
```

```
 F^2^ > 2sigma(F^2^) is used only for calculating R-factors(gt) etc. and
is
 not relevant to the choice of reflections for refinement.  R-factors
based
 on F^2^ are statistically about twice as large as those based on F, and
R-
 factors based on ALL data will be even larger.
;

_refine_ls_structure_factor_coef  Fsqd
_refine_ls_matrix_type            full
_refine_ls_weighting_scheme       calc
_refine_ls_weighting_details
 'calc w=1/[\s^2^(Fo^2^)+(0.0780P)^2^+0.0000P] where P=(Fo^2^+2Fc^2^)/3'
_atom_sites_solution_primary      direct
_atom_sites_solution_secondary    difmap
_atom_sites_solution_hydrogens    geom
_refine_ls_hydrogen_treatment     mixed
_refine_ls_extinction_method      none
_refine_ls_extinction_coef        ?
_refine_ls_number_reflns          7401
_refine_ls_number_parameters      343
_refine_ls_number_restraints      0
_refine_ls_R_factor_all           0.0627
_refine_ls_R_factor_gt            0.0490
_refine_ls_wR_factor_ref          0.1482
_refine_ls_wR_factor_gt           0.1410
_refine_ls_goodness_of_fit_ref    1.184
_refine_ls_restrained_S_all       1.184
_refine_ls_shift/su_max           0.001
_refine_ls_shift/su_mean          0.000

loop_
 _atom_site_label
 _atom_site_type_symbol
 _atom_site_fract_x
 _atom_site_fract_y
 _atom_site_fract_z
 _atom_site_U_iso_or_equiv
 _atom_site_adp_type
 _atom_site_occupancy
 _atom_site_symmetry_multiplicity
 _atom_site_calc_flag
 _atom_site_refinement_flags
 _atom_site_disorder_assembly
 _atom_site_disorder_group
I1 I 0.49755(3) 0.95261(3) 0.131604(19) 0.06503(13) Uani 1 1 d . . .
N1 N 0.2237(4) 0.8249(3) 0.08862(17) 0.0442(7) Uani 1 1 d . . .
C1 C 0.2910(5) 0.9000(4) 0.1920(2) 0.0505(10) Uani 1 1 d . . .
O1 O 0.2479(4) 0.9101(3) -0.02927(17) 0.0645(8) Uani 1 1 d . . .
I2 I 0.59107(4) -0.00035(3) 0.382897(17) 0.06506(13) Uani 1 1 d . . .
N2 N 0.4249(4) 0.3198(4) 0.40633(16) 0.0473(8) Uani 1 1 d . . .
C2 C 0.1861(4) 0.8503(4) 0.1602(2) 0.0453(9) Uani 1 1 d . . .
O2 O 0.3729(4) 0.2951(4) 0.52553(16) 0.0740(10) Uani 1 1 d . . .
```

```
C3 C 0.0471(4) 0.8257(4) 0.2000(2) 0.0498(9) Uani 1 1 d . . .
C4 C 0.0174(5) 0.8438(5) 0.2703(2) 0.0596(11) Uani 1 1 d . . .
H4A H -0.0771 0.8261 0.2972 0.071 Uiso 1 1 calc R . .
C5 C 0.1225(6) 0.8871(5) 0.3026(3) 0.0645(12) Uani 1 1 d . . .
C6 C 0.2579(5) 0.9181(5) 0.2619(3) 0.0603(11) Uani 1 1 d . . .
H6A H 0.3285 0.9520 0.2821 0.072 Uiso 1 1 calc R . .
C7 C 0.3017(4) 0.6813(4) 0.0725(2) 0.0456(9) Uani 1 1 d . . .
H7A H 0.3926 0.6967 0.0364 0.055 Uiso 1 1 calc R . .
C8 C 0.2010(5) 0.6114(5) 0.0406(2) 0.0521(10) Uani 1 1 d . . .
H8A H 0.1329 0.6696 0.0122 0.063 Uiso 1 1 calc R . .
C9 C 0.2034(5) 0.4727(5) 0.0503(3) 0.0590(11) Uani 1 1 d . . .
H9A H 0.1372 0.4365 0.0284 0.071 Uiso 1 1 calc R . .
C10 C 0.3066(6) 0.3694(5) 0.0946(3) 0.0658(12) Uani 1 1 d . . .
H10A H 0.2457 0.3272 0.1380 0.079 Uiso 1 1 calc R . .
H10B H 0.3573 0.2923 0.0682 0.079 Uiso 1 1 calc R . .
C11 C 0.4246(6) 0.4400(5) 0.1139(3) 0.0648(12) Uani 1 1 d . . .
H11A H 0.5057 0.4531 0.0731 0.078 Uiso 1 1 calc R . .
H11B H 0.4701 0.3782 0.1529 0.078 Uiso 1 1 calc R . .
C12 C 0.3564(5) 0.5854(4) 0.1363(2) 0.0550(10) Uani 1 1 d . . .
H12A H 0.2712 0.5748 0.1753 0.066 Uiso 1 1 calc R . .
H12B H 0.4337 0.6260 0.1523 0.066 Uiso 1 1 calc R . .
C13 C 0.2072(5) 0.9316(4) 0.0316(3) 0.0536(10) Uani 1 1 d . . .
C14 C 0.1313(6) 1.0770(5) 0.0490(3) 0.0737(14) Uani 1 1 d . . .
H14A H 0.1250 1.1440 0.0054 0.111 Uiso 1 1 calc R . .
H14B H 0.1909 1.1099 0.0778 0.111 Uiso 1 1 calc R . .
H14C H 0.0296 1.0700 0.0750 0.111 Uiso 1 1 calc R . .
C15 C -0.0720(5) 0.7786(6) 0.1682(3) 0.0676(13) Uani 1 1 d . . .
H15A H -0.0345 0.7716 0.1187 0.101 Uiso 1 1 calc R . .
H15B H -0.1643 0.8475 0.1719 0.101 Uiso 1 1 calc R . .
H15C H -0.0941 0.6862 0.1936 0.101 Uiso 1 1 calc R . .
C17 C 0.0905(8) 0.9005(7) 0.3813(3) 0.0940(19) Uani 1 1 d . . .
H17A H 0.1764 0.9323 0.3941 0.141 Uiso 1 1 calc R . .
H17B H 0.0751 0.8085 0.4094 0.141 Uiso 1 1 calc R . .
H17C H -0.0004 0.9691 0.3905 0.141 Uiso 1 1 calc R . .
C18 C 0.6153(5) 0.1998(5) 0.3213(2) 0.0517(10) Uani 1 1 d . . .
C19 C 0.5357(4) 0.3236(4) 0.34344(19) 0.0458(9) Uani 1 1 d . . .
C20 C 0.5639(5) 0.4556(5) 0.3033(2) 0.0506(9) Uani 1 1 d . . .
C21 C 0.6696(5) 0.4553(5) 0.2416(2) 0.0598(11) Uani 1 1 d . . .
H21A H 0.6894 0.5430 0.2142 0.072 Uiso 1 1 calc R . .
C22 C 0.7466(5) 0.3317(6) 0.2190(2) 0.0646(12) Uani 1 1 d . . .
C23 C 0.7207(5) 0.2047(5) 0.2591(2) 0.0601(11) Uani 1 1 d . . .
H23A H 0.7743 0.1195 0.2448 0.072 Uiso 1 1 calc R . .
C24 C 0.2611(5) 0.3116(5) 0.4029(2) 0.0565(10) Uani 1 1 d . . .
H24A H 0.2311 0.2291 0.4380 0.068 Uiso 1 1 calc R . .
C25 C 0.1575(6) 0.4417(6) 0.4231(3) 0.0669(12) Uani 1 1 d . . .
H25A H 0.1774 0.4816 0.4604 0.080 Uiso 1 1 calc R . .
C26 C 0.0406(6) 0.5032(6) 0.3917(3) 0.0787(15) Uani 1 1 d . . .
H26A H -0.0179 0.5856 0.4071 0.094 Uiso 1 1 calc R . .
C27 C -0.0040(7) 0.4482(7) 0.3327(3) 0.0849(16) Uani 1 1 d . . .
H27A H -0.1148 0.4509 0.3407 0.102 Uiso 1 1 calc R . .
H27B H 0.0239 0.5103 0.2879 0.102 Uiso 1 1 calc R . .
C28 C 0.0713(7) 0.3003(7) 0.3273(3) 0.0856(17) Uani 1 1 d . . .
H28A H 0.0582 0.2753 0.2824 0.103 Uiso 1 1 calc R . .
H28B H 0.0237 0.2343 0.3662 0.103 Uiso 1 1 calc R . .
```

```
C29 C 0.2413(6) 0.2861(6) 0.3309(3) 0.0695(13) Uani 1 1 d . . .
H29A H 0.2918 0.1905 0.3231 0.083 Uiso 1 1 calc R . .
H29B H 0.2882 0.3557 0.2937 0.083 Uiso 1 1 calc R . .
C30 C 0.4657(6) 0.3075(5) 0.4722(2) 0.0559(10) Uani 1 1 d . . .
C31 C 0.6300(6) 0.3130(6) 0.4740(3) 0.0724(14) Uani 1 1 d . . .
H31A H 0.6455 0.3038 0.5228 0.109 Uiso 1 1 calc R . .
H31B H 0.6570 0.4032 0.4480 0.109 Uiso 1 1 calc R . .
H31C H 0.6936 0.2355 0.4524 0.109 Uiso 1 1 calc R . .
C32 C 0.5031(8) 0.6039(5) 0.3257(2) 0.093(2) Uani 1 1 d . . .
H32A H 0.5385 0.6775 0.2882 0.139 Uiso 1 1 calc R . .
H32B H 0.5403 0.6090 0.3688 0.139 Uiso 1 1 calc R . .
H32C H 0.3926 0.6177 0.3342 0.139 Uiso 1 1 calc R . .
C33 C 0.8587(7) 0.3350(8) 0.1495(3) 0.096(2) Uani 1 1 d . . .
H33A H 0.9033 0.2384 0.1429 0.145 Uiso 1 1 calc R . .
H33B H 0.9387 0.3888 0.1512 0.145 Uiso 1 1 calc R . .
H33C H 0.8052 0.3799 0.1103 0.145 Uiso 1 1 calc R . .

loop_
 _atom_site_aniso_label
 _atom_site_aniso_U_11
 _atom_site_aniso_U_22
 _atom_site_aniso_U_33
 _atom_site_aniso_U_23
 _atom_site_aniso_U_13
 _atom_site_aniso_U_12
I1 0.04592(18) 0.0609(2) 0.0939(3) -0.01275(16) -0.02136(15) -0.01130(13)
N1 0.0427(17) 0.0396(16) 0.0523(19) -0.0072(14) -0.0150(14) -0.0040(13)
C1 0.044(2) 0.043(2) 0.067(3) -0.0152(19) -0.0163(19) -0.0005(16)
O1 0.072(2) 0.069(2) 0.054(2) 0.0052(15) -0.0150(16) -0.0230(16)
I2 0.0679(2) 0.0574(2) 0.0637(2) -0.00712(14) -0.00463(15) -0.00129(15)
N2 0.0428(18) 0.062(2) 0.0365(17) -0.0104(15) -0.0044(13) -0.0057(15)
C2 0.044(2) 0.041(2) 0.052(2) -0.0082(16) -0.0145(17) 0.0014(15)
O2 0.084(2) 0.092(2) 0.0349(17) -0.0033(15) -0.0019(16) 0.0025(19)
C3 0.040(2) 0.050(2) 0.059(3) -0.0112(18) -0.0124(18) 0.0022(16)
C4 0.058(3) 0.054(2) 0.062(3) -0.015(2) -0.006(2) 0.004(2)
C5 0.072(3) 0.055(3) 0.067(3) -0.024(2) -0.020(2) 0.013(2)
C6 0.059(3) 0.055(3) 0.075(3) -0.025(2) -0.026(2) 0.000(2)
C7 0.0380(19) 0.046(2) 0.051(2) -0.0081(17) -0.0058(16) -0.0015(15)
C8 0.052(2) 0.059(3) 0.048(2) -0.0086(18) -0.0146(18) -0.0067(19)
C9 0.055(3) 0.056(3) 0.073(3) -0.023(2) -0.014(2) -0.009(2)
C10 0.068(3) 0.048(2) 0.086(4) -0.019(2) -0.018(3) -0.007(2)
C11 0.064(3) 0.051(3) 0.082(3) -0.017(2) -0.025(2) 0.006(2)
C12 0.055(2) 0.053(2) 0.060(3) -0.017(2) -0.022(2) 0.0048(19)
C13 0.045(2) 0.050(2) 0.071(3) -0.002(2) -0.021(2) -0.0136(17)
C14 0.080(4) 0.050(3) 0.097(4) -0.001(2) -0.046(3) -0.003(2)
C15 0.048(3) 0.089(4) 0.072(3) -0.015(3) -0.011(2) -0.025(2)
C17 0.114(5) 0.100(5) 0.069(4) -0.031(3) -0.015(3) 0.000(4)
C18 0.054(2) 0.059(3) 0.042(2) -0.0081(18) -0.0120(18) -0.0034(19)
C19 0.044(2) 0.061(2) 0.0344(19) -0.0093(17) -0.0085(15) -0.0070(17)
C20 0.053(2) 0.061(2) 0.044(2) -0.0058(18) -0.0148(18) -0.0177(19)
C21 0.057(3) 0.075(3) 0.051(3) -0.002(2) -0.012(2) -0.025(2)
C22 0.048(2) 0.100(4) 0.046(2) -0.011(2) -0.0033(19) -0.016(2)
C23 0.051(2) 0.076(3) 0.053(3) -0.022(2) -0.005(2) 0.002(2)
C24 0.045(2) 0.073(3) 0.051(2) -0.007(2) -0.0066(18) -0.012(2)
```

```
C25 0.055(3) 0.080(3) 0.063(3) -0.018(2) 0.002(2) -0.008(2)
C26 0.055(3) 0.083(4) 0.089(4) -0.003(3) -0.010(3) 0.003(3)
C27 0.060(3) 0.097(4) 0.088(4) 0.004(3) -0.014(3) -0.003(3)
C28 0.068(4) 0.113(5) 0.086(4) -0.018(3) -0.027(3) -0.024(3)
C29 0.057(3) 0.086(4) 0.075(3) -0.035(3) -0.013(2) -0.008(2)
C30 0.070(3) 0.057(2) 0.038(2) -0.0047(18) -0.016(2) 0.001(2)
C31 0.071(3) 0.099(4) 0.052(3) -0.014(3) -0.027(2) -0.005(3)
C32 0.161(6) 0.048(3) 0.035(2) -0.0027(19) 0.009(3) 0.046(3)
C33 0.079(4) 0.133(6) 0.067(4) -0.009(3) 0.019(3) -0.024(4)

_geom_special_details
;
 All esds (except the esd in the dihedral angle between two l.s. planes)
 are estimated using the full covariance matrix.  The cell esds are taken
 into account individually in the estimation of esds in distances, angles
 and torsion angles; correlations between esds in cell parameters are only
 used when they are defined by crystal symmetry.  An approximate
(isotropic)
 treatment of cell esds is used for estimating esds involving l.s. planes.
;

loop_
 _geom_bond_atom_site_label_1
 _geom_bond_atom_site_label_2
 _geom_bond_distance
 _geom_bond_site_symmetry_2
 _geom_bond_publ_flag
I1 C1 2.102(4) . ?
N1 C13 1.376(5) . ?
N1 C2 1.426(5) . ?
N1 C7 1.500(5) . ?
C1 C6 1.373(6) . ?
C1 C2 1.412(5) . ?
O1 C13 1.217(5) . ?
I2 C18 2.101(4) . ?
N2 C30 1.375(5) . ?
N2 C19 1.428(5) . ?
N2 C24 1.509(5) . ?
C2 C3 1.382(6) . ?
O2 C30 1.208(5) . ?
C3 C4 1.380(6) . ?
C3 C15 1.506(6) . ?
C4 C5 1.390(7) . ?
C4 H4A 0.9400 . ?
C5 C6 1.377(7) . ?
C5 C17 1.528(7) . ?
C6 H6A 0.9400 . ?
C7 C8 1.499(6) . ?
C7 C12 1.509(5) . ?
C7 H7A 0.9900 . ?
C8 C9 1.314(6) . ?
C8 H8A 0.9400 . ?
C9 C10 1.501(7) . ?
C9 H9A 0.9400 . ?
```

```
C10 C11 1.497(7) . ?
C10 H10A 0.9800 . ?
C10 H10B 0.9800 . ?
C11 C12 1.537(6) . ?
C11 H11A 0.9800 . ?
C11 H11B 0.9800 . ?
C12 H12A 0.9800 . ?
C12 H12B 0.9800 . ?
C13 C14 1.518(7) . ?
C14 H14A 0.9700 . ?
C14 H14B 0.9700 . ?
C14 H14C 0.9700 . ?
C15 H15A 0.9700 . ?
C15 H15B 0.9700 . ?
C15 H15C 0.9700 . ?
C17 H17A 0.9700 . ?
C17 H17B 0.9700 . ?
C17 H17C 0.9700 . ?
C18 C19 1.380(6) . ?
C18 C23 1.391(6) . ?
C19 C20 1.404(6) . ?
C20 C21 1.388(6) . ?
C20 C32 1.551(6) . ?
C21 C22 1.374(7) . ?
C21 H21A 0.9400 . ?
C22 C23 1.359(7) . ?
C22 C33 1.530(7) . ?
C23 H23A 0.9400 . ?
C24 C25 1.496(7) . ?
C24 C29 1.511(6) . ?
C24 H24A 0.9900 . ?
C25 C26 1.311(7) . ?
C25 H25A 0.9400 . ?
C26 C27 1.494(8) . ?
C26 H26A 0.9400 . ?
C27 C28 1.483(9) . ?
C27 H27A 0.9800 . ?
C27 H27B 0.9800 . ?
C28 C29 1.530(7) . ?
C28 H28A 0.9800 . ?
C28 H28B 0.9800 . ?
C29 H29A 0.9800 . ?
C29 H29B 0.9800 . ?
C30 C31 1.501(7) . ?
C31 H31A 0.9700 . ?
C31 H31B 0.9700 . ?
C31 H31C 0.9700 . ?
C32 H32A 0.9700 . ?
C32 H32B 0.9700 . ?
C32 H32C 0.9700 . ?
C33 H33A 0.9700 . ?
C33 H33B 0.9700 . ?
C33 H33C 0.9700 . ?
```

```
loop_
 _geom_angle_atom_site_label_1
 _geom_angle_atom_site_label_2
 _geom_angle_atom_site_label_3
 _geom_angle
 _geom_angle_site_symmetry_1
 _geom_angle_site_symmetry_3
 _geom_angle_publ_flag
C13 N1 C2 122.6(3) . . ?
C13 N1 C7 116.8(3) . . ?
C2 N1 C7 120.1(3) . . ?
C6 C1 C2 120.6(4) . . ?
C6 C1 I1 119.2(3) . . ?
C2 C1 I1 120.2(3) . . ?
C30 N2 C19 121.6(4) . . ?
C30 N2 C24 117.8(3) . . ?
C19 N2 C24 120.2(3) . . ?
C3 C2 C1 118.8(4) . . ?
C3 C2 N1 120.7(3) . . ?
C1 C2 N1 120.6(4) . . ?
C4 C3 C2 119.3(4) . . ?
C4 C3 C15 119.4(4) . . ?
C2 C3 C15 121.3(4) . . ?
C3 C4 C5 122.2(5) . . ?
C3 C4 H4A 118.9 . . ?
C5 C4 H4A 118.9 . . ?
C6 C5 C4 118.3(4) . . ?
C6 C5 C17 120.3(5) . . ?
C4 C5 C17 121.5(5) . . ?
C5 C6 C1 120.8(4) . . ?
C5 C6 H6A 119.6 . . ?
C1 C6 H6A 119.6 . . ?
C8 C7 N1 110.9(3) . . ?
C8 C7 C12 111.2(3) . . ?
N1 C7 C12 112.7(3) . . ?
C8 C7 H7A 107.3 . . ?
N1 C7 H7A 107.3 . . ?
C12 C7 H7A 107.3 . . ?
C9 C8 C7 123.1(4) . . ?
C9 C8 H8A 118.4 . . ?
C7 C8 H8A 118.4 . . ?
C8 C9 C10 123.2(4) . . ?
C8 C9 H9A 118.4 . . ?
C10 C9 H9A 118.4 . . ?
C11 C10 C9 111.8(4) . . ?
C11 C10 H10A 109.3 . . ?
C9 C10 H10A 109.3 . . ?
C11 C10 H10B 109.3 . . ?
C9 C10 H10B 109.3 . . ?
H10A C10 H10B 107.9 . . ?
C10 C11 C12 111.7(4) . . ?
C10 C11 H11A 109.3 . . ?
C12 C11 H11A 109.3 . . ?
C10 C11 H11B 109.3 . . ?
```

```
C12 C11 H11B 109.3 . . ?
H11A C11 H11B 107.9 . . ?
C7 C12 C11 107.4(4) . . ?
C7 C12 H12A 110.2 . . ?
C11 C12 H12A 110.2 . . ?
C7 C12 H12B 110.2 . . ?
C11 C12 H12B 110.2 . . ?
H12A C12 H12B 108.5 . . ?
O1 C13 N1 122.0(4) . . ?
O1 C13 C14 121.9(4) . . ?
N1 C13 C14 116.1(4) . . ?
C13 C14 H14A 109.5 . . ?
C13 C14 H14B 109.5 . . ?
H14A C14 H14B 109.5 . . ?
C13 C14 H14C 109.5 . . ?
H14A C14 H14C 109.5 . . ?
H14B C14 H14C 109.5 . . ?
C3 C15 H15A 109.5 . . ?
C3 C15 H15B 109.5 . . ?
H15A C15 H15B 109.5 . . ?
C3 C15 H15C 109.5 . . ?
H15A C15 H15C 109.5 . . ?
H15B C15 H15C 109.5 . . ?
C5 C17 H17A 109.5 . . ?
C5 C17 H17B 109.5 . . ?
H17A C17 H17B 109.5 . . ?
C5 C17 H17C 109.5 . . ?
H17A C17 H17C 109.5 . . ?
H17B C17 H17C 109.5 . . ?
C19 C18 C23 120.7(4) . . ?
C19 C18 I2 121.2(3) . . ?
C23 C18 I2 117.9(3) . . ?
C18 C19 C20 119.3(4) . . ?
C18 C19 N2 121.2(4) . . ?
C20 C19 N2 119.4(4) . . ?
C21 C20 C19 117.9(4) . . ?
C21 C20 C32 115.6(4) . . ?
C19 C20 C32 126.1(4) . . ?
C22 C21 C20 122.5(4) . . ?
C22 C21 H21A 118.7 . . ?
C20 C21 H21A 118.7 . . ?
C23 C22 C21 119.0(4) . . ?
C23 C22 C33 119.8(5) . . ?
C21 C22 C33 121.2(5) . . ?
C22 C23 C18 120.5(4) . . ?
C22 C23 H23A 119.8 . . ?
C18 C23 H23A 119.8 . . ?
C25 C24 N2 111.4(4) . . ?
C25 C24 C29 110.9(4) . . ?
N2 C24 C29 112.0(3) . . ?
C25 C24 H24A 107.5 . . ?
N2 C24 H24A 107.5 . . ?
C29 C24 H24A 107.5 . . ?
C26 C25 C24 123.8(5) . . ?
```

```
C26 C25 H25A 118.1 . . ?
C24 C25 H25A 118.1 . . ?
C25 C26 C27 123.0(5) . . ?
C25 C26 H26A 118.5 . . ?
C27 C26 H26A 118.5 . . ?
C28 C27 C26 111.8(5) . . ?
C28 C27 H27A 109.3 . . ?
C26 C27 H27A 109.3 . . ?
C28 C27 H27B 109.3 . . ?
C26 C27 H27B 109.3 . . ?
H27A C27 H27B 107.9 . . ?
C27 C28 C29 110.4(5) . . ?
C27 C28 H28A 109.6 . . ?
C29 C28 H28A 109.6 . . ?
C27 C28 H28B 109.6 . . ?
C29 C28 H28B 109.6 . . ?
H28A C28 H28B 108.1 . . ?
C24 C29 C28 109.4(4) . . ?
C24 C29 H29A 109.8 . . ?
C28 C29 H29A 109.8 . . ?
C24 C29 H29B 109.8 . . ?
C28 C29 H29B 109.8 . . ?
H29A C29 H29B 108.2 . . ?
O2 C30 N2 121.3(4) . . ?
O2 C30 C31 122.1(4) . . ?
N2 C30 C31 116.6(4) . . ?
C30 C31 H31A 109.5 . . ?
C30 C31 H31B 109.5 . . ?
H31A C31 H31B 109.5 . . ?
C30 C31 H31C 109.5 . . ?
H31A C31 H31C 109.5 . . ?
H31B C31 H31C 109.5 . . ?
C20 C32 H32A 109.5 . . ?
C20 C32 H32B 109.5 . . ?
H32A C32 H32B 109.5 . . ?
C20 C32 H32C 109.5 . . ?
H32A C32 H32C 109.5 . . ?
H32B C32 H32C 109.5 . . ?
C22 C33 H33A 109.5 . . ?
C22 C33 H33B 109.5 . . ?
H33A C33 H33B 109.5 . . ?
C22 C33 H33C 109.5 . . ?
H33A C33 H33C 109.5 . . ?
H33B C33 H33C 109.5 . . ?

_diffrn_measured_fraction_theta_max    0.994
_diffrn_reflns_theta_full              27.50
_diffrn_measured_fraction_theta_full   0.994
_refine_diff_density_max    1.559
_refine_diff_density_min   -0.605
_refine_diff_density_rms    0.107

++++++++++++++++++++++++++++++++++++++++++++++++++++++++++++++++++++++++++++++
```

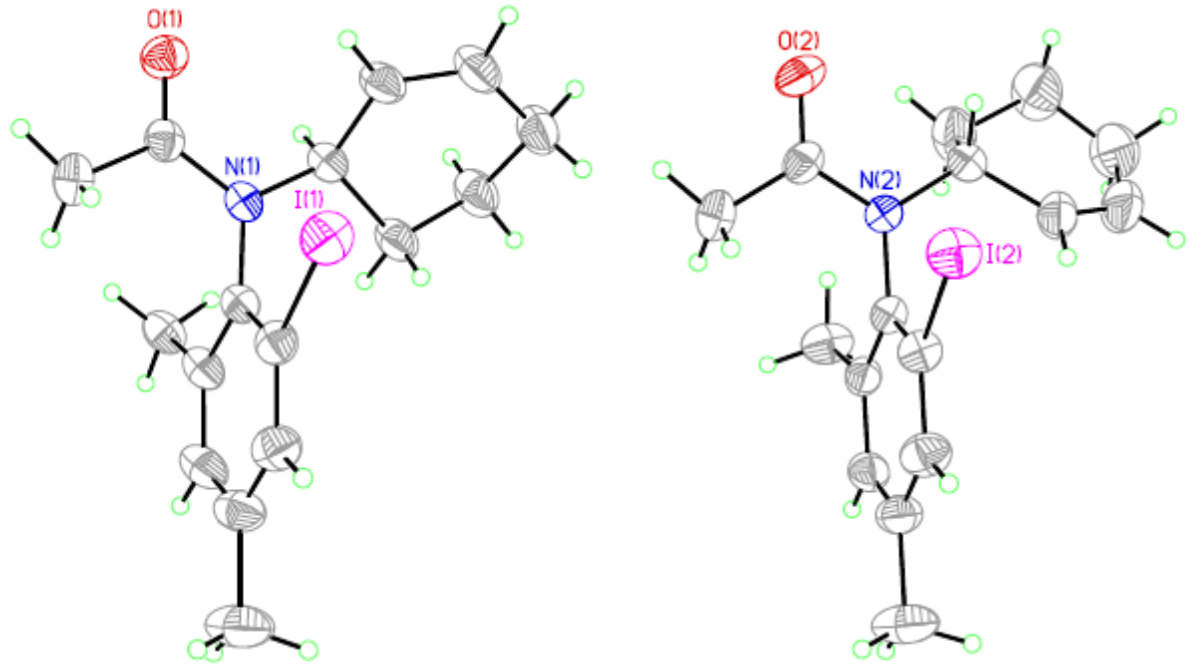

The corresponding CIF file for *syn*-**4.15** is shown below, between the lines of "+" symbols.

```
++++++++++++++++++++++++++++++++++++++++++++++++++++++++++++++++++++++++++++++++

data_dg1012s

_audit_creation_method            SHELXL-97
_chemical_name_systematic
;
 ?
;
_chemical_name_common             ?
_chemical_melting_point           ?
_chemical_formula_moiety          ?
_chemical_formula_sum
 'C16 H20 I N O'
_chemical_formula_weight          369.23

loop_
 _atom_type_symbol
 _atom_type_description
 _atom_type_scat_dispersion_real
 _atom_type_scat_dispersion_imag
 _atom_type_scat_source
 'C'  'C'   0.0033   0.0016
 'International Tables Vol C Tables 4.2.6.8 and 6.1.1.4'
 'H'  'H'   0.0000   0.0000
 'International Tables Vol C Tables 4.2.6.8 and 6.1.1.4'
 'N'  'N'   0.0061   0.0033
 'International Tables Vol C Tables 4.2.6.8 and 6.1.1.4'
```

```
 'O'  'O'   0.0106   0.0060
 'International Tables Vol C Tables 4.2.6.8 and 6.1.1.4'
 'I'  'I'  -0.4742   1.8119
 'International Tables Vol C Tables 4.2.6.8 and 6.1.1.4'

_symmetry_cell_setting            Triclinic
_symmetry_space_group_name_H-M    P-1

loop_
 _symmetry_equiv_pos_as_xyz
 'x, y, z'
 '-x, -y, -z'

_cell_length_a                    9.3192(3)
_cell_length_b                    9.4812(3)
_cell_length_c                    19.0469(7)
_cell_angle_alpha                 98.0530(10)
_cell_angle_beta                  96.6240(10)
_cell_angle_gamma                 101.0690(10)
_cell_volume                      1617.72(9)
_cell_formula_units_Z             4
_cell_measurement_temperature     295(2)
_cell_measurement_reflns_used     7246
_cell_measurement_theta_min       2.18
_cell_measurement_theta_max       27.28

_exptl_crystal_description        ?
_exptl_crystal_colour             ?
_exptl_crystal_size_max           0.29
_exptl_crystal_size_mid           0.25
_exptl_crystal_size_min           0.24
_exptl_crystal_density_meas       0
_exptl_crystal_density_diffrn     1.516
_exptl_crystal_density_method     'not measured'
_exptl_crystal_F_000              736
_exptl_absorpt_coefficient_mu     1.973
_exptl_absorpt_correction_type    none
_exptl_absorpt_correction_T_min   0.5985
_exptl_absorpt_correction_T_max   0.6489
_exptl_absorpt_process_details    ?

_exptl_special_details
;
 ?
;

_diffrn_ambient_temperature       295(2)
_diffrn_radiation_wavelength      0.71073
_diffrn_radiation_type            MoK\a
_diffrn_radiation_source          'fine-focus sealed tube'
_diffrn_radiation_monochromator   graphite
_diffrn_measurement_device_type   'CCD area detector'
_diffrn_measurement_method        'phi and omega scans'
_diffrn_detector_area_resol_mean  ?
```

```
_diffrn_standards_number          ?
_diffrn_standards_interval_count  ?
_diffrn_standards_interval_time   ?
_diffrn_standards_decay_%         ?
_diffrn_reflns_number             21333
_diffrn_reflns_av_R_equivalents   0.0144
_diffrn_reflns_av_sigmaI/netI     0.0217
_diffrn_reflns_limit_h_min        -14
_diffrn_reflns_limit_h_max        14
_diffrn_reflns_limit_k_min        -13
_diffrn_reflns_limit_k_max        14
_diffrn_reflns_limit_l_min        -28
_diffrn_reflns_limit_l_max        28
_diffrn_reflns_theta_min          2.18
_diffrn_reflns_theta_max          32.61
_reflns_number_total              11088
_reflns_number_gt                 8383
_reflns_threshold_expression      >2sigma(I)

_computing_data_collection        'Bruker SMART'
_computing_cell_refinement        'Bruker SMART'
_computing_data_reduction         'Bruker SAINT'
_computing_structure_solution     'SHELXS-97 (Sheldrick, 1990)'
_computing_structure_refinement   'SHELXL-97 (Sheldrick, 1997)'
_computing_molecular_graphics     'Bruker SHELXTL'
_computing_publication_material   'Bruker SHELXTL'

_refine_special_details
;
 Refinement of F^2^ against ALL reflections.  The weighted R-factor wR and
 goodness of fit S are based on F^2^, conventional R-factors R are based
 on F, with F set to zero for negative F^2^. The threshold expression of
 F^2^ > 2sigma(F^2^) is used only for calculating R-factors(gt) etc. and
is
 not relevant to the choice of reflections for refinement.  R-factors
based
 on F^2^ are statistically about twice as large as those based on F, and
R-
 factors based on ALL data will be even larger.
;

_refine_ls_structure_factor_coef  Fsqd
_refine_ls_matrix_type            full
_refine_ls_weighting_scheme       calc
_refine_ls_weighting_details
 'calc w=1/[\s^2^(Fo^2^)+(0.0780P)^2^+0.0000P] where P=(Fo^2^+2Fc^2^)/3'
_atom_sites_solution_primary      direct
_atom_sites_solution_secondary    difmap
_atom_sites_solution_hydrogens    geom
_refine_ls_hydrogen_treatment     mixed
_refine_ls_extinction_method      none
_refine_ls_extinction_coef        ?
_refine_ls_number_reflns          11088
_refine_ls_number_parameters      343
```

```
_refine_ls_number_restraints      0
_refine_ls_R_factor_all           0.0536
_refine_ls_R_factor_gt            0.0390
_refine_ls_wR_factor_ref          0.1298
_refine_ls_wR_factor_gt           0.1177
_refine_ls_goodness_of_fit_ref    1.039
_refine_ls_restrained_S_all       1.039
_refine_ls_shift/su_max           0.001
_refine_ls_shift/su_mean          0.000

loop_
 _atom_site_label
 _atom_site_type_symbol
 _atom_site_fract_x
 _atom_site_fract_y
 _atom_site_fract_z
 _atom_site_U_iso_or_equiv
 _atom_site_adp_type
 _atom_site_occupancy
 _atom_site_symmetry_multiplicity
 _atom_site_calc_flag
 _atom_site_refinement_flags
 _atom_site_disorder_assembly
 _atom_site_disorder_group
I1 I 0.082354(19) 0.53458(2) 0.136297(10) 0.05819(7) Uani 1 1 d . . .
N1 N -0.2580(2) 0.5478(2) 0.08324(10) 0.0419(4) Uani 1 1 d . . .
O1 O -0.2990(2) 0.5602(2) -0.03504(10) 0.0574(4) Uani 1 1 d . . .
C1 C -0.0706(3) 0.6223(3) 0.19130(13) 0.0466(5) Uani 1 1 d . . .
I2 I 0.40251(2) -0.091842(19) 0.382080(10) 0.06055(7) Uani 1 1 d . . .
C2 C -0.2107(2) 0.6212(2) 0.15520(12) 0.0415(4) Uani 1 1 d . . .
N2 N 0.5514(2) 0.2559(2) 0.40194(10) 0.0432(4) Uani 1 1 d . . .
O2 O 0.6019(3) 0.3210(2) 0.52205(10) 0.0656(5) Uani 1 1 d . . .
C3 C -0.3061(3) 0.6932(3) 0.19152(15) 0.0497(5) Uani 1 1 d . . .
C4 C -0.2588(3) 0.7592(3) 0.26230(16) 0.0606(7) Uani 1 1 d . . .
H4A H -0.3216 0.8074 0.2863 0.073 Uiso 1 1 calc R . .
C5 C -0.1238(3) 0.7566(3) 0.29841(15) 0.0605(7) Uani 1 1 d . . .
C6 C -0.0280(3) 0.6887(3) 0.26180(15) 0.0567(6) Uani 1 1 d . . .
H6A H 0.0653 0.6882 0.2850 0.068 Uiso 1 1 calc R . .
C7 C -0.3425(3) 0.3932(2) 0.06832(13) 0.0452(5) Uani 1 1 d . . .
H7A H -0.4355 0.3899 0.0377 0.054 Uiso 1 1 calc R . .
C8 C -0.2594(3) 0.2939(3) 0.02792(15) 0.0567(6) Uani 1 1 d . . .
H8A H -0.2012 0.3310 -0.0045 0.068 Uiso 1 1 calc R . .
C9 C -0.2657(4) 0.1582(3) 0.03654(18) 0.0670(8) Uani 1 1 d . . .
H9A H -0.2123 0.1043 0.0091 0.080 Uiso 1 1 calc R . .
C10 C -0.3517(4) 0.0841(3) 0.08696(19) 0.0655(8) Uani 1 1 d . . .
H10A H -0.2843 0.0680 0.1263 0.079 Uiso 1 1 calc R . .
H10B H -0.4083 -0.0101 0.0623 0.079 Uiso 1 1 calc R . .
C11 C -0.4564(4) 0.1751(3) 0.1164(2) 0.0670(8) Uani 1 1 d . . .
H11A H -0.5424 0.1642 0.0806 0.080 Uiso 1 1 calc R . .
H11B H -0.4897 0.1398 0.1584 0.080 Uiso 1 1 calc R . .
C12 C -0.3814(4) 0.3354(3) 0.13642(17) 0.0604(7) Uani 1 1 d . . .
H12A H -0.2924 0.3469 0.1704 0.072 Uiso 1 1 calc R . .
H12B H -0.4471 0.3899 0.1586 0.072 Uiso 1 1 calc R . .
C13 C -0.2441(3) 0.6190(3) 0.02624(14) 0.0454(5) Uani 1 1 d . . .
```

```
C14 C -0.1566(4) 0.7733(3) 0.04084(17) 0.0650(7) Uani 1 1 d . . .
H14A H -0.1557 0.8115 -0.0032 0.097 Uiso 1 1 calc R . .
H14B H -0.0571 0.7753 0.0614 0.097 Uiso 1 1 calc R . .
H14C H -0.2012 0.8318 0.0737 0.097 Uiso 1 1 calc R . .
C15 C -0.4604(3) 0.7025(3) 0.15444(16) 0.0539(6) Uani 1 1 d . . .
H15A H -0.5086 0.7554 0.1879 0.081 Uiso 1 1 calc R . .
H15B H -0.5191 0.6060 0.1383 0.081 Uiso 1 1 calc R . .
H15C H -0.4490 0.7520 0.1141 0.081 Uiso 1 1 calc R . .
C16 C -0.0768(5) 0.8298(5) 0.37642(18) 0.0935(13) Uani 1 1 d . . .
H16A H -0.1556 0.8708 0.3933 0.140 Uiso 1 1 calc R . .
H16B H 0.0095 0.9058 0.3800 0.140 Uiso 1 1 calc R . .
H16C H -0.0548 0.7589 0.4051 0.140 Uiso 1 1 calc R . .
C17 C 0.3690(3) 0.0661(3) 0.31857(13) 0.0481(5) Uani 1 1 d . . .
C18 C 0.4425(3) 0.2118(2) 0.33867(12) 0.0414(4) Uani 1 1 d . . .
C19 C 0.4064(3) 0.3143(3) 0.29812(13) 0.0458(5) Uani 1 1 d . . .
C20 C 0.3005(3) 0.2682(3) 0.23734(14) 0.0529(6) Uani 1 1 d . . .
H20A H 0.2769 0.3370 0.2101 0.063 Uiso 1 1 calc R . .
C21 C 0.2293(3) 0.1248(4) 0.21590(14) 0.0578(6) Uani 1 1 d . . .
C22 C 0.2632(3) 0.0229(3) 0.25719(15) 0.0587(7) Uani 1 1 d . . .
H22A H 0.2154 -0.0744 0.2440 0.070 Uiso 1 1 calc R . .
C23 C 0.7090(3) 0.2502(3) 0.39875(15) 0.0535(6) Uani 1 1 d . . .
H23A H 0.7408 0.2020 0.4383 0.064 Uiso 1 1 calc R . .
C24 C 0.8095(4) 0.3981(4) 0.4097(3) 0.0833(11) Uani 1 1 d . . .
H24A H 0.8076 0.4498 0.4572 0.100 Uiso 1 1 calc R . .
H24B H 0.7749 0.4539 0.3748 0.100 Uiso 1 1 calc R . .
C25 C 0.9651(4) 0.3842(6) 0.4018(3) 0.1050(16) Uani 1 1 d . . .
H25A H 1.0289 0.4805 0.4119 0.126 Uiso 1 1 calc R . .
H25B H 0.9988 0.3282 0.4369 0.126 Uiso 1 1 calc R . .
C27 C 0.8521(4) 0.1901(5) 0.3022(2) 0.0868(12) Uani 1 1 d . . .
H27A H 0.8589 0.1278 0.2610 0.104 Uiso 1 1 calc R . .
C28 C 0.7306(4) 0.1609(4) 0.33100(18) 0.0667(8) Uani 1 1 d . . .
H28A H 0.6558 0.0824 0.3086 0.080 Uiso 1 1 calc R . .
C29 C 0.5106(3) 0.2901(3) 0.46752(13) 0.0491(5) Uani 1 1 d . . .
C30 C 0.3511(4) 0.2902(4) 0.47089(17) 0.0661(8) Uani 1 1 d . . .
H30A H 0.3372 0.3151 0.5199 0.099 Uiso 1 1 calc R . .
H30B H 0.2924 0.1952 0.4511 0.099 Uiso 1 1 calc R . .
H30C H 0.3213 0.3605 0.4438 0.099 Uiso 1 1 calc R . .
C31 C 0.4732(4) 0.4763(3) 0.31916(17) 0.0662(8) Uani 1 1 d . . .
H31A H 0.5445 0.4923 0.3617 0.099 Uiso 1 1 calc R . .
H31B H 0.3966 0.5281 0.3282 0.099 Uiso 1 1 calc R . .
H31C H 0.5210 0.5107 0.2809 0.099 Uiso 1 1 calc R . .
C32 C 0.1149(5) 0.0765(5) 0.15004(19) 0.0911(13) Uani 1 1 d . . .
H32A H 0.1044 0.1590 0.1274 0.137 Uiso 1 1 calc R . .
H32B H 0.0219 0.0343 0.1634 0.137 Uiso 1 1 calc R . .
H32C H 0.1454 0.0053 0.1173 0.137 Uiso 1 1 calc R . .
C26 C 0.9787(5) 0.3127(6) 0.3294(3) 0.0985(14) Uani 1 1 d . . .
H26A H 0.9830 0.3832 0.2969 0.118 Uiso 1 1 calc R . .
H26B H 1.0698 0.2771 0.3312 0.118 Uiso 1 1 calc R . .

loop_
 _atom_site_aniso_label
 _atom_site_aniso_U_11
 _atom_site_aniso_U_22
 _atom_site_aniso_U_33
```

```
 _atom_site_aniso_U_23
 _atom_site_aniso_U_13
 _atom_site_aniso_U_12
I1 0.04572(10) 0.07246(13) 0.06288(12) 0.01521(9) 0.01161(8) 0.02336(9)
N1 0.0418(9) 0.0354(8) 0.0477(10) 0.0035(7) 0.0074(8) 0.0085(7)
O1 0.0566(11) 0.0664(12) 0.0504(10) 0.0098(8) 0.0041(8) 0.0183(9)
C1 0.0450(12) 0.0466(12) 0.0494(12) 0.0105(10) 0.0127(10) 0.0072(9)
I2 0.07096(13) 0.04767(11) 0.06312(12) 0.01719(8) 0.00559(9) 0.00955(8)
C2 0.0412(11) 0.0377(10) 0.0447(11) 0.0039(8) 0.0086(9) 0.0071(8)
N2 0.0446(10) 0.0460(10) 0.0388(9) 0.0052(7) 0.0053(7) 0.0109(8)
O2 0.0822(15) 0.0719(13) 0.0397(9) 0.0062(8) 0.0029(9) 0.0146(11)
C3 0.0470(12) 0.0398(11) 0.0605(14) -0.0006(10) 0.0152(11) 0.0068(9)
C4 0.0629(17) 0.0477(13) 0.0667(17) -0.0070(12) 0.0238(14) 0.0041(12)
C5 0.0633(17) 0.0574(15) 0.0509(14) -0.0028(12) 0.0136(12) -0.0059(13)
C6 0.0531(15) 0.0593(15) 0.0508(14) 0.0084(11) 0.0045(11) -0.0026(12)
C7 0.0427(11) 0.0399(11) 0.0514(12) 0.0013(9) 0.0105(9) 0.0071(9)
C8 0.0644(16) 0.0485(13) 0.0584(15) -0.0007(11) 0.0251(13) 0.0125(12)
C9 0.079(2) 0.0462(14) 0.080(2) 0.0005(13) 0.0325(16) 0.0183(13)
C10 0.076(2) 0.0428(13) 0.080(2) 0.0092(13) 0.0220(16) 0.0119(13)
C11 0.0723(19) 0.0436(13) 0.084(2) 0.0065(13) 0.0299(16) 0.0005(13)
C12 0.0749(19) 0.0420(12) 0.0664(17) 0.0029(11) 0.0351(15) 0.0072(12)
C13 0.0424(11) 0.0449(11) 0.0526(13) 0.0097(10) 0.0105(9) 0.0153(9)
C14 0.080(2) 0.0484(14) 0.0692(18) 0.0203(13) 0.0144(15) 0.0098(13)
C15 0.0440(12) 0.0479(13) 0.0674(16) -0.0008(11) 0.0117(11) 0.0089(10)
C16 0.108(3) 0.103(3) 0.0533(18) -0.0136(18) 0.0140(18) -0.001(2)
C17 0.0511(13) 0.0447(12) 0.0477(12) 0.0097(10) 0.0068(10) 0.0068(10)
C18 0.0434(11) 0.0427(11) 0.0384(10) 0.0053(8) 0.0079(8) 0.0096(9)
C19 0.0498(12) 0.0468(12) 0.0433(11) 0.0078(9) 0.0102(9) 0.0141(10)
C20 0.0538(14) 0.0631(16) 0.0474(13) 0.0167(11) 0.0077(10) 0.0205(12)
C21 0.0516(14) 0.0739(18) 0.0445(13) 0.0086(12) 0.0010(10) 0.0094(13)
C22 0.0553(15) 0.0566(15) 0.0559(15) 0.0060(12) 0.0028(12) -0.0025(12)
C23 0.0457(13) 0.0643(16) 0.0505(13) 0.0052(11) 0.0040(10) 0.0163(11)
C24 0.0532(17) 0.076(2) 0.110(3) -0.012(2) 0.0173(18) 0.0030(16)
C25 0.055(2) 0.131(4) 0.115(4) -0.009(3) 0.017(2) 0.003(2)
C27 0.073(2) 0.114(3) 0.074(2) -0.005(2) 0.0250(18) 0.028(2)
C28 0.0567(16) 0.074(2) 0.0669(18) -0.0054(15) 0.0116(13) 0.0188(15)
C29 0.0626(15) 0.0451(12) 0.0413(11) 0.0084(9) 0.0127(10) 0.0118(11)
C30 0.0663(18) 0.081(2) 0.0565(16) 0.0072(14) 0.0243(14) 0.0241(16)
C31 0.088(2) 0.0445(13) 0.0618(17) 0.0148(12) -0.0052(15) 0.0082(14)
C32 0.083(2) 0.114(3) 0.0596(19) 0.0132(19) -0.0214(17) 0.000(2)
C26 0.066(2) 0.131(4) 0.102(3) 0.017(3) 0.030(2) 0.019(2)

_geom_special_details
;
 All esds (except the esd in the dihedral angle between two l.s. planes)
 are estimated using the full covariance matrix.  The cell esds are taken
 into account individually in the estimation of esds in distances, angles
 and torsion angles; correlations between esds in cell parameters are only
 used when they are defined by crystal symmetry.  An approximate
(isotropic)
 treatment of cell esds is used for estimating esds involving l.s. planes.
;

loop_
```

```
 _geom_bond_atom_site_label_1
 _geom_bond_atom_site_label_2
 _geom_bond_distance
 _geom_bond_site_symmetry_2
 _geom_bond_publ_flag
I1 C1 2.092(2) . ?
N1 C13 1.362(3) . ?
N1 C2 1.426(3) . ?
N1 C7 1.496(3) . ?
O1 C13 1.227(3) . ?
C1 C6 1.379(4) . ?
C1 C2 1.401(3) . ?
I2 C17 2.098(2) . ?
C2 C3 1.406(3) . ?
N2 C29 1.362(3) . ?
N2 C18 1.439(3) . ?
N2 C23 1.488(3) . ?
O2 C29 1.226(3) . ?
C3 C4 1.387(4) . ?
C3 C15 1.551(4) . ?
C4 C5 1.369(4) . ?
C4 H4A 0.9300 . ?
C5 C6 1.391(4) . ?
C5 C16 1.525(4) . ?
C6 H6A 0.9300 . ?
C7 C8 1.514(3) . ?
C7 C12 1.531(4) . ?
C7 H7A 0.9800 . ?
C8 C9 1.312(4) . ?
C8 H8A 0.9300 . ?
C9 C10 1.486(5) . ?
C9 H9A 0.9300 . ?
C10 C11 1.524(5) . ?
C10 H10A 0.9700 . ?
C10 H10B 0.9700 . ?
C11 C12 1.521(4) . ?
C11 H11A 0.9700 . ?
C11 H11B 0.9700 . ?
C12 H12A 0.9700 . ?
C12 H12B 0.9700 . ?
C13 C14 1.503(4) . ?
C14 H14A 0.9600 . ?
C14 H14B 0.9600 . ?
C14 H14C 0.9600 . ?
C15 H15A 0.9600 . ?
C15 H15B 0.9600 . ?
C15 H15C 0.9600 . ?
C16 H16A 0.9600 . ?
C16 H16B 0.9600 . ?
C16 H16C 0.9600 . ?
C17 C22 1.397(4) . ?
C17 C18 1.398(3) . ?
C18 C19 1.389(3) . ?
C19 C20 1.391(4) . ?
```

```
C19 C31 1.520(4) . ?
C20 C21 1.375(4) . ?
C20 H20A 0.9300 . ?
C21 C22 1.387(4) . ?
C21 C32 1.504(4) . ?
C22 H22A 0.9300 . ?
C23 C28 1.497(4) . ?
C23 C24 1.502(5) . ?
C23 H23A 0.9800 . ?
C24 C25 1.504(5) . ?
C24 H24A 0.9700 . ?
C24 H24B 0.9700 . ?
C25 C26 1.480(6) . ?
C25 H25A 0.9700 . ?
C25 H25B 0.9700 . ?
C27 C28 1.313(5) . ?
C27 C26 1.475(6) . ?
C27 H27A 0.9300 . ?
C28 H28A 0.9300 . ?
C29 C30 1.495(4) . ?
C30 H30A 0.9600 . ?
C30 H30B 0.9600 . ?
C30 H30C 0.9600 . ?
C31 H31A 0.9600 . ?
C31 H31B 0.9600 . ?
C31 H31C 0.9600 . ?
C32 H32A 0.9600 . ?
C32 H32B 0.9600 . ?
C32 H32C 0.9600 . ?
C26 H26A 0.9700 . ?
C26 H26B 0.9700 . ?

loop_
 _geom_angle_atom_site_label_1
 _geom_angle_atom_site_label_2
 _geom_angle_atom_site_label_3
 _geom_angle
 _geom_angle_site_symmetry_1
 _geom_angle_site_symmetry_3
 _geom_angle_publ_flag
C13 N1 C2 121.8(2) . . ?
C13 N1 C7 117.33(19) . . ?
C2 N1 C7 120.41(19) . . ?
C6 C1 C2 120.9(2) . . ?
C6 C1 I1 119.0(2) . . ?
C2 C1 I1 119.98(17) . . ?
C1 C2 C3 118.8(2) . . ?
C1 C2 N1 121.3(2) . . ?
C3 C2 N1 119.9(2) . . ?
C29 N2 C18 120.7(2) . . ?
C29 N2 C23 118.0(2) . . ?
C18 N2 C23 121.00(19) . . ?
C4 C3 C2 118.5(2) . . ?
C4 C3 C15 119.5(2) . . ?
```

```
C2 C3 C15 122.0(2) . . ?
C5 C4 C3 122.9(3) . . ?
C5 C4 H4A 118.6 . . ?
C3 C4 H4A 118.6 . . ?
C4 C5 C6 118.5(3) . . ?
C4 C5 C16 121.1(3) . . ?
C6 C5 C16 120.4(3) . . ?
C1 C6 C5 120.3(3) . . ?
C1 C6 H6A 119.8 . . ?
C5 C6 H6A 119.8 . . ?
N1 C7 C8 111.3(2) . . ?
N1 C7 C12 112.74(19) . . ?
C8 C7 C12 109.8(2) . . ?
N1 C7 H7A 107.6 . . ?
C8 C7 H7A 107.6 . . ?
C12 C7 H7A 107.6 . . ?
C9 C8 C7 123.1(3) . . ?
C9 C8 H8A 118.5 . . ?
C7 C8 H8A 118.5 . . ?
C8 C9 C10 124.8(3) . . ?
C8 C9 H9A 117.6 . . ?
C10 C9 H9A 117.6 . . ?
C9 C10 C11 111.1(3) . . ?
C9 C10 H10A 109.4 . . ?
C11 C10 H10A 109.4 . . ?
C9 C10 H10B 109.4 . . ?
C11 C10 H10B 109.4 . . ?
H10A C10 H10B 108.0 . . ?
C12 C11 C10 111.4(3) . . ?
C12 C11 H11A 109.3 . . ?
C10 C11 H11A 109.3 . . ?
C12 C11 H11B 109.3 . . ?
C10 C11 H11B 109.3 . . ?
H11A C11 H11B 108.0 . . ?
C11 C12 C7 108.7(2) . . ?
C11 C12 H12A 109.9 . . ?
C7 C12 H12A 109.9 . . ?
C11 C12 H12B 109.9 . . ?
C7 C12 H12B 109.9 . . ?
H12A C12 H12B 108.3 . . ?
O1 C13 N1 121.9(2) . . ?
O1 C13 C14 120.6(2) . . ?
N1 C13 C14 117.5(2) . . ?
C13 C14 H14A 109.5 . . ?
C13 C14 H14B 109.5 . . ?
H14A C14 H14B 109.5 . . ?
C13 C14 H14C 109.5 . . ?
H14A C14 H14C 109.5 . . ?
H14B C14 H14C 109.5 . . ?
C3 C15 H15A 109.5 . . ?
C3 C15 H15B 109.5 . . ?
H15A C15 H15B 109.5 . . ?
C3 C15 H15C 109.5 . . ?
H15A C15 H15C 109.5 . . ?
```

```
H15B C15 H15C 109.5 . . ?
C5 C16 H16A 109.5 . . ?
C5 C16 H16B 109.5 . . ?
H16A C16 H16B 109.5 . . ?
C5 C16 H16C 109.5 . . ?
H16A C16 H16C 109.5 . . ?
H16B C16 H16C 109.5 . . ?
C22 C17 C18 120.4(2) . . ?
C22 C17 I2 117.76(19) . . ?
C18 C17 I2 121.70(18) . . ?
C19 C18 C17 119.3(2) . . ?
C19 C18 N2 120.4(2) . . ?
C17 C18 N2 120.3(2) . . ?
C18 C19 C20 119.0(2) . . ?
C18 C19 C31 122.6(2) . . ?
C20 C19 C31 118.4(2) . . ?
C21 C20 C19 122.5(2) . . ?
C21 C20 H20A 118.8 . . ?
C19 C20 H20A 118.8 . . ?
C20 C21 C22 118.6(2) . . ?
C20 C21 C32 121.9(3) . . ?
C22 C21 C32 119.5(3) . . ?
C21 C22 C17 120.2(3) . . ?
C21 C22 H22A 119.9 . . ?
C17 C22 H22A 119.9 . . ?
N2 C23 C28 112.8(2) . . ?
N2 C23 C24 113.3(3) . . ?
C28 C23 C24 109.7(3) . . ?
N2 C23 H23A 106.9 . . ?
C28 C23 H23A 106.9 . . ?
C24 C23 H23A 106.9 . . ?
C23 C24 C25 110.5(3) . . ?
C23 C24 H24A 109.6 . . ?
C25 C24 H24A 109.6 . . ?
C23 C24 H24B 109.6 . . ?
C25 C24 H24B 109.6 . . ?
H24A C24 H24B 108.1 . . ?
C26 C25 C24 112.9(4) . . ?
C26 C25 H25A 109.0 . . ?
C24 C25 H25A 109.0 . . ?
C26 C25 H25B 109.0 . . ?
C24 C25 H25B 109.0 . . ?
H25A C25 H25B 107.8 . . ?
C28 C27 C26 125.9(4) . . ?
C28 C27 H27A 117.1 . . ?
C26 C27 H27A 117.1 . . ?
C27 C28 C23 122.0(3) . . ?
C27 C28 H28A 119.0 . . ?
C23 C28 H28A 119.0 . . ?
O2 C29 N2 121.1(3) . . ?
O2 C29 C30 121.0(2) . . ?
N2 C29 C30 117.9(2) . . ?
C29 C30 H30A 109.5 . . ?
C29 C30 H30B 109.5 . . ?
```

```
H30A C30 H30B 109.5 . . ?
C29 C30 H30C 109.5 . . ?
H30A C30 H30C 109.5 . . ?
H30B C30 H30C 109.5 . . ?
C19 C31 H31A 109.5 . . ?
C19 C31 H31B 109.5 . . ?
H31A C31 H31B 109.5 . . ?
C19 C31 H31C 109.5 . . ?
H31A C31 H31C 109.5 . . ?
H31B C31 H31C 109.5 . . ?
C21 C32 H32A 109.5 . . ?
C21 C32 H32B 109.5 . . ?
H32A C32 H32B 109.5 . . ?
C21 C32 H32C 109.5 . . ?
H32A C32 H32C 109.5 . . ?
H32B C32 H32C 109.5 . . ?
C27 C26 C25 110.7(3) . . ?
C27 C26 H26A 109.5 . . ?
C25 C26 H26A 109.5 . . ?
C27 C26 H26B 109.5 . . ?
C25 C26 H26B 109.5 . . ?
H26A C26 H26B 108.1 . . ?

_diffrn_measured_fraction_theta_max    0.938
_diffrn_reflns_theta_full              32.61
_diffrn_measured_fraction_theta_full   0.938
_refine_diff_density_max    1.207
_refine_diff_density_min   -0.681
_refine_diff_density_rms    0.077
```

++

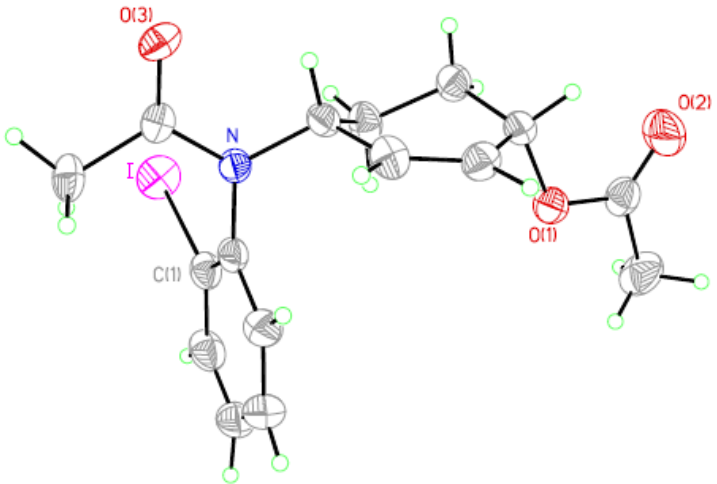

The corresponding CIF file for *anti*-**4.52** is shown below, between the lines of "+" symbols.

```
++++++++++++++++++++++++++++++++++++++++++++++++++++++++++++++++++++++++++++++++

data_dgc922s

_audit_creation_method            SHELXL-97
_chemical_name_systematic
;
 ?
;
_chemical_name_common             ?
_chemical_melting_point           ?
_chemical_formula_moiety          ?
_chemical_formula_sum
 'C16 H18 I N O3'
_chemical_formula_weight          399.21

loop_
 _atom_type_symbol
 _atom_type_description
 _atom_type_scat_dispersion_real
 _atom_type_scat_dispersion_imag
 _atom_type_scat_source
 'C'  'C'   0.0033   0.0016
 'International Tables Vol C Tables 4.2.6.8 and 6.1.1.4'
 'H'  'H'   0.0000   0.0000
 'International Tables Vol C Tables 4.2.6.8 and 6.1.1.4'
 'N'  'N'   0.0061   0.0033
 'International Tables Vol C Tables 4.2.6.8 and 6.1.1.4'
 'O'  'O'   0.0106   0.0060
 'International Tables Vol C Tables 4.2.6.8 and 6.1.1.4'
 'I'  'I'  -0.4742   1.8119
 'International Tables Vol C Tables 4.2.6.8 and 6.1.1.4'

_symmetry_cell_setting            Monoclinic
_symmetry_space_group_name_H-M    P2(1)/c

loop_
 _symmetry_equiv_pos_as_xyz
 'x, y, z'
 '-x, y+1/2, -z+1/2'
 '-x, -y, -z'
 'x, -y-1/2, z-1/2'

_cell_length_a                    9.7112(15)
_cell_length_b                    11.6237(17)
_cell_length_c                    14.127(2)
_cell_angle_alpha                 90.00
_cell_angle_beta                  94.332(3)
_cell_angle_gamma                 90.00
_cell_volume                      1590.1(4)
_cell_formula_units_Z             4
_cell_measurement_temperature     203(2)
_cell_measurement_reflns_used     5306
_cell_measurement_theta_min       0.00
```

```
_cell_measurement_theta_max       0.00

_exptl_crystal_description        ?
_exptl_crystal_colour             ?
_exptl_crystal_size_max           0.34
_exptl_crystal_size_mid           0.25
_exptl_crystal_size_min           0.21
_exptl_crystal_density_meas       0
_exptl_crystal_density_diffrn     1.668
_exptl_crystal_density_method     'not measured'
_exptl_crystal_F_000              792
_exptl_absorpt_coefficient_mu     2.023
_exptl_absorpt_correction_type    none
_exptl_absorpt_correction_T_min   0.5462
_exptl_absorpt_correction_T_max   0.6760
_exptl_absorpt_process_details    ?

_exptl_special_details
;
 ?
;

_diffrn_ambient_temperature       203(2)
_diffrn_radiation_wavelength      0.71073
_diffrn_radiation_type            MoK\a
_diffrn_radiation_source          'fine-focus sealed tube'
_diffrn_radiation_monochromator   graphite
_diffrn_measurement_device_type   'CCD area detector'
_diffrn_measurement_method        'phi and omega scans'
_diffrn_detector_area_resol_mean  ?
_diffrn_standards_number          ?
_diffrn_standards_interval_count  ?
_diffrn_standards_interval_time   ?
_diffrn_standards_decay_%         ?
_diffrn_reflns_number             15074
_diffrn_reflns_av_R_equivalents   0.0444
_diffrn_reflns_av_sigmaI/netI     0.0359
_diffrn_reflns_limit_h_min        -12
_diffrn_reflns_limit_h_max        12
_diffrn_reflns_limit_k_min        -15
_diffrn_reflns_limit_k_max        15
_diffrn_reflns_limit_l_min        -18
_diffrn_reflns_limit_l_max        18
_diffrn_reflns_theta_min          2.10
_diffrn_reflns_theta_max          27.50
_reflns_number_total              3655
_reflns_number_gt                 3144
_reflns_threshold_expression      >2sigma(I)

_computing_data_collection        'Bruker SMART'
_computing_cell_refinement        'Bruker SMART'
_computing_data_reduction         'Bruker SAINT'
_computing_structure_solution     'SHELXS-97 (Sheldrick, 1990)'
_computing_structure_refinement   'SHELXL-97 (Sheldrick, 1997)'
```

```
_computing_molecular_graphics     'Bruker SHELXTL'
_computing_publication_material   'Bruker SHELXTL'

_refine_special_details
;
 Refinement of F^2^ against ALL reflections.  The weighted R-factor wR and
 goodness of fit S are based on F^2^, conventional R-factors R are based
 on F, with F set to zero for negative F^2^. The threshold expression of
 F^2^ > 2sigma(F^2^) is used only for calculating R-factors(gt) etc. and
is
 not relevant to the choice of reflections for refinement.  R-factors
based
 on F^2^ are statistically about twice as large as those based on F, and
R-
 factors based on ALL data will be even larger.
;

_refine_ls_structure_factor_coef  Fsqd
_refine_ls_matrix_type            full
_refine_ls_weighting_scheme       calc
_refine_ls_weighting_details
 'calc w=1/[\s^2^(Fo^2^)+(0.0780P)^2^+0.0000P] where P=(Fo^2^+2Fc^2^)/3'
_atom_sites_solution_primary      direct
_atom_sites_solution_secondary    difmap
_atom_sites_solution_hydrogens    geom
_refine_ls_hydrogen_treatment     mixed
_refine_ls_extinction_method      none
_refine_ls_extinction_coef        ?
_refine_ls_number_reflns          3655
_refine_ls_number_parameters      240
_refine_ls_number_restraints      0
_refine_ls_R_factor_all           0.0433
_refine_ls_R_factor_gt            0.0362
_refine_ls_wR_factor_ref          0.1128
_refine_ls_wR_factor_gt           0.1071
_refine_ls_goodness_of_fit_ref    0.996
_refine_ls_restrained_S_all       0.996
_refine_ls_shift/su_max           0.083
_refine_ls_shift/su_mean          0.006

loop_
 _atom_site_label
 _atom_site_type_symbol
 _atom_site_fract_x
 _atom_site_fract_y
 _atom_site_fract_z
 _atom_site_U_iso_or_equiv
 _atom_site_adp_type
 _atom_site_occupancy
 _atom_site_symmetry_multiplicity
 _atom_site_calc_flag
 _atom_site_refinement_flags
 _atom_site_disorder_assembly
 _atom_site_disorder_group
```

```
I I 0.72654(2) 0.845623(19) 0.818067(16) 0.04560(12) Uani 1 1 d . . .
N N 0.8461(2) 0.58283(19) 0.85798(15) 0.0260(5) Uani 1 1 d . . .
O1 O 0.7107(2) 0.3853(2) 0.55234(14) 0.0362(5) Uani 1 1 d . . .
C1 C 0.6255(3) 0.6898(3) 0.84230(19) 0.0316(6) Uani 1 1 d . . .
O2 O 0.7856(3) 0.3469(2) 0.40915(19) 0.0590(8) Uani 1 1 d . . .
C2 C 0.4822(3) 0.6924(3) 0.8437(2) 0.0413(7) Uani 1 1 d . . .
H2 H 0.437(3) 0.762(3) 0.834(2) 0.031(8) Uiso 1 1 d . . .
O3 O 1.0604(2) 0.60724(19) 0.92997(15) 0.0345(5) Uani 1 1 d . . .
C3 C 0.4116(3) 0.5925(4) 0.8640(2) 0.0449(8) Uani 1 1 d . . .
H3 H 0.318(5) 0.591(4) 0.874(3) 0.056(12) Uiso 1 1 d . . .
C4 C 0.4839(3) 0.4920(3) 0.8833(3) 0.0431(8) Uani 1 1 d . . .
H4 H 0.435(4) 0.431(4) 0.900(3) 0.047(11) Uiso 1 1 d . . .
C5 C 0.6260(3) 0.4895(3) 0.8826(2) 0.0360(7) Uani 1 1 d . . .
H5 H 0.674(4) 0.432(3) 0.891(3) 0.043(10) Uiso 1 1 d . . .
C6 C 0.6994(3) 0.5884(2) 0.86170(18) 0.0281(6) Uani 1 1 d . . .
C7 C 0.9011(3) 0.5290(3) 0.77395(19) 0.0295(6) Uani 1 1 d . . .
H7 H 0.996(4) 0.539(3) 0.785(3) 0.042(10) Uiso 1 1 d . . .
C8 C 0.8440(4) 0.5843(3) 0.6814(2) 0.0361(7) Uani 1 1 d . . .
H8A H 0.870(5) 0.665(3) 0.678(3) 0.061(13) Uiso 1 1 d . . .
H8B H 0.737(4) 0.581(3) 0.677(2) 0.031(8) Uiso 1 1 d . . .
C9 C 0.8955(4) 0.5206(3) 0.5981(2) 0.0342(6) Uani 1 1 d . . .
H9A H 0.860(4) 0.547(3) 0.545(3) 0.046(11) Uiso 1 1 d . . .
H9B H 0.991(4) 0.523(4) 0.604(3) 0.055(11) Uiso 1 1 d . . .
C10 C 0.8543(3) 0.3950(3) 0.5946(2) 0.0316(6) Uani 1 1 d . . .
H10 H 0.907(4) 0.355(3) 0.551(3) 0.027(8) Uiso 1 1 d . . .
C11 C 0.8571(3) 0.3412(2) 0.6908(2) 0.0329(6) Uani 1 1 d . . .
H11 H 0.847(3) 0.250(3) 0.693(2) 0.030(8) Uiso 1 1 d . . .
C12 C 0.8785(3) 0.4013(3) 0.7708(2) 0.0339(6) Uani 1 1 d . . .
H12 H 0.889(4) 0.363(3) 0.833(3) 0.043(10) Uiso 1 1 d . . .
C13 C 0.6926(4) 0.3610(3) 0.4594(2) 0.0362(7) Uani 1 1 d . . .
C14 C 0.5431(4) 0.3552(4) 0.4269(3) 0.0536(10) Uani 1 1 d . . .
H14A H 0.5141 0.4281 0.3985 0.080 Uiso 1 1 calc R . .
H14B H 0.4896 0.3395 0.4807 0.080 Uiso 1 1 calc R . .
H14C H 0.5282 0.2943 0.3803 0.080 Uiso 1 1 calc R . .
C15 C 0.9352(3) 0.6154(2) 0.93288(19) 0.0265(5) Uani 1 1 d . . .
C16 C 0.8715(4) 0.6607(3) 1.0199(2) 0.0347(7) Uani 1 1 d . . .
H16A H 0.8341 0.5970 1.0543 0.052 Uiso 1 1 calc R . .
H16B H 0.7980 0.7142 1.0007 0.052 Uiso 1 1 calc R . .
H16C H 0.9416 0.6998 1.0606 0.052 Uiso 1 1 calc R . .

loop_
 _atom_site_aniso_label
 _atom_site_aniso_U_11
 _atom_site_aniso_U_22
 _atom_site_aniso_U_33
 _atom_site_aniso_U_23
 _atom_site_aniso_U_13
 _atom_site_aniso_U_12
I 0.04962(18) 0.03439(16) 0.05196(18) 0.00805(8) -0.00157(11) 0.00553(8)
N 0.0229(11) 0.0297(11) 0.0249(10) -0.0036(9) -0.0004(8) 0.0030(9)
O1 0.0312(11) 0.0490(12) 0.0282(10) -0.0068(9) -0.0001(8) -0.0028(9)
C1 0.0305(14) 0.0376(15) 0.0262(13) -0.0046(11) -0.0016(11) 0.0068(12)
O2 0.0563(17) 0.086(2) 0.0353(13) -0.0149(12) 0.0063(12) -0.0039(14)
C2 0.0335(16) 0.0545(19) 0.0356(16) -0.0071(14) 0.0003(13) 0.0133(15)
```

```
O3 0.0265(10) 0.0355(11) 0.0404(11) -0.0005(9) -0.0054(8) -0.0032(8)
C3 0.0244(15) 0.067(2) 0.0436(18) -0.0138(16) 0.0041(13) -0.0011(15)
C4 0.0322(16) 0.052(2) 0.0461(18) -0.0044(15) 0.0080(14) -0.0082(15)
C5 0.0334(16) 0.0363(16) 0.0390(16) -0.0032(13) 0.0073(13) -0.0003(13)
C6 0.0271(13) 0.0358(15) 0.0210(12) -0.0039(11) -0.0001(10) 0.0007(11)
C7 0.0239(13) 0.0376(15) 0.0271(13) -0.0051(11) 0.0030(10) 0.0029(11)
C8 0.053(2) 0.0283(15) 0.0287(14) 0.0001(11) 0.0114(13) -0.0030(13)
C9 0.0396(17) 0.0368(16) 0.0265(14) -0.0006(12) 0.0050(12) -0.0062(13)
C10 0.0279(14) 0.0387(16) 0.0285(13) -0.0074(12) 0.0047(11) -0.0013(12)
C11 0.0312(15) 0.0300(15) 0.0370(15) 0.0003(11) 0.0000(12) 0.0000(11)
C12 0.0372(16) 0.0328(15) 0.0314(14) 0.0020(12) 0.0011(12) 0.0083(12)
C13 0.0431(18) 0.0355(16) 0.0296(15) -0.0011(11) 0.0000(13) -0.0056(13)
C14 0.050(2) 0.066(3) 0.043(2) -0.0039(16) -0.0120(17) -0.0129(18)
C15 0.0330(14) 0.0193(12) 0.0266(13) 0.0016(10) -0.0026(10) 0.0017(10)
C16 0.0429(17) 0.0354(16) 0.0244(14) -0.0048(11) -0.0066(12) 0.0073(12)

_geom_special_details
;
 All esds (except the esd in the dihedral angle between two l.s. planes)
 are estimated using the full covariance matrix.  The cell esds are taken
 into account individually in the estimation of esds in distances, angles
 and torsion angles; correlations between esds in cell parameters are only
 used when they are defined by crystal symmetry.  An approximate
(isotropic)
 treatment of cell esds is used for estimating esds involving l.s. planes.
;

loop_
 _geom_bond_atom_site_label_1
 _geom_bond_atom_site_label_2
 _geom_bond_distance
 _geom_bond_site_symmetry_2
 _geom_bond_publ_flag
I C1 2.101(3) . ?
N C15 1.369(3) . ?
N C6 1.432(3) . ?
N C7 1.477(3) . ?
O1 C13 1.341(4) . ?
O1 C10 1.479(3) . ?
C1 C2 1.394(4) . ?
C1 C6 1.396(4) . ?
O2 C13 1.202(4) . ?
C2 C3 1.389(6) . ?
C2 H2 0.92(3) . ?
O3 C15 1.223(3) . ?
C3 C4 1.379(6) . ?
C3 H3 0.93(5) . ?
C4 C5 1.381(4) . ?
C4 H4 0.90(4) . ?
C5 C6 1.396(4) . ?
C5 H5 0.82(4) . ?
C7 C12 1.500(4) . ?
C7 C8 1.524(4) . ?
C7 H7 0.93(4) . ?
```

```
C8 C9 1.507(4) . ?
C8 H8A 0.97(4) . ?
C8 H8B 1.03(3) . ?
C9 C10 1.515(4) . ?
C9 H9A 0.86(4) . ?
C9 H9B 0.93(4) . ?
C10 C11 1.494(4) . ?
C10 H10 0.95(4) . ?
C11 C12 1.332(4) . ?
C11 H11 1.06(3) . ?
C12 H12 0.98(4) . ?
C13 C14 1.491(5) . ?
C14 H14A 0.9700 . ?
C14 H14B 0.9700 . ?
C14 H14C 0.9700 . ?
C15 C16 1.512(4) . ?
C16 H16A 0.9700 . ?
C16 H16B 0.9700 . ?
C16 H16C 0.9700 . ?

loop_
 _geom_angle_atom_site_label_1
 _geom_angle_atom_site_label_2
 _geom_angle_atom_site_label_3
 _geom_angle
 _geom_angle_site_symmetry_1
 _geom_angle_site_symmetry_3
 _geom_angle_publ_flag
C15 N C6 122.2(2) . . ?
C15 N C7 119.5(2) . . ?
C6 N C7 118.0(2) . . ?
C13 O1 C10 117.4(2) . . ?
C2 C1 C6 121.0(3) . . ?
C2 C1 I 117.6(2) . . ?
C6 C1 I 121.3(2) . . ?
C1 C2 C3 119.6(3) . . ?
C1 C2 H2 119(2) . . ?
C3 C2 H2 122(2) . . ?
C4 C3 C2 119.8(3) . . ?
C4 C3 H3 116(3) . . ?
C2 C3 H3 124(3) . . ?
C3 C4 C5 120.7(3) . . ?
C3 C4 H4 117(3) . . ?
C5 C4 H4 122(3) . . ?
C4 C5 C6 120.7(3) . . ?
C4 C5 H5 125(3) . . ?
C6 C5 H5 114(3) . . ?
C5 C6 C1 118.3(3) . . ?
C5 C6 N 119.7(3) . . ?
C1 C6 N 122.0(3) . . ?
N C7 C12 112.4(2) . . ?
N C7 C8 112.4(2) . . ?
C12 C7 C8 110.4(2) . . ?
N C7 H7 103(2) . . ?
```

```
C12 C7 H7 106(2) . . ?
C8 C7 H7 113(2) . . ?
C9 C8 C7 110.0(3) . . ?
C9 C8 H8A 110(3) . . ?
C7 C8 H8A 112(3) . . ?
C9 C8 H8B 109.1(18) . . ?
C7 C8 H8B 109.2(18) . . ?
H8A C8 H8B 107(4) . . ?
C8 C9 C10 113.4(3) . . ?
C8 C9 H9A 112(3) . . ?
C10 C9 H9A 103(3) . . ?
C8 C9 H9B 108(3) . . ?
C10 C9 H9B 107(3) . . ?
H9A C9 H9B 114(4) . . ?
O1 C10 C11 106.7(2) . . ?
O1 C10 C9 109.0(3) . . ?
C11 C10 C9 112.7(2) . . ?
O1 C10 H10 104(2) . . ?
C11 C10 H10 114(2) . . ?
C9 C10 H10 110.2(19) . . ?
C12 C11 C10 123.0(3) . . ?
C12 C11 H11 120.1(17) . . ?
C10 C11 H11 116.8(17) . . ?
C11 C12 C7 123.8(3) . . ?
C11 C12 H12 121(2) . . ?
C7 C12 H12 115(2) . . ?
O2 C13 O1 123.9(3) . . ?
O2 C13 C14 124.7(3) . . ?
O1 C13 C14 111.3(3) . . ?
C13 C14 H14A 109.5 . . ?
C13 C14 H14B 109.5 . . ?
H14A C14 H14B 109.5 . . ?
C13 C14 H14C 109.5 . . ?
H14A C14 H14C 109.5 . . ?
H14B C14 H14C 109.5 . . ?
O3 C15 N 121.6(3) . . ?
O3 C15 C16 121.5(3) . . ?
N C15 C16 116.8(3) . . ?
C15 C16 H16A 109.5 . . ?
C15 C16 H16B 109.5 . . ?
H16A C16 H16B 109.5 . . ?
C15 C16 H16C 109.5 . . ?
H16A C16 H16C 109.5 . . ?
H16B C16 H16C 109.5 . . ?

_diffrn_measured_fraction_theta_max    1.000
_diffrn_reflns_theta_full              27.50
_diffrn_measured_fraction_theta_full   1.000
_refine_diff_density_max    1.623
_refine_diff_density_min   -0.526
_refine_diff_density_rms    0.092
```

++

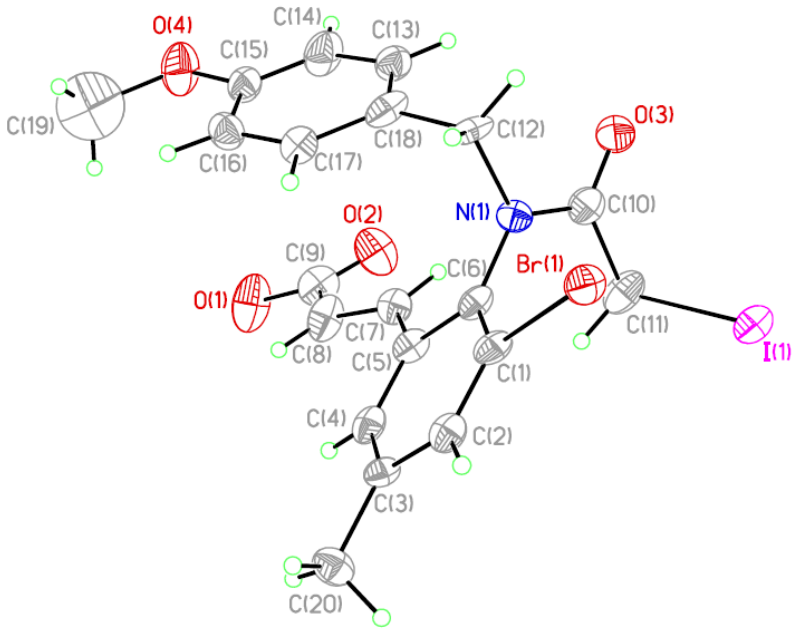

The corresponding CIF file for (*P*)-**5.31** is shown below, between the lines of "+" symbols.

++

```
data_dg7151s

_audit_creation_method            SHELXL-97
_chemical_name_systematic
;
 ?
;
_chemical_name_common             ?
_chemical_melting_point           ?
_chemical_formula_moiety          ?
_chemical_formula_sum
 'C20 H19 Br I N O4'
_chemical_formula_weight          544.17

loop_
 _atom_type_symbol
 _atom_type_description
 _atom_type_scat_dispersion_real
 _atom_type_scat_dispersion_imag
 _atom_type_scat_source
 'C'  'C'   0.0033   0.0016
 'International Tables Vol C Tables 4.2.6.8 and 6.1.1.4'
 'H'  'H'   0.0000   0.0000
 'International Tables Vol C Tables 4.2.6.8 and 6.1.1.4'
 'N'  'N'   0.0061   0.0033
```

```
 'International Tables Vol C Tables 4.2.6.8 and 6.1.1.4'
 'O'  'O'   0.0106   0.0060
 'International Tables Vol C Tables 4.2.6.8 and 6.1.1.4'
 'Br'  'Br'  -0.2901   2.4595
 'International Tables Vol C Tables 4.2.6.8 and 6.1.1.4'
 'I'  'I'  -0.4742   1.8119
 'International Tables Vol C Tables 4.2.6.8 and 6.1.1.4'

_symmetry_cell_setting           Monoclinic
_symmetry_space_group_name_H-M    'P 21'

loop_
 _symmetry_equiv_pos_as_xyz
 'x, y, z'
 '-x, y+1/2, -z'

_cell_length_a                   16.9278(18)
_cell_length_b                   7.4154(8)
_cell_length_c                   35.492(4)
_cell_angle_alpha                90.00
_cell_angle_beta                 95.125(2)
_cell_angle_gamma                90.00
_cell_volume                     4437.4(8)
_cell_formula_units_Z            8
_cell_measurement_temperature    203(2)
_cell_measurement_reflns_used    5106
_cell_measurement_theta_min      2.43
_cell_measurement_theta_max      23.59

_exptl_crystal_description       block
_exptl_crystal_colour            colorless
_exptl_crystal_size_max          0.31
_exptl_crystal_size_mid          0.28
_exptl_crystal_size_min          0.14
_exptl_crystal_density_meas      0
_exptl_crystal_density_diffrn    1.629
_exptl_crystal_density_method    'not measured'
_exptl_crystal_F_000             2128
_exptl_absorpt_coefficient_mu    3.267
_exptl_absorpt_correction_type   Multi-scan
_exptl_absorpt_correction_T_min  0.4308
_exptl_absorpt_correction_T_max  0.6577
_exptl_absorpt_process_details   'Bruker Sadabs'

_exptl_special_details
;
 ?
;

_diffrn_ambient_temperature      203(2)
_diffrn_radiation_wavelength     0.71073
_diffrn_radiation_type           MoK\a
_diffrn_radiation_source         'fine-focus sealed tube'
_diffrn_radiation_monochromator  graphite
```

```
_diffrn_measurement_device_type   'CCD area detector'
_diffrn_measurement_method        'phi and omega scans'
_diffrn_detector_area_resol_mean  ?
_diffrn_standards_number          ?
_diffrn_standards_interval_count  ?
_diffrn_standards_interval_time   ?
_diffrn_standards_decay_%         ?
_diffrn_reflns_number             24977
_diffrn_reflns_av_R_equivalents   0.0000
_diffrn_reflns_av_sigmaI/netI     0.0759
_diffrn_reflns_limit_h_min        -23
_diffrn_reflns_limit_h_max        23
_diffrn_reflns_limit_k_min        -10
_diffrn_reflns_limit_k_max        10
_diffrn_reflns_limit_l_min        -49
_diffrn_reflns_limit_l_max        49
_diffrn_reflns_theta_min          1.73
_diffrn_reflns_theta_max          30.00
_reflns_number_total              24977
_reflns_number_gt                 17531
_reflns_threshold_expression      >2sigma(I)

_computing_data_collection        'Bruker SMART'
_computing_cell_refinement        'Bruker SMART'
_computing_data_reduction         'Bruker SAINT'
_computing_structure_solution     'SHELXS-97 (Sheldrick, 1990)'
_computing_structure_refinement   'SHELXL-97 (Sheldrick, 1997)'
_computing_molecular_graphics     'Bruker SHELXTL'
_computing_publication_material   'Bruker SHELXTL'

_refine_special_details
;
 Refinement of F^2^ against ALL reflections.  The weighted R-factor wR and
 goodness of fit S are based on F^2^, conventional R-factors R are based
 on F, with F set to zero for negative F^2^. The threshold expression of
 F^2^ > 2sigma(F^2^) is used only for calculating R-factors(gt) etc. and
is
 not relevant to the choice of reflections for refinement.  R-factors
based
 on F^2^ are statistically about twice as large as those based on F, and
R-
 factors based on ALL data will be even larger.
;

_refine_ls_structure_factor_coef  Fsqd
_refine_ls_matrix_type            full
_refine_ls_weighting_scheme       calc
_refine_ls_weighting_details
 'calc w=1/[\s^2^(Fo^2^)+(0.0780P)^2^+0.0000P] where P=(Fo^2^+2Fc^2^)/3'
_atom_sites_solution_primary      direct
_atom_sites_solution_secondary    difmap
_atom_sites_solution_hydrogens    geom
_refine_ls_hydrogen_treatment   constr
_refine_ls_extinction_method      none
```

```
_refine_ls_extinction_coef        ?
_refine_ls_abs_structure_details
 'Flack H D (1983), Acta Cryst. A39, 876-881'
_refine_ls_abs_structure_Flack    0.021(10)
_refine_ls_number_reflns          24977
_refine_ls_number_parameters      964
_refine_ls_number_restraints      1
_refine_ls_R_factor_all           0.1007
_refine_ls_R_factor_gt            0.0764
_refine_ls_wR_factor_ref          0.1965
_refine_ls_wR_factor_gt           0.1861
_refine_ls_goodness_of_fit_ref    1.298
_refine_ls_restrained_S_all       1.298
_refine_ls_shift/su_max           0.001
_refine_ls_shift/su_mean          0.000

loop_
 _atom_site_label
 _atom_site_type_symbol
 _atom_site_fract_x
 _atom_site_fract_y
 _atom_site_fract_z
 _atom_site_U_iso_or_equiv
 _atom_site_adp_type
 _atom_site_occupancy
 _atom_site_symmetry_multiplicity
 _atom_site_calc_flag
 _atom_site_refinement_flags
 _atom_site_disorder_assembly
 _atom_site_disorder_group
N1 N 0.4459(3) -0.8211(8) 0.67220(15) 0.0333(12) Uani 1 1 d . . .
Br1 Br 0.46294(5) -0.90311(11) 0.75773(2) 0.04295(18) Uani 1 1 d . . .
I1 I 0.59485(4) -1.20797(8) 0.68950(2) 0.06564(19) Uani 1 1 d . . .
C1 C 0.3791(4) -0.9787(9) 0.72141(19) 0.0353(15) Uani 1 1 d . . .
O1 O 0.1931(4) -0.8804(13) 0.53197(17) 0.080(2) Uani 1 1 d . . .
H1A H 0.1997 -0.8901 0.5092 0.120 Uiso 1 1 calc R . .
N2 N 0.0611(3) -0.8642(8) 0.33039(17) 0.0334(12) Uani 1 1 d . . .
Br2 Br 0.03187(4) -0.95229(11) 0.24549(2) 0.04380(19) Uani 1 1 d . . .
I2 I -0.09332(4) -1.26463(9) 0.32113(2) 0.06561(19) Uani 1 1 d . . .
C2 C 0.3166(4) -1.0704(10) 0.7343(2) 0.0377(16) Uani 1 1 d . . .
H2A H 0.3162 -1.1001 0.7600 0.045 Uiso 1 1 calc R . .
O2 O 0.3252(4) -0.8922(12) 0.53797(17) 0.070(2) Uani 1 1 d . . .
Br3 Br 0.50809(5) 0.60120(11) -0.220050(19) 0.04235(18) Uani 1 1 d . . .
I3 I 0.20534(3) 0.30057(11) -0.20836(2) 0.0715(2) Uani 1 1 d . . .
N3 N 0.3934(3) 0.6393(8) -0.15808(17) 0.0328(12) Uani 1 1 d . . .
C3 C 0.2533(4) -1.1190(9) 0.70822(18) 0.0310(14) Uani 1 1 d . . .
O3 O 0.5616(3) -0.7871(9) 0.64411(17) 0.0540(14) Uani 1 1 d . . .
Br4 Br -0.01832(5) 0.54571(12) 0.22264(2) 0.04402(19) Uani 1 1 d . . .
I4 I 0.26564(5) 0.19256(11) 0.17671(2) 0.0807(2) Uani 1 1 d . . .
N4 N 0.1071(3) 0.5805(8) 0.16504(16) 0.0343(12) Uani 1 1 d . . .
C4 C 0.2571(4) -1.0731(10) 0.6710(2) 0.0376(16) Uani 1 1 d . . .
H4A H 0.2146 -1.1067 0.6535 0.045 Uiso 1 1 calc R . .
O4 O 0.2309(4) -0.3319(12) 0.56005(18) 0.072(2) Uani 1 1 d . . .
O5 O 0.3288(5) -0.8939(15) 0.46327(18) 0.093(3) Uani 1 1 d . . .
```

```
H5A H 0.3211 -0.8940 0.4860 0.139 Uiso 1 1 calc R . .
C5 C 0.3187(4) -0.9818(10) 0.65771(17) 0.0343(15) Uani 1 1 d . . .
O6 O 0.1988(4) -0.9067(12) 0.45861(15) 0.070(2) Uani 1 1 d . . .
C6 C 0.3840(4) -0.9307(9) 0.68312(19) 0.0357(15) Uani 1 1 d . . .
C7 C 0.3196(5) -0.9393(11) 0.6165(2) 0.0407(16) Uani 1 1 d . . .
H7A H 0.3693 -0.9232 0.6071 0.049 Uiso 1 1 calc R . .
O7 O -0.0509(4) -0.8623(10) 0.36152(18) 0.0625(16) Uiso 1 1 d . . .
O8 O 0.2807(4) -0.3663(10) 0.43923(18) 0.0647(18) Uani 1 1 d . . .
C8 C 0.2568(6) -0.9228(13) 0.5924(2) 0.053(2) Uani 1 1 d . . .
H8A H 0.2065 -0.9310 0.6016 0.064 Uiso 1 1 calc R . .
O9 O 0.3685(4) 0.4467(10) 0.01055(15) 0.0589(17) Uani 1 1 d . . .
H9A H 0.3292 0.4357 0.0228 0.088 Uiso 1 1 calc R . .
C9 C 0.2611(6) -0.8919(14) 0.5519(2) 0.056(2) Uani 1 1 d . . .
O10 O 0.2784(4) 0.4748(10) -0.03818(17) 0.0592(17) Uani 1 1 d . . .
C10 C 0.5100(5) -0.8834(12) 0.6547(2) 0.0432(17) Uani 1 1 d . . .
O11 O 0.2724(3) 0.6950(8) -0.18605(16) 0.0469(13) Uani 1 1 d . . .
C11 C 0.5112(6) -1.0868(12) 0.6480(2) 0.054(2) Uani 1 1 d . . .
H11A H 0.5265 -1.1119 0.6225 0.065 Uiso 1 1 calc R . .
H11B H 0.4583 -1.1374 0.6500 0.065 Uiso 1 1 calc R . .
O12 O 0.3141(4) 1.0482(11) -0.00855(17) 0.0623(17) Uani 1 1 d . . .
C12 C 0.4406(5) -0.6258(9) 0.6784(2) 0.0432(18) Uani 1 1 d . . .
H12A H 0.4935 -0.5719 0.6783 0.052 Uiso 1 1 calc R . .
H12B H 0.4214 -0.6031 0.7032 0.052 Uiso 1 1 calc R . .
O13 O 0.1636(3) 0.3801(10) 0.00132(14) 0.0539(17) Uani 1 1 d . . .
H13B H 0.2033 0.4122 -0.0090 0.081 Uiso 1 1 calc R . .
C13 C 0.4099(5) -0.4835(11) 0.6138(2) 0.0452(18) Uani 1 1 d . . .
H13A H 0.4638 -0.4915 0.6096 0.054 Uiso 1 1 calc R . .
O14 O 0.2480(3) 0.4152(9) 0.05253(14) 0.0460(13) Uani 1 1 d . . .
C14 C 0.3576(6) -0.4180(14) 0.5864(3) 0.063(3) Uani 1 1 d . . .
H14A H 0.3766 -0.3797 0.5636 0.076 Uiso 1 1 calc R . .
O15 O 0.2276(3) 0.6595(9) 0.18960(18) 0.0544(15) Uani 1 1 d . . .
C15 C 0.2804(5) -0.4051(12) 0.5901(2) 0.0453(18) Uani 1 1 d . . .
O16 O 0.0655(3) 0.8223(10) -0.00750(15) 0.0575(16) Uani 1 1 d . . .
C16 C 0.2502(5) -0.4572(12) 0.6239(2) 0.0456(18) Uani 1 1 d . . .
H16A H 0.1961 -0.4452 0.6274 0.055 Uiso 1 1 calc R . .
C17 C 0.3036(5) -0.5272(11) 0.6517(2) 0.0401(17) Uani 1 1 d . . .
H17A H 0.2843 -0.5687 0.6742 0.048 Uiso 1 1 calc R . .
C18 C 0.3853(6) -0.5393(10) 0.6482(2) 0.0471(19) Uani 1 1 d . . .
C20 C 0.1851(4) -1.2258(12) 0.7200(2) 0.0449(18) Uani 1 1 d . . .
H20A H 0.1472 -1.2460 0.6983 0.067 Uiso 1 1 calc R . .
H20B H 0.1598 -1.1600 0.7393 0.067 Uiso 1 1 calc R . .
H20C H 0.2041 -1.3408 0.7302 0.067 Uiso 1 1 calc R . .
C21 C 0.1247(4) -0.9983(9) 0.27831(18) 0.0299(13) Uani 1 1 d . . .
C22 C 0.1894(5) -1.0807(11) 0.26253(19) 0.0413(17) Uani 1 1 d . . .
H22A H 0.1858 -1.1150 0.2369 0.050 Uiso 1 1 calc R . .
C23 C 0.2582(4) -1.1096(11) 0.28583(18) 0.0353(15) Uani 1 1 d . . .
C24 C 0.2606(4) -1.0760(9) 0.32355(19) 0.0325(14) Uani 1 1 d . . .
H24A H 0.3059 -1.1089 0.3393 0.039 Uiso 1 1 calc R . .
C25 C 0.1972(4) -0.9937(9) 0.33951(18) 0.0304(13) Uani 1 1 d . . .
C26 C 0.1276(4) -0.9555(9) 0.31602(18) 0.0286(13) Uani 1 1 d . . .
C27 C 0.1996(5) -0.9500(10) 0.38029(18) 0.0386(16) Uani 1 1 d . . .
H27A H 0.1516 -0.9253 0.3907 0.046 Uiso 1 1 calc R . .
C28 C 0.2679(5) -0.9440(15) 0.4031(2) 0.056(2) Uani 1 1 d . . .
H28A H 0.3169 -0.9600 0.3930 0.068 Uiso 1 1 calc R . .
```

```
C29 C 0.2648(5) -0.9123(15) 0.4440(2) 0.057(2) Uani 1 1 d . . .
C30 C 0.0041(5) -0.9458(12) 0.3482(2) 0.0454(18) Uani 1 1 d . . .
C31 C 0.0086(5) -1.1443(12) 0.3521(3) 0.054(2) Uani 1 1 d . . .
H31A H 0.0100 -1.1778 0.3789 0.064 Uiso 1 1 calc R . .
H31B H 0.0573 -1.1887 0.3423 0.064 Uiso 1 1 calc R . .
C32 C 0.0622(5) -0.6621(10) 0.3260(2) 0.0439(18) Uani 1 1 d . . .
H32A H 0.0084 -0.6150 0.3271 0.053 Uiso 1 1 calc R . .
H32B H 0.0794 -0.6317 0.3011 0.053 Uiso 1 1 calc R . .
C33 C 0.0958(5) -0.5545(12) 0.3915(3) 0.051(2) Uani 1 1 d . . .
H33A H 0.0448 -0.5910 0.3968 0.061 Uiso 1 1 calc R . .
C34 C 0.1472(6) -0.4823(13) 0.4205(3) 0.055(2) Uani 1 1 d . . .
H34A H 0.1303 -0.4669 0.4448 0.066 Uiso 1 1 calc R . .
C35 C 0.2236(6) -0.4334(12) 0.4132(2) 0.054(2) Uani 1 1 d . . .
C36 C 0.2464(5) -0.4508(13) 0.3756(2) 0.0483(19) Uani 1 1 d . . .
H36A H 0.2970 -0.4145 0.3696 0.058 Uiso 1 1 calc R . .
C37 C 0.1929(5) -0.5215(10) 0.3489(2) 0.0419(17) Uani 1 1 d . . .
H37A H 0.2079 -0.5360 0.3242 0.050 Uiso 1 1 calc R . .
C38 C 0.1173(5) -0.5731(10) 0.3564(2) 0.0399(16) Uani 1 1 d . . .
C39 C 0.2548(9) -0.368(2) 0.4805(4) 0.123(6) Uani 1 1 d . . .
H39A H 0.2974 -0.3209 0.4978 0.185 Uiso 1 1 calc R . .
H39B H 0.2431 -0.4911 0.4876 0.185 Uiso 1 1 calc R . .
H39C H 0.2079 -0.2942 0.4816 0.185 Uiso 1 1 calc R . .
C40 C 0.3311(5) -1.1939(14) 0.2702(2) 0.0497(19) Uani 1 1 d . . .
H40A H 0.3737 -1.2034 0.2903 0.075 Uiso 1 1 calc R . .
H40B H 0.3481 -1.1186 0.2501 0.075 Uiso 1 1 calc R . .
H40C H 0.3178 -1.3130 0.2604 0.075 Uiso 1 1 calc R . .
C41 C 0.5131(4) 0.4754(10) -0.17276(19) 0.0343(15) Uani 1 1 d . . .
C42 C 0.5740(4) 0.3564(11) -0.1647(2) 0.0385(16) Uani 1 1 d . . .
H42A H 0.6125 0.3397 -0.1818 0.046 Uiso 1 1 calc R . .
C43 C 0.5784(5) 0.2606(11) -0.1311(2) 0.0438(18) Uani 1 1 d . . .
C44 C 0.5216(4) 0.2962(11) -0.1052(2) 0.0369(15) Uani 1 1 d . . .
H44A H 0.5242 0.2344 -0.0820 0.044 Uiso 1 1 calc R . .
C45 C 0.4609(4) 0.4240(10) -0.11400(19) 0.0328(14) Uani 1 1 d . . .
C46 C 0.4572(4) 0.5111(9) -0.14836(19) 0.0300(13) Uani 1 1 d . . .
C47 C 0.4006(4) 0.4498(10) -0.08647(18) 0.0358(15) Uani 1 1 d . . .
H47A H 0.3501 0.4881 -0.0964 0.043 Uiso 1 1 calc R . .
C48 C 0.4107(5) 0.4244(12) -0.0493(2) 0.0416(17) Uani 1 1 d . . .
H48A H 0.4606 0.3888 -0.0380 0.050 Uiso 1 1 calc R . .
C49 C 0.3456(5) 0.4507(13) -0.0256(2) 0.0451(19) Uani 1 1 d . . .
C50 C 0.3229(4) 0.5896(10) -0.17703(19) 0.0347(14) Uani 1 1 d . . .
C51 C 0.3185(5) 0.3892(13) -0.1850(3) 0.054(2) Uani 1 1 d . . .
H51A H 0.3325 0.3237 -0.1614 0.065 Uiso 1 1 calc R . .
H51B H 0.3579 0.3587 -0.2026 0.065 Uiso 1 1 calc R . .
C52 C 0.4104(4) 0.8337(11) -0.1500(2) 0.0394(16) Uani 1 1 d . . .
H52A H 0.4671 0.8554 -0.1517 0.047 Uiso 1 1 calc R . .
H52B H 0.3811 0.9067 -0.1696 0.047 Uiso 1 1 calc R . .
C53 C 0.3113(5) 0.9637(10) -0.1090(2) 0.0426(17) Uani 1 1 d . . .
H53A H 0.2741 0.9711 -0.1303 0.051 Uiso 1 1 calc R . .
C54 C 0.2917(5) 1.0182(14) -0.0747(2) 0.052(2) Uani 1 1 d . . .
H54A H 0.2428 1.0757 -0.0727 0.062 Uiso 1 1 calc R . .
C55 C 0.3430(5) 0.9909(12) -0.0419(2) 0.050(2) Uani 1 1 d . . .
C56 C 0.4186(5) 0.9314(12) -0.0449(3) 0.0492(19) Uani 1 1 d . . .
H56A H 0.4555 0.9260 -0.0235 0.059 Uiso 1 1 calc R . .
C57 C 0.4397(4) 0.8793(11) -0.0800(2) 0.0390(16) Uani 1 1 d . . .
```

```
H57A H 0.4907 0.8313 -0.0817 0.047 Uiso 1 1 calc R . .
C58 C 0.3895(4) 0.8945(10) -0.1127(2) 0.0380(16) Uani 1 1 d . . .
C59 C 0.3602(6) 1.0132(17) 0.0263(3) 0.070(3) Uani 1 1 d . . .
H59A H 0.3326 1.0595 0.0471 0.105 Uiso 1 1 calc R . .
H59B H 0.4113 1.0720 0.0262 0.105 Uiso 1 1 calc R . .
H59C H 0.3678 0.8842 0.0294 0.105 Uiso 1 1 calc R . .
C60 C 0.6421(5) 0.1225(14) -0.1215(3) 0.061(3) Uani 1 1 d . . .
H60A H 0.6767 0.1162 -0.1418 0.092 Uiso 1 1 calc R . .
H60B H 0.6179 0.0055 -0.1183 0.092 Uiso 1 1 calc R . .
H60C H 0.6728 0.1566 -0.0982 0.092 Uiso 1 1 calc R . .
C61 C -0.0161(4) 0.4190(10) 0.17626(19) 0.0328(14) Uani 1 1 d . . .
C62 C -0.0752(4) 0.3050(13) 0.1650(2) 0.0417(17) Uani 1 1 d . . .
H62A H -0.1181 0.2917 0.1799 0.050 Uiso 1 1 calc R . .
C63 C -0.0743(5) 0.2051(11) 0.1313(2) 0.0464(18) Uani 1 1 d . . .
C64 C -0.0087(4) 0.2239(10) 0.11075(19) 0.0349(14) Uani 1 1 d . . .
H64A H -0.0060 0.1541 0.0888 0.042 Uiso 1 1 calc R . .
C65 C 0.0539(4) 0.3437(9) 0.12153(17) 0.0308(13) Uani 1 1 d . . .
C66 C 0.0481(4) 0.4458(9) 0.15481(17) 0.0294(13) Uani 1 1 d . . .
C67 C 0.1179(4) 0.3735(9) 0.09753(17) 0.0284(13) Uani 1 1 d . . .
H67A H 0.1663 0.4152 0.1094 0.034 Uiso 1 1 calc R . .
C68 C 0.1144(4) 0.3471(10) 0.0596(2) 0.0382(16) Uani 1 1 d . . .
H68A H 0.0671 0.3029 0.0470 0.046 Uiso 1 1 calc R . .
C69 C 0.1795(4) 0.3837(11) 0.03830(19) 0.0362(15) Uani 1 1 d . . .
C70 C 0.1772(4) 0.5495(12) 0.18471(19) 0.0398(16) Uani 1 1 d . . .
C71 C 0.1874(5) 0.3649(13) 0.2036(2) 0.0480(19) Uani 1 1 d . . .
H71A H 0.1354 0.3066 0.2034 0.058 Uiso 1 1 calc R . .
H71B H 0.2079 0.3815 0.2301 0.058 Uiso 1 1 calc R . .
C72 C 0.0876(5) 0.7669(11) 0.1522(2) 0.0465(18) Uani 1 1 d . . .
H72A H 0.1280 0.8495 0.1638 0.056 Uiso 1 1 calc R . .
H72B H 0.0365 0.8018 0.1609 0.056 Uiso 1 1 calc R . .
C73 C 0.1475(4) 0.8342(11) 0.0922(2) 0.0423(17) Uani 1 1 d . . .
H73A H 0.1954 0.8581 0.1068 0.051 Uiso 1 1 calc R . .
C74 C 0.1460(4) 0.8508(11) 0.0524(2) 0.0410(17) Uani 1 1 d . . .
H74A H 0.1913 0.8841 0.0405 0.049 Uiso 1 1 calc R . .
C75 C 0.0730(5) 0.8147(11) 0.03180(19) 0.0409(16) Uani 1 1 d . . .
C76 C 0.0075(4) 0.7684(12) 0.0492(2) 0.0474(19) Uani 1 1 d . . .
H76A H -0.0406 0.7453 0.0346 0.057 Uiso 1 1 calc R . .
C77 C 0.0112(4) 0.7552(11) 0.0875(2) 0.0430(17) Uani 1 1 d . . .
H77A H -0.0348 0.7255 0.0991 0.052 Uiso 1 1 calc R . .
C78 C 0.0836(4) 0.7858(10) 0.11037(18) 0.0369(15) Uani 1 1 d . . .
C79 C 0.1317(6) 0.8756(15) -0.0266(3) 0.062(2) Uani 1 1 d . . .
H79A H 0.1173 0.8748 -0.0537 0.093 Uiso 1 1 calc R . .
H79B H 0.1751 0.7922 -0.0206 0.093 Uiso 1 1 calc R . .
H79C H 0.1480 0.9961 -0.0187 0.093 Uiso 1 1 calc R . .
C80 C -0.1399(5) 0.0774(14) 0.1178(3) 0.056(2) Uani 1 1 d . . .
H80A H -0.1808 0.0798 0.1353 0.084 Uiso 1 1 calc R . .
H80B H -0.1188 -0.0439 0.1166 0.084 Uiso 1 1 calc R . .
H80C H -0.1624 0.1139 0.0929 0.084 Uiso 1 1 calc R . .
C19 C 0.1411(11) -0.322(4) 0.5599(6) 0.172(8) Uiso 1 1 d . . .
H19A H 0.1189 -0.2677 0.5365 0.258 Uiso 1 1 calc R . .
H19B H 0.1272 -0.2504 0.5811 0.258 Uiso 1 1 calc R . .
H19C H 0.1199 -0.4432 0.5619 0.258 Uiso 1 1 calc R . .

loop_
```

```
 _atom_site_aniso_label
 _atom_site_aniso_U_11
 _atom_site_aniso_U_22
 _atom_site_aniso_U_33
 _atom_site_aniso_U_23
 _atom_site_aniso_U_13
 _atom_site_aniso_U_12
N1 0.039(3) 0.031(3) 0.029(3) -0.009(2) 0.002(2) -0.004(2)
Br1 0.0494(4) 0.0421(4) 0.0351(3) 0.0014(3) -0.0094(3) -0.0030(3)
I1 0.0577(3) 0.0408(3) 0.0975(5) 0.0162(3) 0.0020(3) 0.0066(3)
C1 0.050(4) 0.022(3) 0.032(3) -0.006(3) -0.001(3) 0.003(3)
O1 0.087(5) 0.116(7) 0.033(3) 0.004(4) -0.010(3) 0.040(5)
N2 0.031(3) 0.025(3) 0.044(3) -0.001(2) 0.003(2) 0.004(2)
Br2 0.0437(4) 0.0480(5) 0.0372(4) -0.0013(3) -0.0105(3) 0.0063(3)
I2 0.0485(3) 0.0472(3) 0.0986(5) -0.0182(3) -0.0075(3) 0.0010(3)
C2 0.046(4) 0.033(4) 0.034(3) -0.006(3) 0.000(3) 0.006(3)
O2 0.063(4) 0.103(6) 0.043(3) -0.012(4) -0.009(3) -0.009(4)
Br3 0.0483(4) 0.0487(5) 0.0312(3) 0.0068(3) 0.0100(3) 0.0005(3)
I3 0.0467(3) 0.0721(4) 0.0923(5) -0.0326(4) -0.0132(3) -0.0051(3)
N3 0.027(3) 0.033(3) 0.039(3) 0.001(2) 0.007(2) -0.001(2)
C3 0.042(4) 0.024(3) 0.027(3) 0.000(2) -0.001(3) -0.002(3)
O3 0.049(3) 0.052(4) 0.061(4) 0.013(3) 0.006(3) -0.002(3)
Br4 0.0491(4) 0.0528(5) 0.0310(3) -0.0032(3) 0.0085(3) 0.0110(4)
I4 0.0806(5) 0.0624(4) 0.1019(6) 0.0212(4) 0.0249(4) 0.0243(4)
N4 0.035(3) 0.034(3) 0.032(3) 0.002(2) -0.006(2) 0.004(2)
C4 0.046(4) 0.029(3) 0.037(4) -0.011(3) -0.004(3) 0.009(3)
O4 0.063(4) 0.098(6) 0.052(4) 0.017(4) -0.007(3) 0.022(4)
O5 0.084(5) 0.146(9) 0.043(3) 0.004(5) -0.022(3) -0.037(6)
C5 0.050(4) 0.032(4) 0.020(3) -0.001(3) 0.000(3) 0.003(3)
O6 0.084(5) 0.096(6) 0.028(3) 0.005(3) 0.001(3) 0.015(4)
C6 0.047(4) 0.026(3) 0.034(3) -0.003(3) 0.003(3) 0.008(3)
C7 0.045(4) 0.041(4) 0.036(3) -0.007(3) 0.005(3) 0.003(3)
O8 0.076(4) 0.068(4) 0.049(3) -0.005(3) -0.001(3) -0.011(4)
C8 0.064(5) 0.061(6) 0.031(4) -0.010(4) -0.012(3) 0.019(4)
O9 0.056(3) 0.088(5) 0.036(3) -0.004(3) 0.020(3) -0.020(3)
C9 0.073(6) 0.056(5) 0.039(4) -0.007(4) -0.003(4) 0.001(5)
O10 0.049(3) 0.083(5) 0.048(3) 0.019(3) 0.022(3) 0.007(3)
C10 0.049(4) 0.044(4) 0.036(4) 0.004(3) 0.003(3) 0.004(4)
O11 0.032(3) 0.056(4) 0.052(3) 0.001(3) 0.001(2) 0.010(3)
C11 0.075(6) 0.042(5) 0.047(5) -0.004(4) 0.013(4) 0.020(4)
O12 0.059(4) 0.081(5) 0.045(3) -0.014(3) -0.004(3) 0.011(4)
C12 0.074(5) 0.018(3) 0.034(4) 0.004(3) -0.011(3) -0.005(3)
O13 0.038(3) 0.098(5) 0.027(2) -0.008(3) 0.008(2) -0.014(3)
C13 0.048(4) 0.042(4) 0.046(4) 0.007(3) 0.006(3) 0.002(4)
O14 0.029(2) 0.074(4) 0.035(3) -0.013(3) 0.004(2) -0.011(3)
C14 0.068(6) 0.066(6) 0.055(5) 0.026(5) 0.006(4) 0.016(5)
O15 0.038(3) 0.058(4) 0.067(4) -0.010(3) 0.000(3) -0.016(3)
C15 0.044(4) 0.043(4) 0.048(4) 0.010(4) 0.002(3) 0.005(4)
O16 0.051(3) 0.082(5) 0.037(3) 0.006(3) -0.009(2) -0.009(3)
C16 0.040(4) 0.050(5) 0.048(4) 0.000(4) 0.010(3) -0.001(4)
C17 0.048(4) 0.041(4) 0.031(3) -0.001(3) 0.005(3) 0.004(3)
C18 0.073(6) 0.028(4) 0.039(4) -0.001(3) -0.003(4) 0.008(4)
C20 0.043(4) 0.054(5) 0.038(4) 0.002(3) 0.004(3) -0.009(4)
C21 0.029(3) 0.030(3) 0.030(3) 0.001(3) -0.006(2) 0.001(3)
```

C22 0.063(5) 0.039(4) 0.022(3) 0.000(3) 0.004(3) -0.017(3)
C23 0.027(3) 0.051(4) 0.028(3) 0.008(3) 0.000(2) 0.001(3)
C24 0.033(3) 0.032(3) 0.031(3) 0.010(3) -0.003(3) -0.003(3)
C25 0.038(3) 0.029(3) 0.025(3) 0.005(2) 0.006(3) 0.001(3)
C26 0.030(3) 0.024(3) 0.032(3) 0.005(3) 0.002(2) -0.005(2)
C27 0.056(4) 0.035(4) 0.024(3) -0.003(3) -0.002(3) 0.008(3)
C28 0.058(5) 0.084(7) 0.025(3) -0.006(4) -0.006(3) -0.006(5)
C29 0.056(5) 0.079(7) 0.032(4) 0.009(4) -0.009(3) -0.012(5)
C30 0.042(4) 0.053(5) 0.041(4) -0.011(4) 0.004(3) -0.001(4)
C31 0.044(4) 0.043(5) 0.072(6) 0.009(4) -0.001(4) -0.003(4)
C32 0.063(5) 0.027(4) 0.041(4) 0.007(3) -0.005(3) 0.007(3)
C33 0.044(4) 0.050(5) 0.060(5) -0.002(4) 0.008(4) -0.001(4)
C34 0.065(5) 0.052(5) 0.052(5) -0.004(4) 0.026(4) -0.001(4)
C35 0.071(6) 0.043(5) 0.044(4) 0.000(4) -0.012(4) -0.008(4)
C36 0.050(4) 0.051(5) 0.045(4) 0.005(4) 0.009(3) -0.001(4)
C37 0.058(5) 0.036(4) 0.033(4) -0.003(3) 0.013(3) -0.007(3)
C38 0.050(4) 0.028(4) 0.041(4) -0.008(3) 0.002(3) 0.001(3)
C39 0.161(14) 0.110(12) 0.087(9) -0.005(9) -0.056(9) -0.032(11)
C40 0.044(4) 0.059(5) 0.046(4) -0.007(4) 0.007(3) 0.008(4)
C41 0.041(4) 0.036(4) 0.026(3) 0.004(3) 0.009(3) -0.008(3)
C42 0.027(3) 0.052(5) 0.037(4) -0.001(3) 0.004(3) -0.001(3)
C43 0.047(4) 0.043(5) 0.042(4) 0.011(3) 0.007(3) 0.011(3)
C44 0.031(3) 0.036(4) 0.043(4) 0.008(3) 0.000(3) 0.005(3)
C45 0.026(3) 0.034(4) 0.038(4) -0.001(3) 0.000(3) -0.003(3)
C46 0.025(3) 0.028(3) 0.036(3) -0.003(3) -0.001(2) -0.004(2)
C47 0.041(4) 0.042(4) 0.025(3) -0.001(3) 0.005(3) -0.002(3)
C48 0.036(4) 0.053(5) 0.036(4) 0.003(3) 0.004(3) -0.005(3)
C49 0.039(4) 0.063(5) 0.033(4) 0.015(3) 0.003(3) -0.014(4)
C50 0.031(3) 0.040(4) 0.034(3) 0.003(3) 0.004(3) 0.000(3)
C51 0.029(4) 0.052(5) 0.081(6) -0.016(5) 0.003(4) -0.013(4)
C52 0.039(4) 0.048(5) 0.032(3) 0.005(3) 0.005(3) -0.003(3)
C53 0.051(4) 0.028(4) 0.048(4) 0.006(3) 0.002(3) 0.000(3)
C54 0.039(4) 0.062(6) 0.055(5) -0.012(4) 0.000(3) 0.001(4)
C55 0.060(5) 0.045(5) 0.042(4) -0.005(3) -0.017(4) 0.010(4)
C56 0.051(5) 0.046(5) 0.050(5) -0.006(4) 0.001(4) -0.005(4)
C57 0.030(3) 0.048(4) 0.037(4) 0.003(3) -0.007(3) -0.004(3)
C58 0.042(4) 0.029(3) 0.044(4) -0.005(3) 0.007(3) -0.016(3)
C59 0.069(6) 0.090(8) 0.047(5) -0.017(5) -0.012(4) 0.032(6)
C60 0.038(4) 0.056(6) 0.091(7) 0.023(5) 0.014(4) 0.024(4)
C61 0.032(3) 0.035(4) 0.030(3) 0.001(3) 0.000(3) 0.006(3)
C62 0.032(3) 0.059(5) 0.035(4) 0.002(3) 0.009(3) -0.003(4)
C63 0.050(4) 0.032(4) 0.057(5) -0.005(4) 0.007(4) 0.001(3)
C64 0.030(3) 0.038(4) 0.037(3) -0.004(3) 0.007(3) -0.004(3)
C65 0.041(4) 0.025(3) 0.026(3) 0.000(2) 0.002(3) -0.006(3)
C66 0.038(3) 0.028(3) 0.021(3) -0.004(2) -0.001(2) 0.004(3)
C67 0.031(3) 0.030(3) 0.024(3) -0.003(2) 0.002(2) 0.003(3)
C68 0.047(4) 0.034(4) 0.034(4) -0.005(3) 0.005(3) -0.007(3)
C69 0.028(3) 0.048(4) 0.031(3) -0.005(3) -0.001(3) -0.002(3)
C70 0.035(4) 0.053(5) 0.033(3) -0.012(3) 0.010(3) 0.006(3)
C71 0.042(4) 0.058(5) 0.044(4) 0.014(4) 0.003(3) 0.007(4)
C72 0.059(5) 0.039(5) 0.041(4) 0.001(3) 0.003(3) 0.000(4)
C73 0.031(3) 0.051(5) 0.043(4) -0.002(3) -0.008(3) -0.003(3)
C74 0.038(4) 0.045(4) 0.038(4) 0.005(3) -0.008(3) -0.008(3)
C75 0.054(4) 0.039(4) 0.027(3) 0.005(3) -0.007(3) 0.002(4)

```
C76 0.040(4) 0.048(5) 0.051(4) 0.013(4) -0.014(3) 0.001(3)
C77 0.027(3) 0.044(4) 0.057(5) 0.001(3) -0.001(3) 0.002(3)
C78 0.049(4) 0.030(3) 0.030(3) 0.002(3) -0.008(3) 0.001(3)
C79 0.078(6) 0.066(6) 0.044(5) 0.007(4) 0.015(4) 0.005(5)
C80 0.034(4) 0.058(6) 0.078(6) -0.008(5) 0.012(4) -0.016(4)

_geom_special_details
;
 All esds (except the esd in the dihedral angle between two l.s. planes)
 are estimated using the full covariance matrix.  The cell esds are taken
 into account individually in the estimation of esds in distances, angles
 and torsion angles; correlations between esds in cell parameters are only
 used when they are defined by crystal symmetry.  An approximate
(isotropic)
 treatment of cell esds is used for estimating esds involving l.s. planes.
;

loop_
 _geom_bond_atom_site_label_1
 _geom_bond_atom_site_label_2
 _geom_bond_distance
 _geom_bond_site_symmetry_2
 _geom_bond_publ_flag
N1 C10 1.377(10) . ?
N1 C6 1.407(9) . ?
N1 C12 1.469(9) . ?
Br1 C1 1.914(7) . ?
I1 C11 2.147(9) . ?
C1 C2 1.371(11) . ?
C1 C6 1.414(10) . ?
O1 C9 1.299(11) . ?
N2 C30 1.345(10) . ?
N2 C26 1.444(9) . ?
N2 C32 1.507(9) . ?
Br2 C21 1.901(6) . ?
I2 C31 2.156(9) . ?
C2 C3 1.399(10) . ?
O2 C9 1.231(12) . ?
Br3 C41 1.915(7) . ?
I3 C51 2.122(8) . ?
N3 C50 1.368(9) . ?
N3 C46 1.457(9) . ?
N3 C52 1.493(10) . ?
C3 C4 1.373(10) . ?
C3 C20 1.489(10) . ?
O3 C10 1.214(10) . ?
Br4 C61 1.899(7) . ?
I4 C71 2.127(9) . ?
N4 C70 1.343(9) . ?
N4 C66 1.436(9) . ?
N4 C72 1.483(10) . ?
C4 C5 1.361(11) . ?
O4 C15 1.405(10) . ?
O4 C19 1.521(19) . ?
```

```
O5 C29 1.236(10) . ?
C5 C6 1.414(10) . ?
C5 C7 1.498(10) . ?
O6 C29 1.275(11) . ?
C7 C8 1.308(11) . ?
O7 C30 1.246(10) . ?
O8 C35 1.370(10) . ?
O8 C39 1.566(16) . ?
C8 C9 1.466(12) . ?
O9 C49 1.308(9) . ?
O10 C49 1.198(10) . ?
C10 C11 1.528(12) . ?
O11 C50 1.182(9) . ?
O12 C55 1.386(11) . ?
O12 C59 1.427(11) . ?
C12 C18 1.504(11) . ?
O13 C69 1.316(8) . ?
C13 C14 1.347(12) . ?
C13 C18 1.386(11) . ?
O14 C69 1.245(8) . ?
C14 C15 1.328(12) . ?
O15 C70 1.181(10) . ?
C15 C16 1.400(11) . ?
O16 C75 1.390(8) . ?
O16 C79 1.418(10) . ?
C16 C17 1.379(11) . ?
C17 C18 1.403(12) . ?
C21 C26 1.372(9) . ?
C21 C22 1.414(11) . ?
C22 C23 1.384(10) . ?
C23 C24 1.359(10) . ?
C23 C40 1.530(10) . ?
C24 C25 1.397(10) . ?
C25 C26 1.410(9) . ?
C25 C27 1.480(9) . ?
C27 C28 1.352(11) . ?
C28 C29 1.475(11) . ?
C30 C31 1.480(13) . ?
C32 C38 1.513(11) . ?
C33 C38 1.337(12) . ?
C33 C34 1.392(13) . ?
C34 C35 1.390(13) . ?
C35 C36 1.427(12) . ?
C36 C37 1.356(12) . ?
C37 C38 1.385(11) . ?
C41 C42 1.368(10) . ?
C41 C46 1.364(9) . ?
C42 C43 1.385(10) . ?
C43 C44 1.412(10) . ?
C43 C60 1.505(11) . ?
C44 C45 1.412(9) . ?
C45 C46 1.376(10) . ?
C45 C47 1.487(10) . ?
C47 C48 1.330(10) . ?
```

```
C48 C49 1.456(11) . ?
C50 C51 1.513(12) . ?
C52 C58 1.469(10) . ?
C53 C54 1.354(11) . ?
C53 C58 1.436(11) . ?
C54 C55 1.403(11) . ?
C55 C56 1.367(12) . ?
C56 C57 1.381(12) . ?
C57 C58 1.383(10) . ?
C61 C62 1.344(11) . ?
C61 C66 1.395(9) . ?
C62 C63 1.407(11) . ?
C63 C64 1.389(10) . ?
C63 C80 1.506(11) . ?
C64 C65 1.410(9) . ?
C65 C66 1.414(9) . ?
C65 C67 1.453(9) . ?
C67 C68 1.358(9) . ?
C68 C69 1.416(10) . ?
C70 C71 1.528(12) . ?
C72 C78 1.487(10) . ?
C73 C78 1.357(10) . ?
C73 C74 1.413(11) . ?
C74 C75 1.406(10) . ?
C75 C76 1.359(11) . ?
C76 C77 1.358(11) . ?
C77 C78 1.427(9) . ?

loop_
 _geom_angle_atom_site_label_1
 _geom_angle_atom_site_label_2
 _geom_angle_atom_site_label_3
 _geom_angle
 _geom_angle_site_symmetry_1
 _geom_angle_site_symmetry_3
 _geom_angle_publ_flag
C10 N1 C6 124.5(6) . . ?
C10 N1 C12 117.4(7) . . ?
C6 N1 C12 118.1(6) . . ?
C2 C1 C6 123.9(7) . . ?
C2 C1 Br1 118.0(5) . . ?
C6 C1 Br1 118.1(6) . . ?
C30 N2 C26 124.8(6) . . ?
C30 N2 C32 120.8(7) . . ?
C26 N2 C32 114.3(6) . . ?
C1 C2 C3 118.5(7) . . ?
C50 N3 C46 122.5(6) . . ?
C50 N3 C52 120.0(6) . . ?
C46 N3 C52 117.3(5) . . ?
C4 C3 C2 118.2(7) . . ?
C4 C3 C20 120.5(6) . . ?
C2 C3 C20 121.2(6) . . ?
C70 N4 C66 125.1(6) . . ?
C70 N4 C72 118.7(7) . . ?
```

```
C66 N4 C72 116.2(6) . . ?
C5 C4 C3 124.1(7) . . ?
C15 O4 C19 123.3(10) . . ?
C4 C5 C6 119.4(6) . . ?
C4 C5 C7 121.1(6) . . ?
C6 C5 C7 119.4(7) . . ?
N1 C6 C5 122.5(6) . . ?
N1 C6 C1 121.2(6) . . ?
C5 C6 C1 115.9(7) . . ?
C8 C7 C5 125.4(8) . . ?
C35 O8 C39 112.8(8) . . ?
C7 C8 C9 123.2(9) . . ?
O2 C9 O1 123.6(8) . . ?
O2 C9 C8 121.1(8) . . ?
O1 C9 C8 115.1(9) . . ?
O3 C10 N1 124.1(8) . . ?
O3 C10 C11 120.8(8) . . ?
N1 C10 C11 115.1(7) . . ?
C10 C11 I1 108.8(6) . . ?
C55 O12 C59 118.5(7) . . ?
N1 C12 C18 110.8(6) . . ?
C14 C13 C18 120.9(8) . . ?
C15 C14 C13 123.0(8) . . ?
C14 C15 C16 120.1(8) . . ?
C14 C15 O4 118.6(7) . . ?
C16 C15 O4 121.2(7) . . ?
C75 O16 C79 119.2(6) . . ?
C17 C16 C15 116.9(7) . . ?
C16 C17 C18 123.2(7) . . ?
C13 C18 C17 115.9(7) . . ?
C13 C18 C12 122.6(8) . . ?
C17 C18 C12 121.2(8) . . ?
C26 C21 C22 121.7(6) . . ?
C26 C21 Br2 120.8(5) . . ?
C22 C21 Br2 117.5(5) . . ?
C23 C22 C21 118.1(6) . . ?
C24 C23 C22 120.6(7) . . ?
C24 C23 C40 118.5(6) . . ?
C22 C23 C40 120.7(6) . . ?
C23 C24 C25 121.6(6) . . ?
C24 C25 C26 118.6(6) . . ?
C24 C25 C27 122.5(6) . . ?
C26 C25 C27 118.8(6) . . ?
C21 C26 C25 119.0(6) . . ?
C21 C26 N2 119.5(6) . . ?
C25 C26 N2 121.4(6) . . ?
C28 C27 C25 122.7(7) . . ?
C27 C28 C29 119.4(8) . . ?
O5 C29 O6 121.9(8) . . ?
O5 C29 C28 117.1(9) . . ?
O6 C29 C28 120.9(8) . . ?
O7 C30 N2 123.2(8) . . ?
O7 C30 C31 119.6(8) . . ?
N2 C30 C31 117.3(7) . . ?
```

```
C30 C31 I2 109.3(6) . . ?
N2 C32 C38 111.8(6) . . ?
C38 C33 C34 121.6(8) . . ?
C35 C34 C33 119.5(8) . . ?
O8 C35 C34 125.5(8) . . ?
O8 C35 C36 115.4(8) . . ?
C34 C35 C36 119.0(8) . . ?
C37 C36 C35 117.9(8) . . ?
C36 C37 C38 122.9(7) . . ?
C33 C38 C37 118.9(7) . . ?
C33 C38 C32 120.6(8) . . ?
C37 C38 C32 120.3(7) . . ?
C42 C41 C46 123.0(6) . . ?
C42 C41 Br3 118.1(5) . . ?
C46 C41 Br3 118.9(5) . . ?
C41 C42 C43 119.6(7) . . ?
C42 C43 C44 118.4(7) . . ?
C42 C43 C60 121.7(7) . . ?
C44 C43 C60 119.8(7) . . ?
C43 C44 C45 120.4(6) . . ?
C46 C45 C44 119.0(6) . . ?
C46 C45 C47 122.9(6) . . ?
C44 C45 C47 118.0(6) . . ?
C41 C46 C45 119.5(6) . . ?
C41 C46 N3 121.2(6) . . ?
C45 C46 N3 119.3(6) . . ?
C48 C47 C45 126.9(7) . . ?
C47 C48 C49 121.1(7) . . ?
O10 C49 O9 123.8(8) . . ?
O10 C49 C48 123.3(7) . . ?
O9 C49 C48 112.9(7) . . ?
O11 C50 N3 122.3(7) . . ?
O11 C50 C51 125.2(7) . . ?
N3 C50 C51 112.5(6) . . ?
C50 C51 I3 113.9(6) . . ?
C58 C52 N3 114.3(6) . . ?
C54 C53 C58 119.4(7) . . ?
C53 C54 C55 121.4(8) . . ?
C56 C55 O12 124.8(7) . . ?
C56 C55 C54 119.6(8) . . ?
O12 C55 C54 115.1(7) . . ?
C55 C56 C57 118.8(8) . . ?
C56 C57 C58 123.1(7) . . ?
C57 C58 C53 117.1(7) . . ?
C57 C58 C52 123.5(7) . . ?
C53 C58 C52 119.4(7) . . ?
C62 C61 C66 121.5(6) . . ?
C62 C61 Br4 119.8(5) . . ?
C66 C61 Br4 118.7(5) . . ?
C61 C62 C63 121.2(7) . . ?
C64 C63 C62 117.7(7) . . ?
C64 C63 C80 119.8(7) . . ?
C62 C63 C80 122.5(7) . . ?
C63 C64 C65 122.5(7) . . ?
```

```
C64 C65 C66 117.2(6) . . ?
C64 C65 C67 121.2(6) . . ?
C66 C65 C67 121.3(6) . . ?
C61 C66 C65 119.7(6) . . ?
C61 C66 N4 121.2(6) . . ?
C65 C66 N4 119.0(6) . . ?
C68 C67 C65 126.3(6) . . ?
C67 C68 C69 122.3(7) . . ?
O14 C69 O13 120.6(6) . . ?
O14 C69 C68 124.1(6) . . ?
O13 C69 C68 115.3(6) . . ?
O15 C70 N4 123.5(8) . . ?
O15 C70 C71 120.2(7) . . ?
N4 C70 C71 116.2(7) . . ?
C70 C71 I4 113.0(5) . . ?
N4 C72 C78 112.5(6) . . ?
C78 C73 C74 123.7(6) . . ?
C75 C74 C73 116.1(7) . . ?
C76 C75 O16 117.4(6) . . ?
C76 C75 C74 121.8(6) . . ?
O16 C75 C74 120.8(7) . . ?
C77 C76 C75 120.4(7) . . ?
C76 C77 C78 121.3(7) . . ?
C73 C78 C77 116.8(6) . . ?
C73 C78 C72 122.2(6) . . ?
C77 C78 C72 120.9(7) . . ?

_diffrn_measured_fraction_theta_max    0.997
_diffrn_reflns_theta_full              30.00
_diffrn_measured_fraction_theta_full   0.997
_refine_diff_density_max    8.357
_refine_diff_density_min   -1.927
_refine_diff_density_rms    0.198

++++++++++++++++++++++++++++++++++++++++++++++++++++++++++++++++++++++++++++++
```

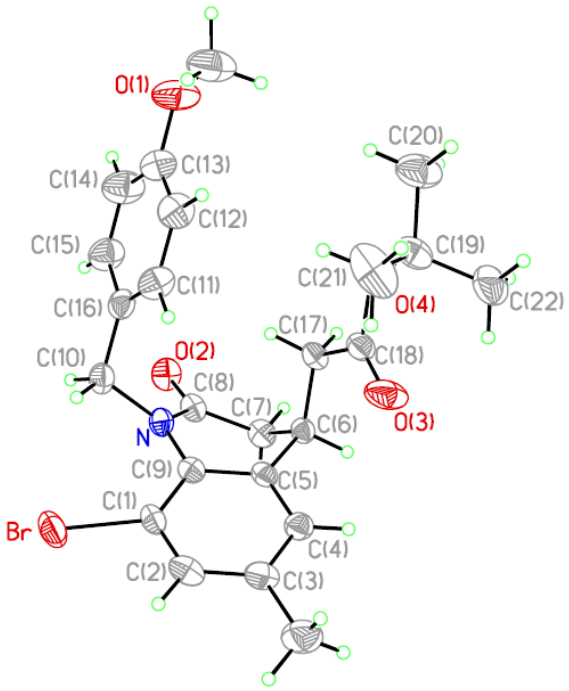

The corresponding CIF file for (*S*)-**5.18f** is shown below, between the lines of "+" symbols.

++

```
data_dg81908s

_audit_creation_method            SHELXL-97
_chemical_name_systematic
;
 ?
;
_chemical_name_common             ?
_chemical_melting_point           ?
_chemical_formula_moiety          'C24 H28 Br N O4'
_chemical_formula_sum
 'C24 H28 Br N O4'
_chemical_formula_weight          474.38
_chemical_absolute_configuration   ad
loop_
 _atom_type_symbol
 _atom_type_description
 _atom_type_scat_dispersion_real
 _atom_type_scat_dispersion_imag
 _atom_type_scat_source
 'C'  'C'   0.0033   0.0016
 'International Tables Vol C Tables 4.2.6.8 and 6.1.1.4'
 'H'  'H'   0.0000   0.0000
 'International Tables Vol C Tables 4.2.6.8 and 6.1.1.4'
 'N'  'N'   0.0061   0.0033
 'International Tables Vol C Tables 4.2.6.8 and 6.1.1.4'
```

```
 'O'  'O'   0.0106   0.0060
 'International Tables Vol C Tables 4.2.6.8 and 6.1.1.4'
 'Br'  'Br'  -0.2901   2.4595
 'International Tables Vol C Tables 4.2.6.8 and 6.1.1.4'

_symmetry_cell_setting           monoclinic
_symmetry_space_group_name_H-M    'P 21'

loop_
 _symmetry_equiv_pos_as_xyz
 'x, y, z'
 '-x, y+1/2, -z'

_cell_length_a                    10.5601(18)
_cell_length_b                    7.3873(13)
_cell_length_c                    14.727(3)
_cell_angle_alpha                 90.00
_cell_angle_beta                  101.490(4)
_cell_angle_gamma                 90.00
_cell_volume                      1125.8(3)
_cell_formula_units_Z             2
_cell_measurement_temperature     203(2)
_cell_measurement_reflns_used     2752
_cell_measurement_theta_min       2.6
_cell_measurement_theta_max       22.6

_exptl_crystal_description       block
_exptl_crystal_colour             colorless
_exptl_crystal_size_max           0.21
_exptl_crystal_size_mid           0.18
_exptl_crystal_size_min           0.10
_exptl_crystal_density_meas       0
_exptl_crystal_density_diffrn     1.399
_exptl_crystal_density_method     'not measured'
_exptl_crystal_F_000              492
_exptl_absorpt_coefficient_mu     1.855
_exptl_absorpt_correction_type    Multi-scan
_exptl_absorpt_correction_T_min   0.6967
_exptl_absorpt_correction_T_max   0.8362
_exptl_absorpt_process_details   'Bruker Sadabs'

_exptl_special_details
;
 ?
;

_diffrn_ambient_temperature       203(2)
_diffrn_radiation_wavelength      0.71073
_diffrn_radiation_type            MoK\a
_diffrn_radiation_source          'fine-focus sealed tube'
_diffrn_radiation_monochromator   graphite
_diffrn_measurement_device_type   'Bruker Smart Apex CCD'
_diffrn_measurement_method        'omega scans'
_diffrn_detector_area_resol_mean  ?
```

```
_diffrn_standards_number          ?
_diffrn_standards_interval_count  ?
_diffrn_standards_interval_time   ?
_diffrn_standards_decay_%         ?
_diffrn_reflns_number             14095
_diffrn_reflns_av_R_equivalents   0.0458
_diffrn_reflns_av_sigmaI/netI     0.0873
_diffrn_reflns_limit_h_min        -15
_diffrn_reflns_limit_h_max        15
_diffrn_reflns_limit_k_min        -10
_diffrn_reflns_limit_k_max        11
_diffrn_reflns_limit_l_min        -21
_diffrn_reflns_limit_l_max        21
_diffrn_reflns_theta_min          1.97
_diffrn_reflns_theta_max          32.35
_reflns_number_total              7315
_reflns_number_gt                 5348
_reflns_threshold_expression      >2sigma(I)

_computing_data_collection        'Bruker SMART'
_computing_cell_refinement        'Bruker SMART'
_computing_data_reduction         'Bruker SAINT'
_computing_structure_solution     'SHELXS-97 (Sheldrick, 1990)'
_computing_structure_refinement   'SHELXL-97 (Sheldrick, 1997)'
_computing_molecular_graphics     'Bruker SHELXTL'
_computing_publication_material   'Bruker SHELXTL'

_refine_special_details
;
 Refinement of F^2^ against ALL reflections.  The weighted R-factor wR and
 goodness of fit S are based on F^2^, conventional R-factors R are based
 on F, with F set to zero for negative F^2^. The threshold expression of
 F^2^ > 2sigma(F^2^) is used only for calculating R-factors(gt) etc. and
is
 not relevant to the choice of reflections for refinement.  R-factors
based
 on F^2^ are statistically about twice as large as those based on F, and
R-
 factors based on ALL data will be even larger.
;

_refine_ls_structure_factor_coef  Fsqd
_refine_ls_matrix_type            full
_refine_ls_weighting_scheme       calc
_refine_ls_weighting_details
 'calc w=1/[\s^2^(Fo^2^)+(0.0780P)^2^+0.0000P] where P=(Fo^2^+2Fc^2^)/3'
_atom_sites_solution_primary      direct
_atom_sites_solution_secondary    difmap
_atom_sites_solution_hydrogens    geom
_refine_ls_hydrogen_treatment     constr
_refine_ls_extinction_method      none
_refine_ls_extinction_coef        ?
_refine_ls_abs_structure_details
 'Flack H D (1983), Acta Cryst. A39, 876-881'
```

```
_refine_ls_abs_structure_Flack    0.008(9)
_refine_ls_number_reflns          7315
_refine_ls_number_parameters      277
_refine_ls_number_restraints      1
_refine_ls_R_factor_all           0.0747
_refine_ls_R_factor_gt            0.0500
_refine_ls_wR_factor_ref          0.1338
_refine_ls_wR_factor_gt           0.1159
_refine_ls_goodness_of_fit_ref    0.823
_refine_ls_restrained_S_all       0.823
_refine_ls_shift/su_max           0.001
_refine_ls_shift/su_mean          0.000

loop_
 _atom_site_label
 _atom_site_type_symbol
 _atom_site_fract_x
 _atom_site_fract_y
 _atom_site_fract_z
 _atom_site_U_iso_or_equiv
 _atom_site_adp_type
 _atom_site_occupancy
 _atom_site_symmetry_multiplicity
 _atom_site_calc_flag
 _atom_site_refinement_flags
 _atom_site_disorder_assembly
 _atom_site_disorder_group
Br Br 0.70134(3) 0.27425(5) 0.31693(2) 0.04584(12) Uani 1 1 d . . .
N N 0.4912(2) 0.5276(3) 0.17956(16) 0.0266(5) Uani 1 1 d . . .
O1 O -0.0922(2) 0.2666(7) 0.02915(15) 0.0580(7) Uani 1 1 d . . .
C1 C 0.6143(3) 0.4885(4) 0.3422(2) 0.0289(6) Uani 1 1 d . . .
O2 O 0.4508(2) 0.6082(3) 0.02853(14) 0.0365(5) Uani 1 1 d . . .
C2 C 0.6505(3) 0.5530(5) 0.4312(2) 0.0356(7) Uani 1 1 d . . .
H2A H 0.7046 0.4827 0.4761 0.043 Uiso 1 1 calc R . .
C3 C 0.6082(3) 0.7203(5) 0.4555(2) 0.0354(7) Uani 1 1 d . . .
O3 O 0.2397(2) 0.8903(5) 0.35234(17) 0.0590(8) Uani 1 1 d . . .
O4 O 0.06552(17) 0.7986(4) 0.24937(12) 0.0332(5) Uani 1 1 d . . .
C4 C 0.5253(3) 0.8181(4) 0.3885(2) 0.0306(7) Uani 1 1 d . . .
H4A H 0.4961 0.9321 0.4038 0.037 Uiso 1 1 calc R . .
C5 C 0.4840(2) 0.7515(4) 0.29883(17) 0.0249(5) Uani 1 1 d . . .
C6 C 0.4054(3) 0.8677(4) 0.22364(19) 0.0251(5) Uani 1 1 d . . .
H6A H 0.4128 0.9954 0.2445 0.030 Uiso 1 1 calc R . .
C7 C 0.4701(3) 0.8490(4) 0.1398(2) 0.0309(6) Uani 1 1 d . . .
H7A H 0.4232 0.9223 0.0885 0.037 Uiso 1 1 calc R . .
H7B H 0.5590 0.8943 0.1559 0.037 Uiso 1 1 calc R . .
C8 C 0.4714(3) 0.6552(4) 0.1097(2) 0.0271(6) Uani 1 1 d . . .
C9 C 0.5282(3) 0.5836(4) 0.27343(18) 0.0254(5) Uani 1 1 d . . .
C10 C 0.4512(3) 0.3402(4) 0.1522(2) 0.0334(6) Uani 1 1 d . . .
H10A H 0.4814 0.2592 0.2047 0.040 Uiso 1 1 calc R . .
H10B H 0.4928 0.3027 0.1014 0.040 Uiso 1 1 calc R . .
C11 C 0.2248(3) 0.3299(5) 0.1842(2) 0.0410(8) Uani 1 1 d . . .
H11A H 0.2603 0.3489 0.2472 0.049 Uiso 1 1 calc R . .
C12 C 0.0892(3) 0.3118(5) 0.1555(2) 0.0438(9) Uani 1 1 d . . .
H12A H 0.0347 0.3198 0.1987 0.053 Uiso 1 1 calc R . .
```

```
C13 C 0.0391(3) 0.2826(7) 0.0638(2) 0.0433(7) Uani 1 1 d . . .
C14 C 0.1175(3) 0.2699(9) 0.0002(2) 0.0544(9) Uani 1 1 d . . .
H14A H 0.0818 0.2479 -0.0625 0.065 Uiso 1 1 calc R . .
C15 C 0.2488(3) 0.2895(7) 0.0292(2) 0.0465(8) Uani 1 1 d . . .
H15A H 0.3018 0.2820 -0.0150 0.056 Uiso 1 1 calc R . .
C16 C 0.3059(3) 0.3201(4) 0.1215(2) 0.0325(6) Uani 1 1 d . . .
C17 C 0.2610(3) 0.8188(4) 0.19704(19) 0.0290(6) Uani 1 1 d . . .
H17A H 0.2199 0.8958 0.1453 0.035 Uiso 1 1 calc R . .
H17B H 0.2528 0.6929 0.1757 0.035 Uiso 1 1 calc R . .
C18 C 0.1906(3) 0.8412(4) 0.2758(2) 0.0318(6) Uani 1 1 d . . .
C19 C -0.0212(3) 0.8001(6) 0.3167(2) 0.0383(8) Uani 1 1 d . . .
C20 C -0.1533(3) 0.7639(9) 0.2556(3) 0.0577(10) Uani 1 1 d . . .
H20A H -0.1705 0.8536 0.2065 0.087 Uiso 1 1 calc R . .
H20B H -0.2193 0.7710 0.2927 0.087 Uiso 1 1 calc R . .
H20C H -0.1540 0.6440 0.2286 0.087 Uiso 1 1 calc R . .
C21 C 0.0175(5) 0.6520(8) 0.3869(3) 0.0698(14) Uani 1 1 d . . .
H21A H 0.0203 0.5375 0.3552 0.105 Uiso 1 1 calc R . .
H21B H -0.0451 0.6447 0.4269 0.105 Uiso 1 1 calc R . .
H21C H 0.1022 0.6785 0.4239 0.105 Uiso 1 1 calc R . .
C22 C -0.0216(4) 0.9837(7) 0.3617(3) 0.0562(11) Uani 1 1 d . . .
H22A H 0.0607 1.0037 0.4033 0.084 Uiso 1 1 calc R . .
H22B H -0.0906 0.9887 0.3964 0.084 Uiso 1 1 calc R . .
H22C H -0.0353 1.0767 0.3143 0.084 Uiso 1 1 calc R . .
C23 C 0.6525(3) 0.7955(8) 0.5525(2) 0.0524(9) Uani 1 1 d . . .
H23A H 0.5878 0.7700 0.5891 0.079 Uiso 1 1 calc R . .
H23B H 0.6644 0.9253 0.5491 0.079 Uiso 1 1 calc R . .
H23C H 0.7336 0.7392 0.5812 0.079 Uiso 1 1 calc R . .
C24 C -0.1764(3) 0.2712(10) 0.0912(3) 0.0656(11) Uani 1 1 d . . .
H24A H -0.1446 0.1914 0.1430 0.098 Uiso 1 1 calc R . .
H24B H -0.2616 0.2315 0.0599 0.098 Uiso 1 1 calc R . .
H24C H -0.1817 0.3938 0.1136 0.098 Uiso 1 1 calc R . .

loop_
 _atom_site_aniso_label
 _atom_site_aniso_U_11
 _atom_site_aniso_U_22
 _atom_site_aniso_U_33
 _atom_site_aniso_U_23
 _atom_site_aniso_U_13
 _atom_site_aniso_U_12
Br 0.04299(18) 0.04097(18) 0.05117(19) 0.00253(18) 0.00365(13) 0.01911(17)
N 0.0298(11) 0.0231(11) 0.0277(11) 0.0031(9) 0.0075(9) 0.0026(9)
O1 0.0408(12) 0.089(2) 0.0403(12) -0.0045(19) -0.0005(10) -0.015(2)
C1 0.0258(13) 0.0260(13) 0.0357(15) 0.0047(11) 0.0085(11) 0.0058(10)
O2 0.0454(13) 0.0398(13) 0.0267(10) 0.0027(9) 0.0129(9) 0.0024(10)
C2 0.0268(14) 0.0475(19) 0.0319(15) 0.0094(13) 0.0047(11) 0.0038(13)
C3 0.0272(14) 0.048(2) 0.0300(14) -0.0005(12) 0.0039(11) -0.0002(12)
O3 0.0294(12) 0.109(3) 0.0376(13) -0.0261(15) 0.0048(10) 0.0018(14)
O4 0.0265(9) 0.0448(14) 0.0288(9) -0.0018(10) 0.0070(7) -0.0020(10)
C4 0.0273(13) 0.0341(18) 0.0303(13) -0.0013(11) 0.0058(10) 0.0000(11)
C5 0.0197(10) 0.0263(15) 0.0290(11) 0.0030(11) 0.0057(9) 0.0008(10)
C6 0.0246(12) 0.0225(13) 0.0286(13) 0.0019(10) 0.0060(10) 0.0013(10)
C7 0.0305(14) 0.0282(14) 0.0353(16) 0.0084(12) 0.0099(12) -0.0010(11)
C8 0.0271(14) 0.0287(15) 0.0283(14) 0.0065(11) 0.0123(11) 0.0021(11)
```

```
C9 0.0232(12) 0.0272(14) 0.0266(12) 0.0037(10) 0.0072(10) -0.0013(10)
C10 0.0373(15) 0.0260(13) 0.0369(15) 0.0000(12) 0.0074(12) 0.0040(12)
C11 0.0460(18) 0.046(2) 0.0314(15) -0.0024(13) 0.0099(13) -0.0081(14)
C12 0.0452(17) 0.051(3) 0.0401(16) -0.0013(15) 0.0197(14) -0.0060(15)
C13 0.0417(15) 0.0466(18) 0.0397(15) -0.0023(19) 0.0033(12) -0.0063(19)
C14 0.0514(18) 0.077(3) 0.0332(15) -0.006(2) 0.0034(13) -0.008(3)
C15 0.0481(17) 0.056(2) 0.0358(15) -0.0091(19) 0.0091(13) -0.005(2)
C16 0.0362(14) 0.0245(15) 0.0375(15) 0.0010(11) 0.0090(12) -0.0014(11)
C17 0.0251(12) 0.0324(17) 0.0298(13) 0.0012(10) 0.0067(10) 0.0054(10)
C18 0.0255(13) 0.0380(15) 0.0319(14) -0.0027(12) 0.0059(11) 0.0038(11)
C19 0.0287(13) 0.054(2) 0.0341(14) 0.0080(15) 0.0124(11) 0.0027(15)
C20 0.0361(16) 0.086(3) 0.0536(19) -0.003(3) 0.0159(14) -0.010(2)
C21 0.067(3) 0.082(3) 0.070(3) 0.038(3) 0.035(2) 0.024(3)
C22 0.044(2) 0.073(3) 0.055(2) -0.014(2) 0.0184(18) 0.011(2)
C23 0.0485(18) 0.067(3) 0.0367(16) -0.006(2) -0.0029(13) 0.004(2)
C24 0.0377(17) 0.099(3) 0.061(2) -0.012(3) 0.0104(15) -0.013(3)

_geom_special_details
;
 All esds (except the esd in the dihedral angle between two l.s. planes)
 are estimated using the full covariance matrix.  The cell esds are taken
 into account individually in the estimation of esds in distances, angles
 and torsion angles; correlations between esds in cell parameters are only
 used when they are defined by crystal symmetry.  An approximate
(isotropic)
 treatment of cell esds is used for estimating esds involving l.s. planes.
;

loop_
 _geom_bond_atom_site_label_1
 _geom_bond_atom_site_label_2
 _geom_bond_distance
 _geom_bond_site_symmetry_2
 _geom_bond_publ_flag
Br C1 1.903(3) . ?
N C8 1.380(4) . ?
N C9 1.421(4) . ?
N C10 1.480(4) . ?
O1 C13 1.384(4) . ?
O1 C24 1.397(4) . ?
C1 C2 1.375(4) . ?
C1 C9 1.407(4) . ?
O2 C8 1.222(4) . ?
C2 C3 1.385(5) . ?
C2 H2A 0.9400 . ?
C3 C4 1.385(4) . ?
C3 C23 1.516(5) . ?
O3 C18 1.200(4) . ?
O4 C18 1.338(3) . ?
O4 C19 1.477(3) . ?
C4 C5 1.395(4) . ?
C4 H4A 0.9400 . ?
C5 C9 1.402(4) . ?
C5 C6 1.512(4) . ?
```

```
C6 C7 1.533(4) . ?
C6 C17 1.539(4) . ?
C6 H6A 0.9900 . ?
C7 C8 1.499(4) . ?
C7 H7A 0.9800 . ?
C7 H7B 0.9800 . ?
C10 C16 1.518(4) . ?
C10 H10A 0.9800 . ?
C10 H10B 0.9800 . ?
C11 C16 1.381(4) . ?
C11 C12 1.416(5) . ?
C11 H11A 0.9400 . ?
C12 C13 1.366(5) . ?
C12 H12A 0.9400 . ?
C13 C14 1.370(5) . ?
C14 C15 1.375(5) . ?
C14 H14A 0.9400 . ?
C15 C16 1.392(4) . ?
C15 H15A 0.9400 . ?
C17 C18 1.506(4) . ?
C17 H17A 0.9800 . ?
C17 H17B 0.9800 . ?
C19 C21 1.504(6) . ?
C19 C22 1.510(6) . ?
C19 C20 1.525(5) . ?
C20 H20A 0.9700 . ?
C20 H20B 0.9700 . ?
C20 H20C 0.9700 . ?
C21 H21A 0.9700 . ?
C21 H21B 0.9700 . ?
C21 H21C 0.9700 . ?
C22 H22A 0.9700 . ?
C22 H22B 0.9700 . ?
C22 H22C 0.9700 . ?
C23 H23A 0.9700 . ?
C23 H23B 0.9700 . ?
C23 H23C 0.9700 . ?
C24 H24A 0.9700 . ?
C24 H24B 0.9700 . ?
C24 H24C 0.9700 . ?

loop_
 _geom_angle_atom_site_label_1
 _geom_angle_atom_site_label_2
 _geom_angle_atom_site_label_3
 _geom_angle
 _geom_angle_site_symmetry_1
 _geom_angle_site_symmetry_3
 _geom_angle_publ_flag
C8 N C9 119.9(2) . . ?
C8 N C10 116.3(2) . . ?
C9 N C10 123.1(2) . . ?
C13 O1 C24 118.6(3) . . ?
C2 C1 C9 122.0(3) . . ?
```

```
C2 C1 Br 114.9(2) . . ?
C9 C1 Br 122.9(2) . . ?
C1 C2 C3 120.9(3) . . ?
C1 C2 H2A 119.6 . . ?
C3 C2 H2A 119.6 . . ?
C4 C3 C2 118.1(3) . . ?
C4 C3 C23 120.8(3) . . ?
C2 C3 C23 121.0(3) . . ?
C18 O4 C19 120.8(2) . . ?
C3 C4 C5 121.6(3) . . ?
C3 C4 H4A 119.2 . . ?
C5 C4 H4A 119.2 . . ?
C4 C5 C9 120.4(2) . . ?
C4 C5 C6 121.0(3) . . ?
C9 C5 C6 118.1(2) . . ?
C5 C6 C7 105.7(2) . . ?
C5 C6 C17 115.1(2) . . ?
C7 C6 C17 110.6(2) . . ?
C5 C6 H6A 108.4 . . ?
C7 C6 H6A 108.4 . . ?
C17 C6 H6A 108.4 . . ?
C8 C7 C6 110.8(2) . . ?
C8 C7 H7A 109.5 . . ?
C6 C7 H7A 109.5 . . ?
C8 C7 H7B 109.5 . . ?
C6 C7 H7B 109.5 . . ?
H7A C7 H7B 108.1 . . ?
O2 C8 N 120.4(3) . . ?
O2 C8 C7 123.3(3) . . ?
N C8 C7 116.2(2) . . ?
C5 C9 C1 116.8(3) . . ?
C5 C9 N 118.4(2) . . ?
C1 C9 N 124.6(3) . . ?
N C10 C16 112.9(2) . . ?
N C10 H10A 109.0 . . ?
C16 C10 H10A 109.0 . . ?
N C10 H10B 109.0 . . ?
C16 C10 H10B 109.0 . . ?
H10A C10 H10B 107.8 . . ?
C16 C11 C12 121.4(3) . . ?
C16 C11 H11A 119.3 . . ?
C12 C11 H11A 119.3 . . ?
C13 C12 C11 118.6(3) . . ?
C13 C12 H12A 120.7 . . ?
C11 C12 H12A 120.7 . . ?
C12 C13 C14 121.2(3) . . ?
C12 C13 O1 122.7(3) . . ?
C14 C13 O1 116.1(3) . . ?
C13 C14 C15 119.4(3) . . ?
C13 C14 H14A 120.3 . . ?
C15 C14 H14A 120.3 . . ?
C14 C15 C16 122.3(3) . . ?
C14 C15 H15A 118.9 . . ?
C16 C15 H15A 118.9 . . ?
```

```
C11 C16 C15 117.1(3) . . ?
C11 C16 C10 121.4(3) . . ?
C15 C16 C10 121.5(3) . . ?
C18 C17 C6 113.2(2) . . ?
C18 C17 H17A 108.9 . . ?
C6 C17 H17A 108.9 . . ?
C18 C17 H17B 108.9 . . ?
C6 C17 H17B 108.9 . . ?
H17A C17 H17B 107.7 . . ?
O3 C18 O4 124.1(3) . . ?
O3 C18 C17 124.7(3) . . ?
O4 C18 C17 111.2(2) . . ?
O4 C19 C21 109.7(3) . . ?
O4 C19 C22 110.9(3) . . ?
C21 C19 C22 112.1(4) . . ?
O4 C19 C20 102.6(2) . . ?
C21 C19 C20 111.7(4) . . ?
C22 C19 C20 109.5(4) . . ?
C19 C20 H20A 109.5 . . ?
C19 C20 H20B 109.5 . . ?
H20A C20 H20B 109.5 . . ?
C19 C20 H20C 109.5 . . ?
H20A C20 H20C 109.5 . . ?
H20B C20 H20C 109.5 . . ?
C19 C21 H21A 109.5 . . ?
C19 C21 H21B 109.5 . . ?
H21A C21 H21B 109.5 . . ?
C19 C21 H21C 109.5 . . ?
H21A C21 H21C 109.5 . . ?
H21B C21 H21C 109.5 . . ?
C19 C22 H22A 109.5 . . ?
C19 C22 H22B 109.5 . . ?
H22A C22 H22B 109.5 . . ?
C19 C22 H22C 109.5 . . ?
H22A C22 H22C 109.5 . . ?
H22B C22 H22C 109.5 . . ?
C3 C23 H23A 109.5 . . ?
C3 C23 H23B 109.5 . . ?
H23A C23 H23B 109.5 . . ?
C3 C23 H23C 109.5 . . ?
H23A C23 H23C 109.5 . . ?
H23B C23 H23C 109.5 . . ?
O1 C24 H24A 109.5 . . ?
O1 C24 H24B 109.5 . . ?
H24A C24 H24B 109.5 . . ?
O1 C24 H24C 109.5 . . ?
H24A C24 H24C 109.5 . . ?
H24B C24 H24C 109.5 . . ?

_diffrn_measured_fraction_theta_max    0.943
_diffrn_reflns_theta_full              30.00
_diffrn_measured_fraction_theta_full   1.000
_refine_diff_density_max    0.776
_refine_diff_density_min   -0.254
```

```
_refine_diff_density_rms    0.073
```

++

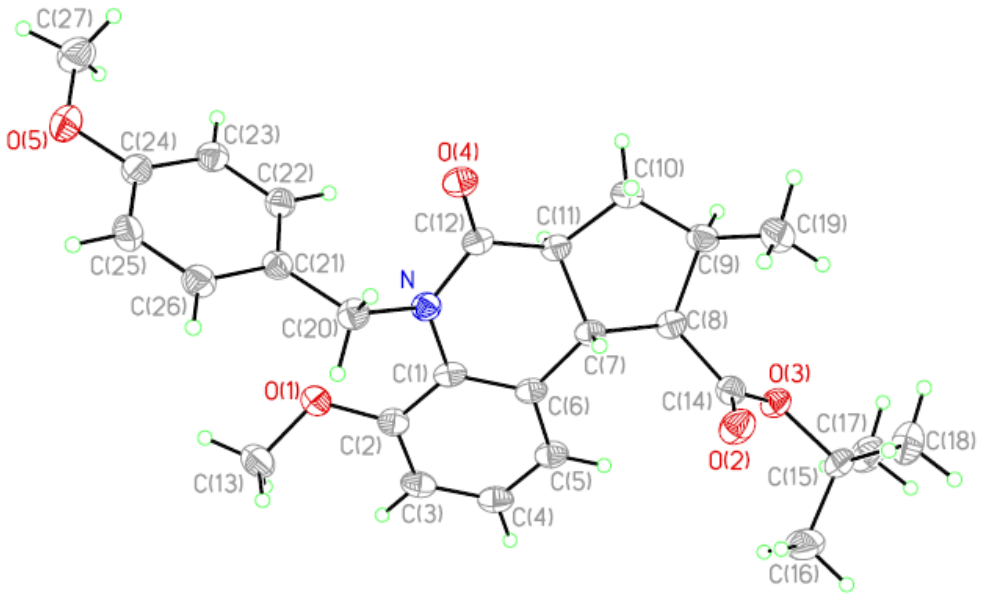

The corresponding CIF file for (*S*)-**5.18f** is shown below, between the lines of "+" symbols.

++

```
data_dgc915s

_audit_creation_method            SHELXL-97
_chemical_name_systematic
;
 ?
;
_chemical_name_common             ?
_chemical_melting_point           ?
_chemical_formula_moiety          ?
_chemical_formula_sum
 'C27 H33 N O5'
_chemical_formula_weight          451.54

loop_
 _atom_type_symbol
 _atom_type_description
 _atom_type_scat_dispersion_real
 _atom_type_scat_dispersion_imag
 _atom_type_scat_source
 'C'  'C'   0.0033   0.0016
 'International Tables Vol C Tables 4.2.6.8 and 6.1.1.4'
 'H'  'H'   0.0000   0.0000
 'International Tables Vol C Tables 4.2.6.8 and 6.1.1.4'
```

```
 'N'  'N'   0.0061   0.0033
 'International Tables Vol C Tables 4.2.6.8 and 6.1.1.4'
 'O'  'O'   0.0106   0.0060
 'International Tables Vol C Tables 4.2.6.8 and 6.1.1.4'

_symmetry_cell_setting            Monoclinic
_symmetry_space_group_name_H-M    P2(1)/c

loop_
 _symmetry_equiv_pos_as_xyz
 'x, y, z'
 '-x, y+1/2, -z+1/2'
 '-x, -y, -z'
 'x, -y-1/2, z-1/2'

_cell_length_a                    12.012(3)
_cell_length_b                    9.305(2)
_cell_length_c                    22.056(5)
_cell_angle_alpha                 90.00
_cell_angle_beta                  101.822(5)
_cell_angle_gamma                 90.00
_cell_volume                      2412.9(10)
_cell_formula_units_Z             4
_cell_measurement_temperature     203(2)
_cell_measurement_reflns_used     1240
_cell_measurement_theta_min       2.29
_cell_measurement_theta_max       20.23

_exptl_crystal_description        ?
_exptl_crystal_colour             ?
_exptl_crystal_size_max           0.25
_exptl_crystal_size_mid           0.21
_exptl_crystal_size_min           0.21
_exptl_crystal_density_meas       0
_exptl_crystal_density_diffrn     1.243
_exptl_crystal_density_method     'not measured'
_exptl_crystal_F_000              968
_exptl_absorpt_coefficient_mu     0.085
_exptl_absorpt_correction_type    none
_exptl_absorpt_correction_T_min   0.9790
_exptl_absorpt_correction_T_max   0.9824
_exptl_absorpt_process_details    ?

_exptl_special_details
;
 ?
;

_diffrn_ambient_temperature       203(2)
_diffrn_radiation_wavelength      0.71073
_diffrn_radiation_type            MoK\a
_diffrn_radiation_source          'fine-focus sealed tube'
_diffrn_radiation_monochromator   graphite
_diffrn_measurement_device_type   'CCD area detector'
```

```
_diffrn_measurement_method        'phi and omega scans'
_diffrn_detector_area_resol_mean  ?
_diffrn_standards_number          ?
_diffrn_standards_interval_count  ?
_diffrn_standards_interval_time   ?
_diffrn_standards_decay_%         ?
_diffrn_reflns_number             18592
_diffrn_reflns_av_R_equivalents   0.0893
_diffrn_reflns_av_sigmaI/netI     0.0730
_diffrn_reflns_limit_h_min        -14
_diffrn_reflns_limit_h_max        14
_diffrn_reflns_limit_k_min        -11
_diffrn_reflns_limit_k_max        11
_diffrn_reflns_limit_l_min        -26
_diffrn_reflns_limit_l_max        26
_diffrn_reflns_theta_min          1.73
_diffrn_reflns_theta_max          25.00
_reflns_number_total              4245
_reflns_number_gt                 2609
_reflns_threshold_expression      >2sigma(I)

_computing_data_collection        'Bruker SMART'
_computing_cell_refinement        'Bruker SMART'
_computing_data_reduction         'Bruker SAINT'
_computing_structure_solution     'SHELXS-97 (Sheldrick, 1990)'
_computing_structure_refinement   'SHELXL-97 (Sheldrick, 1997)'
_computing_molecular_graphics     'Bruker SHELXTL'
_computing_publication_material   'Bruker SHELXTL'

_refine_special_details
;
 Refinement of F^2^ against ALL reflections.  The weighted R-factor wR and
 goodness of fit S are based on F^2^, conventional R-factors R are based
 on F, with F set to zero for negative F^2^. The threshold expression of
 F^2^ > 2sigma(F^2^) is used only for calculating R-factors(gt) etc. and
is
 not relevant to the choice of reflections for refinement.  R-factors
based
 on F^2^ are statistically about twice as large as those based on F, and
R-
 factors based on ALL data will be even larger.
;

_refine_ls_structure_factor_coef  Fsqd
_refine_ls_matrix_type            full
_refine_ls_weighting_scheme       calc
_refine_ls_weighting_details
 'calc w=1/[\s^2^(Fo^2^)+(0.0780P)^2^+0.0000P] where P=(Fo^2^+2Fc^2^)/3'
_atom_sites_solution_primary      direct
_atom_sites_solution_secondary    difmap
_atom_sites_solution_hydrogens    geom
_refine_ls_hydrogen_treatment     mixed
_refine_ls_extinction_method      none
_refine_ls_extinction_coef        ?
```

```
_refine_ls_number_reflns          4245
_refine_ls_number_parameters      298
_refine_ls_number_restraints      0
_refine_ls_R_factor_all           0.1066
_refine_ls_R_factor_gt            0.0570
_refine_ls_wR_factor_ref          0.1537
_refine_ls_wR_factor_gt           0.1323
_refine_ls_goodness_of_fit_ref    0.922
_refine_ls_restrained_S_all       0.922
_refine_ls_shift/su_max           0.004
_refine_ls_shift/su_mean          0.001

loop_
 _atom_site_label
 _atom_site_type_symbol
 _atom_site_fract_x
 _atom_site_fract_y
 _atom_site_fract_z
 _atom_site_U_iso_or_equiv
 _atom_site_adp_type
 _atom_site_occupancy
 _atom_site_symmetry_multiplicity
 _atom_site_calc_flag
 _atom_site_refinement_flags
 _atom_site_disorder_assembly
 _atom_site_disorder_group
O1 O -0.22651(16) 0.3973(2) 0.00797(9) 0.0462(5) Uani 1 1 d . . .
O2 O 0.31427(17) 0.5545(2) 0.19965(9) 0.0491(5) Uani 1 1 d . . .
O3 O 0.25520(15) 0.67436(18) 0.27684(8) 0.0388(5) Uani 1 1 d . . .
O4 O 0.00988(16) 0.04730(18) 0.13943(8) 0.0433(5) Uani 1 1 d . . .
O5 O -0.44740(17) -0.2070(2) -0.03796(9) 0.0547(6) Uani 1 1 d . . .
N N -0.05503(18) 0.2520(2) 0.08834(10) 0.0334(5) Uani 1 1 d . . .
C1 C -0.0617(2) 0.4062(3) 0.08769(12) 0.0328(6) Uani 1 1 d . . .
C2 C -0.1456(2) 0.4783(3) 0.04508(12) 0.0369(7) Uani 1 1 d . . .
C3 C -0.1466(2) 0.6276(3) 0.04417(13) 0.0421(7) Uani 1 1 d . . .
H3A H -0.2018 0.6764 0.0151 0.051 Uiso 1 1 calc R . .
C4 C -0.0676(2) 0.7047(3) 0.08535(13) 0.0418(7) Uani 1 1 d . . .
H4A H -0.0689 0.8057 0.0841 0.050 Uiso 1 1 calc R . .
C5 C 0.0132(2) 0.6352(3) 0.12821(12) 0.0377(7) Uani 1 1 d . . .
H5A H 0.0664 0.6889 0.1565 0.045 Uiso 1 1 calc R . .
C6 C 0.0171(2) 0.4862(3) 0.13032(12) 0.0328(6) Uani 1 1 d . . .
C7 C 0.0992(2) 0.4007(3) 0.17657(11) 0.0320(6) Uani 1 1 d . . .
H7A H 0.1608 0.3667 0.1564 0.038 Uiso 1 1 calc R . .
C8 C 0.1533(2) 0.4678(3) 0.23841(12) 0.0347(6) Uani 1 1 d . . .
H8A H 0.0941 0.5217 0.2542 0.042 Uiso 1 1 calc R . .
C9 C 0.1916(2) 0.3356(3) 0.28256(12) 0.0388(7) Uani 1 1 d . . .
H9A H 0.1628 0.3498 0.3211 0.047 Uiso 1 1 calc R . .
C10 C 0.1290(2) 0.2056(3) 0.24734(12) 0.0390(7) Uani 1 1 d . . .
H10A H 0.1819 0.1458 0.2300 0.047 Uiso 1 1 calc R . .
H10B H 0.0939 0.1465 0.2751 0.047 Uiso 1 1 calc R . .
C11 C 0.0389(2) 0.2694(3) 0.19611(12) 0.0329(6) Uani 1 1 d . . .
H11A H -0.0266 0.3014 0.2136 0.039 Uiso 1 1 calc R . .
C12 C -0.0031(2) 0.1778(3) 0.14021(12) 0.0339(6) Uani 1 1 d . . .
C13 C -0.2767(3) 0.4521(4) -0.05124(13) 0.0577(9) Uani 1 1 d . . .
```

```
H13A H -0.3327 0.3843 -0.0725 0.087 Uiso 1 1 calc R . .
H13B H -0.2183 0.4666 -0.0752 0.087 Uiso 1 1 calc R . .
H13C H -0.3136 0.5431 -0.0466 0.087 Uiso 1 1 calc R . .
C14 C 0.2500(2) 0.5691(3) 0.23468(12) 0.0356(7) Uani 1 1 d . . .
C15 C 0.3441(2) 0.7869(3) 0.28372(13) 0.0426(7) Uani 1 1 d . . .
C16 C 0.3324(3) 0.8701(3) 0.22387(14) 0.0634(10) Uani 1 1 d . . .
H16A H 0.2566 0.9108 0.2129 0.095 Uiso 1 1 calc R . .
H16B H 0.3448 0.8060 0.1912 0.095 Uiso 1 1 calc R . .
H16C H 0.3882 0.9467 0.2291 0.095 Uiso 1 1 calc R . .
C17 C 0.3152(3) 0.8801(3) 0.33495(15) 0.0591(9) Uani 1 1 d . . .
H17A H 0.2406 0.9227 0.3210 0.089 Uiso 1 1 calc R . .
H17B H 0.3716 0.9556 0.3453 0.089 Uiso 1 1 calc R . .
H17C H 0.3149 0.8214 0.3713 0.089 Uiso 1 1 calc R . .
C18 C 0.4605(3) 0.7192(4) 0.30403(16) 0.0624(9) Uani 1 1 d . . .
H18A H 0.4777 0.6613 0.2705 0.094 Uiso 1 1 calc R . .
H18B H 0.4611 0.6588 0.3399 0.094 Uiso 1 1 calc R . .
H18C H 0.5173 0.7941 0.3146 0.094 Uiso 1 1 calc R . .
C19 C 0.3190(3) 0.3109(3) 0.29993(15) 0.0571(9) Uani 1 1 d . . .
H19A H 0.3346 0.2283 0.3272 0.086 Uiso 1 1 calc R . .
H19B H 0.3556 0.3952 0.3210 0.086 Uiso 1 1 calc R . .
H19C H 0.3483 0.2934 0.2627 0.086 Uiso 1 1 calc R . .
C20 C -0.0737(2) 0.1724(3) 0.02922(12) 0.0373(7) Uani 1 1 d . . .
H20A H -0.0081 0.1092 0.0299 0.045 Uiso 1 1 calc R . .
H20B H -0.0750 0.2419 -0.0043 0.045 Uiso 1 1 calc R . .
C21 C -0.1798(2) 0.0825(3) 0.01355(12) 0.0331(6) Uani 1 1 d . . .
C22 C -0.2446(2) 0.0429(3) 0.05583(12) 0.0364(7) Uani 1 1 d . . .
H22A H -0.2265 0.0807 0.0962 0.044 Uiso 1 1 calc R . .
C23 C -0.3355(2) -0.0509(3) 0.04038(13) 0.0395(7) Uani 1 1 d . . .
H23A H -0.3785 -0.0758 0.0700 0.047 Uiso 1 1 calc R . .
C24 C -0.3628(2) -0.1075(3) -0.01862(13) 0.0409(7) Uani 1 1 d . . .
C25 C -0.3014(3) -0.0661(3) -0.06232(13) 0.0452(7) Uani 1 1 d . . .
H25A H -0.3209 -0.1020 -0.1030 0.054 Uiso 1 1 calc R . .
C26 C -0.2114(2) 0.0280(3) -0.04609(13) 0.0428(7) Uani 1 1 d . . .
H26A H -0.1704 0.0558 -0.0762 0.051 Uiso 1 1 calc R . .
C27 C -0.5024(3) -0.2664(3) 0.00774(15) 0.0612(9) Uani 1 1 d . . .
H27A H -0.5600 -0.3344 -0.0117 0.092 Uiso 1 1 calc R . .
H27B H -0.5379 -0.1900 0.0270 0.092 Uiso 1 1 calc R . .
H27C H -0.4467 -0.3153 0.0390 0.092 Uiso 1 1 calc R . .

loop_
 _atom_site_aniso_label
 _atom_site_aniso_U_11
 _atom_site_aniso_U_22
 _atom_site_aniso_U_33
 _atom_site_aniso_U_23
 _atom_site_aniso_U_13
 _atom_site_aniso_U_12
O1 0.0456(12) 0.0463(12) 0.0423(12) 0.0093(10) -0.0013(10) -0.0040(10)
O2 0.0518(13) 0.0552(13) 0.0449(12) -0.0080(10) 0.0211(11) -0.0135(10)
O3 0.0422(11) 0.0328(10) 0.0419(11) -0.0041(9) 0.0101(9) -0.0055(9)
O4 0.0518(12) 0.0261(11) 0.0502(12) 0.0010(9) 0.0060(10) 0.0013(9)
O5 0.0514(13) 0.0547(13) 0.0549(14) -0.0032(11) 0.0037(11) -0.0171(11)
N 0.0376(13) 0.0282(12) 0.0343(13) -0.0011(10) 0.0075(10) 0.0004(10)
C1 0.0377(16) 0.0267(14) 0.0380(16) 0.0032(12) 0.0172(13) 0.0009(12)
```

```
C2 0.0385(16) 0.0382(17) 0.0356(16) 0.0026(13) 0.0116(14) -0.0007(13)
C3 0.0469(18) 0.0362(17) 0.0447(18) 0.0120(14) 0.0128(15) 0.0091(14)
C4 0.0526(19) 0.0308(15) 0.0460(18) 0.0046(14) 0.0197(15) 0.0040(14)
C5 0.0469(17) 0.0276(15) 0.0413(17) -0.0007(13) 0.0155(14) 0.0009(13)
C6 0.0355(15) 0.0306(15) 0.0359(16) 0.0027(12) 0.0161(13) -0.0003(12)
C7 0.0370(15) 0.0272(14) 0.0339(15) 0.0009(12) 0.0125(12) 0.0013(12)
C8 0.0386(16) 0.0317(15) 0.0360(15) -0.0027(12) 0.0127(13) -0.0009(12)
C9 0.0503(18) 0.0359(16) 0.0314(15) 0.0022(13) 0.0109(13) -0.0017(13)
C10 0.0438(17) 0.0334(15) 0.0395(16) 0.0056(13) 0.0080(13) -0.0006(13)
C11 0.0372(15) 0.0291(14) 0.0344(15) 0.0003(12) 0.0121(12) -0.0028(12)
C12 0.0337(15) 0.0283(16) 0.0411(17) 0.0025(13) 0.0111(13) -0.0013(12)
C13 0.056(2) 0.074(2) 0.0400(18) 0.0129(17) 0.0038(16) -0.0061(18)
C14 0.0393(16) 0.0337(15) 0.0336(15) -0.0005(13) 0.0065(13) 0.0008(13)
C15 0.0415(17) 0.0340(16) 0.0507(18) 0.0016(14) 0.0057(14) -0.0109(13)
C16 0.084(3) 0.0424(18) 0.062(2) 0.0060(17) 0.0126(19) -0.0152(18)
C17 0.068(2) 0.0463(19) 0.064(2) -0.0157(17) 0.0151(18) -0.0147(17)
C18 0.0432(19) 0.068(2) 0.073(2) -0.0077(19) 0.0040(17) -0.0072(17)
C19 0.059(2) 0.0464(19) 0.059(2) 0.0090(16) -0.0053(17) 0.0006(16)
C20 0.0403(16) 0.0342(15) 0.0384(16) -0.0023(13) 0.0102(13) 0.0009(13)
C21 0.0364(15) 0.0282(14) 0.0343(15) 0.0009(12) 0.0067(13) 0.0050(12)
C22 0.0423(16) 0.0342(15) 0.0330(15) -0.0019(12) 0.0082(13) 0.0010(13)
C23 0.0396(16) 0.0402(16) 0.0397(17) 0.0037(14) 0.0105(13) -0.0001(14)
C24 0.0374(16) 0.0357(16) 0.0458(18) 0.0040(14) 0.0000(14) 0.0001(13)
C25 0.0502(19) 0.0495(18) 0.0337(16) -0.0053(14) 0.0033(14) -0.0022(15)
C26 0.0481(18) 0.0450(17) 0.0361(17) 0.0015(14) 0.0102(14) -0.0009(15)
C27 0.053(2) 0.058(2) 0.071(2) 0.0070(18) 0.0108(18) -0.0134(17)

_geom_special_details
;
 All esds (except the esd in the dihedral angle between two l.s. planes)
 are estimated using the full covariance matrix.  The cell esds are taken
 into account individually in the estimation of esds in distances, angles
 and torsion angles; correlations between esds in cell parameters are only
 used when they are defined by crystal symmetry.  An approximate
(isotropic)
 treatment of cell esds is used for estimating esds involving l.s. planes.
;

loop_
 _geom_bond_atom_site_label_1
 _geom_bond_atom_site_label_2
 _geom_bond_distance
 _geom_bond_site_symmetry_2
 _geom_bond_publ_flag
O1 C2 1.363(3) . ?
O1 C13 1.417(3) . ?
O2 C14 1.207(3) . ?
O3 C14 1.343(3) . ?
O3 C15 1.481(3) . ?
O4 C12 1.225(3) . ?
O5 C24 1.376(3) . ?
O5 C27 1.425(3) . ?
N C12 1.372(3) . ?
N C1 1.438(3) . ?
```

```
N C20 1.476(3) . ?
C1 C2 1.400(4) . ?
C1 C6 1.404(4) . ?
C2 C3 1.390(4) . ?
C3 C4 1.373(4) . ?
C3 H3A 0.9400 . ?
C4 C5 1.370(4) . ?
C4 H4A 0.9400 . ?
C5 C6 1.388(4) . ?
C5 H5A 0.9400 . ?
C6 C7 1.494(4) . ?
C7 C8 1.520(3) . ?
C7 C11 1.527(3) . ?
C7 H7A 0.9900 . ?
C8 C14 1.511(4) . ?
C8 C9 1.578(4) . ?
C8 H8A 0.9900 . ?
C9 C19 1.516(4) . ?
C9 C10 1.547(4) . ?
C9 H9A 0.9900 . ?
C10 C11 1.516(4) . ?
C10 H10A 0.9800 . ?
C10 H10B 0.9800 . ?
C11 C12 1.499(4) . ?
C11 H11A 0.9900 . ?
C13 H13A 0.9700 . ?
C13 H13B 0.9700 . ?
C13 H13C 0.9700 . ?
C15 C16 1.512(4) . ?
C15 C18 1.516(4) . ?
C15 C17 1.520(4) . ?
C16 H16A 0.9700 . ?
C16 H16B 0.9700 . ?
C16 H16C 0.9700 . ?
C17 H17A 0.9700 . ?
C17 H17B 0.9700 . ?
C17 H17C 0.9700 . ?
C18 H18A 0.9700 . ?
C18 H18B 0.9700 . ?
C18 H18C 0.9700 . ?
C19 H19A 0.9700 . ?
C19 H19B 0.9700 . ?
C19 H19C 0.9700 . ?
C20 C21 1.504(4) . ?
C20 H20A 0.9800 . ?
C20 H20B 0.9800 . ?
C21 C22 1.381(4) . ?
C21 C26 1.388(4) . ?
C22 C23 1.385(4) . ?
C22 H22A 0.9400 . ?
C23 C24 1.380(4) . ?
C23 H23A 0.9400 . ?
C24 C25 1.383(4) . ?
C25 C26 1.380(4) . ?
```

```
C25 H25A 0.9400 . ?
C26 H26A 0.9400 . ?
C27 H27A 0.9700 . ?
C27 H27B 0.9700 . ?
C27 H27C 0.9700 . ?

loop_
 _geom_angle_atom_site_label_1
 _geom_angle_atom_site_label_2
 _geom_angle_atom_site_label_3
 _geom_angle
 _geom_angle_site_symmetry_1
 _geom_angle_site_symmetry_3
 _geom_angle_publ_flag
C2 O1 C13 118.1(2) . . ?
C14 O3 C15 121.1(2) . . ?
C24 O5 C27 117.5(2) . . ?
C12 N C1 121.7(2) . . ?
C12 N C20 116.4(2) . . ?
C1 N C20 119.6(2) . . ?
C2 C1 C6 119.3(2) . . ?
C2 C1 N 121.1(2) . . ?
C6 C1 N 119.6(2) . . ?
O1 C2 C3 122.8(3) . . ?
O1 C2 C1 117.7(2) . . ?
C3 C2 C1 119.4(3) . . ?
C4 C3 C2 120.6(3) . . ?
C4 C3 H3A 119.7 . . ?
C2 C3 H3A 119.7 . . ?
C5 C4 C3 120.4(3) . . ?
C5 C4 H4A 119.8 . . ?
C3 C4 H4A 119.8 . . ?
C4 C5 C6 120.6(3) . . ?
C4 C5 H5A 119.7 . . ?
C6 C5 H5A 119.7 . . ?
C5 C6 C1 119.6(2) . . ?
C5 C6 C7 124.6(2) . . ?
C1 C6 C7 115.8(2) . . ?
C6 C7 C8 119.7(2) . . ?
C6 C7 C11 109.5(2) . . ?
C8 C7 C11 102.4(2) . . ?
C6 C7 H7A 108.2 . . ?
C8 C7 H7A 108.2 . . ?
C11 C7 H7A 108.2 . . ?
C14 C8 C7 113.5(2) . . ?
C14 C8 C9 112.9(2) . . ?
C7 C8 C9 104.5(2) . . ?
C14 C8 H8A 108.6 . . ?
C7 C8 H8A 108.6 . . ?
C9 C8 H8A 108.6 . . ?
C19 C9 C10 111.7(2) . . ?
C19 C9 C8 115.2(2) . . ?
C10 C9 C8 104.4(2) . . ?
C19 C9 H9A 108.4 . . ?
```

```
C10 C9 H9A 108.4 . . ?
C8 C9 H9A 108.4 . . ?
C11 C10 C9 105.5(2) . . ?
C11 C10 H10A 110.6 . . ?
C9 C10 H10A 110.6 . . ?
C11 C10 H10B 110.6 . . ?
C9 C10 H10B 110.6 . . ?
H10A C10 H10B 108.8 . . ?
C12 C11 C10 117.3(2) . . ?
C12 C11 C7 108.8(2) . . ?
C10 C11 C7 102.5(2) . . ?
C12 C11 H11A 109.3 . . ?
C10 C11 H11A 109.3 . . ?
C7 C11 H11A 109.3 . . ?
O4 C12 N 121.6(2) . . ?
O4 C12 C11 123.6(2) . . ?
N C12 C11 114.7(2) . . ?
O1 C13 H13A 109.5 . . ?
O1 C13 H13B 109.5 . . ?
H13A C13 H13B 109.5 . . ?
O1 C13 H13C 109.5 . . ?
H13A C13 H13C 109.5 . . ?
H13B C13 H13C 109.5 . . ?
O2 C14 O3 125.4(2) . . ?
O2 C14 C8 124.4(2) . . ?
O3 C14 C8 110.2(2) . . ?
O3 C15 C16 109.6(2) . . ?
O3 C15 C18 109.8(2) . . ?
C16 C15 C18 112.7(3) . . ?
O3 C15 C17 102.1(2) . . ?
C16 C15 C17 111.3(3) . . ?
C18 C15 C17 110.8(3) . . ?
C15 C16 H16A 109.5 . . ?
C15 C16 H16B 109.5 . . ?
H16A C16 H16B 109.5 . . ?
C15 C16 H16C 109.5 . . ?
H16A C16 H16C 109.5 . . ?
H16B C16 H16C 109.5 . . ?
C15 C17 H17A 109.5 . . ?
C15 C17 H17B 109.5 . . ?
H17A C17 H17B 109.5 . . ?
C15 C17 H17C 109.5 . . ?
H17A C17 H17C 109.5 . . ?
H17B C17 H17C 109.5 . . ?
C15 C18 H18A 109.5 . . ?
C15 C18 H18B 109.5 . . ?
H18A C18 H18B 109.5 . . ?
C15 C18 H18C 109.5 . . ?
H18A C18 H18C 109.5 . . ?
H18B C18 H18C 109.5 . . ?
C9 C19 H19A 109.5 . . ?
C9 C19 H19B 109.5 . . ?
H19A C19 H19B 109.5 . . ?
C9 C19 H19C 109.5 . . ?
```

```
H19A C19 H19C 109.5 . . ?
H19B C19 H19C 109.5 . . ?
N C20 C21 116.7(2) . . ?
N C20 H20A 108.1 . . ?
C21 C20 H20A 108.1 . . ?
N C20 H20B 108.1 . . ?
C21 C20 H20B 108.1 . . ?
H20A C20 H20B 107.3 . . ?
C22 C21 C26 117.4(2) . . ?
C22 C21 C20 124.1(2) . . ?
C26 C21 C20 118.4(2) . . ?
C21 C22 C23 121.8(3) . . ?
C21 C22 H22A 119.1 . . ?
C23 C22 H22A 119.1 . . ?
C24 C23 C22 119.7(3) . . ?
C24 C23 H23A 120.1 . . ?
C22 C23 H23A 120.1 . . ?
O5 C24 C23 124.5(3) . . ?
O5 C24 C25 115.9(3) . . ?
C23 C24 C25 119.6(3) . . ?
C26 C25 C24 119.8(3) . . ?
C26 C25 H25A 120.1 . . ?
C24 C25 H25A 120.1 . . ?
C25 C26 C21 121.7(3) . . ?
C25 C26 H26A 119.2 . . ?
C21 C26 H26A 119.2 . . ?
O5 C27 H27A 109.5 . . ?
O5 C27 H27B 109.5 . . ?
H27A C27 H27B 109.5 . . ?
O5 C27 H27C 109.5 . . ?
H27A C27 H27C 109.5 . . ?
H27B C27 H27C 109.5 . . ?

_diffrn_measured_fraction_theta_max    1.000
_diffrn_reflns_theta_full              25.00
_diffrn_measured_fraction_theta_full   1.000
_refine_diff_density_max    0.171
_refine_diff_density_min   -0.163
_refine_diff_density_rms    0.040


++++++++++++++++++++++++++++++++++++++++++++++++++++++++++++++++++++++++++++++
```

BIBLIOGRAPHY

1. Bogen, S.; Malacria, M. *J. Am. Chem. Soc.* **1996**, *118*, 3992-3993.
2. Cassayre, J.; Quiclet-Sire, B.; Saunier, J.-B.; Zard, S. Z. *Tetrahedron* **1998**, *54*, 1029-1040.
3. Chatgilialoglu, C.; Ferreri, C.; Guerra, M.; Timokhin, V.; Froudakis, G.; Gimisis, T. *J. Am. Chem. Soc.* **2002**, *124*, 10765-10772.
4. Curran, D. P.; Porter, N. A.; Giese, B. *Stereochemistry of Radical Reactions: Concepts, Guidelines, and Synthetic Applications*; VCH Publishers, Inc.: New York, 1996.
5. El Bialy, S. A. A.; Ohtani, S.; Sato, T.; Ikeda, M. *Heterocycles* **2001**, *54*, 1021-1025.
6. Guerrero, M. A.; Cruz-Almanda, R.; Miranda, L. D. *Tetrahedron* **2003**, *59*, 4953-4958.
7. Ishibashi, H.; Kodama, K.; Higuchi, M.; Muraoka, O.; Tanabe, G.; Takeda, Y. *Tetrahedron* **2001**, *57*, 7629-7637.
8. Ishibashi, H.; Matsukida, H.; Toyao, A.; Tamura, O.; Takeda, Y. *Synlett* **2000**, 1497-1499.
9. Ishibashi, H.; Sato, T.; Ikeda, M.; *Synthesis* **2002**, *6*, 695-713.
10. Isobe, K.; Mohri, K.; Tokoro, K.; Fukushima, C.; Higuchi, F.; Taga, J. *Chem. Pharm. Bull.* **1988**, *36*, 1275-1282.
11. Miranda, L. D.; Zard, S. Z. *Org. Lett.* **2002**, *4*, 1135-1138.
12. Parsons, A. F.; *Acad. Sci. Ser.* **2001**, *4*, 391-400.
13. Rama Rao, A. V.; Singh, A. K.; Rao, B. V.; Reddy, K. M. *Tetrahedron Lett.* **1993**, *34*, 2665-2668.
14. Rama Rao, A. V.; Singh, A. K.; Reddy, K. M.; Ravikumar, K. *J. Chem. Soc., Perk. Trans. 1* **1993**, *24*, 3171-3175.
15. Sato, T.; Wada, Y.; Nishimoto, M.; Ishibashi, H.; Ikeda, M. *J. Chem. Soc. Perk. Trans. 1* **1989**, 789-886.
16. Tamura, O.; Matsukida, H.; Toyao, A.; Takeda, Y.; Ishibashi, H. *J. Org. Chem.* **2002**, *67*, 5537-5545.
17. Zard, S. Z. *Radical Reactions in Organic Synthesis*; Oxford University Press: New York, 2003.
18. Park, S.-U.; Varick, T. R.; Newcomb, M. *Tetrahedron Lett.* **1990**, *21*, 2975-2978.
19. Baldwin, J. E. *J. Chem. Soc., Chem. Commun.* **1976**, 738.
20. Beckwith, A. L. J. *Tetrahedron* **1981**, *37*, 3073-3100.
21. Beesley, R. M.; Ingold, C. K.; Thorpe, J. F. *J. Chem. Soc.* **1915**, *107*, 1080.
22. Carey, F. A.; Sundberg, R. J. *Advanced Organic Chemistry Part A: Structure and Mechanisms*; 4th ed.; Kluwer Academic / Plenum Publishers: New York, 2000.
23. Bommezijn, S.; Martin, C. G.; Kennedy, A. R.; Lizos, D.; Murphy, J. A. *Org. Lett.* **2001**, *3*, 3405-3407.

24. Baker, R. S.; Parsons, A. F.; Wilson, M. *Tetrahedron Lett.* **1998**, *39*, 2815-2818.
25. Ikeda, M.; Teranishi, H.; Nozaki, K.; Ishibashi, H. *J. Chem. Soc., Perk. Trans. 1* **1998**, 1691-1697.
26. Sato, T.; Nakamura, N.; Ikeda, K.; Okada, M.; Ishibashi, H.; Ikeda, M. *J. Chem. Soc., Perk. Trans. 1* **1992**, *18*, 2399-2408.
27. Nakamura, E.; Inubushi, T.; Aoki, S.; Machii, D. *J. Am. Chem. Soc.* **1991**, *113*, 8980-8982.
28. Newcomb, M.; Horner, J. H.; Filipkowski, M. A.; Ha, C.; Park, S.-U. *J. Am. Chem. Soc.* **1995**, *117*, 3674-3684.
29. Viehe, H. G.; Janousek, Z.; Merényi, R. *Substituent Effects in Radical Chemistry*; D. Reidel Publishing Co.: Dordrecht, 1986.
30. Curran, D. P.; Chen, M.-H.; Kim, D. *J. Am. Chem. Soc.* **1989**, *111*, 6265-6276.
31. Bremner, J. B.; Sengpracha, W. *Tetrahedron* **2005**, *61*, 941-953.
32. Curran, D. P.; Tamine, J. *J. Org. Chem.* **1991**, *56*, 2746-2750.
33. Stork, G.; Mah, R. *Heterocycles* **1989**, *28*, 723-727.
34. Musa, O. M.; Horner, J. H.; Newcomb, M. *J. Org. Chem.* **1999**, *64*, 1022-1025.
35. Sibi, M. P.; Ji, J. *J. Am. Chem. Soc.* **1996**, *118*, 3063-3064.
36. Spencer, J. N.; Ganunis, T.; Zafar, A.; Eppley, H.; Otter, J. C.; Coley, S. M.; Yoder, C. H. *J. Organomet. Chem.* **1990**, *389*, 295-300.
37. Murakata, M.; Jono, T.; Mizuno, Y.; Hoshino, O. *J. Am. Chem. Soc.* **1997**, *119*, 11713-11714.
38. Feng, H.; Kavrakova, I. K.; Pratt, D. A.; Tellinghuisen, J.; Porter, N. A. *J. Org. Chem.* **2002**, *67*, 6050-6054.
39. Aldabbagh, F.; Bowman, W. R. *Tetrahedron* **1999**, *55*, 4109-4122.
40. Marco-Contelles, J.; Rodriguez-Fernandez, M. *Tetrahedron Lett.* **2000**, *41*, 381-384.
41. Fontana, F.; Kolt, R. J.; Huang, Y.; Wayner, D. D. M. *J. Org. Chem.* **1994**, *59*, 4671-4676.
42. Andrieux, C. P.; Savéant, J.-M.; Tallec, A.; Tardivel, R.; Tardy, C. *J. Am. Chem. Soc.* **1997**, *119*, 2420-2429.
43. Curran, D. P.; Ko, S.-B. *Tetrahedron Lett.* **1998**, *39*, 6629-6632.
44. Miranda, L. D.; Cruz-Almanda, R.; Pavón, M.; Romero, Y.; Muchowski, J. M. *Tetrahedron Lett.* **2000**, *41*, 10181-10184.
45. Lexa, D.; Savéant, J.-M.; Schäfer, H. J.; Su, K.-B.; Vering, B.; Wang, D. L. *J. Am. Chem. Soc.* **1990**, *112*, 6162-6177.
46. Curran, D. P.; Liu, H.; Josien, H.; Ko, S. *Tetrahedron* **1996**, *52*, 11385-11404.
47. Engel, P. S.; Wu, W.-X. *J. Am. Chem. Soc.* **1989**, *111*, 1830-1835.
48. Curran, D. P.; Yu, H.; Liu, H. *Tetrahedron* **1994**, *50*, 7343-7366.
49. Wunderlich, M. D.; Leung, L. K.; Sandberg, J. A.; Meyer, K. D.; Yoder, C. H. *J. Am. Chem. Soc.* **1978**, *100*, 1500-1503.
50. Chupp, J. P.; Olin, J. F. *J. Org. Chem.* **1967**, *32*, 2297-2303.
51. Otani, Y.; Nagae, O.; Naruse, Y.; Inagaki, S.; Ohno, M.; Yamaguchi, K.; Yamamoto, G.; Uchiyama, M.; Ohwada, T. *J. Am. Chem. Soc.* **2003**, *125*, 15191-19199.
52. Sandström, J. *Dynamic NMR Spectroscopy*; Academic Press Inc.: New York, New York, 1982.
53. Ōki, M. *Applications of Dynamic NMR Spectroscopy to Organic Chemistry*; VCH Publishers: Deerfield Beach, 1985; Vol. 4.

54. Ōki, M. *The Chemistry of Rotational Isomers*; Springer-Verlag: New York, 1993; Vol. 30.
55. Reich, H. J. *J. Chem. Ed. Software* **1996**, *3D*, 2.
56. Curran, D. P.; Liu, W.; Chen, C. H.-T. *J. Am. Chem. Soc.* **1999**, *121*, 11012-11013.
57. Mannschreck, A.; Vonderheid, C. *Chem. Lett.* **1977**, *6*, 211-214.
58. Ahlbrecht, H.; Becher, G.; Blecher, J.; Kalinowski, H.-O.; Raab, W.; Mannschreck, A. *Tetrahedron Lett.* **1979**, *24*, 2265-2268.
59. Giese, B. *Angew. Chem. Int. Ed.* **1983**, *22*, 753-764.
60. Laidler, K. J.; Meiser, J. H. *Physical Chemistry*; 3rd ed.; Houghton Mifflin Company: Boston, 1999.
61. Stout, G. H.; Jensen, L. H. *X-Ray Structure Determination: A Practical Guide*; 2nd ed.; John Wiley & Sons: New York, 1989.
62. AcornNMR; Version 3.7.28.14 ed.; Acorn NMR Inc.: Livermore, CA.
63. Newcomb, M. *Tetrahedron* **1993**, *49*, 1151-1176.
64. Musa, O. M.; Choi, S.-Y.; Horner, J. H.; Newcomb, M. *J. Org. Chem.* **1998**, *63*, 786-793.
65. Chatgilialoglu, C.; Dickhaut, J.; Giese, B. *J. Org. Chem.* **1991**, *56*, 6399-6403.
66. Chatgilialoglu, C.; Ingold, K. U.; Scaiano, J. C. *J. Am. Chem. Soc.* **1981**, *103*, 7739-7742.
67. Friedrich, E. C.; Abma, C. B.; Vartanian, P. F. *J. Organomet. Chem.* **1980**, *187*, 203-211.
68. Lund, T.; Wayner, D. D. M.; Jonsson, M.; Larsen, A. G.; Daasbjerg, K. *J. Am. Chem. Soc.* **2001**, *123*, 12590-12595.
69. Wayner, D. D. M.; McPhee, D. J.; Griller, D. *J. Am. Chem. Soc.* **1988**, *110*, 132-137.
70. Burkey, T. J.; Castelhano, A. L.; Griller, D.; Lossing, F. P. *J. Am. Chem. Soc.* **1983**, *105*, 4701-4703.
71. Suga, S.; Suzuki, S.; Yoshida, J.-i. *J. Am. Chem. Soc.* **2002**, *124*, 30-31.
72. Fry, A. J. *Synthetic Organic Electrochemistry*; 2nd ed.; John Wiley & Sons, Inc.: New York, 1989.
73. Baizer, M. M.; Chruma, J. L. *J. Org. Chem.* **1972**, *37*, 1951-1960.
74. *Organic Electrochemistry*; Marcel Dekker, Inc.: New York, 1973.
75. Bard, A. J. *Acyclic Aliphatic Halides et al.*; Marcel Dekker, Inc.: New York, 1984; Vol. 14.
76. Eberson, L. *Electron Transfer Reactions in Organic Chemistry*; 1st ed.; Springer-Verlag: Heidelberg, 1987.
77. Costentin, C.; Robert, M.; Savéant, J.-M. *Chem. Phys.* **2006**, *324*, 40-56.
78. Maryanoff, B. E.; Zhang, H.-C.; Cohen, J. H.; Turchi, I. J.; Maryanoff, C. A.; *Chem. Rev.* **2004**, *104*, 1431-1628, especially 1435-1438 and 1450-1454.
79. Padwa, A.; Lee, H. I.; Rashatasakhon, P.; Rose, M. *J. Org. Chem.* **2004**, *69*, 8209-8218.
80. Harrowven, D. C.; Guy, I. L. *Chem. Commun.* **2004**, 1968-1969.
81. *Reduction*; Pergamon Press, Inc.: New York, 1991; Vol. 8.
82. Kim, M.; Kawada, K.; Gross, R. S.; Watt, D. S. *J. Org. Chem.* **1990**, *55*, 504-511.
83. Nikulin, V. I.; Rakov, I. M.; De Los Angeles, J. E.; Mehta, R. C.; Boyd, L. Y.; Feller, D. R.; Miller, D. D. *Bioorg. Med. Chem.* **2006**, *14*, 1684-1697.
84. Zheng, X.; Wang, X.; Chang, J.; Zhao, K. *Synlett* **2006**, *19*.
85. Keller, A. Ph.D. Dissertation, University of Pittsburgh, 2007.
86. Gervay, J.; Gregar, T. Q. *Tetrahedron Lett.* **1997**, *38*, 5921-5924.
87. Zimmerman, H. E. *J. Am. Chem. Soc.* **1957**, *79*, 6554-6558.

88. Pagni, R. M.; Kabalka, G. W.; Boothe, R.; Gaetano, K.; Stewart, L. J.; Conaway, R.; Dial, C.; Gray, D.; Larson, S.; Luidhart, T. *J. Org. Chem.* **1988**, *53*, 4477-4482.
89. Harrowven, D. C.; Guy, I. L. *J. Chem. Soc., Chem. Commun.* **2004**, 1968-1969.
90. Curran, D. P.; Guthrie, D. B.; Geib, S. J. *J. Am. Chem. Soc.* **2008**, *130*, 8437-8445.
91. Adler, T.; Bonjoch, J.; Clayden, J.; Font-Bardía, M.; Pickworth, M.; Solans, X.; Solé, D.; Vallverdú, L. *Org. Biomol. Chem.* **2005**, *3*, 3173-3183.
92. Ahmed, A.; Bragg, R. A.; Clayden, J.; Lai, L. W.; McCarthy, C.; Pink, J. H.; Westlund, N.; Yasin, S. *Tetrahedron* **1998**, *54*, 13277-13294.
93. Ates, A.; Curran, D. P. *J. Am. Chem. Soc.* **2001**, *123*, 5130-5131.
94. Betson, M. S.; Clayden, J.; Helliwell, M.; Johnson, P.; Lai, L. W.; Pink, J. H.; Stimson, C. C.; Vassiliou, M.; Yasin, S.; Youssef, L. *Org. Biomol. Chem.* **2006**, 424-443.
95. Bringmann, G.; Tasler, S.; Endress, H.; Kraus, J.; Messer, K.; Wohlfarth, M.; Lobin, W. *J. Am. Chem. Soc.* **2001**, *123*, 2703-2711.
96. Cass, Q. B.; Degani, A. L. G.; Tiritan, M. E.; Matlin, S. A.; Curran, D. P.; Balog, A. *Chirality* **1997**, *9*, 109-112.
97. Clayden, J. *Synlett* **1998**, 810-816.
98. Clayden, J. *Chem. Commun.* **2004**, 127-135.
99. Clayden, J.; Foricher, Y. J. Y.; Helliwell, M.; Johnson, P.; Mitjans, D.; Vinader, V. *Org. Biomol. Chem.* **2006**, 444-454.
100. Clayden, J.; Lai, L. W. *Angew. Chem. Int. Ed.* **1999**, *38*, 2556-2558.
101. Clayden, J.; Lai, L. W.; Helliwell, M. *Tetrahedron* **2004**, *60*, 4399-4412.
102. Clayden, J.; Lemiègre, L.; Pickworth, M.; Jones, L. *Org. Biomol. Chem.* **2008**, 2908-2913.
103. Clayden, J.; Turner, H.; Helliwell, M.; Moir, E. *J. Org. Chem.* **2008**, *73*, 4415-4423.
104. Clayden, J.; Vallverdú, L.; Helliwell, M. *Org. Biomol. Chem.* **2006**, 2106-2118.
105. Curran, D. P.; Chen, C. H.-T.; Geib, S. J.; Lapierre, A. J. B. *Tetrahedron* **2004**, *60*, 4413-4424.
106. Curran, D. P.; DeMello, N. C. *J. Chem. Soc. Chem. Comm.* **1993**, 1314-1316.
107. Curran, D. P.; Hale, G. R.; Geib, S. J.; Balog, A.; Cass, Q. B.; Degani, A. L. G.; Hernandes, M. Z.; Freitas, L. C. G. *Tetrahedron: Asymmetry* **1997**, *8*, 3955-3975.
108. Curran, D. P.; Liu, W.; Chen, C. H.-T. *J. Am. Chem. Soc.* **1999**, *121*, 11012-11013.
109. Curran, D. P.; Qi, H.; Geib, S. J.; DeMello, N. C. *J. Am. Chem. Soc.* **1994**, *116*, 3131-3132.
110. Dantale, S.; Reboul, V.; Metzner, P.; Philouze, C. *Chem. Eur. J.* **2002**, *8*, 632-640.
111. Godfrey, C. R. A.; Simpkins, N. S.; Walker, M. D. *Synlett* **2000**, *3*, 388-390.
112. Hata, T.; Koide, H.; Taniguchi, N.; Uemura, M. *Org. Lett.* **2000**, *2*, 1907-1910.
113. Hata, T.; Koide, H.; Uemura, M. *Synlett* **2000**, 1145-1147.
114. Huettel, W.; Nieger, M.; Mueller, M. *Synthesis* **2003**, 1803-1808.
115. Hughes, A. D.; Price, D. A.; Shishkin, O.; Simpkins, N. S. *Tetrahedron Lett.* **1996**, *37*, 7607-7610.
116. Hughes, A. D.; Price, D. A.; Simpkins, N. S. *J. Chem. Soc. Perk. Trans. 1* **1999**, 1295-1304.
117. Hughes, A. D.; Simpkins, N. S. *Synlett* **1998**, *9*, 967-968.
118. Kawabata, T.; Yahiro, K.; Fuji, K. *J. Am. Chem. Soc.* **1991**, *113*, 9694-9696.
119. Kitagawa, O.; Izawa, H.; Sato, K.; Dobashi, A.; Taguchi, T. *J. Org. Chem.* **1998**, *63*, 2634-2640.

120. Kitagawa, O.; Izawa, H.; Taguchi, T. *Tetrahedron Lett.* **1997**, *38*, 4447-4450.
121. Kitagawa, O.; Kohriyama, M.; Taguchi, T. *J. Org. Chem.* **2002**, *67*, 8682-8684.
122. Kitagawa, O.; Momose, S.-i.; Fushimi, Y.; Taguchi, T. *Tetrahedron Lett.* **1999**, *40*, 8827-8831.
123. Kitagawa, O.; Takahashi, M.; Yoshikawa, M.; Taguchi, T. *J. Am. Chem. Soc.* **2005**, *127*, 3676-3677.
124. Kitagawa, O.; Yoshikawa, M.; Tanabe, H.; Morita, T.; Takahashi, M.; Dobashi, Y.; Taguchi, T. *J. Am. Chem. Soc.* **2006**, *128*, 12923-12931.
125. Koide, H.; Hata, T.; Uemura, M. *J. Org. Chem.* **2002**, *67*, 1929-1935.
126. Koide, H.; Hata, T.; Yoshihara, K.; Kamikawa, K.; Uemura, M. *Tetrahedron* **2004**, *60*, 4527-4541.
127. Lapierre, A. J. B. Ph.D. Dissertation, University of Pittsburgh, 2005.
128. Lapierre, A. J. B.; Geib, S. J.; Curran, D. P. *J. Am. Chem. Soc.* **2007**, *129*, 494-495.
129. Nicolaou, K. C.; Mitchell, H. J.; Jain, N. F.; Winssinger, N.; Hughes, R.; Bando, T. *Angew. Chem. Int. Ed.* **1999**, *38*, 240-244.
130. Noyori, R. *Angew. Chem. Int. Ed.* **2002**, *41*, 2008-2022.
131. Oppenheimer, J.; Hsung, R. P.; Figueroa, R.; Johnson, W. L. *Org. Lett.* **2007**, *9*, 3969-3972.
132. Petit, M.; Geib, S. J.; Curran, D. P. *Tetrahedron* **2004**, *60*, 7543-7552.
133. Petit, M.; Lapierre, A. J. B.; Curran, D. P. *J. Am. Chem. Soc.* **2005**, *127*, 14994-14995.
134. Roussel, C.; Vanthuyne, N.; Bouchekara, M.; Djafri, A.; Elguero, J.; Alkorta, I. *J. Org. Chem.* **2008**, *73*, 403-411.
135. Tanaka, K.; Takeishi, K. *Synthesis* **2007**, 2920-2923.
136. Tanaka, K.; Takeishi, K.; Noguchi, K. *J. Am. Chem. Soc.* **2006**, *128*, 4586-4587.
137. Terauchi, J.; Curran, D. P. *Tetrahedron: Asymmetry* **2003**, *14*, 587-592.
138. Vanthuyne, N.; Andreoli, F.; Fernandez, S.; Roman, M.; Roussel, C. *Lett. Org. Chem.* **2005**, *2*, 433-443.
139. Wolf, C.; Köunig, W. A.; Roussel, C. *Chirality* **1995**, *7*, 610-611.
140. McNaught, A. D.; Wilkinson, A. *Compendium of Chemical Terminology*; IUPAC: Cambridge, 1997.
141. Eliel, E. L.; Wilen, S. H. *Stereochemistry of Organic Compounds*; John Wiley & Sons, Inc.: New York, 1994.
142. Cahn, R. S.; Ingold, C.; Prelog, V. *Angew. Chem. Int. Ed.* **1966**, *5*, 385-415.
143. Christie, G. H.; Kenner, J. *J. Chem. Soc., Trans.* **1922**, 614-620.
144. Pinto, B. M. In *Acyclic Organonitrogen Stereodynamics*; Lambert, J., Takeuchi, Y., Eds.; VCH Publishers, Inc.: New York, 1992, p 149-175.
145. Isbrandt, L.; Tung, W. C.-T.; Rogers, M. T. *J. Mag. Reson.* **1973**, *9*, 461-466.
146. Siddall, T. H.; Stewart, W. E.; Knight, F. D. *J. Phys. Chem.* **1970**, *74*, 3580-3583.
147. Lewin, A. H.; Frucht, M.; Chen, K. V. J.; Benedetti, E.; Di Blasio, B. *Tetrahedron* **1975**, *31*, 207-215.
148. Stewart, W. E.; Siddall, T. H. *Chem. Rev.* **1970**, *70*, 517-551.
149. Cuyegkang, M. A.; Mannschreck, A. *Chem. Ber.* **1987**, *120*, 803-809.
150. Pirkle, W. H.; Welch, C. J.; Zych, A. J. *J. Chromatogr. A* **1993**, *648*, 101-109.
151. Bragg, R. A.; Clayden, J.; Morris, G. A.; Pink, J. H. *Chem. Eur. J.* **2002**, *8*, 1279-1289.
152. Pedersen, B. F.; Pedersen, B. *Tetrahedron Lett.* **1965**, *6*, 2995-3001.
153. Ototake, N.; Taguchi, T.; Kitagawa, O. *Tetrahedron Lett.* **2008**, *49*, 5458-5460.

154. Mills, W. H.; Kelham, R. M. *J. Chem. Soc.* **1937**, 274-278.
155. Lapierre, A. J. B. Ph.D. Dissertation, University of Pittsburgh, 2005.
156. Pirkle, W. H.; Welch, C. J.; Hyun, M. H. *J. Chromatogr. A* **1992**, *607*, 126-130.
157. Qi, H. Ph.D. Dissertation, University of Pittsburgh, 1995.
158. Bach, T.; Schröder, J.; Harms, K. *Tetrahedron Lett.* **1999**, *40*, 9003-9004.
159. Fuji, K.; Kawabata, T. *Chem. Eur. J.* **1998**, *4*, 373-376.
160. Zhao, H.; Hsu, D. C.; Carlier, P. R. *Synthesis* **2005**, *1*, 1-16.
161. Kawabata, T.; Fuji, K. In *Topics In Stereochemistry*; Denmark, S. E., Ed.; John Wiley & Sons, Inc.: New York, 2003; Vol. 23, p 175-206.
162. Rychnovsky, S. D.; Dalgard, J. E. *Org. Lett.* **2004**, *6*, 2713-2716.
163. Kondru, R. K.; Chen, C. H.-T.; Curran, D. P.; Beratan, D. N.; Wipf, P. *Tetrahedron: Asymmetry* **1999**, *10*, 4143-4150.
164. Guthrie, D. B.; Curran, D. P., Unpublished results.
165. *Protective Groups in Organic Synthesis*; 3rd ed.; Greene, T. W.; Wuts, P. G. M., Eds.; John Wiley & Sons, Inc.: New York, 1999.
166. Boger, D. L.; Boyce, C. W. *J. Org. Chem.* **2000**, *65*, 4088-4100.
167. Boger, D. L.; Hughes, T. V.; Hedrick, M. P. *J. Org. Chem.* **2001**, *66*, 2207-2216.
168. Boger, D. L.; Santillán Jr., A.; Searcey, M.; Brunette, S. R.; Wolkenberg, S. E.; Hedrick, M. P.; Jin, Q. *J. Org. Chem.* **2000**, *65*, 4101-4111.
169. Jin, W.; Trzupek, J. D.; Rayl, T. J.; Broward, M. A.; Vielhauer, G. A.; Weir, S. J.; Hwang, I.; Boger, D. L. *J. Am. Chem. Soc.* **2007**, *129*, 15391-15397.
170. Patel, V. F.; Andis, S. L.; Enkema, J. K.; Johnson, D. A.; Kennedy, J. H.; Mohamadi, F.; Schultz, R. M.; Soose, D. J.; Spees, M. M. *J. Org. Chem.* **1997**, *62*, 8868-8874.
171. Tichenor, M. S.; MacMillan, K. S.; Stover, J. S.; Wolkenberg, S. E.; Pavani, M. G.; Zanella, L.; Zaid, A. N.; Spalluto, G.; Rayl, T. J.; Hwang, I.; Baraldi, P. G.; Boger, D. L. *J. Am. Chem. Soc.* **2007**, *129*, 14092-14099.
172. Tichenor, M. S.; Trzupek, J. D.; Kastrinsky, D. B.; Shiga, F.; Hwang, I.; Boger, D. L. *J. Am. Chem. Soc.* **2006**, *128*, 15683-15696.
173. Tietze, L. F.; Haunert, F.; Feuerstein, T.; Herzig, T. *Eur. J. Org. Chem.* **2003**, 562-566.
174. Tietze, L. F.; Major, F.; Schuberth, I.; Spiegl, D. A.; Krewer, B.; Maksimenka, K.; Bringmann, G.; Magull, J. *Chem. Eur. J.* **2007**, *13*, 4396-4409.
175. Tietze, L. F.; Herzig, T.; Fecher, A.; Haunert, F.; Schuberth, I. *ChemBioChem* **2001**, *2*, 758-765.
176. Tietze, L. F.; Herzig, T.; Feuerstein, T.; Schuberth, I. *Eur. J. Org. Chem.* **2002**, 1634-1645.
177. Julià, S.; Ginebreda, A.; Sala, P.; Sancho, M.; Annunziata, R.; Cozzi, F. *Org. Magn. Reson.* **1983**, *21*, 573-575.
178. Cooke, M. P., Jr. *J. Org. Chem.* **1984**, *49*, 1144-1146.
179. Cooke, M. P., Jr.; Widener, R. K. *J. Org. Chem.* **1987**, *52*, 1381-1396.
180. Clayden, J. *Organolithiums: Selectivity for Synthesis*; 1st ed.; Pergamon: Boston, 2002.
181. Piers, E.; Harrison, C. L.; Zetina-Rocha, C. *Org. Lett.* **2001**, *3*, 3245-3247.
182. Horne, S.; Taylor, N.; Collins, S.; Rodrigo, R. *J. Chem. Soc. Perk. Trans. 1* **1991**, 3047-3051.
183. Köbrich, G.; Trapp, H. *Chem. Ber.* **1966**, *99*, 670-679.
184. Bordwell, F. G.; Fried, H. E. *J. Org. Chem.* **1991**, *56*, 4218-4223.
185. Kosynkin, D. V.; Tour, J. M. *Org. Lett.* **2001**, *3*, 991-992.

186. Koradin, C.; Dohle, W.; Rodriguez, A. L.; Schmid, B.; Knochel, P. *Tetrahedron* **2003**, *59*, 1571-1589.
187. Hellwinkel, D.; Laemmerzahl, F.; Hofmann, G. *Chem. Ber.* **1983**, *116*, 3375-3405.
188. Dugave, C. In *Cis-trans Isomerization in Biochemistry*; 1st ed.; Dugave, C., Ed.; Wiley-VCH: Weinheim, 2006, p 1-5.
189. Deetz, M. J.; Forbes, C. C.; Jonas, M.; Malerich, J. P.; Smith, B. D.; Wiest, O. *J. Org. Chem.* **2002**, *67*, 3949-3952.
190. Smith, B. D.; Goodenough-Lashua, D. M.; D'Souza, C. J. E.; Norton, K. J.; Schmidt, L. M.; Tung, J. C. *Tetrahedron Lett.* **2004**, *45*, 2747-2749.
191. Kost, D.; Kornberg, N. *Tetrahedron Lett.* **1978**, *19*, 3275-3276.
192. Rablen, P. R. *J. Org. Chem.* **2000**, *65*, 7930-7937.
193. Okano, K.; Tokuyama, H.; Fukuyama, T. *J. Am. Chem. Soc.* **2006**, *128*, 7136-7137.
194. Yamada, K.; Kurokawa, T.; Tokuyama, H.; Fukuyama, T. *J. Am. Chem. Soc.* **2003**, *125*, 6630-6631.
195. Barton, D. H. R.; Crich, D.; Motherwell, W. B. *Tetrahedron* **1985**, *41*, 3901-3924.
196. Beckwith, A. L. J.; Joseph, S. P.; Mayadunne, T. A. *J. Org. Chem.* **1993**, *58*, 4198-4199.
197. Jones, K.; McCarthy, C. *Tetrahedron Lett.* **1989**, *30*, 2657-2660.
198. Alcaide, B.; Almendros, P.; Rodríguez-Vicente, A.; Ruiz, M. P. *Tetrahedron* **2005**, *61*, 2767-2778.
199. Alcaide, B.; Moreno, A. M.; Rodríguez-Vicente, A.; Sierra, M. A. *Tetrahedron: Asymmetry* **1996**, *7*, 2203-2206.
200. Lampard, C.; Murphy, J. A.; Rasheed, F. *Tetrahedron Lett.* **1994**, *35*, 8675-8678.
201. Lampard, C.; Murphy, J. A.; Lewis, N. *J. Chem. Soc. Chem. Comm.* **1993**, *1993*, 295-297.
202. Johnston, L. J.; Lusztyk, J.; Wayner, D. D. M.; Abeywickreyma, A. N.; Beckwith, A. L. J.; Scaiano, J. C.; Ingold, C. K. *J. Am. Chem. Soc.* **1985**, *107*, 4594-4596.
203. Jones, K.; Storey, J. M. D. *J. Chem. Soc. Chem. Comm.* **1992**, 1766-1767.
204. Stambuli, J. P.; Stauffer, S. R.; Shaughnessy, K. H.; Hartwig, J. F. *J. Am. Chem. Soc.* **2001**, *123*, 2677-2678.
205. Mori, M.; Nakanishi, M.; Kajishima, D.; Sato, Y. *Org. Lett.* **2001**, *3*, 1913-1916.
206. Mori, M.; Nakanishi, M.; Kajishima, D.; Sato, Y. *J. Am. Chem. Soc.* **2003**, *125*, 9801-9807.
207. Zhu, G.; Lu, X. *Organometallics* **1995**, *14*, 4899-4904.
208. Mariampillai, B.; Herse, C.; Lautens, M. *Org. Lett.* **2005**, *7*, 4745-4747.
209. Lautens, M.; Tayama, E.; Herse, C. *J. Am. Chem. Soc.* **2005**, *127*, 72-73.
210. Cicchi, S.; Goti, A.; Guarna, A.; De Sarlo, F. *Tetrahedron Lett.* **1990**, *31*, 3351-3354.
211. Li, F.; Brogan, J. B.; Gage, J. L.; Zhang, D.; Miller, M. J. *J. Org. Chem.* **2004**, *69*, 4538-4540.
212. Baeckvall, J. E.; Vaagberg, J. O. *Org. Synth.* **1990**, *69*, 38-43.
213. Cheng, J. C.-Y.; Daves, J., G. Doyle *Organometallics* **1986**, *5*, 1753-1755.
214. Sinou, D.; Bedjeguelal, K. *Eur. J. Org. Chem.* **2000**, 4071-4077.
215. Kimura, Y.; Kusano, M.; Koshino, H.; Uzawa, J.; Fujioka, S.; Tani, K. *Tetrahedron Lett.* **1996**, *37*, 4961-4964.
216. Ito, C.; Itoigawa, M.; Otsuka, T.; Tokuda, H.; Nishino, H.; Furukawa, H. *J. Nat. Prod.* **2000**, *63*, 1344-1348.

217. Ellis, D.; Kuhen, K. L.; Anaclerio, B.; Wu, B.; Wolff, K.; Yin, H.; Bursulaya, B.; Caldwell, J.; Karanewsky, D.; He, Y. *Bioorg. Med. Chem. Lett.* **2006**, *16*, 4246-4251.
218. Patel, M.; McHugh Jr., R. J.; Cordova, B. C.; Klabe, R. M.; Bacheler, L. T.; Erickson-Viitanen, S.; Rodgers, J. D. *Bioorg. Med. Chem. Lett.* **2001**, *11*, 1943-1945.
219. Seitz, W.; Geneste, H.; Backfisch, G.; Delzer, J.; Graef, C.; Hornberger, W.; Kling, A.; Subkowskic, T.; Norbert, Z. *Bioorg. Med. Chem. Lett.* **2008**, *18*, 527-531.
220. El Ali, B.; Okuro, K.; Vasapollo, G.; Alper, H. *J. Am. Chem. Soc.* **1996**, *118*, 4264-4270.
221. Dong, C.; Alper, H. *Tetrahedron: Asymmetry* **2004**, *15*, 35-40.
222. Okuro, K.; Kai, H.; Alper, H. *Tetrahedron: Asymmetry* **1997**, *8*, 2307-2309.
223. Blay, G.; Cardona, L.; Torres, L.; Pedro, J. R. *Synthesis* **2007**, 108-112.
224. McAllister, L. A.; Turner, K. L.; Brand, S.; Stefaniak, M.; Procter, D. J. *J. Org. Chem.* **2006**, *71*, 6497-6507.
225. Turner, K. L.; Baker, T. M.; Islam, S.; Procter, D. J.; Stefaniak, M. *Org. Lett.* **2006**, *8*, 329-332.
226. Bolm, C.; Hildebrand, J. P. *Tetrahedron Lett.* **1998**, *39*, 5731-5734.
227. Clark, A. J.; Jones, K.; McCarthy, C.; Storey, J. M. D. *Tetrahedron Lett.* **1991**, *32*, 2829-2832.
228. Clark, A. J.; Jones, K. *Tetrahedron* **1992**, *48*, 6875-6882.
229. Sato, T.; Ishida, S.; Ishibashi, H.; Ikeda, M. *J. Chem. Soc. Perk. Trans. 1* **1991**, 353-359.
230. Allan, G. M.; Parsons, A. F.; Pons, J.-F. *Synlett* **2002**, 1431-1434.
231. Ishibashi, H.; Sato, T.; Ikeda, M. *Synthesis* **2002**, *6*, 695-713.
232. Itai, A.; Toriumi, Y.; Tomioka, N.; Kagechika, H.; Azumaya, I.; Shudo, K. *Tetrahedron Lett.* **1989**, *30*, 6177-6180.
233. McLaughlin, M.; Palucki, M.; Davies, I. W. *Org. Lett.* **2006**, *8*, 3307-3310.
234. Nakamura, I.; Yamagishi, U.; Song, D.; Konta, S.; Yamamoto, Y. *Angew. Chem. Int. Ed.* **2007**, *46*, 2284-2287.
235. Opatz, T.; Ferenc, D. *Org. Lett.* **2006**, *8*, 4473-4475.
236. Jeffery, T. *Tetrahedron* **1996**, *52*, 10113-10130.
237. Georgiades, S. N.; Clardy, J. *Org. Lett.* **2005**, *7*, 4091-4094.
238. Georgiades, S. N.; Clardy, J. *Org. Lett.* **2006**, *8*, 4251-4254.
239. Campbell, J. B., Jr.; Firor, J. W.; Davenport, T. W. *Synth. Commun.* **1989**, *19*, 2265-2272.
240. See Experimental section for more information.
241. Franz, J. A.; Suleman, N. K.; Alnajjar, M. S. *J. Org. Chem.* **1986**, *51*, 19-25.
242. Musa, O. M.; Choi, S.-Y.; Horner, J. H.; Newcomb, M. *J. Org. Chem.* **1998**, *63*, 786-793.
243. Beckwith, A. L. J. *Tetrahedron* **1981**, *37*, 3073-3100.
244. Bott, G.; Field, L. D.; Sternhell, S. *J. Am. Chem. Soc.* **1980**, *102*, 5618-5626.
245. Bijvoet, J. M.; Peerdeman, A. F.; van Bommel, A. J. *Nature* **1951**, *168*, 271-272.
246. Dunitz, J. D. *Angew. Chem. Int. Ed.* **2001**, *40*, 4167-4173.
247. Maddaluno, J. F.; Gresh, N.; Giessner-Prettre, C. *J. Org. Chem.* **1994**, *59*, 793-802.
248. Roesky, H. W.; Andruh, M. *Coord. Chem. Rev.* **2003**, *236*, 91-119.
249. Strub, W.; Roduner, E.; Fischer, H. *J. Phys. Chem.* **1987**, *91*, 4379-4383.
250. Fremont, S. L.; Belletire, J. L.; Ho, D. M. *Tetrahedron Lett.* **1991**, *32*, 2335-2338.
251. Bryans, J. S.; Large, J. M.; Parsons, A. F. *J. Chem. Soc. Perk. Trans. 1* **1999**, 2897-2904.
252. De Riggi, I.; Gastaldi, S.; Surzur, J.-M.; Bertrand, M. P. *J. Org. Chem.* **1992**, *57*, 6118-6125.

253. Sato, T.; Wada, Y.; Nishimoto, M.; Ishibashi, H.; Ikeda, M. *J. Chem. Soc. Perk. Trans. 1* **1989**, 879-886.
254. Akritopoulou-Zanze, I.; Whitehead, A.; Waters, J. E.; Henry, R. F.; Djuric, S. W. *Tetrahedron Lett.* **2007**, *48*, 3549-3552.
255. Bowry, V. W.; Lusztyk, J.; Ingold, K. U. *J. Am. Chem. Soc.* **1991**, *113*, 5687-5698.
256. Beckwith, A. L. J.; Bowry, V. W. *J. Org. Chem.* **1988**, *53*, 1632-1641.
257. Nonhebel, D. C. *Chem. Soc. Rev.* **1993**, *22*, 347-359.
258. Furxhi, E.; Horner, J. H.; Newcomb, M. *J. Org. Chem.* **1999**, *64*, 4064-4068.
259. Horner, J. H.; Tanaka, N.; Newcomb, M. *J. Am. Chem. Soc.* **1998**, *120*, 10379-10390.
260. Beckwith, A. L. J.; Schiesser, C. H. *Tetrahedron Lett.* **1985**, *26*, 373-376.
261. Spellmeyer, D. C.; Houk, K. N. *J. Org. Chem.* **1987**, *52*, 959-974.
262. Denmark, S. E.; Cottell, J. J. *Adv. Synth. Catal.* **2006**, *348*, 2397-2042.
263. Overman, L. E.; Robertson, G. M.; Robichaud, A. J. *J. Am. Chem. Soc.* **1991**, *113*, 2598-2610.
264. Plat, M.; Hachem-Mehri, M.; Koch, M.; Scheidegger, U.; Potier, P. *Tetrahedron Lett.* **1970**, *39*, 3395-3398.
265. Selig, P.; Bach, T. *Angew. Chem. Int. Ed.* **2008**, *47*, 5082-5084.
266. Skoog, D. A.; Holler, F. J.; Nieman, T. A. *Principles of Instrumental Analysis*; 5th ed.; Harcourt Brace College Publishers: Philadelphia, 1998.
267. Mokotoff, M.; Hill, S. T. *J. Heterocycl. Chem.* **1988**, *25*, 65-71.
268. Allin, S. M.; James, S. L.; Elsegood, M. R. J.; Martin, W. P. *J. Org. Chem.* **2002**, *67*, 9464-9467.
269. Molander, G. A.; Harris, C. R. *J. Am. Chem. Soc.* **1995**, *117*, 3705-3716.
270. Padwa, A.; Rashatasakhon, P.; Rose, M. *J. Org. Chem.* **2003**, *68*, 5139-5146.
271. Leibner, J. E.; Jacobus, J. *J. Org. Chem.* **1979**, *44*, 449.
272. Adams, R.; Sundholm, N. K. *J. Am. Chem. Soc.* **1948**, *70*, 2667-2673.
273. Hiroya, K.; Itoh, S.; Sakamoto, T. *J. Org. Chem.* **2004**, *69*, 1126-1136.
274. Duclos, J.-F.; Outurquin, F.; Paulmier, C. *Tetrahedron Lett.* **1993**, *34*, 7417-7420.
275. Das, B. P.; Begum, N. A.; Choudhury, D. N.; Banerji, J. *J. Ind. Chem. Soc.* **2005**, *82*, 158-160.
276. Howell, J. A. S.; Fey, N.; Lovatt, J. D.; Yates, P. C.; McArdle, P.; Cunningham, D.; Sadeh, E.; Gottlieb, H. E.; Goldschmidt, Z.; Hursthouse, M. B.; Light, M. E. *J. Chem. Soc., Dalton Trans.* **1999**, 3015-3028.